An examination of escape times in a mock residential test house by analyzing smoke filling and detection times for couch fires in a living room

by

Peter Senez

A thesis
presented to the University of Waterloo
in fulfillment of the
thesis requirement for the degree of
Doctor of Philosophy
in
Mechanical and Mechatronics Engineering

Waterloo, Ontario, Canada, 2024

© Peter Senez 2024

Examining Committee Membership

The following served on the Examining Committee for this thesis. The decision of the Examining Committee is by majority vote.

External Examiner:	Patrick van Hees Professor, Head of Department Department of Building and Environmental Technology Lund University, Sweden
Supervisor:	Elizabeth Weckman Professor Department of Mechanical and Mechatronics Engineering University of Waterloo
Internal Members:	Andrea Scott Associate Professor Department of Mechanical and Mechatronics Engineering University of Waterloo
	David Torvi Adjunct Professor Department of Mechanical and Mechatronics Engineering University of Waterloo
Internal-External Member:	Christine Moresoli Associate Dean, Professor Department of Chemical Engineering University of Waterloo

Author's Declaration

I hereby declare that I am the sole author of this thesis. This is a true copy of the thesis, including any required final revisions, as accepted by my examiners.

I understand that my thesis may be made electronically available to the public.

Abstract

A series of full-scale multi-compartment and multi-storey fire experiments are undertaken to evaluate the potential “available safe escape time” (ASET) in fires fueled by different upholstered furniture types, burning under controlled ventilation conditions in a representative multi-storey residential dwelling. Ten different furniture fire experiments are conducted to fill key gaps in current understanding of fire growth and behavior, smoke filling, detection times, and available escape times in limited ventilation conditions as established within the well-instrumented “burn house” at the University of Waterloo Fire Research Laboratory. Findings for mass loss rate, smoke movement and resultant visibility, oxygen consumption, and the evolution of carbon monoxide along the “escape path” are compared across furniture types. An estimate is made for the available escape time accounting for occupant movement while upright, or when the environmental conditions deteriorate, movement out of the house by crawling. Findings show that the North American furniture fires result in crawl-out available escape times between 96 and 238 seconds whereas the UK furniture fires have significantly longer crawl-out available escape times, between 281 – 1487 seconds.

In slower-burning fires, the importance of considering the incipient fire time in comparing detector response highlights the benefit of placing detectors near fuel loads in living areas, which in this study allows for a 127% increase in available escape time. An overall increase in available escape time of 19 – 50% is found for the fast-burning North American furniture. Flame-retardant interliners, combined with flame-retardant treatments, are observed to significantly limit the exposure and participation of the polyurethane foam in the fire, controlling fire growth in one instance and preventing sustained ignition in two other couches. Further examination of key elements of furniture fire behavior illustrates that ignition, incipient fire time, growth period, and peak mass loss rate are critical functional parameters. These can be used to define a scoring system by which to compare the fire performance of different couches.

Through detailed analysis of video evidence, several unique patterns of smoke filling are observed. These include encapsulation of the fire in the burn room, a smoke hazing effect, visual evidence of a smoke layer within the smoke layer, and smoke layers that ascend from floor to ceiling. Due to their importance in the determination of visibility through a given escape route, these are worthy of more in-depth investigation in future research. Overall, the research fills key gaps in our understanding of the evolution of fire environments in limited ventilation residential furniture fires as related to available time for occupant escape. As such, it highlights the need for defined fire safety objectives in house design to improve residential fire safety.

Keywords: escape time, smoke filling, smoke spread, fire detection, upholstered furniture fire testing, fire dynamics, flame retardants, crawl-out, air-aspirated smoke detection, incipient burning, fire growth, ventilation-limited compartment, house fire, single-family home, fire video capture, fire characterization, gas species production.

Acknowledgments

A sincere thank you to my immediate and extended family, whose immense support and encouragement have inspired and motivated me through this extended journey. At the University, sincere appreciation goes to my supervisor, Prof. Weckman, for her overall dedication to fire science; Andy Barber, for his persistence to make things work; and innumerable others, many of whom I never met, and who supported the construction and repair of the test house and all of the corresponding instrumentation. There are a multitude of students who participated in this phase of the research program and immensely helped with the program management, setup, implementation, and compiling data after the tests; including: Bronwyn Forrest, Vusal Ibrahimli, Alex DiPaola, Jennifer Ellingham, Keon Senez, Liam Marshall, and Ayaan Lakhani plus many others who contributed from time to time directly and indirectly, including many York University students. I'd also like to recognize my current and past business partners, colleagues and friends who have been involved in supporting research in this area, especially Keith Calder, Chris Reed, Danusia Figiel, Gordana Tijanic, Mike Bodnar, Yeo Swee Khiank, and Tony Cole. A special recognition also to Harold Locke for his encouragement and mentorship over the past 30 years.

Finally, there have been several financial contributors, both direct and in-kind, that have supported this research through the University, which include: Natural Sciences and Engineering Research Council of Canada, BC Housing, the City of Calgary, the American Chemistry Council's Foundation for Chemistry Research & Initiatives, Mircom, Xtralis, Canada Foundation for Innovation, Southwest Research Institute, York University, Fire & Risk Alliance, the Ontario Centre of Innovation, RDH Building Science Laboratories, Waterloo Fire Rescue, Kitchener Fire Department, and University of Waterloo Plant Operations.

Dedication

This thesis is dedicated to those who have perished or been injured by fire in their homes.

Table of Contents

Examining Committee Membership ii
Author's Declaration iii
Abstract iv
Acknowledgments vi
Dedication vii
List of Figures xi
List of Tables xvi
List of Abbreviations xvii
Chapter 1 Introduction 1
Chapter 2 Literature Review 4
2.1 Residential Fire Experience 4
2.1.1 Fire frequency and fatality in residences 4
2.2 Smoke Alarms and Escape Time for Residential Fires 7
2.2.1 Smoke Alarm Early Placement History (1960 to 1980) 7
2.2.2 Tenability Criteria for Safe Escape During a Fire (1980 – Present) 11
2.2.3 Smoke Alarm Placement and Audibility (1980 – 2000) 13
2.2.4 Smoke Alarm Placement and Audibility (2000 – Present) 15
2.2.5 Smoke Detector Placement Research Observations and Summary 20
2.3 Smoke Filling in a Ventilation-limited Environment 21
2.4 Furniture Ignition Controls 22
2.5 Previous Testing & Research 31
2.5.1 Early House Burns and Ventilation Environment 31
2.5.2 Precursor work at the University of Waterloo 32
2.6 Synopsis of Literature and Research Focus 36
Chapter 3 Objectives and Experimental Design 38
3.1 Research Objectives 39
3.2 Test House Configuration 40
3.3 Test House Instrumentation 43
3.3.1 Furniture Load Cells, Thermocouples & Heat Flux Gages 44
3.3.2 Velocity Probes & Gas Instrumentation Stations 48
3.3.3 Data Acquisition System 51
3.4 Mechanical Ventilation 51
3.5 Smoke Alarms, Detection and Video Camera Visibility 53

3.5.1 Smoke Detection....53
3.5.2 Video Cameras and Light Panels (Checkerboards)....56
Chapter 4 Experimental Test Framework & Procedure....57
4.1 Video Smoke Layer Descent and Visibility Tenability Criteria....57
4.2 Correlating the Developing Smoke Environment to MLR, Temperature, Asphyxiant Gas and Oxygen Depletion....62
4.3 Test Fuel – Furniture Selection and Flame Retardancy....65
4.4 Ignition Sources & Test Procedures....74
Chapter 5 Experimental Results....77
5.1 Temperature & Relative Humidity Outside of Test House....78
5.2 Ignition....78
5.3 Incipient Time Period....85
5.4 Consideration of Heat Release Rates....91
5.5 MLR in the Fire Growth Stage....92
5.6 Detector Response Times....100
5.6.1 Detector data for purposes of determination of escape time....104
5.6.2 Summary of observations relating to fire detectors....106
5.7 Smoke Layer Development....107
5.7.1 Wood Crib Fire Source – Test 1FV....107
5.7.2 Smoke Layer Development with the NFR Couches....111
5.7.3 Fire and Smoke Layer Development with the UK FR Couches....126
5.7.4 US FR Couch Tests....137
5.7.5 Summary of Results....143
5.8 Temperature....143
5.9 Gases....147
Chapter 6 Results & Discussion....155
6.1 Escape Times Based on Camera Visibility....155
6.2 Walk-out Escape Time....160
6.3 Crouch/Crawl-out Escape Time....162
6.4 Detector Location Sensitivity....165
6.5 Graphical Summary of Flaming Fire Tests....165
6.6 Furniture controls....172
Chapter 7 Conclusions....176
Chapter 8 Further Research....181
References....183

Appendices 192
Appendix A : One-minute video output for MV and FV series wood and couch tests 193
Appendix B : Temperature Time Curves for Select Thermocouple Locations 341
Appendix C : Gas Instrumentation Stations (GIS) Graphs 349

List of Figures

Figure 2-1: 10-year fire deaths in the US estimated by the US Fire Administration with a linear trendline. 4
Figure 2-2: 10-year fire deaths from 2012 and 2021 with a linear trendline. 5
Figure 2-3: Armchairs ignited by wastebasket filled with paper in Indiana Dunes Phase I test series. 9
Figure 2-4: FR (left) and NFR (right) couch experiment within a half-sea container in June 2014. 27
Figure 2-5: Early ignition of couches in comparison tests. 27
Figure 2-6: Video capture of burning into the seat cushion 27
Figure 2-7: Flashover occurs in the left cell and is initiated in the right cell. 28
Figure 2-8: Post-test image showing most foam burned while most of the wood framing was intact. 28
Figure 2-9: The time-temperature graph shows each burn cell's top and bottom thermocouple. 29
Figure 2-10: Example of post-incident burn with furniture no longer remaining. 32
Figure 2-11: Heat release rate data from 2015 UWFRL burn tests comparing NFR, FR and LFR materials. 34
Figure 2-12: Ad-hoc test to evaluate response to fabric and foam thermal exposure (samples placed radially equidistant from the fire origin) 34
Figure 2-13: 2015 UWFRL Couch experiments comparing FR and LFR couches. 35
Figure 2-14: 2015 UWFRL couch experiments comparing NFR and FR couches. 35
Figure 2-15: Graphical illustration of thesis research focus areas. 37
Figure 3-1: Visual representation of stages of fire development and viability of escape. 40
Figure 3-2: Floor Plan of Burn House (left) Lower Level (right) Upper Level. 41
Figure 3-3: Burn house with steel framing prior to boarding (left), and after boarding in the LBR (centre and right). 41
Figure 3-4: East facade of burn house showing smoke discharge from test outside Door 1. 42
Figure 3-5: North, West, and South facades of burn house with annotations for reference. 43
Figure 3-6: Image showing the general configuration of the test setup and corresponding instrumentation in the LBR. 43
Figure 3-7: Floor plan showing hypothetical escape path (green line) from upper level (left) through lower level (right) 44
Figure 3-8: Approximate load cell arrangement prior to being thermally protected. 45
Figure 3-9: Thermocouple and heat flux gage locations. 46
Figure 3-10: HFG (indicated by red arrows) in the wall opposite the couch (left) and on the floor on the edge of the burn area in LBR. 46
Figure 3-11: Velocity probes: (left) between LSW and LHA, (Centre) base of stair in LBR, (right) LHA top of stair. 48
Figure 3-12: Locations of velocity probes and Gas Instrumentation Stations 48
Figure 3-13: Sensor configuration in each gas instrumentation station box. 50
Figure 3-14: Example GIS stations (left GIS4 in LHA, centre GIS3 LSW, right GIS2 in LBR). 50
Figure 3-15: Supply and exhaust ventilation locations. 52

Figure 3-16: Exterior ventilation ducts on north wall exhaust (left) and east wall supply (right). 52
Figure 3-17: Supply air locations in yellow circles in USW (top left), LSW (top right), USE (bottom left), LBR (bottom right). 53
Figure 3-18: (left) LBR showing location of smoke detection, (right) typical spot and air aspirating tube devices used in tests. 54
Figure 3-19: (left) Mircom panel connected to dedicated computer, (right) Xtralis VESDA sensors and dedicated computer. 55
Figure 3-20: Video camera and smoke detection locations in the test house. 55
Figure 4-1: Quad video capture of LBR and LHA. 58
Figure 4-2: Quad video capture of the lower level, excluding the burn area in LBR. 58
Figure 4-3: Quad video capture of the upper level. 59
Figure 4-4: Visual data points for interpretation of smoke layer descent in burn room 2MV. 60
Figure 4-5: Example of smoke layer descent reaching 1500 mm above the floor in test 2MV. 60
Figure 4-6: Illustration of lost visibility in CAMs 1, 2 and 7 in Test 2MV with only flaming showing in CAM 4. 61
Figure 4-7: Upper level camera perspectives to estimate smoke development. 62
Figure 4-8: Illustration of MLR data showing stages of fire growth. 63
Figure 4-9: Ikea LACK coffee table (left) and end table (right). 71
Figure 4-10: Illustration of furniture configuration in the burn area of the LBR. 72
Figure 4-11: Different crib types used in the test series. 74
Figure 4-12: Showing placement of crib equidistant (360 mm from edge of couch arm). 76
Figure 5-1: Fire damage to the back cushion (top) and seat cushion (bottom) for each of the tests where the couches did not sustain ignition (documented immediately after removal from the burn house). 81
Figure 5-2: Test 5FV showing subsets with different ignition sources that did not allow the couch to sustain ignition and greater burning at the interface of the back and seat cushions. 82
Figure 5-3: Post-test damage for Test 8aFV (left) and 8bFV (right). 82
Figure 5-4: Positioning of propane burner over burn area of Test 8aFV. 83
Figure 5-5: Mass loss rates for all ignited couches and the wood crib. 85
Figure 5-6: Transition of Tests 4FV and 7FV from incipient to the growth stage of fire. 86
Figure 5-7: Transition of Tests 3FV and 6FV from incipient to the growth stage of fire. 86
Figure 5-8: Transition of Tests 2MV and 9FV from incipient to the growth stage of the fire. 86
Figure 5-9: Transition of Test 1FV from incipient to the growth stage of the fire. 87
Figure 5-10: C3 video capture images of several tests at the point of incipient to growth stages of the fire. 87
Figure 5-11: Early fire growth time progression of fire development in Test 3FV (NFR) captured from CAM 1. 88
Figure 5-12: Progression of fire development on the left couch cushion in Test 6FV captured from CAM 1. 89
Figure 5-13: Continued time progression of fire development on the left couch cushion in Test 6FV captured from CAM 1. 89
Figure 5-14: Remaining components of faux leather couches (left - 3FV NFR, right 6FV FR) 89

Figure 5-15: Approximated HRR estimates for the FV series. 91
Figure 5-16: MLR for Test 2MV showing stages of fire development. 92
Figure 5-17: MLR comparison of different NFR couch materials. 93
Figure 5-18: Video capture at peak MLR time for wood and NFR couches. 94
Figure 5-19: Comparison of MLR in NFR and FR faux leather couches. 95
Figure 5-20: Video capture at peak MLR time for UK FR couches. 96
Figure 5-21: MLR comparison of Tests 4FV and 7FV. 96
Figure 5-22: Video capture at peak MLR for US FR faux leather couch. 97
Figure 5-23: Total mass of each couch consumed by test. 98
Figure 5-24: Comparison of couch damage for all tests. 98
Figure 5-25: Top - seat cushions with lightweight cloth fabric at the back of the cushion for leather and faux leather couches, (Bottom) Back cushion with lightweight fabric on the back. 100
Figure 5-26: Summary of Detector Response times for Mircom and VESDA Systems for Detectors D1 to D6. 102
Figure 5-27: Fire detector response times for MV test series. 103
Figure 5-28: Graphical illustration of D3 response times for MV and FV test series. 105
Figure 5-29: Test 1FV showing select intervals of the burn room quad video. 109
Figure 5-30: Test 1FV showing select intervals of upper level quad video. 110
Figure 5-31: Test 2MV, C4 partial images at 1:00, 2:00, 2:30, and 3:00 show fire progression on the seat cushion. 111
Figure 5-32: Test 2MV at 211 seconds after the start of the fire when the smoke layer reaches approximately 1500 mm. 112
Figure 5-33: Test 2MV showing select intervals of the burn room quad video. 113
Figure 5-34: Test 2MV showing select intervals of upper level quad video. 114
Figure 5-35: Lower level quad showing smoke layer collapse in LHA at 04:45 116
Figure 5-36: Lower level quad showing LL Vis. Lost at 05:47. 116
Figure 5-37: Test 3FV showing select intervals of the burn room quad video. 119
Figure 5-38: Test 3FV showing select intervals of the upper level quad video. 120
Figure 5-39: Test 4FV burn room time capture at 07:13 showing the initial smoke layer. 122
Figure 5-40: Test 4FV at the time of smoke layer interface reaching 1500 mm in the burn room. 122
Figure 5-41: Test 4FV showing select intervals of the burn room quad video. 123
Figure 5-42: Test 4FV showing select intervals of upper level quad video. 124
Figure 5-43: Test 5cFV showing select intervals of the burn room quad video. 128
Figure 5-44: Test 5cFV showing select intervals of upper level quad video. 129
Figure 5-45: Test 7aFV ignited using Crib 5 showing 2 minute intervals of the lower level burn room and upper level quad videos 130
Figure 5-46: Test 6FV showing select intervals of the burn room quad video. 132
Figure 5-47: Test 6FV showing select intervals of upper level quad video. 133

Figure 5-48: Test 7bFV showing select intervals of the burn room quad video. 135
Figure 5-49: Test 7bFV showing select intervals of upper level quad video. 136
Figure 5-50: Test 8aFV showing select intervals of the burn room and upper level quad video. 138
Figure 5-51: Test 8bFV showing select intervals of burn room and upper level quad video. 139
Figure 5-52: Test 9FV showing select intervals of the burn room quad video. 141
Figure 5-53: Test 9FV showing select intervals of the upper level quad video. 142
Figure 5-54: Temperature profiles of T5, T6, and T8 for tests 2MV and 9FV. 144
Figure 5-55: Comparison of T5, T6 and T8 rakes for Tests 4FV and 7FV. 145
Figure 5-56: Comparison of T5, T6 and T8 rakes for Tests 3FV and 6FV. 146
Figure 5-57: Comparison of electrochemical GIS3 O_2 sensor with Novatech IR sensor in LSW at 1.5 m. 148
Figure 5-58: Comparison of electrochemical GIS3 CO sensor with Novatech IR sensor in LSW at 1.5 m. 149
Figure 5-59: Novatech CO_2 results for FV series tests in LSW at 1.5 m. 149
Figure 5-60: O2 and CO Concentrations at 0.3, 0.9 and 1.5 m heights in the UHA at GIS5. 152
Figure 5-61: GIS5 0.9 m sensor height with upper level visibility loss lines for Tests 2MV, and 3,4, 7, and 9FV. 152
Figure 5-62: GIS5 0.9 m for Test 1FV and Test 6FV with upper level visibility loss line superimposed. 153
Figure 5-63: Lower Level O_2 and CO concentrations at GIS4, top 1.5 m, middle 0.9 m, bottom, 0.3 m above the floor. 153
Figure 5-64: GIS4 0.9 m with visibility loss lines for Tests 2MV, and 3,4, 7, and 9FV. 154
Figure 5-65: GIS4 0.9 m for Test 1FV and Test 6FV with lower level visbility loss line superimposed. 154
Figure 5-66: Lower Level O2 and CO concentrations at GIS1, top 0.9 m, bottom, 0.3 m above floor. 154
Figure 6-1: Visual representation of stages of fire development and viability of escape. 155
Figure 6-2: LBR quad video images of several fire tests at different intervals showing smoke hazing. 156
Figure 6-3: Lower level (left) and upper level quad video capture at 14:00 157
Figure 6-4: Reference comparison of CO and CO2 curves at Novatech sensors located at 1.5 m in the LSW. . 157
Figure 6-5: Test 7bFV showing smoke layer within the smoke layer. 158
Figure 6-6: Upper level quad image capture of Test 2MV at 05:09. 159
Figure 6-7: Lower level walk-out escape times. 161
Figure 6-8: Comparing smoke layer at 1500 mm between Tests 1FV and 2MV. 162
Figure 6-9: Comparing smoke layer at 1500 mm between Tests 3FV and 6FV. 162
Figure 6-10: Lower level crouch/crawl-out escape times for all tests. 163
Figure 6-11: Test 2MV all timeline points are overlayed with MLR, O2 and CO versus time. 167
Figure 6-12: Test 9FV all timeline points are overlayed with MLR, O2 and CO versus time. 167
Figure 6-13: Test 3FV; all timeline points are overlayed with MLR, O2, and CO versus time. 168
Figure 6-14: Test 6FV; all timeline points are overlayed with MLR, O2, and CO versus time. 168
Figure 6-15: Test 4FV; all timeline points are overlayed with MLR, O2, and CO versus time. 169
Figure 6-16: Test 7FV; all timeline points are overlayed with MLR, O2, and CO versus time. 169

Figure 6-17: Encapsulation of smoke layer onto the fire – Test 2MV – Part I. 171
Figure 6-18: Encapsulation of the smoke layer onto the fire - Test 2MV - Part 2. 172

List of Tables

Table 2-1: Exposure tenability limits for incapacitation or death from exposures to common asphyxiant products of combustion as determined by Purser and McAllister. 12

Table 2-2: Tenability limits for sensory irritation or death from irritant substances as determined by Purser and McAllister. 12

Table 3-1: Thermocouple heights by location reference. 47

Table 3-2: Summary of sensors and range for gas instrumentation stations 49

Table 4-1: Fuel array for wood crib and liquid fuel tests. 66

Table 4-2: Cloth furniture comparison of Test couches 2MV and 5FV. 67

Table 4-3: Faux leather furniture comparison of Test couches 3FV and 6FV 68

Table 4-4: Leather furniture comparison of Test couches 4FV and 7FV 69

Table 4-5: Furniture comparison of Test couches 8FV and 9FV meeting CA TB 133 standard. 70

Table 4-6: Summary of test samples sent for FTIR testing at 3rd party lab. 72

Table 4-7: FTIR results identifying concentrations of additives frequently associated with flame retardants in furniture, from 3rd party lab. 73

Table 4-8: First ignition used by Test number 75

Table 5-1: Summary of exterior temperature and relative humidity at the start of each test. 78

Table 5-2: Summary of ignition sources used for each test. 84

Table 5-3: Summary of Incipient Fire Duration Times. 87

Table 5-4: Fire growth time and peak MLR for each test 93

Table 5-5: Response time of detectors 100

Table 5-6: Adjusted detection time accounting for the incipient stage of fire. 104

Table 5-7: Summary of smoke filling visibility times for all flaming tests. 143

Table 6-1: Lower level walk-out escape time range based on D1 and D3 activation. 160

Table 6-2: Lower level crouch or crawl-out escape time range based on D1 and D3 activation 160

Table 6-3: Time difference between LBR and LSW detectors (D3 - D1). 165

Table 6-4: Scoring system for couch fire performance ranking. 174

Table 6-5: Risk scoring for all test couches 175

List of Abbreviations

Abbreviation	Meaning
AFF	Above finished floor
ASET	Available Safe Egress (or Escape) Time
ASTM	American Society for Testing & Materials
BS 5852	British Standard 5852 - Methods of test for assessment of the ignitability of upholstered seating by smouldering and flaming ignition sources
CB	Checkerboard, also referred to as Light Board
CH4 or CH_4	Methane
CO	Carbon monoxide
CO2 or CO_2	Carbon dioxide
CPSC	Consumer Product Safety Commission in the United States
CSA	Canadian Standards Association
DNI	Did not ignite
FR	Flame retardant
FV	Fuel Volatility experimental test series at UWFRL
GIS	Gas Instrumentation Station
HCL	Hydrogen Chloride
HCN	Hydrogen Cyanide
HFG	Heat flux gauge
HRR	Heat release rate
LBR	Lower Burn Room, also known as the Living Room, in the UWFRL Burn House
LFR	Lightly flame retardant
LHA	Lower Hallway, in the UWFRL Burn House
LL Vis. Lost	Lower level camera visibility lost
LSW	Lower Southwest room, also known as the kitchen, in the UWFRL Burn House
MLR	Mass loss rate
MV	Mechanical Ventilation experimental test series at UWFRL
NA	North America
NBCC	National Building Code of Canada
NBS	National Bureau of Standards, now the National Institute of Standards and Technology (NIST), USA
NFIRS	US National Fire Incident Reporting System
NH3 or NH_3	Ammonia
NFPA	National Fire Protection Association in the United States

Abbreviation	Meaning
NFPA xx	The number of a standard or guidance document developed by NFPA.
NFR	No flame retardant
NIST	National Institute of Standards and Technology
NO	Nitric Oxide
NOx	General term for reactive Nitrogen Oxides, including nitric oxide and nitrogen dioxide
NRCC	National Research Council of Canada
O2 or O_2	Oxygen
PV	Passive Ventilation test series at UWFRL
RSET	Required Safe Egress (or Escape) Time
SLC	Smoke layer collapse, corresponding to the crawl height escape threshold
TB	California Technical Bulletin
TB 116	California Technical Bulleting 116, Requirements, test procedure and apparatus for testing the flame retardance of upholstered furniture
TB 117	California Technical Bulletin 117 Requirements, test procedure and apparatus for testing the flame retardance of resilient filling materials used in upholstered furniture
TB 133	California Technical Bulletin 133 Flammability Test Procedure for Seating Furniture for Use in Public Occupancies
UHA	Upper Hallway, in the UWFRL Burn House
UL Vis. Lost	Upper level camera visibility lost
USE	Upper Southeast room, also known as the large bedroom, in the UWFRL Burn House
USFA	US Fire Administration
USW	Upper Southwest Room, also known as the small bedroom, in the UWFRL Burn House
UW	University of Waterloo
UWFRL	University of Waterloo Fire Research Laboratory
VOC	Volatile Organic Compounds

Chapter 1
Introduction

A series of full-scale multi-compartment and multi-storey fire experiments were designed and conducted to evaluate the potential "available safe escape time" with different upholstered furniture fuel types using controlled ventilation conditions in a representative multi-storey residential dwelling. Furniture is frequently the catalyst for fire propagation and corresponding smoke spread and oxygen depletion in a structure during a fire. As these conditions evolve during the fire, the environment within the home becomes increasingly dangerous to occupants needing to escape from the fire. Contextualizing the hazard within the dwelling requires correlating fire growth, fire detection time, the onset of dangerous conditions due to smoke and toxic gas spread, the rate of oxygen depletion and the corresponding time for occupants to be notified of the fire, respond and travel through the fire environment to escape to the exterior.

The movement time of occupants to escape a fire varies considerably depending on their agility and cognitive characteristics [1]. Historical data regarding fire fatality has identified that fire deaths are frequently associated with vulnerable populations, such as children and the elderly [2], those with mobility or cognitive limitations, and those impacted by alcohol, drugs or medications. There is a lack of fire data capturing the smoke evolution over prolonged durations in house fires. Thus, it is very difficult to correlate the above parameters to understand available escape times in enclosed and ventilation-limited fire environments as they relate to fuel type, detection and the onset of untenable conditions.

This thesis summarizes data from ten different fire tests and compares findings for visibility, oxygen consumption, and the evolution of carbon monoxide and carbon dioxide along the "escape path" within a well-instrumented "burn house" at the University of Waterloo Fire Research Laboratory (UWFRL). It brings together the above considerations in a comparative fashion for different fuel types and then evaluates the findings relative to the development of an egress-restricting environment. An estimate can then be made for escape times accounting for walking movement while upright or, where the environmental conditions deteriorate, movement out of the building by crawling. Further, and to fully study the above considerations, the following complementary subjects are necessary areas of investigation as part of this research:

a) Smoke alarm response times for different materials and for different detector locations are collected and compared. While a smoke alarm located proximal to the fire source is intuitively expected to respond more quickly than one in a different room or on a different floor, there is limited research on the placement of detectors on non-sleeping room floors to inform available escape time. Data informing detector placement and the corresponding escape time will be generated. Smoke alarms act to both identify a fire condition and alert occupants by initiating a tone or a series of tones to wake occupants. Recent research has focused only on the sounding function of the alarm [3], leading to mandatory interconnectivity and inclusion of the devices in sleeping rooms (to increase the probability of waking the occupants). Early research on the placement of the detectors was focused on placing detectors in the hallways adjacent to the living areas of the house [4]. This appears to be a balance between locating the alarms for early detection and ensuring the device is heard in upstairs bedrooms. In modern systems, multiple alarm devices are interconnected, leaving an opportunity to revisit the placement of the alarms to optimize for early detection.

b) Smoke filling is examined over time within compartments as the fire environment evolves throughout the structure. Recent research in smoke layer descent in single rooms indicates that a smoke layer encapsulates the fire by the extension of the wall jets descending to the floor and then along the floor back toward the fire source [5], while the smoke layer away from the walls descends as a layer. However, the focus in previous research has been predominantly on the heat release rate, temperature, and pressure build-up due to the generation of smoke. This research program further evaluates smoke filling phenomena using solid fuels in a more complex geometrical space. It investigates smoke layer development around the origin of a fire, fueled with solid irregular-shaped fuels. Additionally, it characterizes smoke propagation and layer development throughout different rooms and levels. Understanding the smoke layer and how it interacts with the environment is a key aspect of the research, as it affects the visibility for occupants during escape. The loss of visibility is a key potential driver in reducing the viability of escaping the fire.

c) Mass loss rates for upholstered furniture with different fabric materials and fill protection methods are collected and compared. In particular, comparing the different mass loss and species production rates of leather, faux leather (vinyl) and cloth couch fires with fires fueled by wood and liquid fuels provides a range of environmental conditions to evaluate smoke

alarm activation times and the onset of conditions that may enhance or preclude evacuation. Controls on the ignition and fire development of different materials and fire safety controls may delay alarm sounding and, therefore, potentially reduce or negate the intended effectiveness of the controls. Research correlating detection times and smoke layer development in house fires to types of furniture is currently very limited.

Additional background, a literature search, and the experimental design and methods used are outlined in the following chapters, followed by detailed output and interpretation of data from tests for each of the individual parameters used as a frame of reference for comparison purposes. This research is part of a wider study addressing ventilation-limited fires and the creation and movement of fire gases within a two-storey interconnected structure, dimensionally proportionate to a small single-family home or townhome, common throughout North America.

Chapter 2
Literature Review

2.1 Residential Fire Experience

2.1.1 Fire frequency and fatality in residences

It is generally established that a large proportion of fires occur in residential homes. Recent data from the National Fire Protection Association in the US indicate approximately 26% of all fires originated in home environments between 2015 and 2019. This accounted for 75% of the civilian fire deaths and 72% of the civilian fire injuries [6]. Cooking was found to be the leading cause of injury, and smoking materials caused the most home fire deaths. The single-family home fire death rate per 1,000 reported fires is 8.2, which represented a 16 percent increase from 1980, whereas the equivalent apartment death rate declined by 43% in the same period. The US Fire Administration, who administer the US National Fire Incident Reporting System (NFIRS), has indicated that the 10-year fire death rate trend per million population increased by 18% between 2012 and 2021 [7], and an increasing residential fire death trend as shown in Figure 2-1 [8].

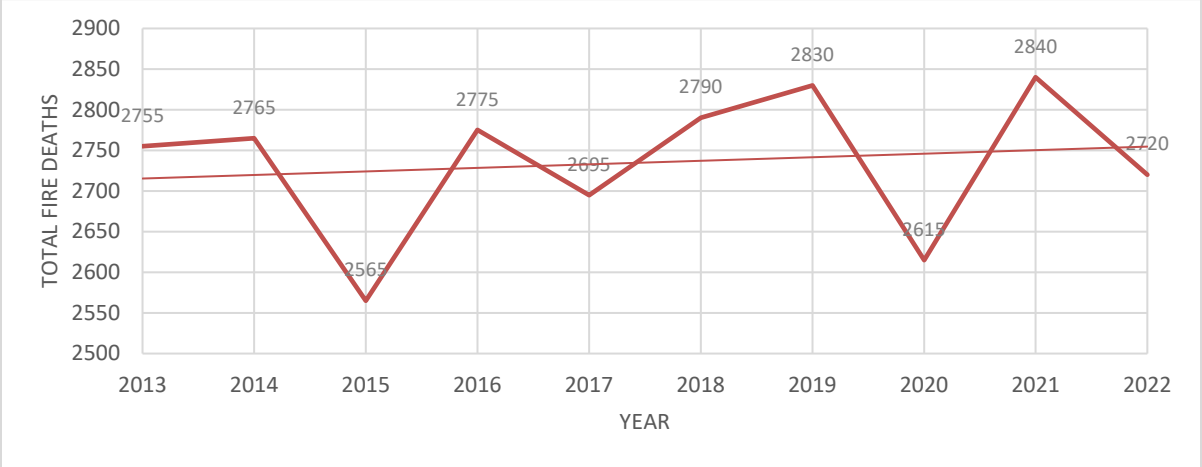


Figure 2-1: 10-year fire deaths in the US estimated by the US Fire Administration with a linear trendline.

Residential fires equally constitute the majority of structure fires in Canada. Residential fires in Canada make up 30% of all reported fires and 66% of all structure fires that occurred in the 10-year period from 2012 to 2021 [9]. Consolidated fire data from all gathered provincial, territorial, and Federal sources for residential fire fatalities in the 10-year period is illustrated in Figure 2-2 [9]. Residential fire deaths constituted an average of 93% of all structural fire deaths, although the data is

not sufficiently granular to differentiate single-family homes from other structure types. The pandemic years of 2020 and 2021 show a spike in fire deaths, likely associated with the increased presence at home during this period [10].

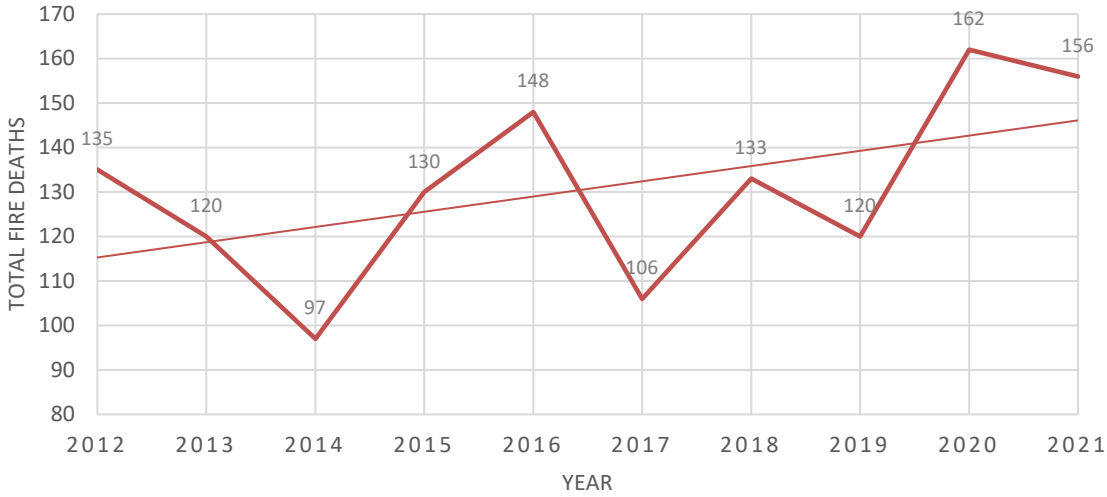


Figure 2-2: 10-year fire deaths from 2012 and 2021 with a linear trendline.

The trend parallels the USFA trend illustrated above, which illustrates increased fatalities over the ten-year period. Statistics Canada also indicates that nearly twice as many unintentional residential fire deaths occurred during colder months between December and March [11], which aligns with the NFPA data that indicates home fires are more common in the cooler months [6], and also highlights that, even though only one-fifth of the fires occur between 11 pm and 7 am, they account for almost half of the fire deaths. This suggests that fire fatalities are most common during the sleeping hours of winter months. Therefore, for both older houses and modern ones, fires are not likely to be subjected to significant ventilation from exterior openings.

Bouanagui determined that, in Ontario, the highest percentage of fire deaths was associated with living room fires [12]. The US statistics correspond, indicating that 16% of fire deaths were associated with fires where upholstered furniture was the item first ignited [6], followed by fires in mattresses/bedding, and historically, this number could be as high as 24% of fire deaths when factored for scenarios where furniture is not the item first ignited but is the primary contributor to fire [13]. This generally aligns with investigation work on 100 living room fires involving furniture, where it was found that 25% of the fires in living rooms had furniture as the catalyst to fire growth but was not the first item ignited [14]. This is consistent with observations by Hall, following changes to data-gathering methods in the US, which found that, between 2006 and 2010, 25% of fires were

from open flames from other fires where the furniture was not the first item ignited [15], and in fact, these exposure fires are the second leading fire scenario causing fire deaths.

Smoke inhalation was the overwhelming leading cause of death, accounting for 68% of unintentional incidents in Canada between 2011 and 2020 [11]. Further, 31% of fire deaths involved the consumption of alcohol, cannabis, or illicit drugs, which is attributed to impaired judgement in either starting the fire or delays in reacting to/escaping the fire. This data is derived from the Canadian Coroner and Medical Examiner Database and provides a unique perspective compared to reports from provincial fire marshals and commissioners. The Canadian data generally aligns with NFPA findings that have 28% of occupants being asleep, 18% being physically disabled, 10% impaired by alcohol, 5% with possibly mental disabilities, 4% impaired by drugs or chemicals, 4% unattended or unsupervised person, and 4% being unconscious [6]. Both US and Canadian data sets have similar profiles of the age of victims, with higher chances of fatality increasing after the age of 50 or 55, with a higher potential for males over females, and an increased risk for elderly and small children. Gilbert draws inference from the data in the context of frailty and rationalizes that nearly all deaths seem to be associated with frailty [2]. This is potentially an oversimplification as a much wider distribution of persons are impacted by fire than provided for in Gilbert's context. Campbell estimates that physical disability was a factor in 18% of home fire deaths per year between 2015 and 2019 [16].

Based on the above, the following is a summary of key findings from published data for consideration in developing a fire research plan focused on residential fires:

1. Fires and fire deaths are most frequent in homes, and in particular single-family homes.
2. Cooking-related fires are the most frequent cause of incidents and personal injury.
3. Exposure to smoke is the most frequent factor in not being able to escape a fire.
4. Fatal fires are more likely to occur in cooler months than in warmer months and overnight when occupants are sleeping.
5. Upholstered furniture and mattresses/bedding are the most frequently ignited first items, leading to fire deaths.
6. Smoke alarms have been effective at reducing the number of deaths in the past 40 years, but many fire fatalities are occurring despite the presence of working smoke alarms.
7. A reduction in fire deaths and injuries is not prevalent in single-family homes in the US between 1980 and 2020 despite the presence of smoke alarms, but a reduction is prevalent in apartment buildings.

8. Other risk factors for vulnerable populations may include cognitive or physical limitations that may delay or prevent an occupant from escaping a fire.

The development of a fire test program studying variations in upholstered furniture in a closed structure (representative of a two-storey house with only minimum ventilation) that investigates smoke spread and the evolution of the fire environment along the escape path aligns with the areas of greatest needs for research (points 1, 3, 5-7 above) to respond to the residential fire problem.

2.2 Smoke Alarms and Escape Time for Residential Fires

Smoke alarms are the primary alerting mechanism in houses to inform occupants of a fire condition. The National Building Code of Canada (NBCC) distinguishes smoke alarms from smoke detectors [17]. Smoke alarms combine detection and sounding, whereas detectors do not sound but instead are connected to a fire alarm system where emergency sounding is done by speakers or bells. In early literature, these terms were often used interchangeably with the same intended meaning. For purposes of this section, either term refers to a device that is both a detector and a sounder, understanding that it is the primary mechanism for alerting occupants of a fire in a house. Similarly, the terms house, home, dwelling, or residence are frequently interchanged and, for purposes of this thesis, mean a single-family detached or semi-detached dwelling unless otherwise specified.

2.2.1 Smoke Alarm Early Placement History (1960 to 1980)

Smoke alarms were first invented in the 1950s and evolved into two prevailing technologies: ionization and photoelectric. Home ionization detectors were first invented by a Swiss scientist, Ernst Meilli, in 1939 looking to detect poisonous gasses and were then adapted for use as smoke alarms [18]. Photoelectric detectors were first developed by Electro Signal Lab [19]. Early work highlighting the potential reduction in fire deaths that could be attributed to the installation of smoke alarms in houses was completed in 1962 by McGuire and Ruscoe [20]. They noted that the provision of fire detectors in residential properties was rare (either smoke or heat detectors), yet residential fires constituted the highest number of fire deaths. Their evaluation considered the potential for the installation of two smoke alarms, one at the head of the basement stairs and another at the head of the main staircase (in a 2-storey dwelling) or one between the living and sleeping areas in a 1-storey dwelling). The proximity to bedrooms was, in part, to identify conditions developing near the bedrooms and the need for the alarm to be sufficiently audible to awaken occupants. They estimated a reduction in the number of fire deaths could be on the order of 41% with the provision of smoke alarms in houses.

According to Bukowski [21], this work was foundational for the National Bureau of Standards (NBS) in the US in developing its "Breakthrough Criteria," which adopted the McGuire and Ruscoe smoke alarm placement. Smoke alarms were subsequently incorporated into 17,000 mobile homes used to support relief efforts following Hurricane Agnes in 1972. In the following several years, when the mobile homes were occupied, no fire deaths were reported in the mobile homes, despite a statistically expected number of fires occurring. This suggested to researchers at the time that smoke alarms were operationally effective at reducing the number of fire deaths, as predicted by McGuire and Ruscoe.

The Committee responsible for the development of NFPA 74 [22] identified four levels of protection for residences and implemented them in the 1974 version of the standard, with the following smoke alarm placement options:

- Level 4: smoke alarms outside the bedrooms and at the head of any basement (essentially the criteria identified by McGuire and Rusco).
- Level 3: as per level 4 plus added heat or smoke detectors in the living or family rooms.
- Level 2: as per level 3, plus head or smoke detectors in the bedrooms.
- Level 1: a full system of heat or smoke detectors in every room.

However, once implemented, the standard left it open to decide which level of protection should be provided (essentially leaving it up to the local jurisdictions). With costs being a factor, Level 4 was the least expensive to implement, and eventually, Level 4 would become the minimum criteria. Up to this mid-70s period, there appears to be no specific research that focused on time to escape from houses. Rather, the provision of detectors represented a starting point, based on a review of historical fire data, to provide early warning where previously there was none. The placement of the devices was a balance between minimizing the number of required detectors (to limit the cost of implementation), placement in proximity to sleeping occupants (so that localized sounders would wake occupants), and placement to normally unoccupied and often unfinished basements (where many houses had their electrical supply and furnaces). The significant fuel hazards within certain areas (furniture and bedding) were acknowledged but not the focal point for the positioning of detectors in this era.

The first comprehensive study of smoke alarm response times and corresponding escape times was the test series performed by the NBS (now the National Institute of Standards and Technology, or NIST), known as the Indiana Dunes tests. These tests were performed in three houses scheduled for demolition in two different test series. The first test series, documented by Bukowski et al. [23],

consisted of 40 experiments with detector locations sited in accordance with NFPA 74 – 1974. Harpe et al. [24] documented the program's second phase, which included an additional 36 tests and focused on windows opening to the exterior. Although not specifically stated as an objective, it also included detectors of both the photoelectric and the ionization type and looked at differences between forced air heating and air-conditioned buildings.

The research found that the forced air heating recirculated the smoke, defeating any passive barriers that prevented doors from being opened or closed. Smouldering fires generally had long development times, limiting the amount of smoke generated and, therefore, providing substantially increased escape times since detectors would respond during this smouldering period. Flaming fires in bedrooms led to degraded conditions within the room itself and, potentially, the immediate area outside of the room if the door was open. If the door was closed, the significantly degraded conditions were primarily limited to that room. The test series included 40 smouldering, kitchen stove and flaming fires, but only a few of the fires were flaming fires in living rooms. These were lit with a waste-paper basket of paper alongside upholstered chairs, as illustrated in Figure 2-3 [23].

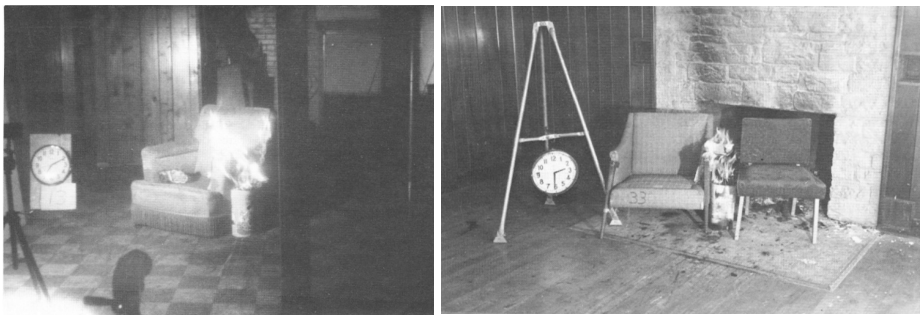


Figure 2-3: Armchairs ignited by wastebasket filled with paper in Indiana Dunes Phase I test series.

Measurements were made at 1.5 m above the floor (5 ft), looking at temperature (150°F or 66°C), visibility (0.3 optical density per ft or 0.09 optical density per m), and carbon monoxide (400 ppm time-averaged concentration over 1 hour). In all the experiments, smoke density was the first criterion reached and was therefore used for the determination of escape time, which was presented as a "success" frequency, considering the probability of escape. Required escape times of 120 – 300 seconds were considered a "reasonable basis" in the graphs that defined percentages of likely successful escape in considering results from all tests (smouldering and flaming). The methodology demonstrated that only small differences between ionization and photoelectric detectors were noted. When forced air heating was operating, smoke recirculated through the house and distributed the smoke and times from detectors activating on the second floor for a fire originating on the first floor did not allow sufficient escape time [25]. This would lead to a recommendation to have a detector on

every floor of a house. However, one interpretation of the findings by a fire safety panel advising the governor of Massachusetts using an arbitrary 3-minute escape time concluded that a smoke detector in every room would only increase the likelihood of escape by 4% (from 89% to 93%) [25]. The specific basis for this assertion is not known.

In 1977, the Standing Committee on Housing and Small Buildings in Canada received a Committee Paper highlighting the following findings from the Indiana Dunes tests [26]:

1. Both basic types of smoke detectors (photoelectric and ionization) are equally effective in providing early warning.
2. Fixed temperature or rate-of-rise heat detectors in the room of fire origin provided little life-saving potential.
3. With forced air heating, there was little difference in smoke levels in bedrooms regardless of whether or not the bedroom doors were closed. With central air conditioning, there were reduced smoke levels in bedrooms with the doors shut.
4. At least one detector should be provided at each end of a long central hall.
5. At least one detector should be provided on each floor level.
6. Detectors mounted on the wall near the ceiling were as effective as those mounted on the ceiling.

The Committee Paper would further highlight changes in codes already in place in the US and in Alberta and Ontario in Canada and propose code language that would require:

- Smoke alarms be installed between the sleeping area and the living area on each storey (and in the hallway where there is a hallway), including the basement,
- Where there are no sleeping areas on a storey, a smoke alarm should be installed near the ceiling adjacent to a stairway serving the storey above, and
- That smoke alarms be connected to electrical power and where more than one smoke alarm is provided, they be wired so that the activation of one smoke alarm will cause all alarms within the dwelling unit to sound.

These recommended code changes were adopted into the 1980 National Building Code of Canada [27] and became the benchmark for smoke detection in houses. The underlying principles, at this point in history, were to have central detectors so alarms could sound to notify sleeping or unaware occupants, who are better off having their bedroom doors open so that they may hear the alarm; given

that central heating systems could distribute the smoke evenly whether bedroom doors were open or closed.

2.2.2 Tenability Criteria for Safe Escape During a Fire (1980 – Present)

The concept of Available Safe Egress Time (ASET) and Required Safe Egress Time (RSET) was formally framed by Cooper in 1983 [28] where detection time initiates the human response to escape as a function of the potentially deteriorating conditions within a fire compartment. Although not explicitly stated, this is essentially the concept applied in the Indiana Dunes tests, where a 2 – 5 min RSET was assumed to be required when comparing the ASET from each of the tests and for each escape routing. The ASET was determined by threshold criteria for visibility, temperature, and carbon dioxide, measured from the start time of the fire.

Of interest from Cooper [28] is the proposed simple qualitative methodology of using the smoke layer interface as the conditional differentiator for tenability, as explained by the following excerpt (underline of phrases added for clarity):

> *Above the interface the gases are smokey, and therefore, potentially obscure and/or debilitating to the point where visibility is significantly impaired. They are contaminated with toxic products of combustion and, therefore, they are themselves at toxicity levels potentially beyond human tenability. Below the interface the gases are modeled as cool, uncontaminated, ambient air. If the interface drops below some pre-assigned level, say some position between one and one and a half meters (three to four feet), it is not practical to expect people to be capable of keeping their faces out of the potentially hazardous upper layer. Thus, a simple, albeit conservative, criterion for hazard can be established which is independent of the details of the toxicity and smoke production properties of the constituent materials making up the fuel assembly. Namely, once the upper layer – lower layer interface drops to a pre-assigned level, hazardous conditions begin to prevail in the component of fire origin and safe evacuation is no longer likely.[29]*

The Indiana Dunes test series did not explicitly focus on smoke layer development but instead on more precise parameters. Visibility was the most relevant parameter, and analysis was based on concepts of light obscuration based on early work in the late 1960s by Jin, which was later consolidated and summarized [30]. Smoke optical density levels of 0.15 m^{-1}, or a roughly translated visibility of 13 m, were determined to be required for safe escape for those unfamiliar with the building and 0.5 m-1 or approximately 4 m, for those familiar with the building. The Indiana Dunes

tests used greater than or equal to 0.23 m^{-1}, as a reference for establishing the visibility threshold at a height of 1.5 m. It was found that visibility was the first of the criteria to fail, which logically aligns with Cooper [28] in assuming that the smoke layer interface is a defining parameter for tenability.

These concepts have been developed into performance-based design methodologies primarily used for managing egress and exiting and evolving the concept of detection, notifying occupants of a condition and leading to various potential evacuation responses where they may be exposed to developing conditions [31-33]. According to Hutchison and Hostikka [34], the recommended tenability limits are based on Purser and McAllister [35]:

1. Visibility through smoke of OD/m is 0.2 (visibility of 5 m for small enclosures),
2. Maximum skin exposure of 2.5 kW/m^2, corresponding approximately to a 200°C maximum smoke layer radiating where occupants are passing below,
3. Maximum temperature of respiratory air of 60°C, and
4. Exposure limits to incapacitation or death as outlined for asphyxiant and irritant gases in Table 2-1 and Table 2-2 respectively.

Table 2-1: Exposure tenability limits for incapacitation or death from exposures to common asphyxiant products of combustion as determined by Purser and McAllister.

	5 min		30 min	
	Incapacitation	Death	Incapacitation	Death
CO	6000–8000 ppm	12,000–16,000 ppm	1400–1700 ppm	2500–4000 ppm
HCN	150–200 ppm	250–400 ppm	90–120 ppm	170–230 ppm
Low O_2	10–13 %	<5 %	<12 %	6–7 %
CO_2	7–8 %	>10 %	6–7 %	>9 %

Table 2-2: Tenability limits for sensory irritation or death from irritant substances as determined by Purser and McAllister.

	Sensory irritation		Death (minutes)		
	a	b	5	10	30
Acrolein (ppm)	1–5	5–95	500–1000	150–690	50–135
HCI (ppm)	75–300	300–11,000	12,000–16,000	10,000	2000–4000

Further, ISO 13571 and 13571-2 outline methodologies for fractional effective dose (FED) for asphyxiating gases and Fractional Effective Concentration (FEC) for irritating gases in terms of determining the time to incapacitation [36, 37]. This is mentioned since some of the research that will be discussed below includes analysis of fractional effective dose in its evaluation of tenability. It involves calculating cumulative exposure or combining concentrations of irritant gases to determine the impact on the individual. However, Purser and McAllister highlight that the visibility design

criteria (or equivalent particulate mass concentration) are intended to represent a low probability that occupants will feel trapped and fail to escape and that “asphyxiant gases present are most unlikely to exceed levels capable of causing incapacitation (loss of consciousness) in exposed occupants within 30 – 60 mins.” [38]

The challenge with estimating the influence of fire effluents on occupants escaping fire in smoke is their environment and their exposure will be a function of many parameters, including the material burning, the fire heat release rate, the yields of toxic gases, building geometry, individual physiology and psychology and decisions made relative to movement, walking, crouching or crawling to leave the building. Further, virtually all of the references identified above caution on the uncertainty associated with the knowledge of physiological response to smoke and toxic products given the limited data and the origin of the same [39], some of which are extrapolated from animal and not human trials.

2.2.3 Smoke Alarm Placement and Audibility (1980 – 2000)

According to Bukowski [21], in the early 80s, after the Indiana Dunes tests, NBS/NIST focused on other areas, including improving detector performance for specialty applications. While they conducted limited studies to improve detector performance and reduce the incidents of nuisance alarms and the influence of mechanical ventilation systems on smoke and heat detector activation times, none of these studies focused on the general placement of detectors in houses or on evacuation times associated with residential applications.

Grand et al. conducted a full-scale mock-up of a motel room and replicated two tests looking at toxic hazards from a furnished room [40]. Smoke detectors were placed on the wall and the ceiling and responded on the order of 15 minutes after smoke was first observed in the smouldering fire ignition scenario and between 18 and 28 seconds after the upholstered chair transitioned to a flaming fire. Flashover was observed to occur approximately 9 min after flaming ignition. While not specifically targeted toward the detection and egress from houses, it highlights short detection times from flaming ignition sources where detectors are in the room of origin.

Halliwal and Sultan published the first in a series of articles on the most effective locations for smoke detectors in residential buildings in 1986 [4, 41, 42]. It highlights the tradeoff for optimizing the location for best detection with the need for audibility of the sounding function of the alarm. It further highlights that the high-priority areas should coincide with the living room, bedroom, and kitchen/dining room, as these locations were (and still are) locations with the highest incidence of fires. The research was more focused on addressing the sound levels of the detectors at different

locations in a home as a function of sound transmission and dampening from different types of rooms in a house. In particular, in the example provided, it was found that adequate sound levels could occur in bedrooms from a hallway smoke alarm where the bedroom doors were open (75 dBA assuming a sound power level of 95 dBA from the alarm device) whereas with the bedrooms doors closed, the sound levels would not be adequate to wake a sleeping person [4]. Although the paper did not give explicit recommendations on detector placement, it highlighted the tradeoff of detector placement versus audibility, but notably did not account for multiple interconnected alarms simultaneously sounding, nor detector placement within the house for earlier warning of the fire event.

The 1995 National Building Code of Canada [43] was amended to include Clause 9.10.18.2.(1)(c), which requires a maximum distance to a smoke alarm of 15 m from any point on a floor area. This means that more than one detector could be required on a non-sleeping room floor if the distance is exceeded, making it more likely that an alarm-sounding function would be audible throughout the house. Appendix language was also added, and is reproduced below (underline added for emphasis):

> *A-9.10.18.2.(1) Location of Smoke Alarms. There are two important points to bear in mind when considering where to locate smoke alarms in dwelling units:*
>
> - *The most frequent point of origin for fires in dwelling units is the living area.*
> - *The main concern in locating smoke alarms is to provide warning to people asleep in bedrooms.*
>
> *Thus a smoke alarm <u>located in the living area and wired so as to sound another smoke alarm located near the bedrooms is the ideal solution</u>. However, it is difficult to define exactly what is meant by "living area." It is felt to be too stringent to require a smoke alarm in every part of a dwelling unit that could conceivably be considered a "living area" (living room, family room, study, etc.). Sentence 9.10.18.2.(1) therefore addresses these issues by requiring at least one smoke alarm on every storey and setting a maximum distance that any point on a floor level can be from a smoke alarm. Thus, in a dwelling unit complying with Sentence 9.10.18.2.(1), every living area will probably be located within a reasonable distance of a smoke alarm. Nevertheless, where a choice arises as to where on a storey to locate the required smoke alarm or alarms, <u>one should be located as close as possible to a living area</u>, provided the requirement for proximity to bedrooms is also satisfied.*

Therefore, by 1995, the NBCC required smoke alarms in proximity to the living areas. However, 15 m is easily the entire width of many houses, and therefore, a single smoke alarm on a floor level is adequate for most average-sized houses, which inherently minimizes the impact of the change. Nevertheless, it remained clear that the focus on detector placement was a balance between the audible and detecting functions of the smoke alarm and not predicated on a targeted escape time.

Other research of interest during this time included an evaluation of the effectiveness of smoke alarm implementation programs, which investigated the individual motivation to maintain smoke alarms in good working order [44]. This is relevant where smoke alarms have failed or not been installed in fatal fires. In the context of occupant escape from fires, Jones conducted research into the potential for hydrogen cyanide from smouldering fires to render victims unconscious and facilitate intoxication by carbon monoxide due to the increasing use of inexpensive synthetic materials associated with building construction and house furnishings [45]. This latter study highlighted early findings of upholstered furniture that will be further elaborated upon in Section 2.4.

2.2.4 Smoke Alarm Placement and Audibility (2000 – Present)

In the early 2000s, both the National Research Council of Canada (NRCC) and the NIST in the US implemented new research programs that studied smoke alarms in houses. Su et al. reported on the "Kemano Studies," where several houses were decommissioned in British Columbia, Canada and made available for fire research [46]. In the NIST "Performance of Home Smoke Alarms – Analysis of the Response of Several Available Technologies in Residential Fire Settings," Technical Note 1455 (the TN1455 Study), Bukowski et al. reported on a series of 24 fires, which included several flaming living room fires [47].

The Kemano Studies consisted of 13 experiments in two houses, one single-storey and one 2-storey. Initiating fires used wood, paper, polyurethane foam, cotton flannel, upholstered furniture and cooking oil. An electric ignitor was used for ignition. According to the report, the fire initiation was deliberately small and with a slow growth to increase the challenge to smoke alarms, which included a comparison of photoelectric, ionization, and dual photoelectric/ionization detectors. The results of the detector comparison confirmed that, as previously established in the Indiana Dunes Tests, ionization smoke detectors respond more quickly in flaming fires, photoelectric devices respond more quickly to smouldering fires, and dual detectors respond at approximately the same shorter time according to whether it was flaming or smouldering, given both technologies were integrated into the same device.

For flaming fires in the living room, the earliest device detection times in the Kemano Tests were between 262 and 319 seconds in the 1-storey house and 329 to 447 seconds in the 2-storey house. Devices outside of the room of origin responded much later, between 343 and 1103 seconds for the 1-storey house and 468 and 754 seconds for the 2-storey house (using the dual detector as a reference). This provides a range of detection times that occurred within the floor area depending on the location of the detector and the geometry of the room space (where different rooms may have transoms above the doorway delaying smoke migration into the room). The visibility in all tests was reported to be

sufficient for evacuation purposes and was measured at 1.65 m above the floor. Optical density was not specifically evaluated for escape purposes but was used as part of the smoke alarm sensitivity portion of the study. CO concentrations were found not high enough or long enough to trigger the CO detectors. In general, however, the small fuel quantities limited the overall fire sizes and generation of smoke meaning the study is limited to early fire development and not fully flaming fires.

In the TN1455 study [47], 24 tests were completed, which included a greater number of flaming fires and one fully furnished fire in living rooms. Evaluating the efficacy of the then-current requirements for the number and location of smoke alarms and incorporating materials and constructions representative of then-current residential furnishings were among the objectives of the test program. Tenability was measured at 1.5 m from the floor, but the interpretation of the results for tenability excluded instrumentation in the same room as the fire since, according to the authors, codes are not designed to protect people intimate with the fire. It should be noted, however, that in evaluating the living room fires in those tests, as well as the Indiana Dunes Test and Kemano Studies, escape from the bedrooms in the single and two-storey layouts of the test houses required that all or most of the occupants escape through the living room. This is an important differentiator between living room fires, likely to impact all escaping occupants, and bedroom fires, which have greater potential to be more localized and not require the occupants to egress through the room with developing fire conditions.

The NIST authors used an ASET/RSET analysis in their evaluation to consider escape times and the tenable environment. A worst-case RSET of 140 seconds was established (see Table 26 in Reference [47]). The tenability criteria are defined as: temperature exceeding 88°C, CO greater than or equal to 0.02 – 0.03% volume fraction for flaming and smouldering fires, respectively, and an optical density (OD) greater than or equal to 0.25 m^{-1} anywhere along the escape path at 1.5 m above the finished floor. This compares with the previous Indiana Dunes test series that used a temperature equal to or exceeding 66°C, a CO greater than or equal to 0.04% volume fraction and an OD greater than or equal to 0.25 m^{-1} (see Table 31 in Reference [47]).

The study had varied and somewhat competing conclusions. It indicates that:

> *In many cases, available escape time would be sufficient only if households follow the advice of fire safety educators, including sleeping with doors closed while using interconnected smoke alarms to provide audible alarm in each bedroom, and pre-planning and practicing escape so as to reduce pre-movement and movement times. [48]*

While also concluding that "Smoke alarms of either type installed on every level generally provided positive escape times for different fire types and locations [49]." The report further suggests that the criteria for tenability were conservative and based on the incapacitation of the most vulnerable occupants and that using "tenability criteria based on incapacitation or death of healthy individuals certainly increase the available safe egress time [50]." However, the above is inconsistent with the methods of flaming ignition, which were used in the test and placed specifically to "minimize the fire growth rate [51]," which in turn would allow for a clearer differentiation of the smoke alarm response times. The study, therefore, precluded investigating faster fire growth scenarios in favour of evaluating alarm response between differing technologies.

Cleary completed a series of 24 follow-up tests to the NIST studies looking specifically at egress times in living room and bedroom tests using optical density, heat and toxic gases as tenability factors [52]. The study concluded that visibility was the first criterion to fail, followed by temperature and then gas, and noted that "Further study is needed to deduce the impact of visibility-limiting smoke levels on the time needed to egress residential fires [52] ." Taber et al. did a series of basement fire tests looking at tenability on the upper two stories [53], which are well documented in a paper by Su et al. [54]. Taber concluded that an "early alert to occupants by the detection system and immediate evacuation by occupants are key elements for occupant life safety [53]." The tests had a large exterior opening to the fire room in the basement, which likely facilitated an accelerated fire growth and induced draft to the upper levels.

Around the same time as the NIST and NRCC work was underway, others were focusing more on the required RSET. Fleischmann identifies premovement times in the range of 5 to 20 plus minutes for dwellings with sleeping occupants from the time of alarm initiation [55] in determining RSET. Proulx similarly suggests RSET times of 2 minutes for the best-case scenario and 16 minutes and 10 seconds for a worst-case scenario and highlights a need for additional research in this area [1, 56]. These are well above the times considered in the simplified ASET/RSET analysis done by NIST. Babrauskas cautions that applying the ASET/RSET context, specifically in the context of the NIST TN1455 report [47] is highly simplistic and omits many behavioural reactions, vulnerable populations, and counterproductive behaviours [57], concerns which were subsequently supported by Chow [58]. Finally, Hall evaluates the potential feasibility of how many people could be saved from home fires if given more time to escape and determines that roughly half of the deaths and two-thirds of the injuries could be prevented if times to incapacitating exposures were lengthened sufficiently [59]. This inherently would provide additional time to react to the fire, to escape, and for emergency responders to become aware of and respond to the fire.

Based on the literature above, it is inaccurate to imply that using smoke alarms was ever intended to provide more than an opportunity for earlier warning of a fire condition. Applying ASET/RSET principles requires that the furnished building be designed as a system, with controls or mitigating measures to manage the environment to allow for escape with fundamental objectives and timelines. For the approach to be effective, the furnished building system must be able to respond to the fire conditions and the distribution of potential RSET times. The work by Fleischman [55] and Proulx [56] suggests 16 - 20 minutes as a potential starting point for RSET times; however, most of the testing has been done over much shorter durations, leaving gaps in understanding of room fire conditions and the tenable environment over longer periods.

The fire studies that correlated detector activation to residential fire escape completed up to 2010 had simplified fuel loads, slower fire growth rates, only studied tenability at head height while discounting the tenability in the room of fire origin [23, 47, 54]. This leaves multiple gaps in the understanding of residential fire escape. If furniture is the primary cause of residential fatalities and egress from the house requires one to pass through the primary area that has the furniture, then a much greater understanding of furniture fire growth relative to detection times and the time to obstruct the escape path warrants further exploration.

Milarcik et al. reviewed the debate and various research efforts focused on ionization and photoelectric detectors and concluded that "instead of continuing to debate which technology is better, efforts should emphasize maximizing the number of detectors in residences …. By focusing on reducing the time to activation and on reducing false alarms, relative time will likely remain unchanged, but overall fire safety for occupants of a residence will be increased [60]." This highlights that the placement of smoke alarms on non-sleeping room floors could benefit from further exploration to address the greater hazard associated with furniture and living room fires blocking egress paths. Other work in this period included the sounding function of smoke alarms. Bruck and Thomas established that a 520 Hz square wave signal was at least 4 -12 times more effective at waking occupants [61] than the originally developed high-pitched alarm. This may shorten the awareness time and, therefore, the time required for escape after a detector activates but does not specifically address detection response or available time to escape.

The 2010 version of the NBCC eliminated the requirement for a maximum of 15 m distance to a detector, changed the requirements for the sound pattern on smoke alarms and required a smoke alarm to be included in each sleeping room [62]. Floors not containing sleeping rooms were still only required to have one smoke alarm, and these would be the last changes to this subsection of the Code, which are the same in the current 2020 version of the NBCC [17].

Additional work has since continued on evaluating programs for the presence of smoke alarms and audibility, as well as additional full-scale tests focused on survivability. Sidman et al. investigated the likelihood of smoke alarms being present and working and found that strategies for maintaining smoke alarms in functional condition and improving compliance with placement recommendations are necessary to achieve universal coverage [63]. Mainuddin et al. reviewed the audibility of alarms in college dormitories and found that even with all of the bedroom doors open, hallway smoke alarms were unlikely to produce a loud enough sound in all rooms, and therefore recommended smoke alarms in every room [64].

In 17 full-scale tests published in 2017 in a one and two-storey house, Traina et al. used ISO 13571 tenability criteria for occupant exposure to heat and toxic gases (CO specifically) [65]. Visibility was not included in the study. Their findings, 11 of which were full-furnished living room fires, indicate that untenable levels were reached at 0.3 and 0.9 m above the floor prior to firefighter intervention (assumed to be 8 minutes), and that the degradation of the fire environment was faster in the single storey structure due to the lower amounts of oxygen as the fire progressed, and the smaller volume for toxic fire gases to fill. The study further suggests that where egress paths may be cut off by the progression of the fire, sheltering behind closed doors would be beneficial. It also notes the importance of teaching the public the value of a comprehensive fire safety plan.

Hutchison and Hostikka consolidate research data on doors in dwellings [34] and conclude that:

> *Any closed door, whether hollow-core, solid-core, solid-wood, or fire rated, can provide protection against the effects of fire, such as heat and smoke, for occupants outside the room of origin. A closed door can extend the tenability time, providing occupants more time to escape and buying time for the fire service to arrive and act on the fire.* [66]

However, it was noted in the original Indiana Dunes tests that recirculatory mechanical systems can influence smoke propagation throughout the house and distribute smoke into other spaces [23]. This could potentially negate the benefit of a closed door, but it was not investigated in the literature referenced in the authors' review. Further, the time available to egress would potentially decrease since occupants would still need to travel through other areas of the house to escape, and closed doors throughout the house could serve to decrease the effective volume of the house for smoke filling, which may accelerate the deterioration of the environment along the path of egress - as observed by Traina [65]. Recent work has also been done on rescue by Kerber [67], who looked at the impact of differing firefighting and ventilation techniques on fire environments. Kobes and Weewer have consolidated the current state of the art and concluded "that survival is mainly related to the location

of the victim, degree of physical vulnerability to the fire, and the physical capacity to escape" [68]. This also assumes that the fire department will be contacted.

Smoke alarms in houses are not required by the NBCC to be connected to the fire department and serve as a local warning only. Common advice from fire departments is only to contact the fire department once you have reached the exterior of the building [69, 70], unless you are trapped. Therefore, while rescue is a potential option if the fire department is contacted by a neighbour or another occupant of the house who has escaped, it is not forthright how quickly rescue operations could occur, especially outside of urban centres. Earlier self-rescue is, therefore, the primary benefit of smoke alarms within houses.

2.2.5 Smoke Detector Placement Research Observations and Summary

The following observations are made based on the above review of the literature:

1. Early testing on smoke alarms balanced the need for devices to address both detection and sounding functions, leading to placements near bedrooms and at the base of stairs in 2-storey houses.
2. The interconnection of devices allowing sounding to occur from multiple devices has not been a consideration in the research on sounding. Decision-making supporting the code direction of the 1980 NBCC and studies done on audibility focus on single devices, and not the combined effect of multiple devices. It remains an open question whether the interconnecting of multiple devices might optimize the position of detectors in living areas without compromising the waking intent of the sounding alarms.
3. The study of flaming and faster-growing fires has been limited when considering smoke alarm location and response times. Much of the research focused on the difference in smoke alarm technologies using small fires to permit the study of the devices' different reaction times. Study of detector response for a wider distribution of fire growth rates in flaming fires would significantly add to the current body of research on alarm activation times relative to the onset of a degraded environment.
4. Studies on smoke alarm placement focused on bedrooms where occupants may be sleeping and whether the bedroom door was left open or closed. Smoke alarms in hallways were found to be insufficient for waking when the bedroom doors were closed. Providing detectors in bedrooms, as is the current requirement of the building code, increases the likelihood of waking when a bedroom door is closed as well as alerting others of the bedroom fire. However, occupants escaping from bedroom fires are moving away from the fire origin if they are required to

escape through the living areas, whereas fires in living rooms are more likely to require occupants to pass through the room of fire origin in order to escape. Additional study on the ASET is warranted when a distribution of detectors is placed on floors without sleeping rooms to determine if the current requirements of the 2020 NBCC need to be reconsidered.

5. The assumption of closed bedroom doors in houses, which are not required by NBCC to be equipped with self-closing devices, is likely optimistic. Doors in houses may be open or closed for various reasons other than fire and could depend on the occupant's age, potential care methods, parenting concerns, ventilation and personal comfort preferences. Such considerations are important in evaluating whether to adopt a defend-in-place approach with potential prolonged exposure to fire/smoke conditions while awaiting rescue in a house fire. At the same time, further understanding of the developing fire environment along the egress path is a useful precursor to evaluating survivability and rescue, particularly given the absence of automated notification to the fire department and the common prevailing advice to only contact the fire department once you are outside.

Based on the above findings, key areas of research that could be incorporated into a fire test program would be to evaluate the room placement of detectors on non-sleeping floors to consider the impact of delayed response where these detectors may be located outside of the living areas. The earlier warning would potentially increase the available escape time for sleeping occupants, and a more comprehensive study could evaluate whether changes are warranted to the current code requirements to require smoke alarms in living areas of the house, where the highest-risk fuel loads are generally present.

2.3 Smoke Filling in a Ventilation-limited Environment

The research findings above generally did not fully capture smoke movement and filling within the houses beyond the head height criteria, especially for larger flaming fires where smoke filling of the house occurred. Particulars of smoke filling in ventilation-limited fires is an area requiring further exploration and is complicated by potential variations in fuel source, fire location and size of the test compartment. There have been studies on fire development in ventilation-limited compartments, which are categorized (with examples) below:

1. Small-scale testing that used relatively small single rooms, some of which incorporated ventilation and predominantly focused on fire extinguishment [71-75].
2. Larger-scale fire tests that address smoke filling within a room or smaller space, where ventilation conditions and/or pressure differentials are studied with a focus on the impact to the

heat release rate (HRR), the thermal environment or species production of toxic gases in the space [76-86].

3. Larger volume spaces where opportunities for smoke control can be evaluated outside of residential applications and houses [87-89].

What is missing from the research, however, is how the smoke is generated with time in a ventilation-limited fire in a multiple-room context. To be complete, the visibility must be well documented, and the evolution of the smoke layer throughout a complex space needs to be captured. Literature on this subject seems to be largely conceptual. For example, according to Mowrer [90], if no sizeable vents are present, "the smoke layer will continue to descend until it reaches either the elevation of the fire source or the floor … Once the smoke layer descends to the elevation of the fire source, the fire source becomes immersed in the smoke layer and further entrainment is assumed to cease." [91]. However, Karlsson and Quintiere [92] compare equations developed by Zukowski [93], and experimental smoke filling times by Hägglund where smoke filling occurs down to floor level [94]. Additional conceptual work on smoke filling was completed by Novozhilov [95] as well as Zhou and Meng [96].

The generally accepted theory is that smoke filling occurs as an approximately horizontal descent of the lower interface of the smoke as it fills from the ceiling in areas outside of the fire plume until the smoke layer drops below the height of the fuel. However, Zhang et al. did an experimental study on the smoke filling with heptane fuel pans at differing heights above the floor and noted stratification of the environment during the early and middle stages of the fire [5]. Afterward, video imaging shows that the smoke does not descend directly from the ceiling to the floor in the center of the room but instead continues filling by jets of smoke down the walls of the compartment, which causes mixing below the interface height. This doesn't align with the theory. Given that smoke and visibility are key parameters in escaping a fire from a house, there is clearly a significant gap in understanding of smoke filling. Further, it is unclear whether Zhang's observations would be equally true for solid fuels with more complex geometry or for those not located in the center of the room. Thus, these types of questions are further explored as part of this research.

2.4 Furniture Ignition Controls

The concept of regulating the fire properties of upholstered furniture in Canada dates at least as far back as 1973 [97]; where the Associate Committee on National Fire Codes identified the concern and the need for standardization of upholstered furniture. A task group was formed to address issues related to fire hazards from building contents and a working group was formed to keep in touch with

the developments taking place to provide regulations and test standards for upholstered furniture, mattresses and pillows.

The role of furniture as a hazard in residential fires was further quantified by NRC's Sumi and D'Souza in 1982 [98]. It was found that smoker's materials accounted for at least 21% of Canadian fire deaths in 1979 and that the residential/furnishings/smoking scenario was by far the most significant cause of fire deaths, whereas the residential/furnishings/open flame scenario was a distant second. The paper explains the complexities of developing ignitability tests due to the variations in materials and geometries and reviews the test methods for evaluating furniture ignition, including the California Technical Bulletin 117 (TB 117) [99] and the British Standard 5852 Part 1 (1979) [100]However, furniture regulations in Canada were never implemented. Given the lack of specific regulations and the much larger US market size, furniture sold in Canada generally complies with US regulations. Therefore, it is necessary to look at the US context to understand furniture in Canada.

A history of US regulations is provided in a white paper by the NFPA [13]. For purposes of this study, two prevailing standards, one in the US and one in the UK, are foundational to residential furniture testing.

1. TB 117 [101] – in 1973, the US Consumer Product Safety Commission (CPSC) created the Flammable Fabrics Act, and the test methods developed by NBS, including a cigarette ignition and a small flame ignition, were implemented by the State of California in TB 117 in 1975. The flame test involved the application of a gas burner flame to the bottom edge of the material when placed in a vertical position, and acceptance was based on afterflame, afterglow, char length or weight loss. The cigarette test involves placing a cigarette at the interface of a material representative of the seat and back cushion. This would go on to become the de facto test standard in North America. Although standards were also developed by others, furniture manufacturers frequently only identified TB 117 [101] on their labeling.
2. BS 5852 Part 1 & 2 (1979 and 1982 respectively) [100, 102] had a cigarette ignition and flaming ignition method using both a gas burner and a miniature wood crib. The furnishing successfully passed the test if no flaming or progressive smouldering were to occur for the duration of the test period. In the case of the miniature wood crib, observations continue after extinguishing or removing the flame for 60 minutes. The test method remains largely unchanged. The two parts were consolidated into one document in 1990, and the current version of the standard is 2006 [103]. The acceptance criteria are not defined in the standard but in the British Regulations [104], which require that manufacturers demonstrate compliance

when exposed to an ignition source 5 wood crib (Crib 5), which is the second smallest of the miniature crib types defined in the standard (Cribs 4 to 7 representing the range).

In 2013, California modified its requirements on furnishing flammability to eliminate the flame test [105]. According to Babrauskas, toxic halogenated flame retardants were being used in products to meet the TB 117 flame ignition test, while the test itself had not shown to have a measurable fire safety benefit [106]. The author identifies two primary considerations: (1) TB 117 compliant materials do not significantly reduce the overall severity of the fire, and (2) the test method is only specific to the foam and does not test the composite material of the foam and fabric. Therefore, flame retardant controls are unlikely to prevent ignition from small flames as the fabric covering the foam is not part of the test. It rationalizes that the fabrics are likely ignitable by a small flame, and therefore, the foam will likely not resist a larger flame attack associated with the fabric burning. A plethora of literature references are included in substantiation of the rationale that the means to achieve compliance with the test method are insufficient to provide meaningful benefit and, therefore, do not warrant the potential increased risk of health exposure due to the use of toxic chemical flame retardants.

In order to address the gap in recognized test methods with the elimination of the small flame test from TB 117, a committee was formed by the NFPA to develop NFPA 277 Standard Methods of Tests for Evaluating Fire and Ignition Resistance of Upholstered Furniture Using a Flaming Ignition Source [107]. The NFPA Standards Council did not approve the draft standard in 2018, citing a fundamental lack of consensus on how to test and evaluate residential upholstered furniture flammability. This was evident in the ballot comments of the committee vote on whether to approve the standard [103]. One concern that was raised was that the ignition source used the propane burner from California Technical Bulletin 133 (TB 133) [108]. This standard, which was repealed in California in 2019 due to similar concerns around flame retardants [109], used a square propane burner applied to the seat of the furniture for 80 seconds. In the public record of the vote to approve the draft standard, the concerns raised by the committee members identified the initiating fire severity as being associated with commercial and institutional occupancies and that a lesser initiating fire was more appropriate for residential considerations. Others identified that the position of the burner on the seat cushion does not adequately address variations in fire exposure to the furniture as well as the absence of any demonstrable life safety benefit to the public for furnishings that met the requirements of the standards versus those that did not. In other words, there is a debate on the efficacy of flame retardants in limiting fire growth versus the potential increased toxicological and environmental risks associated with using them.

This disaccord on environmental risks, fire science and testing methods leaves a gap in North America in actually addressing furniture fire risk, which, according to Ahrens in 2020, continues to be a problem [110]. Specifically, it concludes that "the risk of death in a reported fire is twice what it was in the early 1980's. While smoking remains the leading cause of fires and associated deaths, other causes must also be addressed. [111]" Gann identifies that with a flaming ignition source, or once smouldering transitions to flaming, the fire growth is rapid, and the heat release rate is high and sustained, leaving little time to get out safely [112].

The BS 5852 standard remains current in the UK at the time of this thesis. However, comparable concerns have been identified with respect to the use of certain flame retardants due to toxicity-related concerns [113]. A very comprehensive risk discussion on the subject is provided in a UK report commissioned by the Office for Product Safety & Standards [114]. The report does not clearly provide a path forward on controlling furniture fire risk but does outline methodologies for profiling different risk considerations.

Recent research in furniture performance in fire has focused on the understanding and minimizing of the potential for polyurethane foam to participate in fire, which is the primary factor concerned with rapid fire development, and includes (along with recent associated references):

1. new flame-retardant treatments (that address toxicity concerns) [115-124],
2. barrier solutions that encapsulate the foam to limit its participation in fire [125-133], and
3. controls on the geometric design of furniture that may reduce exposure to the foam and, therefore result in smaller fire growth [134],
4. increased understanding of smoke toxicity [135-137].
5. increased understanding of fire growth on furniture [128, 134, 138-144],

The multiple paths and the considerable research efforts have established that:

- in general, furniture with flame retardants can result in lower peak fire sizes and delayed fire growth [145],
- the utility of flame retardants to limit ignition from small sources does not appear to be in dispute – what is instead of concern is the subsequent fire development when the furniture participates in the fire. When exposed to larger initiating fires, the effectiveness of flame retardants to control combustion becomes muted, and there is a potential increase in smoke production,

- certain barrier technologies are showing promise towards limiting the participation of polyurethane foam and therefore, limiting the rate of heat release and peak sizes of furniture fires, and
- when exposed to fires of equal severity, some research indicates that flame retardant products are observed to release a greater range and quantity of toxic compounds due to less complete combustion and the presence of additional chemicals in the foam, although this assertion is not unanimous as there are competing viewpoints [146].

Both TB 117 and BS 5852 were/are tests designed to limit the potential for ignition when subjected to small ignition sources (as defined in the standards), with the legacy TB 117 being the smallest igniting source, BS 5852 standard crib 5 being a much larger challenge fire, and the legacy TB 133 propane burner being potentially the most severe initiating fire (but for a shorter duration than BS 5852 and not intended for a residential application). There is a challenge, therefore, with much of the intermediate and full-scale testing comparing flame retardant (FR) and non-flame retardant (NFR) products since the standards and regulations do not anticipate a criterion to control fire growth and spread but rather only ignition of the furniture item.

In June 2014, a mock-up burn was prepared to investigate the difference between a couch that complied with TB 117 before and after changes to the standard. The pre-change couch, shown on the left in Figure 2-4, had FR foam meeting the match test of the 2000 version of TB 117 [101]. The post-change couch, shown on the right in Figure 2-4, was reportedly compliant with the 2013 version of TB 117 [105], which did not include the match test and, therefore, would not be expected to have flame retardants in the foam. The foam was not verified through lab testing to confirm the presence of flame retardants. The couch and corresponding armchair were configured inside a sea container used for test burns and located at the Fire and Emergency Services Training Institute in Mississauga, Ontario[1]. The interior dimensions of each cell within the container were 2.8 m wide, 2.1 m deep and with an interior height of 2.6 m. Openings on the front of each cell were 2.1 by 2.0 m high. The wind speed was approximately 24 km/h from the north and, therefore, blowing into the shipping container, further aiding the ventilation of the fires. Each cell was instrumented with a single thermocouple tree and two video cameras, with an additional camera recording both burns from the exterior. The couches were simultaneously ignited with portions of barbeque lighter cubes. Early ignition is shown in Figure 2-5.

[1] Work completed by the author while at Sereca Fire Consulting Ltd, now Jensen Hughes Consulting Canada Ltd., written permission was received on August 15, 2018 to use this information for this thesis work.



Figure 2-4: FR (left) and NFR (right) couch experiment within a half-sea container in June 2014.

The fire was ignited away from the back cushion, and therefore, the fire initially spread down into each of the respective couch seat cushions and then radially outwards, as illustrated in the red circles in Figure 2-5. The fire continued to progress and involved the seat cushion, as shown in Figure 2-6 eventually lighting the back cushion. It then broke through the bottom of the cushion, propagated laterally down the length of the couch, and involved the armchair. Counterintuitively, the FR couch progressed marginally more quickly and reached flashover slightly sooner than the couch without FR, as shown in Figure 2-7.



Figure 2-5: Early ignition of couches in comparison tests.



Figure 2-6: Video capture of burning into the seat cushion.



Figure 2-7: Flashover occurs in the left cell and is initiated in the right cell.

This accurately captures the concern around the use of flame retardants. The original TB 117 test was intended to address ignition from small flames and thus does not extend to addressing the complex interactions associated with full-scale burning. Nevertheless, the need to control large-scale fires is a real issue and will not be solved using materials designed to achieve compliance based on the small flame ignition in earlier versions of the TB 117 standard. Post-test review of the debris field confirmed that the majority of the fuel consumed was the upholstered furniture materials, and only small amounts of the wood frame on both the couch and the armchair participated in the fire as shown in Figure 2-8. The fire did not spread to the coffee table in either test. Thermocouple measurements indicate slightly higher temperatures at the ceiling for the FR couch and slightly higher for the NFR couch at the lower thermocouple, as illustrated in Figure 2-9. The incipient fire period, where limited combustion occurs in a localized area prior to transitioning to a growing fire, was between 3 and 4 minutes, and peak fire temperatures were reached between 5 and 7 minutes. Connecting the furniture performance to the behaviour in limited ventilation situations, however, is not possible since the open burning is not representative of ventilation-limited fires, there is no containment of the smoke as there would be in a room or house, and wind conditions likely impacted the burning rate.



Figure 2-8: Post-test image showing most foam burned while most of the wood framing was intact.

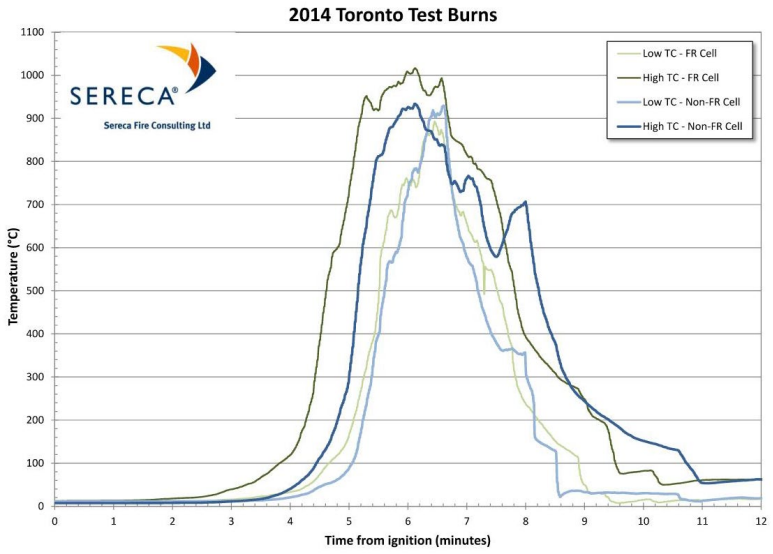


Figure 2-9: The time-temperature graph shows each burn cell's top and bottom thermocouple.

Furthermore, the context of assessing the performance of different options in terms of fire growth and spread requires evaluating a furniture item in consideration of the time to escape, which has not been done in the literature. What is absent is a holistic comparison of time to escape for different furniture constructs with different types of fire controls, where flame retardants, barriers and methods of construction can all be means of reducing fire growth and propagation, with a goal of establishing what level of burning is acceptable before there is a substantial risk to life.

This is accurately captured by Fleming [147], who was not able to identify compelling evidence to indicate there was a benefit to flame retardants and states (underline added for emphasis):

> *In a study [139] comparing furniture that contained flame retardants (UK) and furniture that did not contain flame retardants (FR & US) data was collect on HRR and smoke production … These results indicate the use of flame retardants, delayed the increase in HRR by about 15 minutes. <u>But that does not answer the question, "Do flame retardants provide extra time for occupants to escape?</u>" This study also shows that the rapid increase in smoke is also delayed by 15 minutes. For an alert occupant, the 5 minutes escape time should be more than adequate to escape. For a sleeping occupant, who is relying on a smoke alarm to alert them to the fire, the operation of the smoke alarm may also be delayed by 15 minutes. The same fire scenario occurs, the clock just starts later. [147]*

Part of the rationale against using flame retardants is that the data on fires and fire deaths per 100 fires should have decreased over time since their introduction when the opposite is true. However, the

rationale could equally be applied to the cigarette ignition portion of the TB 117 test standard, and the rationale is more appropriately applied to the test standard as a whole, including cigarette and small flame ignition, rather than debating the use of flame retardants. Anecdotally and experientially, this is likely due to the nature of how data is captured being associated with “smoking materials” but not necessarily capturing the root cause of the ignition. The capture of the data likely includes all forms of smoking materials, including noncommercial cigarettes, and various forms of smoked or heated narcotics or illegal drugs using different ignition methods and means of consumption. However, the TB 117 standard is specific to commercial-grade cigarettes where the tobacco is tightly rolled in paper to finite dimensions and controls. Nevertheless, and returning to the discussion on flame retardants, Fleming’s article accurately captures a primary concern in the flame retardant debate with respect to burning behaviour – specifically that delays to ignition could lead to delays in detection, and the subsequent fire growth is seen as smokier due to the presence of flame retardants acting as combustion inhibitors which could then reduce available egress time. It would be useful to establish if this assertion is accurate for a range of furniture types.

Previous work done by Collier considered incipient fire time as a function of different ignition methods and different locations on furniture [148]. The furniture was tested under a calorimeter, which allowed measurement of the heat release rate, and a criterion of 30 kW was established as a basis for defining the transition beyond the incipient stage of the fire (considering a standard burner would produce about 30 kW. It was found that the ignition source's location influenced the development duration, with ignition sources closer to the centre of the mass of combustibles leading to shorter incipient fire times. The conclusions of the report “reconfirm that the current practice of ignoring the incipient fire development period is conservative for the purpose of calculating ASET based on a fast t-squared design fire [149].” It was further noted that there is a need for case study analysis, including detection times, to evaluate if an incipient period should be further considered in performance-based design. Understanding detector response in real-scale residential applications is relevant to furthering the understanding of a wider distribution of materials than Collier’s tests which repeated tests of a singular material type with no variations on the type of couch materials nor furniture controls [148]. Sundström did a comprehensive tests series on a range of furniture materials, constructs, and controls [134]. In particular, a very wide range of heat release rate curves were observed in 27 European Furniture items. These ranged from very slow fire development to ultrafast fire development. Conversely, Collier’s materials performed only in the fast range. Slower-growing fires would be expected to have a greater opportunity to activate a smoke alarm during the incipient stage, as observed by the various test series studying smouldering fires [23, 46, 47].

One key challenge is that the research as a whole has not had an end objective for establishing an escape time by establishing limits on the fire growth rates, peak burning rate, and duration of fire that define what is permissible to support a safe escape from a house fire. Much of the furniture fire testing shows a very wide range of fire growth rates and peak fire sizes, and there is an overt focus on peak burning rate in well-ventilated conditions and flashover, which is not a representative fire environment of those observed in the research house fires where doors and windows were kept closed prior to the house being ventilated.

Therefore, a comprehensive program is needed that investigates a range of furniture constructed using varying control measures that estimate smoke generation and impact on egress relative to fire detection times in closed houses with representative ventilation.

2.5 Previous Testing & Research

2.5.1 Early House Burns and Ventilation Environment

Opportunities have arisen to conduct burns in full-scale environments working with local fire departments where houses are being used for training prior to demolition. In several tests completed in three different houses in British Columbia in 2003, work was done to better understand the potentially different distributions of fire growth in several different houses under different ventilation conditions, equipped with varying types of furnishings and fuel types [150].

The work focused on the fire development in houses and the corresponding burn patterns that were generated for forensic purposes. However, it was readily identified that, except for where large openings were present to the exterior, the fire would likely become ventilation-controlled, and the rooms/houses would fill with smoke. This aligned with forensic experience that indicated fires that have short incipient fire growth times followed by a growth period through to flashover were less likely than fires that became ventilation-limited and potentially created restricting conditions that could impact escape. Similar work was completed on a decommissioned motel in Sooke, BC in 2010 with consistent findings to the house fire tests, but the findings were not published. In addition, many cubicle burns created for fire investigation courses purposefully identifying differences in fire dynamics associated with fast-growing ignitable liquid fires and the influence of ventilation-limited environments have been completed [151].

All of these burns involved upholstered furniture in the form of sofas, beds, and often varying forms of gasoline and diesel fuels. Given the remote nature of the burn sites and limited electrical power in decommissioned buildings, generally, the instrumentation was limited to thermocouples and video cameras. Nonetheless, some key observations could be made. These include that, for the most

part, couches were easily ignited with a very small amount of liquid fuel or using a small charcoal lighter puck. In all of the upholstered furniture tests, the couches readily ignited and continued to burn, suggesting the ignition and continued burning do not require larger ignition sources. Unfortunately, smoke alarms were not controlled in these tests, precluding analysis of escape times, and in most instances, the houses that were used were blocked off for future tests, making the actual test area quite small relative to the whole area of the house. Even so, based on the relatively limited results, it was clear at the time that additional work was needed.

2.5.2 Precursor work at the University of Waterloo

In 2014 as part of coursework at the University, 100 forensic files involving upholstered furniture fires in living rooms were analyzed to understand better the participation of the furniture in the overall development and final outcome of the fire [14]. It was found that furniture was the primary catalyst for degraded conditions within the structures and is frequently the primary fuel hazard, as illustrated by the absent sofa and burn patterns in Figure 2-10. It also highlighted that while 42% of the fires were related to smoking materials, an additional 25% were related to exposure from other sources of ignition. This suggests that any successful development of fire controls for cigarette ignition remains largely unaddressed and, as outlined above, exposure to nearby fires and ignition sources leads to the ignition and burning of the furniture, precipitating the subsequent degraded fire environment within the dwelling.

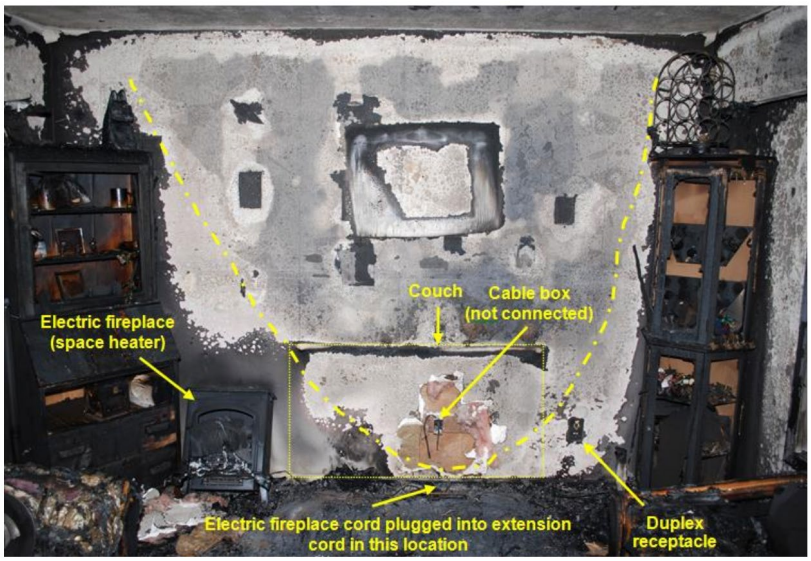


Figure 2-10: Example of post-incident burn with furniture no longer remaining.

The investigation of smouldering fires, discussed in Sections 2.2.1 and 2.2.4, generally did not lead to conditions that would have precluded escape from a fire, even over long periods. A greater

focus on flaming fires is needed, along with an investigation of the smouldering to flaming transition since cigarette fires lead to more pronounced furniture flaming fires, which seems to be at the core of the furniture fire problem.

Nine flaming furniture fires formed part of a test program in 2015 looking at ventilation-limited fires with three tests of three different furniture types, as reported by Forrest [152], Forrest et al.[145], and Senez et al. [153]. The test procedure demonstrated repeatability in overall fire performance for each furniture type and allowed for a comparison of peak heat release rates and the timing thereof for NFR, FR and Lightly Flame Retardant (LFR) fabric and foam. Materials were directly obtained from suppliers, and couches were manufactured to the identical dimensional specifications for all 9 couches by a local furniture supplier in Waterloo. The NFR materials were obtained from the Netherlands. The FR materials were obtained from the UK and were treated with FR to meet the BS 5852 testing requirements. The LFR couch was obtained from the US and was reported to meet the pre-2013 version of TB 117, similar to the couch tested in Mississauga outlined in Section 2.4.

The NFR materials acquired from the Netherlands and the FR materials acquired from the UK were of the same foam and fabric type, with the only difference being that the UK materials were treated with flame retardants. This was verified by a third-party laboratory. To pass the BS 5852 test in the UK, the couch must resist ignition to exposure from Crib 5. To evaluate ignition propensity, the couch was first tested with Crib 4, which is smaller than Crib 5 and, therefore, should have self-extinguished on the FR couch. It only self-extinguished in one of the three tests, and when that test was repeated with Crib 5, which also should have self-extinguished, it proceeded to burn on the same basis as the previous two Crib 4 ignition tests. With this exception, all of the other tests were ignited by Crib 4.

The fire on the NFR couch, Couch A, had the highest peak HRR shown in blue in Figure 2-11. By comparison, a couch made of identical materials but with an FR-treated fabric and foam, Couch B, shown in red, had delayed fire growth and a much lower peak heat release rate. The two overseas materials also had much earlier fire growth when compared to Couch C purchased from the US, which are the black lines in Figure 2-11. This couch had a more gradual fire growth and a lower peak heat release rate than the FR Couch B. Further, an investigation of the differences in fabrics found that the Couch C fabric was more thermally resistant than the other two, with and without FR. An ad-hoc test confirmed the response of the overseas fabric to shrivel up – compared with the US Fabric that had a greater thermal resistance, as illustrated in Figure 2-12.

The better thermal performance of the fabric reduces the rate of exposure of the polyurethane foam to the fire, which in turn reduces the growth rate and peak heat release rate. The FR fabric from the

UK was understood to meet the requirements of BS 5852 and was therefore assumed to have complied with the “match” test requirement of BS 5852, as required by the regulations. However, this was not verified. Materials that don’t comply with the match test requirement are permitted where an “interliner” is intended to provide a fire barrier between the foam and the fabric.

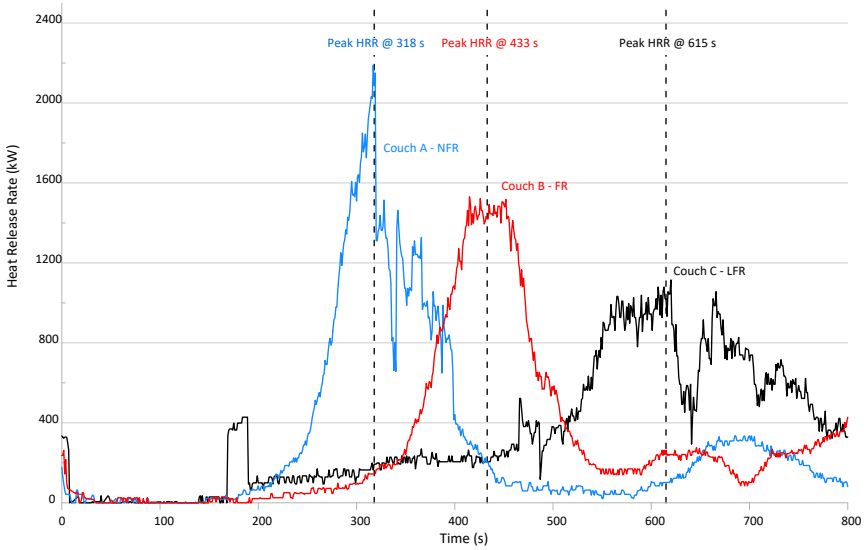


Figure 2-11: Heat release rate data from 2015 UWFRL burn tests comparing NFR, FR and LFR materials.

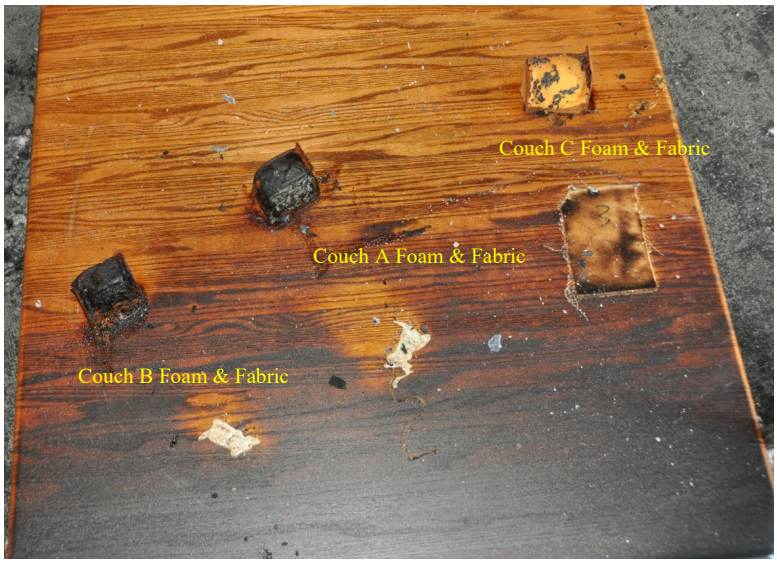


Figure 2-12: Ad-hoc test to evaluate response to fabric and foam thermal exposure (samples placed radially equidistant from the fire origin).

The results suggest that delayed fire growth leading to a lower peak HRR reflects a better fire performance of Couch C. However, the smoke alarm activated at 1.7 minutes for Couch B (red line) and 5.4 minutes Couch C (black line), meaning there was a difference in notification time of 3.7

minutes before the smoke detector responded, and therefore before an occupant would be woken to escape a fire. If the peak heat release rate is used as the outer window for determining escape time, then there is 14% more time available to escape with the FR couch than with the LFR couch, as illustrated in Figure 2-13. If this same rationale is applied to comparing NFR and FR couches of like materials, this percentage increase in escape time is 78%, as illustrated in Figure 2-14.

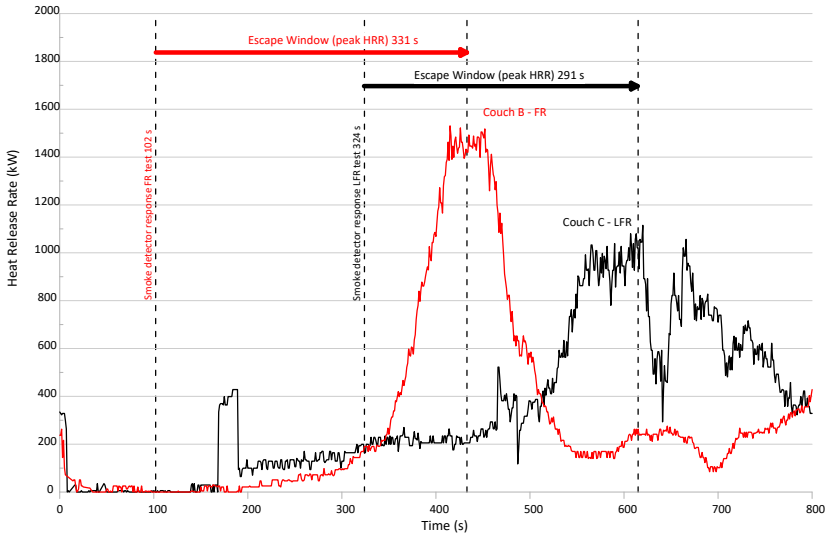


Figure 2-13: 2015 UWFRL Couch experiments comparing FR and LFR couches.

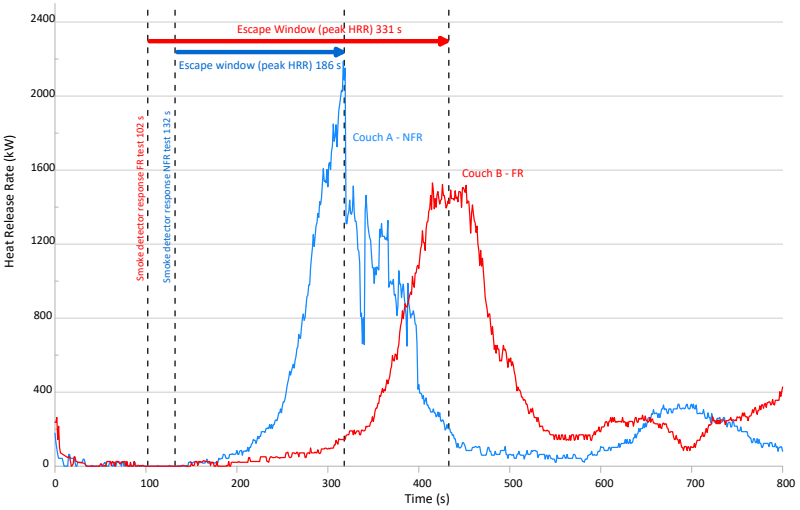


Figure 2-14: 2015 UWFRL couch experiments comparing NFR and FR couches.

This illustrates the difficulty of studying only a single criterion, such as HRR, in quantifying the safety aspects of egress from an enclosed ventilation-limited house. Whether the peak fire size is the appropriate parameter in determining escape time is likely questionable since the peak fire size is an indicator of the onset of ventilation-limited conditions developing in the house, and all of these experiments became oxygen-limited and filled the house with smoke. The extent to which conditions

have degraded along egress routes within the house requires further investigation to quantify the internal conditions along escape routes and highlights the need to evaluate smoke filling, layer height and visibility in future tests.

With good experimental design and relatively well-controlled conditions, the fire behaviour from identical complex solid fuel loadings is repeatable, limiting the need for multiple tests in the controlled environment. Temperature, heat release rate, flame spread rate, carbon monoxide production, and other environmental conditions are measurable and found to be consistent for fires with a given fuel source in the same compartment and reflect the trends in overall fire behaviour. The results also support the consistency in fire trends and heat pattern development in upholstered furniture fires under ventilation-limited conditions. They provide insight into recirculatory trends in the movement of oxygen and fire gases through the compartments, which is an important element since residential fire safety is complicated by the interplay of fire dynamics and the exchange of air and fire gases between the rooms and floor levels. Yet, no full-scale experiments to date have addressed, to any great degree, the variability of fire development with varying ventilation, mechanical systems, and solid fuel sources other than the range of furniture noted above.

Specifically, critical considerations include more in-depth investigations of fires fueled by the types of fuel prone to increased burning (e.g., foam and fabric versus wood frame) and the differences between solid and liquid fuels, including how these impact the responsiveness of smoke alarms and the corresponding internal environmental conditions during the fire. These, in turn, consider the likelihood of detection, occupant awareness, response, and propensity to escape from other areas of the house, namely the upper levels where occupants may be sleeping. It was therefore clear from this test series that additional experiments with a wider variation of fuel and furniture types, and in particular different fabrics, along with an accurate smoke detection system, gas and flow sensors, thermocouples, and video cameras would allow greater interpretation of the evolution of the environment and thus, escape times, during ventilation-limited upholstered furniture fires.

2.6 Synopsis of Literature and Research Focus

In summary, the data on fire deaths affirms the continued problem of furniture fires in residential homes causing the highest number of fire fatalities in Canada and the US. Fires in living rooms impose additional risk due to the accelerated burning rates of upholstered furniture combined with the potential to obstruct escape paths for sleeping occupants needing to move past the living areas to reach an exterior door. Despite this, the location of smoke alarms in houses on non-sleeping floors has not been required to specifically include the living areas of the house, and required detector

numbers are limited to one on nonsleeping floors. Per capita increases in fire deaths in homes in the US since the 1980s highlight the need to revisit safety in houses. It calls into question both the effectiveness of the furniture fire testing standards (i.e., TB117 including both the legacy flame test and the still current cigarette ignition test) and the potential adequacy of the placement of smoke alarms in houses relative to the higher risk fire scenarios.

Controls on furniture construction, inclusive of material fire properties and methods of manufacture, with intent to limit fire growth have not been studied relative to a fully defined level of performance. To do so requires a more involved discussion around the time needed to escape from a fire and, correspondingly, the complex relationships between stages of fire growth relative to the smoke filling and fire detection times in different fires. Further, investigation into whether the positioning of detectors can be optimized to significantly increase early warning to longer times before smoke filling of the environment precludes escape is a key gap in the literature. This interplay between escape time, furniture fire growth, detection time relative to location, and smoke filling leading to an untenable environment is graphically illustrated in Figure 2-15. A detailed experimental investigation into, and the associated analysis of, these parameters and how they combine to determine an available escape time is the focus of this thesis.



Figure 2-15: Graphical illustration of thesis research focus areas.

Chapter 3
Objectives and Experimental Design

A multifaceted large-scale experimental fire program was developed at the UWFRL to investigate different aspects of fire science, including human response to fires, fire heat release rate, gas species production and air movement within a house in varying ventilation environments, and methods of calculating visibility during egress from fires. The program was constructed in three parts: the Mechanical Ventilation Series, the Fuel Volatility Series, and the Passive Ventilation Series, abbreviated MV, FV, and PV, respectively.

The MV series consisted of four fire experiments using the same base fuel type, burning under four different mechanical ventilation conditions: one with the base amount of air supply, one with double the base amount of air supply, one without air supply, and one with 100% recirculating air space. The FV series was focused on varying the fuel type looking at differences in conditions when the ventilation parameter is maintained the same, but the fuel parameter is varied. The MV series focuses on ventilation and is being investigated by others in the UWFRL program. The PV series investigates different ventilation conditions with varying passive ventilation and has been delayed to a future date. The focus of this thesis is on the FV series and the different impacts of furniture fuel packages on the fire environment within, and associated available escape times, from the test house.

Different fires were incorporated into the FV tests to provide a distribution of fire characterization for different materials. Wood cribs are frequently used and well-recognized as an industry standard material in fire testing. Wood represents a naturally occurring material when compared to the synthetic materials that make up upholstered furniture and are considered to contribute to fast fire growth, which is generally defined as reaching 1 MW in 150 seconds [148]. The wood crib fire test, which will be Test 1FV, therefore provides a benchmark that is representative of a naturally occurring organic material yet configured to optimize combustion in a well-ventilated wood crib.

A heptane fire is not expected to have similar burning characteristics as furniture since it is not a solid. Liquid fuels are more easily volatilized in air and, therefore, more readily combusted than solid fuels. They are correspondingly expected to consume oxygen more rapidly during a fire in an enclosed environment than solid fuels. Much of the limited testing that does exist on ventilation-limited fires has used gas burners and liquid pans as fire sources, which do not account for the ventilation differences and delays in fire growth associated with incipient fires established on solids over an extended period. It is known that there are differences in the associated fire dynamics

between liquid/gas and solid fuels, which forms another aspect of research under study as part of the full UWFRL program. However, the present research focuses on the fires established over solid fuels. Test 2FV fueled by heptane is, therefore, only selectively discussed in the sections below, primarily as it relates to oxygen depletion. It is nevertheless included for completeness in many tables and figures.

Therefore, for the FV test series, fuel types were selected as: (1) wood, forming a baseline with well-known burning characteristics, (2) heptane which, as a liquid fuel, is generally more easily volatilized into gas and therefore more likely to degrade the environment more quickly, (3) variations of different couch constructs looking at cloth, faux leather, and leather thereby providing different variations in fabric materials on the couches, with cloth expected to perform the least well, leather expected to resist ignition and limit fire growth, with faux leather in between. This is based on observations of past couches with cloth potentially being more porous, faux leather being less porous but made of synthetic, and leather being less porous and normally resistant to heat. Couches are also constructed to different furniture standards representing different types of burn-limiting controls between test standards TB 117, BS 5852, and TB 133.

To evaluate the end-effectiveness of these different furniture types, this research focuses on the characterization of the overall evolution of the fire environment coupled with the determination of escape time based on camera visibility, with differing fuel arrays from the FV test series, which consists of a total of 10 experimental tests of significance. With one overlapping test between series (known as Test 2MV), nine additional experimental tests were completed comparing 3 different types of furniture purchased from Canada and the UK (5 tests), a wood crib (1 test and a few additional calibration tests), a flammable liquid fire (1 test) and two sets of used furniture that are reported to meet the US TB 133 test. Details on the different fuel arrays are outlined in the next chapter. Below is a synopsis of the research objectives, followed by the details of the experimental design.

3.1 Research Objectives

The primary objective of this research is to estimate escape times from the burn house for a range of flaming fires with different fire growth rates and material responses to ignition and fire propagation. By investigating smoke layer descent, it is anticipated that two levels of escape can be considered: (1) a “walk-out” criterion prior to the smoke layer descending to approximate respiratory height (~1.5 m above the floor); and (2) when the smoke layer has descended to 0.9 m, a “crouch” or “crawl-out” criterion. Generally, the research outlined in the literature review primarily addresses the 1.5 m height range, or the walk-out criteria, and does not account for escape by crouching or crawling below the

smoke. It is nevertheless quite common for fire departments to highlight crouching or crawling as a means of escaping a house fire [69, 70, 154], and therefore, further investigation of this method of escaping is warranted. Based on existing gaps in the field, the present research focuses on the following objectives:

a) to collect detailed time and spatially resolved data on mass loss, visibility, oxygen consumption, and the evolution of carbon monoxide and carbon dioxide during ventilation-limited fires established on leather, faux leather (vinyl) and cloth couches versus wood and liquid fuels in a multi-compartment, two-storey burn house,

b) to evaluate smoke layer development around the origin of fires fueled by solid irregular-shaped fuels throughout the different rooms and levels of the multi-compartment, two-storey structure,

c) to collect new information on the range of environmental conditions occurring at times of smoke alarm activation relative to the onset of conditions that may preclude escape for different materials and different detector locations during the fires, and

d) to evaluate the importance of incipient fire development time and subsequent fire growth rate related to time to escape across a range of furniture designed and built using different fire control strategies.

Comparing the different incipient fire duration, detection times, mass loss rates, smoke layer descent, temperature, and species production rates of leather, faux leather (vinyl), and cloth couches with wood and liquid fuels provides a range of burning environments to better quantify the differences in escape times. A visual representation of the escape timeline relative to smoke filling is presented in Figure 3-1.

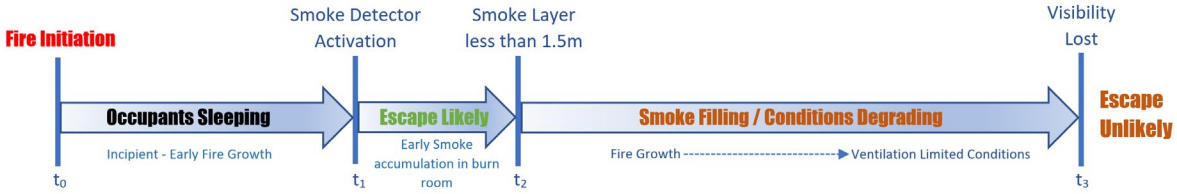


Figure 3-1: Visual representation of stages of fire development and viability of escape.

The details of the test house and instrumentation are summarized in the following sections.

3.2 Test House Configuration

The test rig is a two-storey "Burn House" at the University of Waterloo Fire Laboratory. The multi-room, multi-level test house mimics the size of a small residential house and allows for the study of

escape from the upper level, where a living room fire develops along the path of egress. The test house is a stand-alone exterior steel framed building constructed of 102 mm steel H and I-beams and is clad with 3.18 mm steel on the exterior. The approximate total interior floor area is 100 m^2, plus 5 m^2 (horizontal dimension in plane) stair opening, and the total approximate volume is 275 m^3. Dimensional references are included in Figure 3-2. The lower level was steel framed and boarded with 15.9 mm Type X gypsum board on the walls and ceiling, as shown in Figure 3-3. An additional layer of 12.7 mm cement board was added to the walls and ceiling in the Lower Burn Room (LBR), and 100 mm thick mineral wool insulation was added behind the ceiling. This was found to be functional in the previous burn tests to reduce exposure to the structure and allow for multiple sequential tests before repairs are necessary. The ceiling height of the finished ceiling on the lower level was 2.4 m. The upper level of the house was an unfinished steel structure with a ceiling height of 2.6 m.

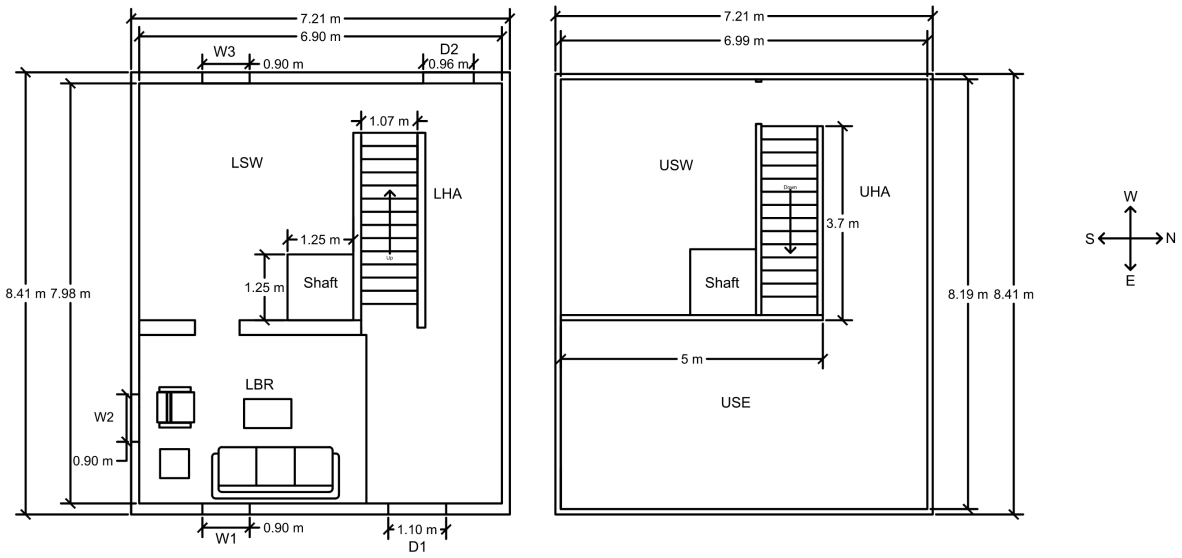


Figure 3-2: Floor Plan of Burn House (left) Lower Level (right) Upper Level.

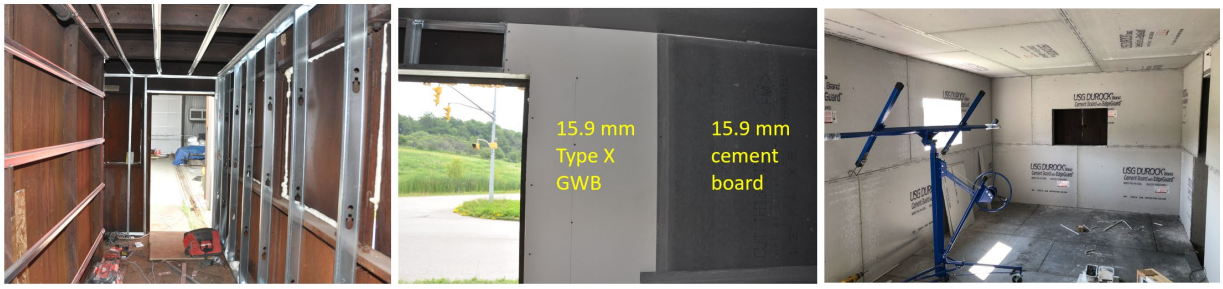


Figure 3-3: Burn house with steel framing prior to boarding (left), and after boarding in the LBR (centre and right).

The lower level LBR connects to the Lower Southwest Room (LSW), also referred to as the kitchen, where a window is located in the west wall (W3). The Lower Hallway (LHA) connects the

door (D2) in the west wall north to the LBR. A stair connects from the LBR to the Upper Hallway (UHA), which opens into the upper southwest room (USW), also referred to as the small bedroom. From the landing at the top of the stairs on the west wall. The UHA extends parallel to the stair along the north wall to the Upper Southeast Room (USE), also referred to as the large bedroom.

A shaft provided access to a crawl space below the lower floor and was continuous through to the upper floor. The shaft, which is separated from the interior of the test house, contains the power supplies and modules for the data acquisition system (DAQ), allowing for temperature or voltage readings on the thermocouples and velocity probes. Penetrations into the shaft were sealed with mineral wool insulation.

The LBR is the primary combustion room. The couch is ignited and has one door (D1) to the exterior and two windows, one immediately behind the couch location (W1) and one behind the chair location (W2). Windows are 0.9 m by 0.6 m, double pane, Low-E slider type, manufactured by Jeld-Wen.

Images of the exterior façade are provided in Figure 3-4, showing the east façade, and Figure 3-5 showing the south, west and north exterior facades with an overlay of relevant test rig particulars to facilitate orientation for the reader. Figure 3-6 illustrates the LBR as fit out for a test overlayed with various details of instrumentation and furniture orientation in yellow text. Thermocouples are located on chains and referenced by a tree number (T#), and gas instrumentation stations are also numbered in the house (GIS#). Further details on the instrumentation are provided in the sections that follow.

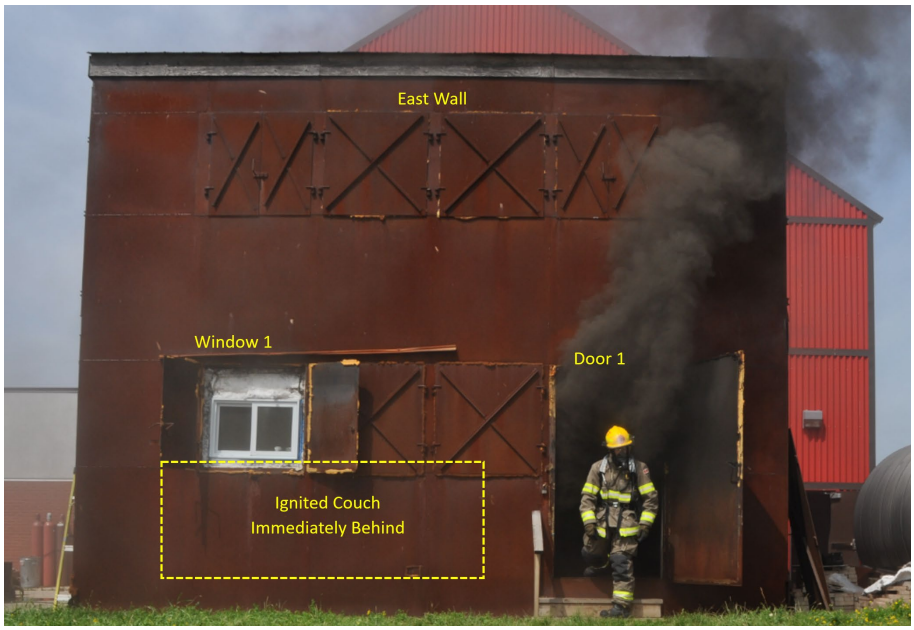


Figure 3-4: East facade of burn house showing smoke discharge from test outside Door 1.

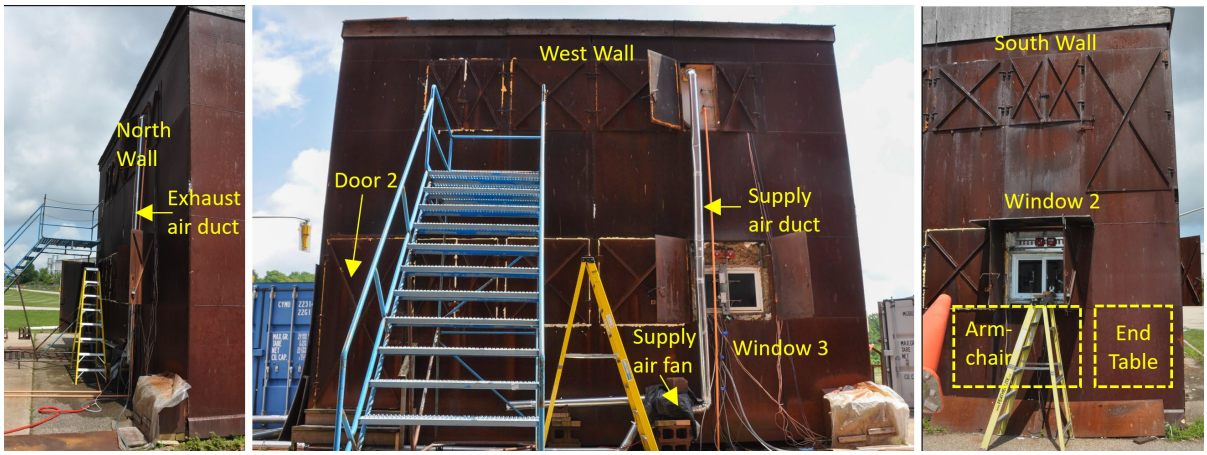


Figure 3-5: North, West, and South facades of burn house with annotations for reference.

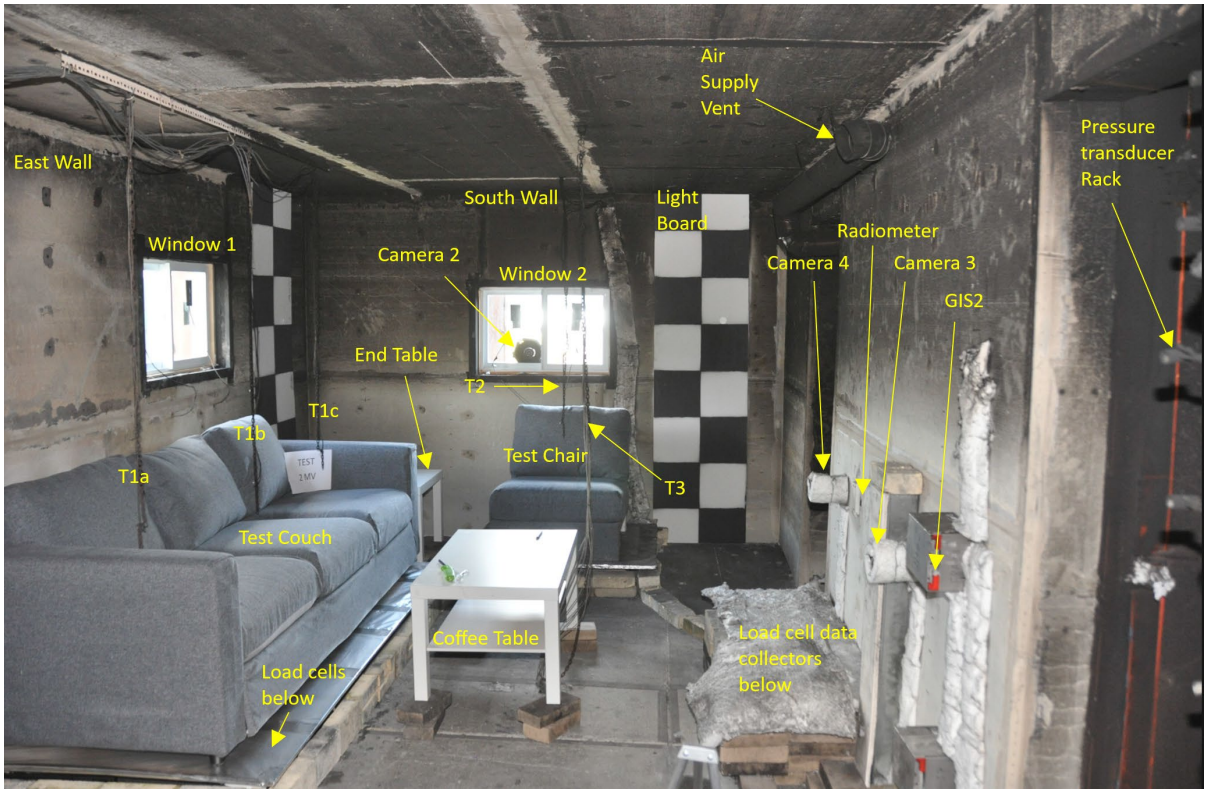


Figure 3-6: Image showing the general configuration of the test setup and corresponding instrumentation in the LBR.

3.3 Test House Instrumentation

The experimental design's instrumentation strategy provided thermal, video, airflow, and gas data throughout the house. For purposes of this study, the path of escape from the upper level rooms (the small and large bedrooms, USW and USE), where sleeping occupants would hypothetically be present and become aware of a fire after a smoke alarm activates, is the primary focus area of study.

Occupants would hypothetically have to descend the stairs where they would encounter developing fire conditions from an upholstered furniture fire on the couch in the living room (LBR) and move away from the fire along the lower hallway (LHA) to reach the exterior door (D2), as depicted in Figure 3-7. Therefore, the corresponding instrumentation focus for this research will be the UHA, the LBR, and the LHA, as this is the path of egress for evaluation. The detailed instrumentation plan is outlined below.

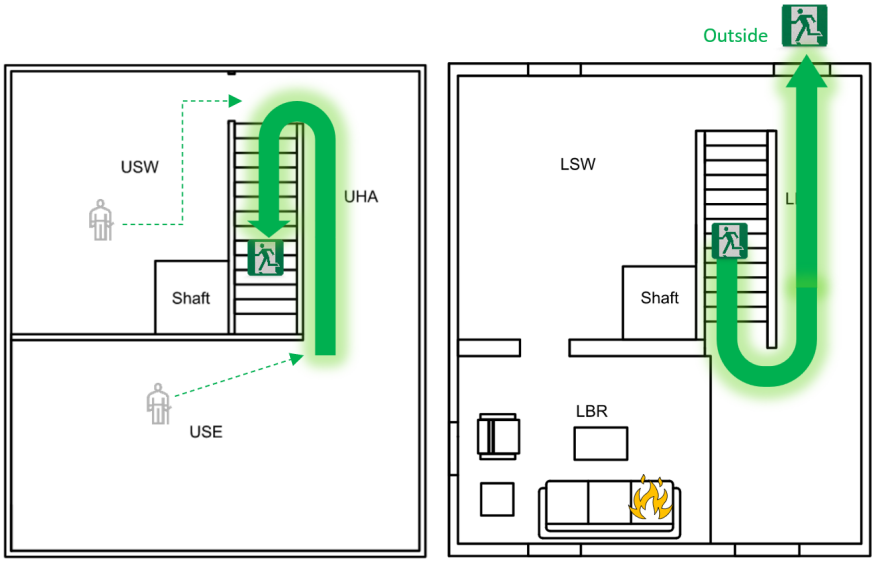


Figure 3-7: Floor plan showing hypothetical escape path (green line) from upper level (left) through lower level (right).

3.3.1 Furniture Load Cells, Thermocouples & Heat Flux Gages

To measure the mass loss of the couch and correspondingly allow for estimates of the heat release rate, four ARS MSB-60 load cells are located and incorporated into a test jig consisting of a foiled 15.9 mm gypsum board protective base (1.2 by 2.4 m) that supported the test couch. Fire bricks, with mineral insulation behind them, are installed around the perimeter and configured to not restrict the movement of the floating base on the load cells. Each load cell is 0.45 m by 0.45 m with a maximum individual capacity of 60 kg (combined 240 kg), and the four load cells are wired to combine the loads of each scale. The test chair is placed on a single MARS MSB-120 load cell, 0.61 by 0.76 m, and is also protected by 15.9 mm gypsum board, fire brick and mineral wool to limit thermal exposure to the load cell test jig during the test. The general arrangement prior to being protected is illustrated in Figure 3-8.

Using weights of known mass, as measured on the calibrated ThermoNobel TAD3 lab scale, the load cells are zeroed prior to placing the furniture at the start of each test. Each furniture item is also weighed on this scale before and after each test, in addition to being continuously measured during

the test on the load cells, which have 0.01 kg resolution and a manufacturer's specified total error of 0.05% [155]. These values were found to be within 3%. A procedure was established to quantify the voltage output on the data acquisition system (DAQ) by first placing the calibrated weights 50% higher than the expected load and then again 25% higher than the expected load for each load cell location (chair and couch).



Figure 3-8: Approximate load cell arrangement prior to being thermally protected.

Type K (chromel-alumel) 20 AWG thermocouples constructed with an exposed bead diameter of 1 mm are placed in thermocouple rakes with 2 to 8 individual thermocouples at different heights. The insulator wires were fed from the DAQ modules in the shaft to individual thermocouples positioned on chains that were anchored to the ceiling with screws into the metal studs and fed back to the shaft in the centre of the house, where they connected to the DAQ instrumentation modules. The thermocouple "rakes" were numbered (T#) as shown in Figure 3-9. Following the 2019 test, T1 was subdivided into three subsets: T1a, T1b, and T1c. This allows additional temperature measurements to evaluate fire spread on each seat cushion, particularly after visibility is lost due to smoke.

Rakes were also included above the Chair (T2) and in front of the coffee table (T3) within the main burn area of the LBR. A raised floor of ~75 mm was included in the main burn area to protect the test house's steel floor and provide a protected path for instrumentation cables with the main burn area. T5 was located away from the main burn area furniture to the north, in the open area of the LBR. Rakes were also placed in the LHA (T6) and the UHA (T8), and each of the non-burn rooms on both levels (T7 in LSW, T9 in USE, and T10 in USW). Thermocouples are also located at each air velocity probe, including in the doorway between the LBR and the LSW (T4). A single thermocouple was added to each interior and exterior pane of glass in the LBR burn rooms. Each thermocouple is rated

for 980°C continuous and 1090°C short-term service and a 1-2 second time response depending on the conditions [156]. Each thermocouple was tested with a hand-held lighter prior to each furniture test. Individual thermocouple heights are shown in Table 3-1.

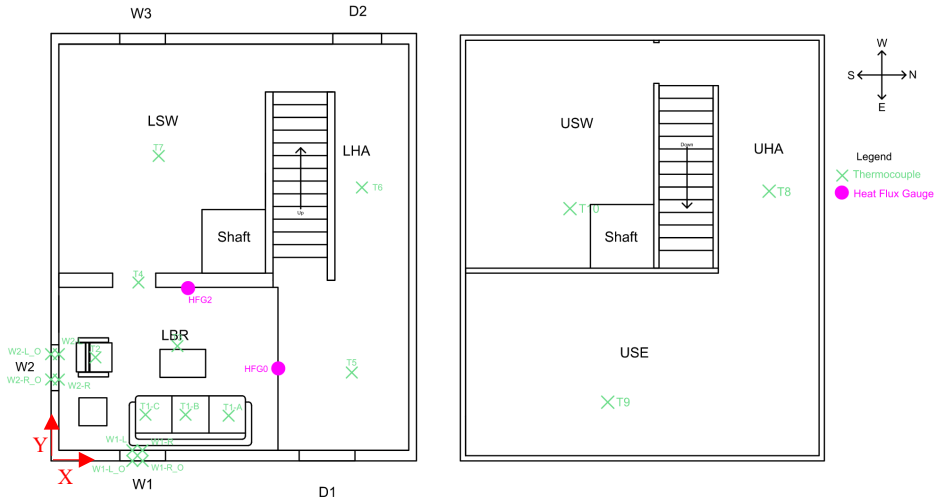


Figure 3-9: Thermocouple and heat flux gage locations.

Also shown in Figure 3-9 are the locations of two water-cooled Vatell TG1000-1 Gardon heat flux gauges (HFG), one located in the wall 2 m opposite the couch, 0.79 m high and 2.55 m from the W2 wall (HFG2). This targets radiation measurement opposite the couch. The other HFG, denoted HFG0 is 4.33 m from W2 wall, 1.61 m from the W1 wall and located within a cored fire brick on the floor and intended to capture radiant heat from the smoke layer. The two locations are illustrated by the red arrows in Figure 3-10. The gauges have a typical accuracy of 3% FS when applying the manufacturer's originally provided voltage-heat flux calibration curve. Similar to the thermocouples, the response of the HFG is tested using a small flame lighter prior to each test.

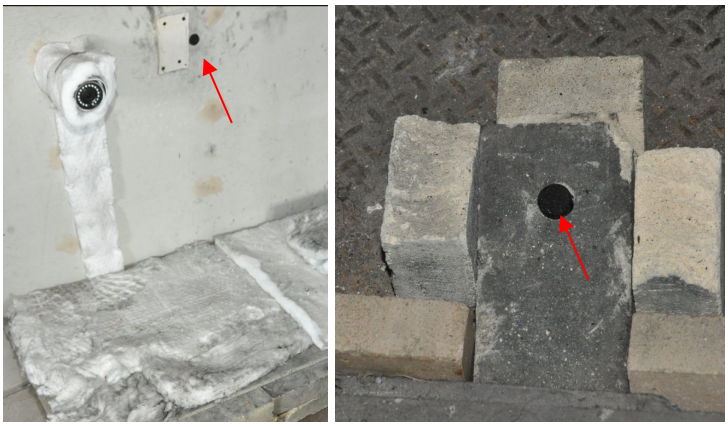


Figure 3-10: HFG (indicated by red arrows) in the wall opposite the couch (left) and on the floor on the edge of the burn area in LBR.

Table 3-1: Thermocouple heights by location reference.

Vertical Position Number	**Height of Thermocouple from floor, and XY position from southeast inside corner** (Refer to Figure 3-9 for X-Y orientation) **Thermocouple Tree Number**																					
	T 1a		T 1b		T 1c		T 2		T 3		T 4		T 5		T 6		T 7		T 8		T 9		T10	
	X	**Y**	**X**	**Y**	**X**	**Y**	**X**	**Y**	**X**	**Y**	**X**	**Y**	**X**	**Y**	**X**	**Y**	**X**	**Y**	**X**	**Y**	**X**	**Y**	**X**	**Y**
	3350	680	2500	700	1710	700	720	1830	2340	2050	1570	2050	5780	1530	5980	5170	1970	5790	5990	5350	2910	1300	2060	1300
1	930		950		880		960		400		880		350		710		370		700		680		600	
2	1310		1290		1270		1350		700		1950		650		1280		680		1320		1290		1310	
3	1860		1890		1890		1890		1000		NA		930		1880		1290		1900		1900		1890	
4	2290		2260		2270		2290		1300		NA		1230		2310		1600		2320		2340		2320	
5	NA		NA		NA		NA		1590		NA		1520		NA		1890		NA		NA		NA	
6	NA		NA		NA		NA		1890		NA		1830		NA		2300		NA		NA		NA	
7	NA		NA		NA		NA		2030		NA		1980		NA		NA		NA		NA		NA	
8	NA		NA		NA		NA		2260		NA		2280		NA		NA		NA		NA		NA	

3.3.2 Velocity Probes & Gas Instrumentation Stations

Gas velocity probes with a Setra 267 differential pressure transducer having a ± 25 kPa range and 0.5% FS accuracy were positioned in racks between the rooms and at the top and bottom of the stairs, shown in Figure 3-11. Probes were also installed in anticipation of the PV test series but are not referenced for the FV series tests since there were no dedicated openings once the door was closed at the start of the test. Each of the stair probe racks (A4 bottom, A8 top) had 8 velocity probes at 0.4, 0.63, 0.9, 1.15, 1.4, 1.6, 1.8, and 2.0 m above the floor. A9, at the interface of UHA and USW, had four probes at 0.4, 0.9, 1.14, and 1.6 m above the floor, with the remaining non-window or door probes, having one at 0.4 and the other at 1.6 m above the floor. Probe locations are shown in Figure 3-12. Additional probes were in each of the supply and exhaust mechanical ducts. Uncertainty for bidirectional probes has been found to be on the order of ±10% [157], inclusive of a probe, pressure transmitter, and thermocouple.



Figure 3-11: Velocity probes: (left) between LSW and LHA, (Centre) base of stair in LBR, (right) LHA top of stair.

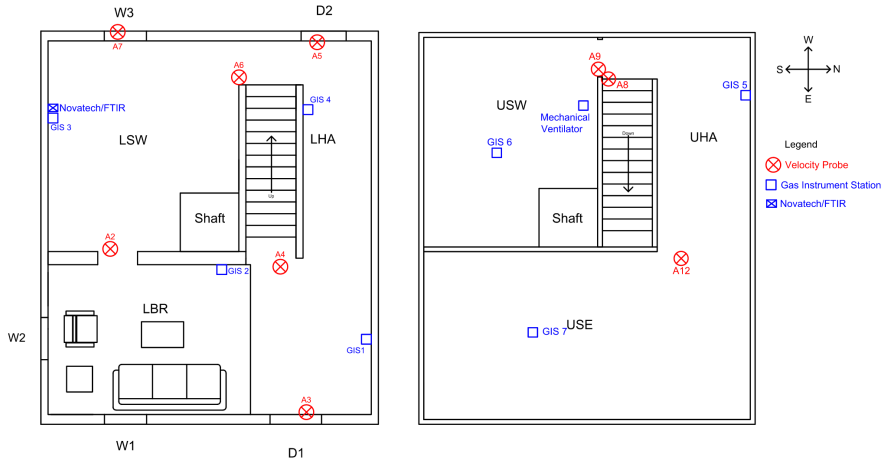


Figure 3-12: Locations of velocity probes and Gas Instrumentation Stations

Seven gas sensing locations are located throughout the house, as shown in Figure 3-12, and allow for the provision of an enhanced profile of gas concentrations throughout the house. Gas sensors were custom manufactured by a third party with a purpose-built circuit board and an imbedded Arduino micro-controller and measure: oxygen (O_2); carbon dioxide (CO_2); carbon monoxide (CO); methane (CH_4); ammonia (NH_3); nitrogen oxides (NO and NO_2); hydrogen cyanide (HCN); Hydrogen Chloride (HCl), volatile organic compounds (VOCs). Relative humidity (RH) and temperature (T) are also recorded to account for the local environment and allow for temperature and relative humidity correction of the gas concentrations, where appropriate.

The onboard controller at each unit connects with an ethernet cable to an electronic switch located in the shaft and was set to send 4 samples per second. An ethernet cable connects from the shaft to a dedicated laptop computer at the test control centre. A purpose-developed script by the manufacturer is used within the LabView software to record and monitor the data. The onboard sensors are summarized in Table 3-2 and schematically illustrated in Figure 3-13. GIS stations 3, 4, 5, and 6 had sensor boxes located at 0.3 m, 0.9 m (crawl-out height), and 1.5 m (walk-out height). GIS sensor stations 1 and 2 in the LBR had only 0.3 and 0.9 m, as shown in Figure 3-14. GIS 7 in the USE only had two sensor boxes at 0.9 and 1.5 m. Previous experiments established that the 1.5 m height gas sensor boxes in the LBR were exposed to excessive heat, causing damage to the boxes, thereby limiting the reuse potential for multiple tests. The USE was found to have relatively homogeneous conditions from previous tests, and therefore, only two sensor boxes were considered necessary at that location, which also allowed boxes to be in reserve should a replacement be necessary. Testing of the sensitivity of the sensor units indicates a potential offset between -0.1% to -4.4%, depending on the sensor type.

Table 3-2: Summary of sensors and range for gas instrumentation stations.

Gas	Type of Sensor	Sensor Name	Range
O_2	Electrochemical	Alphasense O2-A1	0 – 20.95%
CO_2	Metal Oxide	Figaro TGS 4161	350 – 10,000 ppm
CO	Electrochemical	Figaro TGS 5042	0 – 10,000 ppm
NO_2	Electrochemical	Alphasense NO2-AE	0 – >1000 ppm
NO	Electrochemical	Alphasense NO-AE	0 – 5000 ppm
VOCs	Metal Oxide	Figaro TGS 2620	50 – 5,000 ppm
HCL	Electrochemical	Alphasense HCL-A1	0 – 200 ppm
HCN	Electrochemical	Alphasense HCN-A1	0 – 150 ppm
NH_3	Metal Oxide	Figaro TGS 2444	10 – 300 ppm
CH_4	Metal oxide	Figaro TGS 2612-D00	0 – 12,500 ppm
T & RH	Environmental	Silicon Labs Si7021-A20	0 – 100% RH, -4° – 125°C

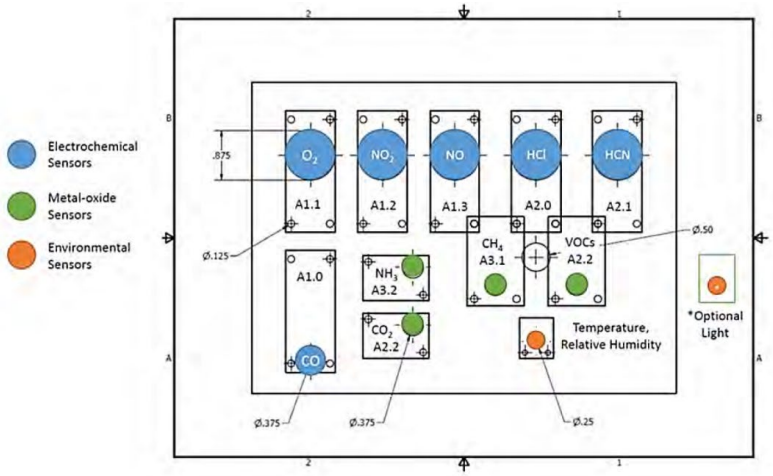


Figure 3-13: Sensor configuration in each gas instrumentation station box.

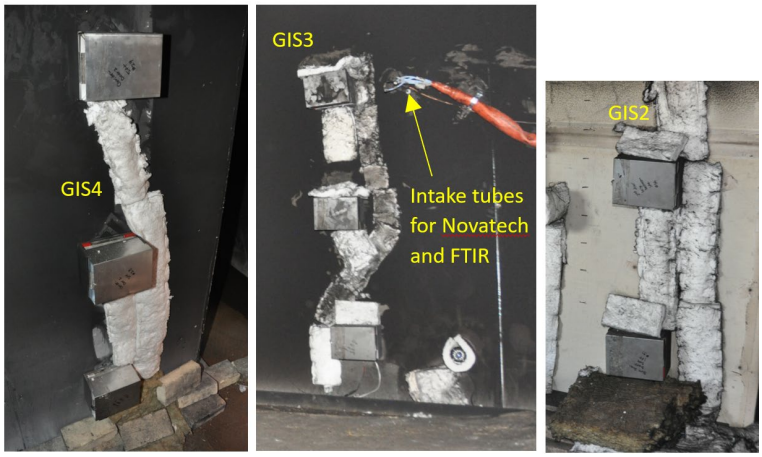


Figure 3-14: Example GIS stations (left GIS4 in LHA, centre GIS3 LSW, right GIS2 in LBR).

Additional complementary sampling was taken from the LSW using:

- a Novatech P-695 gas analysis system, inclusive of Servomex Servopro 4900 paramagnetic and IR analyzers to measure O2, CO, and CO2, a Baseline 8800H to measure Total Hydrocarbons (THC), and a TML-41H chemiluminescence analyzer to measure NO and NO_2.
- a ThermoFisher Scientific Nicolet 6700 Fourier Transform Infrared Spectrometer (FTIR) running OMNIC 8.3 software operating with one sample scan every 9 seconds, with output results for CO_2, CO, HCL, HBR, NO, NO_2, HCN, and graphical results which can be further interpreted for other graphs.

The Novatech intake was initially configured in Tests 1MV, 2MV, and 4MV at 0.3 m in height, but this was subsequently changed in Test 3MV and all FV tests to 1.5 m in height to parallel the location of the FTIR, as shown in Figure 3-14.

3.3.3 Data Acquisition System

The thermocouples, load cells, pressure transducers, heat flux gauges, and the Novatech were all instrumented by a National Instruments Compact FieldPoint data logging system. This allows for shorter lengths of instrumentation cable, limits the potential for interference with analog data cable, and consolidates data collection to simplify the processing of the results. Data is collected at 1.125-second increments (0.89 Hz) and outputs to a comma-separated value (CSV) format, which can readily be investigated with spreadsheet software. Modular backplanes record temperature and analog voltage or current measurements simultaneously and communicate via ethernet cable with a digital switch that transfers back to a laptop computer in the control centre. Raw data is then post-processed to convert the voltage and current output according to the manufacturer's known conversion formulae, which provides output in known references for mass loss, heat flux, gas concentration, and air velocity.

3.4 Mechanical Ventilation

Mechanical airflow is provided in all tests except for Test 1MV, which has no mechanical ventilation. To the extent practical, all penetrations are sealed with polyurethane insulation, mineral wool, or a combination of the two. Leak testing was completed by RDH Building Science, and the information was used to improve the sealing of the house. Before each test, the seals are visually inspected and improved as needed. The baseline ventilation was determined by approximating the minimum flow rates required for houses in Section 9.32. of the 2020 version of the NBCC [17]. This converts to a minimum air exchange of 40 l/s for the house, and it was elected that a balanced supply and exhaust should be used to limit pressurizing or depressurizing the house. Dedicated fans were used to mimic the airflow expected from a heat or energy recovery ventilator, the primary difference being that the fan system used didn't have a heat exchanger that would normally be present in those systems. However, this is considered unnecessary since the majority of the tests are flowing 100% outdoor supply and exhaust. Actual houses may have greater airflows or variations in supply, exhaust, and recirculation depending on heating and cooling methods and occupant preferences.

Accordingly, for the baseline ventilation used in the FV test series, one fan is provided to supply 100% outdoor air, and another is discharged directly to the exterior. Supply is provided to each room at approximately 10 l/s for a total of 40 l/s. Equal exhaust is provided at 20 l/s on each level from the UHA and LHA, respectively, as shown in Figure 3-15. Airflow is provided by two variable speed Continental MBI150/125 centrifugal in-line fans, one in supply feeding fresh air through a 0.127 m (5 in) duct, and one extracting through a 0.127 m (5 in) duct Figure 3-16. The location of the discharge from each supply duct is shown in Figure 3-17.

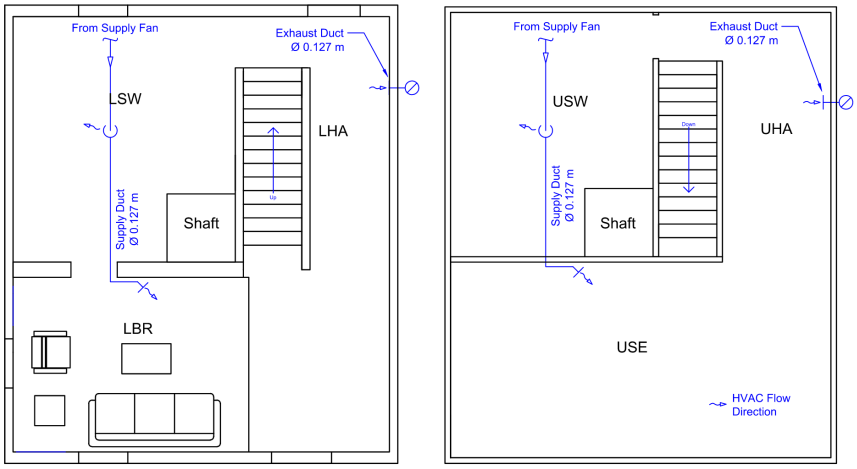


Figure 3-15: Supply and exhaust ventilation locations.



Figure 3-16: Exterior ventilation ducts on north wall exhaust (left) and east wall supply (right).

In the MV series, Test 2MV is the baseline ventilation as described above and is therefore used as a comparison to the FV series, which has the same ventilation configuration. Test 1MV had no ventilation, Test 3MV had approximately double the ventilation supply and exhaust of 2MV, and Test 4MV had 100% recirculation air with no exterior supply air. DiPaola et al. address the differences in the mechanical response in the MV test series [158, 159].

Prior to each test, each supply port was set to have a flow of between 0.011-0.013 m^3/s (port velocity of 0.85 to 1.0 m/s) by measuring with an anemometer and adjusting the damper. Similarly, each exhaust port was set to have 0.043-0.051 m^3/s. This equates to an approximate 0.53 – 0.63 air changes per hour (ACPH) for the house.



Figure 3-17: Supply air locations in yellow circles in USW (top left), LSW (top right), USE (bottom left), LBR (bottom right).

3.5 Smoke Alarms, Detection and Video Camera Visibility

A significant part of this study is predicated on fire detection and video camera smoke visibility. The sections below outline the basis for the smoke alarm positioning and the methodology for interpreting the video output using the checkerboards.

3.5.1 Smoke Detection

In the NBCC, a "smoke detector" is a device that connects to a building alarm system that will then activate the building fire alarm through speakers or bells. Conversely, a "smoke alarm" includes its own sounder, which activates locally when smoke is identified by any one of a possible network of required smoke alarms. According to Subsection 9.10.19. of the NBCC [17], at least one smoke alarm is required to be: on each storey not containing sleeping rooms, in each sleeping room, and in any hallways between sleeping rooms. Smoke alarms are also required to be interconnected, meaning that if any one smoke alarm is activated, all smoke alarms are required to sound. Accordingly, in the test house floor plan, three alarms are required on the upper floor, and only one is required on the lower floor. However, smoke alarms are not addressable devices that record their response time. For this reason, an addressable system is needed to differentiate the response time of detectors in each room, and the need for a sounding function is outside the scope and, therefore, non-essential for the purposes of the test.

Accordingly, the test house includes two commercial-grade fire alarm and detection systems for electronic capturing of the detection time at each location and the study of the sensitivity of the devices

with different technologies. These devices are connected to a fire alarm control panel or computer. The Mircom panel was programmed to generate an audible alarm with sounders outside the test house to identify the alarm activations. The two types of detection systems are installed at ceiling level adjacent to each other at all six locations in the house: 1) addressable spot-type photoelectric smoke/heat detectors (Mircom MIX-4020-ISO) connected to a Mircom FX-2000 fire alarm control panel, and, 2) an air aspirated detection technology known as VESDA (an acronym for Very Early Smoke Detection Apparatus), manufactured by Xtralis. The VESDA-E VEA system draws air samples back to a sensor box through microbore tubing, where the air is sampled for smoke. Devices were programmed to have 7.2% and 8% optical density per meter for the Mircom and VESDA systems, respectively. Figure 3-18 provides a photographic image of the detectors as installed prior to a test.



Figure 3-18: (left) LBR showing location of smoke detection, (right) typical spot and air aspirating tube devices used in tests.

The Mircom panel has addressable devices that allow for identification and recording of each device's activation time. Since the detection was local, the timing aligns with the near-immediate recording of the device response on the control panel. The VESDA system has two sensors with three zones connected to each sensor (clustered with 3 microbore tubes on the upper level and 3 on the lower level of the house, respectively). In the case of the VESDA system, the detection occurs at the sensor box located outside of the control area, and the air aspirating tubes pull smoke from the house back to the sensor box. The two systems installed in the control area are shown in Figure 3-19. Each VESDA tube was approximately 33 m long, which is likely longer than would be required in most houses were such a system to be installed in a house. Smoke travel times were generally on the order of 40 seconds and are documented for each of the six smoke sensor intakes as part of the startup procedure for each test. The data output provided for the VESDA system will not be adjusted for the smoke travel time, but this may be a consideration if shorter microbore tube lengths were used.

In the test house, smoke detectors are provided in each room, as shown in Figure 3-20. Smoke detectors D4, D5 and D6 are provided on the upper level, with D5 being in the UHA, 4 in the USE and D6 in the

USW. This aligns with the requirements of the NBCC. Three detectors are also provided on the lower level in a similar arrangement, with D1 in the LBR, D2 in the LHA, and D3 in the LSW room. Assuming no sleeping rooms are present on the lower level, then only one of these three detectors is required by the NBCC, and the location is non-specific, meaning the detector is permitted to be located in any room on this level. This will be considered later when interpreting the findings as a detector located in proximity to the fire is expected to respond more quickly, but understanding a range of detector responses will allow for a range of escape time considerations. Therefore, the test program has the advantage of further investigating time influences on non-sleeping floors and the corresponding impact on escape time from a fire.

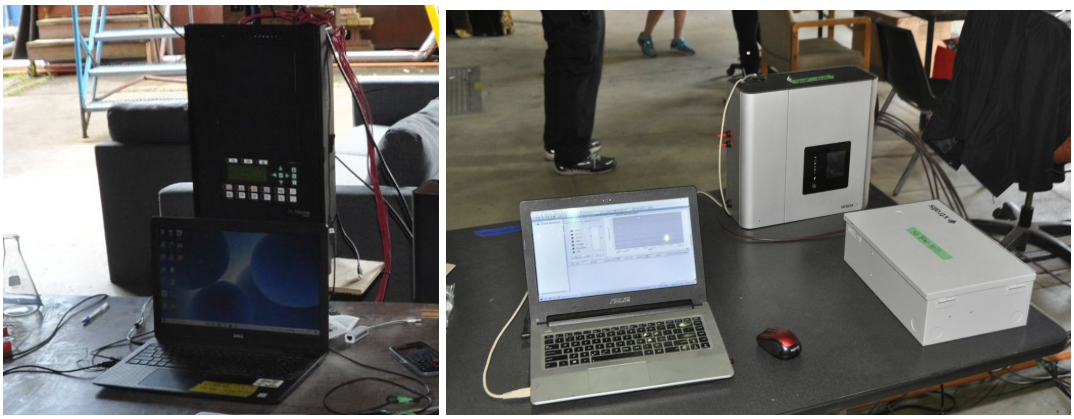


Figure 3-19: (left) Mircom panel connected to dedicated computer, (right) Xtralis VESDA sensors and dedicated computer.

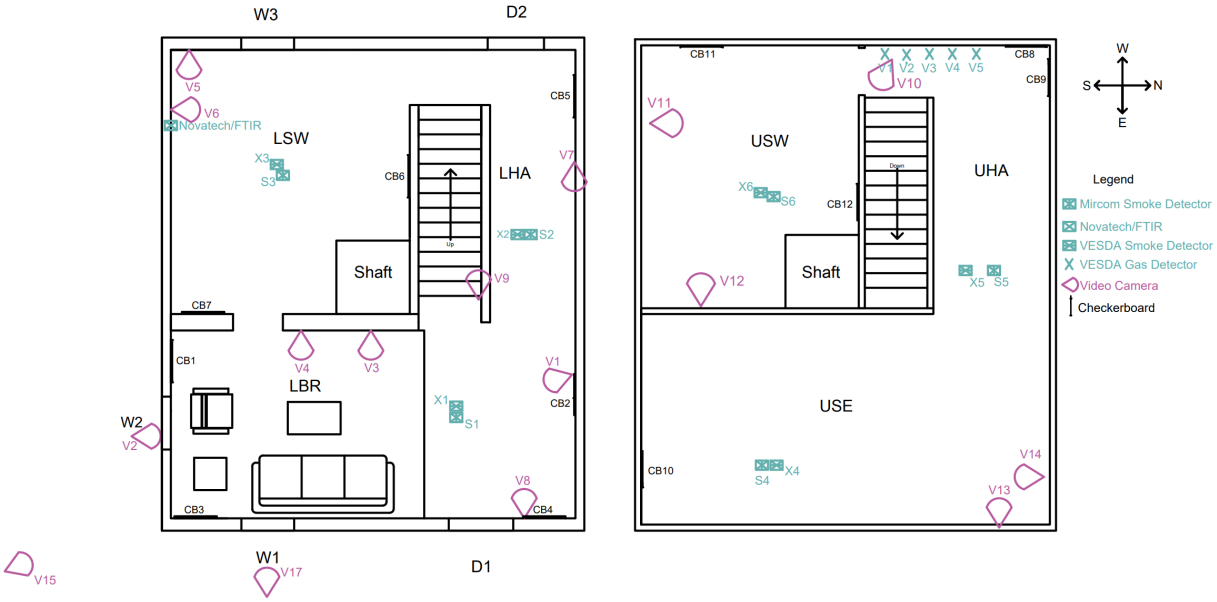


Figure 3-20: Video camera and smoke detection locations in the test house.

Many residential smoke alarms use photoelectric detection technology, and the dual Mircom photoelectric/heat detectors used in this study are expected to provide a comparable response to

photoelectric devices that would typically be expected in single-family homes. Past literature has significantly compared ionization and photoelectric detectors. This work compares photoelectric detection with air aspirated detection, which is seldom used in residential applications, and therefore supplements the existing literature. Comparing detector responses between technologies also allows for cross-validation.

Prior to each test, each smoke detection device was tested using a smoke pen to verify functionality and the delay time of the air aspirated system. The Mircom alarm panel and VESDA computer were reset, and clocks synchronized immediately prior to each test. After each test, the alarm wiring and tubes, in the case of the air aspirated system, were replaced where damaged. Generally, this included all of the devices on the lower level after a full burn of any couch and segments. For purposes of this study, D1, D2, and D3 are of greatest significance. Automatic sprinkler protection is not required by the NBCC in single-family homes and is outside the scope of the study.

3.5.2 Video Cameras and Light Panels (Checkerboards)

Video output is an essential part of this investigation in order to capture the smoke layer conditions from different perspectives. From previous tests, this has proven to be very effective at monitoring the interior conditions. Video cameras are positioned throughout the house and located within 1 m of the floor. The test timeline is synced through the DVR, which is aligned with the master time for the test program, as determined by the official time of Canada on the National Research Council clock[2]. The synchronization of clocks is a key aspect of the testing, and all time data is considered to be captured within a maximum clock differential of ± 1 second.

Video output is captured using two QSee high-definition analog video recorders (DVR). Seventeen Lorex CVC7572-780p hybrid colour-night vision cameras are positioned at strategic locations within and around the perimeter of the test house, as shown in Figure 3-20. An eighteenth camera monitored local environmental conditions by recording the graphical output from a La Crosse Technology S81120-INT wireless combo weather station. The weather station was positioned on top of a recycled sea container, used for other fire testing at the lab, and located immediately south of the test house. It was sufficiently separated to limit any proximity impact associated with the test house.

[2] https://nrc.canada.ca/en/web-clock/ (last accessed October 1, 2023)

Chapter 4
Experimental Test Framework & Procedure

This Chapter describes the experimental test framework and procedure, including how the environment will be analyzed. Then, the furniture arrays that will be used are defined, and finally, the test procedure that will be applied using different ignition sources is outlined.

4.1 Video Smoke Layer Descent and Visibility Tenability Criteria

Previous experiments found that analysis of the video traces is simplified by creating quadrant-based consolidated videos (herein referred to as quad videos) of pertinent regions within the test house. The videos are first created into 3 primary quads: one for the burn area and the lower hallway leading to the burn area, another for the lower level excluding the burn area, and a third for the upper level. This allows visualization of the smoke layer progression using the video and a series of light panels. The light boards, referred to as checkerboards and abbreviated as CB#, are a novel method of readily differentiating the smoke layer developed in the Fire Research Laboratory and are currently under further study by Ellingham [160]. The checkerboards consist of a series of 305 mm black and white alternating squares painted onto gypsum board, mounted vertically from the floor and positioned as shown in Figure 3-20.

Video images are captured at 30 frames per second (fps) and abbreviated as CAM# or C#. The quad videos are first compiled and synchronized by frame to the time of ignition, as determined by the frame showing the first ignition. The quad videos are then overlayed with a test number and timer in the bottom right corner. Four perspectives are merged into one video file for the:

- Burn room (LBR and LHA) using cameras CAMS 1, 2, 4 and 7 (Figure 4-1);
- Lower level (LSW and LHA) using CAMS 5-8 (Figure 4-2); and
- Upper level (USE, UHA and USW) using CAMS 11-14 (Figure 4-3).

These figures are intended to orient the reader, as they will be used to break down smoke layer development in later sections. Overlayed on the above-referenced figures in yellow are checkerboard numbers, room information, and wall references (the test number and timer are part of the captured video image).

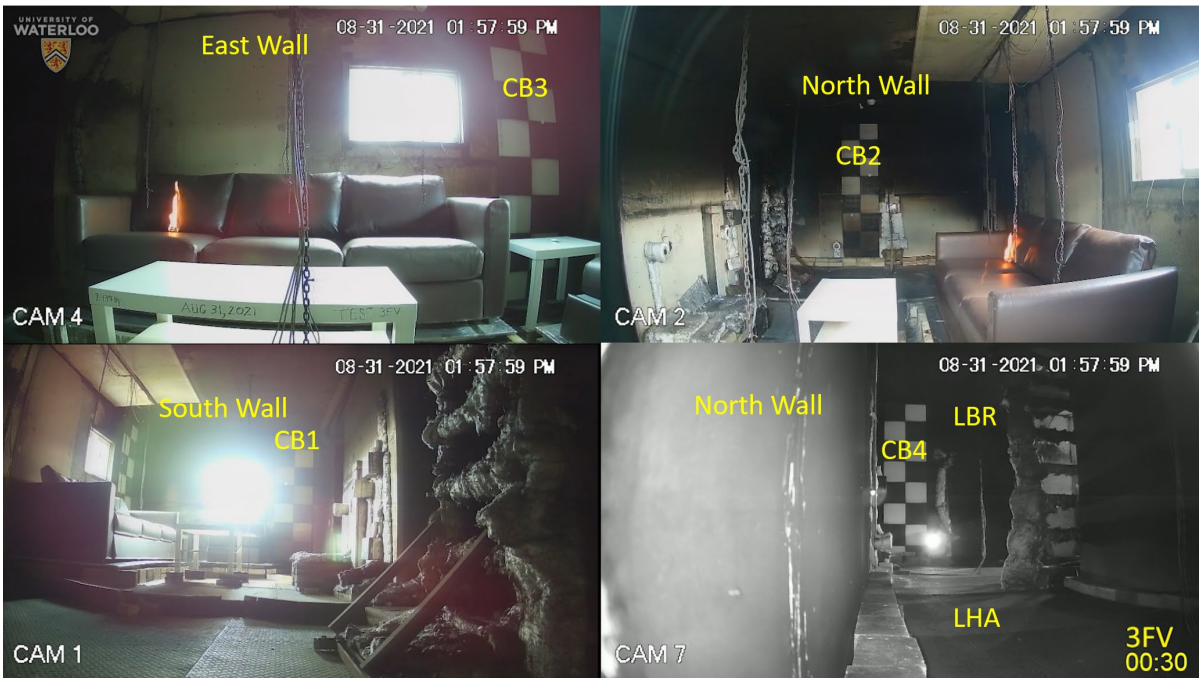


Figure 4-1: Quad video capture of LBR and LHA.

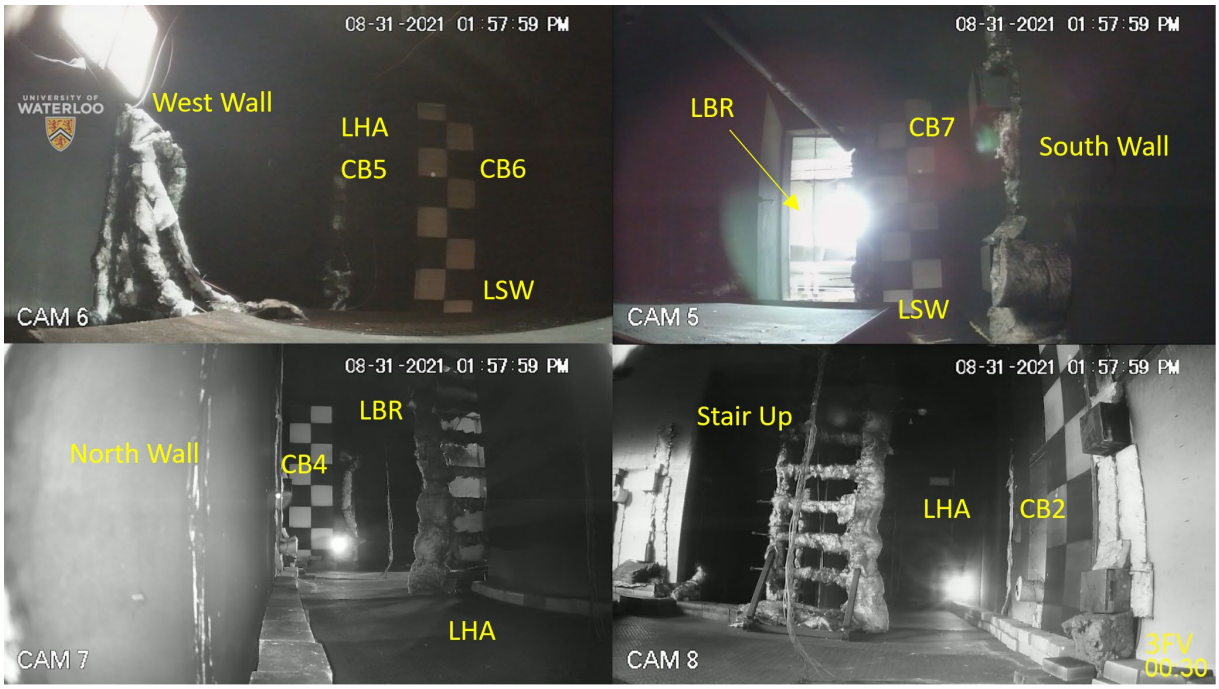


Figure 4-2: Quad video capture of the lower level, excluding the burn area in LBR.

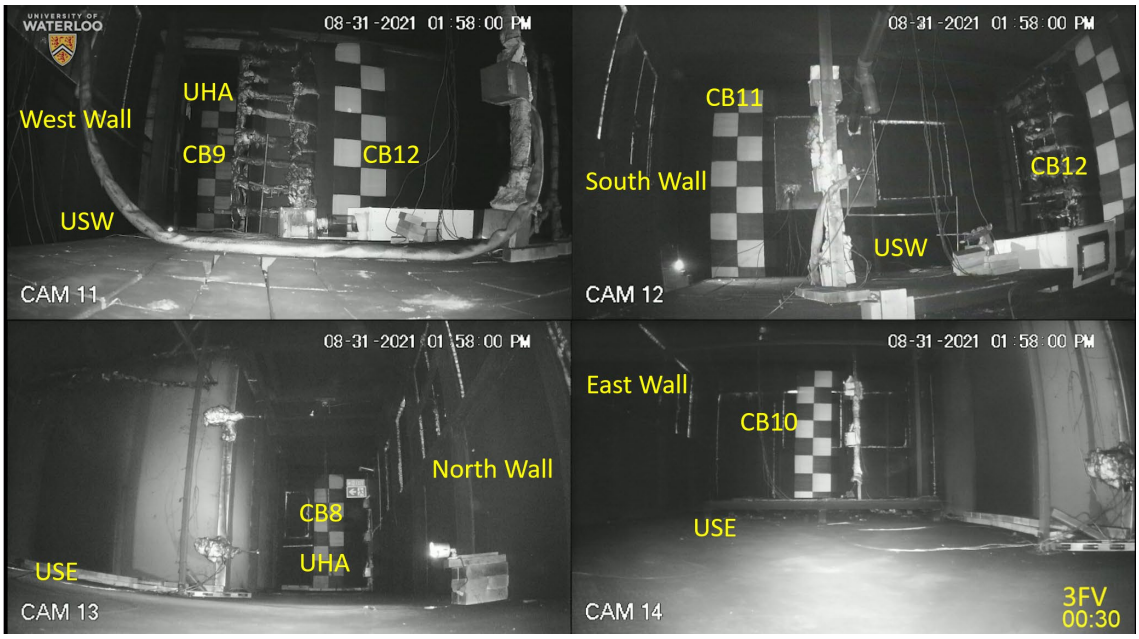


Figure 4-3: Quad video capture of the upper level.

To establish visibility and smoke layer descent within different building areas, the burn room quad video compares the LBR and LHA spaces. Unfortunately, the west end of the LHA was not well captured by CAM 8 (which was looking down the hall from the burn room). Once D2 was closed after initiating the fire, the contrast in lighting between the LSW and the west end of the LHA left the hallway too dark for interpretation, with the day/night cameras adjusting for lighting in the different spaces. Similarly, cameras in the LSW room facing towards the LHA and D2 had limited visual potential due to contrasting lighting and simultaneous fire effects within LSW, obscuring direct visual access to the LHA.

Since the LHA ceiling is flush with the burn room and no door/vent opening thresholds restrict the movement of smoke between the rooms, the combined burn room quad video provides a good reference to estimate smoke conditions developing within the two areas of the house (LHA and LBR). Therefore, the burn room quad video is used to estimate the time to 1) smoke layer development, 2) smoke layer descent to 1500 mm above the floor, 3) smoke layer descent to 900 mm above the floor, and 4) loss of all camera visibility on the quad video, except for the fire. This combination represents the time window and steps where an occupant is increasingly likely to be impeded in escaping the house due to smoke obscuring the path of travel towards a main door.

The primary visual points that are used to determine these milestones are shown in Figure 4-4. The early smoke layer development is considered to have occurred when smoke started to obscure the checkerboard at the southwest corner of the LSE, as marked in the CAM1 image in the figure. There are then smoke layer fluctuations since the interface height between the upper and lower layers is not always uniform and also depends on the camera perspective. The smoke layer descent is therefore approximated

by evaluating the progression of the smoke in the images from CAM 2 and CAM 7 simultaneously to establish when each of the marked heights is reached, as illustrated in Figure 4-5 for the smoke descending to the level 1500 mm above the finished floor (AFF). In this example, the bottom of the smoke layer appears higher on the fire side of the room (CAM 2) and lower on the opposite wall (CAM 7, illustrated by the position of the smoke layer in CAM 7 appearing higher than that in CAM 2).



Figure 4-4: Visual data points for interpretation of smoke layer descent in burn room 2MV.

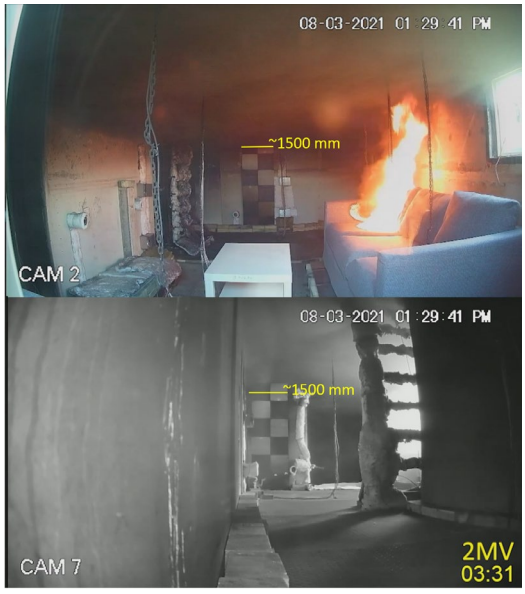


Figure 4-5: Example of smoke layer descent reaching 1500 mm above the floor in test 2MV.

Due to the camera perspectives, interpretation is required to determine when the smoke layer has descended to a given height. The use of the two checkerboards is found to be sufficiently consistent in

evaluating the smoke reaching the 1500 mm height. The same methodology is applied to the descent to 900 mm above the floor; however, as will be outlined later, the smoke often does not reach this position due to the premature collapse of the smoke layer interface. In most instances, the smoke layer interface starts to collapse just as the smoke descends past the 1500 mm line, a height that corresponds to when the smoke layer started to encroach in the flaming region of the fire.

Example images of different representative modes of camera obscuration due to the smoke layer are illustrated in Figure 4-6. At this time interval, CAM 1 has just become fully obscured, CAM 2 has been obscured for a period of time, and the image is now a reflection of the inside of the camera, and CAM 7 has previously become obscured and remains so. In the image from CAM 4, all of the objects to the right of the image are fully obscured, with only the flaming region of the fire remaining in the image. At these stages of the fire, visibility is assumed to be lost in these areas of the house.



Figure 4-6: Illustration of lost visibility in CAMs 1, 2 and 7 in Test 2MV with only flaming showing in CAM 4.

The upper level of the house, which is not finished and is not lit during the tests[3], has a series of checkerboards that can be used as reference points to follow smoke evolution in that part of the structure as illustrated in Figure 4-7. The key milestones that mark the descent of the smoke layer in the upper level are: 1) Smoke at the top of the stair shaft, 2) Smoke layer descent to 1500 mm in the UHA [with a focus on CAM 13], 3) Collapse or fully mixed smoke layer throughout the upper level, and 4) loss of visibility on all cameras in the upper level.

[3] Note that the cameras on the upper level all operate on night mode for the duration of the tests since no exterior windows or lighting are provided on the upper level. Since the test program is comparative in nature and the condition is the same between tests, the operation of cameras in night mode is considered sufficient for purposes of the investigation.

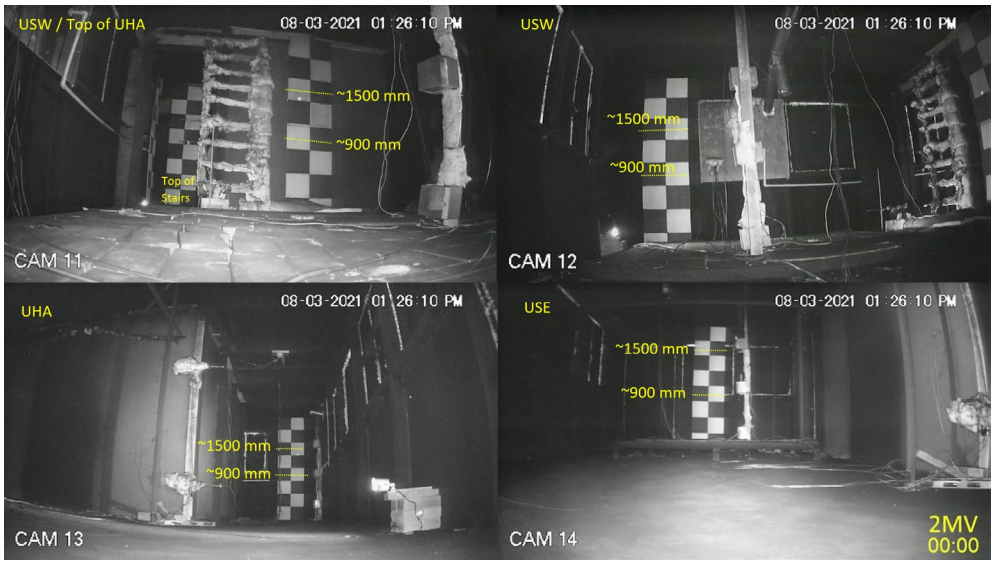


Figure 4-7: Upper level camera perspectives to estimate smoke development.

4.2 Correlating the Developing Smoke Environment to MLR, Temperature, Asphyxiant Gas and Oxygen Depletion

The smoke layer descent can be evaluated against the onset of asphyxiant gases, temperature, and oxygen depletion that may influence the escape environment in each test. It is appropriate to verify that the assumption of using visibility as the escape window corresponds to a thermal and respiratory environment where escape would be possible. Consequently, using the Purser and McAllister (the PA Criteria) recommended thresholds discussed in Section 2.2.2, the following data will be consolidated for further analysis:

1. Mass Loss Rate (MLR). The MLR, as measured on the load cells, will be graphed against time to capture the stages of fire growth using a 10-point forward-moving average in units of kg/s (roughly a 10 s average). This was done to reduce the oscillating variability (i.e., noise) from the sensors and is sufficient without compromising the results, given the time period of interest is measured over many minutes and not seconds. The MLR data can obtain a high-level estimate of the incipient fire duration for each test by defining a transition period from the incipient fire stage (immediately after ignition) to the fire growth stage. The incipient stage can be estimated by interpreting oscillations on the MLR curve where cycling occurs between 0 kg/s and a threshold mass loss value (which will be explained in Section 5.3). The transition to the fire growth stage is observed when the MLR jumps and no longer descends to 0 kg/s. The progression of the growth stage continues to the peak MLR, marking the transition to the ventilation-limited burning stage, where the MLR then decays. This data can be used to estimate the transition from the incipient stage of the fire to the growth stage, the duration of the stages, and the peak MLR, which will assist in differentiating the burning

behaviour of each fuel type. The stages are graphically illustrated in Figure 4-8. Unlike fire curves in well-ventilated environments, flashover is not expected to occur, and there is no stage of full-room involvement followed by a natural (well-ventilated) decay stage.

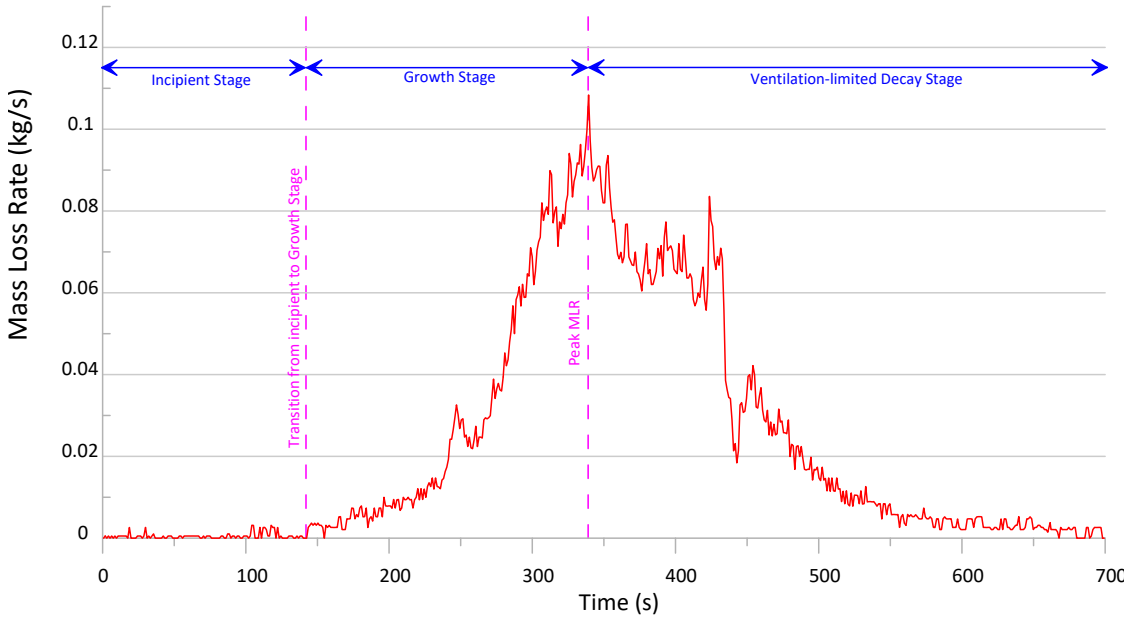


Figure 4-8: Illustration of MLR data showing stages of fire growth.

2. Smoke Detector Activation Times. Differences in the detector response times will be used to establish the range of escape times. The focus will be on the response at D1, representing the detector closest to the fire and, therefore, potentially providing the highest available escape times compared with the response of D3, which is more remote from the fire origin and is therefore expected to take longer to respond and provide the shortest escape time. This represents a reasonable range of potential detector placements and correspondingly allows for evaluation of detector location relative to different fire development conditions and influence on escape time for each furniture type.

3. Temperature along the egress path. Temperatures recorded at the thermocouple rakes along the escape path are presented to consider the exposure of occupants that may evacuate along the UHA, down the stairs through the burn room, and along the LHA to the exterior, as defined in Section 3.3. A 200°C smoke layer above an occupant corresponding to radiant heat skin exposure and a maximum respiratory temperature of 60°C is considered based on the PA Criteria. Specifically, the following thermocouples rakes are considered in the analysis:

    - T8 in the UHA as occupants in the bedroom need to move through this space to reach the top of the stair,

- T5 in the LBR as occupants pass this position after descending the stair, and
- T6 in the LHA as occupants move away from the fire to escape through D2.

The thermocouple locations on the rakes do not align perfectly with the 0.9 and 1.5 m target heights and GIS heights at all locations. Measured temperatures in the UHA and the LHA from positions at approximately 700 mm (0.7 m) and 1300 mm (1.3 m) above the floor are used for comparative analysis and evaluation of conditions at the crawl and walk heights, respectively.

4. Seven Gas Instrument Stations (GIS) are set up throughout the house as outlined in Section 3.3.2. The metal oxide and electrochemical type sensors allow for a cost-effective way of including gas detection equipment throughout the burn house at pertinent heights to account for walk-out (1.5 m) and crawl-out (0.9 m/smoke layer collapse) methods of escaping from a house fire. They also include a number of low-level sensors to capture the conditions nearer to the floor level (0.3 m), which may be considered a low point for respiratory air. These sensors are supplemented with Novatech and FTIR systems located in the LSW on the south wall at 1.5 m above the floor, which is proximal to GIS3 and positioned at 1.5 m off the floor to allow for comparison. This provides different gas sensing technologies with which to verify underlying trends in gas concentrations, which aligns with the level of understanding sought in this experimental research. Determination of precision of the measurements is an ongoing initiative at UWFRL but is not necessary here, where the aim is to obtain a comparative understanding of the differences in gas species distribution between tests. Peak incapacitation thresholds considered are 150 ppm for HCN, 6000 ppm for CO, and a depleted oxygen level of 13%, representing the lower bound of exposure for a 5 min incapacitation per the PA Criteria. Since smoke is expected to be the leading indicator, it is not anticipated that these conditions will be reached during the escape time window in the egress path, but this can be verified or otherwise further reviewed relative to degrading conditions by plotting the data against the smoke layer descent conditions. Although there are gas detectors throughout the house, the focus will be on GIS 1, 4 and 5, which represent the LBR, the LHA and the UHA, respectively, and correspond to the location of the egress path defined in Section 3.3. Further, the sensors at 1.5 m and 0.9 m are used to align with the smoke layer descent criteria, except for respiratory air in the LHA, where the 0.3 m sensors will be used as a lower crawl-out breathing level.

When combined, the results will substantially supplement the video observations and characterize the developing fire conditions for each test in a manner that can be graphically presented.

4.3 Test Fuel – Furniture Selection and Flame Retardancy

The selection of furniture is predicated on obtaining a variety of material types tested to different standards, with the intention of reviewing the differences between material types and testing regimes relative to incipient fire development, smoke detector activation in different rooms, the fire growth rate and smoke filling within the house. Couches are selected for differences in material and general overall dimensions for consistency between couches to the greatest extent practical. Unlike the 2015 UWFRL tests, where materials were purchased and custom-manufactured [153], all comparative couches are purchased from Ikea Canada, representing North American (NA) furniture tested to TB 117 [105]; Ikea UK for furniture tested according to BS 5852 [103]; and from a commercial supplier of furniture from the US that had used stock of furniture tested according to TB 133 (which was a best-fit for purposes of having a third set of materials tested to a different standard) [108].

Much of the investigation relates to fire environments that become ventilation-limited, and therefore, testing also included two baseline tests, a wood crib fire distributed to represent a similar length and weight of one of the couches, and a heptane fire, which represents a rapidly developing fire event. Table 4-1 shows the wood crib and heptane ignition sources positioned on the couch load cells for Tests 1FV and 2FV, respectively.

Since the furniture was purchased blind, meaning that no furniture control particulars were specified for Ikea Canada or Ikea UK, it was not known what flame retardant or barrier-type controls might be present. Given the difference in standards between the US and the UK, the Canadian-purchased furniture was not expected to include a significant FR component, whereas the UK-purchased furniture was. The US couches were specifically purchased for compliance with TB 133 and, therefore, were expected to have FR materials.

In total, there are 10 tests as part of the FV test series. There are two reference tests, 1FV (wood crib, 2FV (heptane), summarized above. There are three Ikea “Comparables” tests: Test 2MV (US Cloth) compares with Test 5FV (UK Cloth), both shown in Table 4-2; Tests 3FV and 6FV compare the US and UK faux leather couches, shown in Table 4-3; and lastly, tests 4FV and 7FV compare two leather couches, which are summarized in Table 4-4. Tests 8FV (US FR Leather) and 9FV (US FR – suede) are summarized in Table 4-5. Each of the tables summarizes the construction of the couches. All of the UK couches have labels to indicate compliance with BS 5852 [103], in accordance with the British Regulations [104], but are not explicit with respect to any flame retardant chemicals or strategies that may have been used.

Table 4-1: Fuel array for wood crib and liquid fuel tests.

Test 1FV	Test 2FV
Wood Crib	**Heptane pan fire**
	
Wood crib positioned along the length of the furniture weigh scales to allow for lateral fire extension. 6 sticks per row with 6, 3 and 3 rows from left to right respectively. Constructed with nominal 2 x 2 inch spruce lumber, cut 24 inches (0.61 m) in length. The cribs are placed to the approximate location of the three cushions on the couch.	5 litres of heptane equally distributed between trays measuring 0.38 x 0.27 m, and positioned to approximate the first cushion of the couch, first tray is 300 mm from east wall and 2.65 m from south wall. The fuel is ignited in the front left tray using the spark from a handheld torch.

The UK Cloth couch for Test 5FV incorporates a Schedule 3 interliner, which is required by British Regulations [104] where the fabric cover does not meet the match test required in BS 5852 [103]. This contains at least 75% by weight of cotton, flax, viscose, modal, silk and wool (whether used separately or together). The interliner is located between the fabric and the cushioning on both the seat cushion, protecting the polyurethane foam slab and the back cushion, which protects the polyester fill. The interliner consists of an FR cotton and polyester exterior with a Levapren backing. Levapren is a trade name for a proprietary copolymerization of ethylene and vinyl acetate and is considered to be a halogen-free and non-corrosive flame retardant[4]. Therefore, this is presumed to be an FR liner and, as shown in Table 4-2, wraps around the polyurethane in its entirety, forming a barrier for the polyurethane foam. All of the polyurethane foam slabs had a polyester wrap around the foam. This was identified in the 2015 tests, which showed that working with the furniture manufacturer, the use of polyester wrap is a standard practice to improve comfort and function. From there, an additional liner can or may not be provided, depending on the construction of the couch. The leather couches did not have an additional liner, whereas the cloth and faux leather couches did. The observed difference in liners is suggestive of both the cloth and the faux leather couches having FR liners, which have the potential to act as barriers to limit the participation of the polyurethane foam. The liner has the potential benefit of slowing the rate of exposure of the PU foam slab or the polyester-filled cushions and, by extension, slowing the mass loss rate and corresponding heat release, which, in turn, has the potential to slow the generation of smoke and toxic gases and reduce the depletion rate of oxygen.

[4] https://www.arlanxeo.com/en/brands/levapren, accessed July 3, 2022

Table 4-2: Cloth furniture comparison of Test couches 2MV and 5FV.

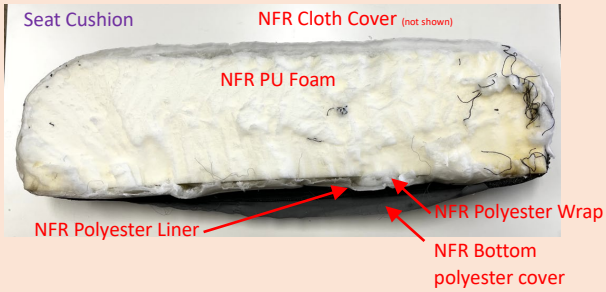
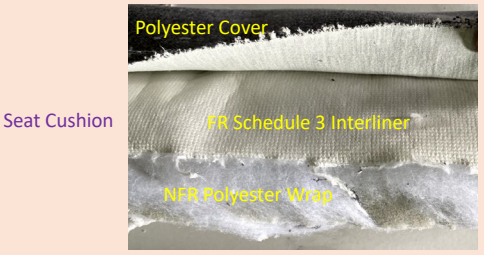
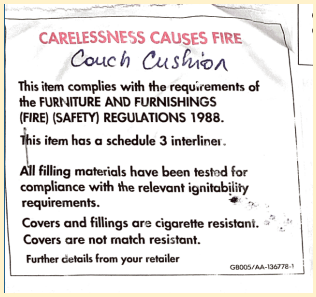
Test 2MV	Test 5FV
Cloth Couch and Armchair **Ikea Canada – Vimle 3 seat couch and armchair Gunnared medium grey**	**Cloth Couch and Armchair** **Ikea UK – Vimle 3 seat couch and armchair – Gunnared medium grey**
	
Seat cushion – NFR polyurethane foam with NFR polyester top cover and a NFR polyester wrap and liner with a polyester bottom cover. **Back cushion** – NFR polyester fill with NFR polyester liner and NFR polyester cover.	**Seat cushion** – FR Polyurethane foam slab with NFR FR polyester wrap, FR Schedule 3 Interliner and FR Cloth cover with NFR polyester bottom cover. **Back cushion** – NFR Polyester fill with FR polyester cloth cover and FR Schedule 3 Interliner
	
	 
Labels: reference compliance with test standard: TB 177 – 2013 with no added flame retardants.	**Labels:** reference compliance with: UK Furniture and Furnishings Regulations 1988 (i.e., BS 5852) **with** a schedule 3 interliner. Covers and fillings are cigarette-resistant, covers are not match resistant.
	

Table 4-3: Faux leather furniture comparison of Test couches 3FV and 6FV.

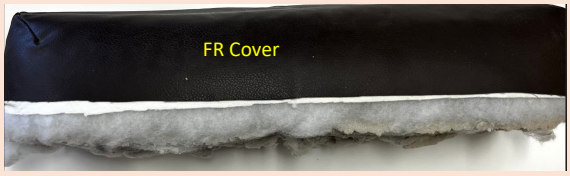
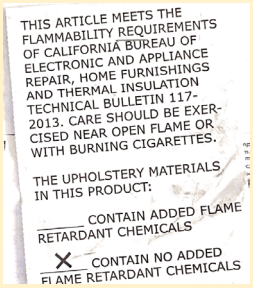
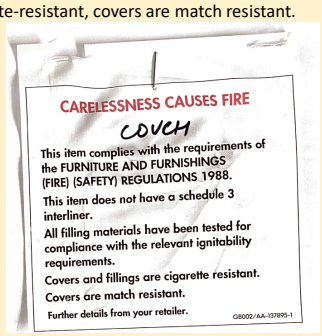
Test 3FV	Test 6FV
Faux-leather Couch and Armchair **Ikea Canada – Vimle 3 seat couch and armchair – Farsta Dark Brown**	**Faux-leather Couch and Armchair** **Ikea UK - Vimle 3 seat couch and armchair – Farsta Dark Brown**
	
Seat cushion – NFR polyurethane foam slab with NFR polyester wrap and NFR polyester liner, and Lycra/polyester primary cover and NFR polyester bottom cover. **Back cushion** – NFR polyester filled with polyester wrap and NFR Lycra/polyester cover. Seat Cushion  Back Cushion 	**Seat cushion** – FR polyurethane foam slab with NFR polyester wrap, an FR Rayon fiber/acetate interliner, and FR Bayhydrol UH 340/polyester primary cover and NFR polyester bottom cover. **Back cushion** – NFR polyester fill with FR Cotton Polyester liner and FR Bayhydrol UH 340/polyester primary cover and NFR polyester back cover. Seat Cushion  Back Cushion 
Labeling references compliance with test standard: TB 177 – 2013 with no added flame retardants. 	Labeling references compliance with: UK Furniture and Furnishings Regulations 1988 (i.e., BS 5852) with **no** schedule 3 interliner. Covers and fillings are cigarette-resistant, covers are match resistant. 

Table 4-4: Leather furniture comparison of Test couches 4FV and 7FV

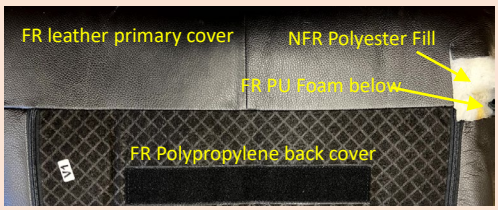
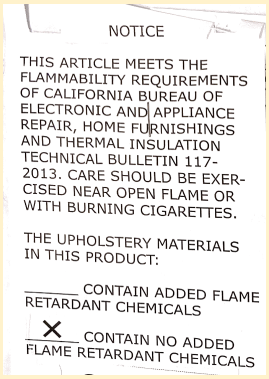
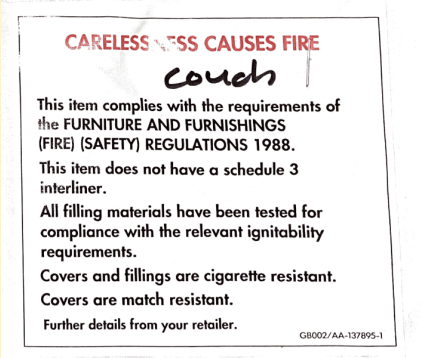
Test 4FV	Test 7FV
Leather Couch and Armchair **Ikea Canada – Landskrona Grann Bomstad Black**	**Leather Couch and Armchair** **Ikea UK – Landskrona Grann Bomstad Black**
	
Seat cushion – NFR polyurethane foam slab wrapped with an NFR polyester liner, an NFR leather primary cover (through dyed grain leather from cattle, with a treated, embossed and pigmented surface). **Back cushion** – NFR polyurethane foam with an NFR polyester liner and a NFR synthetic leather cover. 	**Seat cushion** – FR polyurethane foam slab with NFR polyester wrap, and NFR leather primary cover (Through dyed grain leather from cattle, with a treated, embossed and pigmented surface), and a NFR polypropylene bottom cover. **Back cushion** – FR polyurethane foam wrapped with an NFR polyester polyester cover and an FR synthetic leather. 
Labeling references compliance with test standard: TB 177 – 2013 with no added flame retardants. 	Labeling references compliance with: UK Furniture and Furnishings Regulations 1988 (i.e., BS 5852) with **no** schedule 3 interliner. Covers and fillings are cigarette-resistant, covers are match resistant. 

Table 4-5: Furniture comparison of Test couches 8FV and 9FV meeting CA TB 133 standard.

Test 8FV	Test 9FV
US Sectional Cloth Couch and Armchair **Cort Funiture - Swoop Chairs w/Fire Barrier**	**US Synthetic Leather Couch and Armchair** **Cort Furniture - Unknown manufacturer**
	
Materials tests – NFR polyurethane foam with FR acrylic fiber and FR polyester, and FR cotton/polyester. 	**Seat cushion** – FR polyurethane foam with NFR polyester polyester wrap and an FR polysiloxane/wool/cotton/acrylic/nylon cover. **Back cushion** –NFR polyester fill with FR polypropylene liner and FR Polysiloxane/Wool cover. 
No label referencing compliance with a test standard This furniture was purchased for compliance with TB133 and was only available used.	No label referencing compliance with a test standard. This furniture was purchased for compliance with TB133 and was only available used.

The couch in test 8FV is substantially different than the other couches. This commercial-grade couch is targeted at applications outside of the residence and only has a thin polyurethane slab in the seat cushion. Therefore, although included in the test plan, it is noted that it is likely to perform differently by design than the other couches, given the comparative reduction of materials.

Further, flame retardancy of the couches was verified to confirm that the Ikea Canada couches do not have flame retardants as indicated on the labels, and that the Ikea UK and US couches do have flame retardants, as expected given their origin. Table 4-6 illustrates samples sent for third-party testing using FTIR methods. Only the test number was provided to the lab; therefore, the results are independent of knowing which materials are suspected to have flame retardants. The results are provided in Table 4-7, which largely affirms that the US and UK couches include flame retardants and the Canadian-purchased couches from Ikea do not. For example, the UK couch used in Test 5V matches those purchased from the same manufacturer in Canada, making the couches in Tests 2MV and 5FV directly comparable. For these, the base material of the cover fabric and foam are the same (polyester and polyurethane), but evidence of flame retardants is present in the UK couch (Test 5FV) with phosphorous, chloride, antimony and aluminum in specific fabric materials and phosphorous, chloride, tris-phosphate, melamine and tin in the polyurethane foam. The specifics of flame retardant treatments are much more complex than as simplified

here, but these details are outside the focus of this thesis. For purposes of this testing, the couches are simply differentiated as FR or NFR, which simply means that, where designated as FR, all or most of the primary elements have been treated in manufacture or subsequent coating with flame retardants. The intended purpose of the FR additives is to reduce the propensity of the couch to ignite when exposed to smaller ignition sources up to the size presented in the test. This is accomplished by the exterior fabric resisting the flaming ignition source and "opening up," thereby exposing the foam slab or polyester cushion fille. Where it opens up and exposes the foam, the flame retardants further resist the participation of the foam in accelerating the growth. It should also be noted that other minor elements of these couches have not necessarily been treated with FR, even when the final couch is listed as an FR couch.

Further, it is noted that the liner for the faux leather couch used in Test 6FV was confirmed to be an FR liner, even though it is not designated as such on the labels. However, the materials used between the liners (5FV and 6FV) differ according to the FTIR testing.

As illustrated in Figure 4-10, the couch is positioned approximately 150 mm from the east wall and 1250 mm from the south wall. The chair is 250 mm from the south wall and 1500 mm from the east wall. In addition to the couches and corresponding chairs, an Ikea "LACK" coffee table (0.90 x 0.55 x 0.45 m) and "LACK" side table (0.44 x 0.44 x 0.45 m), weighing 8.5 kg and 3.5 kg respectively, as shown in Figure 4-9, are incorporated into each test. The coffee table is positioned approximately 350 mm from the front of the couch and 2000 mm from the south wall, and the end table is 200 mm from the side of the couch and 400 mm from the side of the chair.



Figure 4-9: Ikea LACK coffee table (left) and end table (right).

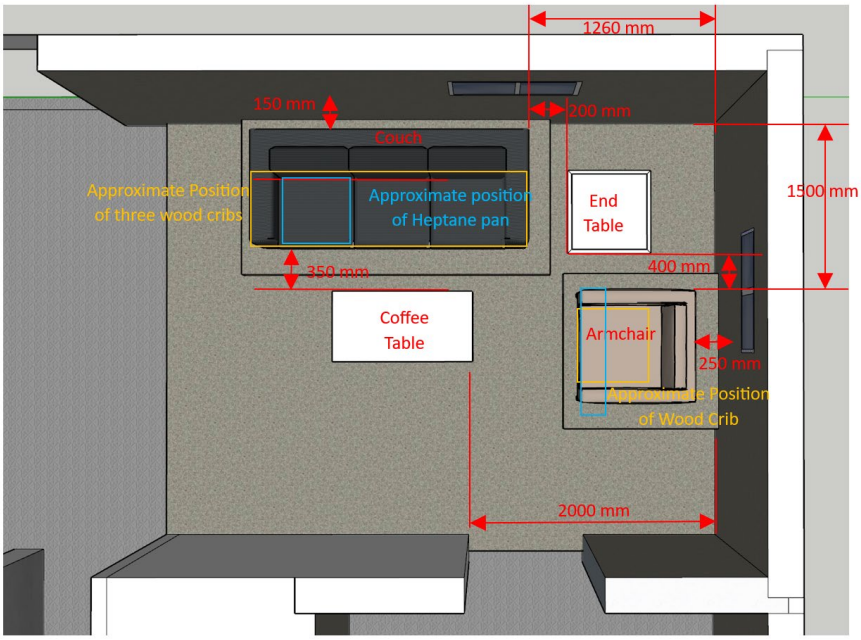


Figure 4-10: Illustration of furniture configuration in the burn area of the LBR.

Table 4-6: Summary of test samples sent for FTIR testing at 3rd party lab.

Test Number	Seat Cushion	Back Cushion	Total Samples
3FV	1. Piece of faux leather cover and the bottom fabric of the cover 2. Inner Cushion liner fabric 3. Cushion Stuffing	1. Piece of faux leather cover and the bottom fabric of the cover 5. Inner Cushion liner fabric 6. Cushion Stuffing	6
4FV	1. Piece of leather cover 2. First layer of stuffing piece 3. Second layer of Stuffing piece	4. Piece of leather cover 5. First layer of stuffing piece 6. Second layer of Stuffing piece	6
5FV	1. Piece of cloth cover 2. bottom fabric of the cover 3. Inner Cushion liner fabric 4. First layer of cushion stuffing 5. Second layer of Cushion Stuffing	6. Piece of cloth cover 7. Inner Cushion liner fabric 8. Cushion Stuffing	8
6FV	1. Piece of faux leather cover and the bottom fabric of the cover 2. Inner Cushion liner fabric 3. Cushion Stuffing	1. Piece of cover and the bottom fabric of the cover 2. Inner Cushion liner fabric 3. Cushion Stuffing	6
7FV	1. Piece of leather cover 2. Bottom fabric of the cover 3. First layer of cushion stuffing 4. Second layer of Cushion Stuffing	5. Piece of cover 6. Bottom fabric of the cover 7. First layer of cushion stuffing 8. Second layer of Cushion Stuffing	8
8FV	N/A	1. Piece of lower cover material 2. Piece of upper cloth-like cover material 3. Piece of liner material 4. Piece of seat/back cushion foam	4
9FV	1. Piece of cover 2. First layer of cushion stuffing 3. Second layer of cushion stuffing	4. Piece of cover 5. Piece of liner material 6. Cushion stuffing	6
1MV	1. Piece of cloth cover 2. Bottom fabric of the cover 3. Inner Cushion liner fabric 4. First layer of cushion stuffing 5. Second layer of Cushion Stuffing 6. Discoloured part of second layer of cushion stuffing	7. Piece of cloth cover 8. Inner Cushion liner fabric 9. Cushion Stuffing	9

Table 4-7: FTIR results identifying concentrations of additives frequently associated with flame retardants in furniture, from 3rd party lab.

Test		Sample		FT-IR ID		ppm P	ppm Br	ppm Cl	ppm Sb	wt% Ti	wt%Al	wt%TCPP	wt% Melamine	ppm Sn	wt% Mg	wt% Ti	wt% Fe	wt% Ca	wt% Al	ppm Zn	Comments
2MV	US	2282-72-1 MV 5	2nd layer foam	Polyurethane		<100	nd	nd				-	nd	290							
2MV	US	2282-72-1 MV 6	discolored foam	Polyurethane		<100	nd	200				-	nd	300							
2MV	US	2282-72-1 MV 1	cloth cover	Polyester		<100	nd	<100	180	0.06											
2MV	US	2282-72-1 MV 2	bottom fabric cover	Polyester		<100	nd	nd	130	0.17											
2MV	US	2282-72-1 MV 3	liner	Polyester		<100	nd	nd	210	0.07											
2MV	US	2282-72-1 MV 4	stuffing	Polyester		<100	nd	nd	210	0.13											
2MV	US	2282-72-1 MV 7	cloth cover	Polyester		<100	nd	<100	200	nd											
2MV	US	2282-72-1 MV 8	inner liner	Polyester		<100	nd	nd	210	nd											
2MV	US	2282-72-1 MV 9	stuffing	Polyester		<100	nd	nd	240	0.06											
3FV	US	2282-72-3 FV 2	Inner cushion liner	Polyester		<100	nd	130	210	0.09											
3FV	US	2282-72-3 FV 5	Inner cushion liner	IRISE Polyester		<100	nd	120	210	0.14											
3FV	US	2282-72-3 FV 6	stuffing	Fortrel Polyester		<100	nd	100	230	0.15											
3FV	US	2282-72-3 FV 3	Cushion PU	Polyurethane		<100	nd	110				-	nd	310							
3FV		2282-72-3 FV 1	Faux leather	Lycra (front) Polyester (back)	Fortrel	<100	nd	490							1.7	0.17	0.42	0.16			
3FV		2282-72-3 FV 4	Faux leather	Lycra (front) Polyester (back)	Cotton	<100	nd	450							1.6	0.20	0.45	0.23			
4FV	US	2282-72-4 FV 2	1st layer stuffing	Fortrel Polyester		<100	nd	<100	260	0.13											
4FV	US	2282-72-4 FV 5	1st layer stuffing	Fortrel Polyester		<100	nd	<100	240	0.14											
4FV	US	2282-72-4 FV 3	2nd layer PU	Polyurethane		<100	nd	180				-	7.4	240							
4FV	US	2282-72-4 FV 6	2nd layer PU	Polyurethane		<100	nd	140				-	12	290							
4FV		2282-72-4 FV 1	Faux leather	Polyacrylic Ethylene (front) Leather Polyamide (back)	Synthetic	0.10 wt%	nd	480							100 ppm	280 ppm	140 ppm	0.13			
4FV		2282-72-4 FV 4	Faux leather	Persoftal OE (front) Leather Polyamide (back)	Synthetic	0.11 wt%	nd	270							<100 ppm	320 ppm	130 ppm	<100 ppm			
5FV	UK	2282-72-5 FV 1	Cloth cover	Polyester (front) (back)	Cotton	<100	nd	4.6 wt%	~1 wt%	0.04											
5FV	UK	2282-72-5 FV 2	Bottom fabric cover	Wellon Polyester		<100	nd	440	130	0.16	wt% Al										
5FV	UK	2282-72-5 FV 3	Inner cushion liner	Cotton Polyester (front) (back)	Levapren	5.0 wt%	nd	650	<100	0.16	0.7 wt%										
5FV	UK	2282-72-5 FV 4	1st layer stuffing	Polyester		100	nd	210	200	0.09											
5FV	UK	2282-72-5 FV 6	Cloth cover	Avlin Polyester		100	nd	4.3 wt%	~0.8 wt%	0.04	wt% Al										
5FV	UK	2282-72-5 FV 7	Inner cushion liner	Coton Polyester		3.8 wt%	nd	290	<100	0.11	0.7 wt%										Probably 12% APP in backcoating
5FV	UK	2282-72-5 FV 8	Cushion stuffing	Fortrel Polyester		<100	nd	<100	230	0.13											
5FV		2282-72-5 FV 5	2nd layer PU	Polyurethane		0.53 wt%	nd	1.7				5.9	5.8	190							
6FV		2282-72-6 FV 4	PU foam	Polyurethane		0.56 wt%	nd	1.7				6.3	6.5	180							
6FV		2282-72-6 FV 1	Faux leather	Bayhydrol UH 340 (front) Polyester (back)	Cotton	0.41 wt%	nd	1900							<100 ppm	0.12	0.18	<100 ppm			
6FV		2282-72-6 FV 2	Inner cushion liner	Rayon fiber (front) acetate (back)	Polyvinyl	5.1 wt%	nd	740	<100	0.20								<100 ppm	0.59	nd	Probably 16% APP in backcoating
6FV		2282-72-6 FV 6	Inner cushion liner	Cotton Polyester		5.7 wt%	nd	150	<100	0.15								<100 ppm	0.41	nd	Probably 18% APP in backcoating
6FV		2282-72-6 FV 3	Cushion stuffing	IRISE Polyester		170	nd	300	390	0.17								320 ppm	<100 ppm		
6FV		2282-72-6 FV 7	Cushion stuffing	Fortrel Polyester		<100	nd	190	460	0.28								<100 ppm	<100 ppm		
6FV		2282-72-6 FV 5	Bottom fabric cover	Bayhydrol UH 34 (side 1) polyester (side2)	Cotton	0.41 wt%	nd	230	<100	0.14					100		0.22	150 ppm	0.12		
7FV		2282-72-7 FV 4	2nd layer PU	Polyurethane		0.26 wt%	nd	0.81				2.4	4.2	360							
7FV		2282-72-7 FV 8	Cushion stuffing PU	Polyurethane		0.49 wt%	nd	1.6				5.1	4.6	200							
7FV		2282-72-7 FV 1	Faux leather	Polyacrylic acid ethylene (front) leather polyamide based (back)	Syn	890	md	1100							<100 ppm	<100 ppm	<100 ppm	0.19			
7FV		2282-72-7 FV 2	Bottom fabric cover	Polypropylene fiber		110	nd	310	690	<100 ppm								~200 ppm	<100 ppm	nd	
7FV		2282-72-7 FV 5	Cover	Polyacrylic ethylene (front) synthetic leather polyamide (back)		840	nd	740	nd	nd								0.18	140 ppm	350	
7FV		2282-72-7 FV 3	1st layer stuffing	Polyester		<100	nd	240	380	0.19								<100 ppm	<100 ppm		
7FV		2282-72-7 FV 7	1st layer stuffing	Polyester		<100	nd	140	300	0.23								0.10	<100 ppm		
7FV		2282-72-7 FV 6	Bottom fabric cover	sample missing		-	-	-	-	-					-		-	-	-		
8FV	TB133	2282-72-8 FV 4	Cushion PU	Polyurethane		<100	nd	150				-	nd	240							
8FV		2282-72-8 FV 1	Cover	polyester		1.4 wt%	nd	21 wt%	0.61 wt%	0.61								0.90	0.50	0.39 wt%	APP and chloroparaffin in backcoating
8FV		2282-72-8 FV 2	Cover	Cotton polyester		<100	nd	1000	160	0.19								~200 ppm	<100 ppm	nd	
8FV		2282-72-8 FV 3	Liner	Acrylic fiber		160	nd	15 wt%	3.6 wt%	<100 ppm					<100		<100	0.090	330 ppm		
9FV	TB133	2282-72-9 FV 3	2nd layer PU	Polyurethane		0.43 wt%	nd	0.92				0.6	9.3	210							
9FV		2282-72-9 FV 2	1st layer stuffing	Polyester		<100	nd	300	430	0.055								210 ppm	<100 ppm		
9FV		2282-72-9 FV 6	Cushion stuffing	Polyester		<100	nd	160	380	0.28								400 ppm	<100 ppm		
9FV		2282-72-9 FV 1	Cover	polysiloxane (side 1) cotton,acrylic, nylon (side 2)	Wool,	0.12 wt%	nd	350	<100	<100 ppm					<100		<100	230 ppm	<100 ppm		
9FV		2282-72-9 FV 4	Cover	polysiloxane (side 1) (side 2)	Wool	0.10 wt%	nd	930	<100	<100 ppm					ppm Mg		100 ppm	270 ppm	<100 ppm		
9FV		2282-72-9 FV 5	Liner	Polypropylene		<100	nd	350	<100	<100 ppm							140 ppm	2.6	260 ppm		

4.4 Ignition Sources & Test Procedures

To ignite the couch, premanufactured miniature wood cribs, as specified within the BS 5852 standard, are used [104]. Cribs 4, 5 and 7 are illustrated in Figure 4-11, and are approximately 8.8, 24, and 128 g respectively[5]. Cribs 4 and 5 have a base of 40 mm x 40 mm. Crib 7, which consists of a base crib and an ignition crib inside, has a larger base of approximately 80 x 80 mm. The different mass of fuel burning associated with each crib type alters the fire exposure to the couches during the ignition and very early growth period by scaling the initiating fire size from smallest (Crib 4) to largest (Crib 7). The total energy released from each of the cribs in the standard is 142, 285[6] and 2110 kJ for Cribs 4, 5, and 7, respectively [161]. Per the standard, ignition is initiated by dispensing 1.4 ± 0.1 ml of isopropanol onto the centre of the lint at the base of the wood crib and then igniting using a gas flame. The same amount of isopropanol is used for all crib sizes and cribs are kept in a conditioning room at 21°C and approximately 50% relative humidity. Furniture was removed from packaging at least 24 hours prior to the test and held in the large test facility at UWFRL but was not explicitly conditioned prior to the test.

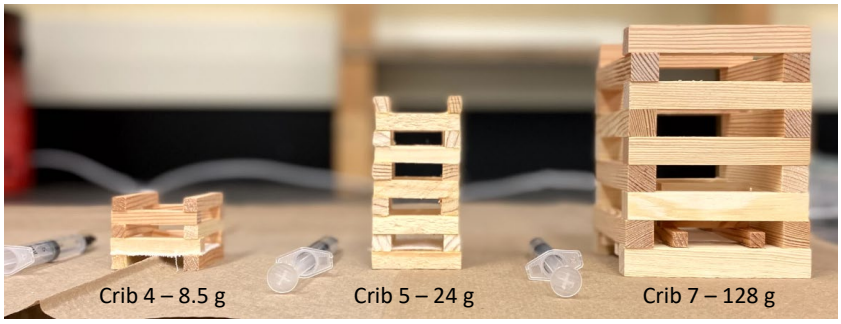


Figure 4-11: Different crib types used in the test series.

For these tests, if a couch does not sustain combustion and extinguishes, then the test is halted, the house is vented, the couch cushions are switched, and the test rig is reset to ignite using the next larger crib until the couch catches on fire. If the couch does not catch on fire with Crib 7, then the tests are discontinued for that couch type. If a test is reset due to self-extinguishment, it is given a letter reference; for example, 5aFV would correspond to Crib 4, 5bFV Crib 5, and 5cFV Crib 7.

The UK Regulations for the flammability of furniture [104] only require a test with ignition by Crib 5, and therefore all of the UK couches purchased would be expected to resist ignition until tested to the Crib

[5] The calibrated wood cribs were purchased from an external provider. Although the appropriate number of sticks were used and all cribs were proportionately the same size, the weight of one Crib 5 was found to exceed the BS 5852 standard's maximum of 18 g. Given dimensional proportionality, all Crib 5s are assumed to be on the order of 24 g. Cribs 4 and 7 were found to be consistent with the standard. The objective of having different ignition exposures is still maintained and the discrepancy is considered minor in nature.
[6] Adjusting for the increased weight, 402 kJ is an appropriate approximation for Crib 5 in these tests.

5 ignition source. The wood ignition cribs used in this test series included Crib 4, used in tests to evaluate ignition underperformance relative to the UK Regulations, Crib 5, used to validate performance relative to the UK Regulations; and Crib 7, to initiate combustion at a higher fire exposure than would be used in the UK Regulations. Crib 4 is therefore used first as the primary ignition source for all of the MV tests and FV tests, with a number of exceptions in the FV series, as summarized and documented in Table 4-8. This allows for consideration of the propensity of the couch materials and construction to resist ignition and, therefore, provides direct context for achieving the BS5852 standard's intended objective of resisting ignition. The standard does not have objectives for controlling fire growth, and therefore, the propensity for the fire to grow and spread is quantified separately from ignition in Chapter 5.

Table 4-8: First ignition used by Test number.

Test Number	Primary Fuel	First Ignition Method
1MV	NFR Cloth Couch	Crib 4
1FV	Wood cribs	Crib 5[1]
2FV	Heptane	Spark
3FV	NFR Faux-leather	Crib 4
4FV	NFR Leather	Crib 5[2]
5FV	UK FR Cloth	Crib 4
6FV	UK FR Faux-leather	Crib 4
7FV	UK FR Leather	Crib 5[2]
8FV	US FR Cloth	Crib 7[3,4]
9FV	US FR Faux-leather	Crib 7[3,5]

Notes:
1. In calibration tests, Crib 4 was insufficient to ignite the larger wood crib, and therefore Crib 5 was used in Test 1FV.
2. Leather is anticipated to be more resistant to ignition and given the couches only had two seat cushions, the program was adapted to use Crib 5 and 7, instead of 4, 5, and 7.
3. The US couches were first ignited with Crib 7 since the expectation was a higher level of ignition resistance due to compliance with the TB133 standard.
4. The couch was sectional which precluded using different seat cushions without altering the shape of the couch. Therefore, if the couch self-extinguishes with Crib 7 then the TB133 burner will be applied over top of the burned area from Crib 7.
5. The couch cushions were stitched into the couch which precluded switching cushions without potentially damaging the couch condition. Therefore, if the couch self-extinguishes with Crib 7 then the TB133 burner will be applied over top of the burned area from Crib 7.

Before initiating a test, a series of established procedures are implemented to control the test environment, identified and included on the test sheets purpose-developed for these experiments. All of the instrumentation has standard operating procedures that allow for a consistent set of instrumentation and data gathering for each test. Therefore, prior to a test, all of the instrumentation is checked, operational testing of the fire alarm systems is completed, any dust or debris is removed from the test couches, chairs, and tables, the mechanical system is initiated, the required airflows are verified, and repairs to any damaged components of the test house or new openings are completed.

All instrumentation is connected at least 5 minutes prior to a test to provide baseline data. The house is sealed, and the window positions are verified as closed. Once the baseline data is complete, an ignition crew enters the house from D2. The fire is ignited using the designated wood crib placed approximately 320 mm from the left arm of the couch, as shown in Figure 4-12. The ignition crew leaves within 30 seconds, and the house is sealed by closing D2. All key times are recorded on the test sheets.



Figure 4-12: Showing placement of crib equidistant (360 mm from edge of couch arm).

The fire is then left to burn and is monitored using video and real-time data from the instrumentation installed throughout the house. In the case of self-extinguishment, the fire development is observed on video, and a decision is taken to halt the test, at which point the test house is opened and reset for the next ignition scenario with the larger initiating crib size. Otherwise, conditions in the house are continuously recorded, and the test is halted when there is no further suggestion of continued burning. This is determined based on real-time temperature data falling below a value of 100°C, as recorded and verified using a manual thermocouple probe inserted into the LBR.

At the conclusion of the test, the fire service on-site enters through D1 and ventilates the house with positive pressure ventilation from D2 and opening W4 on the upper level. The couch is removed, and a water spray bottle is used to extinguish any remaining hot spots. Data logging continues for 30 minutes after the test to capture the baseline measurements post-fire. The remaining fuel is then weighed on the calibration scale, which cross-checks the information provided on the load cells. The post-test procedure is then initiated to capture and store the test data from all equipment.

Chapter 5
Experimental Results

Several aspects of fire development are pertinent to evaluating the smoke layer and smoke filling and, therefore, the escape time from a house fire. Smoke is generated by combustion processes within the fire, making the investigation of the stages of fire development important in determining escape time. The first stage is to determine whether the furniture ignites. During this stage, smoke is primarily generated by the ignition source itself (i.e., the igniting of the wood crib in this research) as opposed to significant burning of the couch materials. This research investigates a range of ignition sources to compare the propensity of the different furniture to ignite.

If ignited, the next question is whether the fire progresses rapidly to a growth stage or whether there is a prolonged incipient fire stage with limited fire growth. During an incipient stage, smoke may be generated in smaller quantities and may or may not be sufficient to cause the activation of a smoke alarm. This is important in considering whether delays in fire growth associated with different furniture flammability controls, such as flame retardants and barriers, equally delay the activation of detection and thereby potentially negate the desired benefit of that furniture control. Finally, if the fire transitions past the incipient stage into the growth stage, the fire growth rate can be quantified by changes in the MLR. The growth rate is then a consideration in the rate and volume of smoke released by the fire and, therefore, the rate at which the house is filled with smoke. Differences in the peak MLR could characterize the differences between material types, but large MLR's and peak fire sizes are likely to be controlled by oxygen availability in ventilation-limited conditions unless a window breaks. Exploration of the ventilation-limited conditions on the smoke filling through the house and the impact of visibility and tenability along escape routes are significant considerations for review in this research.

Externally influenced ventilation changes are not considered further in this study, although they can certainly play a role in other situations. In fact, the interior panes of the windows did crack during these tests, but the glass did not fall away, and the outer panes generally did not crack, so the windows did not fail in a manner that allowed for a significant change in the ventilation environment. Therefore, the smoke environment is primarily characterized by the fuel's MLR (and corresponding HRR) relative to the interior geometry and ventilation-limited conditions in the test house.

Smoke detection is expected to occur during either the incipient or the growth stages of the fire. If there is a prolonged delay in the onset of the growth stage, it is important to confirm whether detection will occur during this delay or whether insufficient smoke is generated such that fire detection is also delayed. This is relevant in evaluating whether burning controls in furniture are effective at increasing the ASET, or whether there is merely a time shift in detector response and fire growth stage, potentially not impacting the ASET. To study this, the response of the smoke detector on the lower level is considered relative to the evolution of the smoke layer and the smoke filling of the house, which in turn affects the visibility along the escape path. Detailed video imaging allows for a thorough step-by-step analysis of the smoke layer descent from different camera perspectives, providing an excellent profile of the smoke filling within different house sections. This level of detail has not been observed in other literature and provides a practical holistic basis for comparing the smoke layer descent between tests. As outlined earlier, camera visibility will be used as the basis for determining ASET for this analysis, but temperature and gas profiles are supplemented, as appropriate, for additional context and reference. For this, the work of Purser is followed, which indicates that focus should be placed on concentration distributions of a small number of asphyxiant gases, namely carbon monoxide (CO), hydrogen cyanide (HCN), carbon dioxide (CO_2) and reduced oxygen [162].

In light of the above considerations, the following chapter sections describe the results across all tests in more detail. Still capture images of the burn room and upper level quad videos are provided at 1-minute intervals for the wood crib and all couch fire tests in Appendix A as a general reference.

5.1 Temperature & Relative Humidity Outside of Test House

The exterior temperature and relative humidity at the start of each test or series of tests are summarized in Table 5-1.

Table 5-1: Summary of exterior temperature and relative humidity at the start of each test.

Test	1FV	2FV	2MV	3FV	4FV	5FV	6FV	7FV	8FV	9FV
Temperature	24.1	24.7	24.1	23.8	28.6	26.8	29.3	30.6	17.2	16.8
Relative Humidity	33	60	37	38	54	59	32	39	84	57

5.2 Ignition

Two large wood crib tests are initially completed. The first is for calibration and configuration of the wood crib (Test 0FV). This test is generally not reported in the data except for here, as it is used as the basis for determining the method of ignition for the large wood crib. The calibration test was first run using Crib 4, but the large wood crib did not ignite. Therefore, the test was reset with Crib 5 as

the igniting source, which ignited the large wood crib, and burning ensued. Test 1FV, the official wood crib fire test, is therefore initiated with Crib 5 (not Crib 4). Also, between the initial calibration and final configuration, the wood crib design is altered to include additional levels of sticks on the source crib. This is due to the lack of lateral fire spread to the middle and far right wood cribs observed during the calibration run, with corresponding uncertainty as to whether the crib configuration or the ventilation-limited environment precludes full fire spread. The final test, 1FV, is then used to compare the ignition of the various couch types.

The cloth couch is the baseline test couch for the MV test series, and it has also been tested on three other occasions under different ventilation conditions. Test 2MV from this series is an overlapping test with the same ventilation configuration as the FV series and, therefore, becomes the NFR-comparable cloth couch. The FV series has 3 different types of NFR couches: cloth, faux leather and leather. The NFR couches, except the leather couch in Test 4FV, are all ignited with Crib 4, the smallest of the crib sources, including all of the MV series tests. Crib 5 is used instead of Crib 4 for ignition in Test 4FV. This is because the couch has only two seat cushions, and knowledge that leather is inherently resistant to flame precluded a first, and most probably failed, ignition attempt using Crib 4. Otherwise, all of the NFR couches proceed to burn from the first ignition without reset to a larger ignition crib type. Thus, the ignition threshold for all NA NFR couches is below the expected threshold to meet the British Regulations. Compared with the wood crib in Test 1FV, which ignites with Crib 5, the cloth and faux leather couches ignite at a lower input energy threshold (Crib 4), implying a greater ease of ignition for NA couches than for wood.

The Test 5FV FR couch is the only couch of the FR comparison series that does not sustain ignition despite three attempts using Cribs 4, 5 and 7 (Test 5aFV, 5bFV, and 5cFV, respectively). In contrast, both Tests 6FV and 7FV FR couches ignite. Test 6FV ignites using Crib 4, which is below the specified ignition threshold and thus does not meet the expectations of a couch that has been constructed to meet the British Regulations [104]. Test 7aFV does not ignite with the Crib 5 ignition source and, therefore, resists ignition in a manner that meets the expectations of the British Regulations. The crib necessary to ignite this couch is also larger than the Crib 5 ignition crib needed to ignite the reference larger wood crib in Test 1FV. It is only with a much larger Crib 7 that the 7FV couch ignites (Test 7bFV) and sustains burning with flames, eventually spreading to the cushions in a similar fashion to the Test 4FV couch.

In general, the UK couches demonstrate a lower propensity for ignition than the NFR comparable couches since a larger crib size is required for all of the UK couches to ignite and continue burning. Given the relative ease of ignition of the NFR cloth couch in Test 2MV, the FR cloth couch in Test

5FV initially appears to be an anomaly as it was also expected to ignite fairly easily. In this case, it is thought that the details of the specific design become important. Specifically, the presence of a Schedule 3 interliner in the FR couch in Test 5FV appears to be a differentiating factor in limiting the propensity of this couch to ignite. According to British Regulations [104], an interliner is required where the fabric does not resist the match or cigarette ignition test forming part of the BS 5852 standard. It is not known whether the 5FV cloth couch was tested to this part of the standard or if the interliner was added to limit the need for testing, but either way, it appears to have played a large role in the propensity for ignition of the couch. Thus, in comparing UK and NA furniture tests on the basis of ignition propensity, the UK cloth couch (with an interliner) is the most resistant to ignition, followed by the UK leather couch, and then the UK faux leather couch.

The Test 8FV US FR cloth couch is less comparable to the other couches as it is sectional and commercial grade and, therefore, more characteristic of furniture in the waiting room of an office than a couch in a residential environment. Unlike the thickly cushioned seats and pillowed back cushions of the previous couches, this couch is constructed with three seat sections that are very firm and have a limited depth of cushioned area in the seat. As expected, couch 8FV did not ignite, either with Crib 7 (Test 8aFV) or with the propane burner (Test 8bFV), despite the propane burner being applied to the already damaged couch from the Crib 7 ignition attempt. In contrast, the US FR faux leather couch in Test 9FV ignited with Crib 7, which was not expected given the FR treatment of the couch and the ignition resistance observed on the couch in Test 8FV. This low ignition resistance may be related to the observed peeling of the fabric during the test, suggesting low thermal/flame resistance of the cover fabric, which retracts away from the heat and leaves the underlying cushion open to ignite and burn. Since there is no NFR couch that is directly comparable to that used in Test 9FV, and the couch in 9FV ignited with the initial ignition source, it is difficult to quantify and compare the ignition resistance of these FR couches relative to those in the previous tests. Nonetheless, this couch exhibits rather poor resistance to ignition relative to that anticipated, somewhat comparable to results found during tests of the FR fabric in the 2015 test series discussed in Section 2.5.2.

In contrast to the tests that developed into full flaming combustion, Figure 5-1 illustrates the burn damage area for the individual cushions from the UK FR cloth couch tests, which did not sustain flaming combustion after ignition. In Test 5aFV, the burn damage area on the seat cushion is slightly larger than the wood ignition crib's bottom surface area and extends around the perimeter of the crib in all directions with slightly greater propagation of fire towards the front of the couch (Figure 5-1). The interliner on the seat cushion is charred but has not fully exposed the polyurethane foam slab. Nevertheless, there is measurable mass loss of the polyurethane foam, indicating some participation of the foam in the combustion process. The burn area on the back seat of the cushion also aligns with

the flaming region of the wood ignition crib. The cloth fabric has burned away and exposed the charred interliner on the back seat cushion, but the interliner is still in place on the front surface, with the fill only slightly exposed towards the bottom of the cushion where the degree of interliner charring is greatest. Similar but increasing degrees of damage are observable in Tests 5bFV and 5cFV, also shown in Figure 5-1. Tests 5bFV and 5cFV have a wider base of burning due to the larger wood crib ignition source and, like Test 5aFV, have the greatest charring on the back seat cushion at the base. The full outcome of the ignition tests on the reassembled couch is observable in Figure 5-2, where, after replacing the cushions of the couch and documenting post-test, the greatest burn area is along the interface between the back and seat cushions. The small amount of damage to this couch, even with an ignition attempt with the largest wood ignition crib, highlights the effectiveness of an interliner in reducing potential ignition of the loose polyester fill within the pillowed back seat cushion, as intended by the British Regulations (refer back to Table 4-2 for the different layering of the couch components). In the same manner, the interliner appears to adhere to the PU slab on the main seat cushion, possibly in combination with the cover fabric and polyester wrap, thereby resisting the foam's participation. However, given the increasing visible mass loss of the PU slab with the ignition source, it appears that the combination of the interliner and flame retardance of the foam are the key factors in limiting the full combustion of the couch in these tests. The impact of these should be noted in comparison to the fire growth exhibited by the comparable couch without FR strategies in Test 2MV.

Similar behaviour to that seen in Test 5FV is observed in Test 7aFV, also included in Figure 5-1 for comparison. This test uses Crib 5 as an igniting source on the UK leather couch and self-extinguishes at approximately 6:30 seconds into the test, which is much quicker than Test 5bFV that used the same ignition crib on the cloth couch (which continues to burn until 17:27).

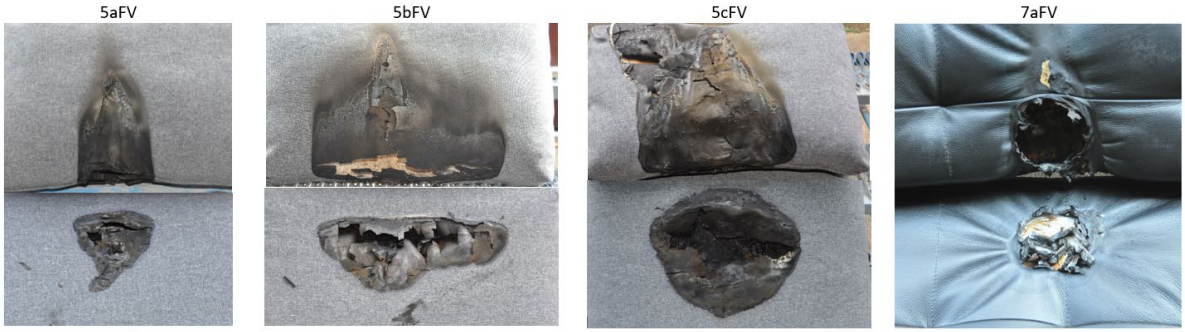


Figure 5-1: Fire damage to the back cushion (top) and seat cushion (bottom) for each of the tests where the couches did not sustain ignition (documented immediately after removal from the burn house).

The physical damage to the cushions of the 7FV leather couch is very localized in an area proportionate to the dimensions of the Crib 5. The thicker leather cover material appears to resist

flame penetration and delays exposure of the underlying FR PU foam slab, thus mitigating against continued combustion and fire growth. This aligns well with expectations of the British regulations for couches, which mandate resistance to ignition with a Crib 5. However, this protection does not persist when the couch is ignited with the larger Crib 7 wood ignition crib since the couch catches fire and burns.



Figure 5-2: Test 5FV showing subsets with different ignition sources that did not allow the couch to sustain ignition and greater burning at the interface of the back and seat cushions.



Figure 5-3: Post-test damage for Test 8aFV (left) and 8bFV (right).

Photographs of the burn patterns from Tests 8aFV and 8bFV are shown Figure 5-3. The test was first initiated with Crib 7, but the fire self-extinguished, leaving the remains of the charred Crib 7 on the seat cushion. The fire did not extend significantly beyond the flaming region of the small initiating Crib 7 fire. Examination of the cushion materials determined that the fire penetrated through the FR Polyester cover of the seat and back but did not penetrate the FR interliner that covered the FR PU foam beneath. Since the cushions on this couch could not be reconfigured, the propane furniture burner ignition source was applied over the top of the burn area shown for Test 8aFV in Figure 5-4.

The fire again penetrated through the FR Polyester cover of the seat and back but did not penetrate the FR interliner to reach the foam beneath. Accordingly, the two attempts at igniting the couch were

unsuccessful despite the use of the two largest ignition sources in the test program. This performance is attributed to the protection of the PU foam by the interliner coupled with the FR treatment of the foam itself.



Figure 5-4: Positioning of propane burner over burn area of Test 8aFV.

Table 5-2 consolidates the results from the ignition tests described above. Based on the Table, the following observations are noted:

1. All of the NFR furniture ignites at an ignition crib threshold below that listed in the British Regulations and readily progresses to open flame burning. Since the NFR furniture is not tested according to British Regulations, this series of tests illustrates the comparative difference in ignition characteristics for this furniture set between North America and the UK. In general, the ignition propensity in North America is below the threshold corresponding to ignition with wood Crib 4 (noting that the leather couch was not tested with Crib 4).
2. The UK faux leather couch ignites with Crib 4, which is below the ignition acceptance threshold under British Regulations. In addition, the presence of an FR interliner, which is not defined as a Schedule 3 interliner in labelling the couch according to British Regulations, does not prevent ignition. However, the couch does not readily or quickly progress to flaming fire growth. Reasons associated with this behaviour will be explored further in the following sections on the incipient and growth stages of the fire.
3. The UK leather couch does not ignite with Crib 5, reflecting an expected level of ignition resistance based on the British Regulations. It demonstrates greater ignition resistance than the NFR leather couch, requiring the use of Crib 7 as an ignition source. This is thought to be due to the effects of the flame retardant additives in the foam, as no interliner is present in this couch.

Table 5-2: Summary of ignition sources used for each test.

Test Number	Primary Fuel	First Ignition Method	Ignition Sources Used	Result
1MV	NFR Cloth Couch	Crib 4	Crib 4	Ignition
1FV	Wood cribs	Crib 5[1]	Crib 5	Ignition
2FV	Heptane	Spark	Spark	Ignition
3FV	NFR Faux-leather	Crib 4	Crib 4	Ignition
4FV	NFR Leather	Crib 5[2]	Crib 5	Ignition[6]
5FV	UK FR Cloth	Crib 4	Cribs 4, 5, and 7	Self-extinguished[7]
6FV	UK FR Faux-leather	Crib 4	Crib 4	Ignition
7FV	UK FR Leather	Crib 5[2]	Crib 5, 7	Ignition[8]
8FV	US FR Cloth	Crib 7[3,4]	Crib 7, Propane Burner	Self-extinguished[9]
9FV	US FR Faux-leather	Crib 7[3,5]	Crib 7	Ignition

Notes:

1. In calibration tests, Crib 4 was insufficient to ignite the larger wood crib, and therefore Crib 5 was used in Test 1FV.
2. Leather is anticipated to be more resistant to ignition and given the couches only had two seat cushions, the program was adapted to use Crib 5 and 7, instead of 4, 5, and 7.
3. The US couches were first ignited with Crib 7 since the expectation was a higher level of ignition resistance due to compliance with the TB133 standard.
4. The couch was sectional which precluded using different seat cushions without altering the shape of the couch. Therefore, if the couch self-extinguishes with Crib 7 then the TB133 burner will be applied over top of the burned area from Crib 7.
5. The couch cushions were stitched into the couch which precluded switching cushions without potentially damaging the couch condition. Therefore, if the couch self-extinguishes with Crib 7 then the TB133 burner will be applied over top of the burned area from Crib 7.
6. This couch ignited and continued burning when exposed to a Crib 4 initiating source, which is below the Crib 5 threshold expected.
7. This couch did not sustain ignition with any of the cribs and further testing was stopped.
8. This couch met its design exposure for Crib 5 and burned with the larger Crib 7 fire exposure.
9. This couch did not ignite from either the Crib 7 exposure or the TB133 propane burner.

4. The UK cloth couch exceeds the ignition resistance threshold anticipated under British Regulations and self-extinguishes in all fires. The presence of a Schedule 3 FR interliner and FR foam are likely contributing factors in limiting the ignition of this couch.

5. The US FR cloth couch achieves the ignition resistance anticipated by the US legacy California TB 133 regulations. This exceeds British Regulations (for residential furniture). This FR couch has an interliner, and limits on ignition are likely attributed to the interliner, the flame retardants in the materials, and the limited thickness of the foam slab used in the cushions.

6. The US FR cloth couch can be used as a reference as it resists both Crib 7 and the TB 133 propane torch. Relative to this, the US FR faux leather couch does not display comparable ignition resistance as it readily ignites with a Crib 7 ignition source. Although not quantifiable given the very different ignition sources used in North American and UK standards, the general ignition performance of the US faux leather couch is surmised to be well below the expected performance of both the US legacy California TB 133 standard and the UK regulations.

Given that ignition is the starting point of a fire, it is now important to correlate the above characteristics of ignition on the couches that ignited to the incipient fire development and growth to allow further evaluation of the fire performance of the different couches. These connections will be explored in the following sections.

5.3 Incipient Time Period

Once ignition is sustained and fire develops, an incipient period ensues where the fire can smoulder or fester for a brief or extended period before taking hold and significantly growing. This can be investigated by examining the stages of fire growth through the measured mass loss rate (MLR) curves, illustrated for each test in Figure 5-5. Tests 5FV and 8FV are not included in the graph since there is no sustained flaming after ignition in either of these tests. Initial analysis of the curves indicates that the MLR curves trend between 0.000 and 0.002 kg/s during the incipient stage, while the fire transitioned into a stage of continued growth after a clearly definable increase in MLR to a value above 0.002 kg/s and no corresponding return to 0 kg/s.

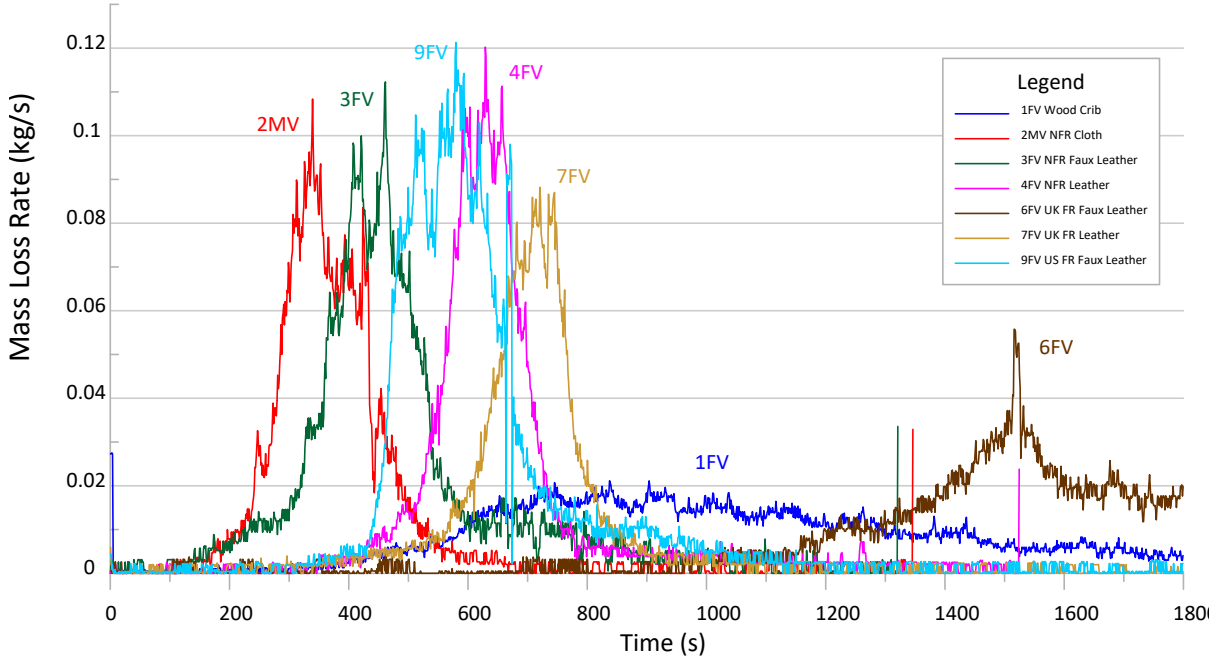


Figure 5-5: Mass loss rates for all ignited couches and the wood crib.

Figure 5-6 illustrates the step transition for Tests 4FV and 7FV. In the case of Test 4FV, the fire grows quickly after the transition when compared with the longer, shallower steps seen in the expanded MLR with time for Test 7FV. Similar transitions, albeit with differing timelines dependent on the growth profile of each fire, are observed when comparing the MLR with time data from tests 3FV and 6FV, as shown in Figure 5-7 and Tests 2MV and 9FV in Figure 5-8. The measured MLR with time from the wood crib in Test 1FV is shown in Figure 5-9. This fire has a somewhat less pronounced, but still distinctive jump, given its slower increase in MLR with time.

Thus, analyzing the transition of the MLR fluctuations from a minimum value of 0.000 kg/s to a value above 0.002 kg/s aligns well with the transition of the fire to an early phase of growth in all tests. Following these initial transition periods, the fires continue to grow, suggesting the observed transition can be used, for purposes of these experiments, to define the incipient fire time. The times to reach the end of the incipient phase, as determined based on the above methodology, are summarized for each test in Table 5-3. These establish the times the fire spent in this first stage of fire development, important for correlating the smoke detector response time to the stage of the fire as will be outlined in Section 5.7.

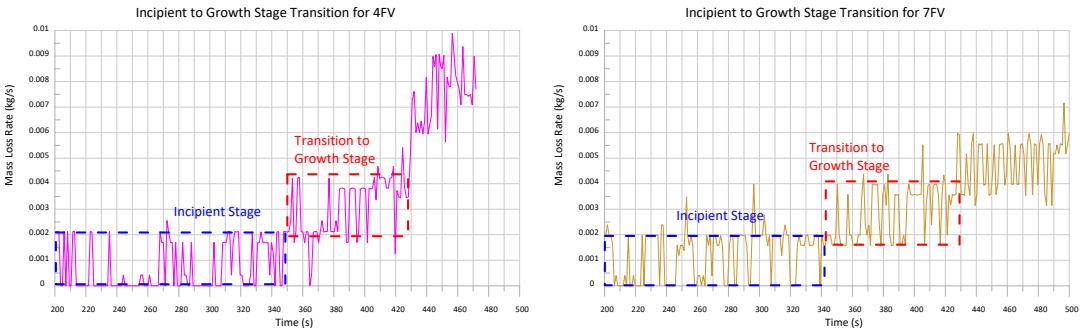


Figure 5-6: Transition of Tests 4FV and 7FV from incipient to the growth stage of fire.

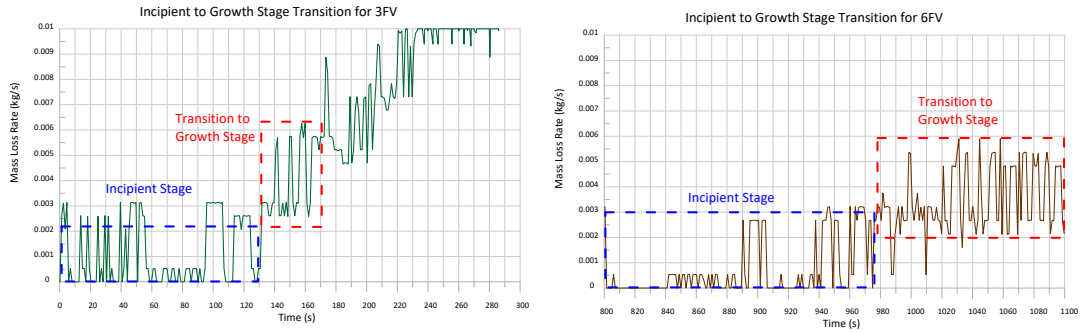


Figure 5-7: Transition of Tests 3FV and 6FV from incipient to the growth stage of fire.

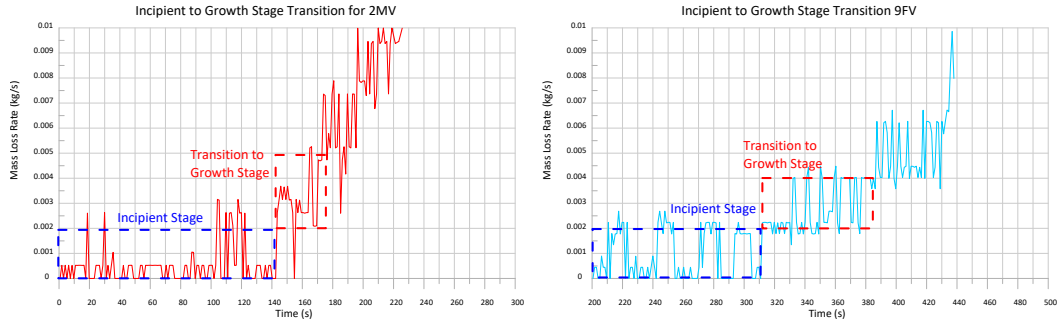


Figure 5-8: Transition of Tests 2MV and 9FV from incipient to the growth stage of the fire.

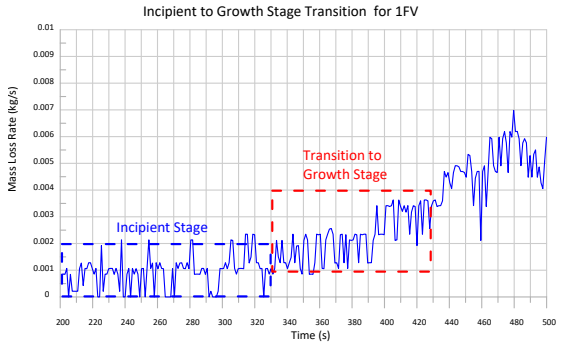


Figure 5-9: Transition of Test 1FV from incipient to the growth stage of the fire.

Table 5-3: Summary of Incipient Fire Duration Times.

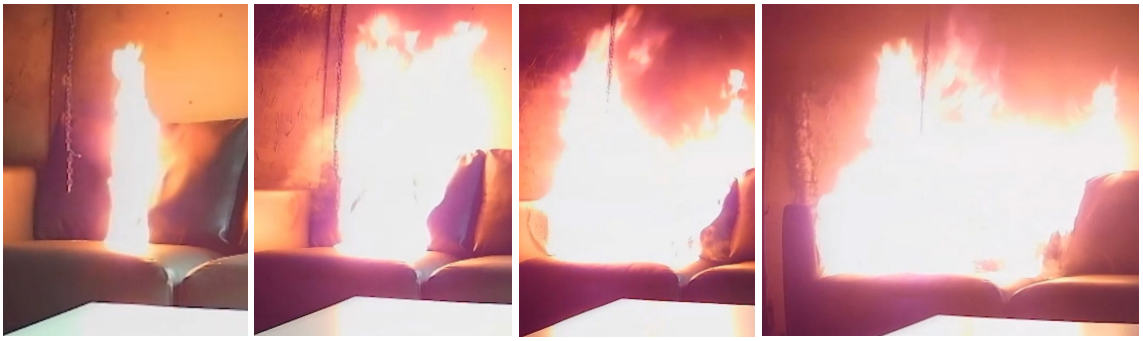
Test Number	Time of transition to growth stage after ignition (seconds)
1FV	328
2MV	142
3FV	130
4FV	370
6FV	998
7bFV	350
9FV	331

The MLR analysis from the measured data was qualitatively compared with observations of the fire growth at the corresponding times from the test videos with very good qualitative alignment. Images of the fire as captured by Camera 3 at the transition times listed in Table 5-3 for the NA and UK faux leather and NA and UK leather comparison couches are illustrated in the Figure 5-10 composite image. Although there are differences in geometry, shape, and location of burning, the overall size of the flaming regions is proportionate, which qualitatively suggests the fires have reached similar stages of fire growth and development.



Figure 5-10: C3 video capture images of several tests at the point of incipient to growth stages of the fire.

The growth of the flames in the faux leather couches used in Test 6FV and Test 3FV are quite distinct, so they merit further discussion and comparison here. Initially in both tests, burning is slightly larger than the flaming area of the ignition Crib 4 with a vertical flame extending most of the height of the cushion and seemingly extending into the back cushion. Following this, the fire in Test 3FV develops from the crib origin in the approximate centre of the back cushion and propagates vertically and then laterally on the face of the back cushion by 03:00 into the test, as shown in Figure 5-11. It then propagates towards the front on the seat cushion and fully involves the left third of the couch by 04:00 after ignition. Following this, the fire increases in magnitude horizontally and begins propagating laterally to the middle back cushion near 05:00 into the tests before under-ventilating and self-extinguishing over the next minute or so.



01:30 03:00 04:00 05:00

Figure 5-11: Early fire growth time progression of fire development in Test 3FV (NFR) captured from CAM 1.

In contrast, it appears as if the fire is going to take hold and progress to full burning in a fashion comparable to the growth observed in the tests with NFR furniture after ignition using the wood ignition Crib 4 in the FR Test 6FV. Instead, at 03:00 after ignition, the shape of the flame starts to transition from a localized vertical source to a wider and less vertically extended flame shape, leading to a prolonged incipient burning phase, as illustrated in Figure 5-12. By 05:00 into the test, a shorter and wider flame propagates laterally on the seat cushion material's surface and at the back cushion's base. This is directly comparable to the burn pattern observed in Test 5bFV on the unignited cloth couch. The primary difference in this instance is that the fire continues to propagate on the faux leather couch via a shorter and wider flaming region along the interface of the seat and back cushions different than is observed for other MV and FV couches. Following this, there is little vertical flame propagation after 05:00 into the test while the fire continues to progress laterally. At 10:00, the fire appears to be at the point of self-extinguishment. The full sequence is illustrated in Figure 5-12.

Rather than extinguishing, the fire progression instead takes a different direction, as shown in the sequence in Figure 5-13. At 12:00 into the test, continued burning at the seat and back cushion interface can be observed along the length of the cushion until, at 13:30, the fire starts to propagate

vertically up the arm of the couch at the interface of the back cushion, shifting the location of fire development from the center to the left side of the cushion. The fire then progresses in a manner consistent with it being ignited on the left side of the back cushion, with the right side of the left cushion subsequently collapsing into the burned-away left side at 20:00 in Figure 5-13. This is a substantially different trend in fire propagation from that seen in either the NFR faux leather couch in Test 3FV or the cloth couches in any of the other tests.

Since couches meeting British regulations are required to withstand Crib 5, it was unexpected that ignition and propagation would occur in Test 6FV when ignited with Crib 4. Nevertheless, it is clear from the fire timeline that fire growth over the UK FR version of the faux leather couch is substantially delayed relative to the NFR version, leading to a reduction in the overall propagation of the fire, as well as in the total consumption of couch materials, as illustrated in the post-fire comparison images contained in Figure 5-14.

P

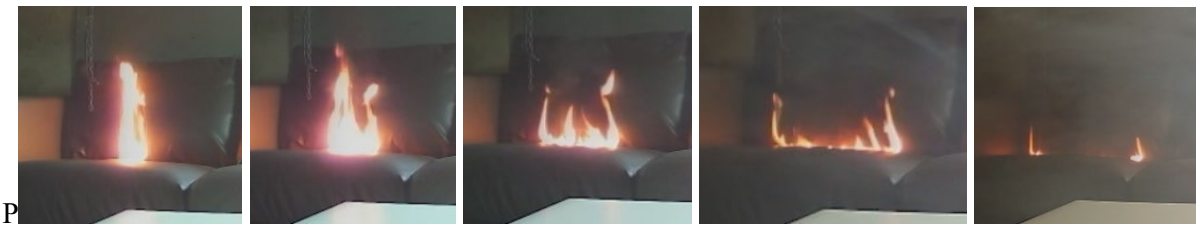


Figure 5-12: Progression of fire development on the left couch cushion in Test 6FV captured from CAM 1.



Figure 5-13: Continued time progression of fire development on the left couch cushion in Test 6FV captured from CAM 1.



Figure 5-14: Remaining components of faux leather couches (left - 3FV NFR, right 6FV FR)

A comparison of the burning behaviour observed for the FR and NFR faux leather and cloth couches suggests that the flame retardant additives in the couch materials alter how the fire propagates. In one case, the couch does not ignite at all, while in the other, the fire growth is contained for an extended period of time, unlike the NFR comparable versions, which have a consistent ignition and growth sequence.

Based on the above, the following observations are noted:

- Using the MLR data, a clear time at which the fire transitions from the incipient to the growth stage is established for all tests where ignition is sustained.
- The couch with the longest incipient time is the FR faux leather couch, which has a prolonged period with small flames characterizing the combustion process before transitioning to continued fire growth. The transition between the incipient and the growth phase of fire development occurs much later in Test 6FV than in Test 3FV despite both tests being ignited with a wood ignition Crib 4. This suggests that ignition should not be taken in isolation to the post-ignition fire growth and development when evaluating overall fire controls. A prolonged incipient stage or very slow growth stage may delay the loss of visibility while still generating sufficient signals to alert occupants to the presence of a fire.
- The two leather couches, the US faux leather, and the wood crib tests, each have incipient times greater than 5 minutes. However, the couches in Tests 7bFV (leather) and 9FV (faux leather) are ignited with a much larger Crib 7 ignition source compared with the Crib 5 ignition source used in Tests 1FV (wood crib) and 4FV (leather).
- The NFR cloth and faux leather couches in Tests 2MV and 3FV have significantly lower incipient fire development times than the other couches.
- The presence of interliners, and potentially the interliners in combination with FR PU foam, appears to reduce the ignition potential in Tests 5FV and 8FV, as well as limiting the transition from the incipient stage to the fire growth stage in Test 6FV.

The results suggest that there is a wide variation in incipient fire development times that appear decoupled from the propensity of ignition. As these may influence detection times and, therefore, escape times, correlating these with the growth stage of the fires will allow for a more complete picture and greater understanding of the full fire risk profiles of the couches used in this study.

5.4 Consideration of Heat Release Rates

One of the methods for estimating fire HRR is to multiply the MLR of fuel by the effective heat of combustion for the fuel. The heat of combustion for the present experiments is estimated for the NFR cloth couch as 20 MJ/kg through cone calorimeter testing at UWFRL. This value is applied for all of the NFR materials, a value of 17.5 MJ/kg is applied for the wood crib [163], and the value for the UK and US furniture with flame retardants is taken as 11.9 MJ/kg - based on past UWFRL work documented by Forrest [152]. Using these values and measured MLR during each fire, Figure 5-15 illustrates the approximated HRR profiles interpreted from these tests.

The use of fire HRR instead of MLR in the present context increases the potential error in the determination of overall fire development since the effective heat of combustion varies as a function of oxygen concentration local to the fire and, therefore, will be constantly changing in value in a ventilation-limited fire environment [140]. The estimation of uncertainty associated with the heat of combustion, and thus HRR and the corresponding changes in a ventilation-limited environment, are the subject of further work at the UWFRL, but for purposes of this analysis, the necessary comparative context of the overall fire growth can be established without converting the measured MLR to HRR. Thus, the specific MLR for each of the different furniture couches is used in the remainder of this thesis.

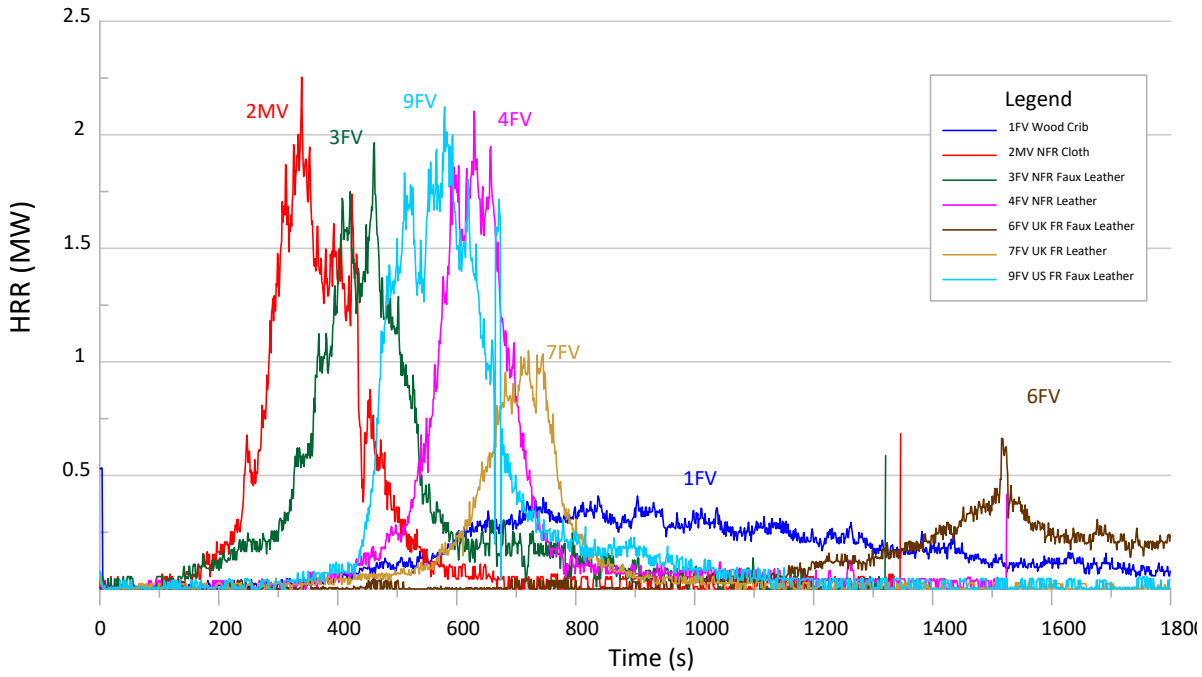


Figure 5-15: Approximated HRR estimates for the FV series.

5.5 MLR in the Fire Growth Stage

The fuel mass loss rates for the NFR couches all peak at values within 0.08 to 0.12 kg/s. The stages of fire growth are illustrated in Figure 5-16 using Test 2MV, which shows an initial 142 s incipient stage growing to a peak MLR at 339 seconds, meaning the duration of the fire growth stage is 197 seconds. The relatively fast growth is followed by a similar decline once ventilation becomes limited and oxygen availability within the house controls the burning characteristics. It should be noted that the fire does not propagate to the armchairs and tables in any of the tests. Although there is some charring of the coffee table and the chair in some instances, it does not add value to the overall findings presented here and, therefore, has not been documented in more detail.

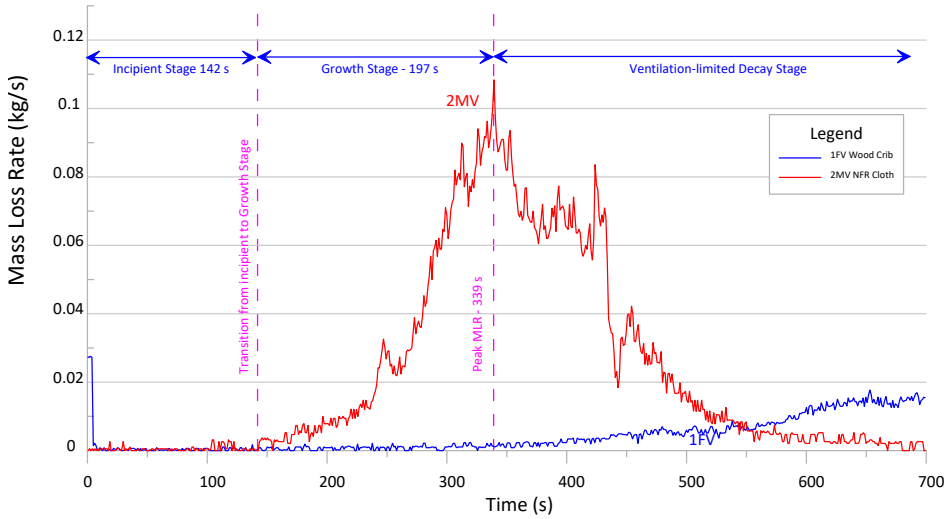


Figure 5-16: MLR for Test 2MV showing stages of fire development.

Figure 5-17 illustrates the comparative evolution with time of the MLRs for the three NFR couch types, with key results also tabulated in Table 5-4. The NFR cloth couch (Test 2MV) fire has a short incipient time before growing to a peak MLR of approximately 0.1 kg/s by 339 seconds after ignition. Test 3FV, the NFR faux leather couch, unexpectedly has a shorter incipient development time than Test 2MV, but this is followed by a much slower period of fire growth so that it does not reach peak MLR until 461 s after ignition. Lastly, the NFR leather couch in Test 4FV has a much longer incipient time than that of either 3FV or 2MV. Following this, it exhibits a shorter growth time than Test 3FV and a slightly longer growth time than Test 2MV. Slower fire growth rates may delay the generation of smoke and, therefore, change the evolution of smoke filling within the house, which in turn will affect the available escape time.

As can be seen in Figure 5-17 and Table 5-4, all of the NFR couch fires grow to similar values of peak MLR, so the distinguishing elements between the fires lie in differences in delay times

associated with incipient fire development and growth before reaching the peak fire size. In the case of Test 3FV, a longer period of fire growth compared with Test 2MV is the primary factor in offsetting the peak, whereas, for Test 4FV, the longer incipient time is the primary contributing element.

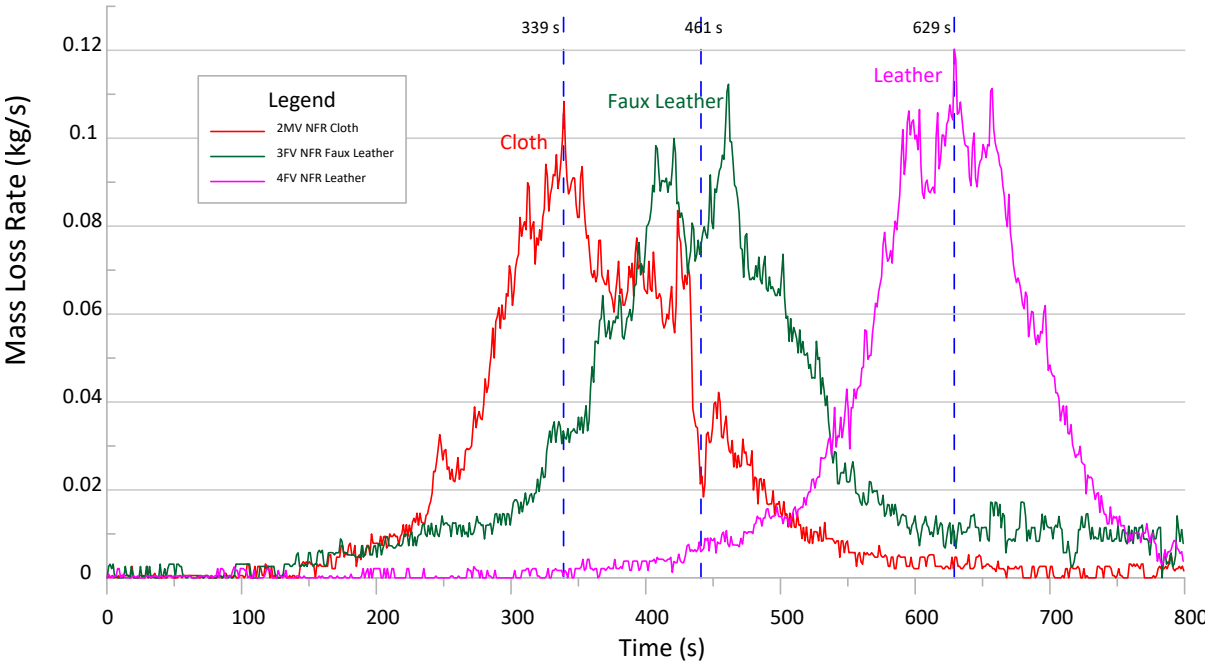


Figure 5-17: MLR comparison of different NFR couch materials.

Table 5-4: Fire growth time and peak MLR for each test.

Test Number	Primary Fuel	Ignition Crib Size	Incipient Stage	Time to Peak MLR	Growth Time to Peak MLR
1FV	Wood cribs	Crib 5	328	837	509
2MV	NFR Cloth Couch	Crib 4	142	339	197
3FV	NFR Faux-leather	Crib 4	130	461	331
4FV	NFR Leather	Crib 5	370	629	259
5FV	UK FR Cloth	Crib 4	Did not Ignite (DNI)	DNI	DNI
6FV	UK FR Faux-leather	Crib 4	998	1516	518
7FV	UK FR Leather	Crib 7	350	720	370
8FV	US FR Cloth	Crib 7	DNI	DNI	DNI
9FV	US FR Faux-leather	Crib 7	331	580	249

The observable differences in couch involvement are illustrated in the video capture images for the wood crib and NFR couch fires from CAM 4 at their respective peak MLR, as shown in Figure 5-18. In Test 1FV for the wood crib fire, the fire did not significantly spread from the original crib ignited to the immediately adjacent cribs. The edge of the middle crib eventually ignites, but ventilation conditions appear to limit the fire's spread laterally, such that the majority of burning takes place in the first crib, equivalent to the first couch cushion on the left (facing a couch) when compared with the couch fires.



Figure 5-18: Video capture at peak MLR time for wood and NFR couches.

In Test 2MV, the fire initially develops primarily in the first cushion on the left. It burns predominantly on the back cushion until it later spreads across the seat cushion. At this point, a portion of the seat cushion is observed to drop down and burn on the floor of the test rig. This increases the local fuel burning area and initiates fire spread laterally across the seat cushion of the middle seat and along the top of the back cushion, with the fire eventually extending to the third cushion before retracting due to ventilation-limited conditions in the structure.

The couch in Test 3FV burns similarly to that in Test 2MV, with the fire initially developing on the back cushion and spreading laterally only after some fuel drops down to the floor. Burning extends further down to at least the middle of the third seat cushion in this test, and the fire continues to burn along the length of the couch, with all of the seat cushions being largely consumed before the fire becomes ventilation-controlled and dies down.

In Test 4FV, with the slightly larger Crib 5 initiating source, the fire first burns through the back cushion. Unlike the other NFR couches, this cushion is constructed from a polyurethane foam slab rather than a polyester fill material. Vertical burning on the back cushion ensues for an extended period without significant propagation of the fire across the first seat cushion. Flaming then increases behind the back cushion, and burning material drops down to the floor as the back cushion collapses down onto the still fairly localized burning area on the first cushion (still without significant horizontal extension). The burning of material below the couch then increases, exposing the underside of the seat cushion, but there is still no significant propagation of flame across the first seat cushion. As the burning of the back of the couch and below the couch increases, the seat cushion curls up from the front corners and sides, presumably due to the drying of the leather seat cover. At this point, the

left half of the couch becomes engulfed in flames. This, in turn, increases radiative exposure to the right cushion of the couch, causing the leather to shrink and the cushion to curl up, exposing the underside of the seat cushion. The fire then spreads to the right cushion for a period of time before it becomes ventilation-controlled and dies down.

The overall MLR of the FR faux leather couch in Test 6FV is compared to that of the NFR faux leather couch (Test 3FV) in Figure 5-19. The incipient stage is 7.7 times longer, the fire growth time is 56% longer, and the peak MLR is at least 30% lower for the FR faux leather couch despite igniting at the same ignition exposure. As previously described, the FR faux leather couch ignites and, after a prolonged incipient period, propagates into the corner of the back cushion and arm of the couch, where the wood frame is covered with a polyester wrap under the faux leather cover without any polyurethane foam slab or polyester fill. The fire in the corner involves the back cushion and seat cushion until the seat cushion collapses. The flames and burning rate then slowly increase, with flames propagating along the back cushion most of the way across to the middle cushion but not fully extending outwards to the front of the seat cushions. The fabric on the arm of the couch also burns through exposing, and subsequently burning, the frame and eventually dropping burning fuel onto the floor. Some burning is observed underneath the couch, but significantly less than in the other tests. As the fire progresses further, flames are observed on the outside of the seat cushion, propagating across the back of the couch and extending to the back middle cushion. At this stage, the fire becomes ventilation-controlled and begins to reduce in size. This slower pattern of fire growth and spread is evidenced by the initial growth, followed by an apparent plateau in the MLR curves of Figure 5-19.

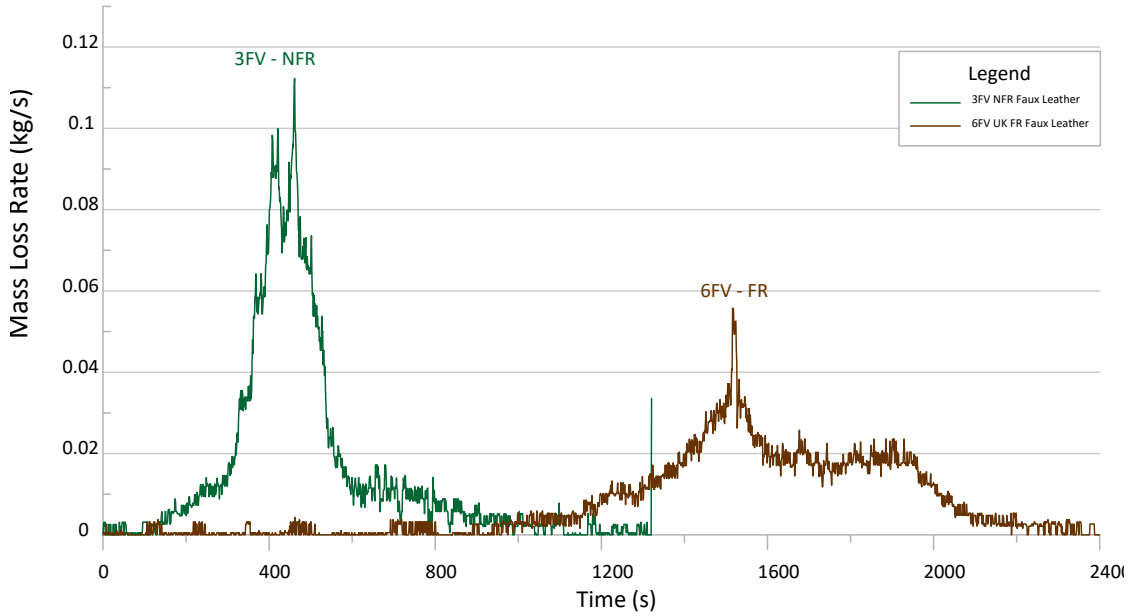


Figure 5-19: Comparison of MLR in NFR and FR faux leather couches.

The overall MLR of the FR couch in Test 7FV is compared to that of the NFR couch (Test 4FV) in Figure 5-21. Overall trends in the pattern of burning are similar, with clearly slower fire growth and 20-25% reduced peak MLR for the FR couch (Test 7FV), even though a much larger Crib 7 ignition source is needed to ignite the couch in Test 7FV. The FR couch's time to peak MLR is 720 seconds compared with 629 seconds after ignition. This is in part due to the difference in fire growth times of 259 seconds versus 370 for the NFR and FR couches, respectively. These observations further support a primary conclusion that the FR couch materials lowered and delayed the peak MLR, as shown in Figure 5-21, and similar to results obtained in the 2015 UWFRL tests described in Section 2.5.2.

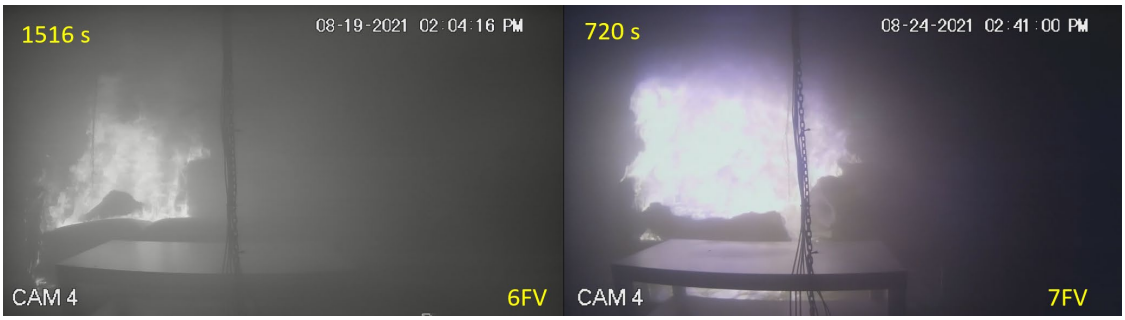


Figure 5-20: Video capture at peak MLR time for UK FR couches.

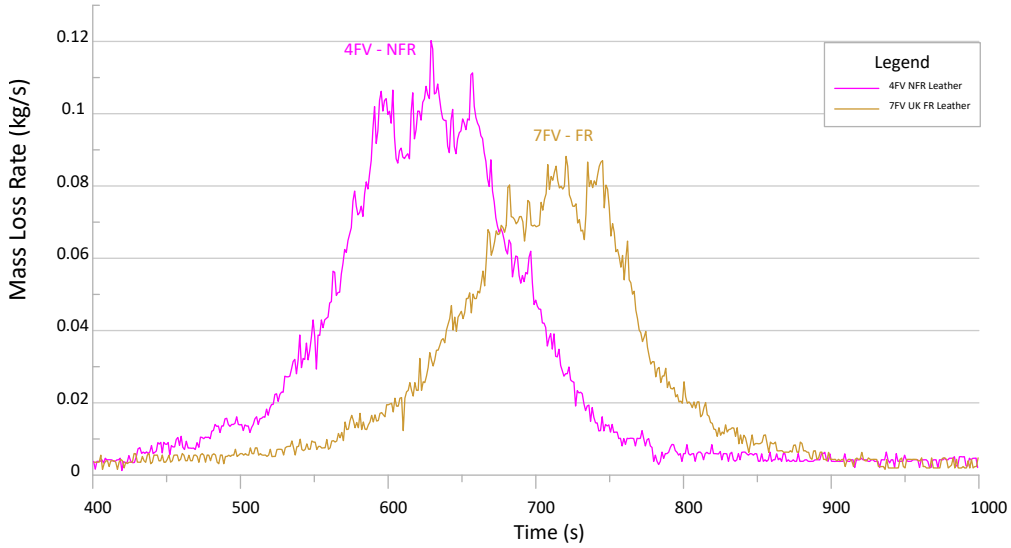


Figure 5-21: MLR comparison of Tests 4FV and 7FV.

The faux leather US FR Test 9FV couch ignites using a wood ignition Crib 7. The fire first burns through the back cushion until that cushion is fully involved, but at the same time, it propagates across to nearly the front of the seat cushion, with burning debris dropping onto the floor. After the incipient period, the fire grows quickly, resulting in flames that propagate to and along the ceiling. Under the heat load, the fabric covering the middle back and seat cushion visibly crumples and peels

away from the seat cushion, exposing the PU foam slab underneath and allowing the fire to propagate on the surface of the seat cushion to the opposite end of the couch, as shown in Figure 5-22. In this fire, the comparatively limited thermal performance of the fabric cover appears to be a significant contributing factor in the fire growth and propagation, resulting in the most extensive and largest fuel mass loss of all tests.



Figure 5-22: Video capture at peak MLR for US FR faux leather couch.

In addition to the above observations of fire development and spread, it is useful to examine the overall fuel mass loss that occurred in each of the above fires. Figure 5-23 illustrates the total mass reduction with time for each fire to show this in more detail, while Figure 5-24 provides an overhead perspective of the post-test damage to all couches. There is a clear differentiation between the amount of mass consumed between the NFR and FR couches in Tests 2MV and 5FV, particularly since the cloth couch in Test 5FV does not sustain flaming combustion even with ignition using the largest wood crib ignition source. Similarly, considerably greater mass remains after burning of the faux leather FR couch in Test 6MV in comparison to the faux leather NFR couch in Test 3FV, where two-thirds of the couch burned away completely, and there is considerable mass lost from the remaining 1/3 of the couch as well. The largest mass loss of any of the comparable couches occurs for the couch in Test 3FV. Only the fire using the couch in Test 9FV, which underperformed relative to expectations, results in a higher mass loss, illustrating a possible limitation of poorly performing fabric covers in terms of overall fire growth and spread. This is consistent with the poor relative performance observed for one of the FR cover fabrics in the 2015 UWFRL test series.

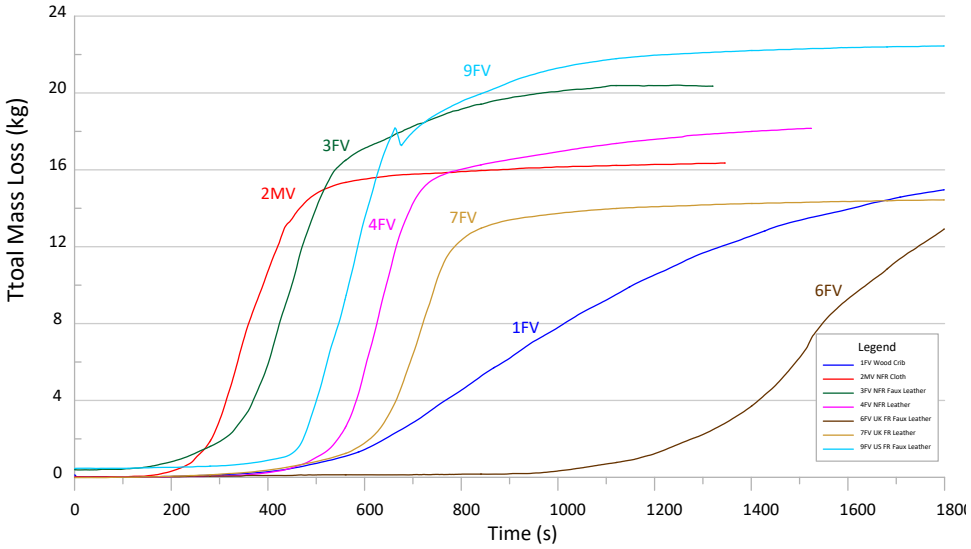


Figure 5-23: Total mass of each couch consumed by test.

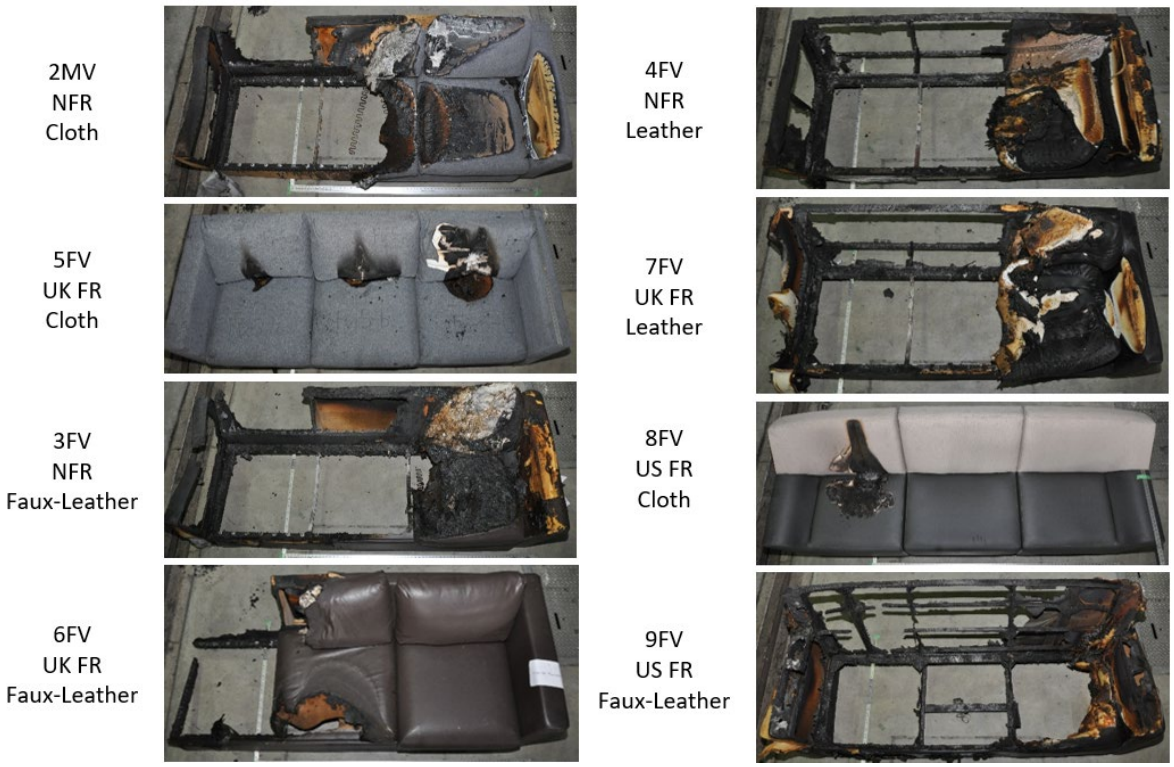


Figure 5-24: Comparison of couch damage for all tests.

Based on the above discussion, key observations relative to the performance of the couches during the growth stage of the fires are as follows:

1. Fires established on all of the NFR couches exhibit much higher growth rates and values of peak MLR in comparison to the slow-burning wood crib fire with a moderately long incipient stage,

very long growth stage and considerably lower MLR. This illustrates the significant difference in fuel volatility between a material such as wood and the foamed plastic materials used in couches.

2. Burning that takes place due to the drop down of fuel to the floor appears to contribute substantially to the overall fire development in all NFR tests, the leather FR test, and the US FR faux leather test. In contrast, there is very limited drop-down of burning fuel with the FR faux leather couch in Test 6FV, which had an interliner. This test has the most comparable test results to that of the wood crib in Test 1FV. The fire fueled by this couch has a long incipient time and a long fire growth time and is characterized by the lowest MLR and overall least total mass loss. The directly comparative fire in Test 3FV has a shorter incipient time, faster fire growth time, and a higher peak MLR.

3. Protective membranes built into the NFR couches are seen to either lengthen the incipient phase and/or slow the fire growth rate, which delays the time taken for the fire to grow to peak MLR values. Despite the differences in development time, the final values of peak MLR in the fires are not remarkably different across the tests. However, irrespective of the similarity in final fire size, the slower developing fires may delay the time to loss of visibility within a structure.

4. In comparing the NFR and the FR leather couches in Tests 4FV and 7FV, both without an interliner, the burning behaviour may be impacted by the larger ignition source for the FR couch, but otherwise, the two couches appear to have comparable incipient fire times. Following this, the FR couch exhibits a slightly longer growth time, a lower peak MLR, and correspondingly lower total mass loss. Whether the additional time afforded by the protective measures in the FR versus NFR leather couches is of benefit during an escape from the fire will be addressed later in this thesis.

5. The three best-performing couches are constructed with interliners (5FV UK FR cloth, 6FV UK FR faux leather, and 8FV US FR cloth). In these couches, interliners are wrapped fully around the foam slab before the fabric cover is installed so that the interliner encapsulates all sides of the cushion foam, including the bottom. This appears to reduce the potential for fuel to drop down while at the same time limiting the acceleration of fire growth on the underside of the couch. In contrast, the fires on all of the NFR, the UK leather, and the NA faux leather couches, without interliners, result in drop-down burning on the floor. In these cases, any protection associated with the leather cover or the treatment of a fabric wrap may be negated due to the discontinuity of protection on the underside of the cushions. As shown in Figure 5-25, the leather (Test 7FV) and faux leather (Test 3FV) couches have different covers on the back, 2/3 of the cushion and the seat, though this could not be confirmed for Test 9FV. These changes in cushion covering materials likely allow the fire to penetrate the foam cushions more readily, thereby accelerating the overall fire growth.



Figure 5-25: Top - seat cushions with lightweight cloth fabric at the back of the cushion for leather and faux leather couches, (Bottom) Back cushion with lightweight fabric on the back.

5.6 Detector Response Times

The detector response times of the Mircom and Vesda systems for each test are provided in Table 5-5. A cable to the photoelectric detectors on the lower level failed in Test 7bFV; therefore, photoelectric detection times are unavailable for the three detectors during this test. Similarly, in Tests 3MV and 4FV, complications occurred with the air aspirated system due to sensor error issues, which limited the data to one device in Test 3MV and resulted in no data for 4MV. Due to the fouling of the sensors and potential soot accumulation within the air tubes associated with the multiple tests, the test procedure was modified to shut down the detection of the air aspirated system after all of the devices responded. This limited the amount of soot fouling that occurred within the tubes and sensors in future tests.

Table 5-5: Response time of detectors.

Detector Location	System	1MV	2MV	3MV	4MV	1FV	2FV	3FV	4FV	5aFV	5bFV	5cFV	6FV	7aFV	7bFV	8FV	9FV
1	Mircom	122	141	107	125	488	16	127	403	97	268	313	138	242	E	149	353
	Vesda	141	140	133	129	436	124	153	N	153	338	293	200	214	297	151	314
2	Mircom	147	159	137	131	525	36	133	415	128	292	325	185	243	E	185	365
	Vesda	210	203	E	197	496	124	225	N	225	166	354	200	265	361	211	363
3	Mircom	177	189	173	173	537	37	183	433	691	430	385	748	758	E	305	407
	Vesda	210	203	E	197	496	53	225	N	225	461	354	559	617	361	344	495
4	Mircom	279	291	275	281	764	103	306	N	DNA	DNA	1634	1326	DNA	642	DNA	521
	Vesda	339	335	E	327	628	124	356	N	DNA	DNA	873	1329	DNA	DNA	DNA	626
5	Mircom	234	273	276	233	981	106	299	581	DNA	DNA	1652	1260	DNA	557	990	479
	Vesda	339	335	E	327	628	124	225	N	DNA	DNA	1004	1065	DNA	491	344	495
6	Mircom	261	279	239	263	748	109	289	577	DNA	DNA	DNA	1250	DNA	604	DNA	528
	Vesda	339	464	E	327	628	124	225	N	DNA	DNA	DNA	1197	DNA	491	DNA	495
		E - Device Error or Equipment Malfunction						N - Device Not Used (Fouled Sensor)						DNA - Did Not Activate			

The response times are presented graphically in Figure 5-26 for visual comparison by system, test number, and detector location. It should be noted that these times should be considered relative as they do not account for the approximate 42-second travel time due to the 30 m length of tubes going

back to the sensor box on the VESDA system or the fact that both technologies could be readily adapted to detect at lower levels of smoke obscuration. In general, the detector response times between the two systems follow similar trends in the sequence of detector response, but there is variability as to which system responds more quickly depending on overall fire development. In the faster-growing fires, including those on all of the NFR (except 4FV where the Vesda is not used) couches, the D1 photoelectric spot detectors of the Mircom system respond first, except for Test 2MV where the air-aspirated Vesda system responds 1 s faster. In contrast, the VESDA responded faster in the wood crib tests and in the FR furniture Tests 5cFV, 7aFV, and 9FV.

The first system to respond on D1 does not necessarily correlate with the system with the fastest response for the other detectors in the house. For example, in Test 6FV, the Mircom spot detector responds at 138 s for D1 versus 200 s for the VESDA, but the difference in response time between the two systems at D2 is only 15 seconds, and the VESDA responds 151 seconds sooner than the Mircom at D3. Similarly, the VESDA responds 39 seconds sooner at D1 in Test 9FV, but the detection times are only 2 seconds apart at D2, and the Mircom spot detector responds 88 seconds sooner at D3. Mircom spot detectors respond much sooner in Test 2FV with the heptane pan, but only on the lower floor. Detection times are nearly identical on the upper floor for the same test. The reverse is true for the more slowly developing wood crib fire in Test 1FV, in which the Vesda responds much sooner on both levels.

For purposes of this study, the photoelectric smoke detector response data will be used since they are one of the common technologies currently used in houses and, therefore, the most appropriate comparative device. The response of the VESDA system will be used for Test 7bFV due to the cable failure to the photoelectric detector in that test and given the relative consistency in detector response by location between the two systems.

The timeline sequence of response times for the MV test series, in which the same cloth couch is burned with slightly varying ventilation conditions, is provided in Figure 5-27 to indicate the variability of detector response for tests with relatively small differences in the fire development on the couch. An average response time on the order of 124 seconds is observed for D1, 144 seconds for D2, and 169 seconds for D3. Since this data does not account for local variations in smoke evolution at the detectors due to specifics of fire development, it illustrates a wider range of detector response times for each individual detector than would be expected if these variabilities could be accounted for.

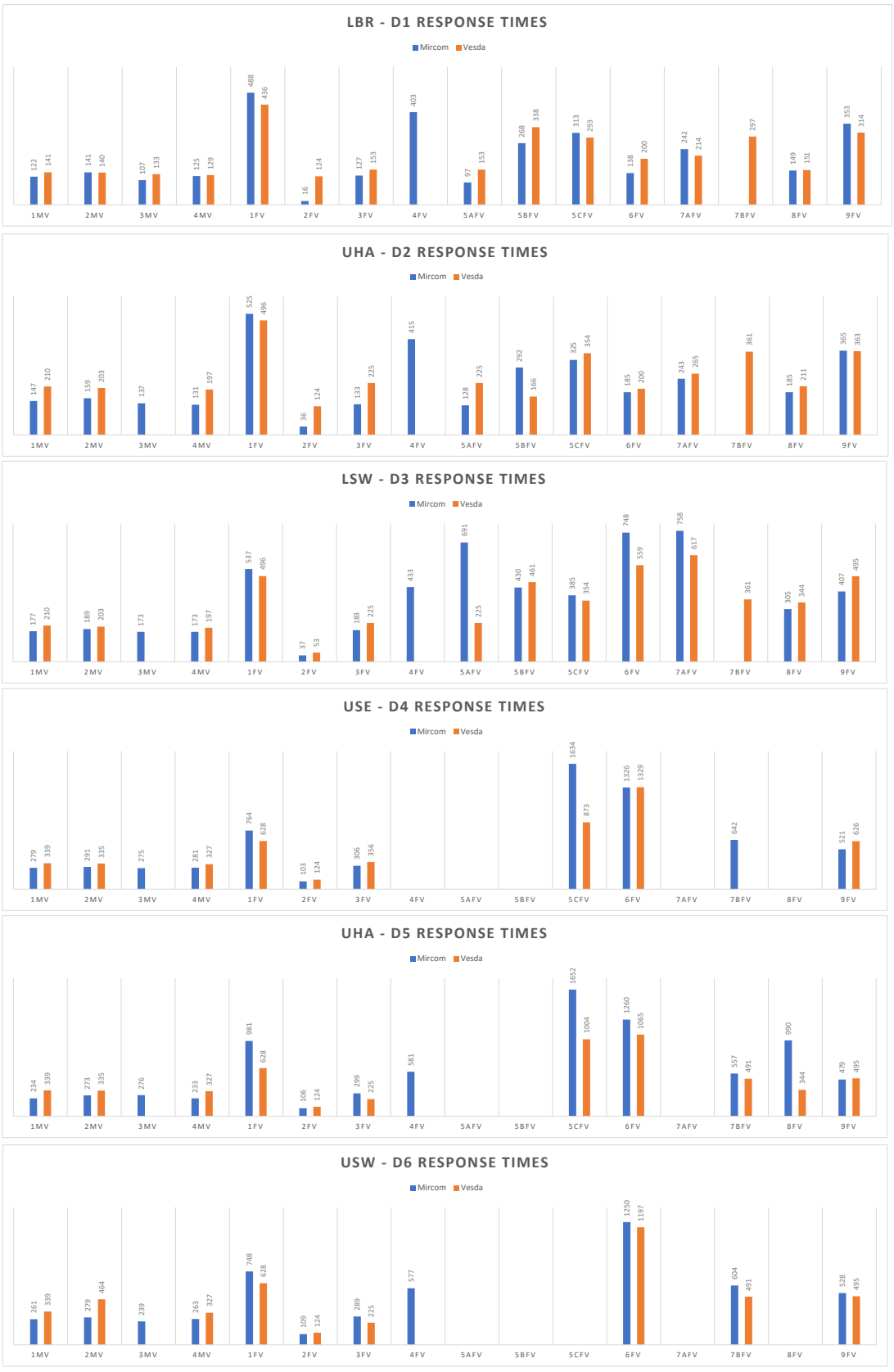


Figure 5-26: Summary of Detector Response times for Mircom and VESDA Systems for Detectors D1 to D6.

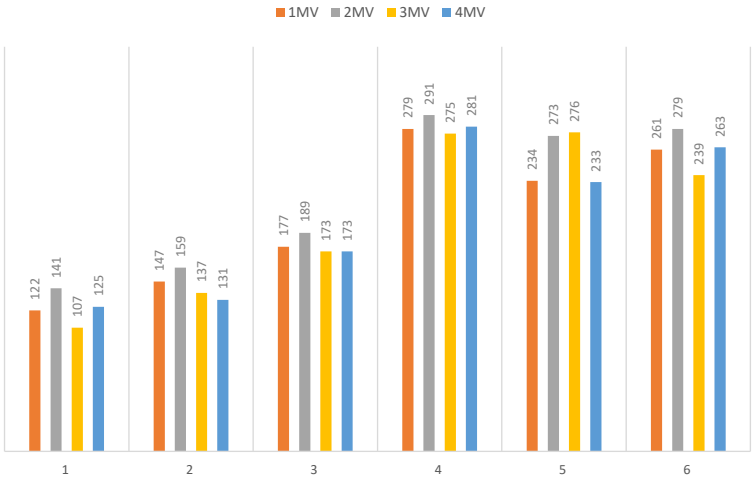


Figure 5-27: Fire detector response times for MV test series.

To address the sensitivity, a review of the D1 response in Figure 5-27 is compared to and adjusted for the length of incipient fire development in the corresponding tests. While the raw data shows that there is a 38 s range in response, this range narrows to only 5 s when the detector response time is referenced to the differences in the length of the incipient fire stage. Applying the same correction reduces the variability in response at D2 to approximately 21 s and 15 s for D3, as tabulated in Table 5-6. Thus, the differences in detector response time across the MV series of tests appear to be linked directly to the differences in incipient fire time at D1 and D2, while less so at D3. This highlights the significance of the incipient stage, or more specifically, the time to start the fire growth stage, in interpreting results relative to emergency egress time. Applying the same approach to results from all remaining tests, also included in Table 5-6, indicates that for faster-growing fires, detection also aligns to either just near or slightly after the transition from incipient to growth stages of the fire.

In contrast to the cases above, the first detector response times in Table 5-6, shown with red shading for Tests 1FV, 4FV, and 9FV, indicate first detector responses (D1) well after the transition from incipient to growth stage, suggesting definite differences in the evolution of smoke to the detector in these fires. The wood crib is a distinct case in this respect, as discussed later. However, the implications of this in Tests 4FV and 9FV should be considered in concert with the fire growth time, as outlined in the MLR discussions above. For these tests, although the incipient fire time is quite long due to the leather and FR fabrics (as shown in Figure 5-17), the time of fire growth to peak MLR is quite short and the corresponding peak MLR is relatively high. The delayed time for fire detection in this situation, then, has the potential to negate any benefit derived from the fabric coverings and the offset that they create in terms of overall fire development. Given the short growth time to peak MLR, summarized in Table 5-4 for these two tests, the correspondingly fast smoke filling is likely to occur in these fires, suggesting that escape times (after detection) may also be lower for these two couches.

Thus, despite the NFR leather couch demonstrating a delayed fire growth and the US FR faux leather couch being chemically treated with flame retardants, it may be difficult to realize any benefit toward reduction in escape times given the smoke detector response. This issue will be explored further in subsequent sections through a more detailed analysis of smoke evolution and gas generation.

Table 5-6: Adjusted detection time accounting for the incipient stage of fire.

Test Number	Primary Fuel	Ignition Crib Size	Incipient Stage (s)	D1 (s)	D2 (s)	D3 (s)	ΔD1 (s)	ΔD2 (s)	ΔD3 (s)
1MV	NFR Cloth Couch	Crib 4	128	122	147	177	-6	19	55
2MV	NFR Cloth Couch	Crib 4	142	141	159	189	-1	17	47
3MV	NFR Cloth Couch	Crib 4	113	107	137	173	-6	24	60
4MV	NFR Cloth Couch	Crib 5[2]	128	125	131	173	-3	3	45
1FV	Wood Crib	Crib 5	328	488	525	537	160	197	209
2FV	Heptane Pan	Spark	0	16	36	37	16	36	37
3FV	NFR Faux Leather	Crib 4	130	127	133	183	-3	3	53
4FV	NFR Leather	Crib 5	370	403	415	433	33	45	63
6FV	FR Faux Leather	Crib 4	998	138	185	748	-860	-813	-250
7bFV	FR Leather	Crib 7	350	297	361	361	-53	11	11
9FV	US FR Faux Leather	Crib 7	331	353	365	407	22	34	76

Conversely, during the UK FR faux leather and UK FR leather couch fires in tests 6FV and 7FV, smoke is detected during the incipient stage or very nearly thereafter (11 s), as shown by the yellow cells in Table 5-6. In the case of the UK leather couch, D1 activated 53 s before the transition to fire growth. Compared with the NFR leather couch, this is an 86 s difference in time to the first detection, potentially contributing to earlier escape time. This increase in escape time due to earlier detection at D1 is 857 s when comparing the two faux leather couches, which is directly related to the long incipient phase for the UK couch. However, similar to the leather couches, the time differential decreases to 303 s for the D3 location, likely due to the slower generation and propagation of smoke during the incipient fire to the adjoining room. The differences in D1 and D3 activation are further discussed below.

5.6.1 Detector data for purposes of determination of escape time

The determination of available safe egress time (the ASET) is predicated on a smoke alarm being the first cue to initiate awareness of fire and reaction by occupants, under the assumption that occupants are sleeping. In a house fire situation, since the NBCC does not require detectors to be located throughout the lower level of the house, relying on detection times measured by detectors that are in close proximity to the fuel source provides an overly optimistic expectation of potential response time, whereas considering only detectors on the upper level of a house would provide an overly

pessimistic timeline, especially given current requirements to interconnect detectors throughout a house.

The present results show a consistency in detector response as located in the burn structure. Not surprisingly, D1 responds first, followed by D2 and D3. Timing aligns with the proximity to the fire and the presence of the door threshold between the LBR and the LSW rooms. Specifically, there is no door threshold between the LBR (D1) and LHA (D2), and the ceiling is flush between these spaces. Thus, LHA D2 responds to the presence of the fire shortly following the LBR D1 detector as expected. In contrast, a threshold between LBR (D1) and LSW (D3) delays the activation of D3 since sufficient smoke has to accumulate in LBR to descend below the door threshold and enter LSW. It potentially follows that response times measured by D3 are the appropriate selections for evaluating escape time since they are representative of delayed conditions before smoke accumulates at a detector that is neither overly optimistic nor pessimistic and is representative of the NBCC requirements. The time delay associated with the response of D3 after D1 for faster-growing fires averages approximately 49 s, with the range being 21 to 66 s, not accounting for the very long time obtained during the slower UK FR faux leather fire, but including detection time for the wood crib fire. On this basis, the response time for D3 across all fire tests is graphically illustrated in Figure 5-28. It will be used later for the determination of a baseline escape time in consideration of the sensitivity of response to the positioning of a detector[7].

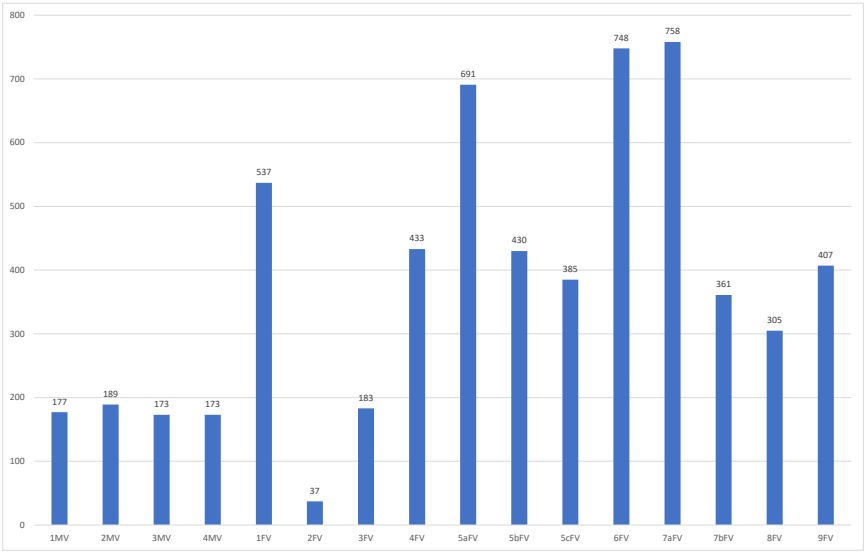


Figure 5-28: Graphical illustration of D3 response times for MV and FV test series.

[7] Test 2FV is a heptane test and therefore has the earliest (shortest) detection time aligning with the rapid fire growth of a liquid fuel. This value is included for the reader's reference but is not directly comparable to those for the other solid fuel fires.

5.6.2 Summary of observations relating to fire detectors

The key takeaways from the review of the detection data, aside from establishing times for initiation of escape, are:

- Detectors activate in the sequence anticipated on the lower floor and can be used to establish the basis for notification of occupants in the determination of available comparative escape times.
- D3 is determined to be the most appropriate detector to use as a lower bound for the start time for escape. This results in a potential delay on the order 49 s for faster growing fires, and much longer for fires with a prolonged incipient stage, which only applies in one instance in this test series.
- In some instances, parameters anticipated to limit fire growth on the couches do not translate into earlier detector response, potentially negating the benefit (e.g., Tests 4FV and 9FV). However, other couches with fire controls (Tests 6FV and 7FV) result in earlier fire detection when compared to the reference NFR tests, suggesting a benefit of potentially increasing overall escape time.
- No particular inference is identified that differentiates variations in response time attributable to the presence or absence of flame retardants. The detection response of fast-growing fires aligns well with the transition from incipient to fire growth, irrespective of flame retardants.
- Variability in detector response times is found to be primarily associated with the duration of the incipient fire. When detection time is adjusted to consider the length of the incipient fire stage, the detector response times are very close for nearfield D1. The gaps in response time widened for detectors located further away from the fire. However, a definitive comparison is much more difficult at further distances, given potential variations in airflow currents, amongst other factors.
- Good agreement in trends of response time is observed between the Mircom spot detectors and the VESDA air aspirated detection. The spot detectors are observed to be advantageous for faster-growing fires, likely due to proximity to the growing smoke layer. The VESDA is observed to be effective in slower and cooler fires, likely since there is a greater dispersion of cooler smoke throughout the space, leading to a less prominent smoke layer at the ceiling.

The following section will explore the relationships between fire growth, smoke evolution, and potential egress time in more detail.

5.7 Smoke Layer Development

The following sections describe the smoke layer descent through the test house for each test, with a view to establishing the time when the smoke layer height reaches 1.5 m, 0.9 m above the floor (commonly referred to as AFF for "above finished floor"). Video time is recorded in minutes and seconds, so reference is made accordingly to match the timer as it appears on the video. References to cameras are depicted by a C#, which corresponds to the CAM# in the video. In addition to the documentation in this section, which is more refined around the time of smoke layer descent, exports of test videos at 1-minute intervals of the wood crib and couch fires are included in Appendix A and provide the whole fire timeline for reference.

5.7.1 Wood Crib Fire Source – Test 1FV

After ignition of the large wood crib, an extended period of time is taken for the fire to grow significantly, as illustrated in the time-interval capture provided in Figure 5-29. At 05:00 after ignition, the crib shows flames out the top. At 10:00, the fire progresses to the entire width of the wood crib, with a peak height of flames occurring between 12 and 16 minutes. After this, the fire size noticeably declines to 26 minutes, when the fire is mainly glowing with only small flames near the surface of the remaining wood.

Corresponding to the fire's growth with time, limited smoke builds up within the LBR until about 10:00 when a light smoke layer is accumulating dominantly above the fire and is not necessarily uniform across the room, as evidenced by the checkerboards in C2 compared with C1 and C7 at 10:00. The smoke cloud is translucent, allowing some of the checkerboards to be discernable through the smoke.

All camera perspectives show the smoke layer progressing downward through to 12:00 after ignition, but by 14:00, the smoke layer interface is no longer discernible, and instead, there is a relatively uniform smoke dispersion, or a "haze" of smoke, throughout the space. This is evident in C1 at 16:00, which shows W2 and the checkerboard becoming much more visible, and in the minutes that follow, the smoke appears relatively uniform throughout the space. The smoke then continues to thicken through the entire space as the fire self-extinguishes, presumably due to oxygen depletion. In summary, the wood crib fire is slow to develop, and the smoke layer does not remain as a stratified layer. Instead, it quickly goes from being a smoke cloud to a mixed haze throughout the space, with similar visibility through LSE and LHA.

By comparison, compartments on the upper level, shown in Figure 5-30, stay relatively clear of any smoke until between 8 and 9 minutes after ignition. Smoke is first observed near the floor in USE and UHA without evidence of the formation of an upper smoke layer or interface height marking the smoke-air transition in the compartments. This seems to suggest that the smoke travels as a cloud and mixes when going up the stairs – potentially cooling down and becoming less buoyant. Visibility in the USW room deteriorates next, with smoke evident shortly after 10 minutes. Visibility is lost in the USE and UHA by 13:29 and in USW by 19:50. Objects are no longer discernable by this time, but lights from the cameras operating in night mode remain visible through the duration of the test, and recirculating smoke and particulate are still observable in all upper level cameras through the duration of the test. It should be noted that the absence of lighting on the upper floor compared with the lower floor, which was lit by light from the windows and from the fire itself, likely impacts the apparent degree of translucency of the smoke layer and the ability to discern objects in these areas as well.

In summary, the smoke layer in the wood crib fire does not stratify into a distinct smoky upper and clear lower layer as originally anticipated. Instead, the smoke forms and mixes, becoming somewhat uniform through the whole height of the lower level. Camera visibility on the lower level is never fully lost, and sight lines in all rooms allow for visually distinguishable furniture and equipment from all camera angles in the burn room. Comparatively, visibility is lost on the upper level of all cameras. Further, the absence of a clearly marked smoke layer precludes the determination of the smoke layer height necessary for defining visibility along an escape route as was originally envisioned.



Figure 5-29: Test 1FV showing select intervals of the burn room quad video.

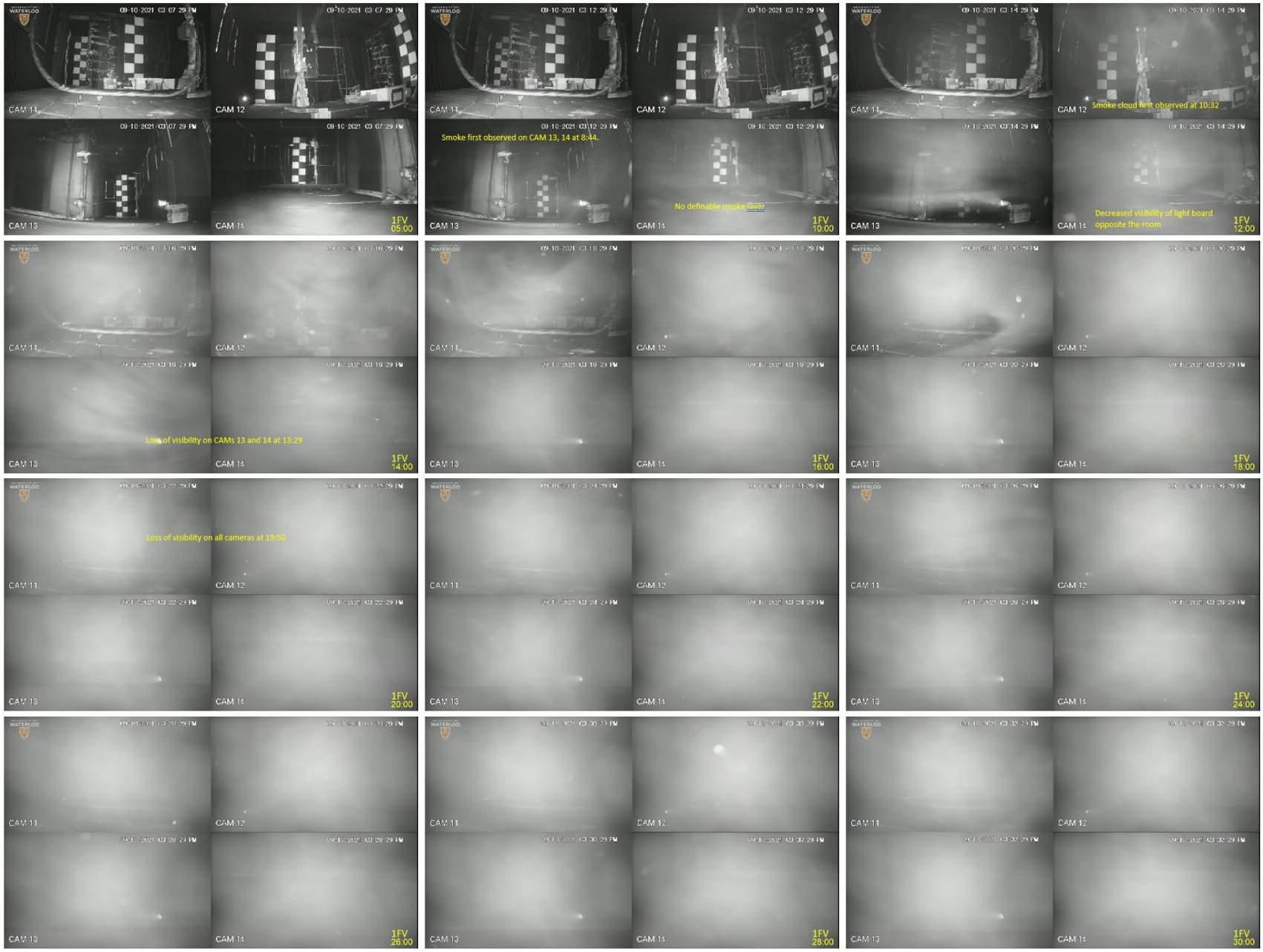


Figure 5-30: Test 1FV showing select intervals of upper level quad video.

5.7.2 Smoke Layer Development with the NFR Couches

In Test 2MV, after ignition, the Crib 4 initiating source penetrates the polyester cloth cover and ignites both the seat and back pillow cushions within the first minute. Between 1 and 3 minutes, the back pillow cushion cover fabric continues to increasingly participate in the fire, as shown in Figure 5-31. The vertical flame from the initiating wood crib, which is positioned near the back of the seat cushion, favours propagation of the fire to the back pillow cushion first until greater penetration and extension can occur into and on the seat cushion. The cover fabric of the back pillow does not resist ignition and readily opens to expose the loose polyester fill that makes up the inside of the cushion. This readily accelerates the burning. As the fire size increases, the fire extends horizontally across the seat cushion in a pattern radially from the location of the igniting wood crib. This burns away the cloth fabric on the surface of the seat and ignites the PU foam slab in the cushion, allowing both the leftmost seat and back pillow cushions on the couch to become fully involved.

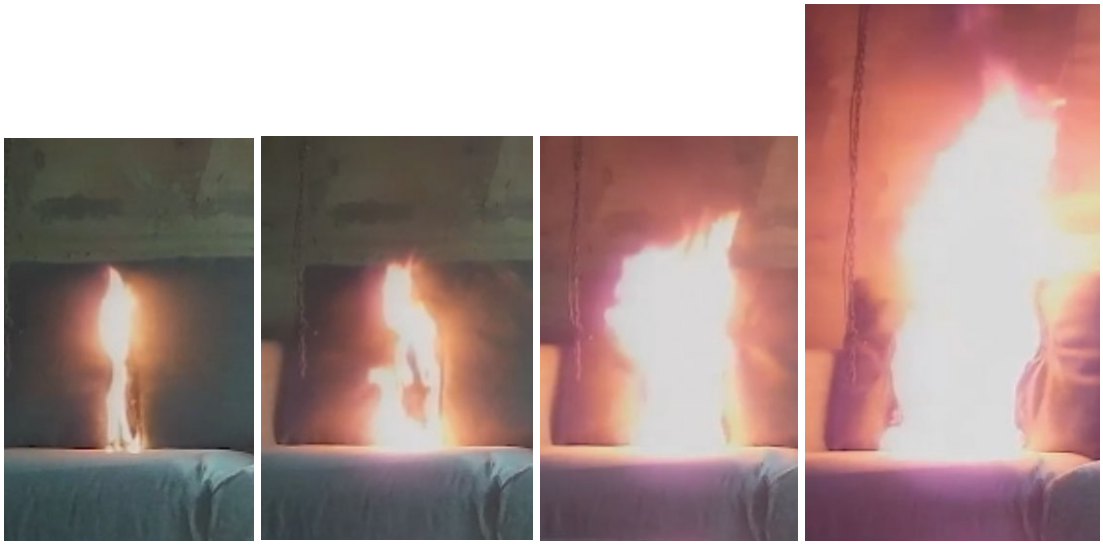


Figure 5-31: Test 2MV, C4 partial images at 1:00, 2:00, 2:30, and 3:00 show fire progression on the seat cushion.

A smoke layer develops on the ceiling of the LBR by approximately 02:17 after ignition. The smoke layer descends to 1500 mm at approximately 03:31, as shown in Figure 5-32. By 04:00, the fire involves the entire back cushion and has propagated across most of the seat cushion. Figure 5-33 shows the quad for the burn room and Figure 5-34 shows the upper level quad for reference.

and 80 capture clips at different intervals for the burn room and upper level quad videos from 04:00 to 06:45, which is the critical time window for this test. Additional 1-minute video captures of the 2MV test are included in Appendix A.



Figure 5-32: Test 2MV at 211 seconds after the start of the fire when the smoke layer reaches approximately 1500 mm.

From 04:00, visibility deteriorates over the next two minutes through the whole house. The smoke layer in the LBR at 04:00 is relatively horizontal, as overlayed with the dashed yellow line on C2 in Figure 5-33. At this point, most of the top side of the seat cushion is burning along with the back cushion, extending to the arm of the couch but not yet involving the middle cushion. The smoke layer descends low enough that it starts to interact with the flaming region of the fire. Burning fuel drops down and burns on the floor below the couch at 04:10, continuing to burn on the floor for the duration of the fire. Above the couch, flames extend to a level even with the top of the W1 frame and intermittently to the ceiling.

From the images captured by C2, the smoke layer interface starts to descend lower on the west side of the room opposite the fire at 04:15 after ignition, sloping downward as illustrated by the superimposed yellow line on C2 in Figure 5-33. In C4, it further descends within the room into the flaming region of the fire on the couch and reaches the top of W1 at 04:30. Simultaneously, the interface line between the upper and lower layers becomes less defined. Following C2 from 04:45, where the smoke layer first starts to collapse to 05:15 into the test, the smoke layer interface transitions from sloped downward toward the west, to losing all visibility on the west side of the room and then increasingly losing visibility towards the fire until all visibility is lost on the camera at 05:30.



Figure 5-33: Test 2MV showing select intervals of the burn room quad video.

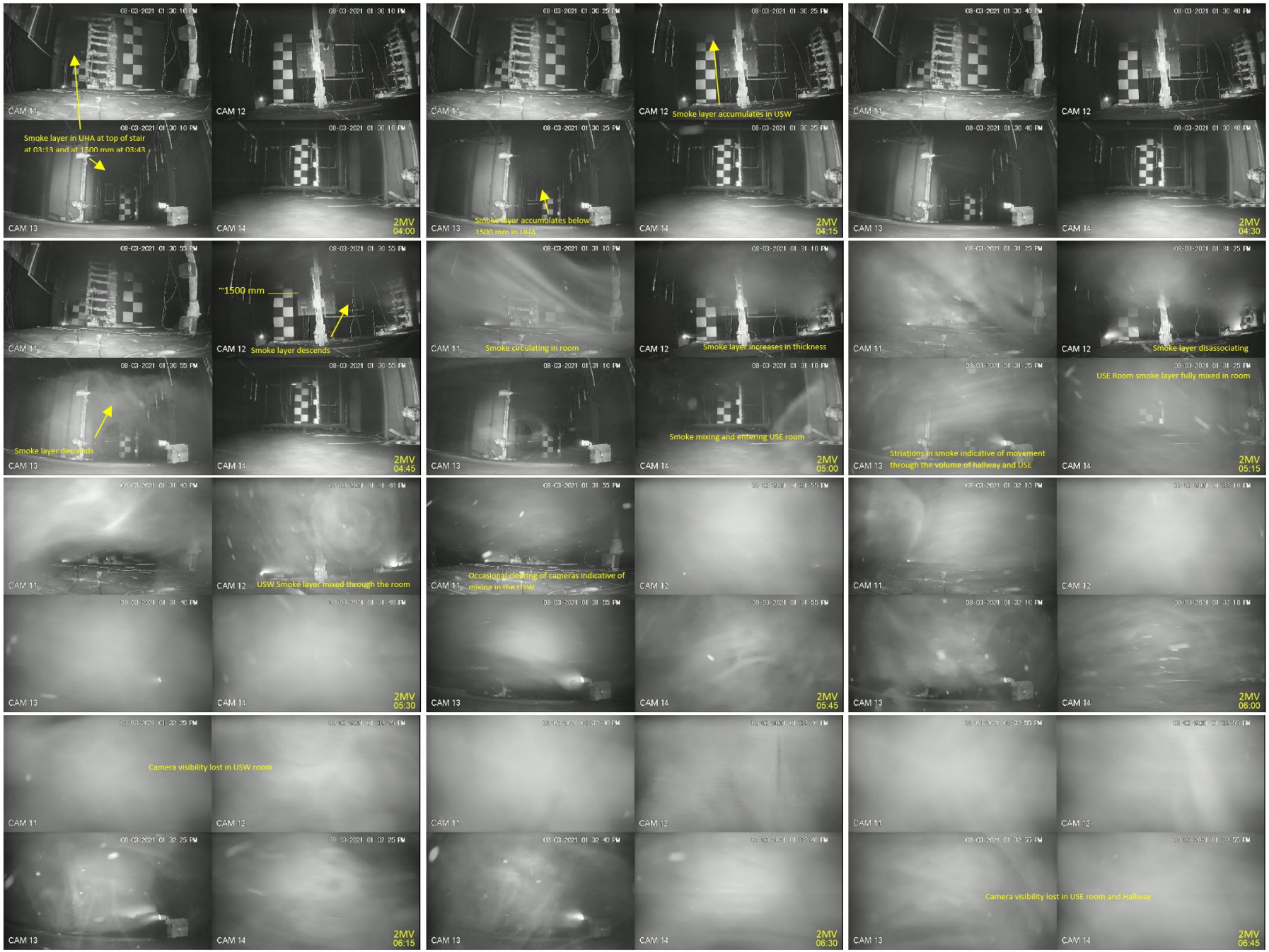


Figure 5-34: Test 2MV showing select intervals of upper level quad video.

During this same time window, the flames extended to the middle back pillow cushion at 04:15 and the middle seat cushion on the top surface at 04:45, propagating across the surface of both the seat and pillow cushions by 05:30. At 05:45, the left seat cushion falls to the floor and burning takes place underneath the bottom half of the couch. At this point, visibility within the lower level has mostly deteriorated, and only the flaming region is visible in the cameras.

As the room conditions deteriorate around the fire and smoke builds from ceiling to floor, the smoke layer gradually pushes into the flaming region of the fire, reducing visible flaming and eventually leading to self-extinguishment of the fire. Described another way, the video captures an “encapsulating and smothering effect” of the smoke layer as it extends from the perimeter into the burning regions of the fire. Rather than the smoke layer descending from the ceiling in a horizontal layer down over the fire until the fire burns within the smoke layer, the smoke descends to the floor around the perimeter of the fire, and then the surrounding volume of smoke pushes into or encapsulates the burning region of the fire.

The same observations of smoke layer evolution are observable on C1 and C4, which are located at a lower position above the floor and within the burn house. From C4, during the same time period, the smoke layer interface is observed on W1 as slightly sloped to increasingly sloped toward the south end of the house (right side of the image). The windows are advantageous in determining the smoke layer height due to the uniform backlighting that distinguishes the layer and illustrates the angle. From this perspective, the encapsulation and smothering effect is observed from south to north. On C1, W2 decreases visibility on both sides (possibly due to the proximity of room corners), creating a bending of the smoke layer with increasing smoke density on the room's west side (right side of the image). The resultant smoke observations align again with observations from the C2 video captures that indicate that smoke descends down the walls on the west side of the burn room and then turns back towards the fire, encapsulating and smothering the fire. These interesting interactions between the smoke layer and the fire plume are observable from three camera perspectives, all with different lighting from the fire. This is substantially different from the more simplified smoke filling dynamics in the literature described by Mowrer [90] or Karlsson and Quintiere [92].

Also observed in video images from the other cameras is the collapse of the smoke layer interface, which results in no clear delineation between the upper and lower layers. C7 provides the perspective from the end of the hall and shows the progression of the breakdown of the smoke layer interface, which initially takes on the appearance of smoke leaking from the upper to the lower layer, followed by progressively increased mixing between the layers until the smoke appears fully mixed. This is annotated in images from C7 and C2 in Figure 5-33 and aligns with the same time period as the smoke layer encapsulation of the flaming region. The smoke layer's collapse point is shown in more detail for the lower level quad in Figure 5-35, as is observable in C6, C7 and C8. The interface is maintained at the

LBR and LSW doorway, as shown on C5. However, visibility is lost on all cameras by 05:47, as shown in Figure 5-36.

Ultimately, the smoke layer interface never descends to 900 mm in the LHA prior to significant smoke mixing from the upper to the lower layer. This makes the concept of defining a "crawl-out" period, where the smoke layer interface remains above 900 mm, not demonstrable or workable. Instead, there is a transitory period of smoke layer collapse, during which mixing between the upper and lower layer progressively increases. During this time, smoke and other contaminants can increase in concentration in the lower layer until the interface is no longer present and the lower layers are more clearly filled with smoke. As a consequence, and considering the similar observations in Test 1FV with the large wood crib fuel source, determining the time between the smoke layer interface descending to 1500 mm above the floor and the loss of camera visibility may be preferable in defining an escape period. During this time, there will most likely be an increasing at-risk component as the smoke mixes, affecting visibility and leading to increasing CO and CO_2 concentrations throughout the lower 900 mm escape path (through the LBR and out the LHA).

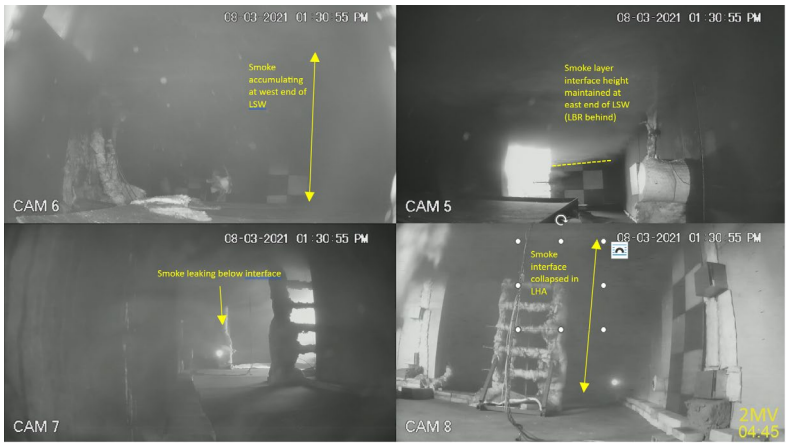


Figure 5-35: Lower level quad showing smoke layer collapse in LHA at 04:45.

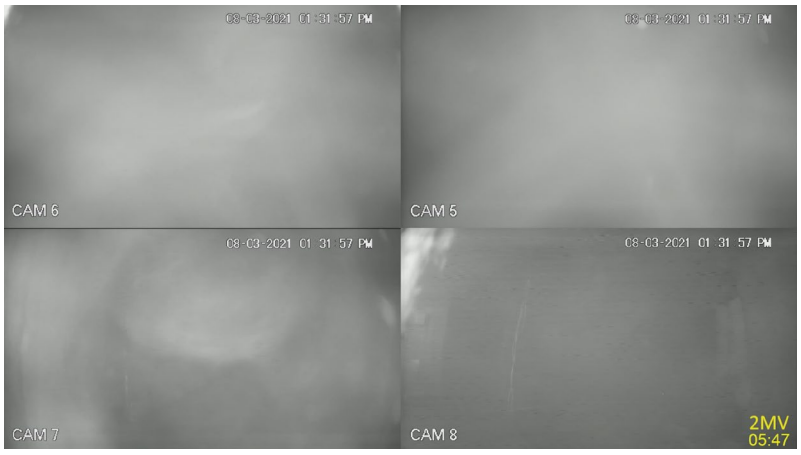


Figure 5-36: Lower level quad showing LL Vis. Lost at 05:47.

On the upper level, smoke first reaches the top of the stair shaft at approximately 03:13 and then reaches 1500 mm at the top of the stair shaft at 03:40. Figure 5-34 shows the conditions at 04:00 through 06:00 and the progressive deterioration of visibility conditions on the upper level. At 04:00, smoke is accumulating at the top of the stairs below 1500 mm and into the USW by 04:15. The smoke layer continues to descend in both spaces at 04:30, but by 04:45, evidence of smoke layer collapse is present in UHA, and smoke is propagating into the USE. By 05:15, smoke is mixing through the entire upper level, and no discernable smoke layer is visible on any of the cameras. Visibility on all cameras is lost by 06:35. Prior to this point, mixing allows for occasional clearing of the cameras. The visibility at the top of the stairs and within the stair enclosure is difficult to quantify with the current test rig and camera angles. A stratified two-zone smoke layer is only present at the top of the stairs for a short period of time, following which determination of the layer height is limited by camera obscuration.

Test 3FV, with the NFR Faux Leather material made of Lycra and having a polyester backing, exhibits very similar overall fire development. After ignition with Crib 4, the Lycra cover on both the seat cushion and the back pillow begins burning within the first minute. Between 1 and 4 minutes, the fire continues to penetrate the back pillow cover fabric and progresses gradually into the polyurethane foam of the seat cushion. A smoke layer can be seen slightly earlier in this test than in Test 2MV at approximately 02:06 after ignition. The smoke layer descends to 1500 mm by 03:45, which is only a few seconds different than in Test 2MV. By 4 minutes into the test, the entire back cushion is involved in the fire, which has propagated across most of the seat cushion, again very similar to Test 2MV. These early stages of fire development are depicted in the minute-interval video captures for Test 3FV, included in Appendix A.

Conditions deteriorate significantly within the house over the next 2 - 3 minutes of this test, as captured at 15 s intervals in Figure 5-37. As in Test 2MV, the smoke layer interface in 3FV does not remain delineated after around 04:30 into the test and begins collapsing at 06:05. During this period, the upper and lower layer interface is initially relatively well defined but then slopes lower on the west side of the room away from the fire, and remains higher on the east side of the room closer to the fire. Based on images from C2 between 04:30 to 06:45 after ignition, the smoke layer interface transitions from sloping lower to the west to conditions with no visibility on the west side of the room and then growing increasingly towards the fire, until all visibility is lost on the camera at 07:19. The collapse of the smoke layer and the encapsulation of the fire occur over a longer duration in this test, taking approximately 2.5 minutes instead of 62 seconds in Test 2MV.

On the upper level in Test 3FV, smoke is initially observed in the UHA at the top of the stair and propagates down the UHA into the USE room, as captured in Figure 5-38. A period over which there is a clear distinction between the upper and lower smoke layer is relatively short. Smoke is first observed near the ceiling at the top of the stairs at 03:18 and descends to 1500 mm above the floor by 04:18. By 04:45

seconds, smoke circulates through the entire height of both USE and USW rooms and can be observed drifting through the full height of the door opening by 05:00. Following that, smoke can be observed circulating and moving past all of the cameras with sporadic clear lines until camera visibility is lost in all rooms at 06:35 after ignition, approximately 44 s prior to the loss of visibility on the lower level at 7:19.



Figure 5-37: Test 3FV showing select intervals of the burn room quad video.

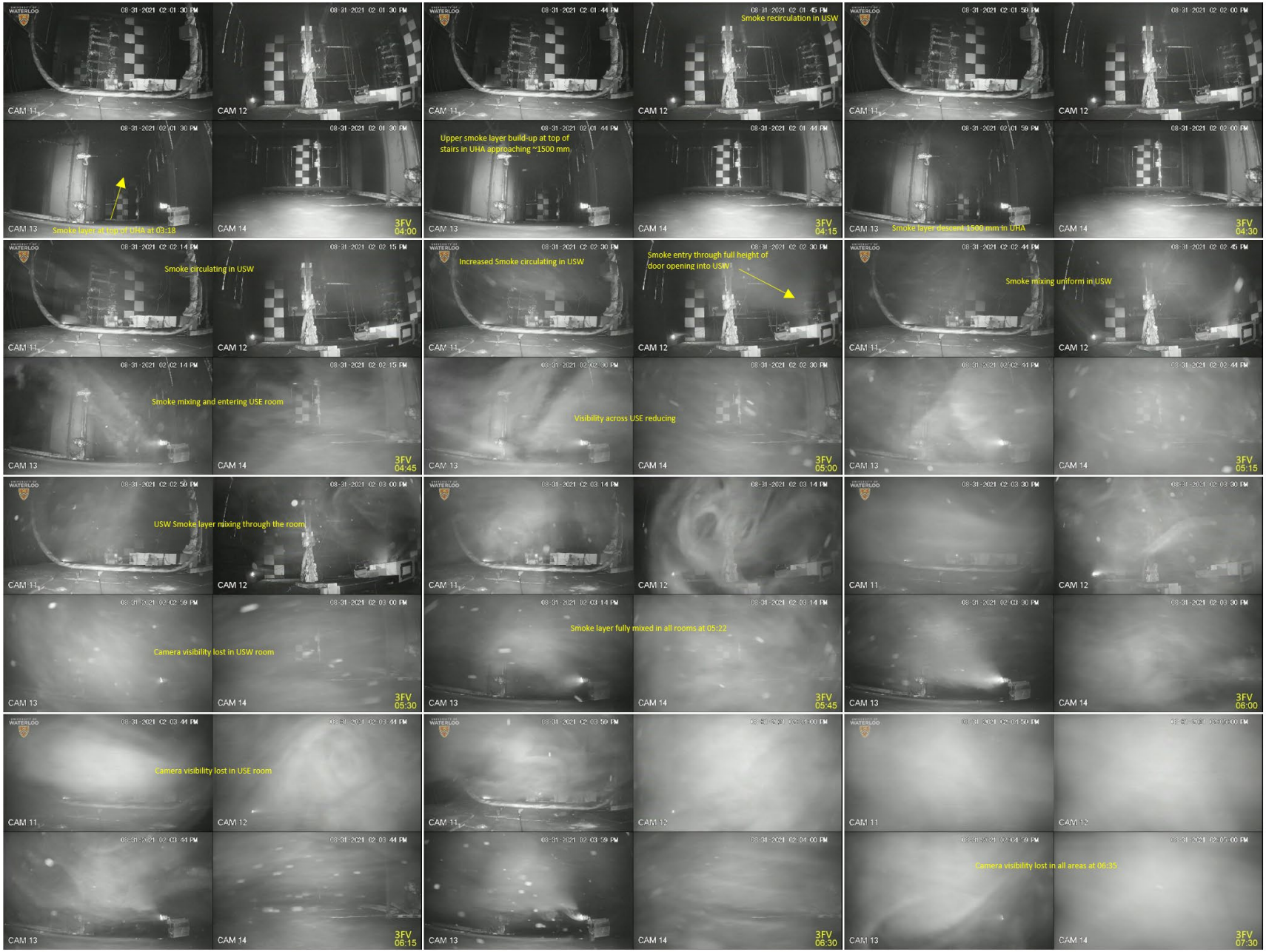


Figure 5-38: Test 3FV showing select intervals of the upper level quad video.

Given that the NFR leather sofa in Test 4FV has only two cushions and that leather inherently can be more resistive to ignition than cloth fabrics, it was elected to ignite the 4FV sofa with a Crib 5. Even with the larger ignition source, the fire growth is substantially delayed compared to that observed in the 2MV and 3FV tests. The back seat cushion begins to burn at approximately 06:00 after ignition, at which point a narrow flame burns through the back cushion with the limited horizontal extension of the fire on the seat cushion. The flame height then starts to increase and smoke starts to accumulate at the ceiling. The smoke layer is initially more prevalent at the room's north end, closer to the fire. This is illustrated in Figure 5-39 along with the initial formation of the ceiling smoke layer at approximately 07:13. The fire continues to grow, burning predominantly into the back cushion. By the time the smoke layer reaches 1500 mm at 08:23, shown in Figure 5-40, the left and right sides of the back cushion have collapsed, significantly increasing the observed burning area of the fire. At this time, the fire starts to propagate along the seat cushion towards the front of the sofa. By 9 minutes, the left seat cushion curls up on both sides and lines are observable on the leather, suggesting the surface material is drying and shrinking, causing the cushion to bend and deform, as well as exposing it to the less protected underside of the couch cushion and facilitating propagation of the fire.

The period between 9:00 – 11:45 is captured in 15 s increments in Figure 5-41. After the initial delay, the fire develops in a manner similar to Tests 2MV and 3FV. The collapse of the smoke layer interface initially occurs at approximately 09:51, and smoke then progressively proceeds to floor level at the perimeter of the room before enveloping the fire. The second seat cushion on the right side of the couch shrinks, leading to the left corner, peeling up and exposing the underside of the cushion, which is polyester and not leather. This facilitates the participation of the second seat cushion in the fire. Lower level visibility is lost at 11:03. In comparing the results with Tests 2MV and 3FV, the leather sofa has an approximately 2.5-minute period from the time the smoke layer deteriorates to the time visibility at C2 is lost, consistent with the faux leather couch in Test 3FV and much longer than for the cloth couch in Test 2MV.

Unlike Tests 2MV and 3FV, no definable smoke layer is observed in the upper level during Test 4FV. The first signs of smoke are at approximately 08:26, with smoke drifting into all rooms by 08:41. This progression of smoke through the upper level is captured in the 15 s time steps in Figure 5-42. Visibility is lost in all rooms by 11:00 after ignition, which aligns reasonably well with the loss of visibility in the lower level, indicating that visibility throughout the whole house is compromised at approximately the same time.



Figure 5-39: Test 4FV burn room time capture at 07:13 showing the initial smoke layer.



Figure 5-40: Test 4FV at the time of smoke layer interface reaching 1500 mm in the burn room.



Figure 5-41: Test 4FV showing select intervals of the burn room quad video.

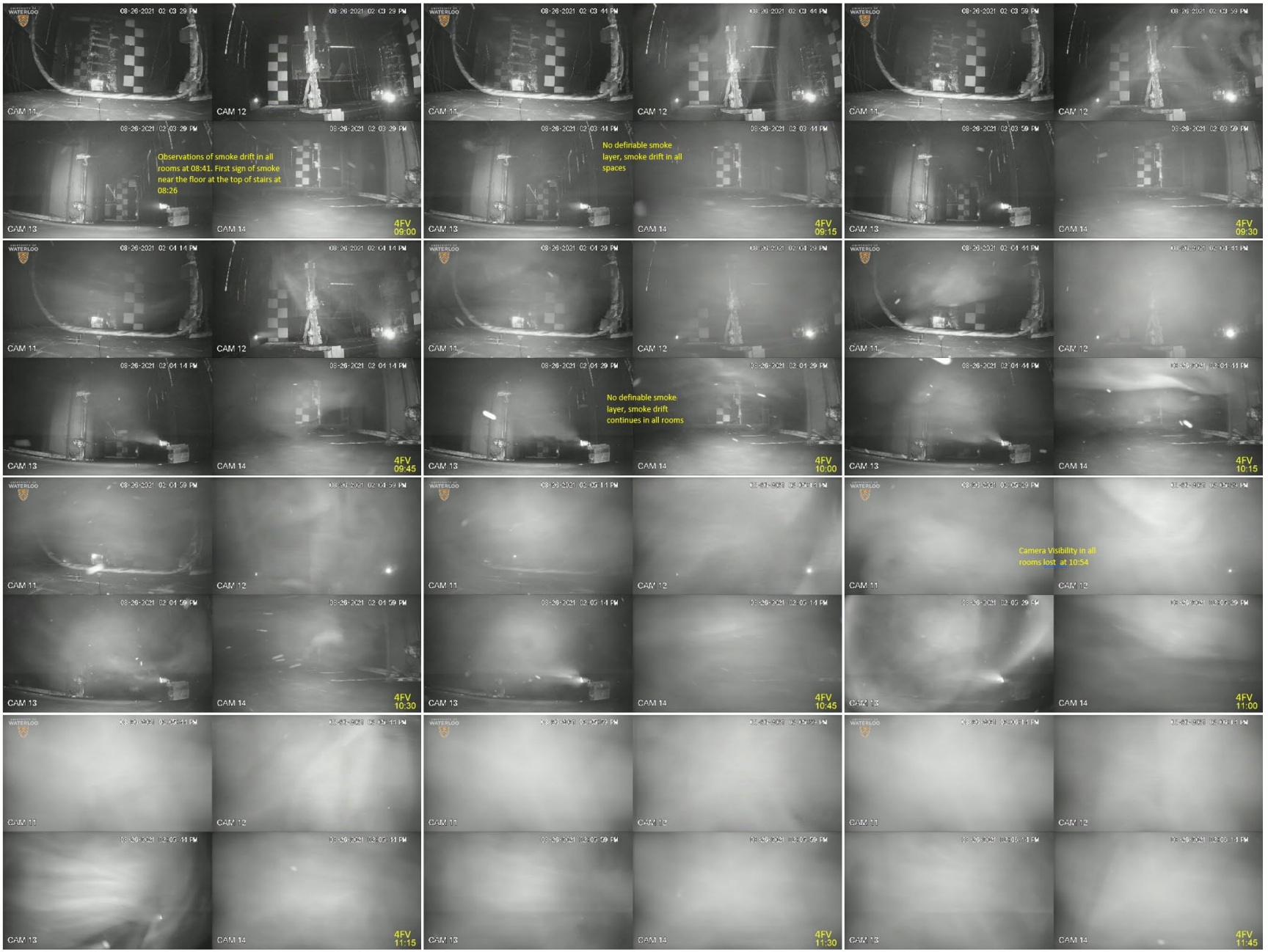


Figure 5-42: Test 4FV showing select intervals of upper level quad video.

The development of the fires established on the NFR furniture follows consistent trends, which can be summarized as follows.

1. A smoke layer develops in all tests. The layer accumulates at the ceiling of the LBR and then spills to adjacent rooms. Eventually, the smoke layer interface dissipates, and smoke mixes through the whole house until visibility is lost on both levels at differing times depending on furniture type. Since the fire is in the living area, smoke pushes down LHA and across the house into the LSW through the door opening. It descends down the walls first at the west end, as illustrated in Test 2MV, Figure 5-35. Therefore, even though there is some visibility in portions of the LBR and the east end of the LSW, visibility is entirely lost in the critical egress path close to D2.
2. Early stages of smoke layer development in the NFR furniture fire tests are consistent with the literature regarding forming a distinct upper layer (smoke) and lower layer (clear). However, once the interface layer height drops below 1500 mm above the floor, the layer does not continue to progress downward as might be anticipated. Instead, the interface remains intact for differing lengths of time dependent on the progression of fire development and then the upper layer smoke dissipates into the lower layer to create a single volume of mixed smoke and ambient air. Consequently, the descent of the smoke layer interface to the 0.9 m height was not observable in any of the tests. This requires that the criterion for crawl-out as related to the smoke layer descending to 0.9 m off the floor be modified to be instead based on the timing of the collapse of the smoke layer and obstruction of visibility along the egress path. This required a review of different camera perspectives as local conditions at the west end of the LHA were not easily observable with the lighting configuration of the house.
3. The smoke layer evolves from a demarcated interface at a given height above the floor to a smoke cloud around the perimeter of the fire. This then appears to encapsulate and smother the flaming region of the fire. These observations are notably different from the picture of the smoke layer interface descending from the ceiling over the flames to the base of the fire or to the floor, as described in the literature. Thus, the nature and timing of the events leading to smoke layer collapse and interaction with the fire plume will be reviewed further relative to measured oxygen and gas species concentrations later in the thesis.
4. The time evolution of visibility on the upper floor largely mirrors that observed on the lower floor in terms of the time at which visibility is lost. In general, limited quantities of smoke were collected on the upper level prior to the smoke layer dropping below 1500 mm on the lower level. Mixing and circulating of smoke from floor to ceiling are apparent in all tests and in all rooms on the upper level, making the evaluation of visibility relative to smoke layer height

somewhat irrelevant. Further, the degree of mixing of smoke throughout the spaces complicates the use of the checkerboards to assess visibility since smoke frequently obstructs the camera's sight lines as it circulates, presenting camera images that are not reflective of the overall smoke behaviour.

5.7.3 Fire and Smoke Layer Development with the UK FR Couches

5.7.3.1 UK couch tests where burning was not sustained

The limited participation of the couches in the fire growth when the burning is not sustained after application of the ignition source, unsurprisingly, corresponds to more limited smoke generation. Smoke conditions within the house are, therefore, more favourable in Tests 5abcFV and 7aFV when compared with any of the NFR tests. For Test 5cFV, with the largest Crib 7 ignition source, a smoke layer initially develops at the ceiling and drops to 1500 mm at approximately 08:02, but shortly after dissipates and white translucent smoke mixes through the floor area. The smoke layer becomes relatively uniformly distributed throughout the space by the end of the test. Visibility is never fully lost during the test, although as larger ignition sources are applied, the degree of visual obscuration correspondingly increases. None of the cameras switch to night mode, and the windows are observable from their respective camera angles throughout the test, which reflects a less dense smoke layer. For reference, Test 5cFV is reproduced in Figure 5-43. Tests 5aFV and 5bFV, corresponding to Cribs 4 and 5, respectively, are comparable but with less smoke. The one-minute intervals from those tests are available in Appendix A.

Limited smoke also accumulates on the upper level during the three experimental subsets of Test 5FV. In Test 5aFV, no significant smoke accumulation in any of the rooms on the upper level during the test. Some smoke migrates upstairs in Test 5bFV. The smoke mixes throughout the height of the USW room, but no smoke layer develops. Towards the end of the test, smoke movement is apparent across C13 and C14 in the USW, but no smoke is present in the USE. This is similar to Test 5cFV, shown in Figure 5-44, in which smoke predominantly migrates into the USW with minimal smoke in the USE. Note that during the reset between subsets 5b and 5c, not all of the smoke is purged from the upper level, and therefore, there is preexisting residual smoke, particularly in the USW room in Test 5cFV but also in the USE. Visibility on the upper level becomes compromised around 12 minutes into Test 5cFV, but the video observations show that smoke is circulating, and full visibility is never lost on any of the cameras on the upper level. Interestingly, circled in yellow at 10:00 on Figure 5-44, smoke can be seen on the floor at the top of the stairs in the UHA and propagating into

the USE from the bottom of the door opening, which perhaps explains why there is no upper layer development and smoke layer interface.

The smoke layer development in Test 7aFV follows similar trends to 5aFV and 5bFV but does not become as dense as in Test 5cFV, as illustrated in Figure 5-45.

To conclude, camera visibility is never fully lost since none of the couches in all subsets of Test 5FV and Test 7aFV ignite. In all cases, a haze of smoke disperses through the lower level with increasing density as a function of the size of the miniature wood crib used to ignite the fire. There is also some extension of smoke into the upper level. However, for purposes of this thesis, visibility is assumed to have been maintained for the duration of all of these tests.



Figure 5-43: Test 5cFV showing select intervals of the burn room quad video.

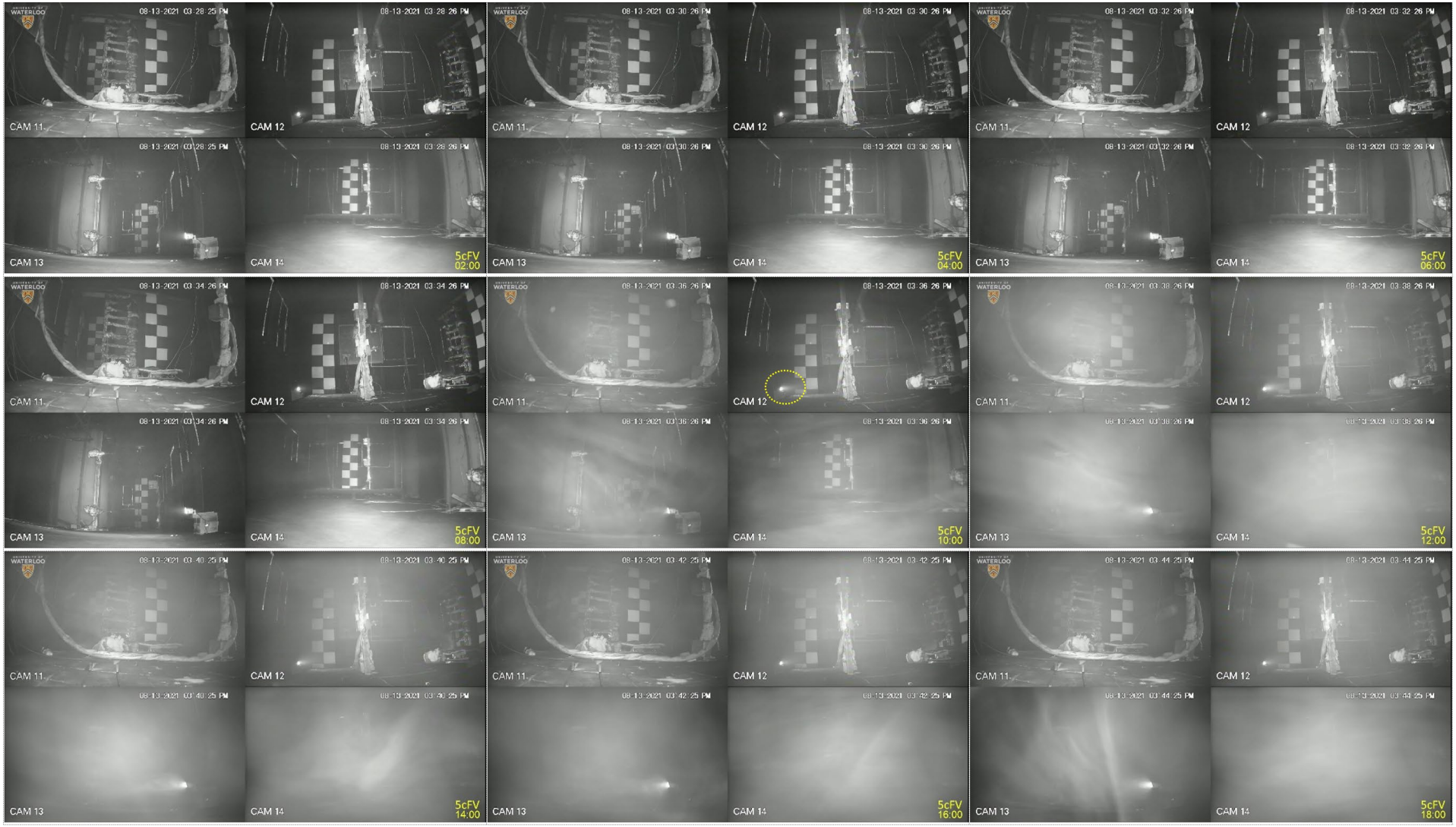


Figure 5-44: Test 5cFV showing select intervals of upper level quad video.

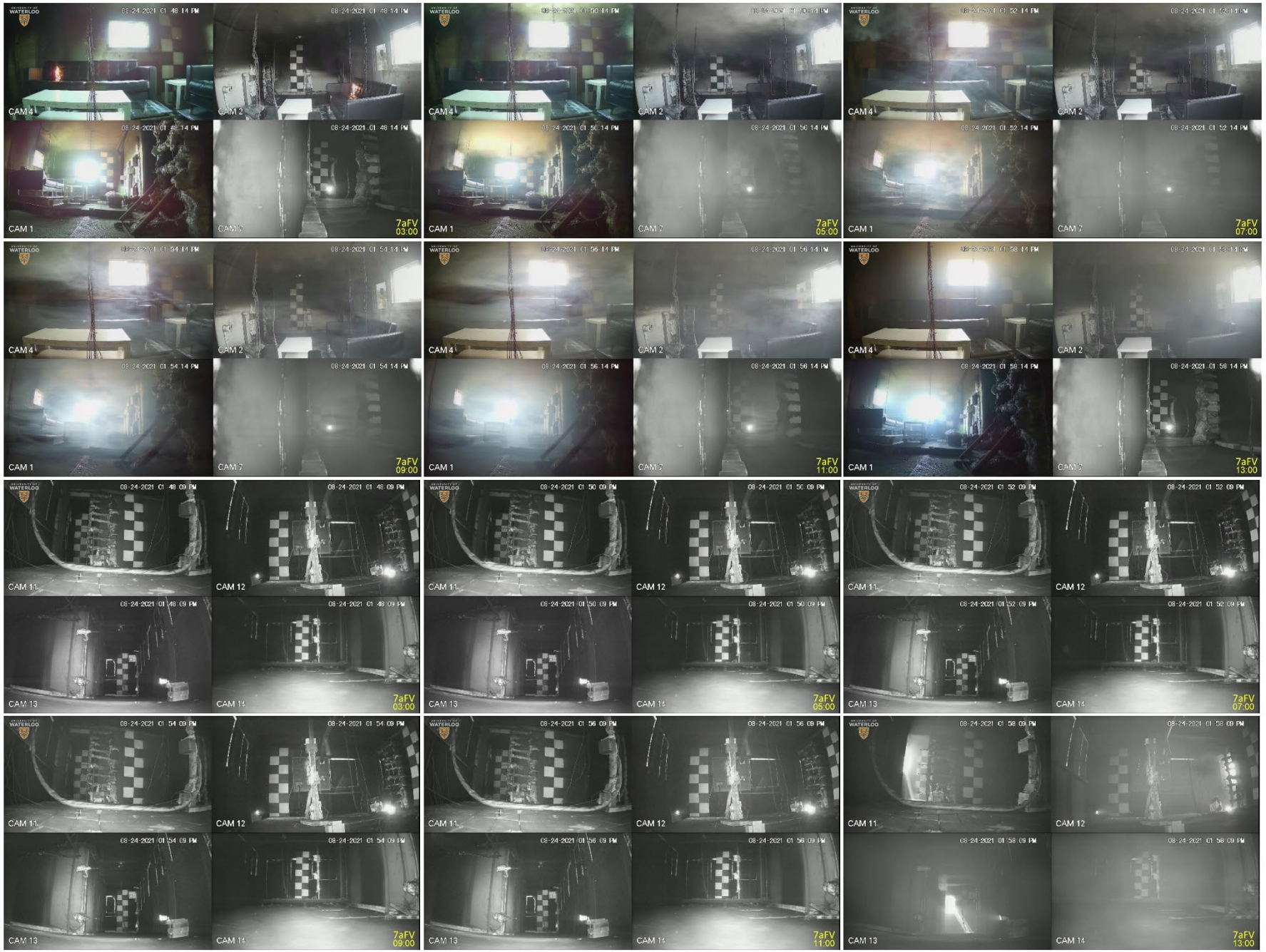


Figure 5-45: Test 7aFV ignited using Crib 5 showing 2 minute intervals of the lower level burn room and upper level quad videos

5.7.3.2 UK couch tests where combustion was sustained

Test 6FV ignites with Crib 4, though at many points in the first several minutes, it is anticipated that the couch will self-extinguish, as would be expected for the lower Crib 4 ignition, relative to the requirements of the British Regulations. However, combustion persists over a prolonged incipient stage. Smoke disperses within the house despite the limited combustion during this incipient period. A light smoke layer forms by 02:33 after ignition and descends for the first five minutes, reaching 1500 mm above the floor at approximately 06:38. However, at that point, the smoke layer interface is already dissipating in the LBR and by 10:00, smoke is mixed through the entire lower level, as shown in Figure 5-46. This generally persists until 20:00 into the test, when the fire starts burning on the left side and arm of the couch.

A heated smoke layer then begins to develop within the cooler smoke layer. Although difficult to fully visualize, darkened smoke is observed through the smoke haze. It extends down to the tops of W1 and W2, which are darkened in C1 and C4 at 20:15 in Figure 5-46 and progressively become blackened by 23:00. The smoke layer with the smoke haze collapses at approximately 20:30, and loss of lower level visibility occurs at 24:30, with camera visibility lost by 25:00. It appears that the darkening within the smoke haze occurs in a similar manner to the fire encapsulation described earlier, but there is not sufficient visual depth through the smoke to readily define the extent of the new heated smoke layer within the existing hazy smoke layer throughout the process.

On the upper level, smoke is visible at the floor at the top of the stairs, as illustrated at 05:00 and 10:00 after ignition in Figure 5-47. Smoke is first visible at this location at 03:09 and remains visible right through to 19:20 into the test before the smoke mixes sufficiently in the upper level and obscures the camera view of the top of the stairs. Since the smoke is filling the upper level from the floor level instead of the ceiling level, as would normally be expected, there is no obvious smoke layer accumulation at 1500 mm in the upper level. Instead, there is a uniform mixing of smoke on that level until camera visibility is lost at 23:00 after ignition.



Figure 5-46: Test 6FV showing select intervals of the burn room quad video.

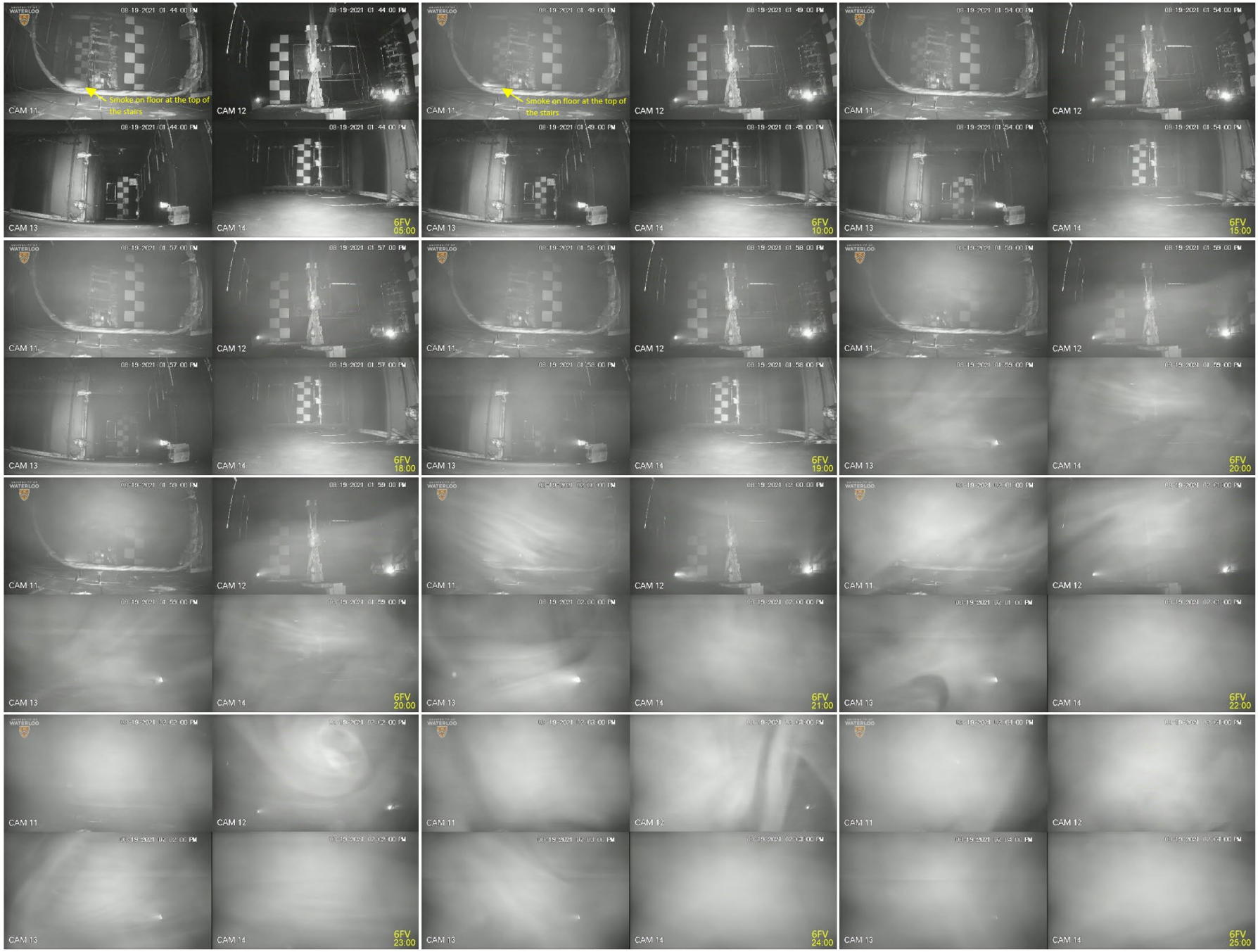


Figure 5-47: Test 6FV showing select intervals of upper level quad video.

The final UK furniture test is Test 7bFV with the UK FR Leather. This test is ignited with Crib 7 in contrast to the comparable NFR leather furniture Test 4FV, which is ignited with the smaller Crib 5. The larger ignition source likely explains the rapid development of the initial ceiling layer, which occurs in Test 7bFV in 04:14 after ignition in comparison to 07:33 taken for a smoke layer to initially form in Test 4FV (see Figure 5-48). However, it is interesting to note that despite the larger ignition source and more rapid growth of the smoke layer, the fire spread on the couch in Test 7bFV is slower than in Test 4FV. Smoke continues to build more rapidly in Test 7bFV, descending to 1500 mm above the floor in 07:16 in 7bFV, compared with 08:23 in Test 4FV. However, the collapse of the smoke layer is more gradual in Test 7bFV. At 07:43, whisps of smoke circulate below the smoke layer interface, but the smoke layer interface remains distinct through to 11:42, when it collapses compared to the smoke layer collapse at 09:50 after ignition in Test 4FV, respectively. Finally, loss of camera visibility occurs slightly later, at 12:16, for 7bFV compared with 11:03 for the 4FV test. In brief, the FR leather couch performed comparably to the NFR leather couch in terms of smoke distribution on the lower level, with smoke from the FR couch dropping below 1500 mm but remaining layered, with associated lower risk, for a longer period of time.

One notable difference between 7bFV and 4FV is on the upper level, where in Test 7bFV, the smoke appears to collect at both the floor level and ceiling at the top of the stairs, whereas in 4FV, smoke is collected only at the ceiling. The different smoke development in Test 7bFV can be seen at 08:00 after ignition in Figure 5-49. It is then followed by a continuous mixing of smoke and fresh air in the upper level and a loss of camera visibility at 12:30 into the test.

To summarize the UK FR couch tests:

1. Since tests 5abcFV and 7aFV did not ignite and no significant smoke layer developed that would preclude escape from the house.
2. Fires in Tests 6FV and 7bFV develop more slowly than for the comparable NFR furniture fires in Tests 3FV and 4FV. As a consequence, there is greater cooling of the smoke, creating a smoke haze throughout the house. In the case of 7bFV, this haze disperses below the smoke interface line for a period of time prior to the collapse of the smoke layer interface.
3. When the fire takes hold in Test 6FV, it develops a smoke layer within the smoke haze created during the fire's incipient period.
4. Smoke develops on the floor at the top of the stairs in both Tests 6FV and 7bFV and at the top and bottom of the stairs in Test 7bFV. This suggests that considerable mixing occurs in the stair shaft.



d

Figure 5-48: Test 7bFV showing select intervals of the burn room quad video.

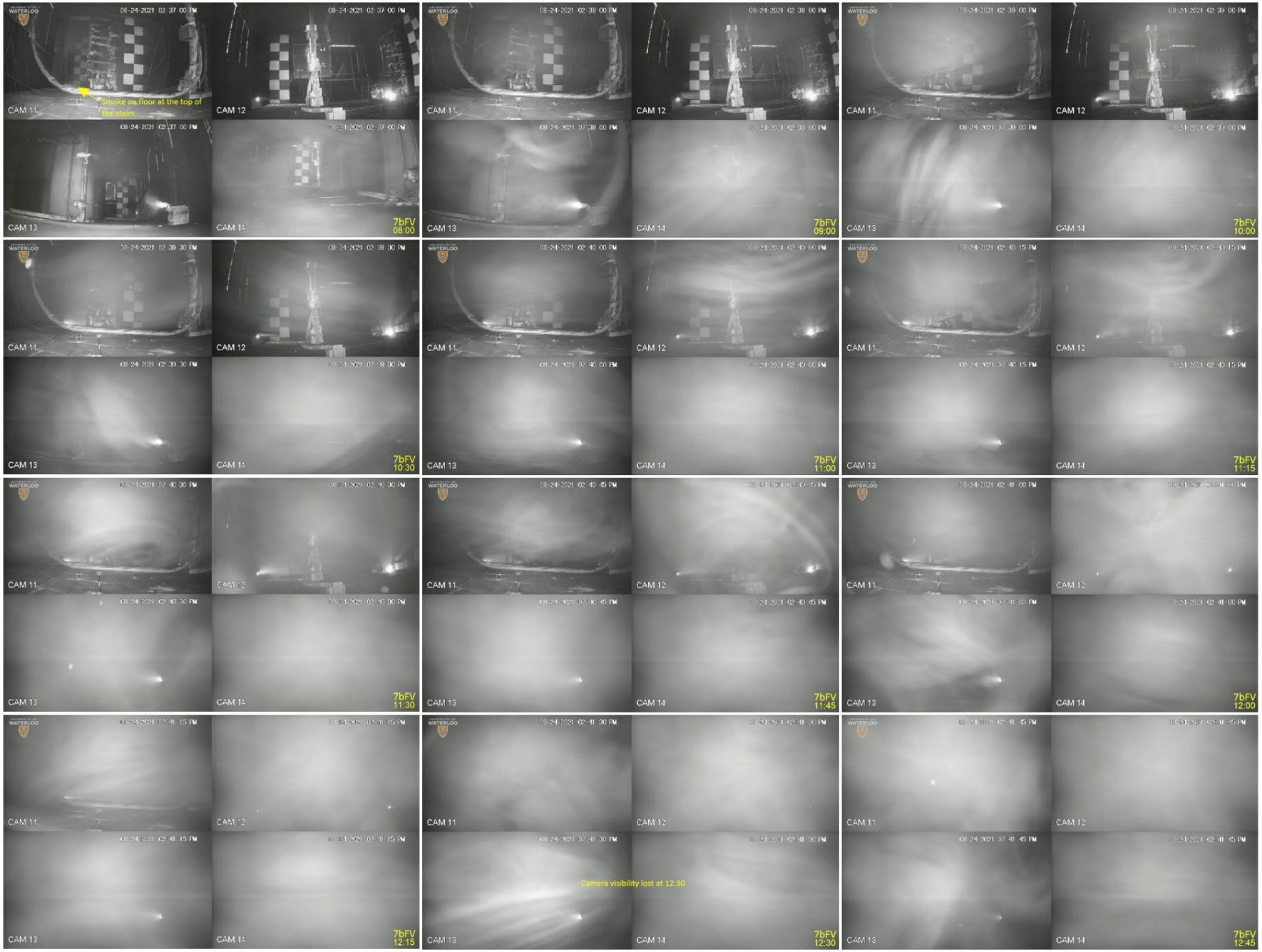


Figure 5-49: Test 7bFV showing select intervals of upper level quad video.

5.7.4 US FR Couch Tests

Images from 8aFV and 8bFV are included in Figures 5-50 and 5-51, respectively. The smoke layer development in 8aFV with the Crib 7 and 8bFV with the propane burner are consistent with the description for Test 5FV, where the couch does not ignite. An initial smoke layer dissipates and mixes through the lower and upper levels. The reset between 8aFV and 8bFV is done quickly, and not all smoke is purged from the upper level following the 8aFV test. Despite this, visibility is never lost on the upper level in 8bFV. In general, this test parallels results seen in the UK FR tests that do not ignite and therefore, no further discussion is added with respect to this test.



Figure 5-50: Test 8aFV showing select intervals of the burn room and upper level quad video.



Figure 5-51: Test 8bFV showing select intervals of burn room and upper level quad video.

The final fire in the series is established on a faux leather couch with a Polysiloxane (silicone) cover with a wool, cotton and acrylic backing and an FR PU seat cushion but NFR cushion fill. The couch is ignited with a Crib 7 and burns with a comparable timeline to the NFR and UK FR leather couches in Test 4FV and 7FV, respectively. The larger wood crib initially takes time to penetrate into the back cushion of the couch. At 04:00 after ignition, the back cushion exhibits striations on the cover fabric from thermal exposure. At 05:00, the flame height grows, and the width of the fire increases, but it is still burning in the original line of the wood crib. The fire continues to progress laterally along the back cushion and push towards the front of the cushion until 07:00, after which the burning rate accelerates, and the smoke layer begins to drop.

The smoke layer starts to accumulate at 06:08 and drops to 1500 mm at 07:45 after ignition. By 08:00, flames are hitting the ceiling, creating a ceiling jet. Figure 5-52 shows the burn room, starting at 08:00, where the fire extends across the middle seat and back cushions. The smoke layer appears largely uniform across the room and starts to collapse at 09:08. By 09:15, the fire extends to the right cushions and by 09:45 reaches the far end of the couch. At this point, camera visibility is fading on C2 and C7, and is ultimately lost on all cameras, except for areas illuminated by the fire, by 10:05.

Smoke is seen in Figure 5-53 at the top of the upper-level stair at 07:48 after ignition. Unlike the other FR furniture fires, smoke collects at the top of the stair and not at the floor. It drops to a level of 1500 mm above the floor by 08:28. However, the smoke layer collapses approximately 30 seconds after ignition and starts mixing in all rooms, leading to a loss of visibility on all cameras by 09:40 into the test.

In general, the 9FV couch underperforms compared to the other FR couches. It does not resist ignition to the same extent as the 5FV or 8FV couches, and, when compared with the 6FV couch, does not resist flame spread and fire growth nearly as well. Further, the greatest total involvement in burning the couch occurs in Test 9FV as the fire extends the full length of the couch (see Figure 5-24), and heat from the fire also damages the chair. One explanation is that there is no evidence of flame retardants in the polyester fill in the back cushions, which are clearly the catalyst for fire growth prior to the involvement of the PU slab in the seat cushion, which does show evidence of flame retardants. As observed in other tests, overall fire development has a significant impact that depends on interactions between the back cushions, the seat cushion and the igniting wood cribs.



Figure 5-52: Test 9FV showing select intervals of the burn room quad video.

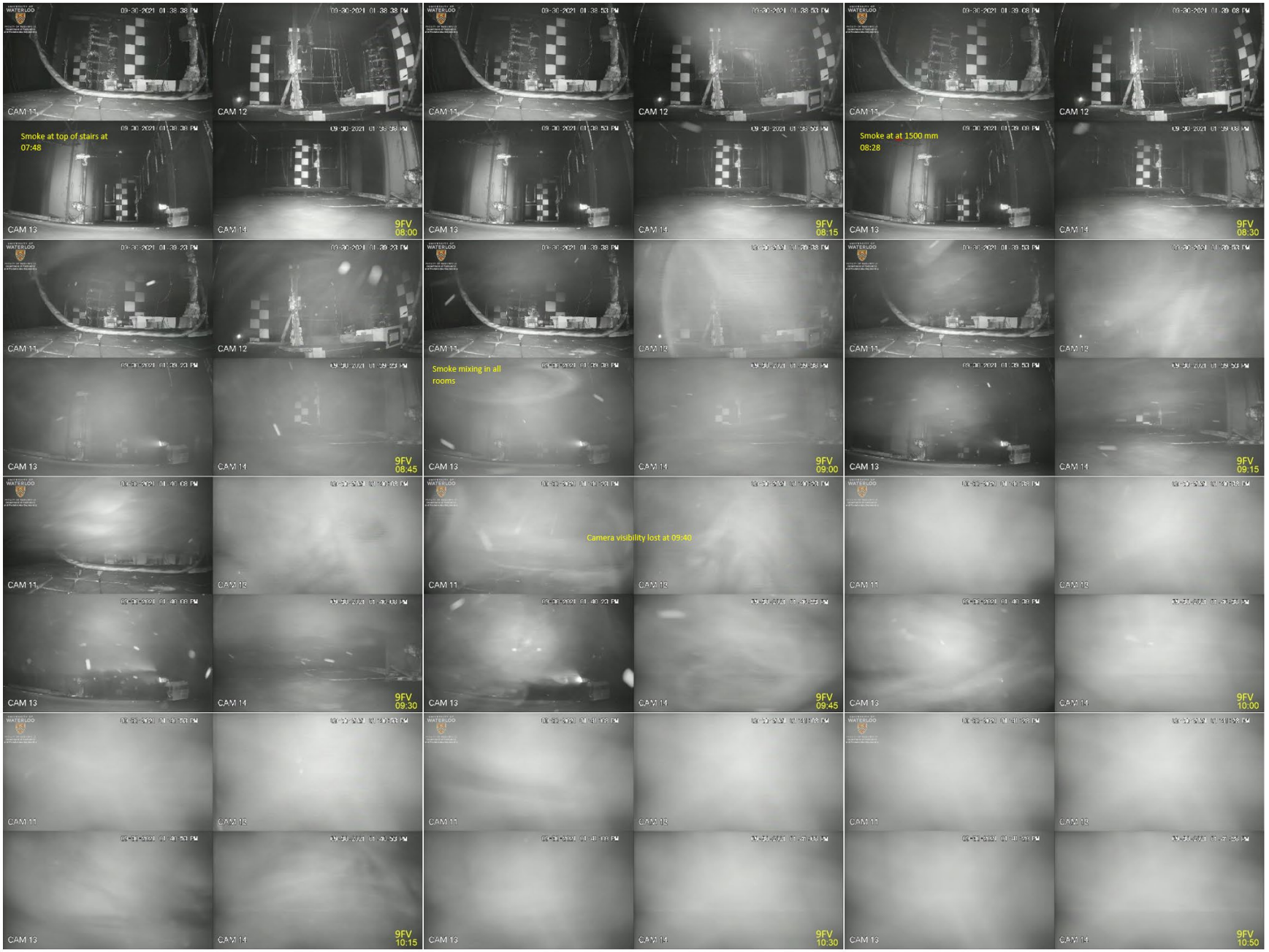


Figure 5-53: Test 9FV showing select intervals of the upper level quad video.

5.7.5 Summary of Results

At the onset of this research, it was anticipated that three smoke layer heights would be used to indicate overall smoke evolution within the fire compartment. These are when the smoke layer descends to 1.5 m above the floor, to 0.9 m above the floor, and then reaches the floor. However, the above discussion shows that the smoke layer collapses in several tests before descending to 0.9 m above the floor. Therefore, the interpretation of smoke layer evolution must be adapted to consider when the smoke layer descends to a 0.9 m height or when the smoke layer descends to a 1.5 m height and subsequently collapses to fill the space. Based on the assessments above, the differences appear to be due to the combination of the enclosed fire environment and the onset of ventilation-limited conditions. These will be explored further in later sections. Nonetheless, for the purposes of estimating evacuation times, Table 5-7 illustrates reference times determined from the video analysis. Where visibility is never lost, an arbitrary value of 1800 s (30 minutes) is assigned for comparative purposes of escape times and as an upper bound for purposes of this analysis. This is well beyond the 16 – 20 minute timelines described in Section 2.2.4.

Table 5-7: Summary of smoke filling visibility times for all flaming tests.

Test	Smoke Layer at 1.5 m (s)	Lower Level 0.9 m or Smoke Layer Collapse	Lower Level Visibility Lost (s)	Upper level Visibility Lost (s)	First Level to Lose Visibility
1FV	685	1800	1800	1190	Upper
2MV	211	285	347	395	Lower
3FV	225	365	439	395	Upper
4FV	503	590	663	654	Upper
5cFV	482	1800	1800	1800	n/a
6FV	398	1230	1510	1380	Upper
7bFV	436	642	736	750	Lower
8FV	369	1800	1800	1800	n/a
9FV	465	548	605	580	Upper

Notably, visibility is lost on the upper level first in 5 of the 7 tests. The times for loss of visibility in the upper and lower levels are often quite close such that it could be inferred that the loss of visibility occurs, more or less, simultaneously between the upper and lower levels. Further, the time taken for smoke to descend to 0.9 m above the floor or for the smoke layer to collapse is shorter than the times to loss of visibility on either upper or lower floors, so it can be used as the primary basis for determining escape times.

5.8 Temperature

This section presents temperatures recorded at the thermocouple rakes along the escape path to consider the exposure of occupants that may evacuate along the UHA, down the stairs and along the LHA to the exterior. All temperatures for this discussion are approximated in the graphs. For

completeness, temperature time profiles for all thermocouple rakes within the house are provided in Appendix B.

Further, comparing profiles of compartment temperatures with time and key locations and aligning these with the timelines to loss of visibility in Table 5-7 provides a basis for considering the developing thermal conditions at key points in time within the burn house. The temperature profiles above can also be compared with the suggested 60°C exposure temperature tenability limit proposed by Purser and McAllister [35].

Temperature profiles measured during Tests 2MV and 9FV, with the two fastest growth times to peak MLR, are compared in Figure 5-54. On the left of the figure are the LBR temperature profiles. The two tests have similar temperature ranges between lower and upper measurement locations, between 160°C at 0.9m and 360°C at 1.5 m, with Test 9FV having a slightly lower peak temperature. The smoke layer height descends to 1500 mm above the floor in the burn room just as temperatures within the compartment begin to increase at both positions. Afterwards, the temperature profiles continue to increase until the peak temperatures are reached, corresponding to the time when peak MLR is also measured.

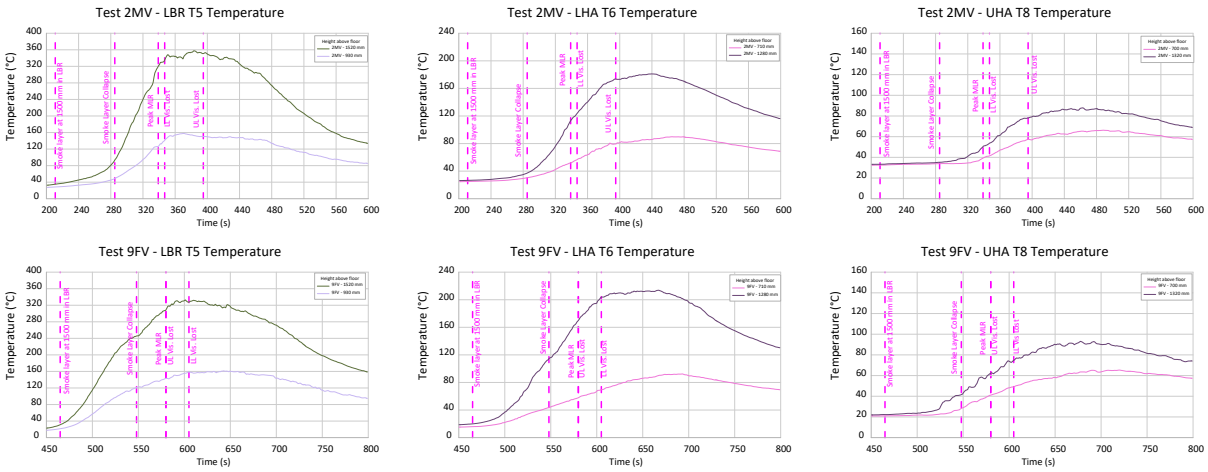


Figure 5-54: Temperature profiles of T5, T6, and T8 for tests 2MV and 9FV.

Taking a tenability endpoint that corresponds with the crawl-out criteria based on the collapse of the smoke layer in these tests, the temperatures remain below 60°C at the LHA T6 location at 710 mm for both tests, with temperatures below 40°C for Test 2MV and just above 40°C for Test 9FV. The same is true for T5 in the LBR for Test 2MV, but temperatures have increased to approximately 120°C at the same location in Test 9FV. Occupants escaping past this location could, therefore, be exposed to significantly elevated temperatures for an intermittent period when passing through the LBR to reach the LHA. Occupants would not need to be as close to the fire as the position of the T5

rake, and airflow down the stair may result in local cooling nearer the stairwell side of LBR, thus allowing occupants to travel towards the LHA with less exposure.

Upper level temperatures do not increase as quickly as those on the lower level. Peak temperatures are on the order of 80 to 90°C in both tests and temperatures at 0.7 m above the floor do not exceed 60°C until well after visibility is lost on both levels.

Similar temperature profiles are measured during Test 4FV, with 70°C to 180°C the range of temperatures measured on the T5 tree in the LBR at 0.9 and 1.5 m, respectively at the time of smoke layer collapse, as illustrated in Figure 5-55 below. Temperatures for Test 7bFV are 50°C and 85°C at the time of smoke layer collapse. Temperatures in Test 7bFV at T6 in the LHA are also lower than in Test 4FV, with Test 7BFV ranging between 38° and 45°C for 0.7 m and 1.3 m thermocouples at the time of smoke layer collapse, compared with 44°C and 58°C at that time for Test 4FV. This suggests a lower potential thermal exposure for occupants passing through the LBR and LHA in the fire on the FR couch versus the NFR couch. On the upper level, the temperature ranges measured by thermocouples on the T8 rake are 42°C and 47°C at 0.7 and 1.3m for Test 4FV and 41°C and 45°C for Test 7FV. On the upper level, the temperature difference between locations is much less dominant.

It should also be noted that peak temperatures at 1.3 m were hotter at 5 of the 6 locations shown here for the NFR couch. The exception is in the LHA, where the peak measured temperature for the FR couch was 190°C versus 163°C at this height for the NFR couch.

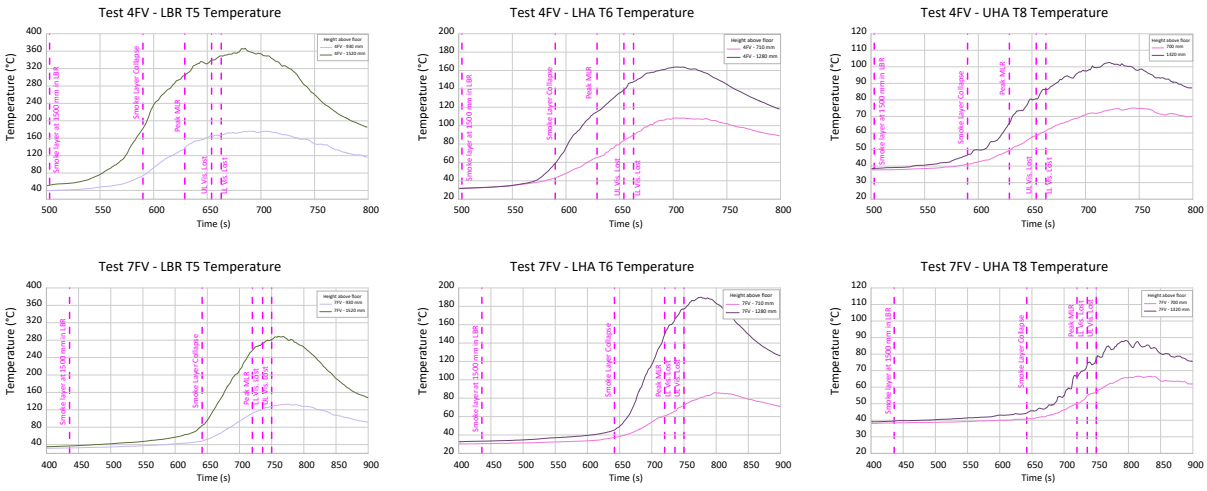


Figure 5-55: Comparison of T5, T6 and T8 rakes for Tests 4FV and 7FV.

Lastly, comparing the evolution of the temperature time profiles at the same heights in Tests 3FV and 6FV, there is a significant time delay in Test 6FV before thermal conditions develop due to the long incipient stage of the fire. The peak temperatures reached in this test are also significantly lower

on all three thermocouple rakes, as illustrated in Figure 5-56. Measured temperatures during Test 3FV range between 125°C and 340°C at 0.7 and 1.3m heights in the LBR, whereas they lie between approximately 70°C and 230°C in Test 6FV at the time when visibility is lost on the lower level. In the LHA, measured temperatures range between approximately 50°C and 85°C for Test 6FV and between 60°C and 165°C for Test 3FV when the lower level visibility is lost. The temperatures at the time of smoke layer collapse in the LBR are between 50°C and 125°C for Test 3FV and 38°C and 110°C for Test 6FV, at the 0.7 and 1.3 m locations, respectively. Corresponding temperatures in the LHA at the time of smoke layer collapse are notably lower, at 37°C and below 65°C in Test 3FV and 32°C and 38°C for Test 6FV, indicating substantially cooler temperatures for the FR faux leather couch at this location. This is similar to the difference between tests 4FV and 7FV, suggesting that cooler temperatures may be present away from the fire for the FR couches versus NFR comparables. The peak temperatures in Test 6FV are the lowest of any of the tests in which the couches burned.

In the UHA, the temperature range at the time that visibility is lost on the upper level is 39°C to 48°C for Test 3FV and 39°C to 45°C for Test 6FV. These temperature ranges are very close and noticeably lower for both tests than those measured during the other flaming fire tests. Temperatures across both height intervals at the time of smoke layer collapse on the upper level are below 40°C for both tests.

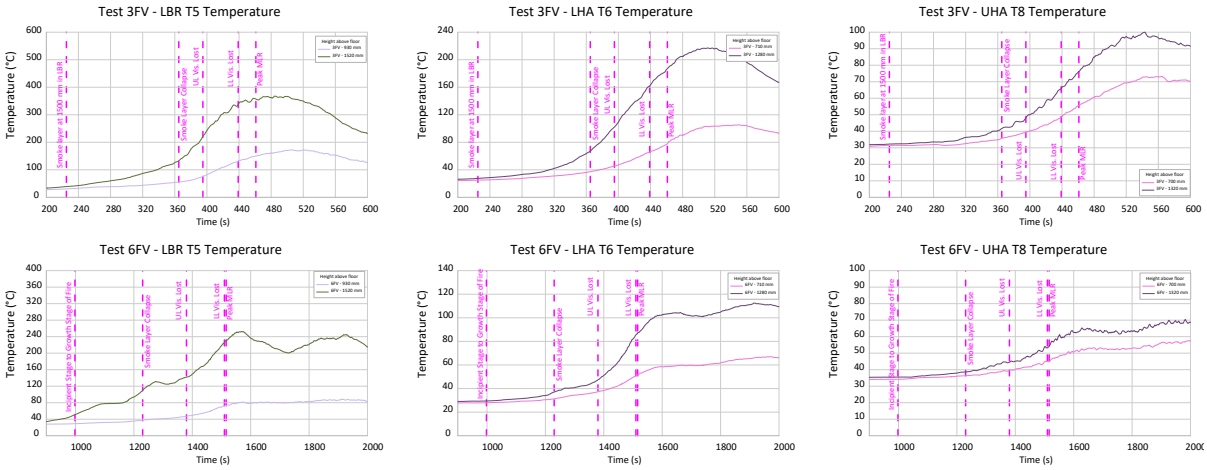


Figure 5-56: Comparison of T5, T6 and T8 rakes for Tests 3FV and 6FV.

In summary, the thermal exposure on the upper level is significantly lower than on the lower level for all tests. If the time period corresponding to smoke layer collapse and a threshold temperature of 60°C are used as a basis for estimating an ASET, it is reasonable to conclude for this test series that the thermal conditions on the upper level are not likely to be the impeding factor in occupant egress. As occupants descend the stairs and progress into the LBR while escaping, particularly for the fast-

developing couch fires, there is a potential period of greater exposure, but if occupants move away from the fire down the LHA, the thermal exposure is substantially reduced for the duration prior to the smoke layer collapsing, below the maximum proposed thresholds of 200°C in the thermal layer and 60°C for respiratory air advanced by Purser and McAllister [35].

5.9 Gases

Certain gas sensors are located in environments with gas concentrations beyond their saturation ranges, including ammonia (NH_3), hydrogen chloride (HCl), and carbon dioxide (CO_2). This cannot be avoided, as the ranges for all gas sensors are the highest that were commercially available at the time the sensor suites were built. The NH_3 concentrations increase to values beyond the sensor saturation limits, but the data remain continuous and consistent in trend, allowing for comparative analysis. In contrast, the sensor output data for CO_2 and HCl is useful until the point of saturation. It then becomes sporadic and inconsistent past this point. Unfortunately, saturation of the sensors occurs too early in the tests for the resulting data to be useful in the comparative analysis sought in this portion of the research. Therefore, CO_2 and HCl results are not considered in evaluating the gaseous environment in this section.

Some sensors have cross-sensitivities with other gases, which may impact the results. The development of corrections to address these are the subject of active research and will likely lead to equipment modification in future tests. These will be discussed further as the results are presented. In other instances, individual sensors cannot respond fast enough to follow rapidly changing transient environments during the full growth stage of the fire but subsequently stabilize to consistent values. In these situations, the peak or trough values can still be used as reference values and relative differences compared between experiments to account for overall trends of the environment at key measurement locations throughout the structure.

The challenges of making gas species measurements in the present fire environments are illustrated by comparing the oxygen concentration measured by the sensor at GIS3 with the Novatech concentration results, shown in Figure 5-57. The GIS sensors are situated at approximately the same height above the floor as the intake tube for the Novatech sensor; however, the oxygen concentrations measured by the GIS3 sensors, shown by the dashed lines, decrease to values much lower than those measured by the Novatech gas analysis system, shown by the solid lines, for all tests[8]. At the same time, the oxygen curves follow consistent trends between sensing technologies, and the timing of the

[8] Note that oxygen concentrations for Test 3MV are plotted here instead of those from Test 2MV since the Novatech is positioned at a different height than the gas sensor suite in Test 2MV.

troughs on the curve are reasonably consistent. Corrections for temperature and relative humidity effects are very small for the GIS3 sensors, even in the harsh measurement environment. Instead, it is thought that the depressed values of oxygen are due to the high cross-sensitivity of the sensors to the presence of hydrogen, which can be preferentially formed in fuel-rich fire environments via the water-gas reaction [164]. For the current oxygen sensors, the presence of hydrogen at levels previously measured in ventilation-limited fire gases can result in a significant decrease (2-3%) in measured oxygen concentration. This is also consistent with the good agreement between the measurements at high values of oxygen concentration, with deviations increasing as concentrations fall below about 12% oxygen. Further investigation is underway at UWFRL to fully clarify these considerations, but it is out of the scope of the present research as outlined above. Instead, for purposes here, a greater focus is placed on the trend of the curve in considering the areas of interest at GIS1, GIS4, and GIS5 in the remaining discussions.

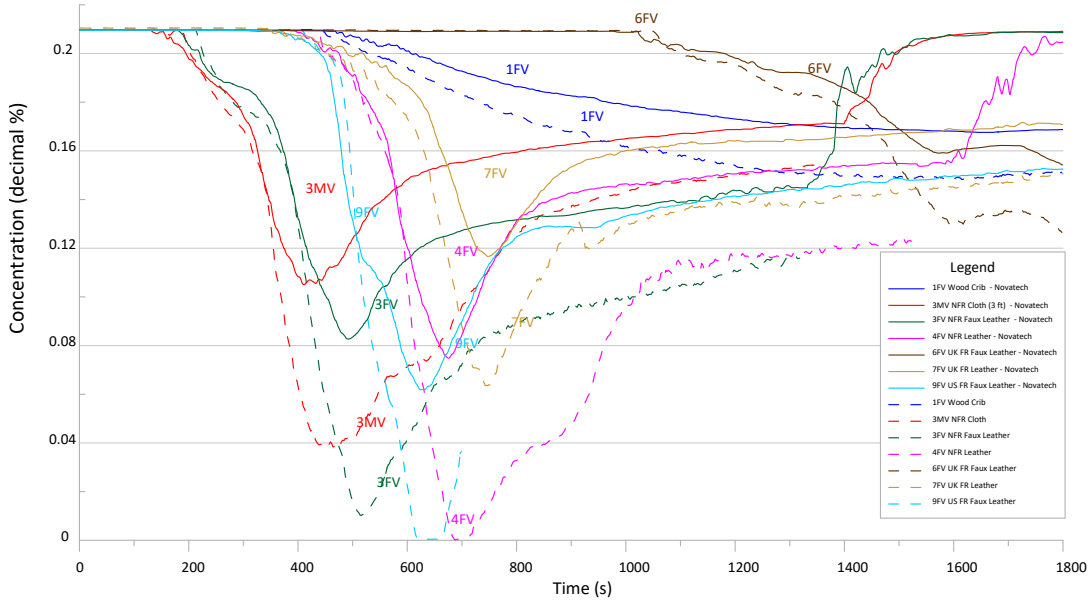


Figure 5-57: Comparison of electrochemical GIS3 O_2 sensor with Novatech IR sensor in LSW at 1.5 m.

Peak scaling, due to a combination of sensor gain, cross-sensitivities and response characteristics, is observed between the GIS3 CO sensors and the Novatech analysis system, as shown in Figure 5-58. After stabilizing from the peak, there is very good agreement between measured CO concentrations from the two sensing technologies, suggesting measurements from the GIS3 sensor after the initial high transient concentrations are quite good. Further, measured CO concentrations in fires with slower changes in concentration do not exhibit the scaling issue, as observed for Tests 1FV and 6FV. Thus, the measured CO concentrations at all GIS locations are anticipated to follow trends in the fire environment well, particularly after the fire becomes ventilation-limited.

The CO_2 data measured using the Novatech system is graphed over time in Figure 5-59. There is no comparative data from the GIS sensors due to the issues with the saturation of these sensors at concentrations of 10,000 ppm (1%) that occurred in these fires before the period of interest. Based on the Novatech measurements, CO_2 concentrations range from approximately 3.8% to exceeding 10%, depending on the test. While saturation of the GIS sensor occurs at 1% concentration, the Novatech results follow concentrations as they evolve in LSW at the south wall, 1.5 m above the floor, and as expected, indicate significantly higher concentrations of CO_2 than 1% during the tests.

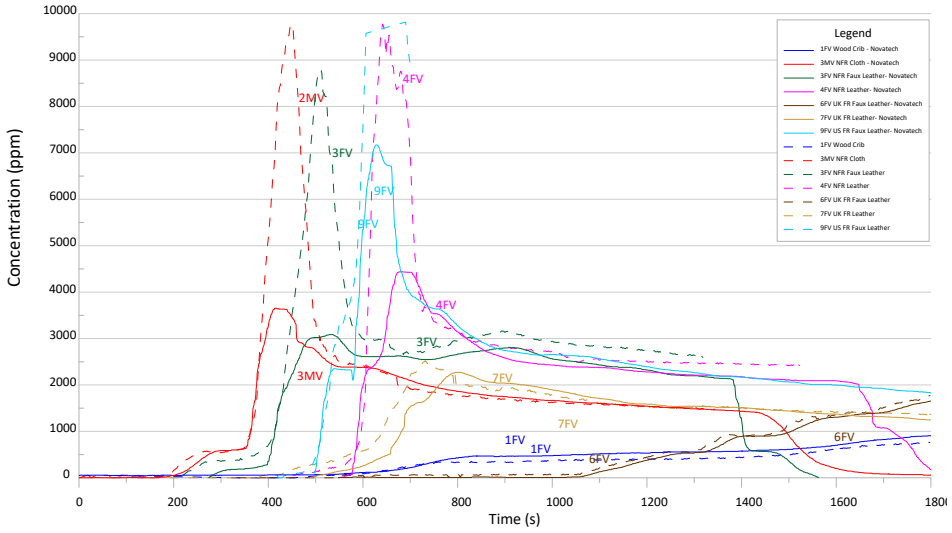


Figure 5-58: Comparison of electrochemical GIS3 CO sensor with Novatech IR sensor in LSW at 1.5 m.

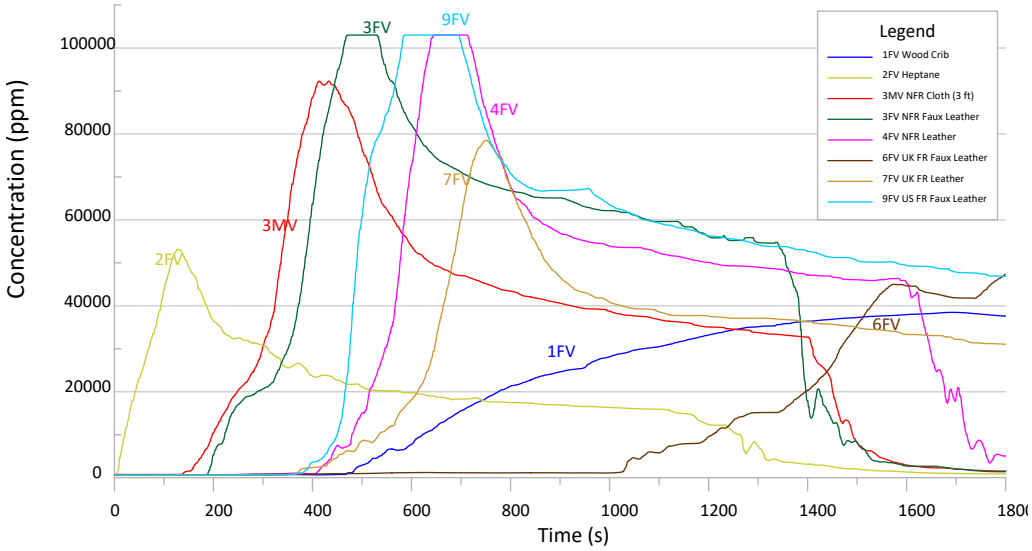


Figure 5-59: Novatech CO_2 results for FV series tests in LSW at 1.5 m.

Data for GIS stations are provided in Appendix C and plotted for a 30 minute period for all GIS locations (missing plots for GIS2 at 0.3 m). Note that where data is not included in the graphs, either

no sensor for that gas is installed in the sensor suite for that particular test, or problems with the sensor reactivity make the data unreadable, and measured data are, therefore, removed.

Turning to locations of interest along the egress path, O_2 and CO concentrations are provided in Figure 5-60 for GIS5 located in the UHA, which is the first point of travel along the escape path when leaving a bedroom in the test house. Looking at the lowest measured oxygen concentration values, there is very close agreement across the three heights at this location, with only a minor difference in concentration (on the order of 1% between low points of 14 and 15%) using 2MV (red) as an example. The minimum measured oxygen concentrations for Tests 3FV (green), 4FV (pink), and 9FV (light blue) were lower, on the order of 13%, and for Test 7FV (gold), slightly higher. Tests 1FV and 6FV indicated the least oxygen consumption with minimum measured values of oxygen concentration on the order of 17% occurring only 30 minutes into the test. The spikes in oxygen concentration at the end of any of the tests correspond to the return of oxygen to ambient values as D1 is opened and the house is ventilated. The CO concentrations plotted in Figure 5-60 appear to stabilize at between 2000 and 2750 ppm for Tests 2MV, 3FV, 4FV and 9FV at all heights, with Test 7FV exhibiting lower maximum CO concentrations of just under 1500 ppm, Test 6FV reaching only approximately 1000 ppm at the end of 30 minutes and Test 1FV reaching just 500 ppm at the end of 30 minutes.

The test-to-test differences in both oxygen and CO concentrations are consistent with differences in MLR, and thus combustion and generation of fire effluents amongst the tests as would be anticipated. The relative consistency in the concentration of each species between the lower and upper GIS positions is of interest, which further suggests the mixing of fire gases throughout the space occurs instead of a stratified smoke layer, consistent with observations noted in the smoke filling discussion above. This appears to occur as a result of the ventilation-limited environment. Figure 5-61 illustrates the times at which upper-layer visibility is lost for each of the fast-growth fires. Figure 5-62 shows the same for the slower-growing fires. In all cases, visibility is lost before the oxygen levels have reached their lowest concentrations, suggesting that mixing is also associated with the ventilation-limited environment.

A comparison of measured gas concentrations at three heights above the floor is also possible at GIS4, located in the LHA. Results are included in Figure 5-63. The sensitivity of sensor response is more apparent on these curves, with greater apparent variability (noise) on the O_2 and CO output. Concentrations of O_2 decrease further and more rapidly at the lowest levels of the compartment than at GIS5. Loss of visibility in the lower layer occurs much closer to the time of the lowest measured oxygen concentration as well. At a height of 0.9 m, oxygen concentrations decrease to approximately 9% for two tests (2MV and 3FV), on the order of 11% for 4FV and 9FV and 13% for 7FV. At this

location, lower level visibility is lost just before the minimum in O_2 concentration for tests 2MV, 3FV, and 9FV but after the minimum for the two leather couches in Tests 4FV and 7FV, as shown in Figure 5-64. In contrast, for the slower-growth fires included in Figure 5-65, visibility is lost approximately mid-way to the minimum oxygen concentration of 15.5% for test 6FV. A reduction in oxygen concentration to just above 19% is observed for Test 1FV, noting that the sensor fails prior to the end of the test (see Figure 5-65), and visibility is never lost in this test.

CO levels at GIS4 peak at an order of magnitude higher to those measured at GIS5, but there is clearly more variation (noise) on the graphs. Nevertheless, the steady-state values appear to range between 1000 – 3000 ppm for all tests, except for the approximate 1000 ppm at 30 minutes after ignition in Test 6FV and about 500 ppm for Test 1FV.

Similar patterns and trends in measured concentrations, as shown in Figure 5-66, can be observed at GIS1 in the LBR, a location that occupants would have to pass after descending the stairs. This location only has sensors at two heights, 0.3 m and 0.9 m above the floor. Measured O_2 concentrations at this location are lower than at GIS4 and 5, given the proximity of GIS1 to the fire's origin. On the other hand, measured CO concentrations are consistent with those measured at GIS4 in Figure 5-63.

The observations of the O_2 and CO concentration measurements at key locations indicate that when visibility within the structure is lost, oxygen depletion and resultant accumulation of CO and CO2 are significant. Concentrations of other measured gases follow similar trends. The faster-growing fires generate greater amounts of toxic gases with trends in time similar to those observed for CO concentrations described above. One exception to these trends appears to be in measured HCN concentrations, which are not shown here. Notably, higher levels of HCN concentration than in the other tests are measured during Test 4FV and the FR couch fires in Tests 9FV and 7FV. In contrast, the other gas concentrations, including CO, in Test 9FV are within the range seen in the other faster fires, while those in Test 7FV are notably lower. Since these three couches are leather couches, one explanation for these apparent differences in trends could be related to the specific combustion characteristics of leather.

Taking all results together, it can be concluded that when camera visibility is lost, the conditions along the egress path have significantly degraded to hazardous levels. This means that after the smoke drops below 0.9 m or the smoke layer collapses, occupants escaping the house will likely have a significantly diminished chance of survival due to loss of visibility, increased temperature exposure, degraded oxygen availability, and increased exposure to asphyxiant gases.

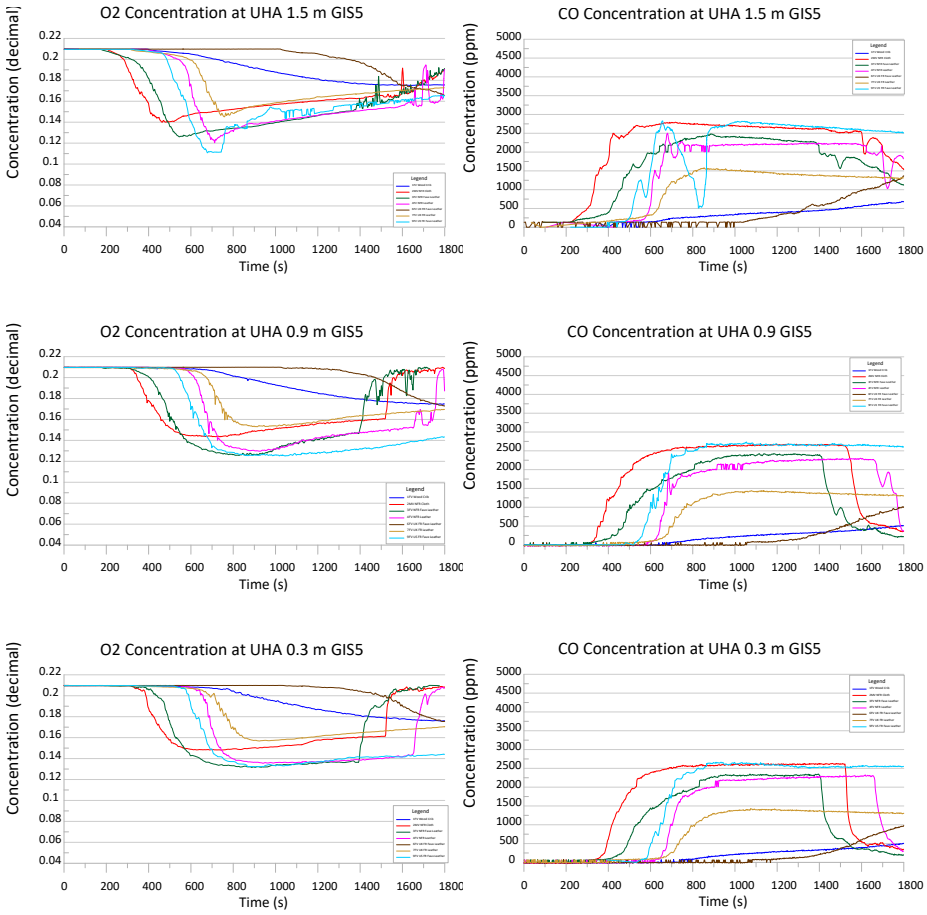


Figure 5-60: O2 and CO Concentrations at 0.3, 0.9 and 1.5 m heights in the UHA at GIS5.

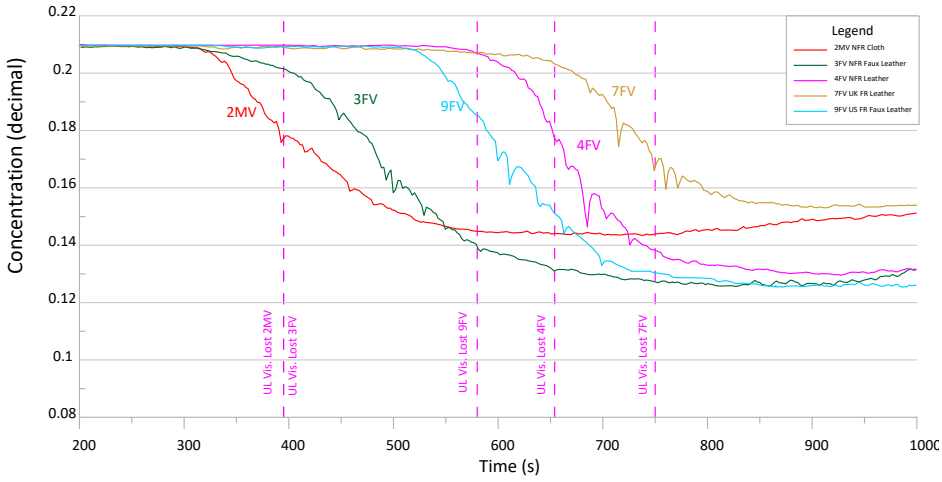


Figure 5-61: GIS5 0.9 m sensor height with upper level visibility loss lines for Tests 2MV, and 3,4, 7, and 9FV.

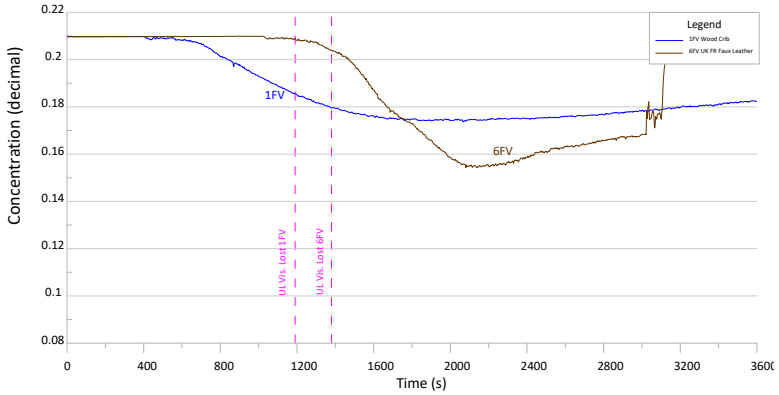


Figure 5-62: GIS5 0.9 m for Test 1FV and Test 6FV with upper level visibility loss line superimposed.

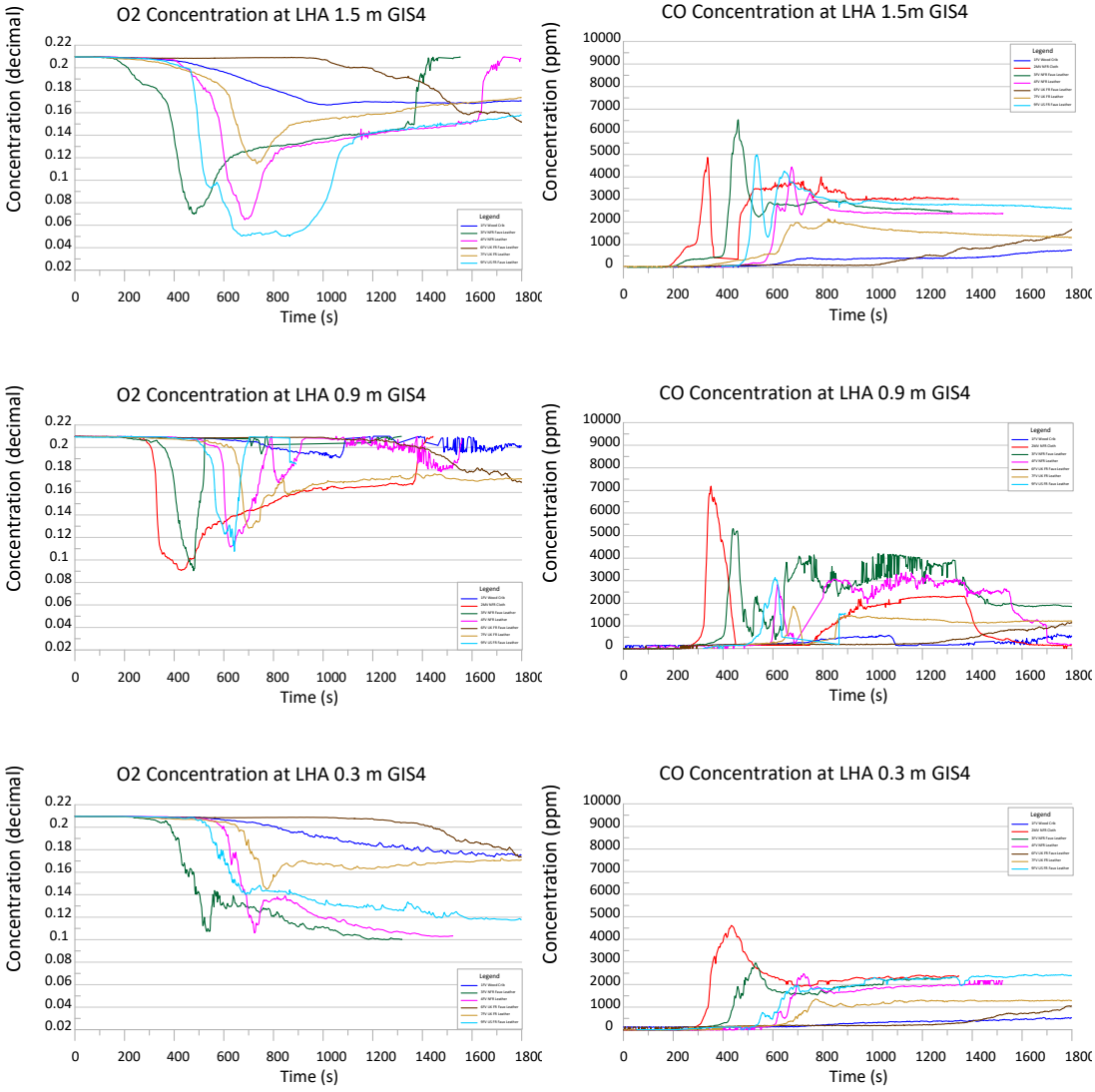


Figure 5-63: Lower Level O_2 and CO concentrations at GIS4, top 1.5 m, middle 0.9 m, bottom, 0.3 m above the floor.

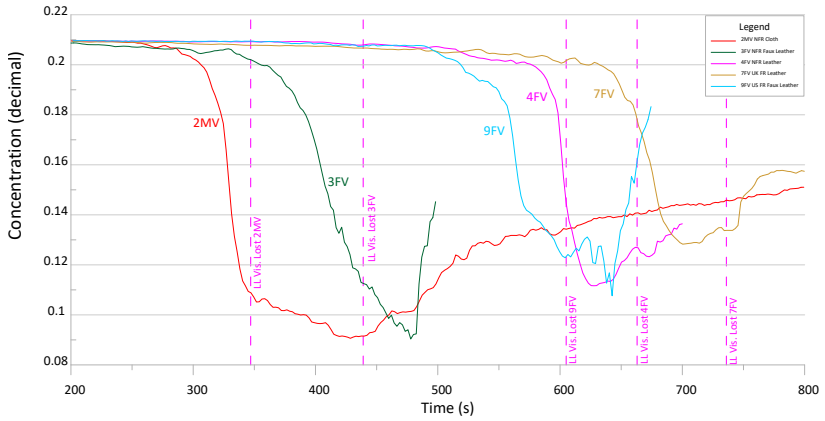


Figure 5-64: GIS4 0.9 m with visibility loss lines for Tests 2MV, and 3,4, 7, and 9FV.

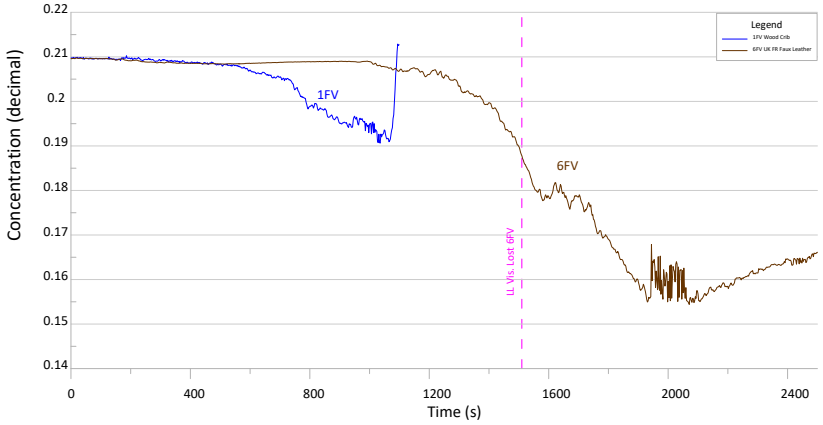


Figure 5-65: GIS4 0.9 m for Test 1FV and Test 6FV with lower level visbility loss line superimposed.

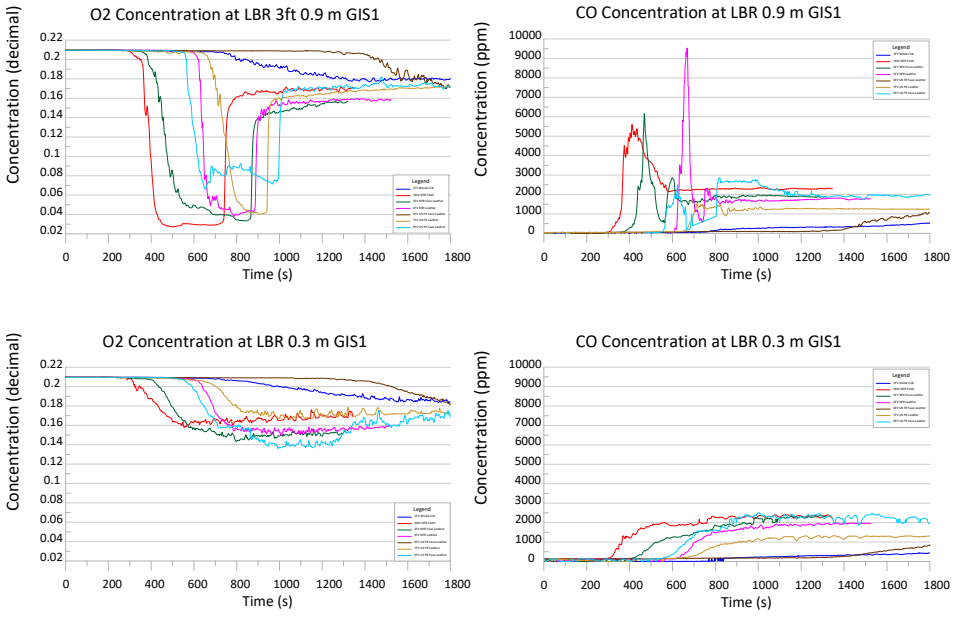


Figure 5-66: Lower Level O2 and CO concentrations at GIS1, top 0.9 m, bottom, 0.3 m above floor.

Chapter 6
Results & Discussion

The previous chapter summarized the experimental findings on a component basis and documented the developing conditions within the burn house. This Chapter develops the linkages of the burning conditions to determine the walk-out and crawl-out escape times for each fire scenario and identifies the interrelated context associated with smoke filling, detection, furniture ignition, and fire growth. Further consideration is also provided on observed conditions of smoke layer development and disassociation, methods of evaluating ignition, fire growth on couches, and differences in detection response for near and far devices. A contextualization of the fire environment is provided over time for each test accounting for critical timeline events and the degradation of the environment, affirming the use of visibility as a threshold for the onset of degraded conditions.

6.1 Escape Times Based on Camera Visibility

As discussed earlier, escape time is estimated by comparing the visibility for different incipient fire durations, detection times, mass loss rates, levels of smoke layer descent, temperature distributions and species production rates in fires fueled by leather, faux leather (vinyl) and cloth couches with those fueled by wood and liquid fuels. A visual representation of the escape timeline relative to smoke filling is replicated from an earlier Figure 3-1 as Figure 6-1. For purposes of this discussion, t_0 represents the fire initiation time and is normalized to 0 in all instances, t_1 is the time of smoke detector activation, t_2 is the point where the smoke layer reaches 1.5 m above the floor. and t_3 is the time when visibility is lost on a given level.

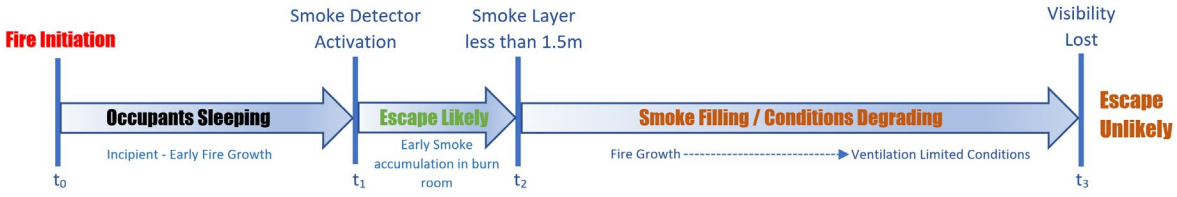


Figure 6-1: Visual representation of stages of fire development and viability of escape.

The following key considerations need to be factored into this analysis:

1. The Hazing Effect - for tests with slower fire growth or fires that did not ignite, particularly Tests 1FV, 5abcFV, 6FV, 7abFV and 8avFV, the smoke layer initially develops at the ceiling level with limited flaming that does not extend close to the ceiling layer. The smoke that is generated is white and mostly translucent in contrast to the grey, dense smoke formed in the

faster-growing flaming fires. In these cases, it is observed that the integrity of the interface between the upper (smoke) and lower (clearer) layers becomes less defined. Smoke leaks into the lower layer, leading to mixing and, in many cases, a full degradation of the smoke layer interface, creating a single zone instead of two layers. This is illustrated in Figure 6-2 for several tests at different intervals after the start of the fire. This creates a "smoke haze" that becomes the end condition for the non-ignition tests, including all of the subsets of Test 5FV and 8FV, as well as 7aFV. Aside from the haze, these tests do not result in significant oxygen depletion and do not exhibit elevated temperatures or significant accumulation of toxic gases. For this reason, they are not included in most of the graphs to limit clutter and processing time.



Figure 6-2: LBR quad video images of several fire tests at different intervals showing smoke hazing.

2. For Tests 1FV, 6FV and 7bFV, the hazing effect created a "new normal" environment within the house. As an example, a haze throughout all rooms on both levels is present for Test 6FV at 14:00 after ignition as illustrated in Figure 6-3. The haze appears to be denser on the lower level versus the upper level, but the distribution within each floor area appears relatively consistent. Figure 6-4 provides the Novatech curves for the three tests in the LSW at 1.5 m. Compared with Figure 6-3 at 14:00 (840 s), Test 6FV has no appreciable increase in CO and CO_2 despite the haze. This equally applies to Test 1FV and 7bFV, where increases in toxic gases do not start until the fire transitions into a growth stage. Even then, concentrations of CO and CO_2 in Tests 1FV and 6FV stay well below the thresholds for exposure over 30 minutes (1500 s) summarized in Table 2-1 [35]. Measured gas concentrations in Test 7bFV eventually

exceed the thresholds due to the degree of burning of the fuel. Regardless, results affirm the limited exposure to toxic gases that occupants may encounter during this hazing period prior to the transition of the situation to a growing fire. The rationale can equally be applied in terms of temperature exposure based on the curves in Section 5.8 and Appendix B. This suggests that, aside from a minor loss in visibility, there is limited additional risk from low oxygen, elevated temperature or high toxic gas concentrations during the haze prior to the transition to the growth stage of the fire. The increased duration of the hazing period, corresponding to the incipient fire stage, equally increases the likelihood of detection during this stage of the fire, which increases evacuation time, as observed in Test 6FV.



Figure 6-3: Lower level (left) and upper level quad video capture at 14:00.

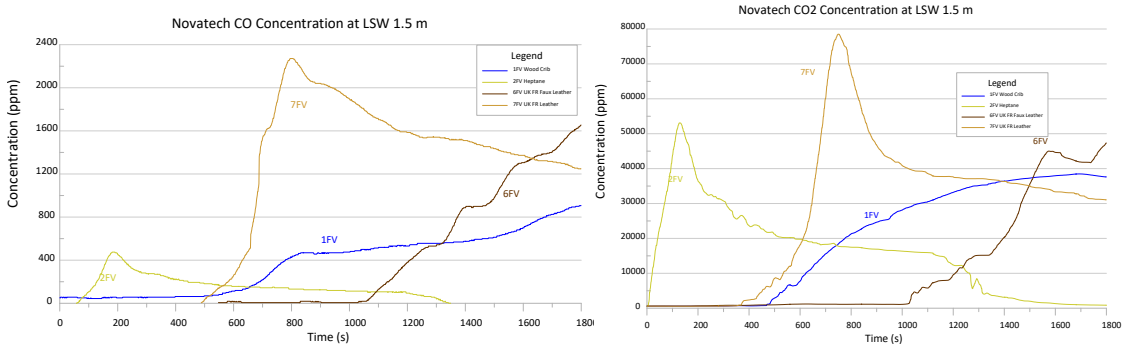


Figure 6-4: Reference comparison of CO and CO2 curves at Novatech sensors located at 1.5 m in the LSW.

3. The "Smoke Layer within the Smoke Layer." The presence of the "new normal" hazing effect throughout the house means that when the fire transitions to a growth stage, a new smoke layer develops within the LBR independent of the smoke haze. This is illustrated for Test 7bFV in Figure 6-5. It is necessary to differentiate between the existing hazing and the new smoke layer descent from the growing fire when determining the time for the smoke to reach 0.9 m above the floor and any subsequent smoke layer collapse. This requires a detailed analysis of video images, particularly in Test 6FV and 7bFV, and the use of multiple camera perspectives to quantify the new smoke layer evolution before and after fire growth. Generally, hazing and

smoke drift occur in all tests to varying degrees. For purposes of analyzing escape, these are considered to present limited risk and, therefore, are not counted in determining times to smoke layer collapse and walk-out escape times.



Figure 6-5: Test 7bFV showing smoke layer within the smoke layer.

4. Upper Level Smoke Clouds – the concept of a developing and descending smoke layer is not realized on the upper level. A smoke layer is formed in hotter fires (e.g., 2MV) at the top of the stairs and in the UHA. However, smoke can readily be seen mixing and swirling across the cameras, making a meaningful determination of the formation of a distinct smoke layer difficult (see Figure 6-6). In cooler fires, the smoke layer does not rise to the ceiling on the upper level, and smoke is observed on the floor at the top of the stairs and is dispersed upwards from there. Unfortunately, no imaging is available from within the stair enclosure. However, it is suspected that the smoke cloud and floor level smoke layer development that leads to a more homogenous mixture on the upper level is due to one or a combination of cooling of the smoke layer as it progresses away from the origin of the fire; mixing of gases in the stair enclosure with cooler gases from the upper level; and/or the inducement of airflow between the upper and lower level due to development of ventilation-limited conditions. DiPaola made a similar observation of mixing in the stairs when studying the MV test series [159]. However, as a consequence, using criteria such as smoke layer descent to 1.5 or 0.9 m heights, as described in Section 4.1, is not feasible for analysis of smoke layer development in the upper level. Instead, given that the loss of visibility in the upper layer occurs after the smoke descends to 0.9 m or

the smoke layer collapses on the lower level, it is reasonable to use this benchmark to determine the upper and lower bounds for crawl-out escape time, without further consideration of conditions on the upper level.



Figure 6-6: Upper level quad image capture of Test 2MV at 05:09.

5. The responding detector for this analysis was originally considered to be D3, located in the LSW. As such, it is more remote from the fire source than either D1 or D2 located in the LBR and LHA, respectively, but is reflective of the minimum level of compliance for detection required by the NBCC for this particular floor layout. The analysis presented below considers the response time from both D1 and D3 as they respectively form an upper and lower bound for detection and evacuation time for each test and, therefore, can be combined to provide walk-out and crawl-out escape times as a range. D2, although on the same level, responds at times between response times for D1 and D3 and, therefore, is not included further in the analysis here.

6. A maximum time of 1800 s (30 mins) is applied for tests where visibility is not lost, including Tests 1FV, 5FV, 6FV and 8FV. This is considered a reasonable outer window for identification and response to a developing house fire.

With the qualifications described above and throughout this thesis, the escape times can be determined. The estimated "Walk-out" escape times (t_2-t_1 in Figure 6-1) and "Crouch or Crawl-out" escape times (t_3-t_1 Figure 6-1) for the lower level are determined using the observation analysis in

Section 5.7 and summarized in Table 5-7. Escape time results for the lower level conditions are compiled in Table 6-1 for walk-out and Table 6-2 for crouch/crawl-out, which are further discussed in the following sections.

Table 6-1: Lower level walk-out escape time range based on D1 and D3 activation.

Test	D1 (t_{1a}) Activation (s)	D3 (t_{1b}) Activation (s)	Smoke Layer 1.5 m AFF (t_3) (s)	Walk-out Escape Time Upper Bound $t_2 - t_{1a}$ (s)	Walk-out Escape Time Lower Bound $t_2 - t_{1b}$ (s)	Percentage Difference
1FV	488	537	685	197	148	33%
2MV	141	189	211	70	22	218%
3FV	127	183	225	98	42	133%
4FV	403	433	503	100	70	43%
5cFV	313	385	482	*	*	-
6FV	138	748	398	*	*	-
7bFV	297	361	436	139	75	85%
8FV	149	305	369	*	*	-
9FV	353	407	465	112	58	93%

* Not determined - smoke mixing occurs, occupants are evacuating through smoke haze

Table 6-2: Lower level crouch or crawl-out escape time range based on D1 and D3 activation.

Test	D1 (t_{1a}) Activation (s)	D3 (t_{1b}) Activation (s)	Smoke Layer Collapse (t_3) (s)	Crawl or Crouch Escape Time Upper Bound $t_3 - t_{1a}$ (s)	Crawl or Crouch Escape Time Lower Bound $t_3 - t_{1b}$ (s)	Percentage Difference
1FV	488	537	1800*	1312	1263	4%
2MV	141	189	285	144	96	50%
3FV	127	183	365	238	182	31%
4FV	403	433	590	187	157	19%
5cFV	313	385	1800*	1487	1415	5%
6FV	138	748	1230	1092	482	127%
7bFV	297	361	642	345	281	23%
8FV	149	305	1800*	1651	1495	10%
9FV	353	407	548	195	141	38%

* Not determined - smoke mixing occurs, occupants are evacuating through smoke haze

6.2 Walk-out Escape Time

Escape times determined based on the walk-out 1500 mm criteria on the lower level are graphically depicted in Figure 6-7[9] This criterion is intended to align with average mouth and nose heights above the floor. Therefore, using this value as a threshold means that smoke is already below average head heights of 1.8 m for occupants escaping through the LBR. An initial observation is that all escape times are quite short, ranging from 22 s for Test 2MV to 197 s for Test 1FV. When applying this criterion to smoke layer development, the wood crib fire in Test 1FV clearly performs the best in terms of time for occupant escape. However, if the wood crib fire is excluded, the walk-out escape times are well below 2 minutes for the lower bound, and three tests are below 1 minute. Only the FR

[9] The criteria is not applied to Tests 5, 6 and 8FV for reasons described above.

leather couch in Test 7bFV has a longer possible escape time. One factor for the short escape times is the ceiling height of 2.4 m in the burn structure. This is potentially on the lower end of typical ceiling heights in modern houses, which have trended more towards 2.7 m or 3.0 m high ceilings. This directly limits the volume of the smoke reservoir that exists above head height and, thus, the volume of smoke that can accumulate before impacting occupants, which in turn may decrease the walk-out escape time.

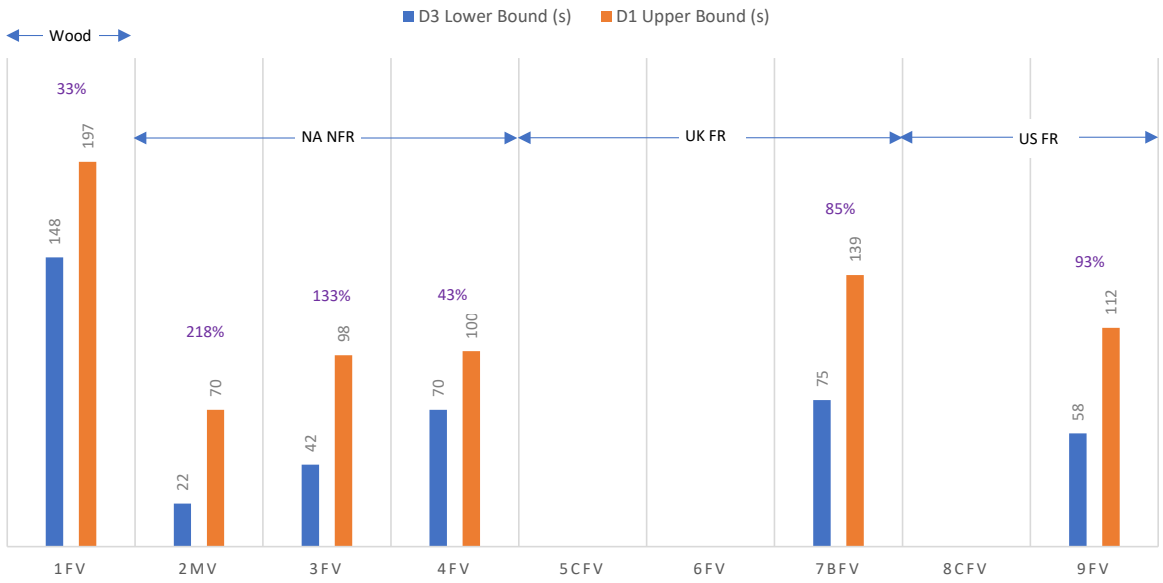


Figure 6-7: Lower level walk-out escape times.

Another key point to note regarding occupant escape is that the different tests had different smoke layer visibility characteristics, likely due to relatively low fire sizes and the presence of ventilation within the house. In Test 1FV, the density of smoke is lower, and there is greater mixing through the whole lower floor when compared with Test 2MV, which has a dense and definable smoke layer with no significant hazing below the smoke line. This illustrated in Figure 6-8 by comparing the burn room quad videos. On the left is Test 1MV, where, looking at C4, there is less obscuration on CB3 than C4 at the very top of the board. Looking at C7 in Test 1FV, the top of CB4 is still visible through the smoke, unlike the comparable image in Test 2MV. However, the same observation does not extend through CB1, where the smoke hazing appears lower in Test 2MV versus Test 1FV.

The hazing and smoke layer density differences are even more pronounced when comparing Test 3FV and 6FV. As shown in the video images in Figure 6-9, the visibility at C7 looks uniform from floor to ceiling when smoke in the LBR has reached 1500 mm on CB2 in Test 6FV. In C1 on CB1, streaking of smoke north/south across the camera is evident in C4 of Test 6FV. Test 3FV has a traditional smoke layer build-up, much like Test 2MV.

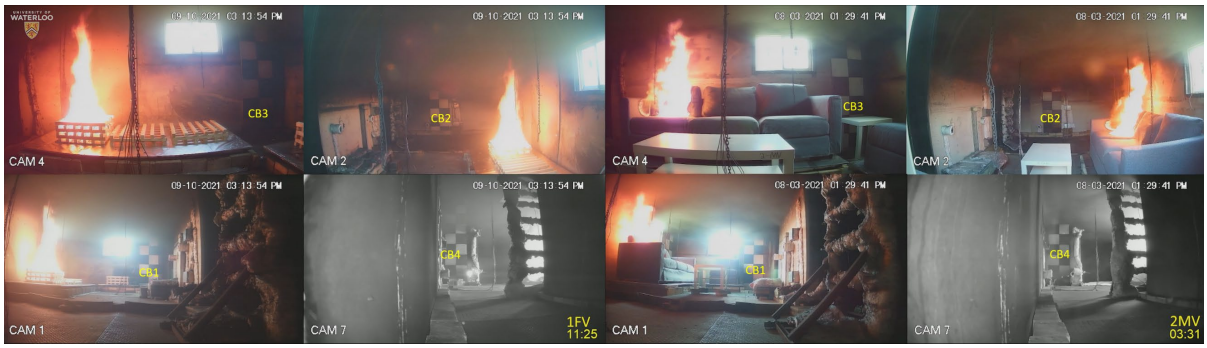


Figure 6-8: Comparing smoke layer at 1500 mm between Tests 1FV and 2MV.



Figure 6-9: Comparing smoke layer at 1500 mm between Tests 3FV and 6FV.

Considering the different fabric covers in the NFR tests, the results align with the general performance predicted in the introduction of Chapter 3. The cloth couch performs worst with a time of only 22 seconds, the faux leather has improved performance at 42 seconds, and the leather couch increases the escape time to 70 seconds using this criterion. These differences potentially highlight the importance of the couch cover fabric in terms of fire performance. Escape time improves if the cover fabric resists participation of the polyurethane foam couch cushions in the fire, similar to what was observed in the MLR comparisons for fire growth and spread. However, as will be outlined, this doesn't hold true for the crouch or crawl out escape time.

In summary, the walk-out safe escape timelines are short and do not afford a significant time to escape. For this house configuration, this likely means that occupants will have to evacuate by crouching or crawling unless their response to a detector is instantaneous and their escape travel is immediate and definitive.

6.3 Crouch/Crawl-out Escape Time

The original concept for determining crouch or crawl escape times is to evaluate the time that it takes for the smoke layer to descend to 0.9 m above the floor, effectively representing a height where one could maintain their head below the smoke layer to escape the house following common advice from

the fire service. However, the criterion is adapted for the present fires since the smoke layer collapses before descending to 0.9 m in some tests, as presented in Subsection 5.7.2 and illustrated on Figure 5-33 and several subsequent figures showing the descent of the smoke layer. This proves to be a relatively consistent phenomenon when visibility loss times are evaluated relative to oxygen depletion through the house, as discussed in Section 5.9 and illustrated in Figure 5-64, it is found that there is likely a correlation between the ventilation-limited environment and an increase in mixing throughout the house, effectively eliminating the buoyancy of the heated smoke layer and essentially filling the house with smoke.

Using the adapted criteria of smoke layer collapse or 0.9 m, escape times for the crouch or crawl are established based on camera visibility, where the loss of visibility is t_3 referenced in Table 6-2 above. The estimated escape times using this threshold are graphically illustrated in Figure 6-10. As a baseline, wood has a 1263 s lower bound escape time, which is less predicated on the visibility (since the wood fire never reached a full loss of visibility) and more based on the artificial 30 min maximum time than the detection time. Nevertheless, the wood-fueled fire, representing a naturally occurring material optimized for combustion, exceeds the worst-case evacuation time identified by Proulx as a range of 120 - 970 s [1]. Amongst the couch fires, the only tests for which the escape time exceeds this worst-case range are the couches that did not ignite.

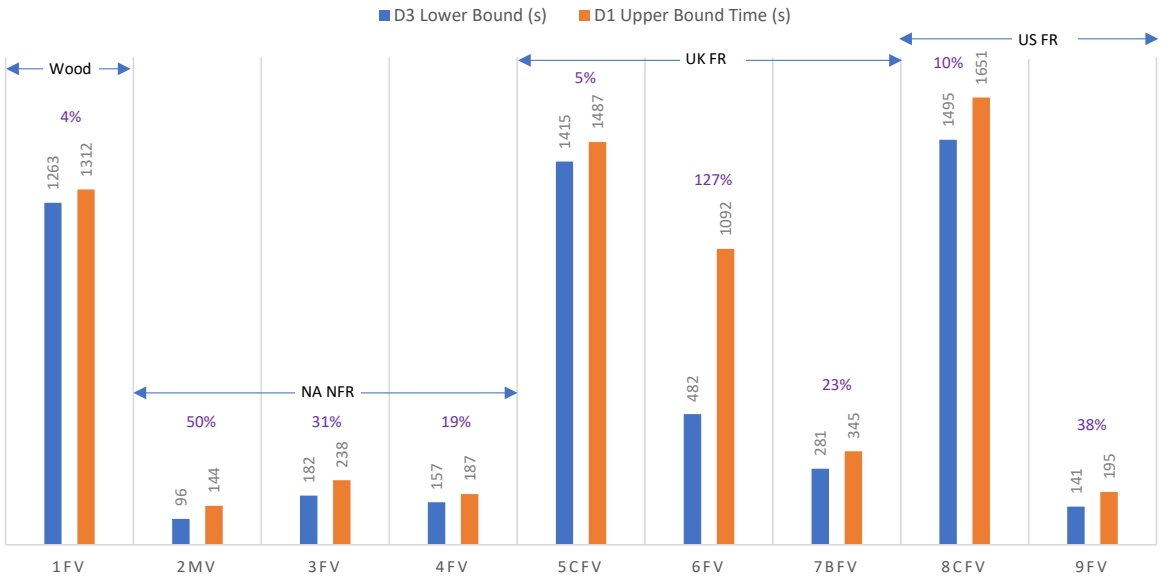


Figure 6-10: Lower level crouch/crawl-out escape times for all tests.

At the same time, there is a significant difference in the performance of the different couches when looking at crouch or crawl visibility compared to the 1500 mm criteria. The couches with high fire growth rates have very short escape times, ranging from 96 seconds for Test 2MV to 238 seconds for

the faux leather couch in Test 3FV. Looking first at the difference across NFR couches, the cloth couch has the shortest available escape time, and the faux leather couch has the longest available escape time. Recall from Figure 5-17 that the time to peak MLR is shortest for cloth, faux leather, and then leather couches. Based on this, the intuitive expectation would be that the leather couch will have a higher ASET when compared with the faux leather based on MLR alone. However, when the delay of the smoke alarm response and the subsequent rate of fire growth are factored in, the leather couch fire actually results in a 15 s shorter escape time on the upper bound (D1) and a 51 s shorter time on the lower bound (D3), illustrating how time evolution of MLR, and correspondingly HRR, do not necessarily correlate to escape time without consideration of the detector response time as well.

Comparing the different NA NFR and UK FR couches, the NFR cloth couch fire that has the shortest ASET obviously cannot readily be compared with the UK FR cloth couch since the UK couch did not ignite. The absence of ignition of the UK cloth couch, and therefore the continuous visibility throughout the test, is indicative of superior comparative performance to the NFR cloth couch, which readily combusted and lost visibility faster than any other couch after the start of ignition. Similarly, but not quite as contrasting a difference, the UK FR faux leather Test 6FV has an escape time of 300 s (5 min) longer than the 182 s escape time for NFR faux leather Test 3FV on the lower bound. On the upper bound, this difference increases to 854 s (1092 – 238 s, over 14 minutes). While not quite reaching the worst-case timeframe of 970 s [1]This upper bound is the closest of the flaming fires to meeting this target. The effect of the UK FR controls on the leather couch in Test 7bFV is more muted than the cloth and faux leather couches. When compared with the NFR leather couch in Test 4FV, however, there is still a 124 s greater ASET in Test 7bFV over Test 4FV on the lower bound and 158 s on the upper bound, not accounting for the substantially larger ignition source in Test 7bFV.

Lastly, with the US FR furniture, there is a clear contrast between the performance of Test 8FV, which did not ignite despite two attempts and Test 9FV, which compares better with Test 2MV in terms of fast fire growth and rate of smoke filling. While Test 9FV demonstrates the highest fire spread and the greatest release of toxic gases, it still does not have the shortest escape time. It is reasonable to conclude that the couch in Test 8FV performed as expected, given the compliance with the TB 133 standard, but that in Test 9FV, it underperformed. This is likely attributed to the poor performance of the fabric covering the foam cushions, as the material readily peels when exposed to the flaming fire ignition source.

In considering comparable couches, the findings illustrate the potential positive effectiveness of fire controls in UK furniture over the NA NFR furniture, but to differing degrees. Comparing the

overall escape times for Tests 3FV versus 6FV and 4FV versus 7bFV, there is between a 79% and 359% increase in escape time. This does not account for the larger igniting source used in Test 7bFV, nor the non-ignition of Test 5FV when compared with Test 2MV, where the latter is the fastest burning fire and has the lowest escape time versus a couch that does not ignite and, therefore has an extended escape time. Further, the couch in Test 5FV is exposed to a Crib 7 initiating source much larger than the Crib 4 igniting source used in Test 2MV. Due to such differences, the controls used are further discussed in the section on furniture below.

6.4 Detector Location Sensitivity

By establishing the upper and lower bounds of detector response times, the detector position is incorporated into the analysis of the experimental findings. As discussed in Section 2.2.5, the impact of detector position on increasing the time to escape requires further study. The difference between the D1 and D3 detector response times is superimposed in Figures 6-7 and 6-10 and is presented as percentage changes in Tables 6-1 and 6-2. The effect of the proximal detector in this research results in an escape time increase of 33 – 217% based on the walk-out criteria and 4 – 127% for the crawl-out criteria. The difference between the tests for each of the systems is provided in Table 6-3. As shown, the increase in evacuation time is between 21 and 610 s for the Mircom system, and -71 and 359 for the VESDA system. In general, for the flaming fires in the NFR tests, the increase in evacuation time is on the order of 50 – 60 seconds, which is significant given the relatively low 96 to 238 s escape times for these tests. In the slow-growing fire in Test 6FV, there is a much larger increase in escape time to 610 s for the Mircom and 359 s for the VESDA system.

Table 6-3: Time difference between LBR and LSW detectors (D3 - D1).

D3-D1	1MV	2MV	3MV	4MV	1FV	2FV	3FV	4FV	5aFV	5bFV	5cFV	6FV	7aFV	7bFV	8FV	9FV
Mircom	55	48	66	48	49	21	56	30	594	162	72	610	516		156	54
Vesda	69	63		68	60	-71	72		72	123	61	359	403	64		181

The key point is that while past research has focused on the sounding function of house smoke alarms, the interlocking of alarms now allows the placement of the devices to be optimized for fuel load without compromising the ability to wake occupants.

6.5 Graphical Summary of Flaming Fire Tests

The use of a crawl-out escape time is not in alignment with the accepted ASET/RSET methods, which assume a walk-out escape time and smoke layer descent to 1.5 m above the floor or higher. Consequently, a criterion based on the occupant having to crawl out represents a disadvantaged situation where an occupant needs to move with their head low and breathing air below 0.9 m. However, during the time period when the smoke layer collapses, and the lower layer visibility is lost,

the escapee is no longer evacuating through a clear path and instead is moving through an increasingly risky environment. For this reason, the 0.9 m/smoke layer collapse condition is used as a basis for determining the escape times.

To further investigate these conditions, Figures 6-11 to 6-16 provide summary overviews for each flaming fire test, comparing the O_2 conditions at 0.9 m above the floor, the CO conditions at 0.3 m above the floor and the fire MLR with time, overlaid with key times for detection, smoke layer collapse and upper layer and lower layer lost of visibility as established through the experimental series. The CO sensor at 0.3 m was selected in lieu of 0.9 m due to the better-quality concentration data from the sensor and given that, while crawling, the mouth and nose of the head can actually be much lower than 0.9 m above the floor. These two conditions, therefore, provide a sense of the overall environment through the duration of the fire near the escape point from the house through D2.

The graphs are superimposed with the time between D1 and D3 activation, the escape window based on a D3 activation, and the period between the smoke layer collapse and loss of visibility in the lower layer, which represents a period in which an escaping occupant is at significant risk.

The following additional observations are noted based on the graphical summaries:

1. Loss of visibility in the upper and lower layers occurs around the time of peak fire MLR and thus the minimum O_2 concentrations, although there is variability, with some criteria being marginally before or after the high MLR and low O_2 conditions.
2. The collapse of the smoke layer occurs just after the oxygen level starts to decrease in all tests, generally before any significant accumulation of CO, and therefore CO_2, as well as other toxic gases. This further rationalizes the criterion as the escape threshold for crawl-out.
3. The window of increasing risk to an occupant is relatively short, between 57 s for Test 9FV to 240 s for Test 6FV. During this period, oxygen concentrations drop to low levels, and toxic gas generation increases. Beyond this, conditions are not favourable for escape.
4. Comparing the UK and NFR couch fires, the UK couches are characterized by considerably lower concentrations of CO and higher concentrations of O2 than the NFR comparables, likely attributable to their lower MLR.

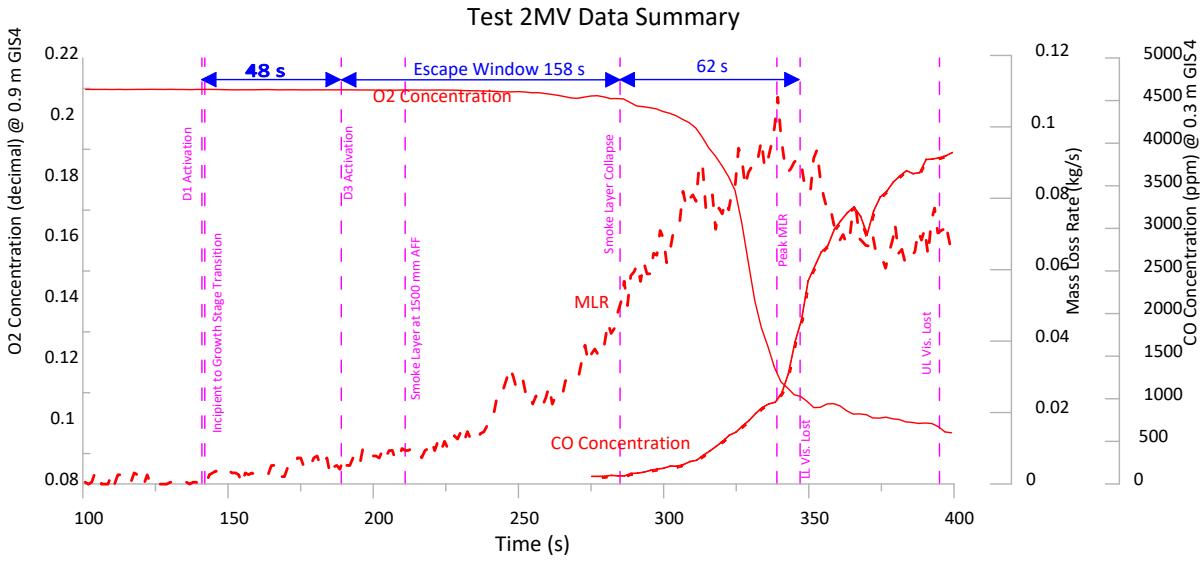


Figure 6-11: Test 2MV all timeline points are overlayed with MLR, O2 and CO versus time.

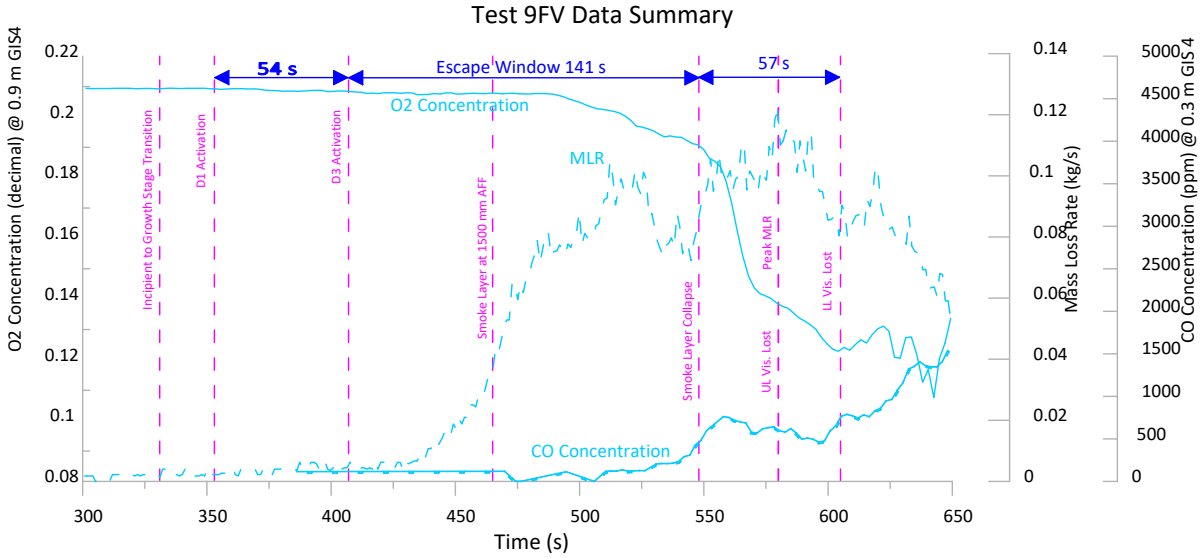


Figure 6-12: Test 9FV all timeline points are overlayed with MLR, O2 and CO versus time.

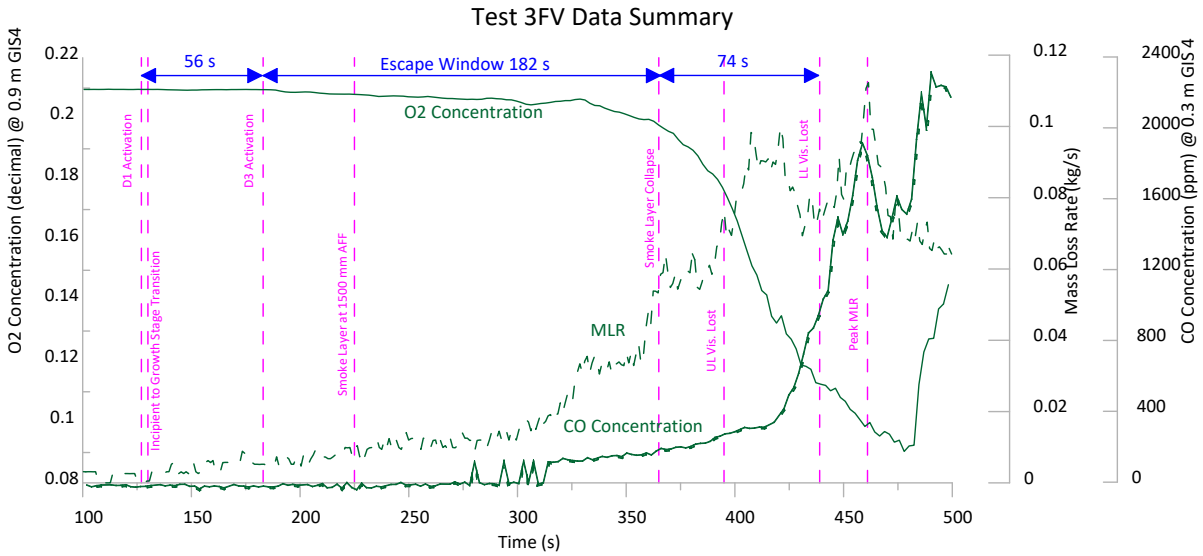


Figure 6-13: Test 3FV; all timeline points are overlayed with MLR, O2, and CO versus time.

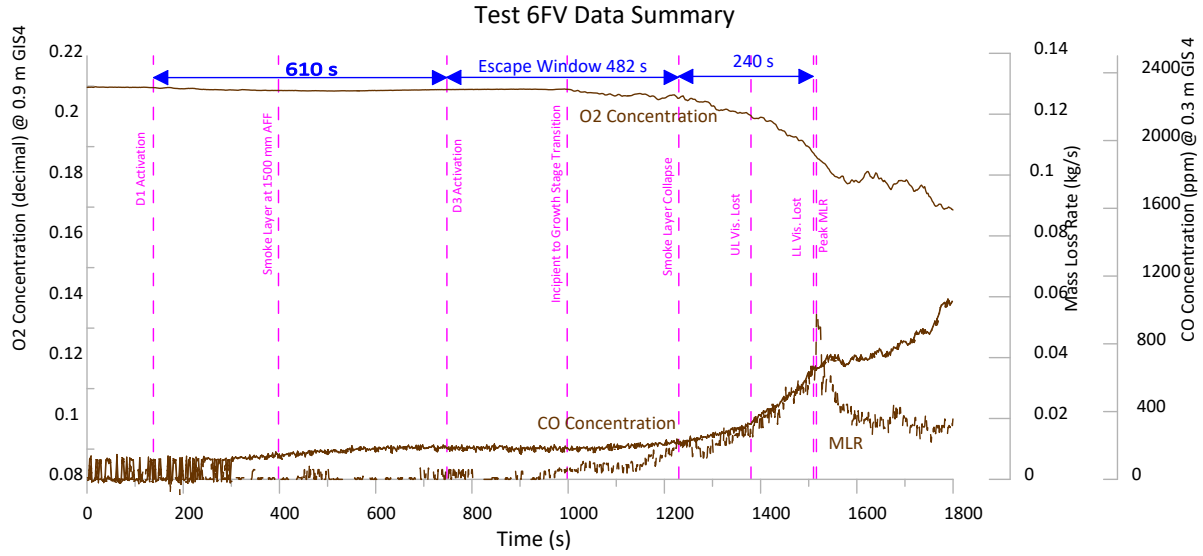


Figure 6-14: Test 6FV; all timeline points are overlayed with MLR, O2, and CO versus time.

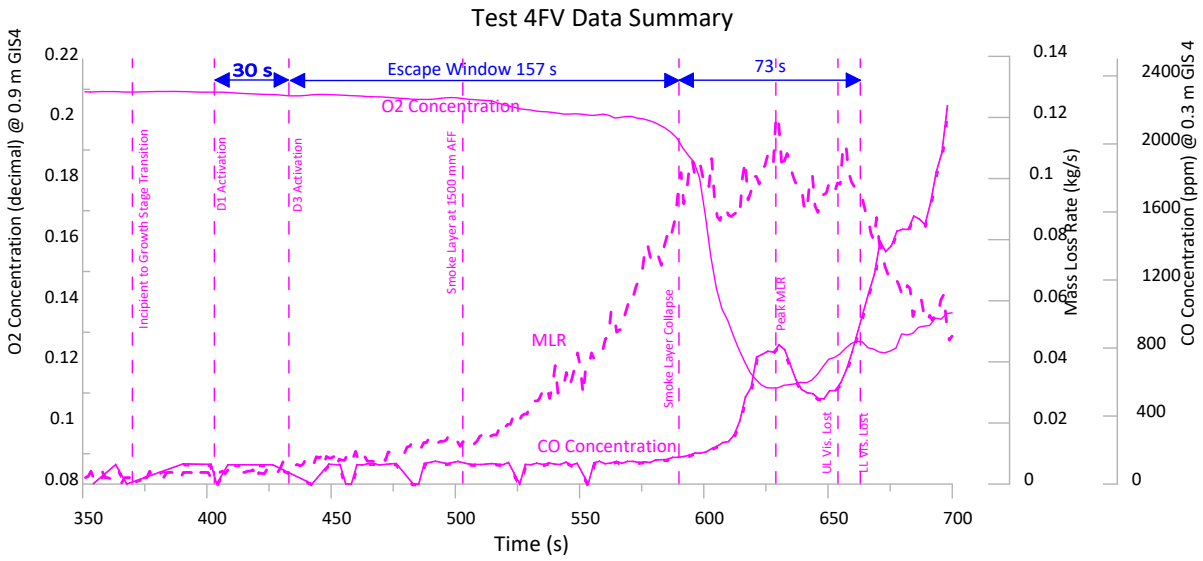


Figure 6-15: Test 4FV; all timeline points are overlayed with MLR, O2, and CO versus time.

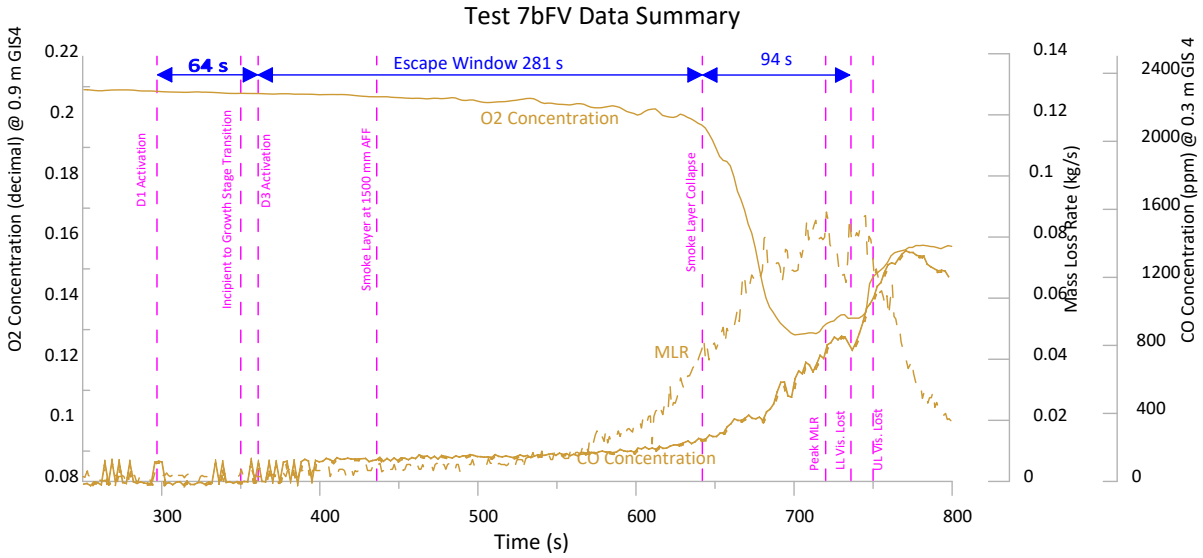


Figure 6-16: Test 7FV; all timeline points are overlayed with MLR, O2, and CO versus time.

Section 5.7.2 provides a detailed description of the smoke encapsulating the flaming region of the fire. Figures 6-17 and 6-18 further illustrate this phenomenon by superimposing yellow lines delineating the observations in 10 s increments in Test 2MV, showing the progressive encapsulation. From C4 and C1 at 04:50 after ignition, the smoke layer descended lower in both corners on the south side of the room. On C4, the end table and the checkerboard are visible and progressively disappear along the right side of the couch and, eventually, the coffee table. The window remains partially visible until 5:50 into the test, after which the entire right side of the couch disappears. On C1, the bottom of the window shows the southwest corner of the room disappearing, and progressively, the east wall starts to disappear from view by 5:50 into the test, at which point, the whole of the west side of the room is no longer visible and only the flaming region of the fire is observable. Further, C7 loses visibility just before C4 and C1 and smoke is observed recirculating in front of the camera just before visibility is lost.

Zhang et al. analyzed elevated pool fires in a 3 m x 3 m x 1.95 m compartment and noted that the smoke layer descended down to the level of the fuel surface but then descended to the floor along the walls via wall jets [5]. In their experiment, the wall jets extended past the smoke layer interface and then circulated back, filling the lower layer. Their experimental design was symmetrical in the compartment and had a simplified fuel load with an elevated fuel tray. The present experiments involve a more complex couch fire with a wider burn area, burning fuel that drops to near floor level and is established in a much larger compartment (more oxygen) where the fuel is positioned on one side of one of the rooms. The observations of smoke layer development during the limited ventilation fires in the present experiments are also different, as they align better with a progressive collapse of the smoke layer interface from the top down with time after ignition. This may involve some mixing from wall jets, as observed by Zhang, but appears to be more like the formation of a smoke cloud around the fire's perimeter due to the ceiling jet flows and thermal conditions within the compartment. The influence of the other rooms within the structure also requires further exploration as, in some instances, lighting conditions limited observations of smoke movement within the space.



Figure 6-17: Encapsulation of smoke layer onto the fire – Test 2MV – Part I.



Figure 6-18: Encapsulation of the smoke layer onto the fire - Test 2MV - Part 2.

The above substantially characterize the conditions that develop during ventilation-limited, flaming couch fires across the different furniture growth rates and conditions in this test series. The findings reflect what occurs during fires in more modern, fully enclosed houses, where the windows do not break and the house fills with smoke, limiting visibility and impacting the interior environment with decreased O_2 levels and increased concentrations of various toxic gases. This "smoke filling" in an enclosed house can negatively impact escape time, and understanding the environmental conditions allows for a greater determination of how to place detectors and how much time is available to escape a house fire. Further, the multi-perspective video capture of the smoke layer development in the burn room and the smoke filling extending to the corridor and upper level offer a unique perspective of real-scale smoke layer development not previously identified in the literature.

6.6 Furniture controls

Clear objectives for controlling fire growth in furniture are not well established. Rather, the scope of each of the three test standards considered in this research is to prevent the ignition of the furniture,

whether that be from a cigarette (TB 117 post-2013), a cigarette and a small flame (TB 117 pre-2013), a cigarette and a small flame and a small flaming ignition source (BS 5852), or a fairly large burner flame for a shorter duration (TB 133). Nevertheless, considerable research has focused on quantifying the effectiveness of furniture controls in limiting fire growth post ignition, whether that be in the form of small-scale testing, such as the cone-calorimeter, or in the form of intermediate-scale testing, such as single-burning items in a furniture calorimeter or in small scale room fire tests.

Since furniture tested to the above standards is designed to limit the potential for "ignition" of the furniture item, the consideration of full-scale testing with ignition sources that overcome the ignition controls as a mechanism to evaluate the overall performance of the furniture item is absent as there is not sufficient context nor goals to define whether the performance of one item is better than another in a real-scale situation. Rather, scientific debate has ensued over the use of certain flame retardants in furniture items and whether the trade-off of health risks is sufficiently beneficial to justify their use. This dichotomy of thinking is independent of the fact that there is still a general acknowledgement by the industry that there is a need to control furniture fires, but there are no agreed-upon objectives for assessing performance in terms of rate of fire growth, peak fire size or duration of burning, nor establishing escape times across furniture designs.

Based on this work, the following additions can be made to the discussion:

1. No direct correlation is found between ignition and burning rate. On the one hand, the best-performing fire growth on an ignited couch is in Test 6FV. However, it ignites with the lowest Crib 4 ignition source. It was hoped that scaling the ignition sources might allow for some way to correlate ignition source thresholds with the ignition of different furniture controls, but this is not evident from the results.
2. Using the peak MLR or, correspondingly, HRR as a sole indicator is also not informative when furniture will be installed in fully enclosed structures, given that all ignited tests became ventilation-limited, and the true peak MLR was likely never realized in these tests, nor was flashover. Therefore, using open-burn tests to determine fire evolution with time and peak fire size is likely not reflective of the end-use condition but could be a useful consideration as part of a scoring method.
3. A couch's prolonged incipient fire development time and a slower fire growth rate are positive attributes to increase available escape time. Delays in combustion reaching the fire growth stage increase the time available for the smoke haze to recirculate and reach smoke detectors. Therefore, a detector will eventually respond even when a prolonged incipient time occurs. In

the case of a slower fire growth rate, the buildup of smoke, toxic gases, and oxygen depletion is slower and therefore more preferable for escape, as observed in Tests 6FC and 7bFV when compared with the equivalent NFR couches, as presented in Figures 6-13 to 6-16.

The key parameters for couch burning (ignition source, incipient fire period, growth period and peak MLR) are considered relative to a potential scoring system for ranking the couches. The scoring system is developed independently of the detection time since it is inherent in the incipient fire and growth times. Data to inform a scoring system can be found from the experimental data from earlier sections of this report, as follows:

- Ignition size, Section 5.1 Table 5-2
- Incipient fire stage, Section 5.3, Table *5-3*
- Fire growth time to peak MLR, Section 5.5, Table 5-4
- Peak MLR, Section 5.3, Figure 5-5

A scoring system is then developed that aligns with logical transition thresholds and rounded to convenient numbering for each of the criteria above. This is presented as an example for these tests in Table 6-4. The score in each of the four categories is then added to achieve a total, which in turn allows the couches to be ranked.

Table 6-4: Scoring system for couch fire performance ranking.

Ignition Size		Incipient Fire Time		Fire Growth Time to Peak MLR		Peak MLR	
Crib Size	Score	Time (s)	Score	Time (s)	Score	(kg/s)	Score
DNI	1	≥ 600	1	≥ 500	1	<0.02	0
4	2	≥ 450	3	≥ 400	2	≥ 0.02	1
5	3	≥ 300	3	≥300	3	≥0.04	2
7	4	≥ 150	4	≥200	4	≥ 0.06	3
-	-	< 150	5	<200	5	≥ 0.08	4
-	-	DNI	0	DNI	0	≥0.1	5

Applying the data from Chapter 5, as outlined above, and scoring each of the values based on Table 6-4, the results of the analysis are presented in Table 6-5. Not surprisingly, given the consolidation of information above, the NFR couches rank at the bottom, along with the US FR leather couch from Test 9FV. The UK FR cloth couch that did not ignite and the US FR cloth couch that did not ignite rank at the top. The mock wood crib couch was next, with a total score of 7, followed by the FR faux leather in Test 6FV and the FR leather couch in Test 7FV. Using a ranking system allows full consideration of the fire parameters influencing detection and escape time. It addresses variations in ignition sources and appropriately ranks the risk profiles. Since it does not address detection time, the NFR leather couch ranks higher than the faux leather, while escape times are actually the other way around. Otherwise, the ranking of the couches is consistent with all of the findings.

Table 6-5: Risk scoring for all test couches

Test Number	Primary Fuel	Ignition Sources Used	Result	Ignition Rank	Incipient	Fire Growth Rate	Peak MLR	Total	Rank
1FV	Wood cribs	Crib 5	Ignition	3	3	1	0	7	3
2MV	NFR Cloth Couch	Crib 4	Ignition	4	5	5	5	19	9
3FV	NFR Faux-leather	Crib 4	Ignition	4	5	3	5	17	8
4FV	NFR Leather	Crib 5	Ignition	3	3	4	5	15	6
5FV	UK FR Cloth	Cribs 4, 5, and 7	DNI	1	0	0	0	1	1
6FV	UK FR Faux-leather	Crib 4	Ignition	4	1	1	2	8	4
7FV	UK FR Leather	Crib 5, 7	Ignition	2	3	3	3	11	5
8FV	US FR Cloth	Crib 7, Propane Burner	DNI	1	0	0	0	1	1
9FV	US FR Faux-leather	Crib 7	Ignition	3	3	4	5	15	6

The ranking also differentiates fire controls that may be used in couch design. Underperforming cover fabrics, as observed in Test 9FV, become appropriately ranked. Further, the method differentiates between the FR leather couch, with delayed fire growth, and the interliner-protected FR faux leather couch. The three couches with FR interliners are the best-performing couches. In the case of Test 6FV, the interliner significantly delays the PU foam's participation but also limits drop-down burning and protects the cushion's underside to limit the couch foam's participation in the fire when drop-down burning occurs. This increases incipient fire time, slows fire growth, and limits the peak MLR while still providing the longest available escape time, all of which demonstrate the potential effectiveness that furniture controls can achieve.

Where certain flame retardants are determined to be of sufficiently limited risk to justify their use or whether different products can be developed should be established by determining the potential efficacy of improving the risk to life by increasing the available safe escape time. Therefore, it is important to understand how furniture fire controls work and how controls may limit the participation of the furniture in a fire. As such, this research has provided a holistic perspective to potentially guide the future development of objectives associated with fire escape from houses.

Chapter 7
Conclusions

This research aimed to estimate escape times from the UWFRL burn house for a range of flaming fires with different material responses to ignition, fire growth rates and fire propagation characteristics under a continuous ventilation supply to the house. Detailed time and spatially resolved data on mass loss, visibility, oxygen consumption, and the evolution of carbon monoxide during ventilation-limited fires established on leather, faux leather (vinyl) and cloth couches versus wood and liquid fuels were obtained in a multi-compartment, two-storey burn house. The results detail the interplay between smoke filling, furniture fire growth, and detection time relative to limiting the available escape time along the egress path of the house.

A detailed analysis of the smoke layer development around the fires fueled by solid irregular-shaped fuels and its migration through the different rooms and levels of the multi-compartment, two-storey structure was obtained. Specifically, new and unique patterns of smoke layer generation were observed when fires developed more slowly, and a smoke haze was generated throughout the house, establishing a new normal room condition prior to the fire growth stage where a more conventional smoke layer developed within the smoke haze. Such conditions have not been reported in past literature. Similarly, on the upper level of the house, the smoke layer development was not as anticipated. A smoke layer formed initially in faster-growing fires, then diffused and readily mixed through the rooms on the upper level, limiting the ability to interpret a distinct layer of smoke and, correspondingly, the potential to estimate walk-out or crawl-out available escape times. Smoke, in some instances, appeared at the floor of the upper level near the top of the stairs either concurrent with or instead of at the ceiling as would normally be anticipated, and subsequently would progress into a room as a smoke cloud through the entire door opening, from floor to ceiling. Cooling, mixing, and air exchange due to the ventilation-limited conditions in the fire room and flow characteristics of the staircase are anticipated explanations for these events.

The differing fire conditions allowed the collection of new information for a range of environmental conditions occurring at times of smoke alarm activation relative to the onset of conditions that may preclude escape for different materials and different detector locations during the fires. The two detector technologies included in the study had comparable response trends but differences in their exact response times. Nevertheless, the placement of the detector in the house was found to be a significant factor in early warning of occupants of a developing fire condition, and the

data can be used to consider current and future code requirements for smoke alarm placement in houses, in consideration of potential to escape. Fires developing in living areas of the home where sleeping occupants are likely to pass during escape are afforded greater time to evacuate if the detectors are proximal to the fuel that is creating the hazard, in this case, furniture.

The importance of the size of the ignition source, incipient fire development in combination with subsequent fire growth rate and peak fire size were determined to be important parameters relative to detection and escape time across a range of furniture designed and built using different fire control strategies. Although it was difficult to establish a direct correlation between ignition, incipient and growth stages of the fire, the use of a scoring system provided a mechanism through which to weigh differences and, with further development, could provide a future context to consider a holistic way of evaluating furniture fire performance versus the current standards focused exclusively on ignition.

By investigating smoke layer descent, walk-out and crawl-out criteria were defined to establish the time to escape using an array of video imaging on both levels of the house.

In characterizing the smoke characteristics of the house,

1. Fires with longer incipient stages had cooler smoke that dissipated throughout the floor before the fire growth stage was reached, leading to a “hazing effect” throughout the house. Analysis of the conditions during this incipient and early fire growth period did not identify a significant accumulation of toxic gases, elevated temperatures, or depleted oxygen.
2. The hazing effect created a “new normal” baseline of smoke concentration on both levels of the house. For fires that continued to develop, a new heated smoke layer developed in the smoke haze. The new heated smoke layer from the growing fire behaved more traditionally with an upper layer of smoke but was contained within the new normal hazed environment.
3. When smoke layers in the upper level did develop, they readily dissipated and mixed throughout the floor level. Smoke layer analysis was found not to be practical due to smoke mixing and circulating around the rooms and frequently in front of cameras, creating a somewhat homogeneous environment.
4. Smoke migrating to the upper layer was observed in slow-developing fires to appear at floor level at the top of the stairs. The migration of smoke from the stairs and UHA was more characteristic of a smoke cloud than a hot smoke layer that would descend in a room. This is attributed to the mixing and cooling of air in the stair shaft geometry, the distance from the fire, and ventilation-limited conditions increasing the exchange of air from the upper to the lower level.

5. In the lower burn room, although the smoke layer initially developed as a relatively horizontal layer in the room, as the fire increased in size and the smoke layer descended, it arched away from the flaming regions, sloping down away from the fire toward the floor. The smoke layer eventually surrounded the fire and then pushed inwards to the fire plume from the perimeter of the room.

6. In establishing the escape criteria, it was found that the average to low ceiling height of the burning house (2.4 m) means the walk-out escape criteria of 1.5 m above the floor is reached relatively quickly after ignition. In fast-growing couch fires, using this criterion provided only a very short window of time for escape, with the lowest being 22 s and the highest 139 s. This would require a relatively immediate response from occupants to escape without delay which is unrealistic in most circumstances.

7. When evaluating the crouch/crawl-out escape time, the use of the 0.9 m and smoke layer collapse criteria timed well with potential for escape when all parameters that may affect tenability during evacuation were considered, albeit at a crawl height and not a head height. Beyond the time of the smoke layer collapse, occupants would be at risk of considerably worsening conditions of elevated temperature, depleted oxygen, and increased toxic gas concentrations. This reasonably validated the use of the 0.9 m/smoke layer collapse criteria as a basis for the analysis.

8. The crouch/crawl-out escape times were determined to be between:

    a. 1263 and 1312 s for the wood crib fire

    b. 96 and 238 s for the NFR tests

    c. 281 and 1487 for the UK FR tests

    d. 141 and 1651 for the US FR tests.

9. Compared with 1.5 m level evacuation times of 60 to 660 s, as considered by Proulx [1], only the two couches that did not ignite provided evacuation times longer than the higher time listed in this criterion. Depending on the detector location, the UK faux leather could provide a much higher level of protection. The remaining couches, including the UK leather couch, led to times for smoke layer descent to 1.5 m, that are well below 660 s. This affirms that if the furniture fire problem is to be solved, it will likely require a combination of flammability controls, which are achievable, and better detection along critical egress paths, also readily achievable based on current technologies.

Two detection systems were incorporated into the tests: a spot-type photoelectrical detector connected to a Mircom Panel system and a VESDA-E VEA microbore tubing system (approximately 33 m in length). With respect to detection, it was found that:

10. Both technologies effectively detected all fires and had comparable trends in response timing. Similar to tests that considered ionization and photoelectric detectors in the past [23, 46, 47], the focus should be on detector placement and optimizing the response of the technologies to effectively identify a fire while limiting the potential for nuisance alarms.

11. Earlier detection at D1 increased the escape time by 33 – 218% compared with D3 for the walk-out escape time. For the crouch/crawl-out escape time, earlier notification of D1 increased the escape time by 19 – 127% compared with D3 (discounting the wood crib fire and tests that did not ignite).

12. The two leather couches had the longest delays in detector activation, which reduced the available escape time. As a result, the fire established on the NFR leather couch led to a longer escape time than for the NFR faux leather couch fire while the opposite was expected.

The available escape time was, not surprisingly, determined to be very dependent on the fuel on fire. Home fires in furniture continue to be a frequent cause of fire death throughout North America, and one of the objectives of this research was to understand the impacts that furniture controls have on the time to escape a fire. The recent North American approach has been to eliminate flame retardants due to toxicological and environmental concerns. This research found that the design of effective controls for flammability and fire performance of furniture is likely more complex than will be solved through the current simple focus on flame retardants. Rather, the question should be asked as to whether there are controls that can limit both the propensity to ignite a couch fire and the propensity for the fire to quickly grow and spread. The salient conclusions of this research regarding furniture controls are as follows:

13. All of the NFR couches ignited using the smallest ignition source and subsequently exhibited much higher growth rates and peak MLR than the slow-burning wood crib fire and the UK FR comparable couches.

14. Drop-down burning appears to substantially contribute to fire progression in all NFR tests, the FR leather test, and the US FR faux leather test. However, limited drop-down burning was observed in the FR faux leather couch fire, Test 6FV, which had an interliner between the covering and the foam cushion. The least amount of couch material burned on this couch compared with all other couches that sustained combustion. Further, the fire was

characterized by a long incipient time, the lowest MLR, and a long growth time, all contributing to the longest available escape time of any of the couches that ignited and burned. In contrast, in couches where drop-down burning occurred, the bottoms of the seat cushions were covered with polyester liners and not protected with the same fabric as the top of the cushion that would be exposed to flaming during any of the test regimes discussed above. This allowed the fire to spread into the foam cushion from below through the polyester material, with consequential increases in fire growth.

15. In comparing the NFR leather and the FR leather couches, the NFR couch had a 370 s incipient time, and the FR couch had a 350 s incipient time. However, the FR couch had a longer growth time, a lower peak MLR, and correspondingly a lower total mass loss, leading to a longer escape time (281 s versus 157 s for the NFR crawl-out time). This is consistent with the 2015 tests that concluded that the FR materials increase the delay in participation of the couch materials in the fire through longer incipient times, slower growth and lower peak fire size. The question is whether this delay increases the escape time, which, in this series of experiments, it did by 79 – 84%. This length of time would further increase when it is also factored in that the couch self-extinguished with the Crib 5 ignition source and was therefore ignited with the larger Crib 7, which is a much larger initiating fire source than used in the NFR test. In a real-world context, it would take additional time for the larger igniting source to reach that point, further increasing the escape time. Combining such factors might move the FR leather couch closer to having a 660 s escape window.

16. Ultimately, not all FR couches perform the same, as observed with the US FR faux leather couch with the second lowest escape time, a value close to that found for the NFR cloth couch. This finding also aligns with the 2015 tests in which fabric covers that were poor thermal performers were found to retract and peel due to heat, thereby exposing the foam cushion materials and leading to faster fire growth.

17. The three best-performing couches were constructed with interliners (5FV, 6FV, and 8FV). All of the NFR, UK leather, and US faux leather couches had drop-down flaming and burning on the platforms under them. In contrast, although there was also drop-down burning in Test 6FV with the interliner but it did not further develop the fire from underneath.

Chapter 8
Further Research

Fire protection in houses is currently treated in a somewhat simplistic fashion, with smoke alarms being the primary means of alerting occupants and with generally limited requirements for additional protection in the forms of controlling smoke propagation. With the advent of new technologies, there appears to be an opportunity to improve fire safety in homes at a relatively low cost. This thesis investigates some of the impacts of detector type and location, as well as furniture fire performance controls, as one means of addressing the most well-known risks to life in houses. In addition, it furthers understanding of the movement and transfer of smoke and hot gases in fires. But many questions remain. Additional investigations would further increase the scientific knowledge that is needed to make informed fire safety and protection decisions. Specifically, with energy-efficient and controlled air environments reflective of modern homes, there are likely opportunities to interlock systems with smoke alarms to better respond to fires. This could include increasing or decreasing air supply, stopping recirculation of air handling systems, or control of fire suppression systems. However, the foundational requirement in adopting any of these measures would focus on which components will most likely add value to occupant safety.

A greater understanding of air movement during fires is needed. From this experimental series, further elaboration on the exchange of smoke and gases between rooms and, in particular, within the burn room is needed to quantify not only the conditions that may be encountered by occupants but also those that might be encountered by firefighters. Additional experiments are warranted to look at fire development under different ventilation scenarios, including both active and passive ventilation. This would assist in establishing the impact of ventilation on both incipient and fire growth stages and smoke movement to better inform safety controls and fire fighting response and potentially define evidence-driven stay-in-place strategies where mobility-limited persons may be living in their homes. Recirculatory air handling systems should also be studied as they could have the potential to spread smoke, but at the same time, there may also be opportunities to leverage these systems to control the smoke in the environment and use these systems to increase available escape time.

Considerable thought has been put into the instrumentation of the present research. However, further work is needed in this area to better quantify the conditions within the space. In particular, measurements of CO_2 concentration at appropriate levels are needed, as are sensor technologies and corrections to address the fluctuating thermal and gaseous environment. Further resolution of the

distribution of toxic and combustible gases throughout the burn house should be investigated, coupled with studies of the impacts of fire gas exposures on escaping occupants and their consequential neurobehavioural response. Finally, additional work on establishing the heat release rates observed and comparing these heat release rates to well ventilated environments will further allow for evolving methods of transposing data from a free-burn experiment into an enclosed environment.

The use of video cameras provided an exceptional avenue to visually record what was happening in the fire and facilitate comparison to past research results. Developing methods to analyze the video to measure smoke characteristics, such as optical density, in a three-dimensional domain would offer an even more detailed resolution of the potential visual environment experienced by escaping occupants. Similarly, video could evolve as a predictive tool to measure fire size and growth rate. The work also provides a known measurement benchmark for smoke formation in fires that could more readily be incorporated into computer models and potentially into machine learning environments. Computer fire modelling has become commonplace in the fire safety industry. Thus, providing detailed experimental data such as those collected in the present research is extremely beneficial in comparing it with modelled results and ensuring these models represent fire dynamics as closely as possible. Limited multi-storey experiments have been characterized in this level of detail, and it is hoped that this work will assist in forming a basis for calibrating, validating, or developing advanced computational fluid dynamics models. Comparison with model results will equally be important in directing future experimental studies.

Lastly, within current methods for house construction, the only two aids to increasing escape time due to furniture fires are to 1. implement controls to limit the participation of the furniture in fires and 2. provide earlier detection to maximize the opportunity for escape. Many suggest that automatic sprinklers would also successfully manage the risk. However, sprinklers may not find a place in much of the global building stock and can also present issues with readily available water supply in some jurisdictions, whereas controls on furniture would avoid water supply issues and could find global acceptance. The observed positive effect of interliners on fire performance in the present experiments and the UK standard furniture used in this research suggest that the design of furniture controls to limit the risk of furniture fires is an achievable goal. At the same time, it is recognized that present test methods may have to be adapted to determine relative fire performance using these strategies. Therefore, the development of methods for testing new designs will require research to review, build on and adapt current methods to determine acceptance criteria that, in particular, address fire growth. Combined with appropriate controls, this appears to be a 60-year-old problem that is readily solvable.

References

[1] G. Proulx, "Evacuation from a single family house," *Proceedings of the 4th International Symposium on Human Behaviour in Fire,* pp. 255-266, July 13 2009 2009, doi: 10.4224/20375064.

[2] S. W. Gilbert and D. T. Butry, "Identifying vulnerable populations to death and injuries from residential fires," *Inj Prev,* vol. 24, no. 5, pp. 358-364, Oct 2018, doi: 10.1136/injuryprev-2017-042343.

[3] J. B. Dinaburg, "Audible Alarm Signal Waking Effectiveness: Literature Review," Fire Protection Research Foundation - Report FPRF-2020-04, Quincy, MA, March 2020 2020.

[4] R. E. Halliwell and M. A. Sultan, "Guide to the most effective locations for smoke detectors in residential buildings," in "Building Practice Note; no. 62," National Research Council of Canada. Institute for Research in Construction, 0701-5216, 1986.

[5] J. Zhang *et al.*, "Smoke filling in closed compartments with elevated fire sources," *Fire Safety Journal,* vol. 54, pp. 14-23, 2012, doi: 10.1016/j.firesaf.2012.08.003.

[6] M. Ahrens and R. Maheshwari, "Home Structure Fires," National Fire Protection Association, Quincy, MA, USA, 2021.

[7] "Fire Death and Injury Risk." United States Fire Administration. https://www.usfa.fema.gov/statistics/deaths-injuries/ (accessed July 6, 2024).

[8] "Residential building fire deaths (2013 - 2022)." United States Fire Administration. https://www.usfa.fema.gov/statistics/residential-fires/ (accessed July 6, 2024).

[9] "Incident-based fire statistics, by type of fire incident and type of structure," vol. Table: 35-10-0192-01, ed: Statistics Canada, 2023.

[10] "Fire incidents increase during the pandemic." Statistics Canada. https://www150.statcan.gc.ca/n1/daily-quotidien/230608/dq230608a-eng.htm (accessed December 27, 2023).

[11] "Circumstances surrounding unintentional fire-related deaths, 2011 to 2020." The Daily. https://www150.statcan.gc.ca/n1/daily-quotidien/220616/dq220616b-eng.htm (accessed.

[12] A. Bounagui, N. Bénichou, and E. Victor, "Residential Fire Scenario Analysis in Ontario 1995-2003.pdf," 2004, doi: 10.4224/20377999.

[13] "White Paper on Upholstered Furniture Flammability," National Fire Protection Association, Quincy, MA, USA, 2013.

[14] P. Senez, "The Fire Risk of Upholstered Furniture in Canada," University of Waterloo, A work completed in fulfillement of ME770 - Advanced Fire Science I, 2014.

[15] J. R. Hall, "Estimating Fires When a Product is the Primary Fuel But Not the First Fuel, With an Application to Upholstered Furniture," *Fire Technology,* vol. 51, no. 2, pp. 381-391, 2014, doi: 10.1007/s10694-014-0391-8.

[16] R. Campbell, "Physical Disability as a Factor in Home Fire Deaths," National Fire Protection Association, Quincy, MA, USA, 2022.

[17] *National Building Code of Canada*, National Research Council of Canada, Canadian Commission on Building and Fire Codes, Ottawa, ON, Canada, 2020.

[18] "History of Smoke Detectors." Inspect Point. https://www.inspectpoint.com/smoke-detectors-history/ (accessed September 10, 2023.

[19] D. F. Steele and R. B. Enemark, "Optical Smoke Detector," United States of America Patent US3863076 (A) Patent Appl. US19730382058 19730724, [Online]. Available: https://worldwide.espacenet.com/publicationDetails/biblio?CC=US&NR=3863076&KC=&FT=E&locale=en_EP

[20] J. H. McGuire, Ruscoe, B.E., "Value of a fire detector in the home," National Research Council of Canada, Ottawa, ON, 1962.

[21] R. W. Bukowski, "A History of NBS/NIST Research on Fire Detectors," in *12th International Conference on Automatic Fire Detection*, Gaithersburg, MD, USA, March 26-28, 2001 2001: National Institute of Standards and Technology, pp. 1-12.
[22] *NFPA 74 - Standard for the Installation, Maintenance, and Use of Household Fire Warning Equipment*, National Fire Protection Association, Boston, MA, USA, 1974.
[23] R. W. Bukowski, Waterman, T.E., Christian, W.J., "Detector Sensitivity and Siting Requirements for Dwellings," National Bureau of Standards, Washington, D.C., 1975.
[24] S. W. Harpe, Waterman, T.E., Christian, W.J., "Detector Sensitivity and Siting Requirements for Dwellings - Phase 2," U.S. National Bureau of Standards, Washington, DC, 1977.
[25] R. W. Bukowski, "Field Investigation of Residential Smoke Detectors.pdf," *Fire Journal,* vol. 71, no. No. 2, pp. 18-41, 1976.
[26] "Smoke Detectors in Residential Occupancies," National Research Council of Canada, Canadian Commission on Building and Fire Codes, Associate Committee on the National Building Code, Standing Committee on Housing and Small Buildings, Ottawa, ON, Committee Paper 1977.
[27] *National Building Code of Canada*, National Research Council of Canada, Associate Committee on the National Building Code, Ottawa, ON, Canada, 1980.
[28] L. Y. Cooper, "A concept for estimating available safe egress time in fires," *Fire Safety Journal,* no. 5, pp. 135-144, 1983.
[29] L. Y. Cooper, "A concept for estimating available safe egress time in fires," *Fire Safety Journal,* no. 5, p. 138, 1983.
[30] T. Jin, "Studies on Human Behavior and Tenability in Fire Smoke," in *Fire Safety Science - Fifth International Symposium* 1997: International Association of Fire Safety Science, pp. 3-21, doi: 10.3801/IAFSS.FSS.5-3.
[31] *NFPA 101 Life Safety Code*, National Fire Protection Association, Quincy, Massachusetts, 2018.
[32] *International Fire Engineering Guidelines - Edition 2005*, Australian Government, State and Territorries of Australia, 2005.
[33] *ISO-TS-21602 - Fire safety engineering - Estimating the reduction in movement speed based on visibility and irritant species concentration*, ISO, Geneva, Switzerland, 2022.
[34] V. N. Hutchison and S. Hostikka, "Impact of Interior Doors on Residential Fire Safety," in *Residential Fire Safety*, (The Society of Fire Protection Engineers Series), 2023, ch. 9, pp. 143-158.
[35] D. A. Purser and J. L. McAllister, "Assessment of Hazards to Occupants from Smoke, Toxic Gases, and Heat," in *SFPE Handbook of Fire Protection Engineering*. New York Heidelberg Dordrecht London: Springer, 2016, ch. 63, pp. 2308-2428.
[36] *ISO 13571 Life-threatening components of fire - Guidelines for the estimation of time to compromised tenability in fires*, ISO, Geneva, Switzerland, 2012.
[37] *ISO/TR 13571-2 Life-threatening components of fire - Part 2: Methodology and examples of tenability assessment.* , ISO, Geneva, Switzerland, 2016.
[38] D. A. Purser and J. L. McAllister, "Assessment of Hazards to Occupants from Smoke, Toxic Gases, and Heat," in *SFPE Handbook of Fire Protection Engineering*. New York Heidelberg Dordrecht London: Springer, 2016, ch. 63, p. 2413.
[39] O. F. Thompson, E. R. Galea, and L. M. Hulse, "A review of the literature on human behaviour in dwelling fires," *Safety Science,* vol. 109, pp. 303-312, 2018, doi: 10.1016/j.ssci.2018.06.016.
[40] A. F. Grand., H. L. Kaplan, J.J. Beitel Ill, W.G. Switzer, and G. E. Hartzell., "An Evaluation of Toxic Hazards from Full-Scale Furnished Room Fire Studies," *Fire Safety: Science and Engineering, ASTM STP 882,* pp. 330-353, 1985.
[41] R. E. Halliwell, "Où installer les détecteurs de fumée dans les habitations," National Research Council of Canada, Ottawa, ON, Note sur la construction, 1986.

[42] M. A. Sultan, and Halliwell, R.E., "Optimum Location for Fire Alarms in Apartment Buildings," in "Fire Technology," 1990, vol. November 1990.
[43] *National Building Code of Canada*, National Research Council of Canada, Canadian Commission on Building and Fire Codes, Ottawa, ON, Canada, 1995.
[44] S. Hygge, " Smoke Detectors in Apartments and One-family Houses: A Comparison Between the Maintenance, Care and Performance of Free and Purchased Smoke Detectors," *Fire Safety Journal,* no. 15, pp. 195-210, 1989.
[45] G. R. N. Jones, "Cyanide and Fire Victims: A Hazard Focus," *Fire Technology,* vol. May 1990, pp. 141-148, 1990.
[46] J. Z. C. Su, G. P.; Carpenter, D. W.; McCartney, C. J.; Leroux, P., "Kemano Studies - Part 1 Response of Residential Smoke Detectors.pdf," 2003, doi: 10.4224/20378519.
[47] R. W. Bukowski, Peacock, R.D., Averill, J.D., Cleary, T.G., Bryner, N.P., Walton, W.W., Reneke, P.R., Kuligowski, E. D., "Performance of Home Smoke Alarms - Analysis of the Response of Several Available Technologies in Residential Fire Settings," National Institute of Standards and Technology, Washington, DC, Technical Note 1455, 2007.
[48] R. W. Bukowski, Peacock, R.D., Averill, J.D., Cleary, T.G., Bryner, N.P., Walton, W.W., Reneke, P.R., Kuligowski, E. D., "Performance of Home Smoke Alarms - Analysis of the Response of Several Available Technologies in Residential Fire Settings," National Institute of Standards and Technology, Washington, DC, Technical Note 1455, p. 253, 2007.
[49] R. W. Bukowski, Peacock, R.D., Averill, J.D., Cleary, T.G., Bryner, N.P., Walton, W.W., Reneke, P.R., Kuligowski, E. D., "Performance of Home Smoke Alarms - Analysis of the Response of Several Available Technologies in Residential Fire Settings," National Institute of Standards and Technology, Washington, DC, Technical Note 1455, p. 259, 2007.
[50] R. W. Bukowski, Peacock, R.D., Averill, J.D., Cleary, T.G., Bryner, N.P., Walton, W.W., Reneke, P.R., Kuligowski, E. D., "Performance of Home Smoke Alarms - Analysis of the Response of Several Available Technologies in Residential Fire Settings," National Institute of Standards and Technology, Washington, DC, Technical Note 1455, p. 254, 2007.
[51] R. W. Bukowski, Peacock, R.D., Averill, J.D., Cleary, T.G., Bryner, N.P., Walton, W.W., Reneke, P.R., Kuligowski, E. D., "Performance of Home Smoke Alarms - Analysis of the Response of Several Available Technologies in Residential Fire Settings," National Institute of Standards and Technology, Washington, DC, Technical Note 1455, p. 70, 2007.
[52] T. Cleary, "Full-scale Residential Smoke Alarm Performance," in *14th International Conference on Automatic Fire Detection*, University of Duisburg-Essen, Duisburg, Germany, 2009.
[53] B. C. S. Taber, J. Z.; Bénichou, N.; Bwalya, A. C.; Lougheed, G. D.; and G. L. Proulx, P., "Smoke Detection in Full-Scale House Experiments," in *Suppression and Detection Research and Applications: A Technical Working Conference (SUPDET 2009)*, Orlando, FL, USA, 2009, pp. 1-3.
[54] J. Z. Su, N. Bénichou, A. Bwalya, G. Lougheed, B. Taber, and P. Leroux, "Unprotected Floor Assemblies and Tenability Conditions in a Test House Under Two Basement Fire Scenarios," *Fire Technology,* vol. 47, no. 3, pp. 631-664, 2010, doi: 10.1007/s10694-010-0158-9.
[55] C. M. Fleischmann, "Prescribing the Input for the ASET versus RSET Analysis: Is This the Way Forward for Performance Based Design?," University of Canterbury, Christchurch, New Zealand, 2008.
[56] G. N. Proulx, R.; Cavan, N. R.; Tonikian, R., "Egress Times from Single Family Homes," National Research Council of Canada, Institute for Research in Construction, Fire Research Program, Ottawa, ON, Canada, 2006.
[57] V. Babrauskas, J. M. Fleming, and B. Don Russell, "RSET/ASET, a flawed concept for fire safety assessment," *Fire and Materials,* vol. 34, no. 7, pp. 341-355, 2010, doi: 10.1002/fam.1025.

[58] W. K. Chow, "Letter to the Editor: Comment on 'RSET/ASET, a flawed concept for fire safety assessment' by V. Babrauskas, J.M. Fleming and B.D. Russell, Fire and Materials, Vol. 34, pp. 341-355 (2010)," *Fire and Materials,* vol. 37, no. 3, pp. 257-258, 2013, doi: 10.1002/fam.2134.
[59] J. R. Hall, "How Many People Can Be Saved from Home Fires if Given More Time to Escape," *Fire Technology,* no. 40, pp. 117-126, 2004.
[60] E. L. Milarcik, S. M. Olenick, and R. J. Roby, "A Relative Time Analysis of the Performance of Residential Smoke Detection Technologies," *Fire Technology,* vol. 44, no. 4, p. 349, 2008, doi: 10.1007/s10694-008-0046-8.
[61] D. Bruck and I. Thomas, "Towards a better smoke alarm signal - an evidence based approach," *Fire Safety Science,* vol. 9, pp. 403-414, 2008, doi: 10.3801/iafss.Fss.9-403.
[62] *National Building Code of Canada*, National Research Council of Canada, Canadian Commission on Building and Fire Codes, Ottawa, ON, Canada, 2010.
[63] E. A. Sidman, D. C. Grossman, and B. A. Mueller, "Comprehensive smoke alarm coverage in lower economic status homes: alarm presence, functionality, and placement," *J Community Health,* vol. 36, no. 4, pp. 525-33, Aug 2011, doi: 10.1007/s10900-010-9337-3.
[64] K. A. M. Moinuddin, D. Bruck, and L. Shi, "An experimental study on timely activation of smoke alarms and their effective notification in typical residential buildings," *Fire Safety Journal,* vol. 93, pp. 1-11, 2017, doi: 10.1016/j.firesaf.2017.07.003.
[65] N. Traina, S. Kerber, D. C. Kyritsis, and G. P. Horn, "Occupant Tenability in Single Family Homes: Part I—Impact of Structure Type, Fire Location and Interior Doors Prior to Fire Department Arrival," *Fire Technology,* vol. 53, no. 4, pp. 1589-1610, 2017, doi: 10.1007/s10694-017-0651-5.
[66] V. N. Hutchison and S. Hostikka, "Impact of Interior Doors on Residential Fire Safety," in *Residential Fire Safety*, (The Society of Fire Protection Engineers Series), 2023, ch. 9, p. 156.
[67] S. Kerber, J. W. Regan, G. P. Horn, K. W. Fent, and D. L. Smith, "Effect of Firefighting Intervention on Occupant Tenability during a Residential Fire," *Fire Technology,* vol. 55, no. 6, pp. 2289-2316, 2019, doi: 10.1007/s10694-019-00864-2.
[68] M. Kobes and R. Weewer, "Residential Fire Rescues: Building a Model of Rescue Types for Supporting the Fire Service," in *Residential Fire Safety*, (The Society of Fire Protection Engineers Series), 2023, ch. Chapter 12, pp. 197-219.
[69] "Home Fire Escape Planning." City of Toronto. https://www.toronto.ca/community-people/public-safety-alerts/safety-tips-prevention/home-high-rise-school-workplace-safety/home-fire-escape-planning/ (accessed November 13, 2023).
[70] "Home Escape Plans." City of Calgary. https://www.calgary.ca/emergencies/preparedness/home-escape-plan.html (accessed November 13, 2023).
[71] Y. Utiskul, J. G. Quintiere, A. S. Rangwala, B. A. Ringwelski, K. Wakatsuki, and T. Naruse, "Compartment fire phenomena under limited ventilation," *Fire Safety Journal,* vol. 40, no. 4, pp. 367-390, 2005, doi: 10.1016/j.firesaf.2005.02.002.
[72] H. Takeda and K. Akita, "Critical Phenomenon in Compartment Fires with Liquid Fuels," in *Eighteenth Symposium (Internaional) on Combustion*, Waterloo, Canada, 1981, vol. 18, no. 1: The Combustion Institue, pp. 519-527.
[73] A. Coppalle, A. Loo, and P. Ainé, "Pool Fire Behavior in a Small and Mechanically Ventilated Compartment," in *Fire Science and Technology 2015*: Springer, 2017, ch. 9, pp. 97-104.
[74] C. Fourneau, C. Delvosalle, H. Breulet, and S. Brohez, "Characterization of highly under-ventilated fires using the cone calorimeter," *Fire and Materials,* vol. 40, no. 3, pp. 434-444, 2016, doi: 10.1002/fam.2298.

[75] Q. He, O. A. Ezekoye, C. Li, and S. Lu, "Ventilation limited extinction of fires in ceiling vented compartments," *International Journal of Heat and Mass Transfer,* vol. 91, pp. 570-583, 2015, doi: 10.1016/j.ijheatmasstransfer.2015.07.080.
[76] J. Li, H. Prétrel, S. Suard, T. Beji, and B. Merci, "Experimental study on the effect of mechanical ventilation conditions and fire dynamics on the pressure evolution in an air-tight compartment," *Fire Safety Journal,* vol. 125, 2021, doi: 10.1016/j.firesaf.2021.103426.
[77] S. Brohez and I. Caravita, "Fire induced pressure in airthight houses: Experiments and FDS validation," *Fire Safety Journal,* vol. 114, 2020, doi: 10.1016/j.firesaf.2020.103008.
[78] S. Hostikka, R. K. Janardhan, U. Riaz, and T. Sikanen, "Fire-induced pressure and smoke spreading in mechanically ventilated buildings with air-tight envelopes," *Fire Safety Journal,* vol. 91, pp. 380-388, 2017, doi: 10.1016/j.firesaf.2017.04.006.
[79] H. Prétrel, W. Le Saux, and L. Audouin, "Pressure variations induced by a pool fire in a well-confined and force-ventilated compartment," *Fire Safety Journal,* vol. 52, pp. 11-24, 2012, doi: 10.1016/j.firesaf.2012.04.005.
[80] T. Tanaka, "Vent Flows," in *SFPE Handbook of Fire Protection Engineering*. New York Heidelberg Dordrecht London: Springer, 2016, ch. Chapter 15, pp. 455-485.
[81] B. Merci, J. Li, and G. Maragkos, "On the importance of the heat release rate in numerical simulations of fires in mechanically ventilated air-tight enclosures," *Proceedings of the Combustion Institute,* vol. 39, no. 3, pp. 3647-3672, 2023, doi: 10.1016/j.proci.2022.06.011.
[82] A. Chaudhary, M. K. Tiwari, A. Gupta, and S. Kumar, "Effect of ventilation on fire growth in diesel fueled compartment fire," *Experimental Heat Transfer,* vol. 35, no. 6, pp. 737-757, 2021, doi: 10.1080/08916152.2021.1946210.
[83] H. Y. Wang, "Numerical study of under-ventilated fire in medium-scale enclosure," *Building and Environment,* vol. 44, no. 6, pp. 1215-1227, 2009, doi: 10.1016/j.buildenv.2008.09.011.
[84] L. Songyang, Z. Ruowen, C. Lvyi, W. Tao, and L. Guangxuan, "Effect of Different Fuels on Confined Compartment Fire," *Journal of Fire Sciences,* vol. 28, no. 4, pp. 383-403, 2009, doi: 10.1177/0734904109350192.
[85] A. Lock *et al.*, "Experimental Study of the Effects of Fuel Type, Fuel Distribution, and Vent Size on Full-Scale Underventilated Compartment Fires in an ISO 9705 Room," Gaithersburg, MD, Technical Note 1603 - National Institute of Standards and Technology 2008.
[86] A. J. Wolfe, C. L. Mealy, and D. T. Gottuk, "Fire Dynamics and Forensic Analysis of Limited Ventilation Compartment Fires Volume 1: Experimental," US Department of Justice Report No.: 230164, Award Number 2007-DN-BX-K240, 2010.
[87] V. Gupta *et al.*, "Ventilation effects on the thermal characteristics of fire spread modes in open-plan compartment fires " *Fire Safety Journal,* no. 120 (2021) 103072, 2021.
[88] E. Guillaume, F. Didieux, A. Thiry, and A. Bellivier, "Real-scale fire tests of one bedroom apartments with regard to tenability assessment," *Fire Safety Journal,* vol. 70, pp. 81-97, 2014, doi: 10.1016/j.firesaf.2014.08.014.
[89] S. Vaux and H. Prétrel, "Relative effects of inertia and buoyancy on smoke propagation in confined and forced ventilated enclosure fire scenarios," *Fire Safety Journal,* vol. 62, pp. 206-220, 2013, doi: 10.1016/j.firesaf.2013.01.013.
[90] F. W. Mowrer, "Enclosure Smoke Filling and Fire-Generated Environmental Conditions," in *SFPE Handbook of Fire Protection Engineering*. New York Heidelberg Dordrecht London: Springer, 2016, ch. 33, pp. 1066-1101.
[91] F. W. Mowrer, "Enclosure Smoke Filling and Fire-Generated Environmental Conditions," in *SFPE Handbook of Fire Protection Engineering*, 2016, ch. 33, p. 1071.
[92] B. Karlsson and J. G. Quintiere, *Enclosure Fire Dynamics*, Second ed. Boca Raton London New York: CRC Press, 2022.
[93] E. E. Zukoski, "Development of a stratified ceiling layer in the early stages of a closed-room fire," *Fire and Materials,* vol. 2, no. 2, pp. 54-62, 1978, doi: 10.1002/fam.810020203.

[94] B. Hägglund, R. Jansson, and K. Nireus, "Smoke filling experiments in a 6x6x6 meter enclosure," Sweden, FOA Report C 20585-D6, 1985.
[95] V. Novozhilov, "A brief note on the smoke filling equation," *Fire Safety Journal,* vol. 47, pp. 16-17, 2012, doi: 10.1016/j.firesaf.2011.09.004.
[96] Y. Zhou and Q. Meng, "A Simple Solution of the Smoke Filling Equation," *Fire Technology,* vol. 53, no. 3, pp. 1479-1484, 2017, doi: 10.1007/s10694-017-0648-0.
[97] "Minutes of the Special Liaison Meeting on Regulation of Building Contents," in *The Associate Commmitee on the National Fire Code of Canada*, ed. Ottawa, Canada: National Research Council of Canada, 1973.
[98] K. Sumi, D'Souza, V. , "Fire Safety of Soft Furnishings - An Overview," *Fire and Materials,* vol. 6, no. 1, pp. 16-22, 1982.
[99] *Technical Bulletin 117 - Requirements, Test Procedure and Apparatus for Testing the Flame Retardance of Resilient Filling Materials Used in Upholstered Furniture*, State of California - Department of Consumer Affairs - Bureau of Home Furnishings and Thermal Insulation, CA, 1980.
[100] *BS5852 - Fire tests for furniture - Part 1. Methods of test for the ignitability by smokers materials of upholstered composites for seating*, British Standards Institution, 1979.
[101] *TB117 Requirements, Test Procedure and Apparatus for Testing the Flame Retardance of Resilient Filling Materials Used in Upholstered Furniture*, Department of Consumer Affairs - Bureau of Home Furnishings, California, USA, 2000.
[102] *BS 5852 - Fire tests for furniture - Part 2. Methods of test for the ignitability of upholstered composites for seating by flaming sources*, British Standards Institution, 1982.
[103] *BS 5852 Methods of test for assessment of the ignitability of upholstered seating by smouldering and flaming ignition sources*, British Standards Institution, 2006.
[104] (1988). *Secretary of State, UK Government, No. 1324, The Furniture and Furnishings (Fire) (Safety) Regulations 1988*. [Online] Available: legislation.gov.uk
[105] *TB117 Requirements, Test Procedure and Apparatus for Testing the Smolder Resistance of Materials Used in Upholstered Furniture*, Department of Consumer Affairs, California, USA, 2013.
[106] V. Babrauskas, A. Blum, R. Daley, and L. Birnbaum, "Flame Retardants in Furniture Foam: Benefits and Risks," *Fire Safety Science,* vol. 10, pp. 265-278, 2011, doi: 10.3801/iafss.Fss.10-265.
[107] *NFPA 277 Standard Methods of Tests for Evaluating Fire and Ignition Resistance of Upholstered Furniture Using a Flaming Ignition Source*, National Fire Protection Association, Quincy, MA, USA. [Online]. Available: https://www.nfpa.org/codes-and-standards
[108] *TB133 - Flammability Test Procedure for Seating Furniture for Use in Public Occupancies*, State of California, California, USA, 1991.
[109] "Final Statement of Reasons - Amendment to Flammability Standards," Department of Consumer Affairs, Bureau of Electronic and Appliance Repair, Home Furnishings and Thermal Insulation, 2018. Accessed: September 9, 2023. [Online]. Available: https://bhgs.dca.ca.gov/laws/famability_fsor.pdf
[110] M. Ahrens, "Soft furnishing fires: They're still a problem," *Fire and Materials,* vol. 45, no. 1, pp. 8-16, 2020, doi: 10.1002/fam.2874.
[111] M. Ahrens, "Soft furnishing fires: They're still a problem," *Fire and Materials,* vol. 45, no. 1, p. 15, 2020, doi: 10.1002/fam.2874.
[112] R. G. Gann, "Solving the soft furnishings fire problem (without incurring collateral damage)," *Fire and Materials,* vol. 45, no. 1, pp. 3-7, 2020, doi: 10.1002/fam.2936.
[113] S. T. McKenna *et al.*, "Flame retardants in UK furniture increase smoke toxicity more than they reduce fire growth rate," *Chemosphere,* vol. 196, pp. 429-439, Apr 2018, doi: 10.1016/j.chemosphere.2017.12.017.

[114] N. Bell, S. Harrad, R. Hull, and P. Whaley, "Fire Risks of Upholstered Products - Research Report," Office for Product Safety & Standards, United Kingdom, 2023.
[115] Y. Y. Chan, C. Ma, F. Zhou, Y. Hu, and B. Schartel, "Flame retardant flexible polyurethane foams based on phosphorous soybean-oil polyol and expandable graphite," *Polymer Degradation and Stability,* vol. 191, 2021, doi: 10.1016/j.polymdegradstab.2021.109656.
[116] Q. Gong, L. Qin, L. Yang, K. Liang, and N. Wang, "Effect of flame retardants on mechanical and thermal properties of bio-based polyurethane rigid foams," *RSC Adv,* vol. 11, no. 49, pp. 30860-30872, Sep 14 2021, doi: 10.1039/d1ra05519d.
[117] R. H. Krämer, M. Zammarano, G. T. Linteris, U. W. Gedde, and J. W. Gilman, "Heat release and structural collapse of flexible polyurethane foam," *Polymer Degradation and Stability,* vol. 95, no. 6, pp. 1115-1122, 2010, doi: 10.1016/j.polymdegradstab.2010.02.019.
[118] C. Ma *et al.*, "Fabrication of flexible polyurethane/phosphorus interpenetrating polymer network (IPN) foam for enhanced thermal stability, flame retardancy and mechanical properties," *Polymer Degradation and Stability,* vol. 189, 2021, doi: 10.1016/j.polymdegradstab.2021.109602.
[119] A. B. Morgan, "Revisiting flexible polyurethane foam flammability in furniture and bedding in the United States," *Fire and Materials,* vol. 45, no. 1, pp. 68-80, 2020, doi: 10.1002/fam.2848.
[120] Y. X. Thong, X. Li, and X. J. Yin, "Determining the best flame retardant for rigid polyurethane foam—Tris(2-chloroisopropyl) phosphate, expandable graphite, or silica aerogel," *Journal of Applied Polymer Science,* vol. 139, no. 14, 2021, doi: 10.1002/app.51888.
[121] V. Trovato *et al.*, "How to Address Flame-Retardant Technology on Cotton Fabrics by Using Functional Inorganic Sol–Gel Precursors and Nanofillers: Flammability Insights, Research Advances, and Sustainability Challenges," *Inorganics,* vol. 11, no. 7, 2023, doi: 10.3390/inorganics11070306.
[122] A. Yadav, F. M. de Souza, T. Dawsey, and R. K. Gupta, "Recent Advancements in Flame-Retardant Polyurethane Foams: A Review," *Industrial & Engineering Chemistry Research,* vol. 61, no. 41, pp. 15046-15065, 2022, doi: 10.1021/acs.iecr.2c02670.
[123] X. Yu *et al.*, "Effects of graphene nanosheets decorated by cerium stannate on the enhancement of flame retardancy and mechanical performances of flexible polyurethane foam composites," *Polymers for Advanced Technologies,* vol. 33, no. 1, pp. 290-302, 2021, doi: 10.1002/pat.5516.
[124] S. Zhang *et al.*, "The improvement of fire safety performance of flexible polyurethane foam by Highly-efficient P-N-S elemental hybrid synergistic flame retardant," *J Colloid Interface Sci,* vol. 606, no. Pt 1, pp. 768-783, Jan 15 2022, doi: 10.1016/j.jcis.2021.08.069.
[125] I. Kim *et al.*, "Demonstration of an all-in-one solution for fire safe upholstery furniture: A benign backcoating for smoldering and flame-resistant cover fabrics," *Fire and Materials,* vol. 46, no. 4, pp. 677-693, 2021, doi: 10.1002/fam.3015.
[126] S. Nazaré, W. Pitts, S. Flynn, J. R. Shields, and R. D. Davis, "Evaluating fire blocking performance of barrier fabrics," *Fire and Materials,* vol. 38, no. 7, pp. 695-716, 2014, doi: 10.1002/fam.2210.
[127] S. Nazare *et al.*, "Assessing fire-blocking effectiveness of barrier fabrics in the cone calorimeter," *Journal of Fire Sciences,* vol. 37, no. 4-6, pp. 340-376, 2019, doi: 10.1177/0734904119863011.
[128] W. M. Pitts *et al.*, "Effects of upholstery materials on the burning behavior of real-scale residential upholstered furniture mock-ups," *Fire and Materials,* vol. 45, no. 1, pp. 127-154, 2020, doi: 10.1002/fam.2915.
[129] R. Shen *et al.*, "Thermal stability and flammability of cotton fabric with TiO2 coatings based on biomineralization," *Materials Chemistry and Physics,* vol. 282, 2022, doi: 10.1016/j.matchemphys.2022.125986.

[130] K. Storesund, F. Amon, A. Steen-Hansen, S. Haghighatpanah, and I. Larsson, "Fire safe, sustainable loose furnishing," *Fire and Materials,* vol. 45, no. 1, pp. 181-190, 2020, doi: 10.1002/fam.2859.
[131] A. L. Thompson, I. Kim, A. Hamins, M. Bundy, and M. Zammarano, "Performance and Failure Mechanism of Fire Barriers in Full-Scale Chair Mock-ups," *Fire and Materials,* vol. 46, no. 1, 2021, doi: 10.1002/fam.3007.
[132] M. Zammarano *et al.*, "Reduced-scale test to assess the effect of fire barriers on the flaming combustion of cored composites: An upholstery-material case study," *Fire and Materials,* vol. 45, no. 1, pp. 114-126, 2020, doi: 10.1002/fam.2910.
[133] M. Zammarano *et al.*, "Full-scale Experiments to Demonstrate Flammability Risk of Residential Upholstered Furniture and Mitigation Using Barrier Fabric," National Insitute of Standards and Technology, Washington, DC, NIST Technical Note 2129, 2020.
[134] B. Sundström, "Combustion behavior of upholstered furniture. Important findings, practical use, and implications," *Fire and Materials,* vol. 45, no. 1, pp. 97-113, 2020, doi: 10.1002/fam.2920.
[135] D. Harris *et al.*, "Chemical exposure and flammability risks of upholstered furniture," *Fire and Materials,* vol. 45, no. 1, pp. 167-180, 2020, doi: 10.1002/fam.2907.
[136] K. Permentier, S. Vercammen, S. Soetaert, and C. Schellemans, "Carbon dioxide poisoning: a literature review of an often forgotten cause of intoxication in the emergency department," *Int J Emerg Med,* vol. 10, no. 1, p. 14, Dec 2017, doi: 10.1186/s12245-017-0142-y.
[137] K. M. Rodgers *et al.*, "Flame Retardant Concentrations Are Lower in College Spaces Meeting the New Furniture Flammability Standard TB117-2013," *Environmental Science & Technology Letters,* vol. 7, no. 11, pp. 833-839, 2020, doi: 10.1021/acs.estlett.0c00483.
[138] V. Babrauskas, K. M. Rodgers, D. Lucas, and R. Fuoco, "Questions and Comments about the Methodology and Conclusions in 'Comparative Room Burn Study of Furnished Rooms from the United Kingdom, France and the United States', by Blais et al. 2019," *Fire Technology,* vol. 57, no. 2, pp. 497-502, 2021, doi: 10.1007/s10694-020-01087-6.
[139] M. S. Blais, K. Carpenter, and K. Fernandez, "Comparative Room Burn Study of Furnished Rooms from the United Kingdom, France and the United States," *Fire Technology,* vol. 56, no. 2, pp. 489-514, 2019, doi: 10.1007/s10694-019-00888-8.
[140] A. Bwalya, E. Gibbs, G. Lougheed, and A. Kashef, "Heat release rates of modern residential furnishings during combustion in a room calorimeter," *Fire and Materials,* vol. 39, no. 8, pp. 685-716, 2015, doi: 10.1002/fam.2259.
[141] E. Guillaume, R. Feijter, and L. Gelderen, "An overview and experimental analysis of furniture fire safety regulations in Europe," *Fire and Materials,* vol. 44, no. 5, pp. 624-639, 2020, doi: 10.1002/fam.2826.
[142] A. Hofmann, A. Klippel, T. Gnutzmann, S. Kaudelka, and F. Rabe, "Influence of modern plastic furniture on the fire development in fires in homes: large-scale fire tests in living rooms," *Fire and Materials,* vol. 45, no. 1, pp. 155-166, 2020, doi: 10.1002/fam.2934.
[143] M. Weinbrenner, R. Weber, T. Neumeyer, and V. Altstädt, "Influence of foam density on burning behavior of polymer bead foams," *Journal of Applied Polymer Science,* vol. 139, no. 4, 2021, doi: 10.1002/app.51558.
[144] K. Wilkens Flecknoe-Brown and P. Hees, "Experimental investigation into the influence of ignition location on flame spread and heat release rates of polyurethane foam slabs," *Fire and Materials,* vol. 45, no. 1, pp. 81-96, 2020, doi: 10.1002/fam.2921.
[145] B. Forrest, E. Weckman, M. DiDomizio, P. Senez, and N. Ryder, "Smoke development and movement during ventilation-limited fires in a multi-storey house," *Fire and Materials,* vol. 45, no. 8, pp. 1063-1074, 2020, doi: 10.1002/fam.2860.
[146] M. M. Hirschler. (2023) Fire Retardant and Associated Toxicity. *PolyFlame*. Available: http://gcf-scf.lmops.univ-lorraine.fr/

[147] J. M. Fleming. (2023) Could Flame Retardants in Furniture be Increasing the Fire Risk. *Poly Flame*. Available: http://gcf-scf.lmops.univ-lorraine.fr/
[148] P. Collier; and P. Whiting, "Timeline for Incipient Fire Development," BRANZ, New Zealand, BRANZ Study Report No.194, 2008.
[149] P. Collier; and P. Whiting, "Timeline for Incipient Fire Development," BRANZ, New Zealand, BRANZ Study Report No.194, 2008.
[150] P. L. Senez and K. D. Calder, "Experimental and Simulated Analysis of Room Fire Theory for Forensic Applications," presented at the Fire & Materials Conference 2005, San Francisco, California, 2005.
[151] P. L. Senez. (2019) Defining Trends in Fire Dynamics. *Fire Protection Engineering*. pp. 19-24. Available: magazine.sfpe.org
[152] B. Forrest, "Heat Release Rate in Ventilation-Limited Furniture Fires," Master of Applied Science, Mechanical Engineering, University of Waterloo, Waterloo, ON, Canada, 2020.
[153] P. Senez, P. Mulherin, and E. Weckman, "Repeatability of Underventilated Compartment Fire Testing with Complex Fuel Packages," presented at the 15th International Conference on Fire and Materials, San Francisco, CA, USA, 2017.
[154] "Fire Escape Plans." Ontario Association of Fire Chiefs. https://www.oafc.on.ca/public-safety/fire-escape-plans (accessed November 13, 2023).
[155] "Load Cells Specifications." Mars Scale Corp. http://www.marsscale.com/load_cells.html (accessed September 30, 2023).
[156] "Comparison of Time Constant* vx. Overall Outside Diameter of Bare Thermocouple Wires or Grounded Junction Thermocouples In Air." Omega Sensing Solutions ULC. www.omega.com/temperature/z/pdf/z051.pdf (accessed September 30, 2023).
[157] J. P. Crocker, A. S. Rangwala, N. A. Dembsey, and D. J. LeBlanc, "Investigation of Sprinkler Sprays on Fire Induced Doorway Flows," *Fire Technology,* vol. 46, no. 2, pp. 347-362, 2009, doi: 10.1007/s10694-009-0081-0.
[158] A. DiPaola, E. Weckman, and P. Senez, "Impacts of Oxygen Deprivation and Noxious Gas CirculationDuring Fire Development in Energy Efficient Homes," University of Waterloo - Faculty of Engineering, Fire Research Group, Department of Mechanical and Mechatronics Engineering, Waterloo, ON, 2022.
[159] A. DiPaola, "Furniture Fire Dynamics and Smoke Flow in a Two-Story House with Mechanical Ventilation," M.Sc., Mechanical and Mechatronics Engineering, University of Waterloo, 2023. [Online]. Available: http://hdl.handle.net/10012/20150
[160] J. Ellingham, "Measuring Smoke Evolution at Full-Scale with Video Recordings," MASc, Mechanical and Mechatronics Engineering, University of Waterloo, Waterloo, Canada, 2021.
[161] M. L. Janssens, "Reducing Uncertainty of Quantifying the Burning Rate of Upholstered Furniture," Southwest Research Institute, San Antonio, TX, USA, 2012.
[162] D. A. Purser, "Toxic product yields and hazard assessment for fully enclosed design fires," *Polymer International,* vol. 49, no. 10, pp. 1232-1255, 2000, doi: 10.1002/1097-0126(200010)49:10<1232::Aid-pi543>3.0.Co;2-t.
[163] A. I. Bartlett, R. M. Hadden, and L. A. Bisby, "A Review of Factors Affecting the Burning Behaviour of Wood for Application to Tall Timber Construction," *Fire Technology,* vol. 55, no. 1, pp. 1-49, 2018, doi: 10.1007/s10694-018-0787-y.
[164] W. M. Pitts, "The Global Equivalence Ratio Concept and the Prediction of Carbon Monoxide Formation in Enclosure Fires," in "NIST Monograph 179," Building and Fire Research Laboratory, National Institute of Standards and Technology, Washington, DC, 1994.

Appendices

Appendix A:

One-minute video output for MV and FV series wood and couch tests

1MV - Burn Room (US Standard Cloth Couch – Crib 4)	**1MV** – Upper Level (US Standard Cloth Couch – Crib 4)

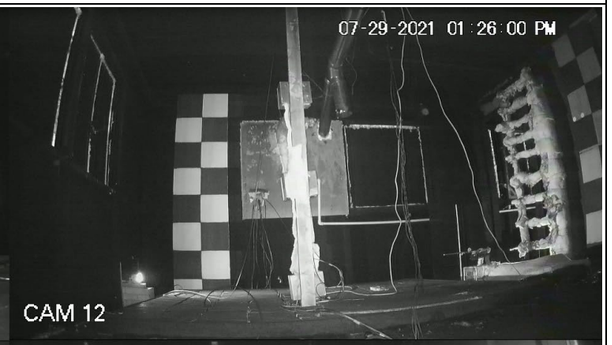
















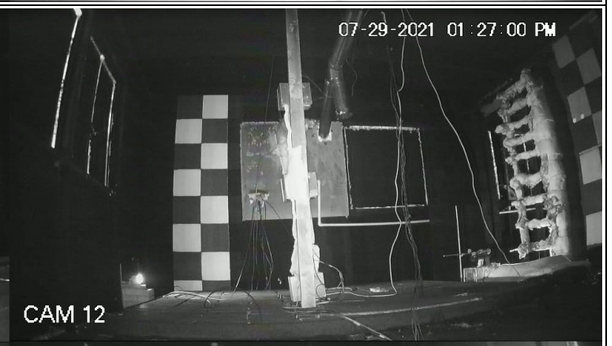
















1MV - Burn Room (US Standard Cloth Couch – Crib 4)	**1MV** – Upper Level (US Standard Cloth Couch – Crib 4)

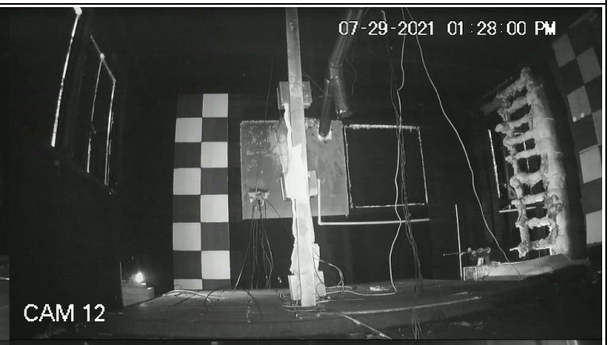
















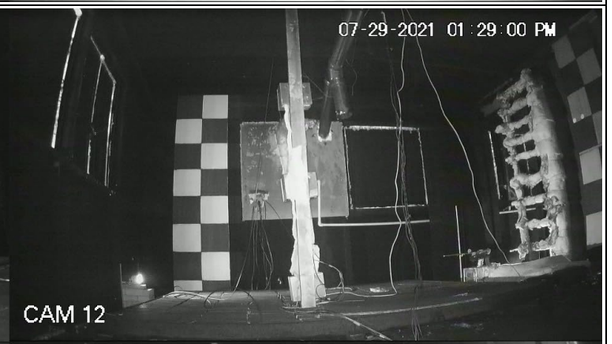
















1MV - Burn Room (US Standard Cloth Couch – Crib 4)	**1MV** – Upper Level (US Standard Cloth Couch – Crib 4)









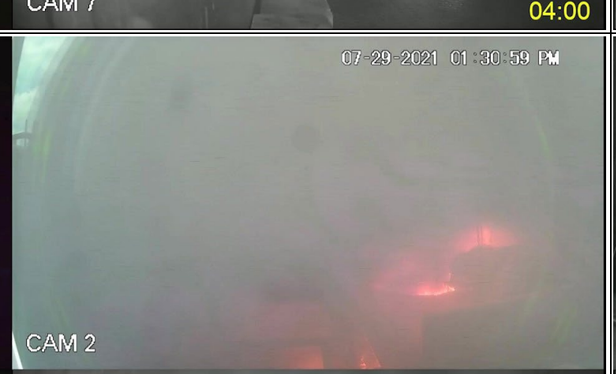
















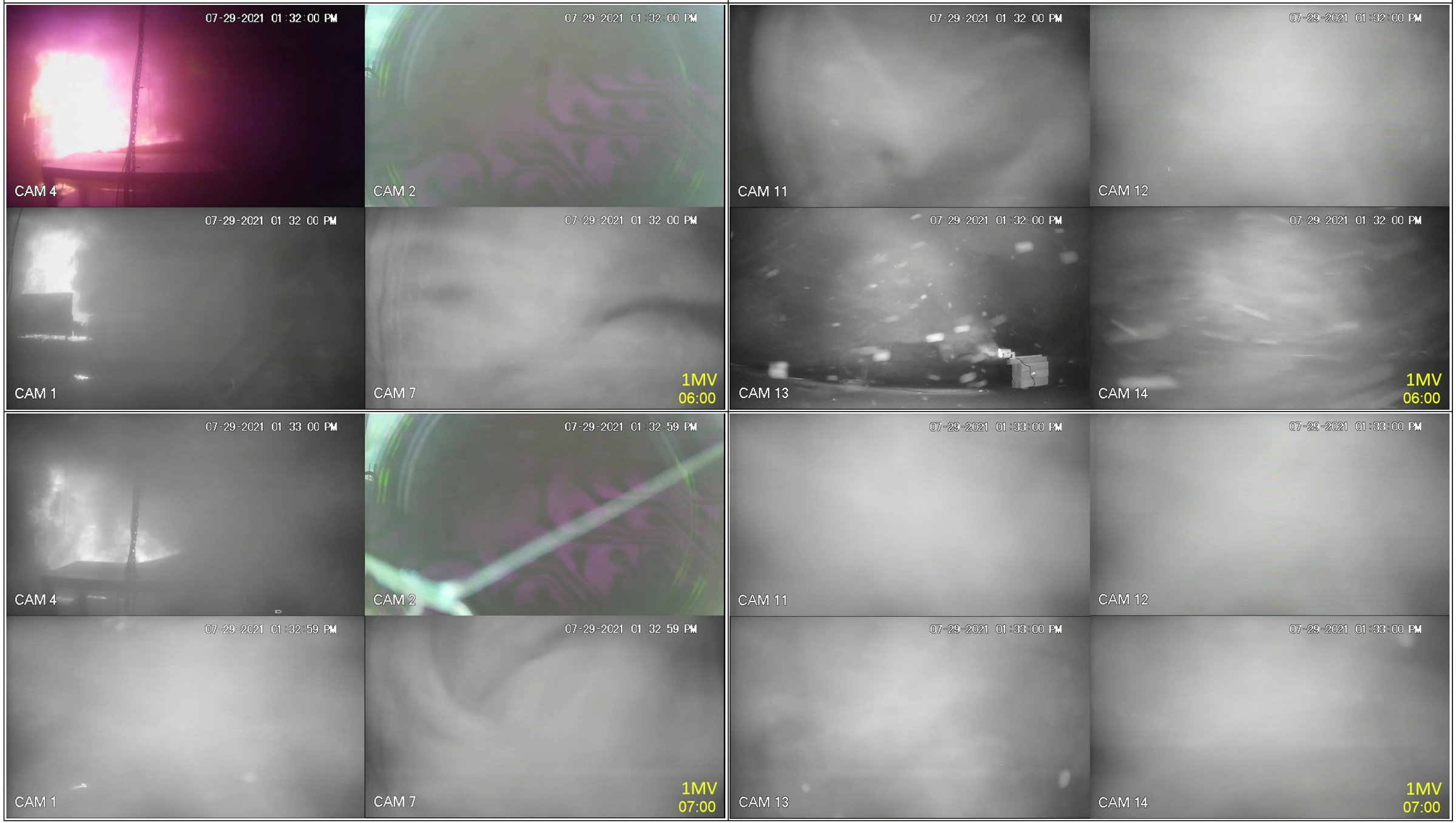








1MV - Burn Room (US Standard Cloth Couch – Crib 4)	**1MV** – Upper Level (US Standard Cloth Couch – Crib 4)

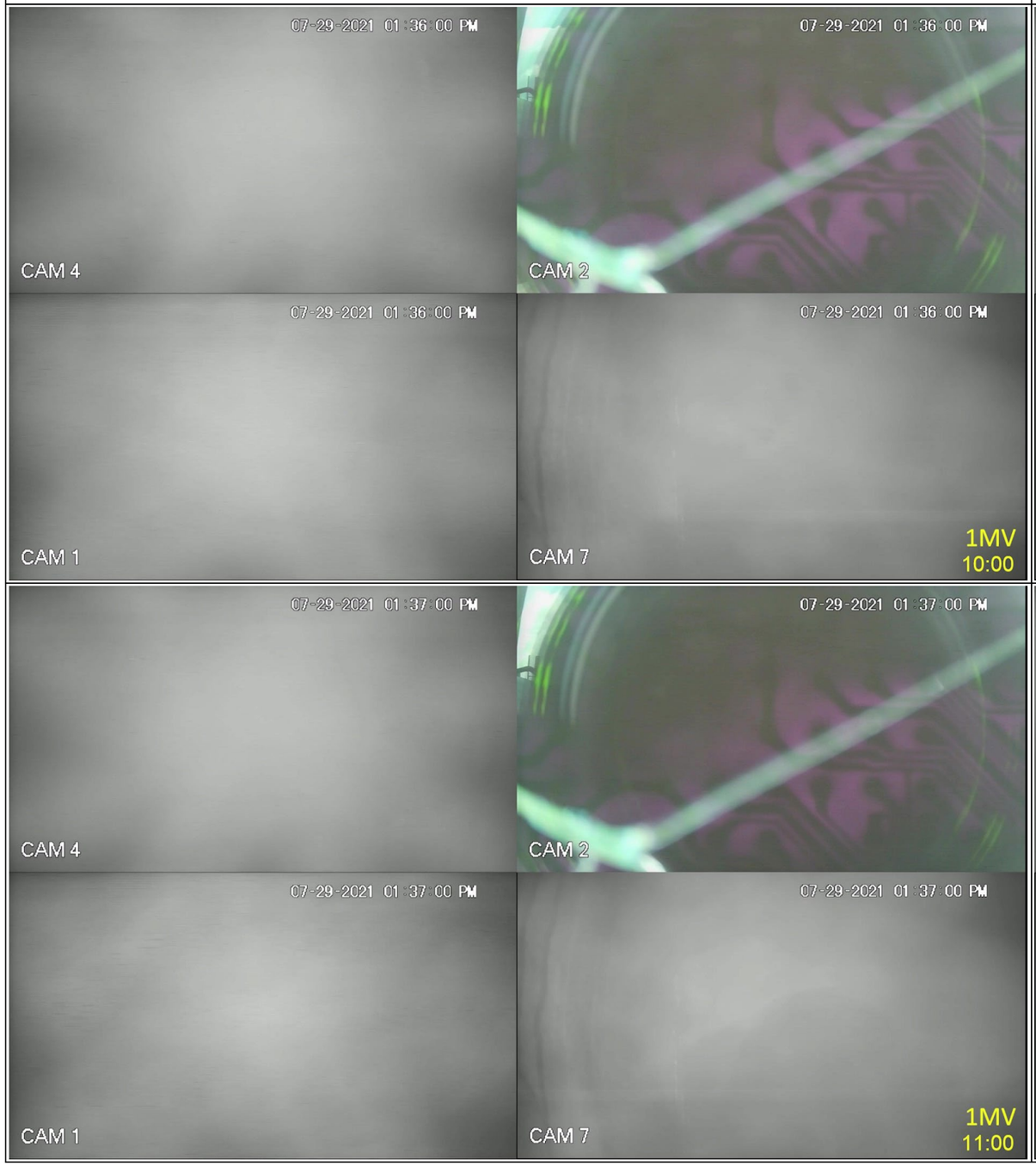


1MV - Burn Room (US Standard Cloth Couch – Crib 4)	**1MV** – Upper Level (US Standard Cloth Couch – Crib 4)



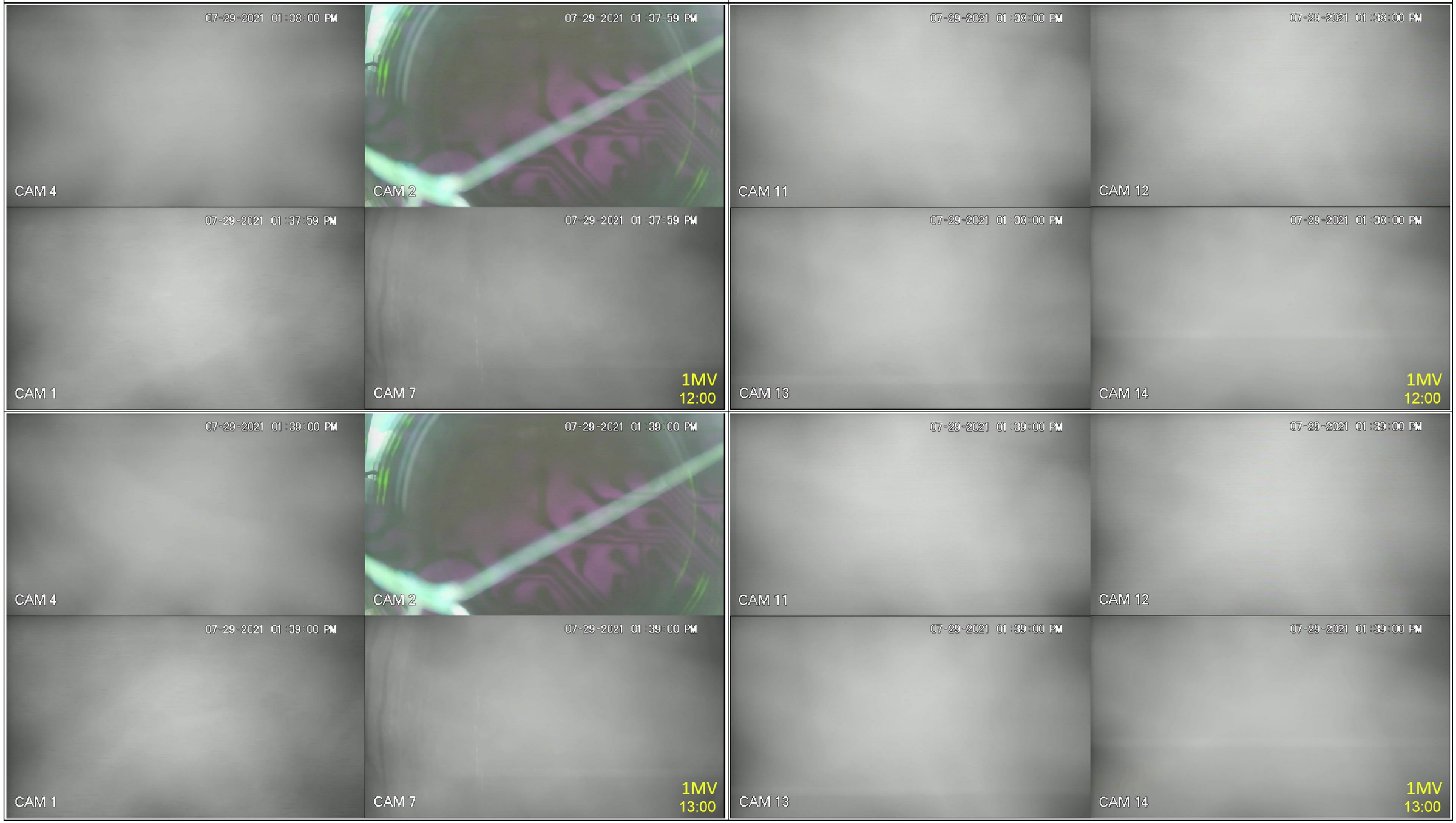


1MV - Burn Room (US Standard Cloth Couch – Crib 4)	**1MV** – Upper Level (US Standard Cloth Couch – Crib 4)



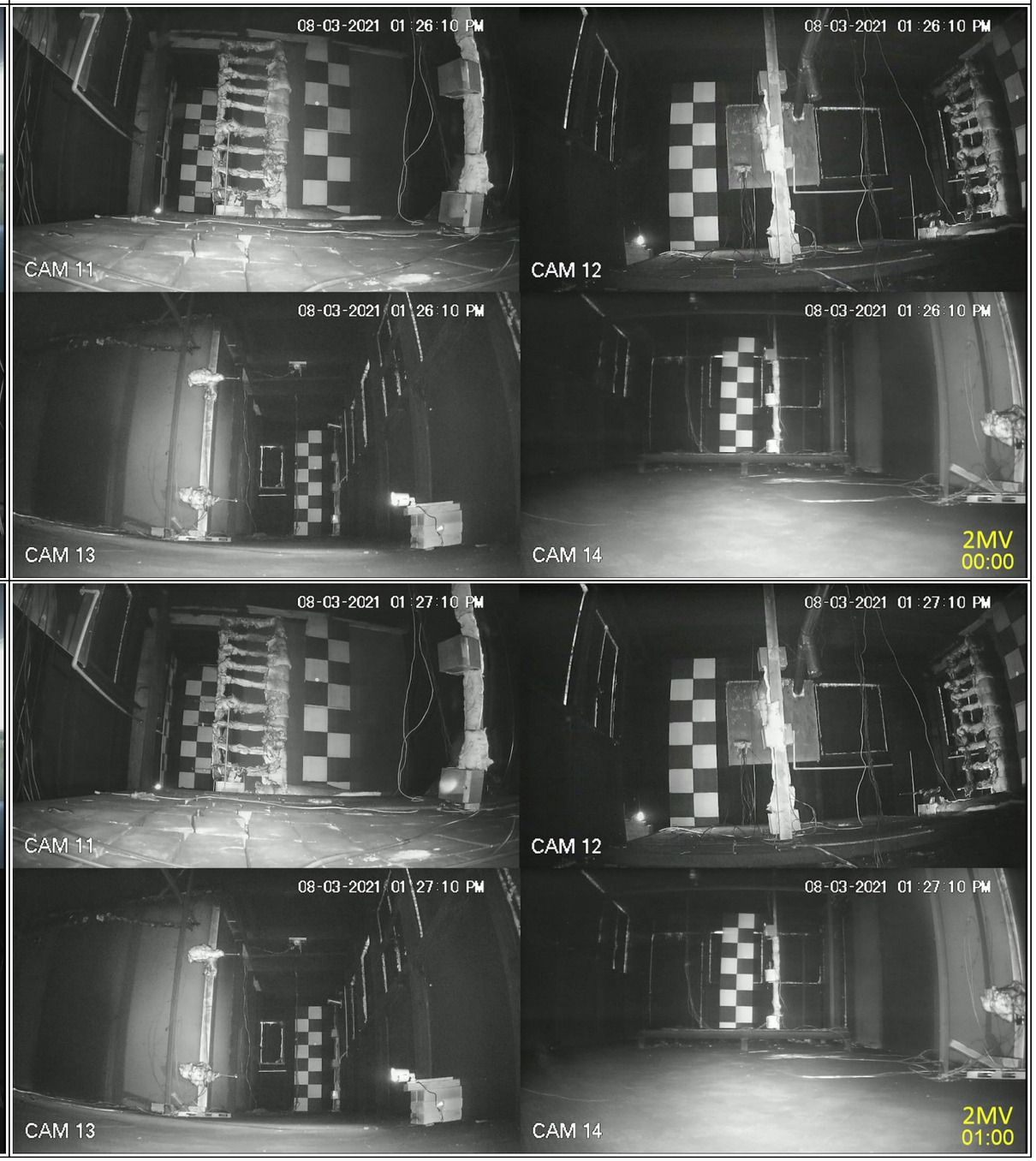


1MV - Burn Room (US Standard Cloth Couch – Crib 4)	**1MV** – Upper Level (US Standard Cloth Couch – Crib 4)



2MV - Burn Room (US Standard Cloth Couch – Crib 4)	**2MV** – Upper Level (US Standard Cloth Couch – Crib 4)





2MV - Burn Room (US Standard Cloth Couch – Crib 4)	**2MV** – Upper Level (US Standard Cloth Couch – Crib 4)

































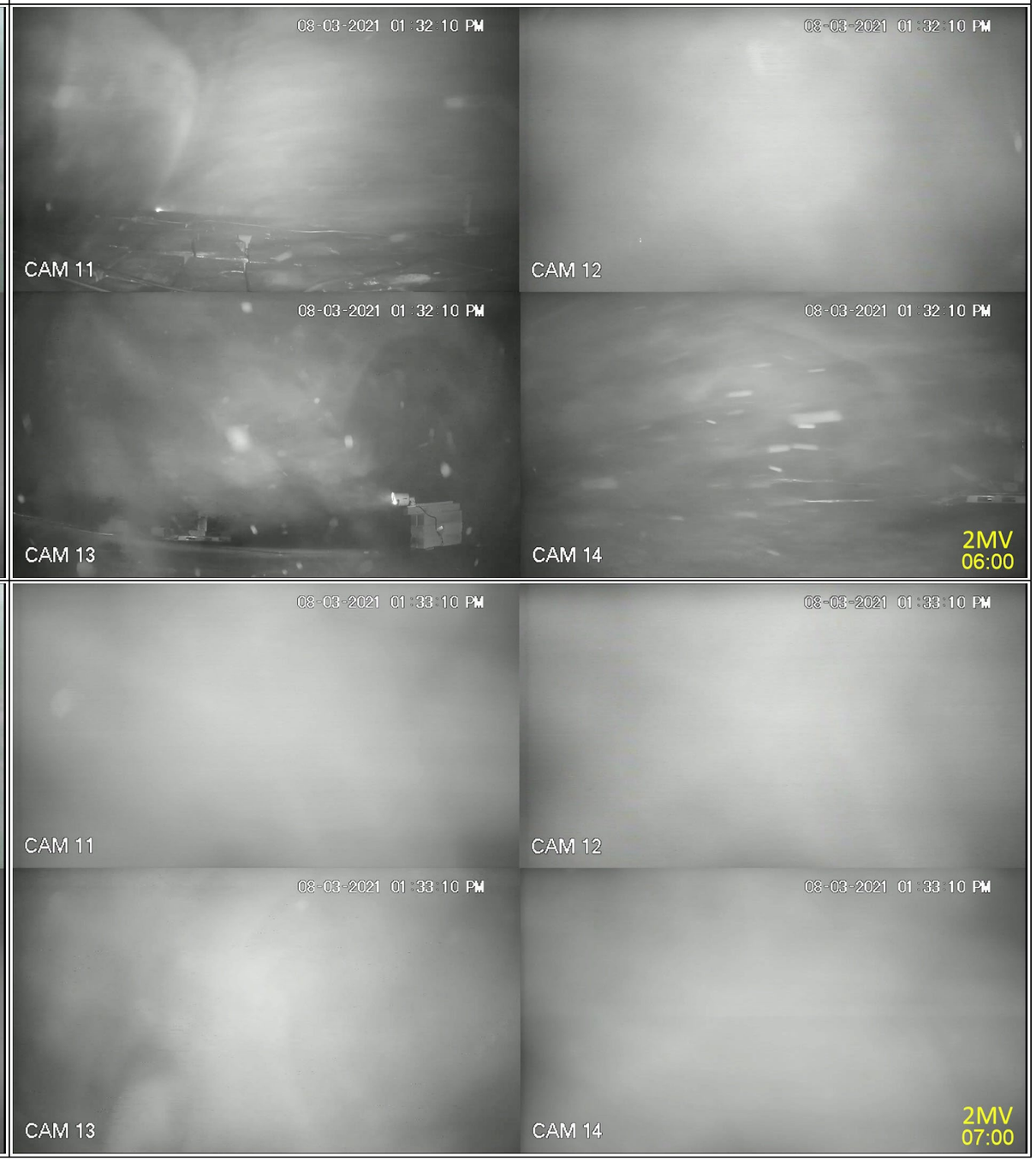
2MV - Burn Room (US Standard Cloth Couch – Crib 4)	**2MV** – Upper Level (US Standard Cloth Couch – Crib 4)





2MV - Burn Room (US Standard Cloth Couch – Crib 4)	**2MV** – Upper Level (US Standard Cloth Couch – Crib 4)





2MV - Burn Room (US Standard Cloth Couch – Crib 4)	**2MV** – Upper Level (US Standard Cloth Couch – Crib 4)









2MV - Burn Room (US Standard Cloth Couch – Crib 4)	**2MV** – Upper Level (US Standard Cloth Couch – Crib 4)





2MV - Burn Room (US Standard Cloth Couch – Crib 4)	**2MV** – Upper Level (US Standard Cloth Couch – Crib 4)









3MV - Burn Room (US Standard Cloth Couch – Crib 4)	**3MV** – Upper Level (US Standard Cloth Couch – Crib 4)

































3MV - Burn Room (US Standard Cloth Couch – Crib 4)	**3MV** – Upper Level (US Standard Cloth Couch – Crib 4)

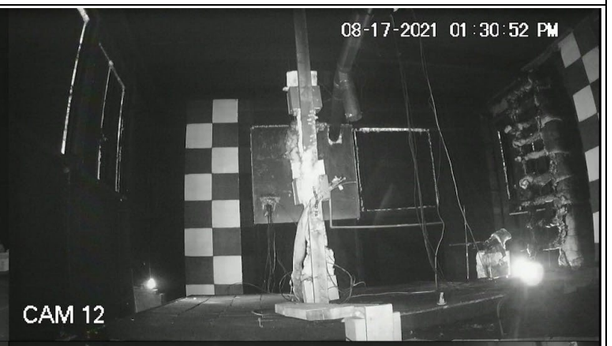












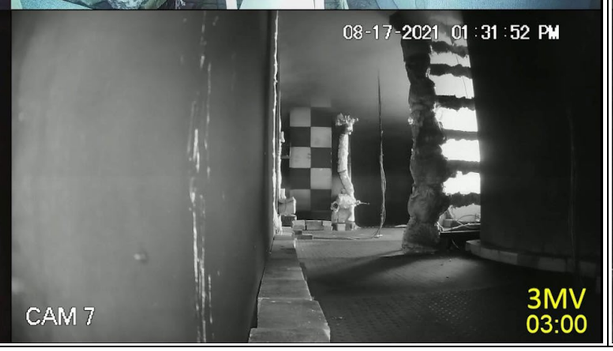


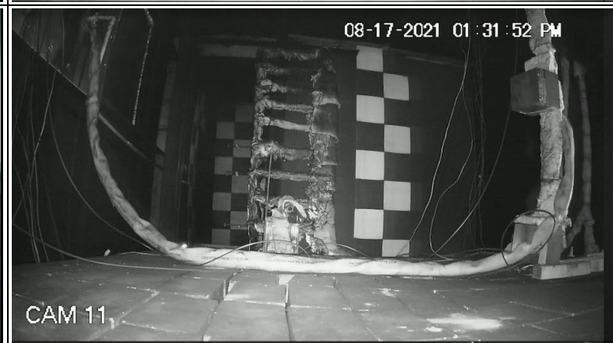


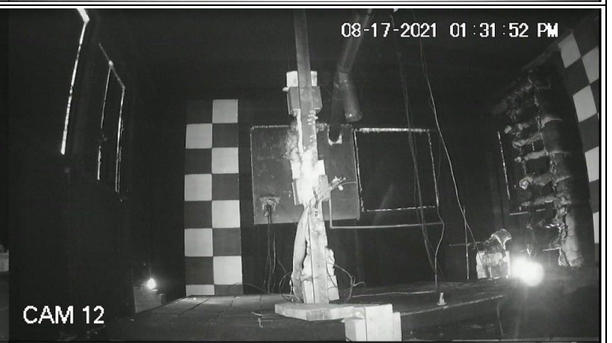
















3MV - Burn Room (US Standard Cloth Couch – Crib 4)











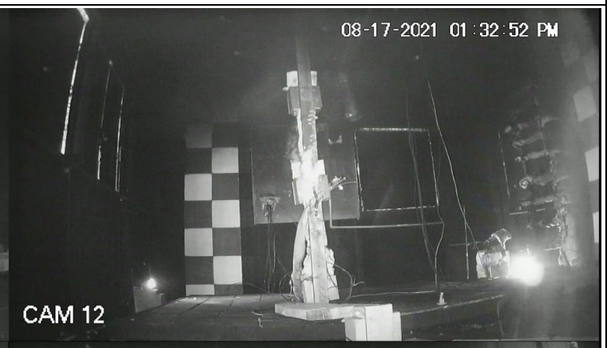






3MV – Upper Level (US Standard Cloth Couch – Crib 4)









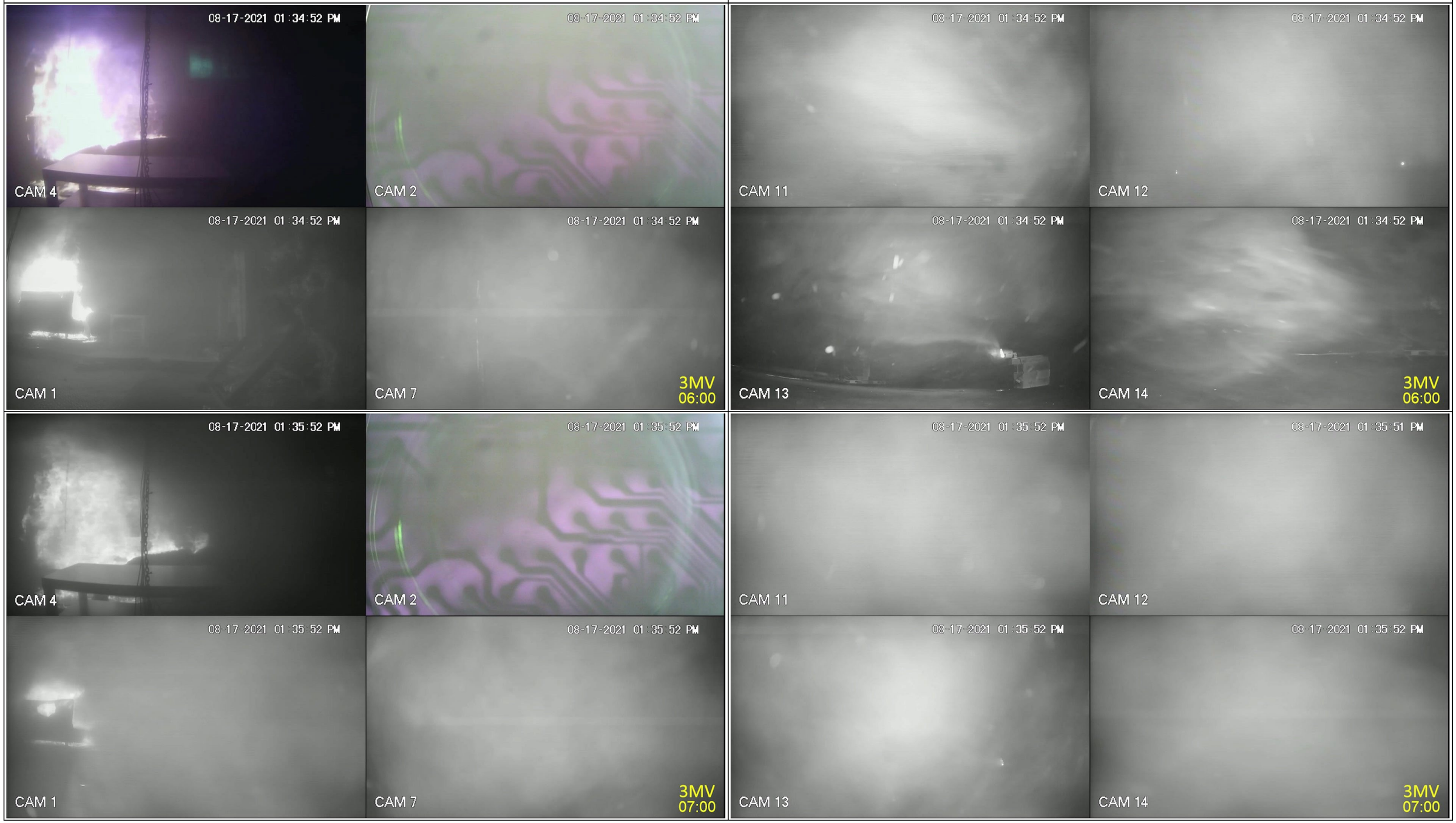




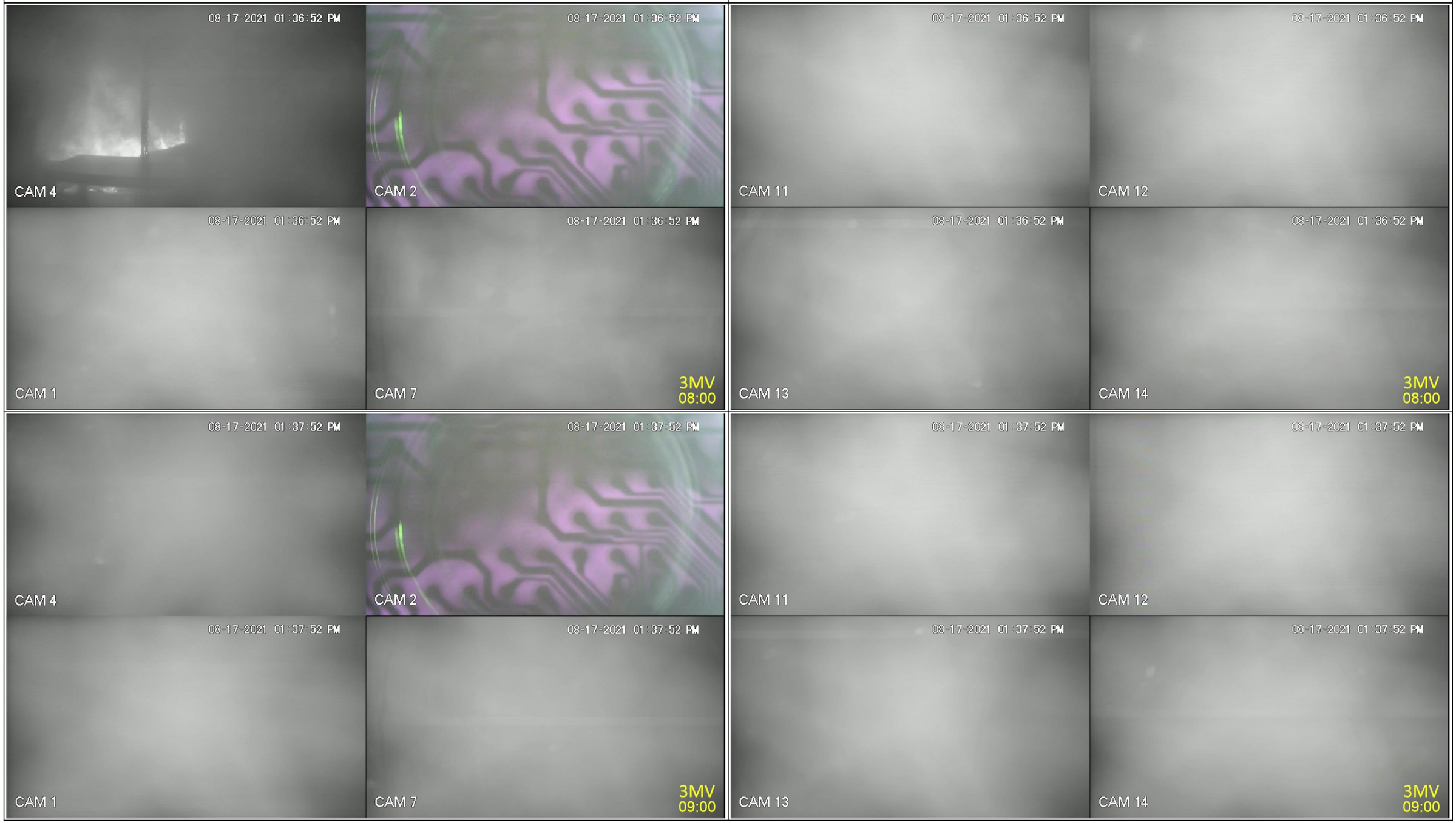




3MV - Burn Room (US Standard Cloth Couch – Crib 4)	**3MV** – Upper Level (US Standard Cloth Couch – Crib 4)



3MV - Burn Room (US Standard Cloth Couch – Crib 4)	**3MV** – Upper Level (US Standard Cloth Couch – Crib 4)



3MV - Burn Room (US Standard Cloth Couch – Crib 4)	**3MV** – Upper Level (US Standard Cloth Couch – Crib 4)



3MV - Burn Room (US Standard Cloth Couch – Crib 4)	**3MV** – Upper Level (US Standard Cloth Couch – Crib 4)



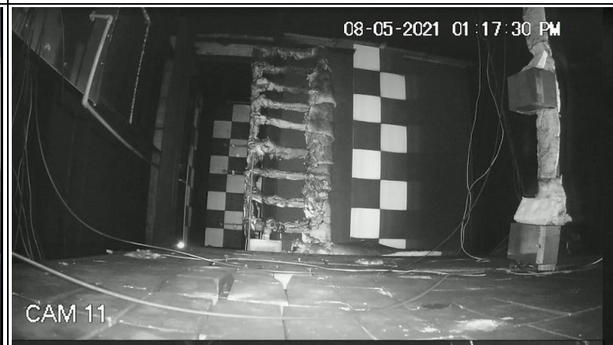
4MV - Burn Room (US Standard Cloth Couch – Crib 4)	**4MV** – Upper Level (US Standard Cloth Couch – Crib 4)















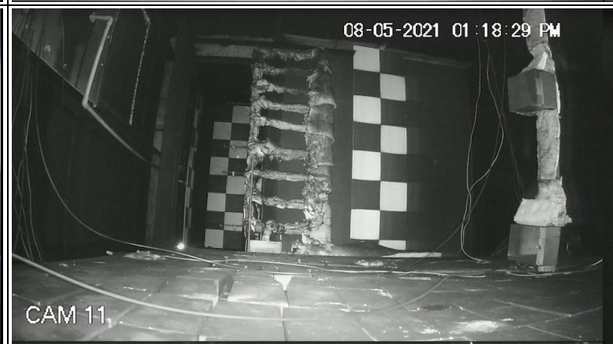












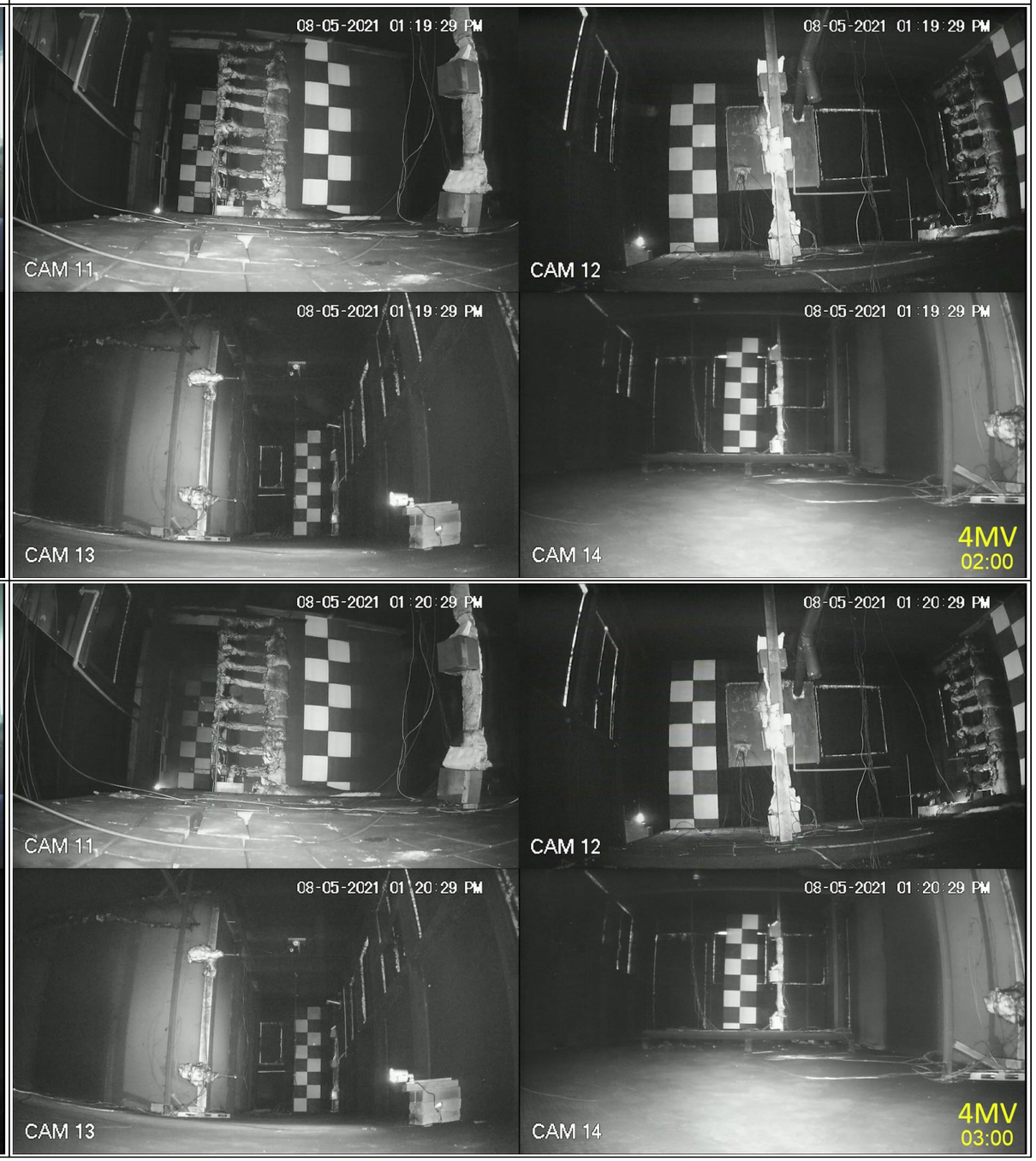






4MV - Burn Room (US Standard Cloth Couch – Crib 4)	**4MV** – Upper Level (US Standard Cloth Couch – Crib 4)





4MV - Burn Room (US Standard Cloth Couch – Crib 4)	**4MV** – Upper Level (US Standard Cloth Couch – Crib 4)





























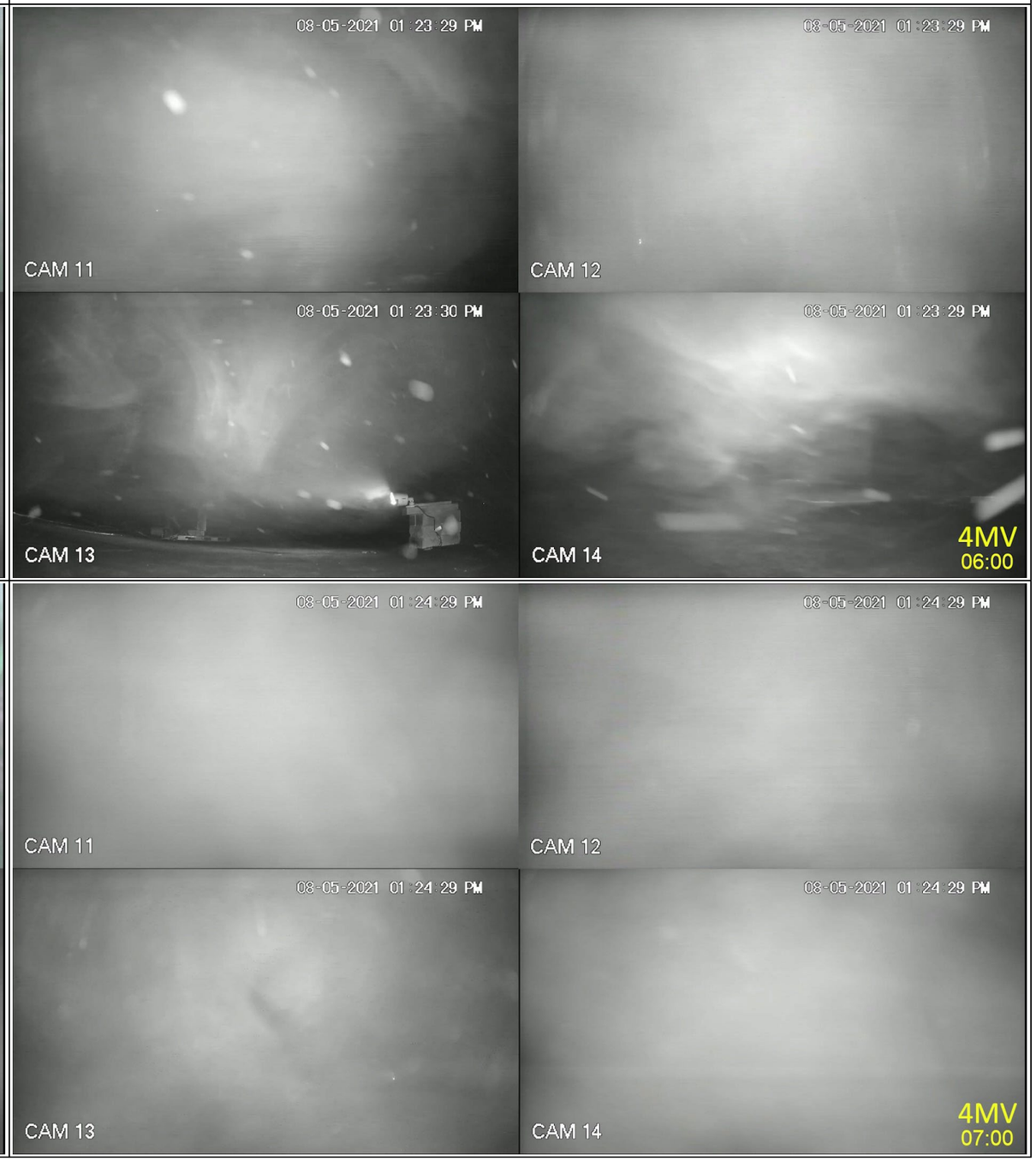




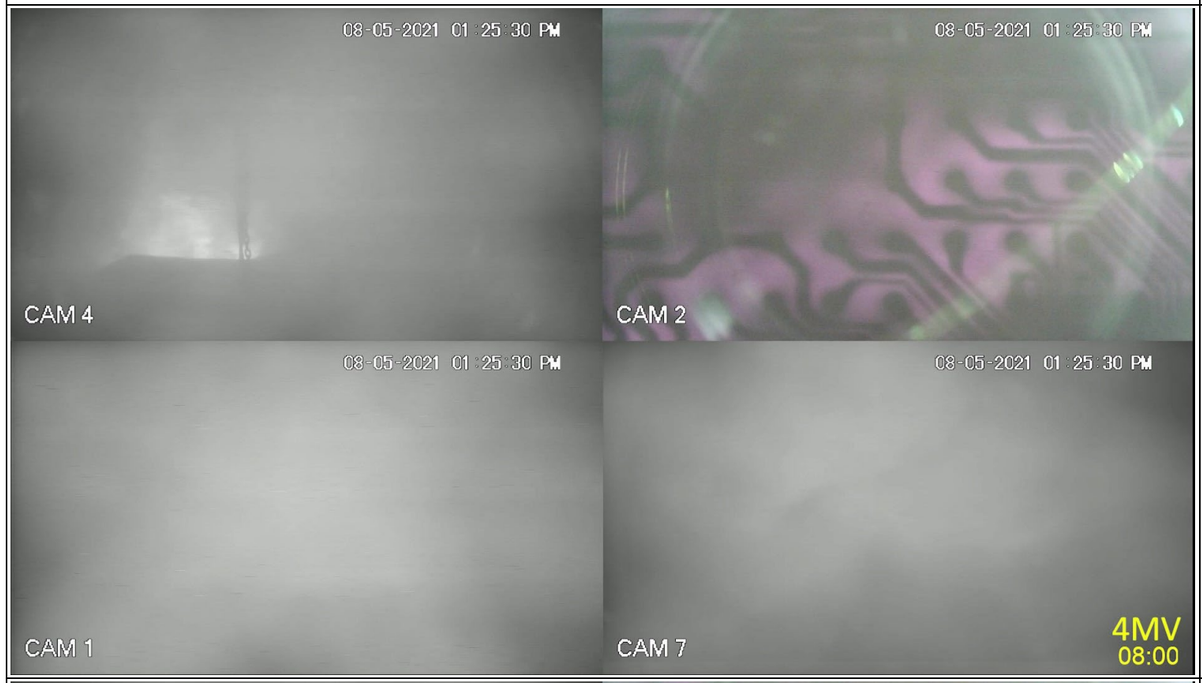
4MV - Burn Room (US Standard Cloth Couch – Crib 4)



4MV – Upper Level (US Standard Cloth Couch – Crib 4)



4MV - Burn Room (US Standard Cloth Couch – Crib 4)	**4MV** – Upper Level (US Standard Cloth Couch – Crib 4)





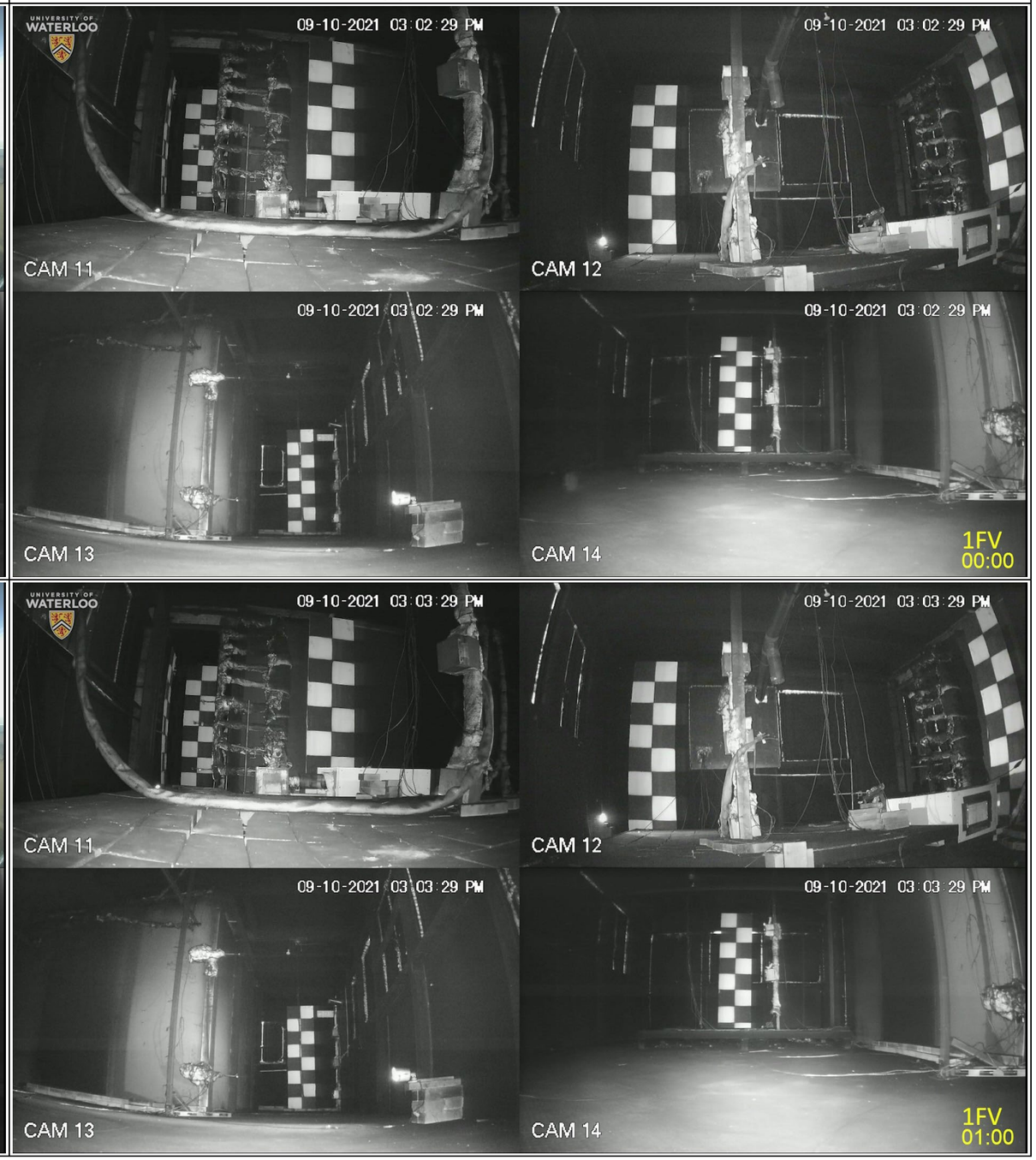
4MV - Burn Room (US Standard Cloth Couch – Crib 4)	**4MV** – Upper Level (US Standard Cloth Couch – Crib 4)

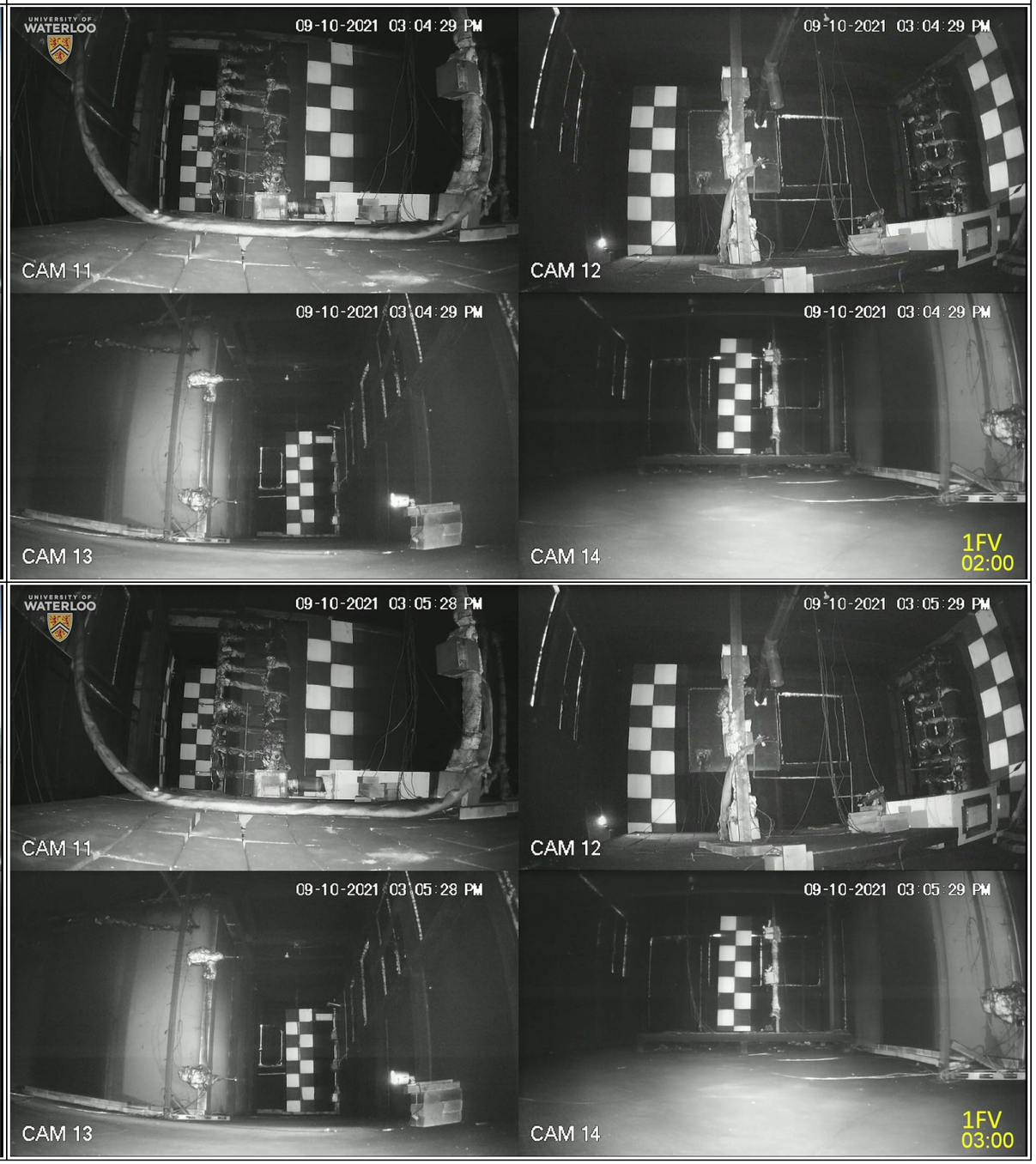


4MV - Burn Room (US Standard Cloth Couch – Crib 4)	**4MV** – Upper Level (US Standard Cloth Couch – Crib 4)





1FV - Burn Room (Wood Crib – Crib 5)	**1FV** – Upper Level (Wood Crib – Crib 5)
	

1FV - Burn Room (Wood Crib – Crib 5)	**1FV** – Upper Level (Wood Crib – Crib 5)
	

1FV - Burn Room (Wood Crib – Crib 5)	**1FV** – Upper Level (Wood Crib – Crib 5)

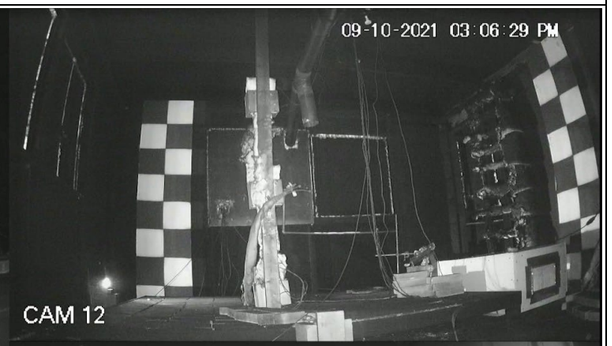
















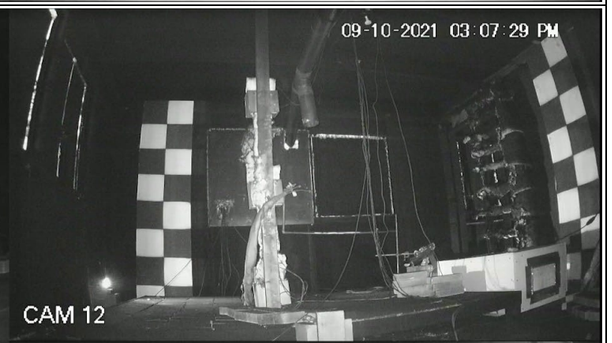






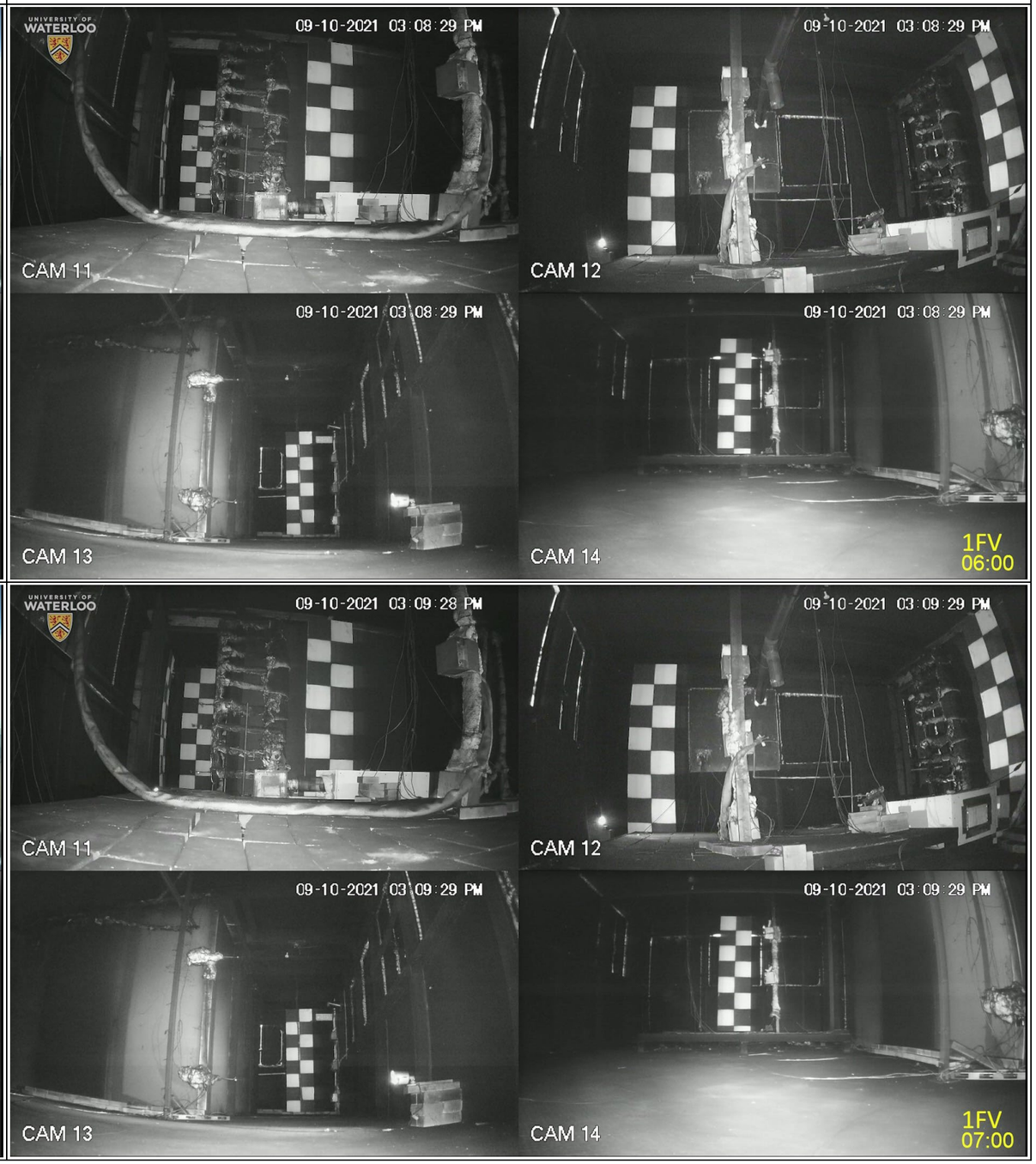






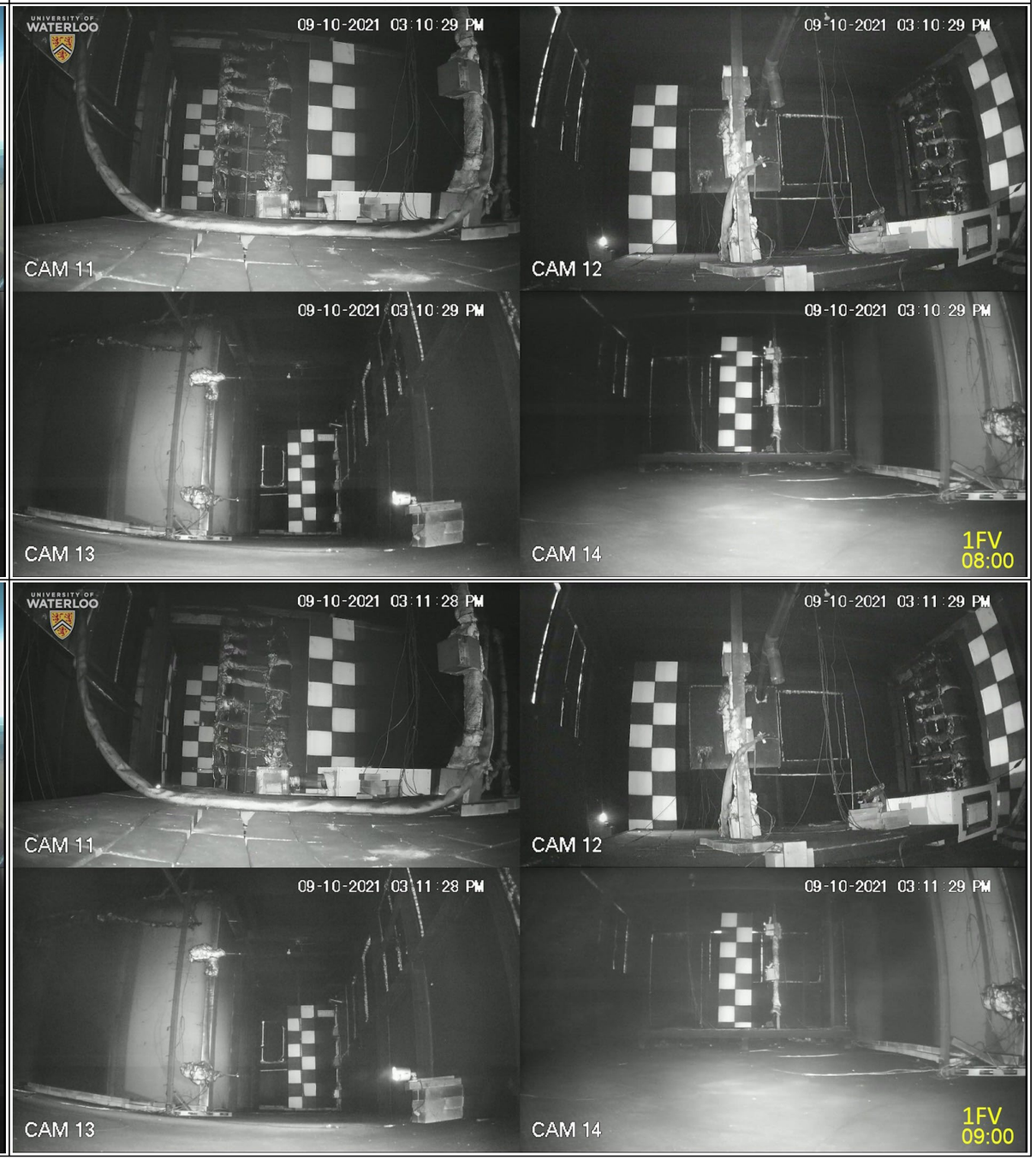




1FV - Burn Room (Wood Crib – Crib 5)	**1FV** – Upper Level (Wood Crib – Crib 5)
	

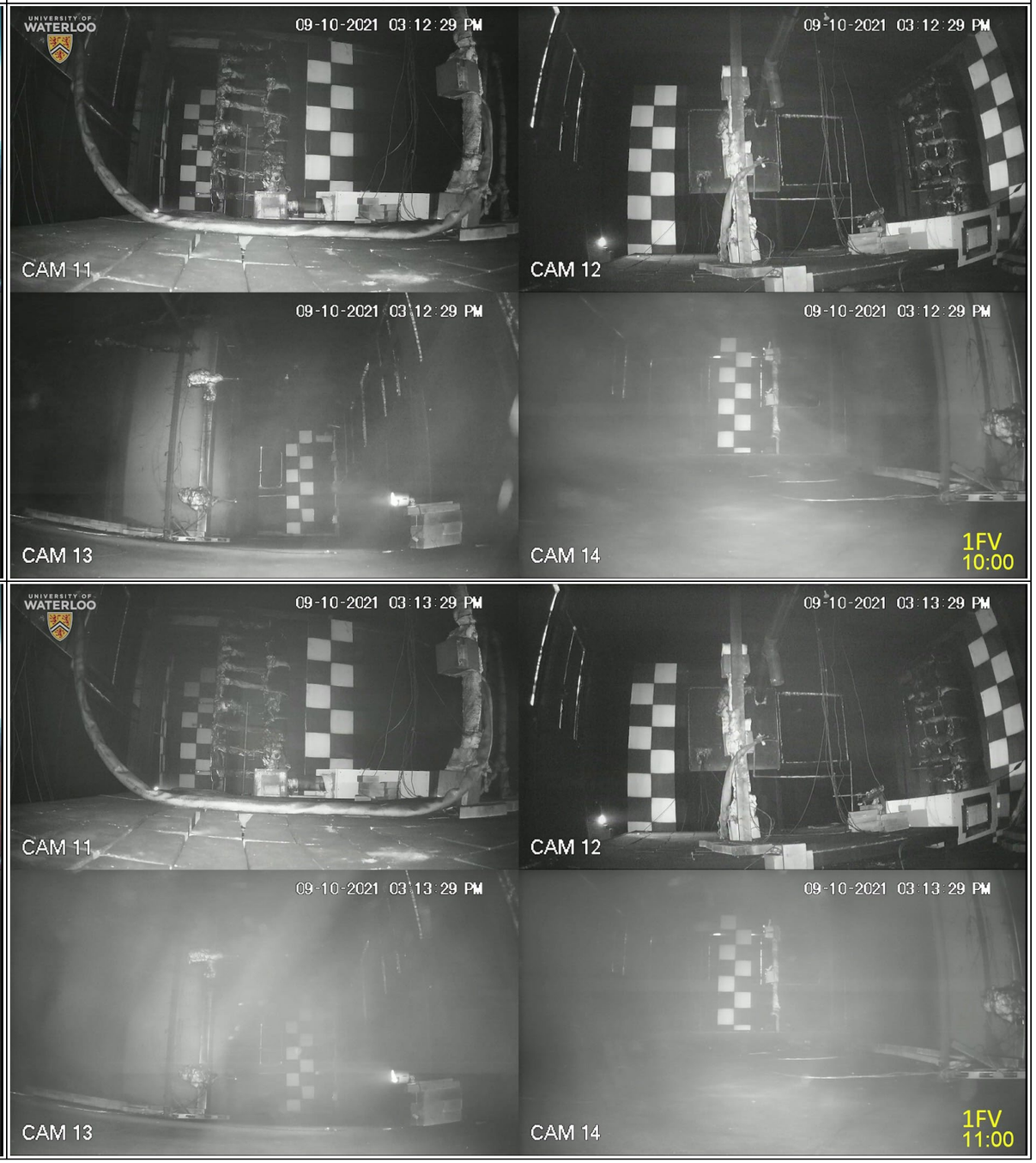
1FV - Burn Room (Wood Crib – Crib 5)	**1FV** – Upper Level (Wood Crib – Crib 5)





1FV - Burn Room (Wood Crib – Crib 5)	**1FV** – Upper Level (Wood Crib – Crib 5)





1FV - Burn Room (Wood Crib – Crib 5)	**1FV** – Upper Level (Wood Crib – Crib 5)



























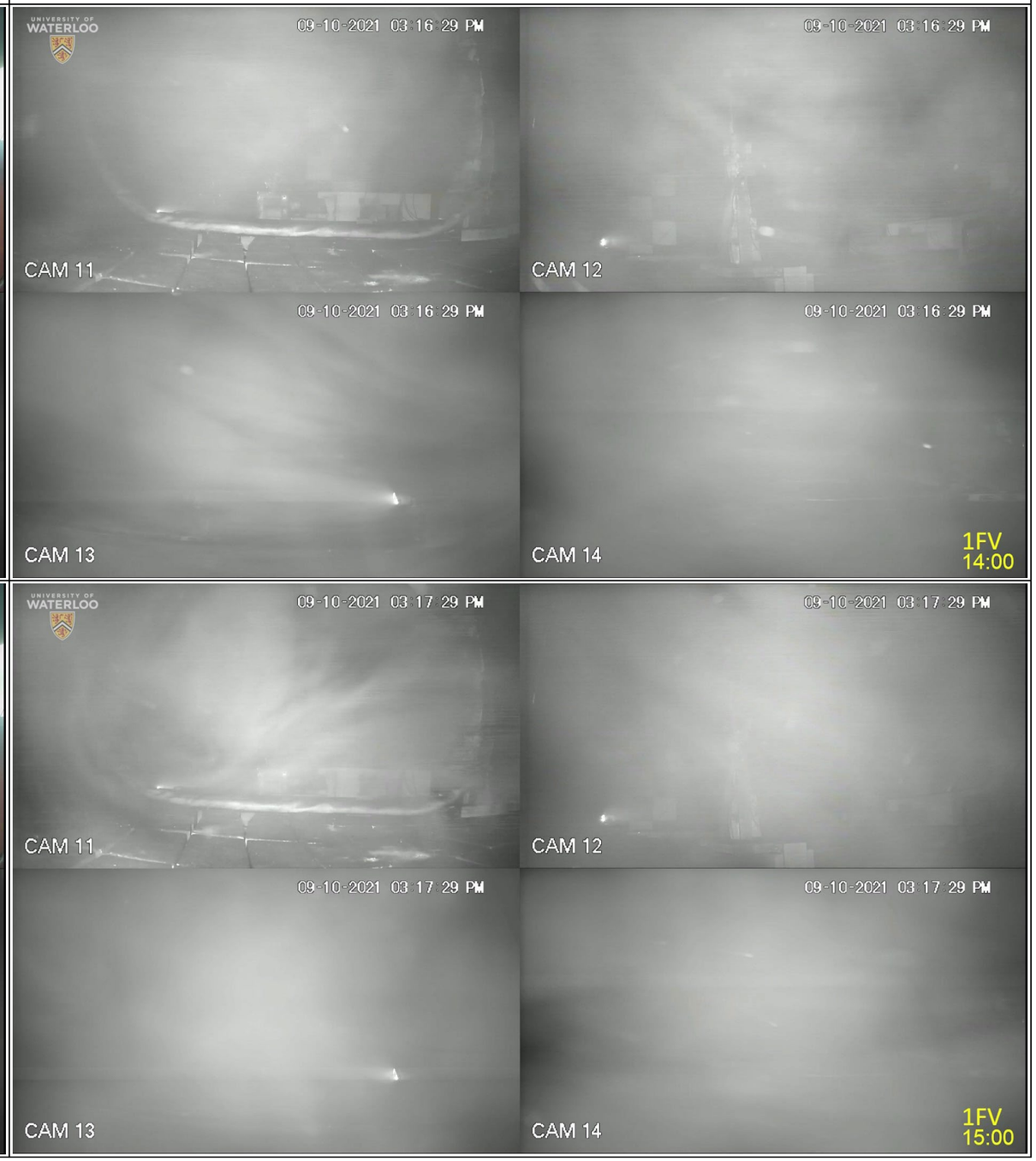




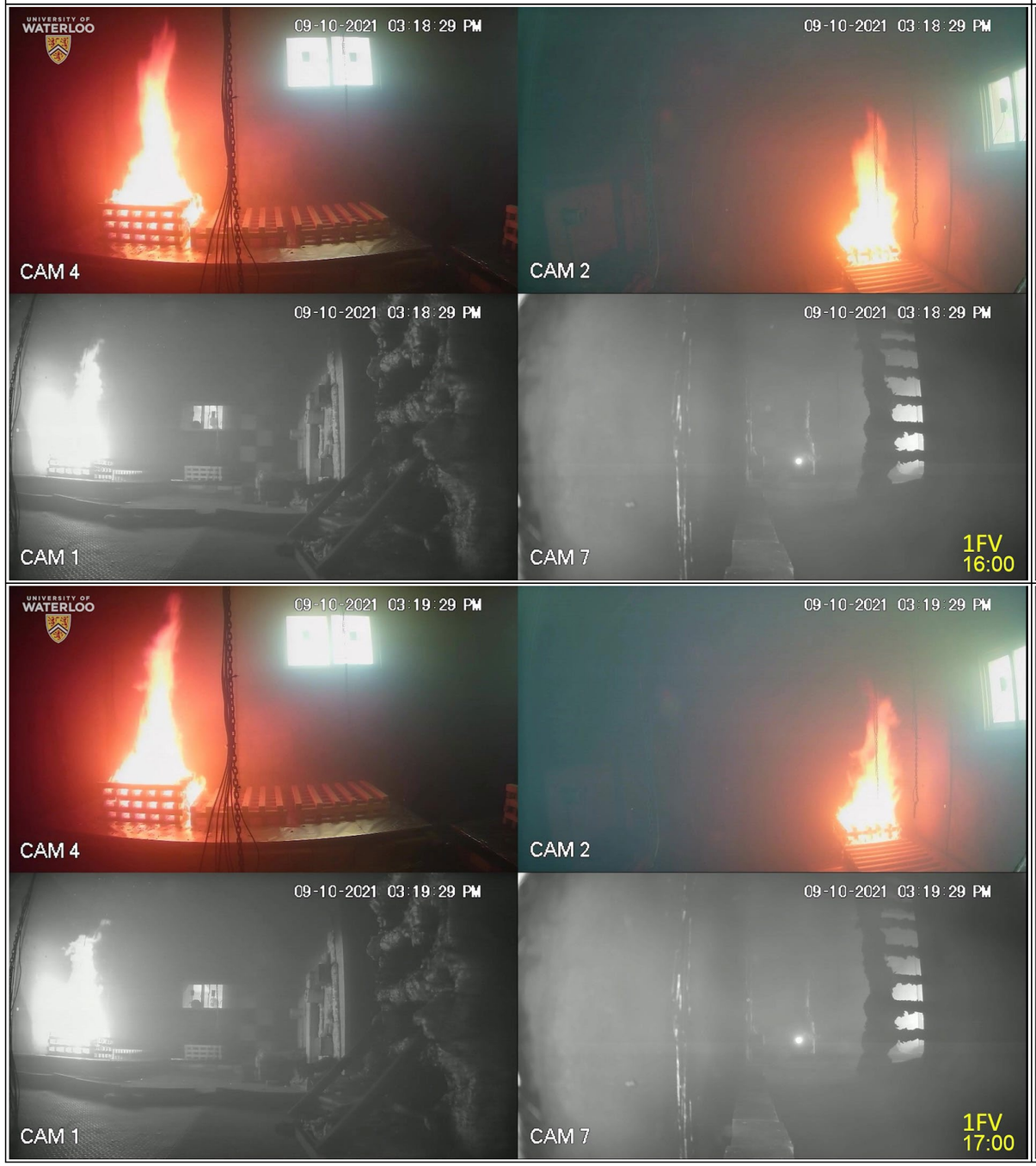


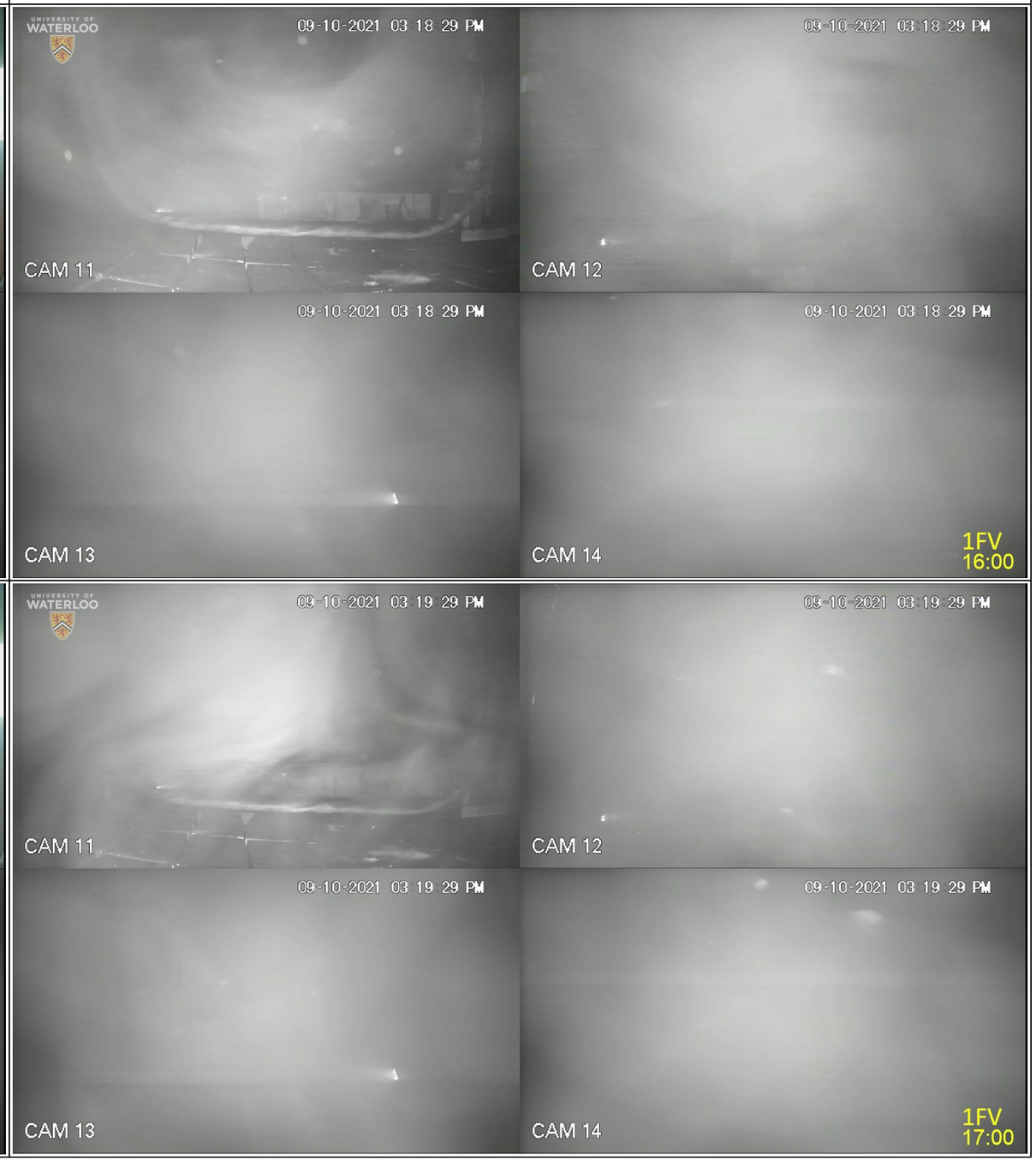
1FV - Burn Room (Wood Crib – Crib 5)	**1FV** – Upper Level (Wood Crib – Crib 5)





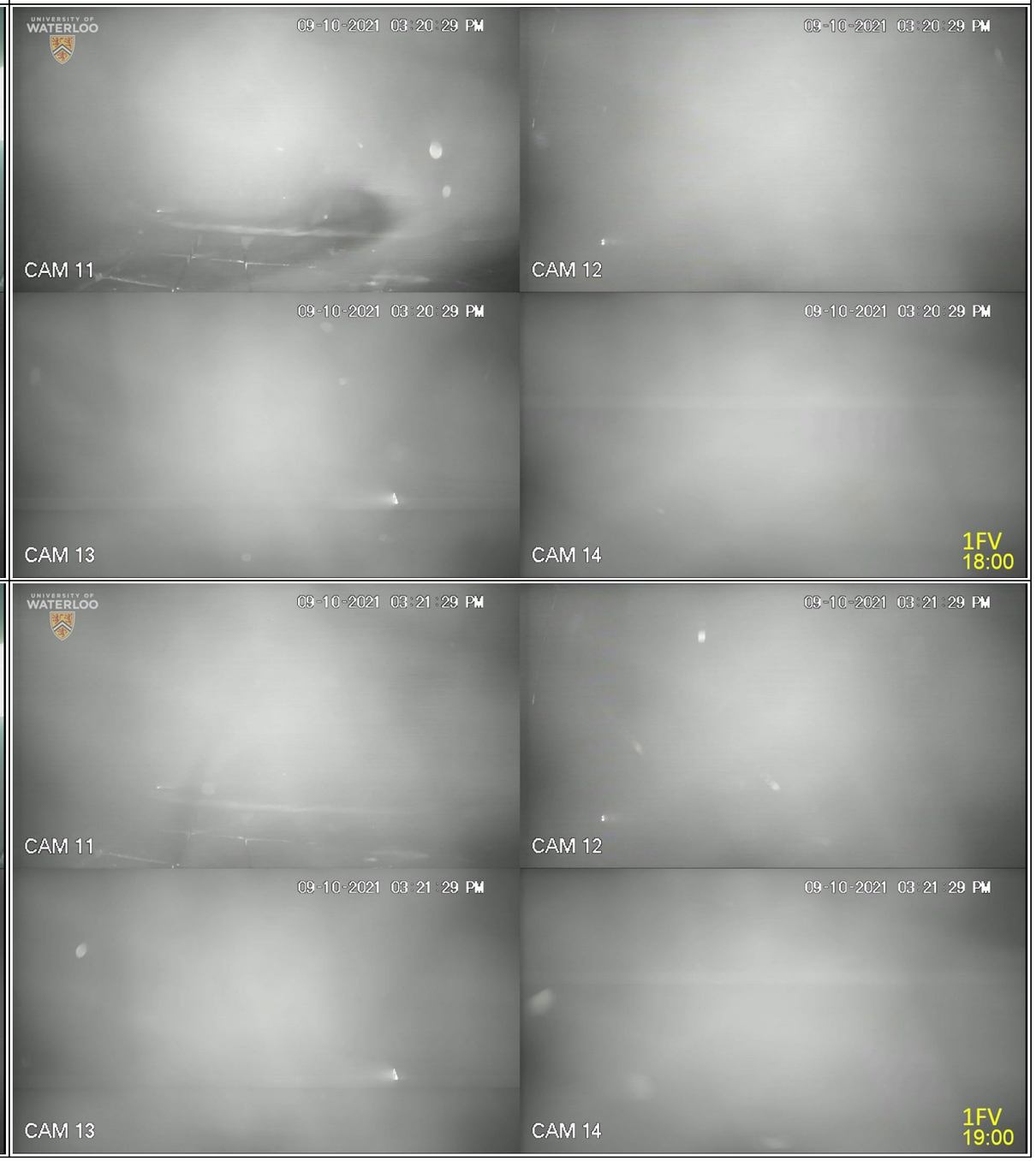
1FV - Burn Room (Wood Crib – Crib 5)	**1FV** – Upper Level (Wood Crib – Crib 5)





1FV - Burn Room (Wood Crib – Crib 5)	**1FV** – Upper Level (Wood Crib – Crib 5)





1FV - Burn Room (Wood Crib – Crib 5)	**1FV** – Upper Level (Wood Crib – Crib 5)
	
	

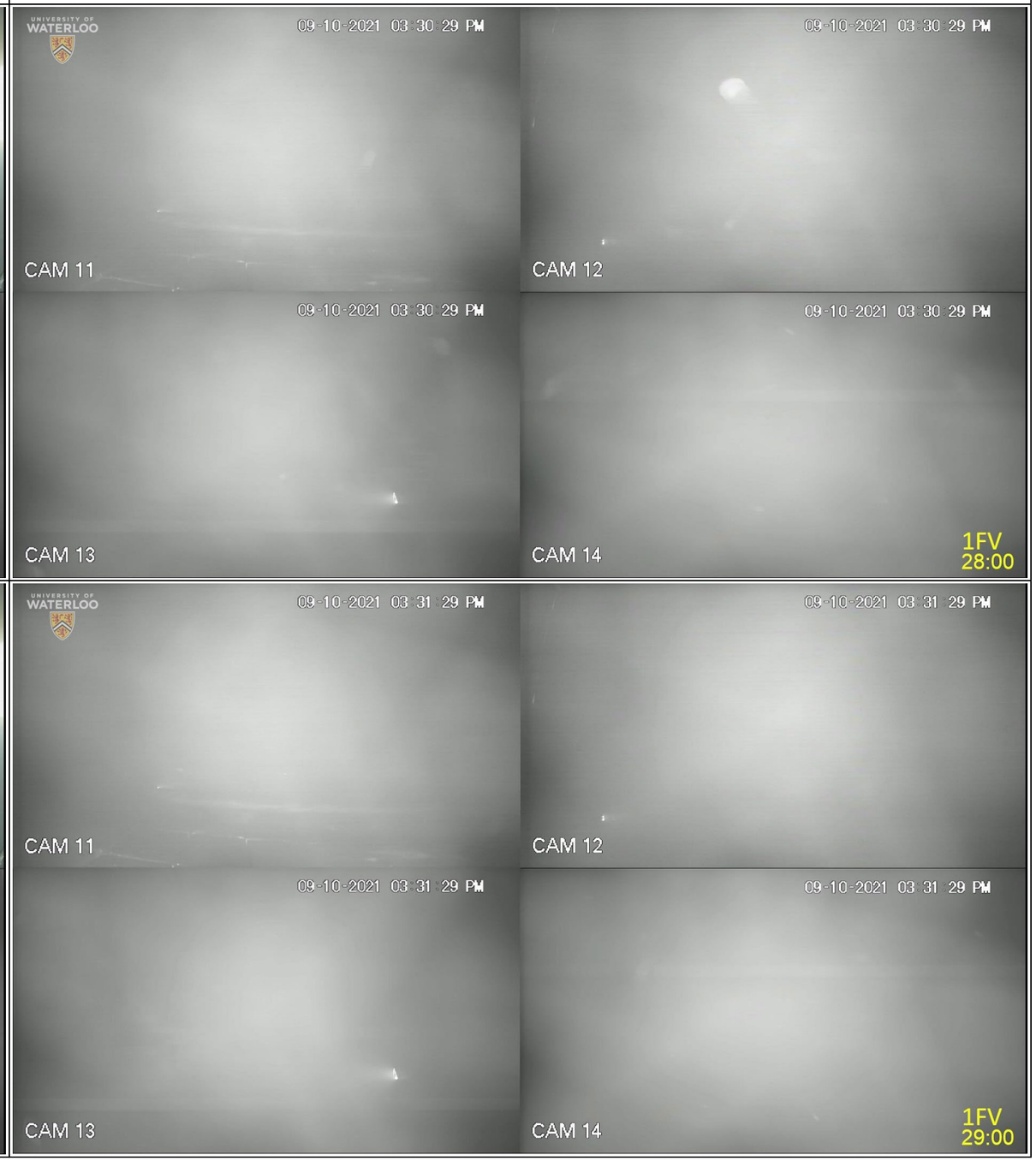
1FV - Burn Room (Wood Crib – Crib 5)	**1FV** – Upper Level (Wood Crib – Crib 5)
	
	

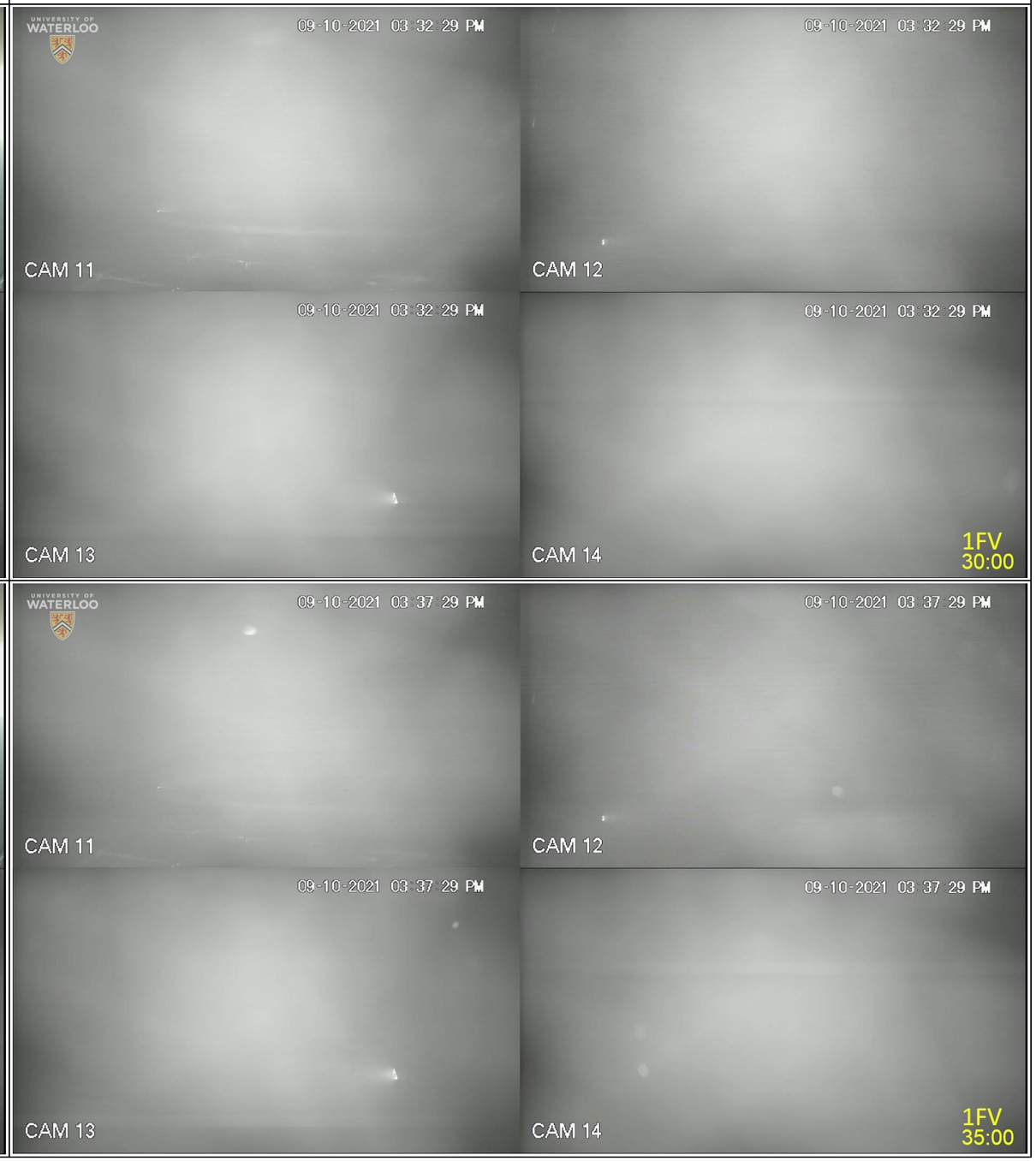
1FV - Burn Room (Wood Crib – Crib 5)	**1FV** – Upper Level (Wood Crib – Crib 5)

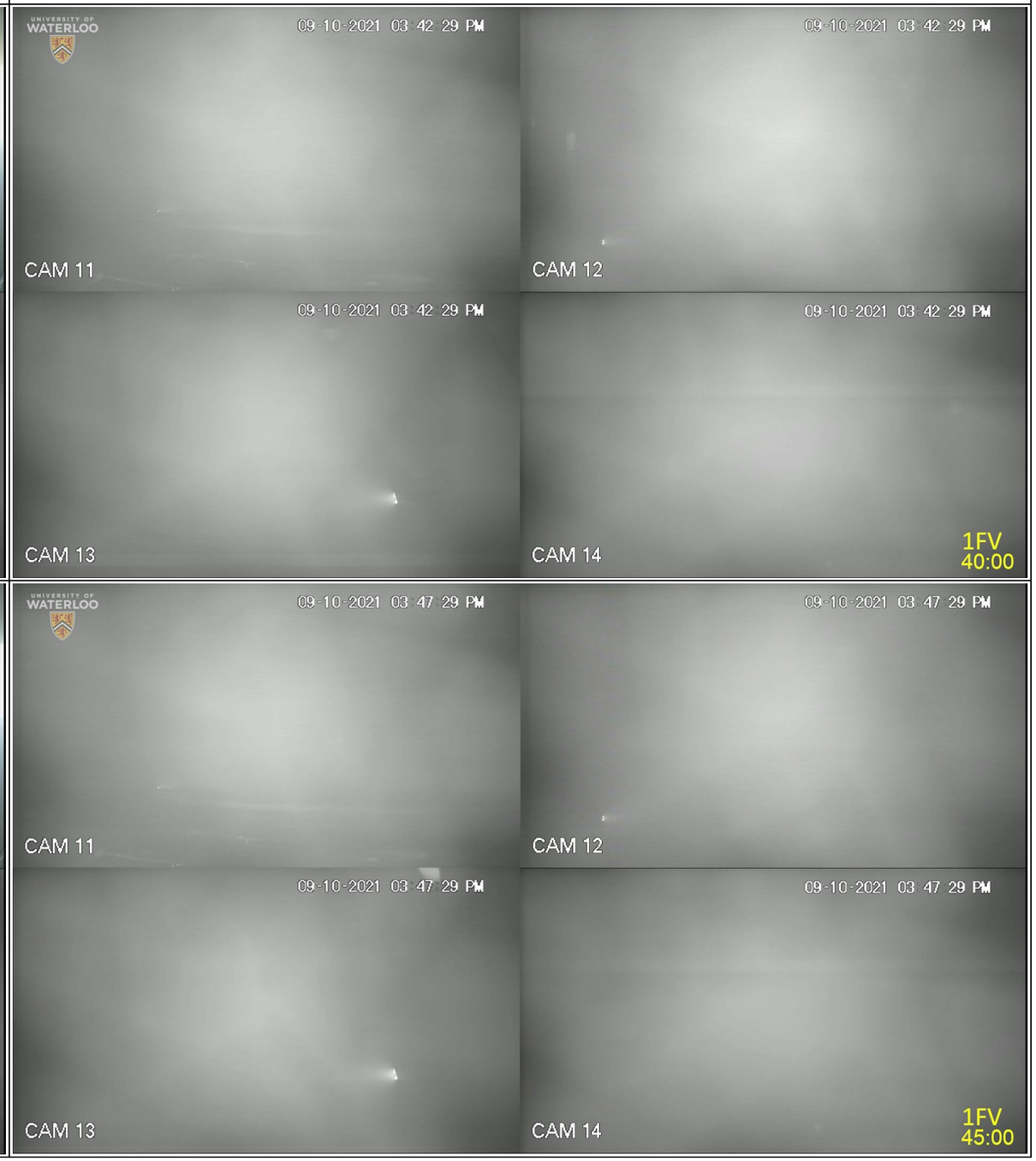




1FV - Burn Room (Wood Crib – Crib 5)	**1FV** – Upper Level (Wood Crib – Crib 5)
	

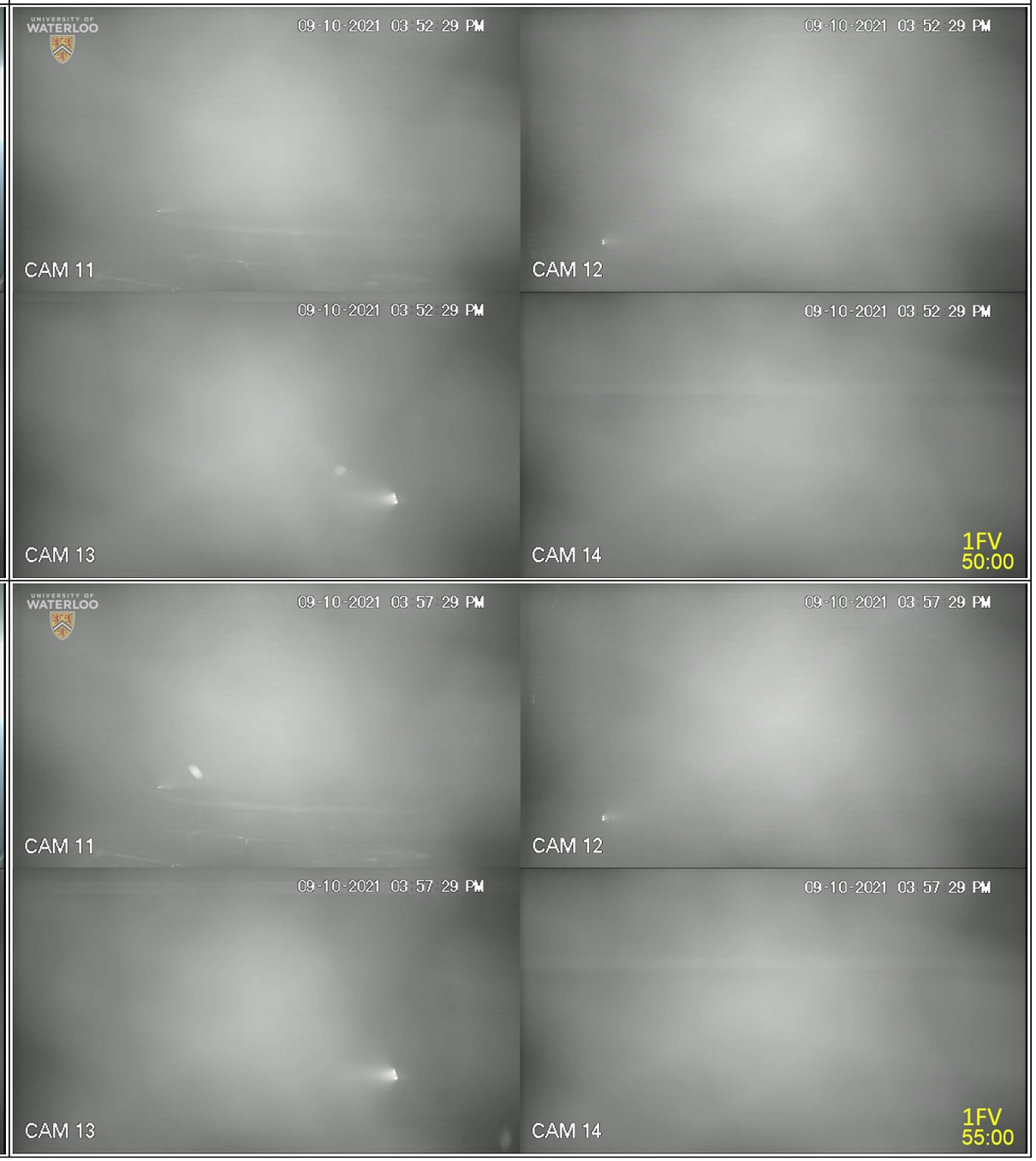
1FV - Burn Room (Wood Crib – Crib 5)	**1FV** – Upper Level (Wood Crib – Crib 5)
	

1FV - Burn Room (Wood Crib – Crib 5)	**1FV** – Upper Level (Wood Crib – Crib 5)
	

1FV - Burn Room (Wood Crib – Crib 5)	**1FV** – Upper Level (Wood Crib – Crib 5)
	

1FV - Burn Room (Wood Crib – Crib 5)	**1FV** – Upper Level (Wood Crib – Crib 5)





3FV - Burn Room (US Standard Faux Leather Couch – Crib 4)	**3FV** – Upper Level (US Standard Faux Leather Couch – Crib 4)

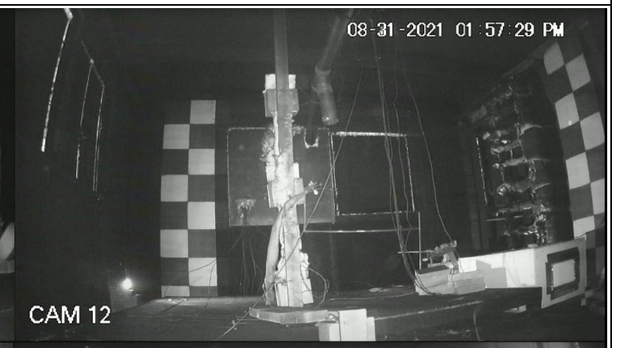
















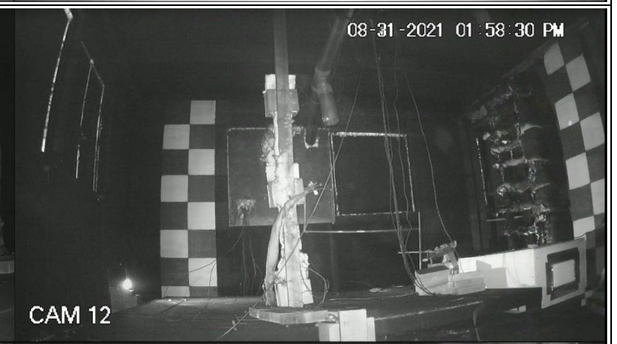














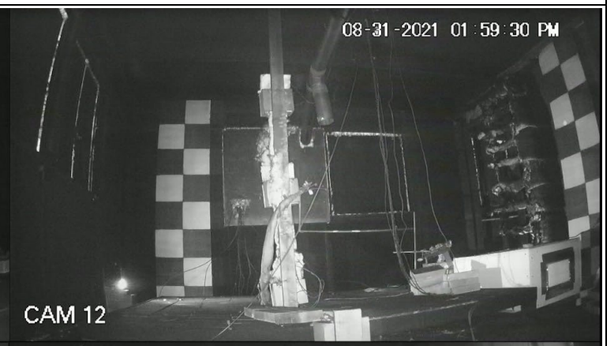


3FV - Burn Room (US Standard Faux Leather Couch – Crib 4)	**3FV** – Upper Level (US Standard Faux Leather Couch – Crib 4)

















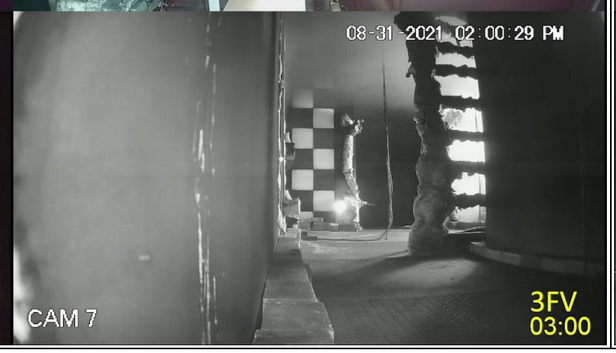
















3FV - Burn Room (US Standard Faux Leather Couch – Crib 4)	**3FV** – Upper Level (US Standard Faux Leather Couch – Crib 4)

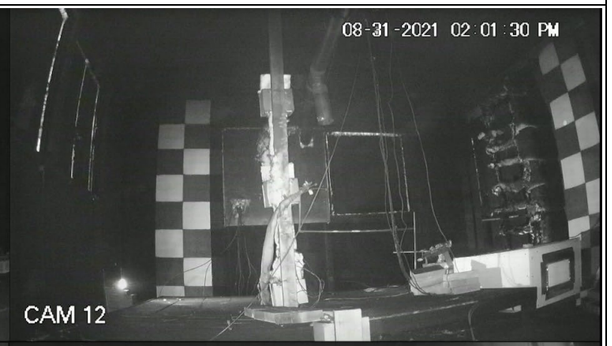




























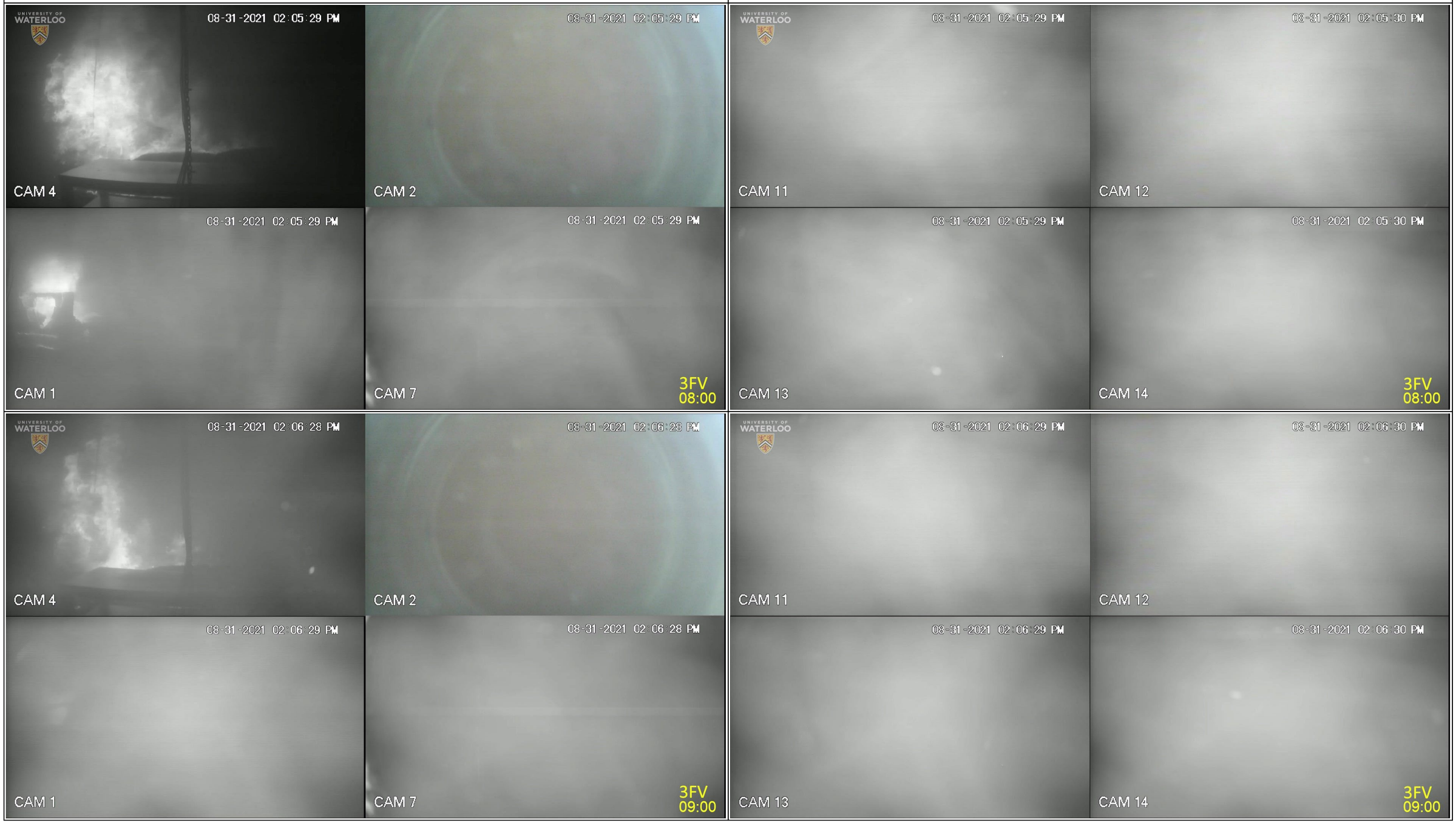




3FV - Burn Room (US Standard Faux Leather Couch – Crib 4)	**3FV** – Upper Level (US Standard Faux Leather Couch – Crib 4)



3FV - Burn Room (US Standard Faux Leather Couch – Crib 4)	**3FV** – Upper Level (US Standard Faux Leather Couch – Crib 4)

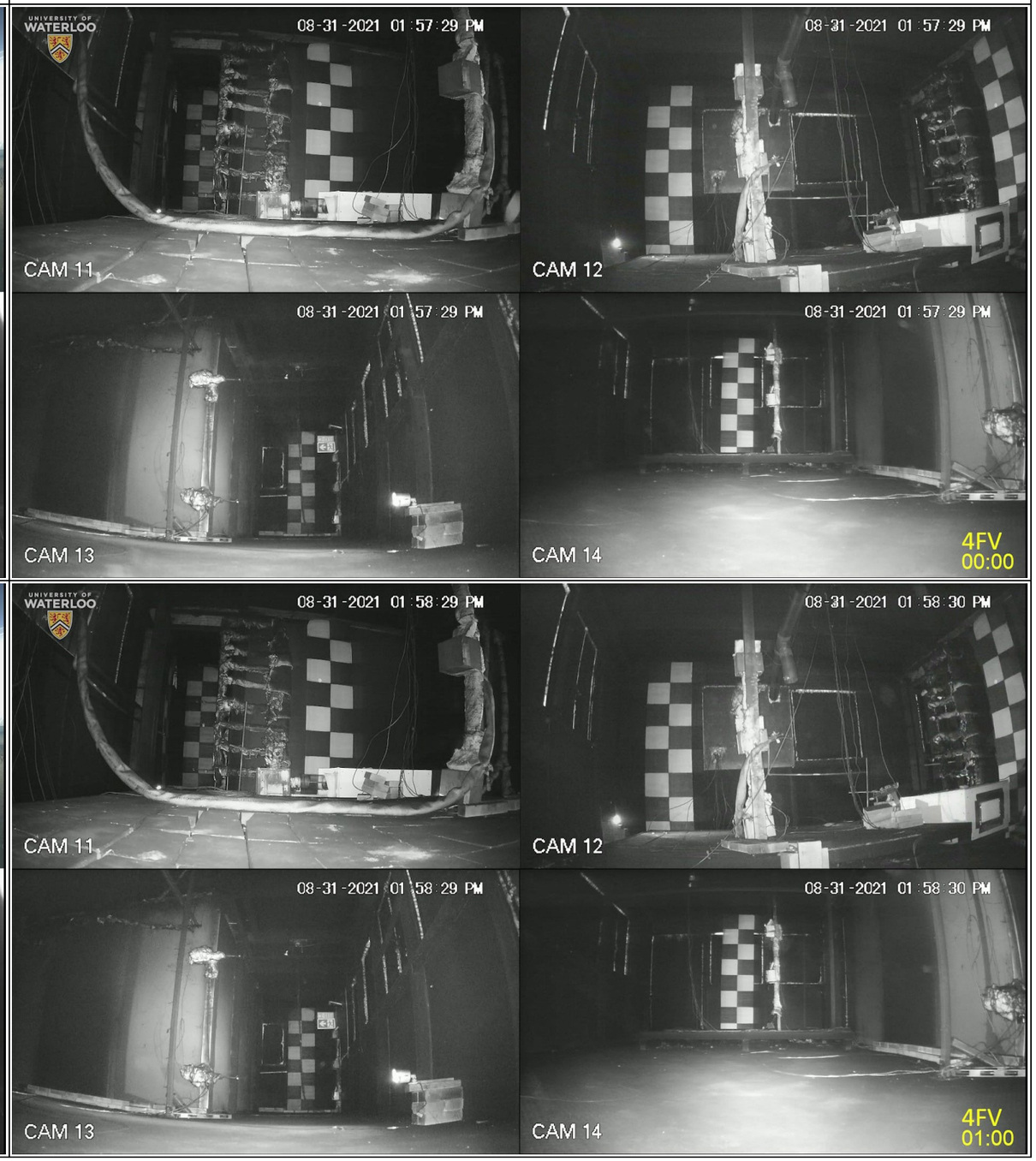


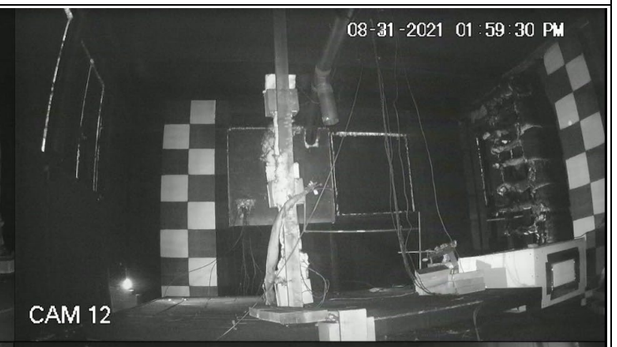
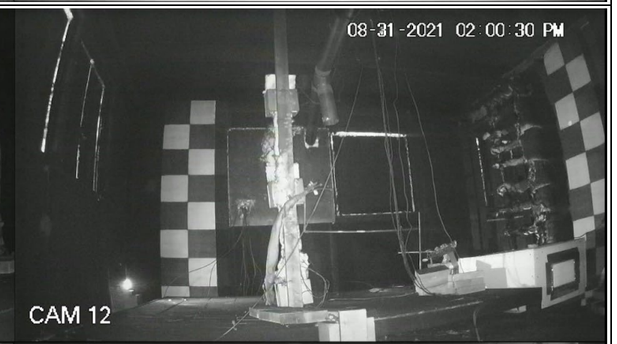
3FV - Burn Room (US Standard Faux Leather Couch – Crib 4)	**3FV** – Upper Level (US Standard Faux Leather Couch – Crib 4)



3FV - Burn Room (US Standard Faux Leather Couch – Crib 4)	**3FV** – Upper Level (US Standard Faux Leather Couch – Crib 4)

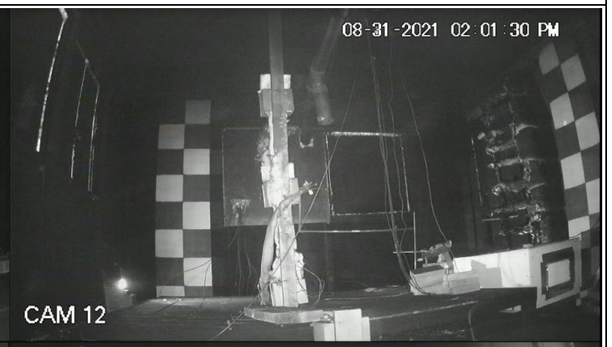


4FV - Burn Room (US Leather Couch – Crib 5)	**4FV** – Upper Level (US Leather Couch – Crib 5)
	

4FV - Burn Room (US Leather Couch – Crib 5)	**4FV** – Upper Level (US Leather Couch – Crib 5)
	
	
	
	
	
	
	
	

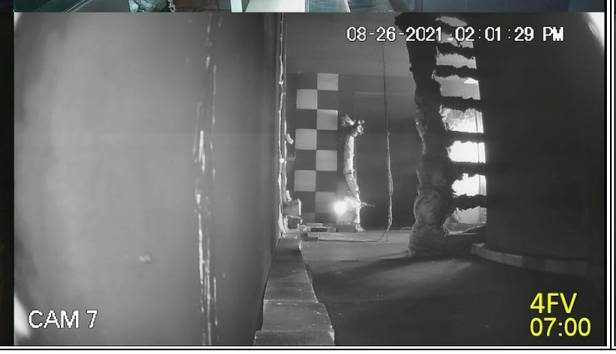
4FV - Burn Room (US Leather Couch – Crib 5)	**4FV** – Upper Level (US Leather Couch – Crib 5)
	
	
	

4FV – Upper Level (US Leather Couch – Crib 5)







4FV - Burn Room (US Leather Couch – Crib 5)	**4FV** – Upper Level (US Leather Couch – Crib 5)
	
	
	
	
	
	
	
	

4FV - Burn Room (US Leather Couch – Crib 5)	**4FV** – Upper Level (US Leather Couch – Crib 5)









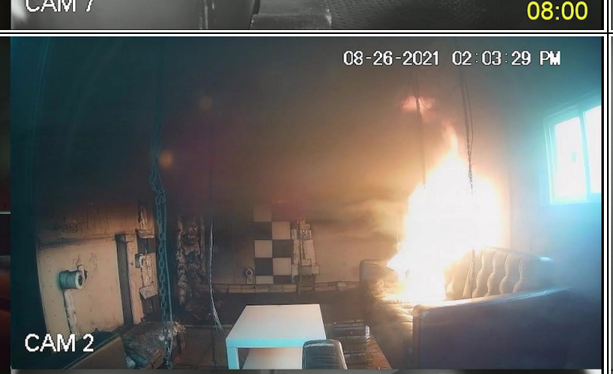


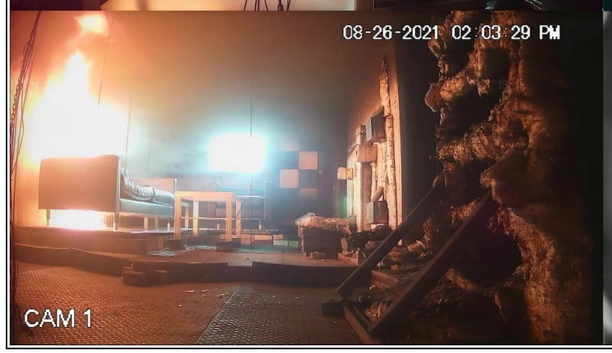


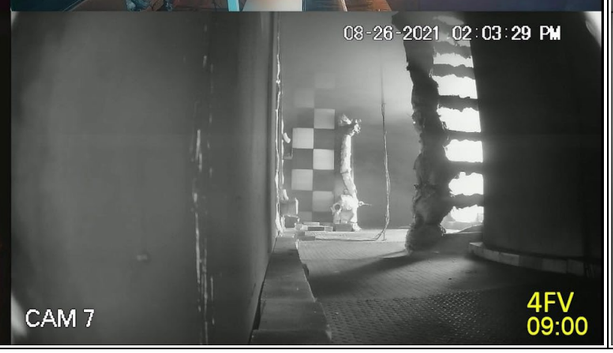




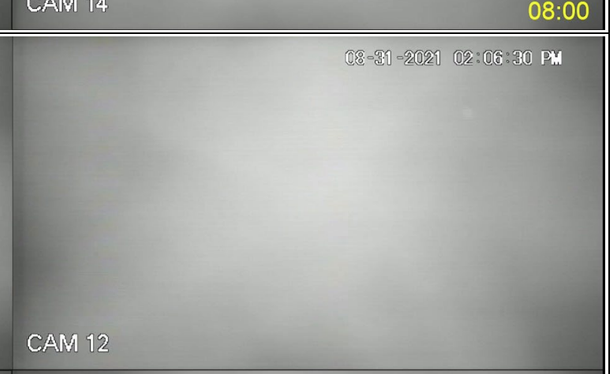








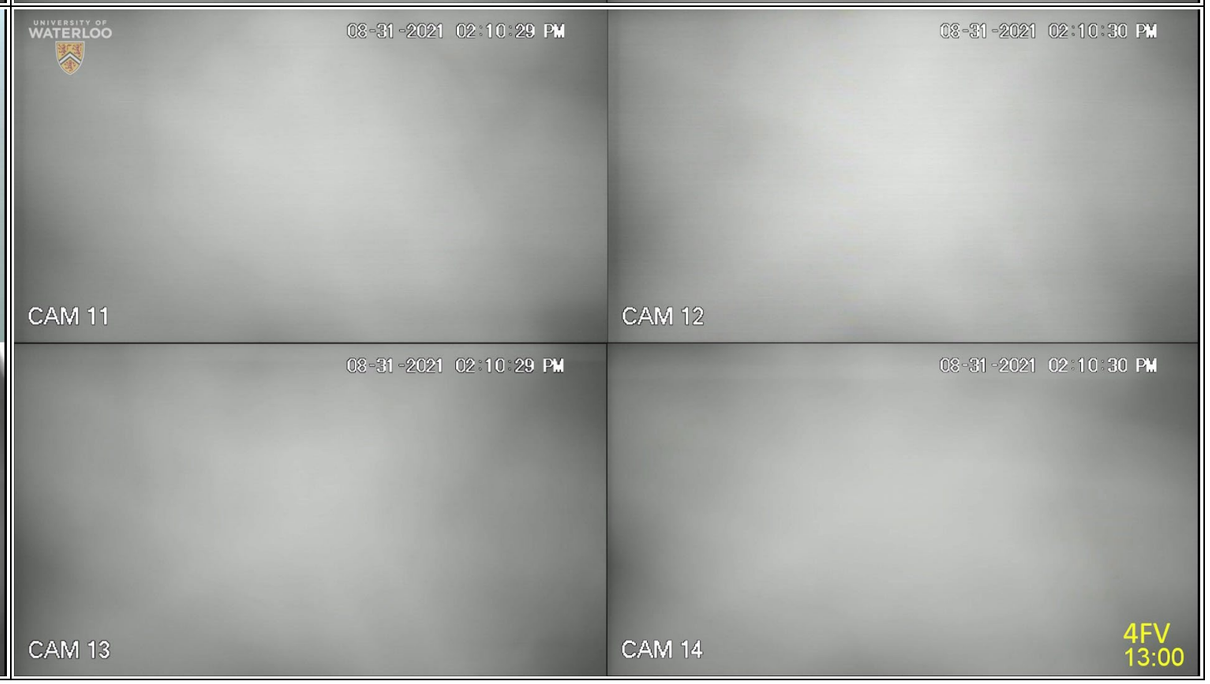




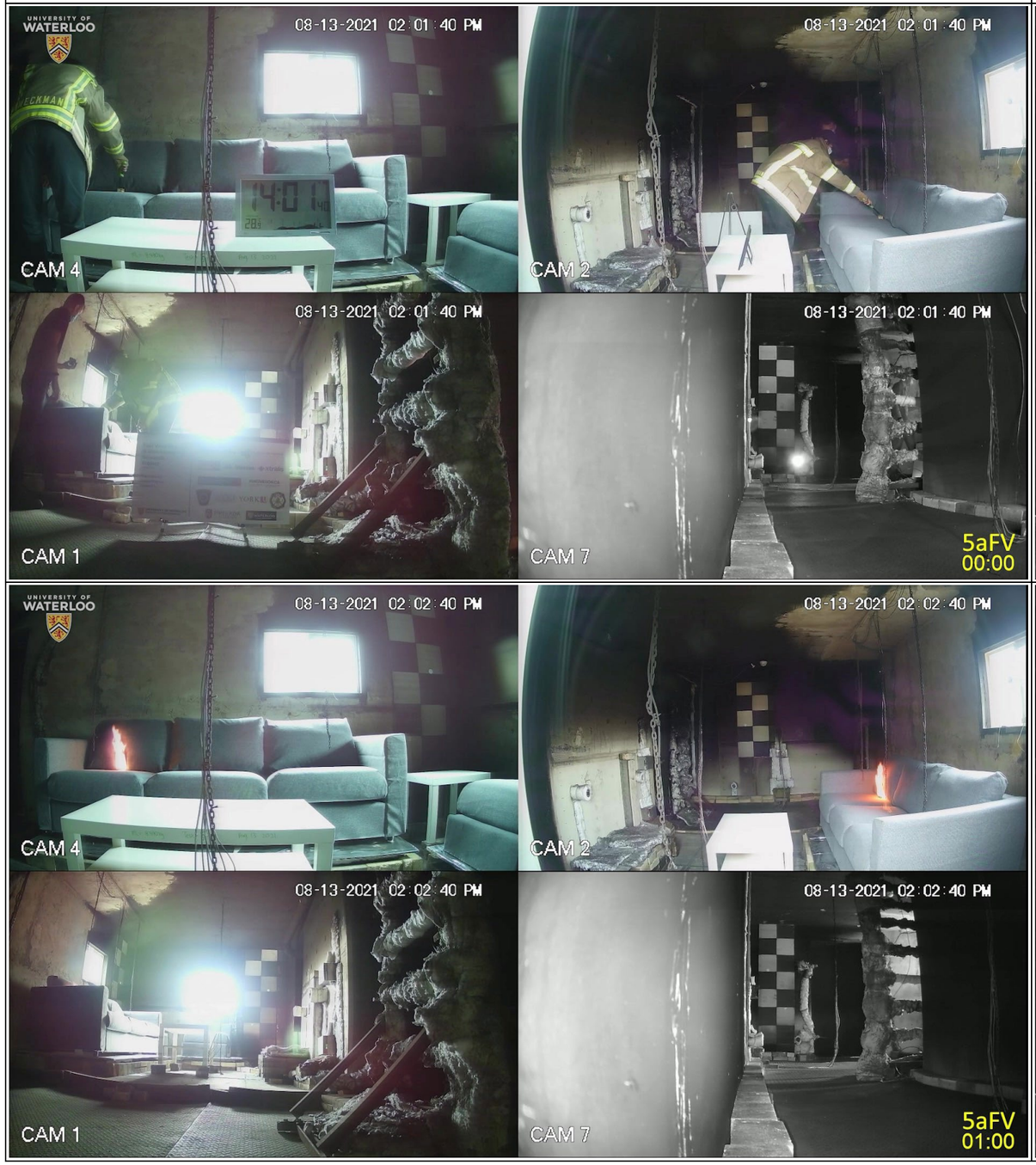




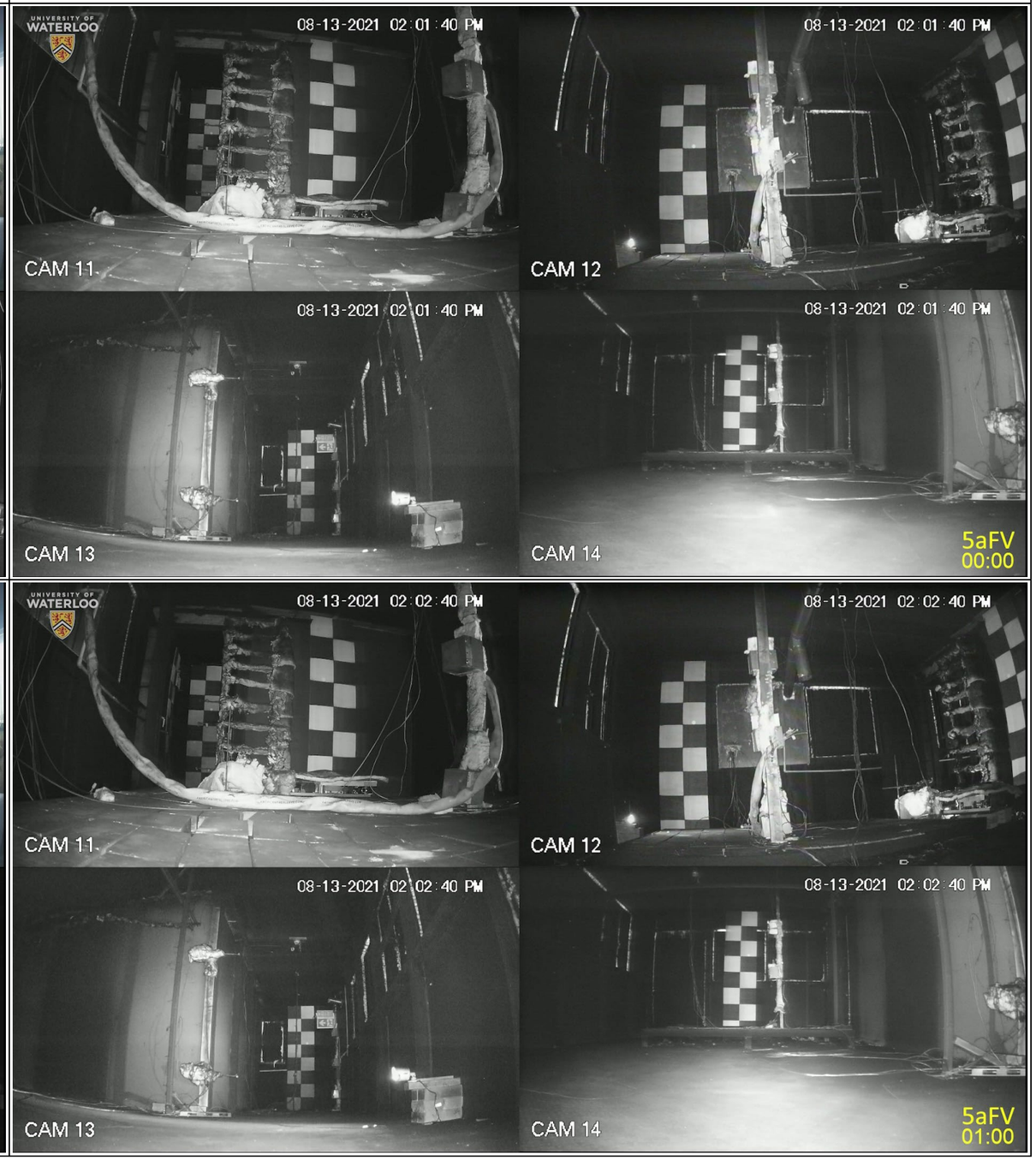
4FV - Burn Room (US Leather Couch – Crib 5)	**4FV** – Upper Level (US Leather Couch – Crib 5)
	

4FV - Burn Room (US Leather Couch – Crib 5)	**4FV** – Upper Level (US Leather Couch – Crib 5)
	
	

5aFV – Burn Room (UK Standard Cloth Couch – Crib 4)



5aFV – Upper Level (UK Standard Cloth Couch – Crib 4)



5aFV – Burn Room (UK Standard Cloth Couch – Crib 4)	**5aFV** – Upper Level (UK Standard Cloth Couch – Crib 4)

















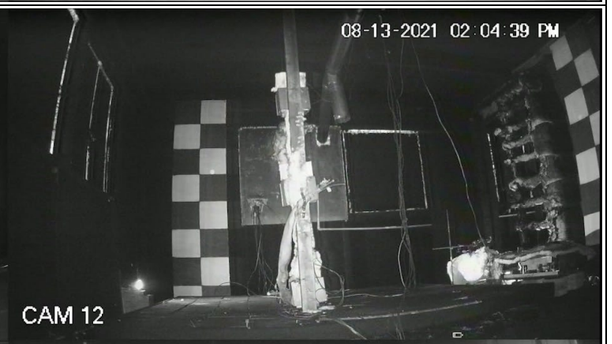










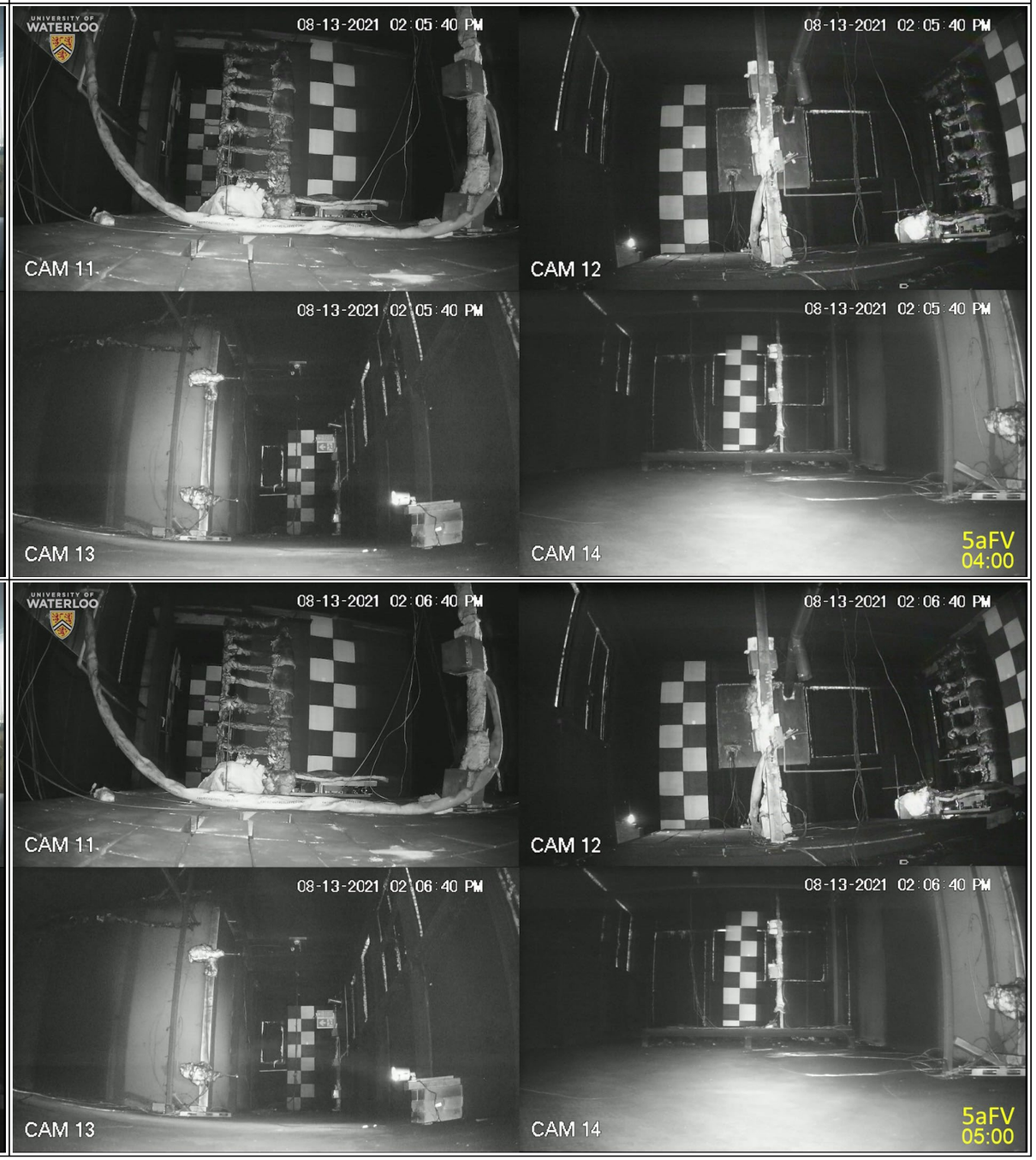






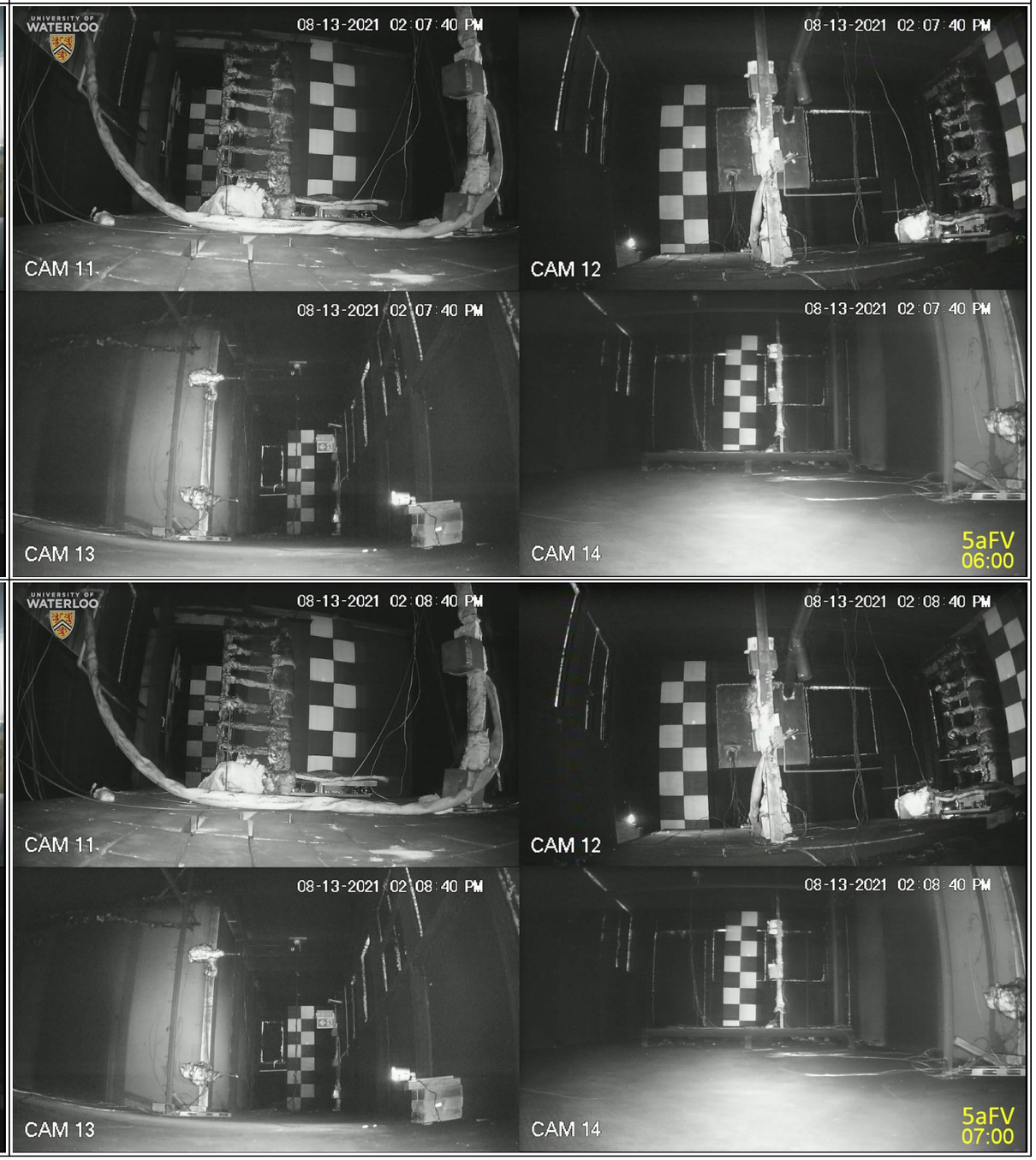
5aFV – Burn Room (UK Standard Cloth Couch – Crib 4)	**5aFV** – Upper Level (UK Standard Cloth Couch – Crib 4)





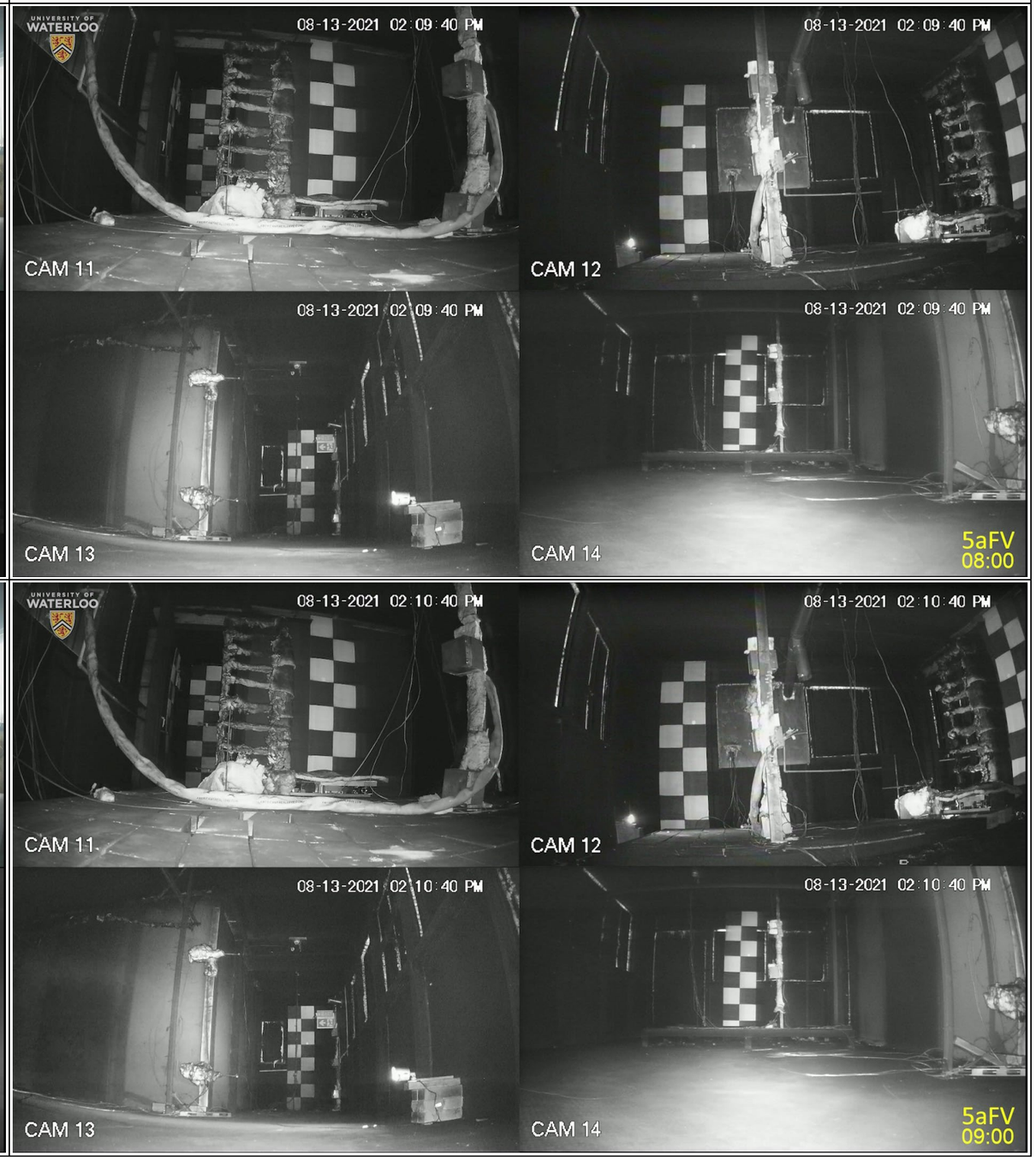
5aFV – Burn Room (UK Standard Cloth Couch – Crib 4)	**5aFV** – Upper Level (UK Standard Cloth Couch – Crib 4)





5aFV – Burn Room (UK Standard Cloth Couch – Crib 4)	**5aFV** – Upper Level (UK Standard Cloth Couch – Crib 4)

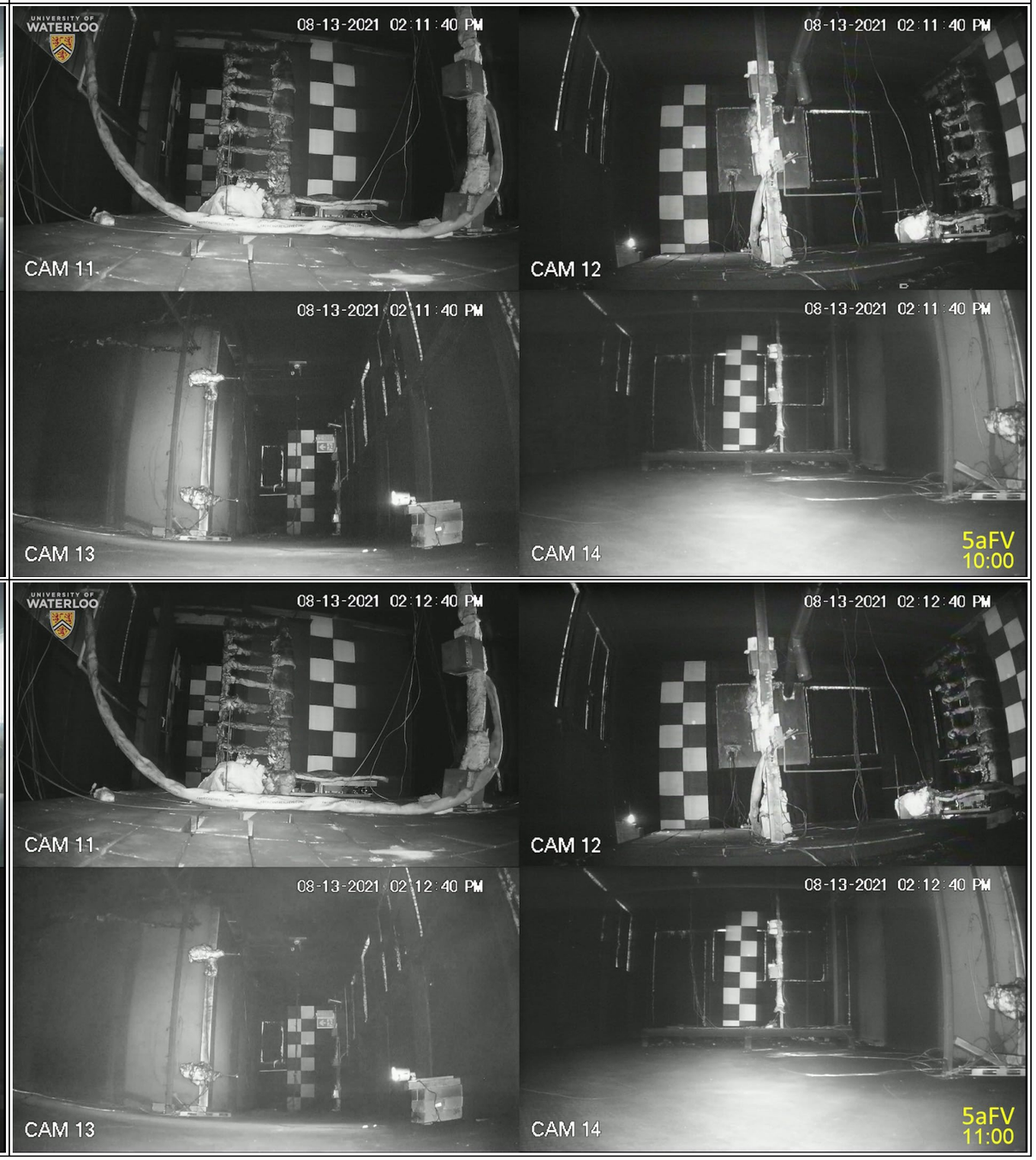




5aFV – Burn Room (UK Standard Cloth Couch – Crib 4)



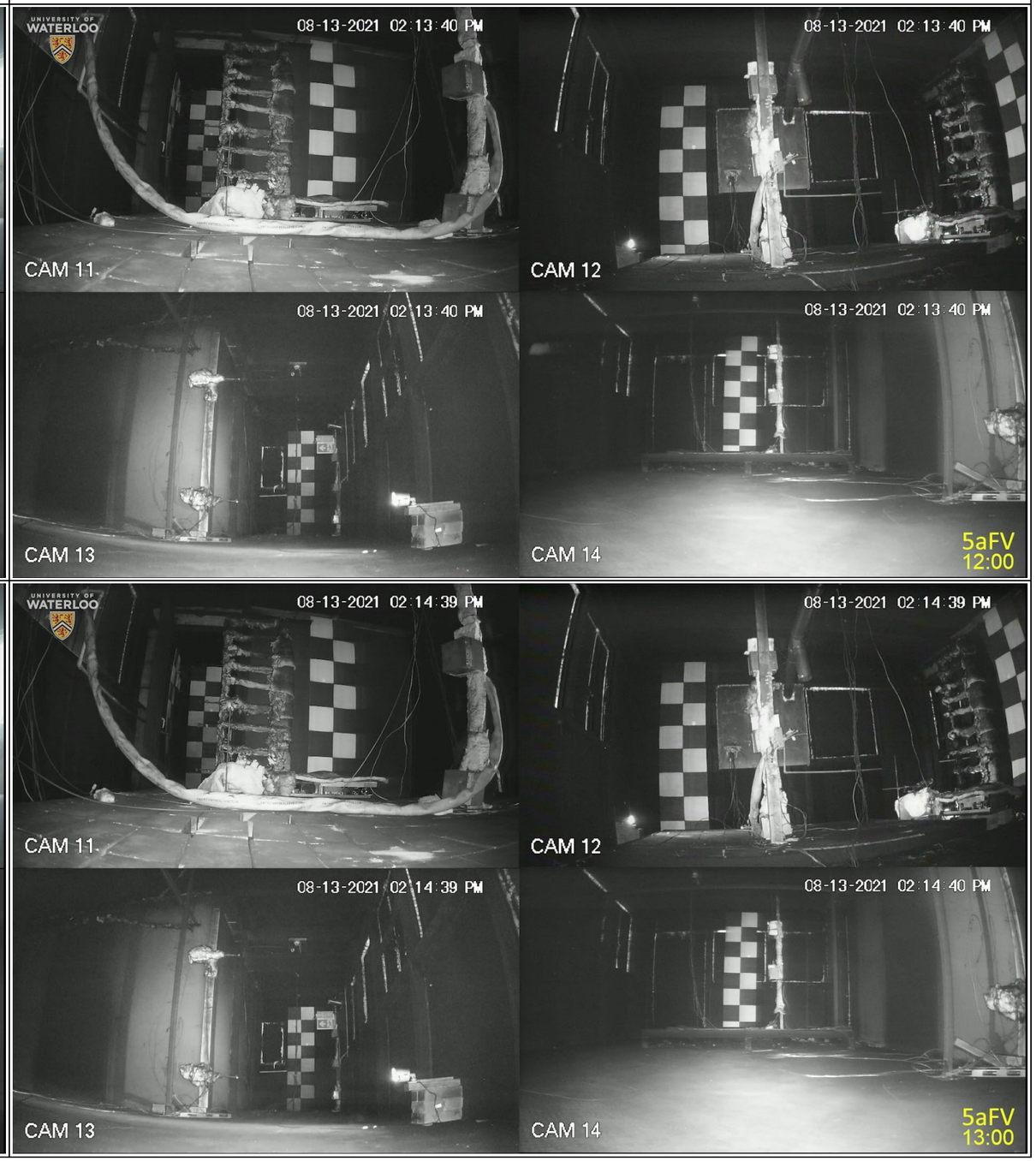
5aFV – Upper Level (UK Standard Cloth Couch – Crib 4)



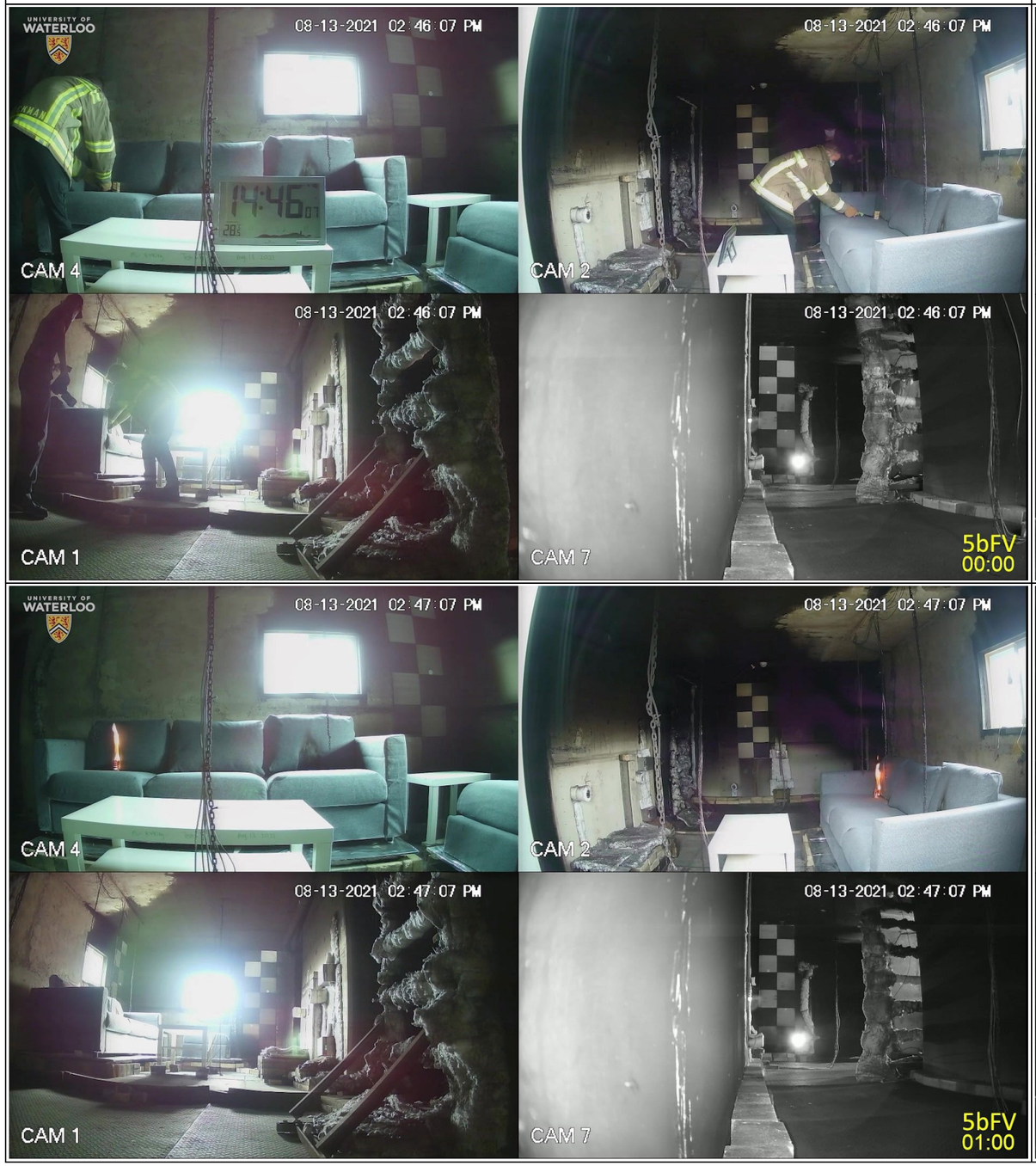
5aFV – Burn Room (UK Standard Cloth Couch – Crib 4)

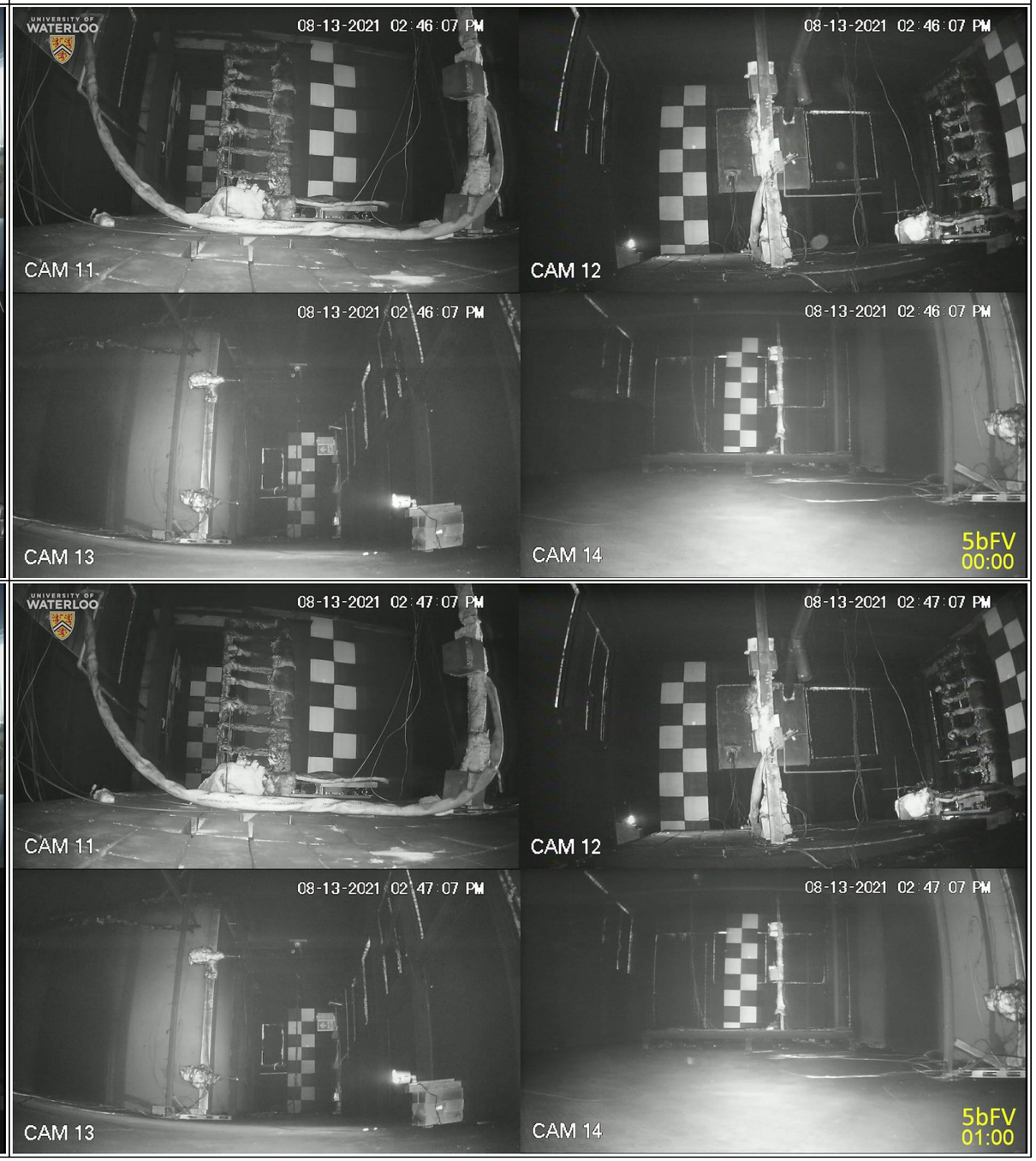


5aFV – Upper Level (UK Standard Cloth Couch – Crib 4)



5bFV – Burn Room (UK Standard Cloth Couch – Crib 5)	**5bFV** – Upper Level (UK Standard Cloth Couch – Crib 5)

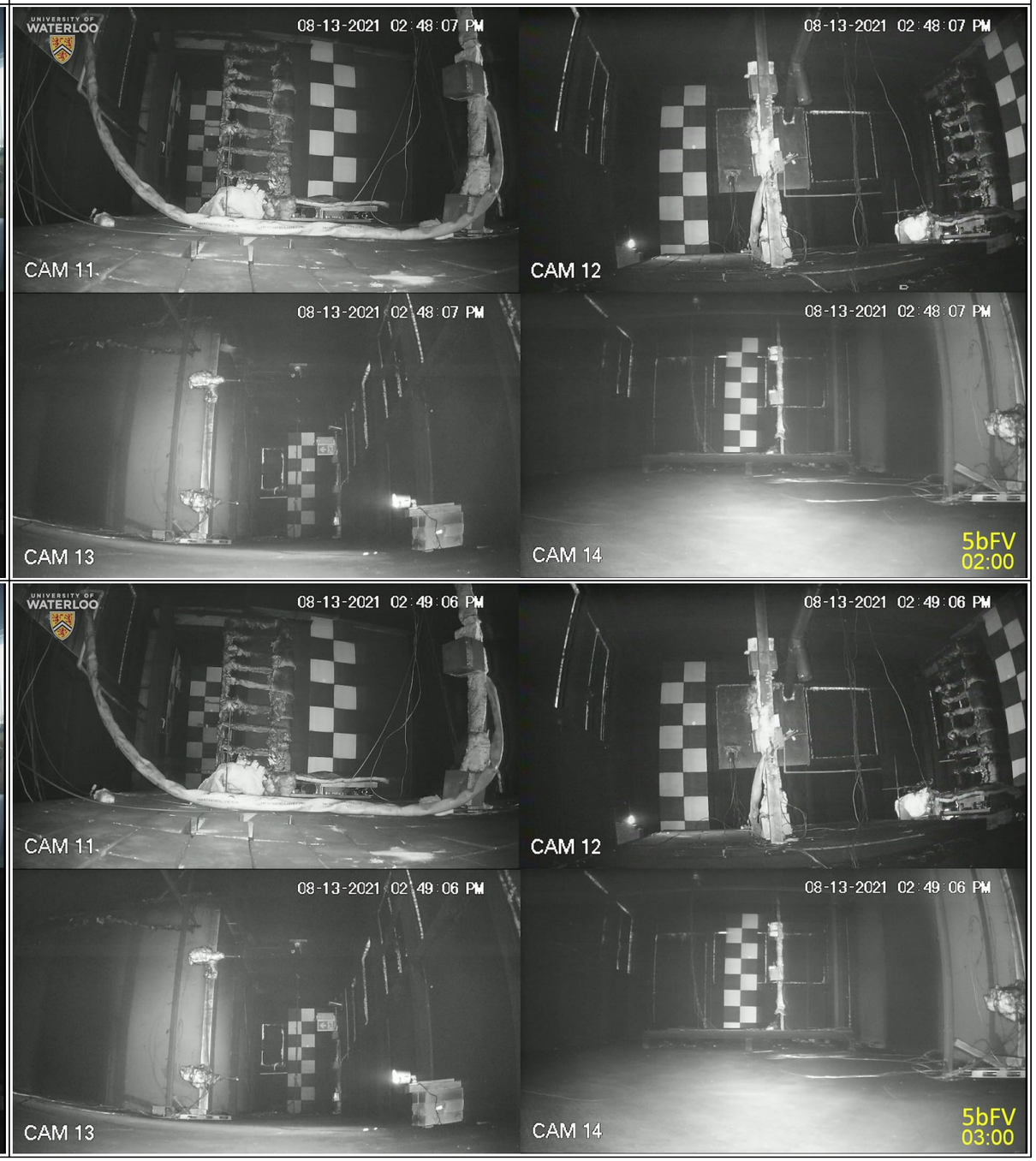




5bFV – Burn Room (UK Standard Cloth Couch – Crib 5)

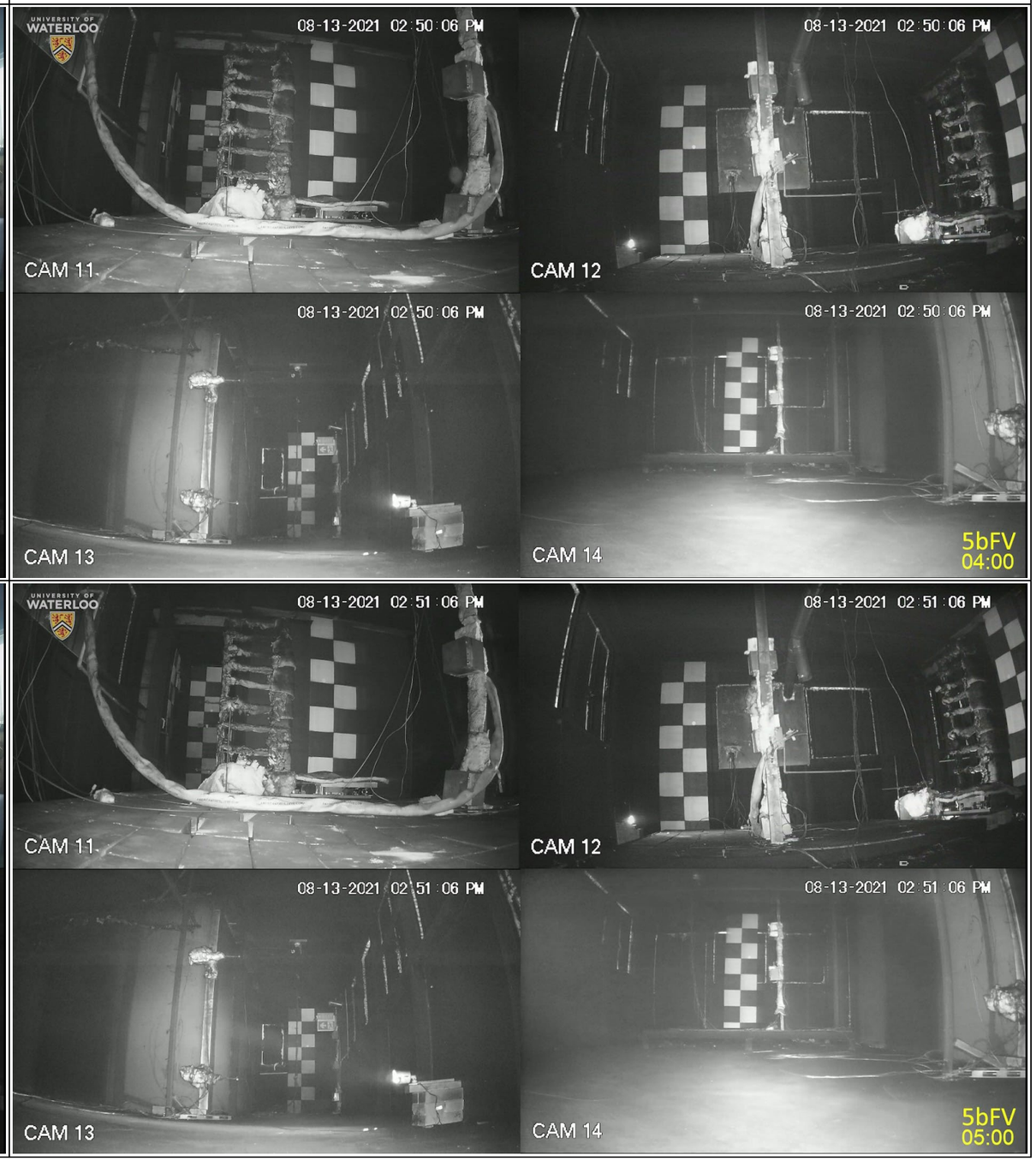


5bFV – Upper Level (UK Standard Cloth Couch – Crib 5)



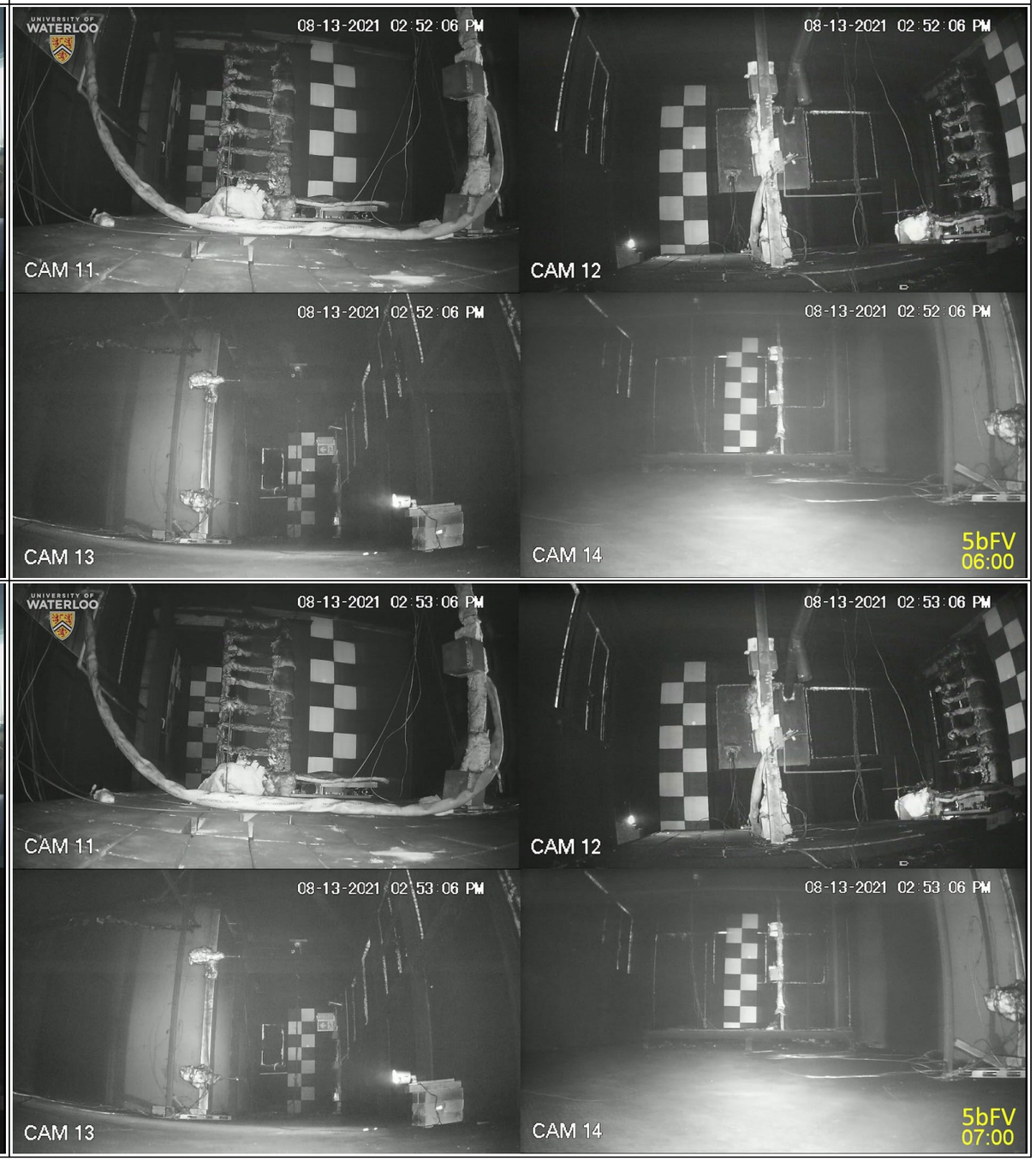
5bFV – Burn Room (UK Standard Cloth Couch – Crib 5)	**5bFV** – Upper Level (UK Standard Cloth Couch – Crib 5)





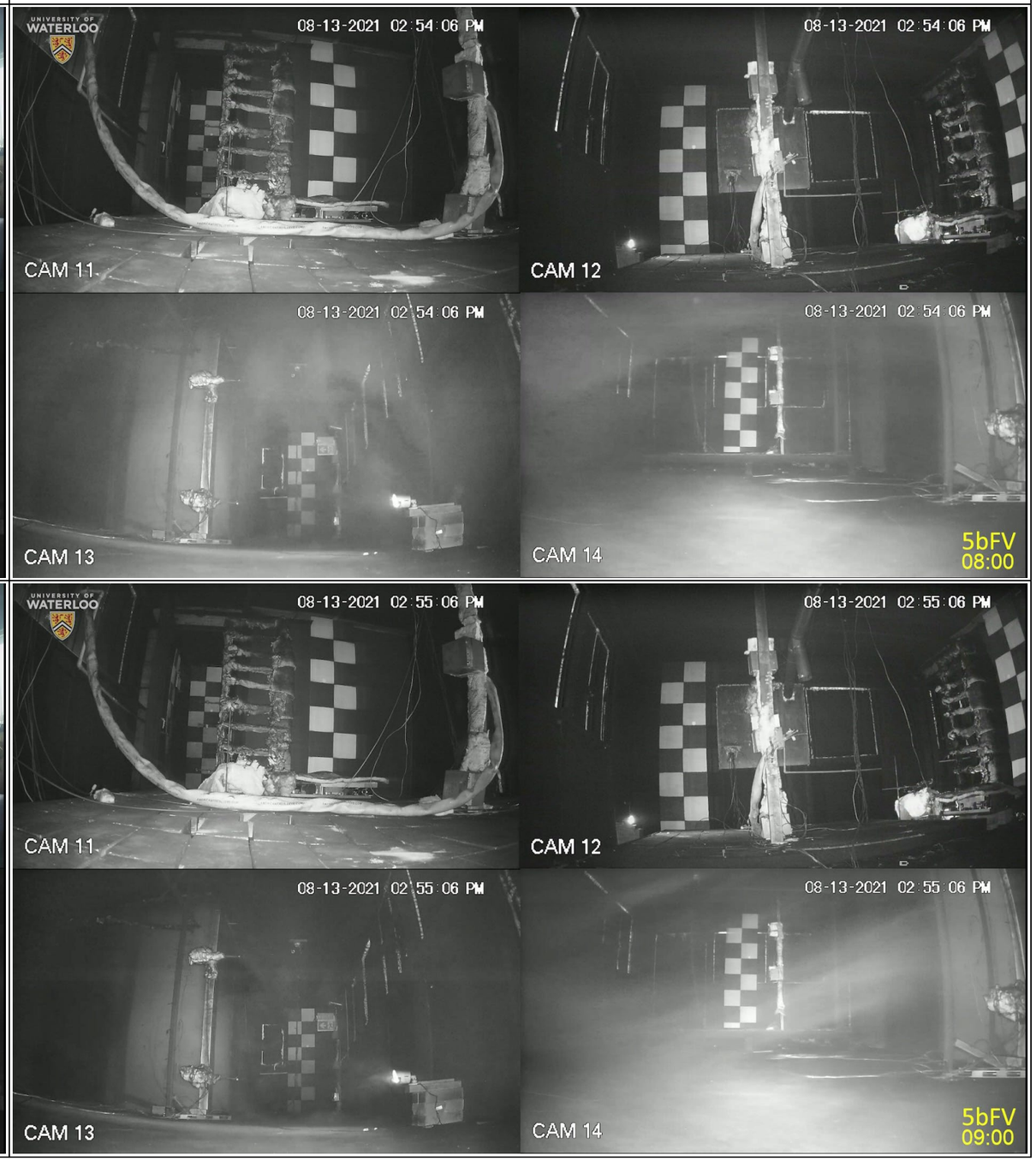
5bFV – Burn Room (UK Standard Cloth Couch – Crib 5)	**5bFV** – Upper Level (UK Standard Cloth Couch – Crib 5)





5bFV – Burn Room (UK Standard Cloth Couch – Crib 5)	**5bFV** – Upper Level (UK Standard Cloth Couch – Crib 5)





5bFV – Burn Room (UK Standard Cloth Couch – Crib 5)

















5bFV – Upper Level (UK Standard Cloth Couch – Crib 5)

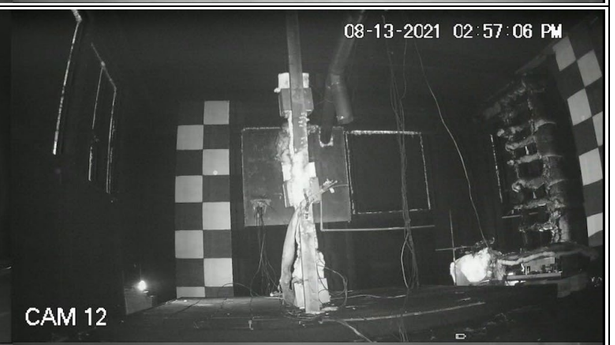










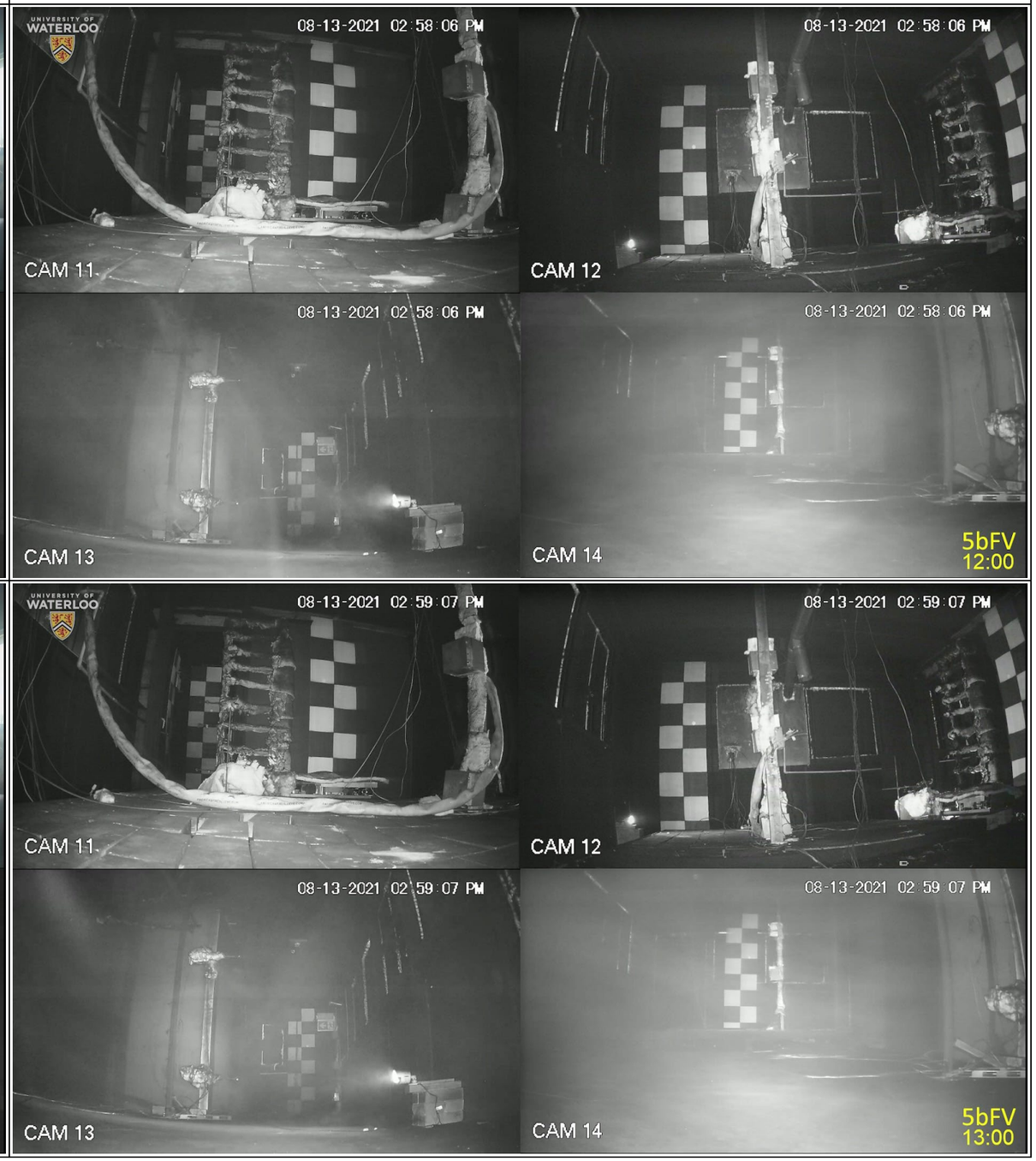






5bFV – Burn Room (UK Standard Cloth Couch – Crib 5)	**5bFV** – Upper Level (UK Standard Cloth Couch – Crib 5)





5bFV – Burn Room (UK Standard Cloth Couch – Crib 5)	**5bFV** – Upper Level (UK Standard Cloth Couch – Crib 5)

































5bFV – Burn Room (UK Standard Cloth Couch – Crib 5)	**5bFV** – Upper Level (UK Standard Cloth Couch – Crib 5)

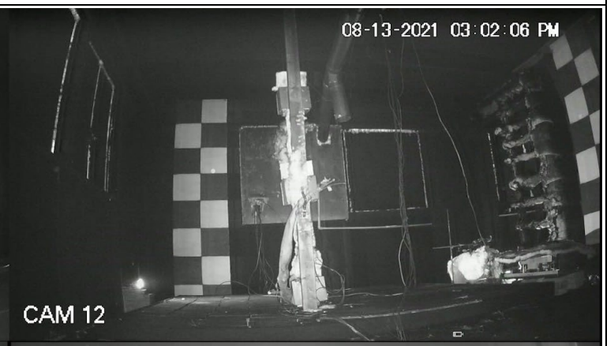
















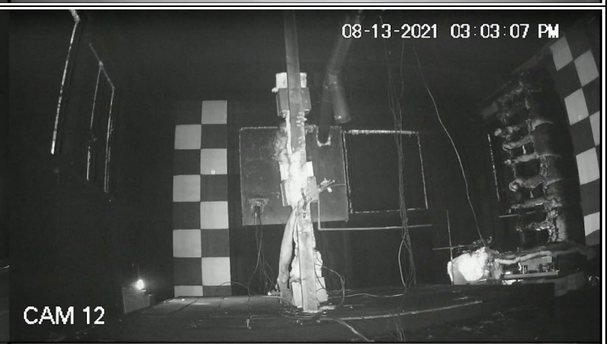
















5bFV – Burn Room (UK Standard Cloth Couch – Crib 5)











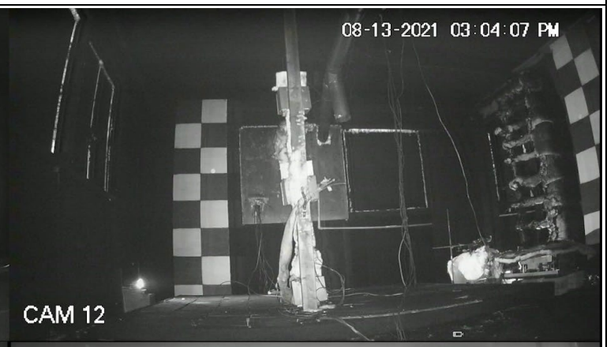






5bFV – Upper Level (UK Standard Cloth Couch – Crib 5)

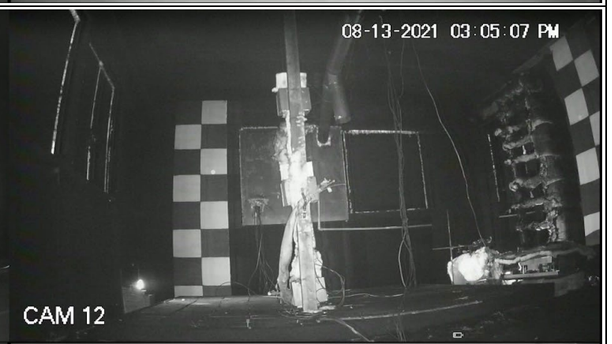
















5bFV – Burn Room (UK Standard Cloth Couch – Crib 5)









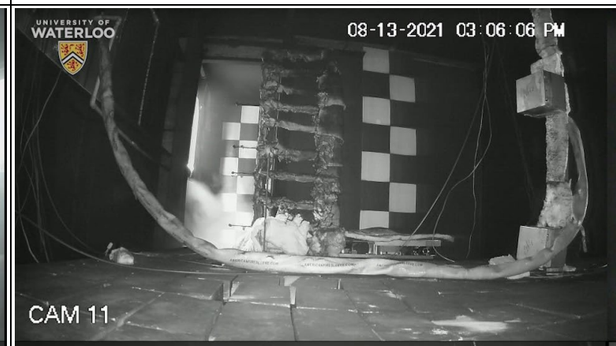








5bFV – Upper Level (UK Standard Cloth Couch – Crib 5)







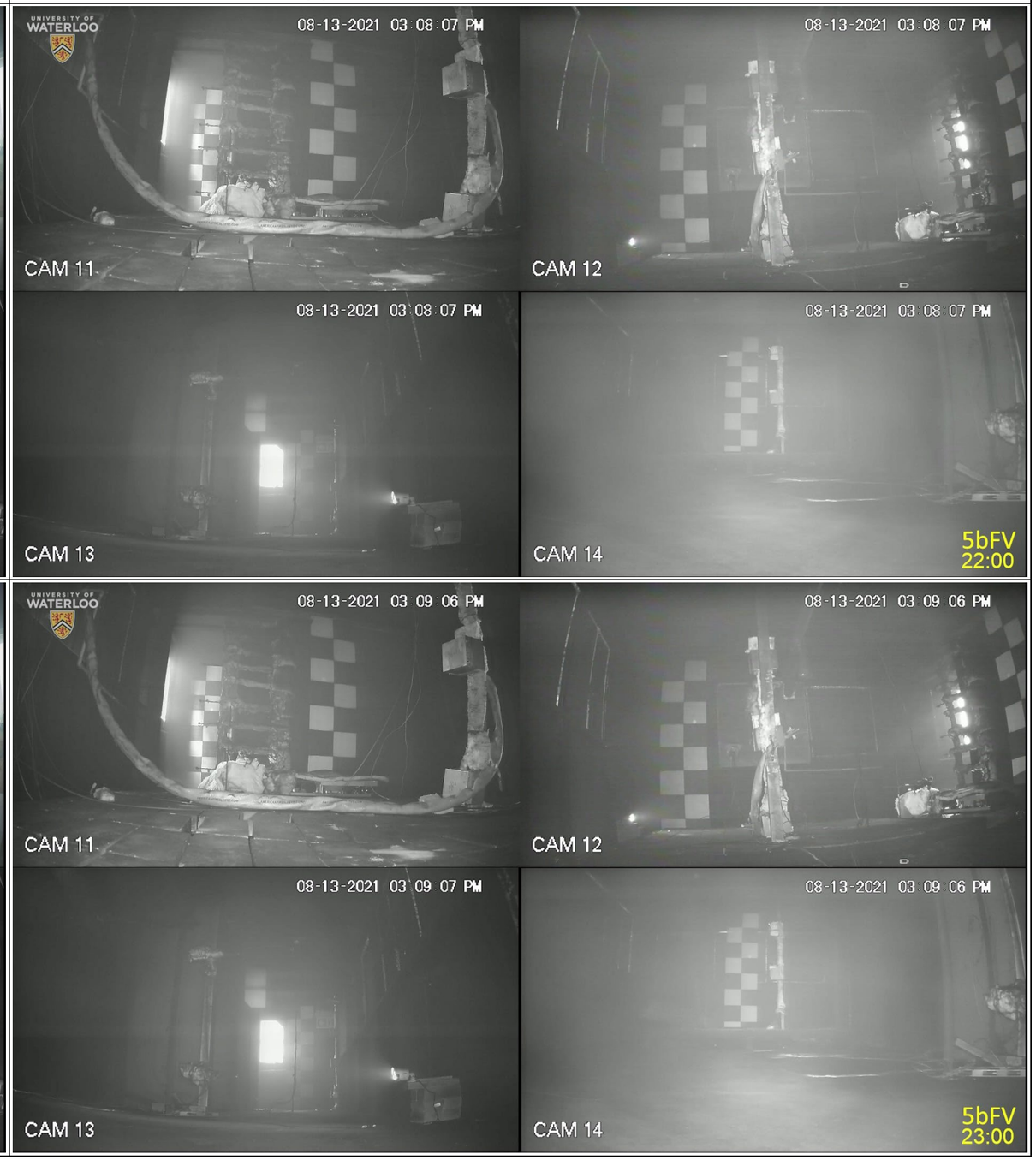










5bFV – Burn Room (UK Standard Cloth Couch – Crib 5)	**5bFV** – Upper Level (UK Standard Cloth Couch – Crib 5)
	

5cFV – Burn Room (UK Standard Cloth Couch – Crib 7)	**5cFV** – Upper Level (UK Standard Cloth Couch – Crib 7)

















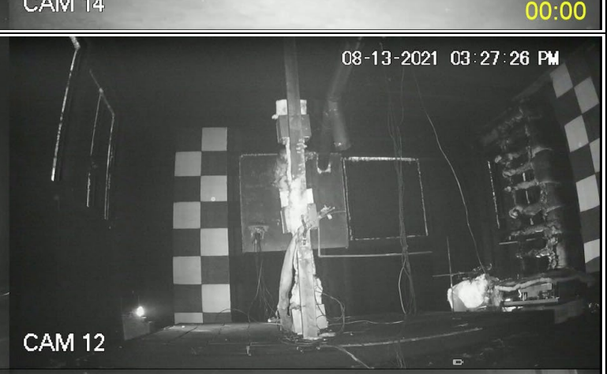










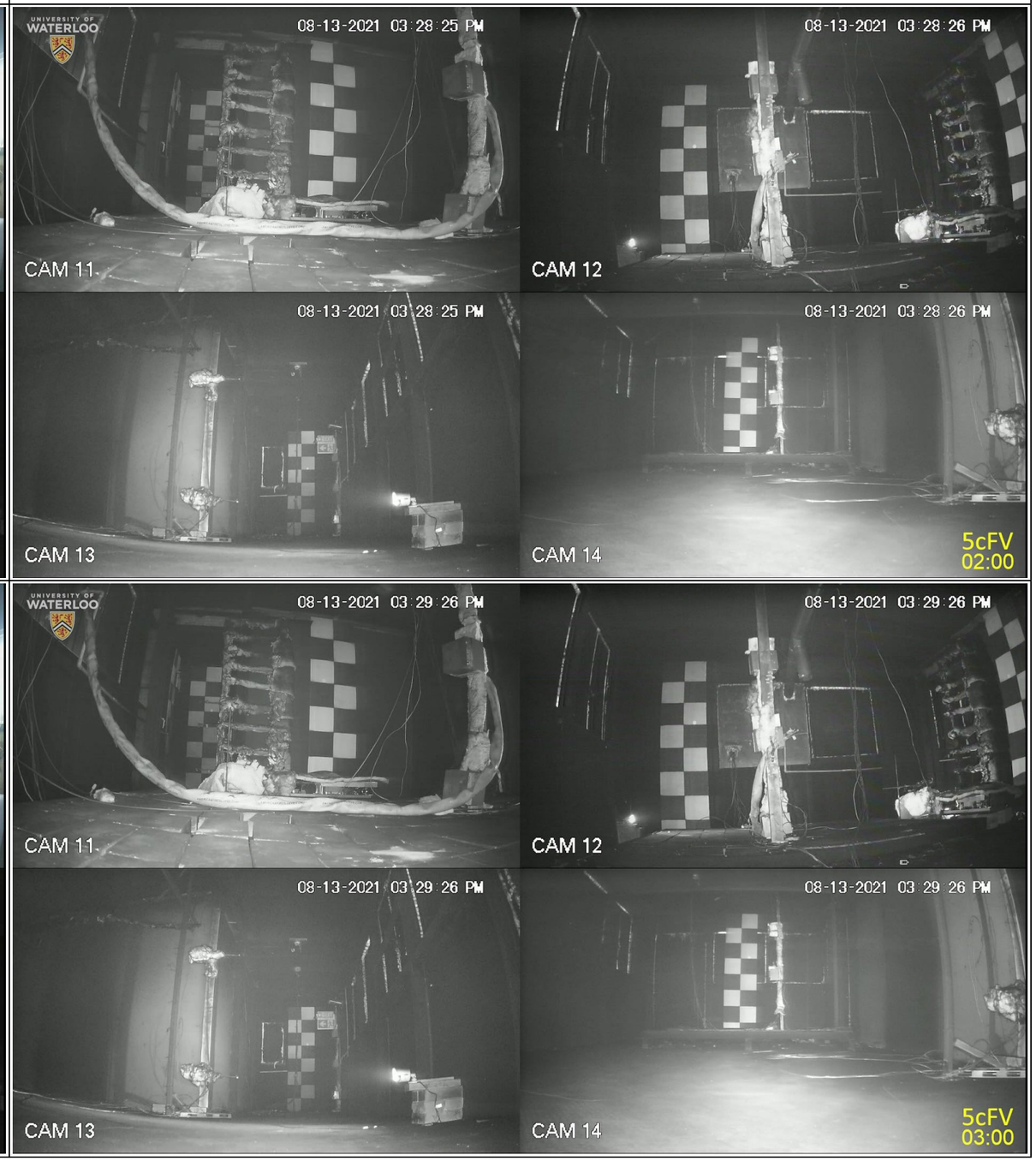




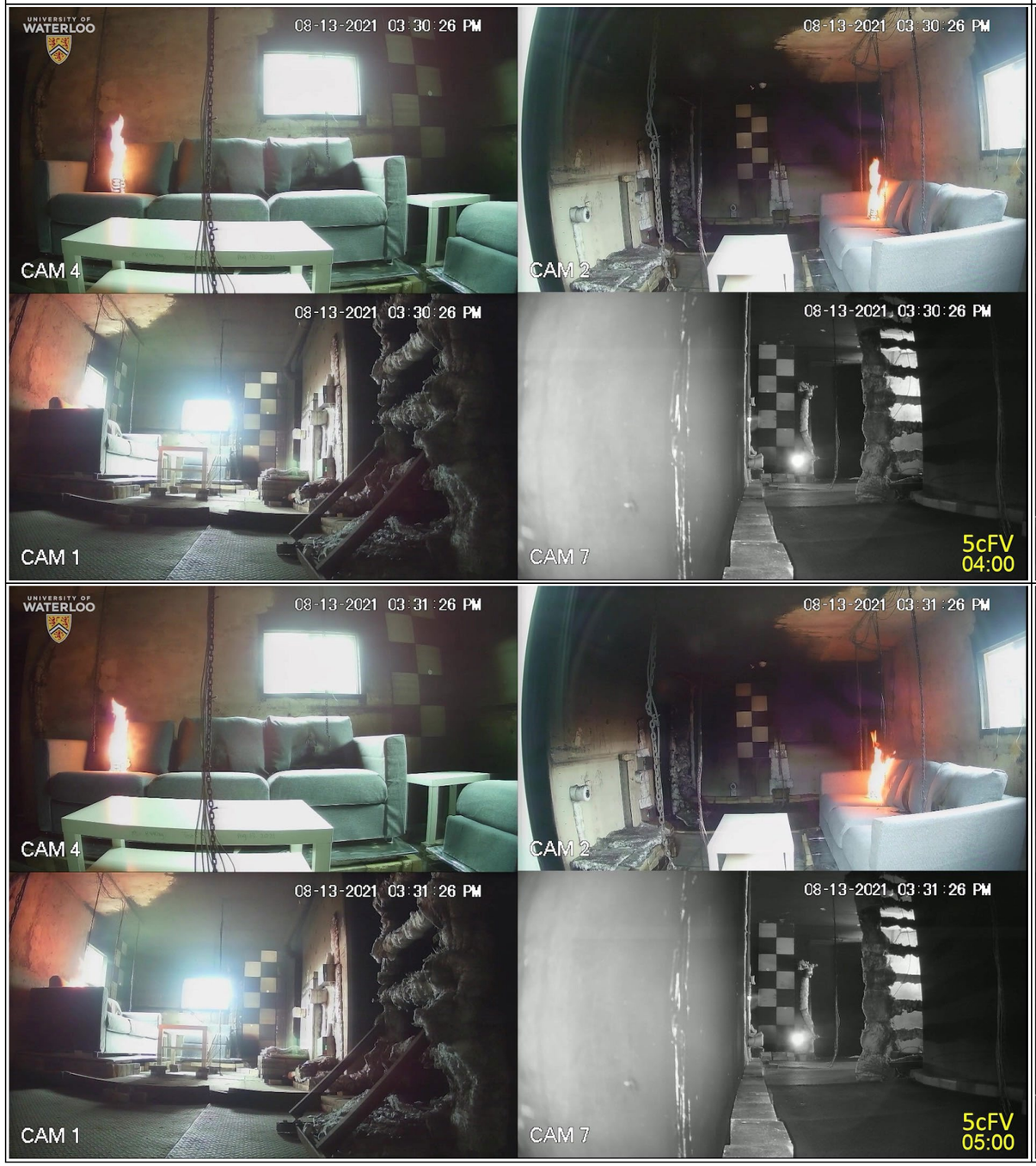


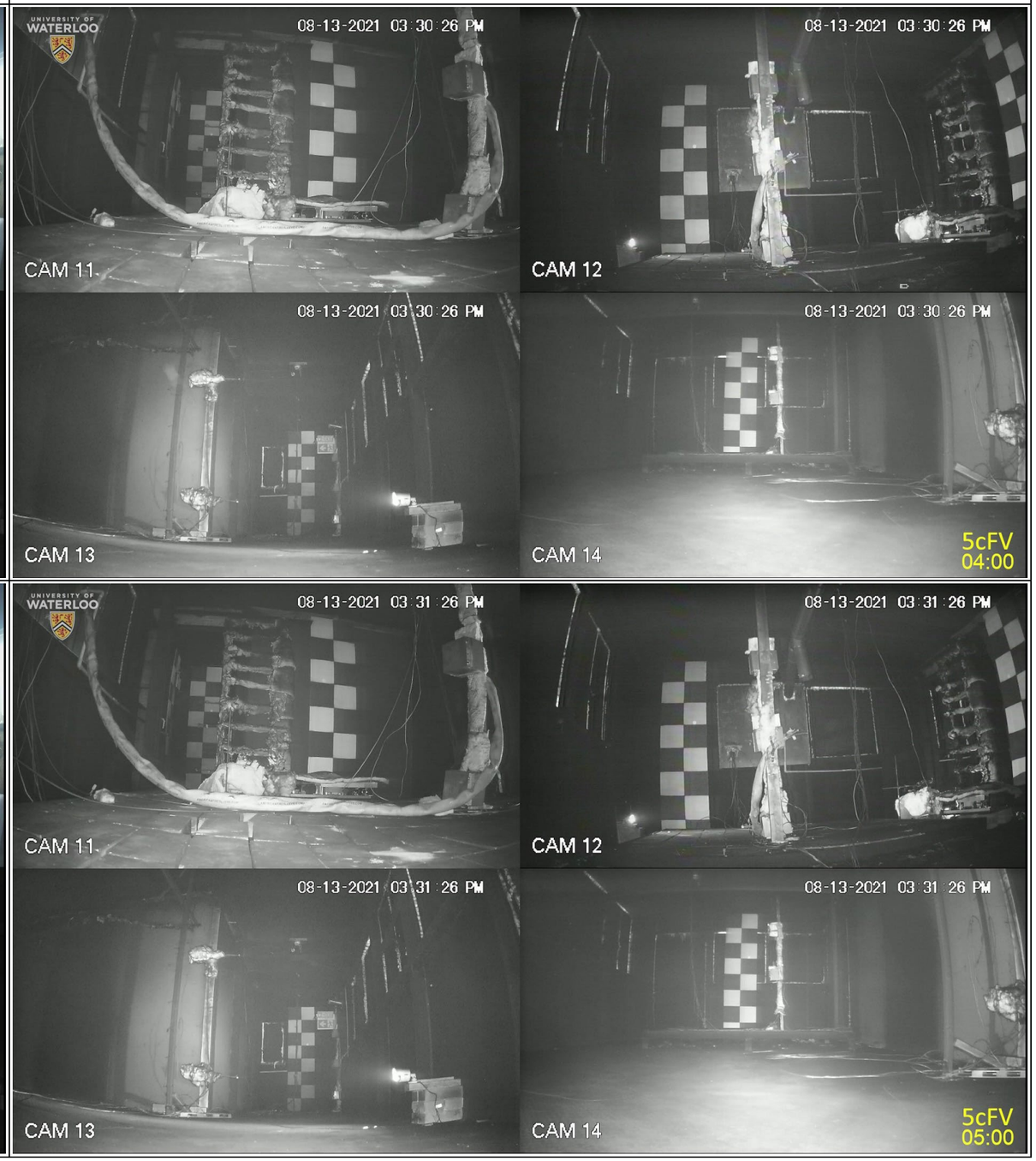
5cFV – Burn Room (UK Standard Cloth Couch – Crib 7)	**5cFV** – Upper Level (UK Standard Cloth Couch – Crib 7)





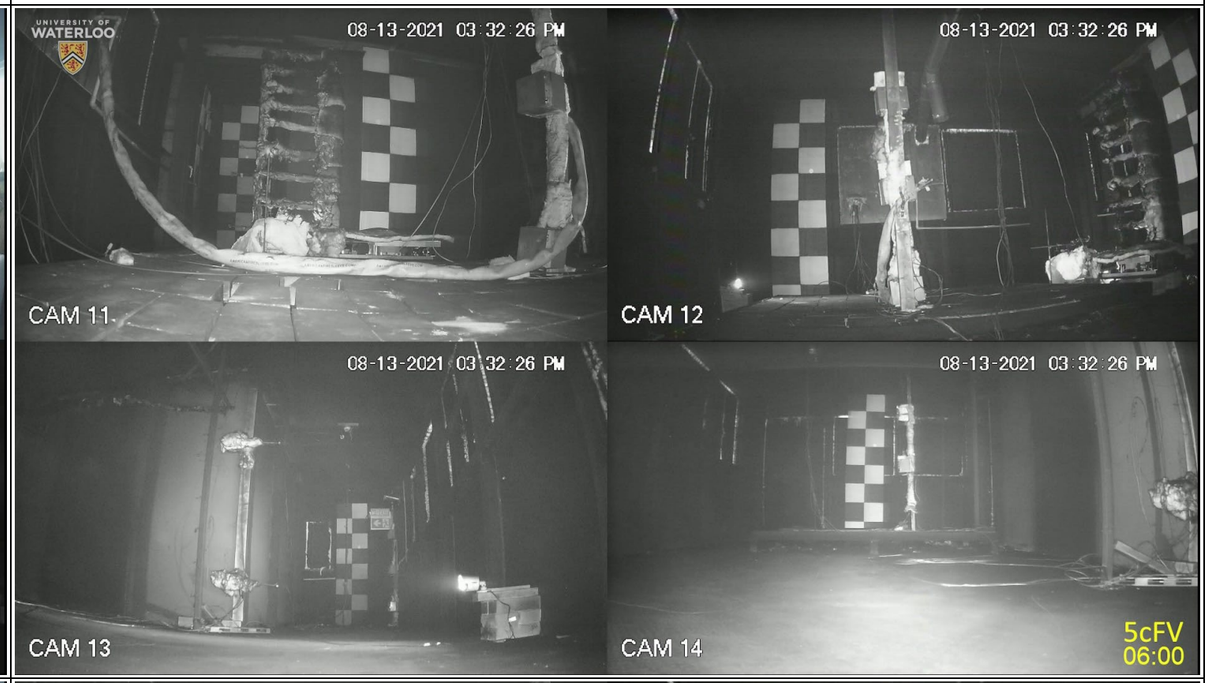
5cFV – Burn Room (UK Standard Cloth Couch – Crib 7)	**5cFV** – Upper Level (UK Standard Cloth Couch – Crib 7)





5cFV – Burn Room (UK Standard Cloth Couch – Crib 7)	**5cFV** – Upper Level (UK Standard Cloth Couch – Crib 7)





5cFV – Burn Room (UK Standard Cloth Couch – Crib 7)	**5cFV** – Upper Level (UK Standard Cloth Couch – Crib 7)

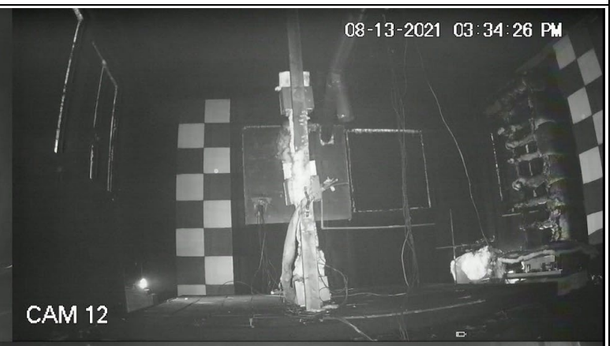




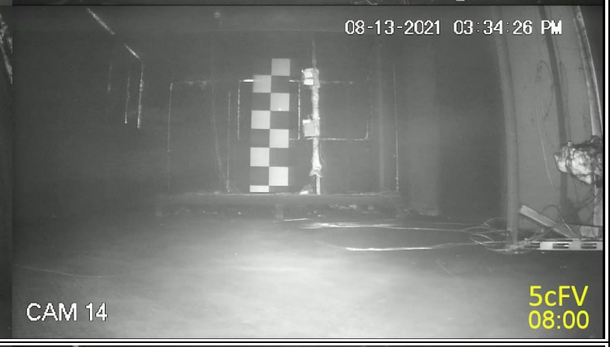




























5cFV – Burn Room (UK Standard Cloth Couch – Crib 7)	**5cFV** – Upper Level (UK Standard Cloth Couch – Crib 7)





5cFV – Burn Room (UK Standard Cloth Couch – Crib 7)	**5cFV** – Upper Level (UK Standard Cloth Couch – Crib 7)











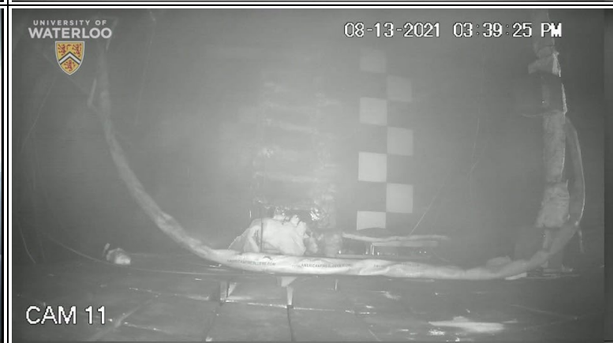
















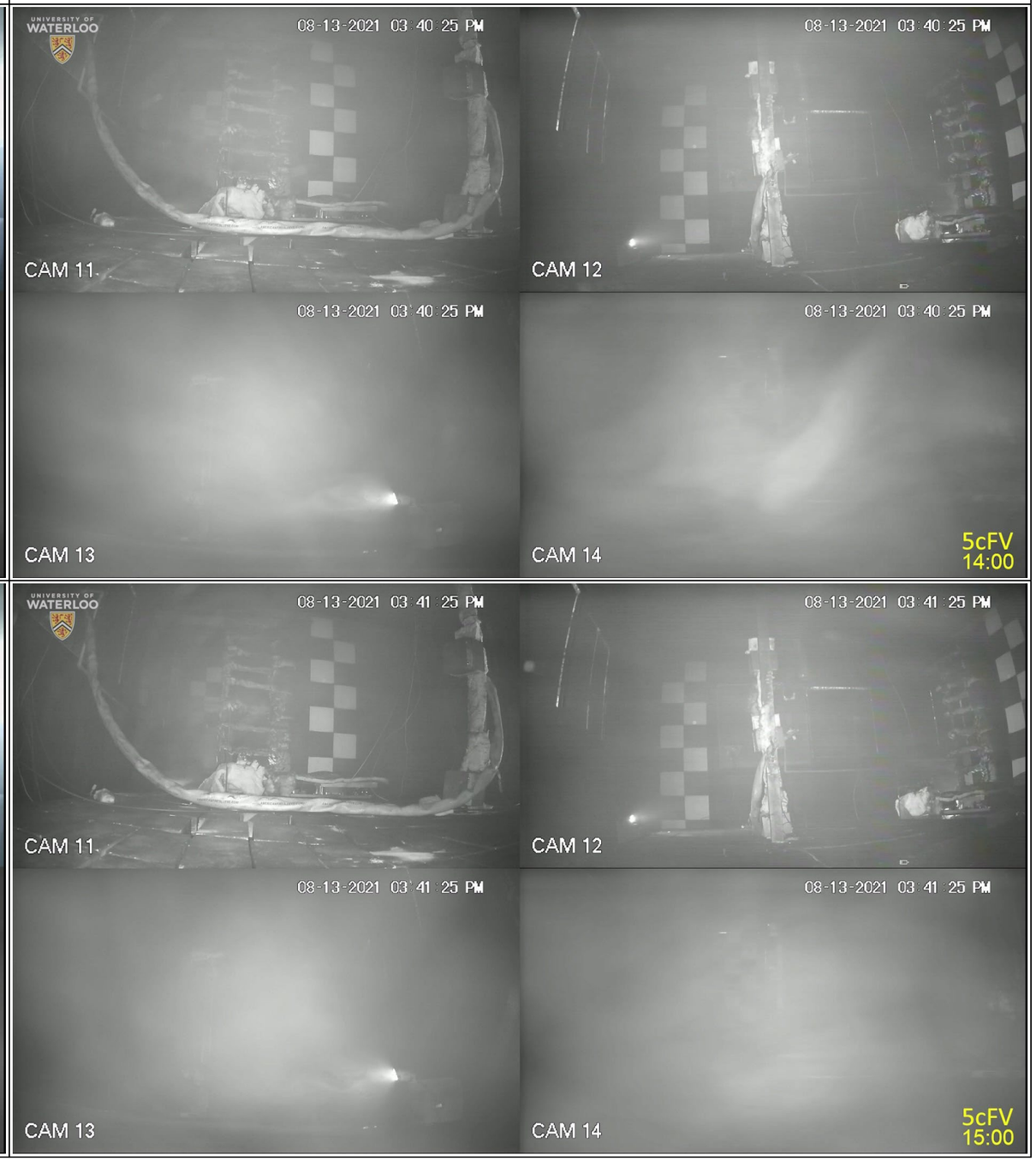






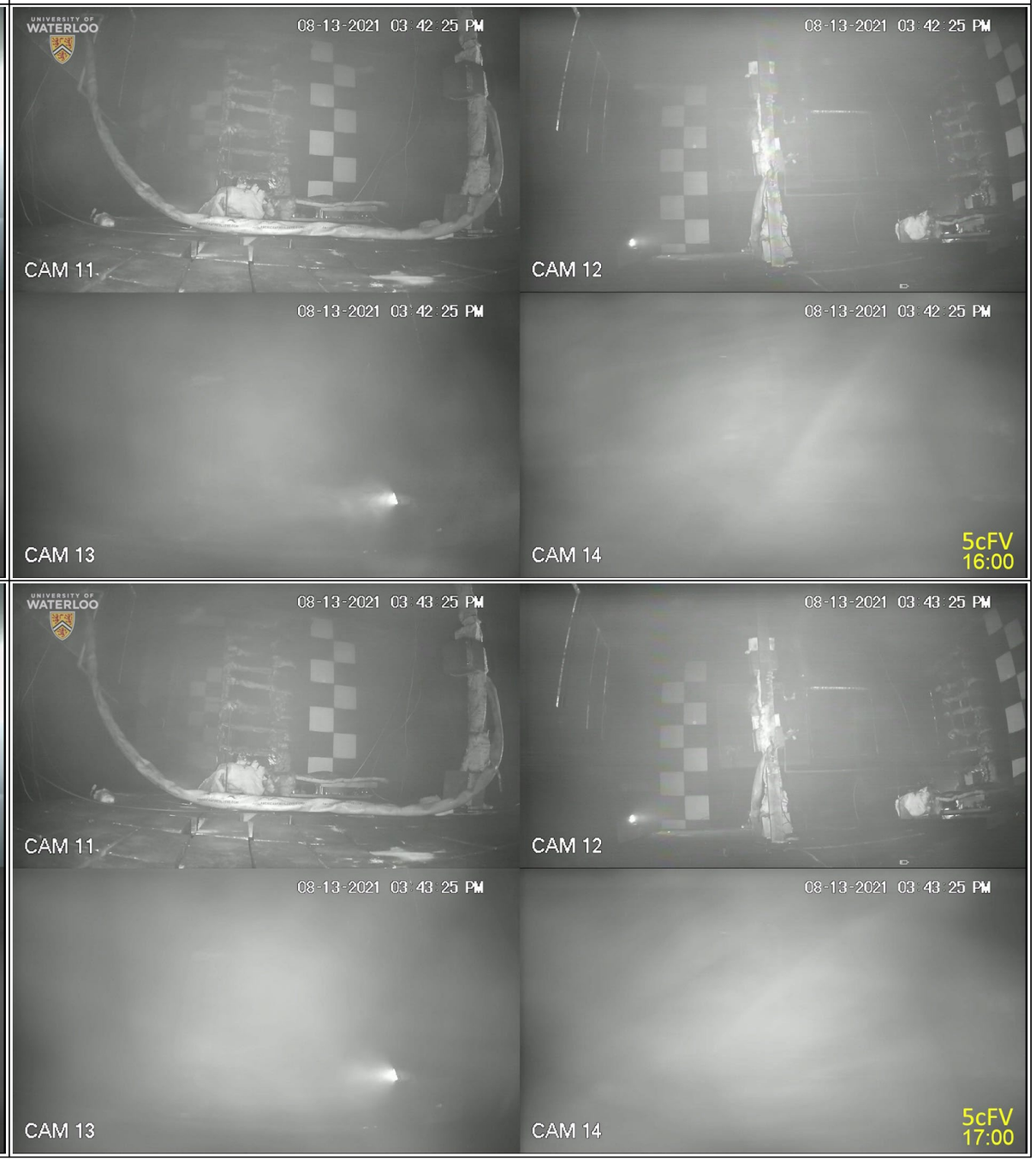
5cFV – Burn Room (UK Standard Cloth Couch – Crib 7)	**5cFV** – Upper Level (UK Standard Cloth Couch – Crib 7)





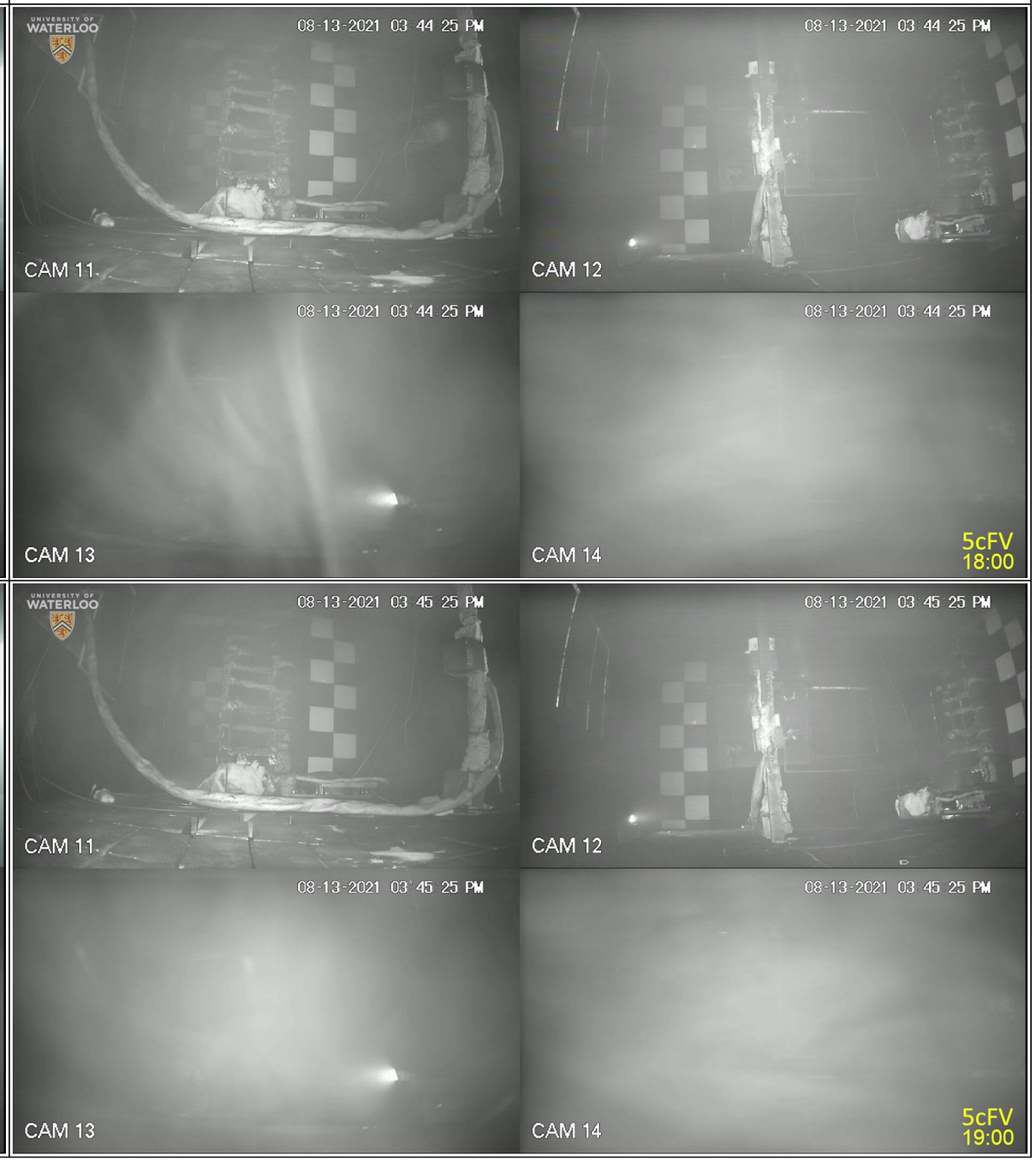
5cFV – Burn Room (UK Standard Cloth Couch – Crib 7)	**5cFV** – Upper Level (UK Standard Cloth Couch – Crib 7)





5cFV – Burn Room (UK Standard Cloth Couch – Crib 7)	**5cFV** – Upper Level (UK Standard Cloth Couch – Crib 7)





5cFV – Burn Room (UK Standard Cloth Couch – Crib 7)	**5cFV** – Upper Level (UK Standard Cloth Couch – Crib 7)



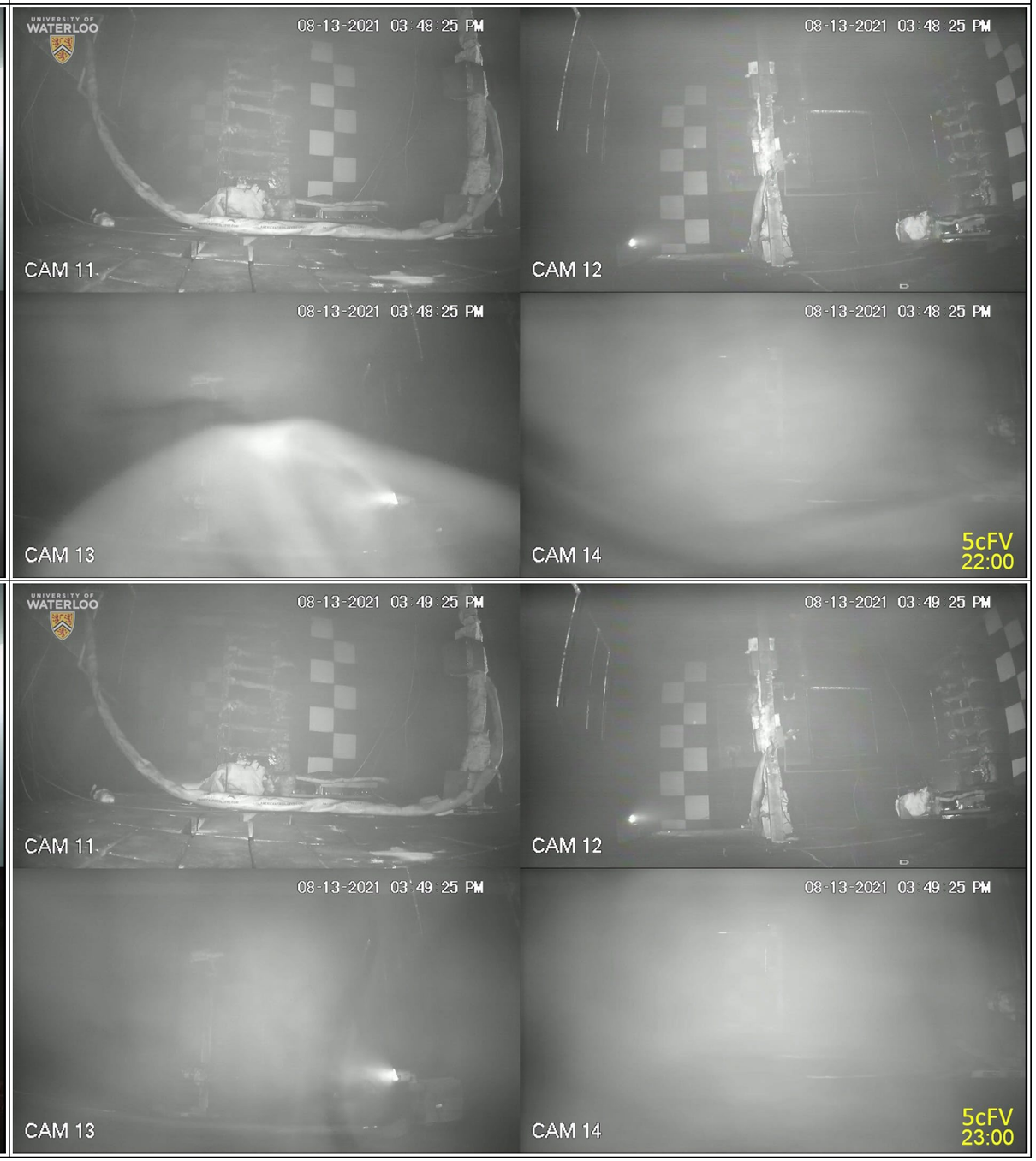






5cFV – Burn Room (UK Standard Cloth Couch – Crib 7)	**5cFV** – Upper Level (UK Standard Cloth Couch – Crib 7)





6FV – Burn Room (UK Standard Faux Leather Couch – Crib 4)	**6FV** – Upper Level (UK Standard Faux Leather Couch – Crib 4)

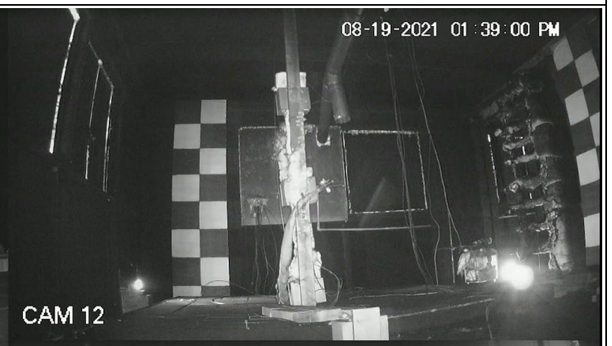
















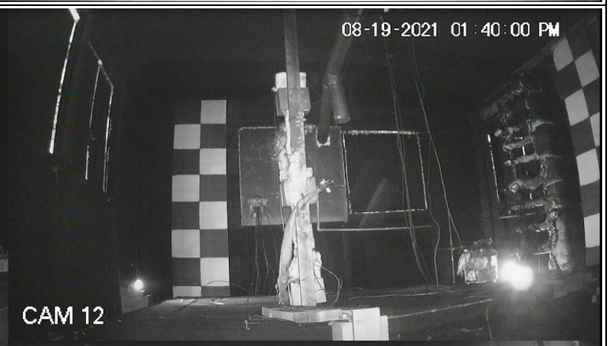
















6FV – Burn Room (UK Standard Faux Leather Couch – Crib 4)	**6FV** – Upper Level (UK Standard Faux Leather Couch – Crib 4)













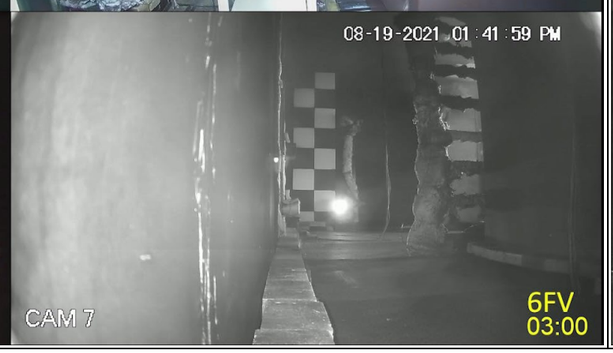


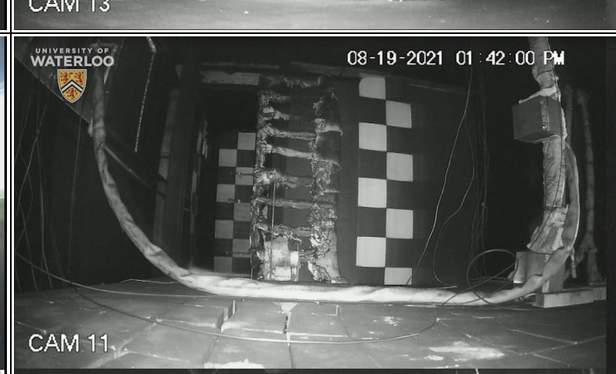


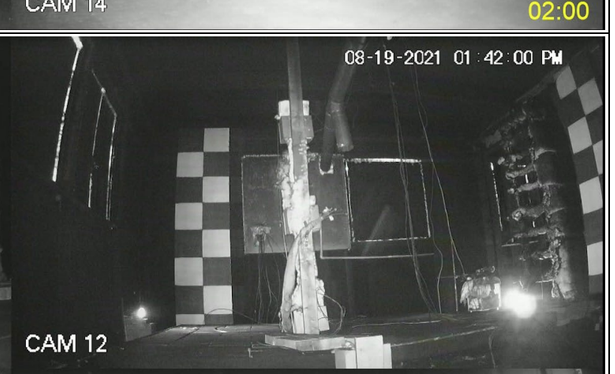
















6FV – Burn Room (UK Standard Faux Leather Couch – Crib 4)	**6FV** – Upper Level (UK Standard Faux Leather Couch – Crib 4)

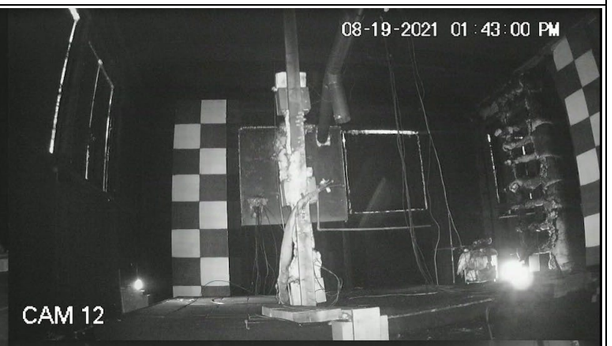
















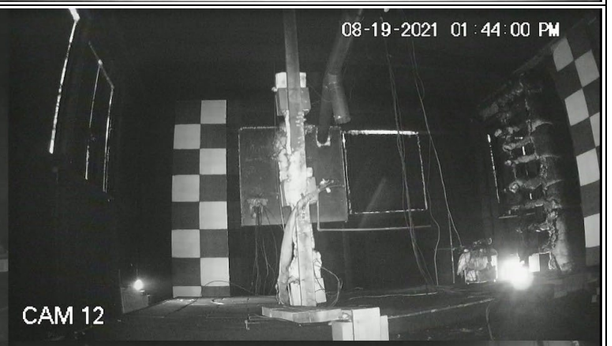
















6FV – Burn Room (UK Standard Faux Leather Couch – Crib 4)	**6FV** – Upper Level (UK Standard Faux Leather Couch – Crib 4)

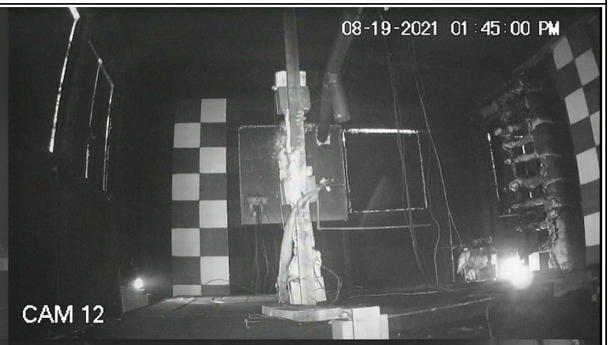
































6FV – Burn Room (UK Standard Faux Leather Couch – Crib 4)	**6FV** – Upper Level (UK Standard Faux Leather Couch – Crib 4)

































6FV – Burn Room (UK Standard Faux Leather Couch – Crib 4)	**6FV** – Upper Level (UK Standard Faux Leather Couch – Crib 4)

































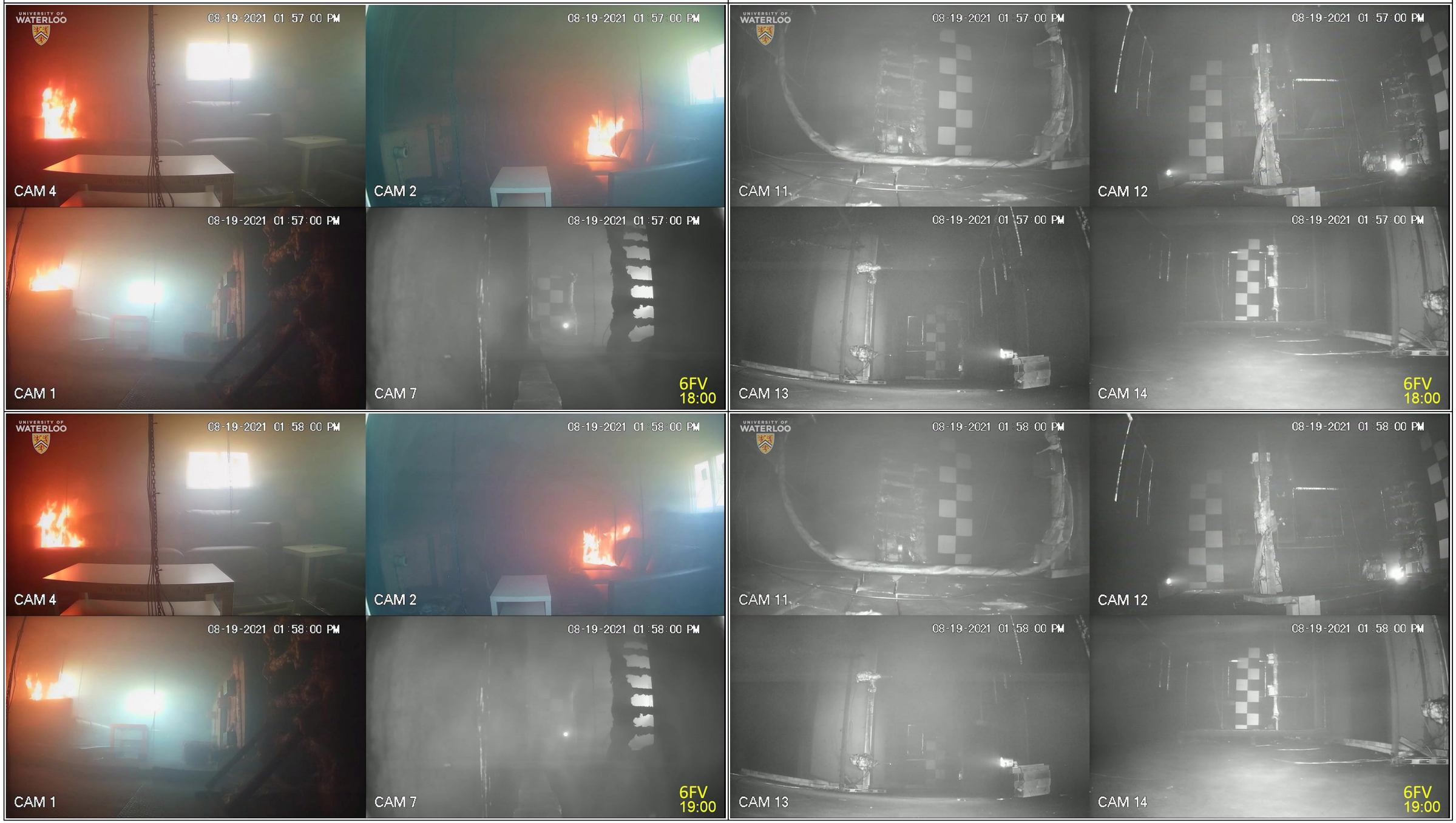
6FV – Burn Room (UK Standard Faux Leather Couch – Crib 4)	**6FV** – Upper Level (UK Standard Faux Leather Couch – Crib 4)
	

6FV – Burn Room (UK Standard Faux Leather Couch – Crib 4)	**6FV** – Upper Level (UK Standard Faux Leather Couch – Crib 4)



6FV – Burn Room (UK Standard Faux Leather Couch – Crib 4)	**6FV** – Upper Level (UK Standard Faux Leather Couch – Crib 4)
	

6FV – Burn Room (UK Standard Faux Leather Couch – Crib 4)	**6FV** – Upper Level (UK Standard Faux Leather Couch – Crib 4)

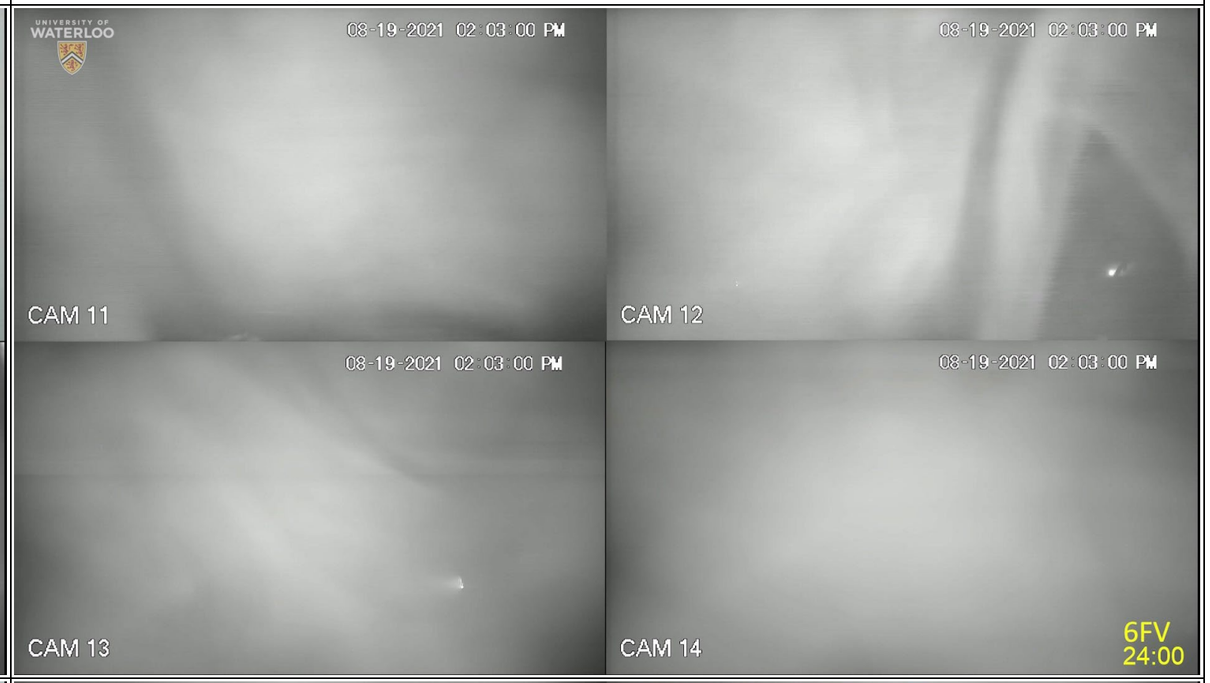
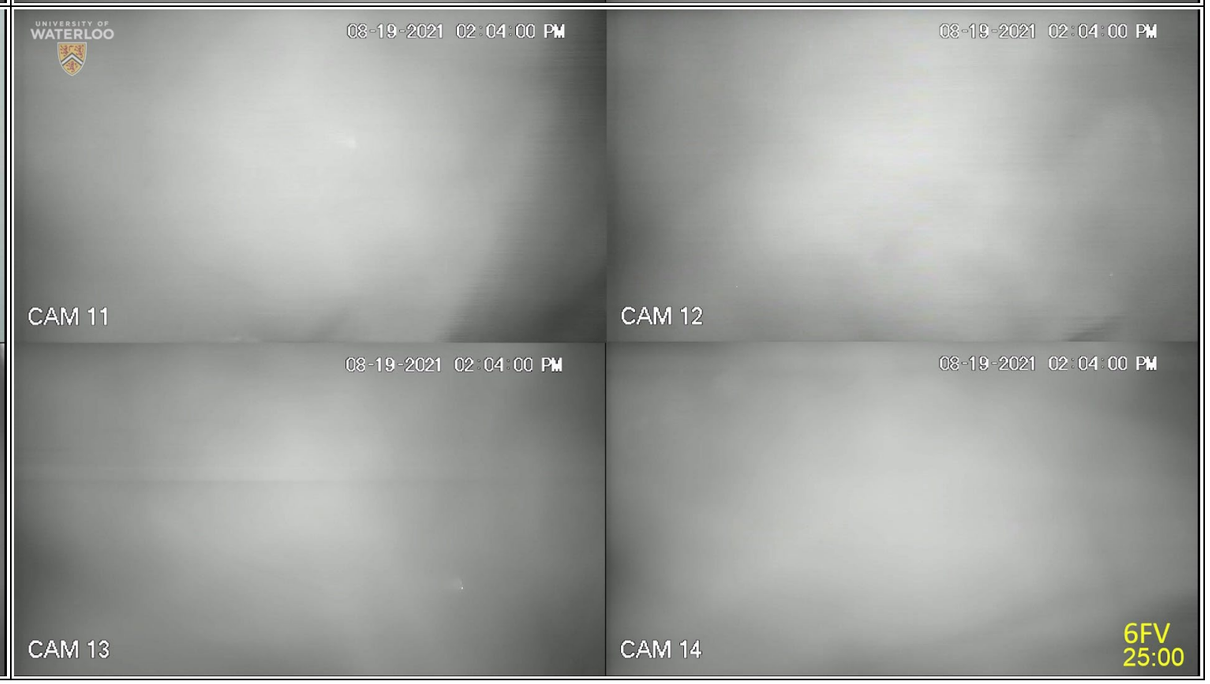


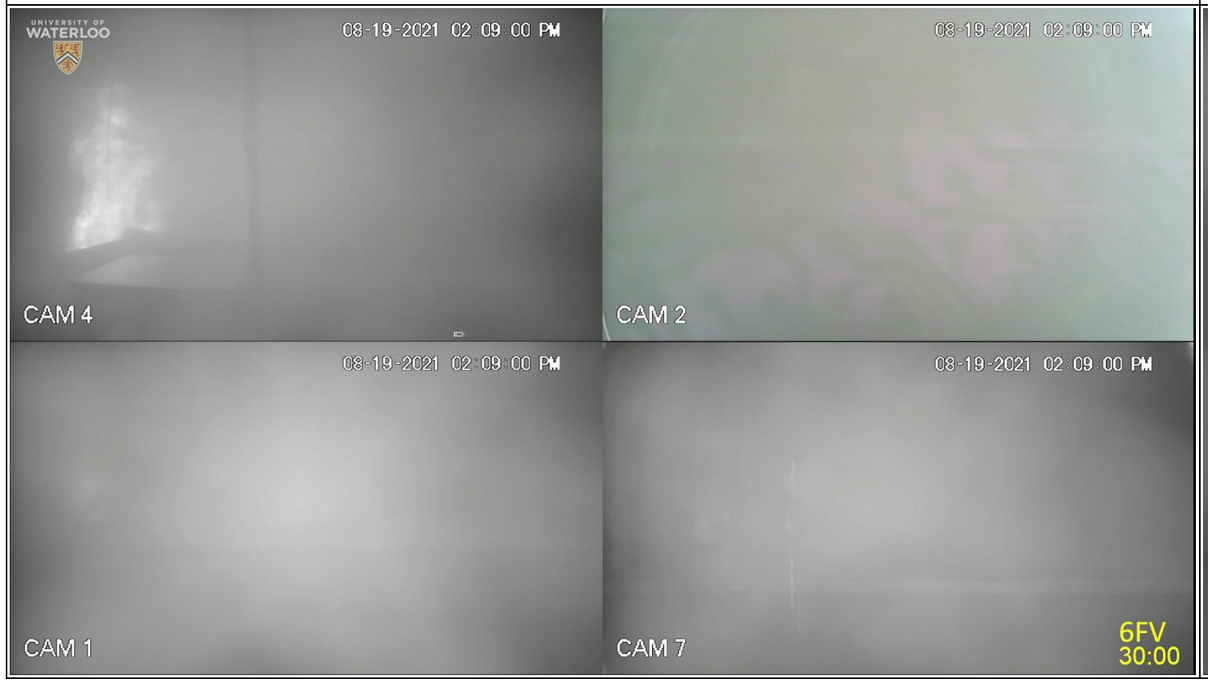
6FV – Burn Room (UK Standard Faux Leather Couch – Crib 4)	**6FV** – Upper Level (UK Standard Faux Leather Couch – Crib 4)



6FV – Burn Room (UK Standard Faux Leather Couch – Crib 4)	**6FV** – Upper Level (UK Standard Faux Leather Couch – Crib 4)



6FV – Burn Room (UK Standard Faux Leather Couch – Crib 4)	**6FV** – Upper Level (UK Standard Faux Leather Couch – Crib 4)
	
	

6FV – Burn Room (UK Standard Faux Leather Couch – Crib 4)	**6FV** – Upper Level (UK Standard Faux Leather Couch – Crib 4)
	

7aFV - Burn Room (UK Leather Couch – Crib 5)	**7bFV** – Upper Level (UK Leather Couch – Crib 5)

















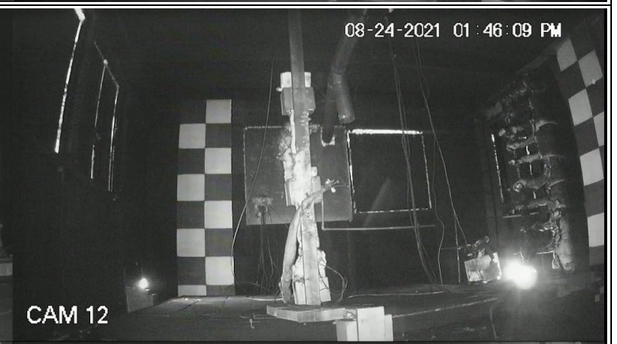










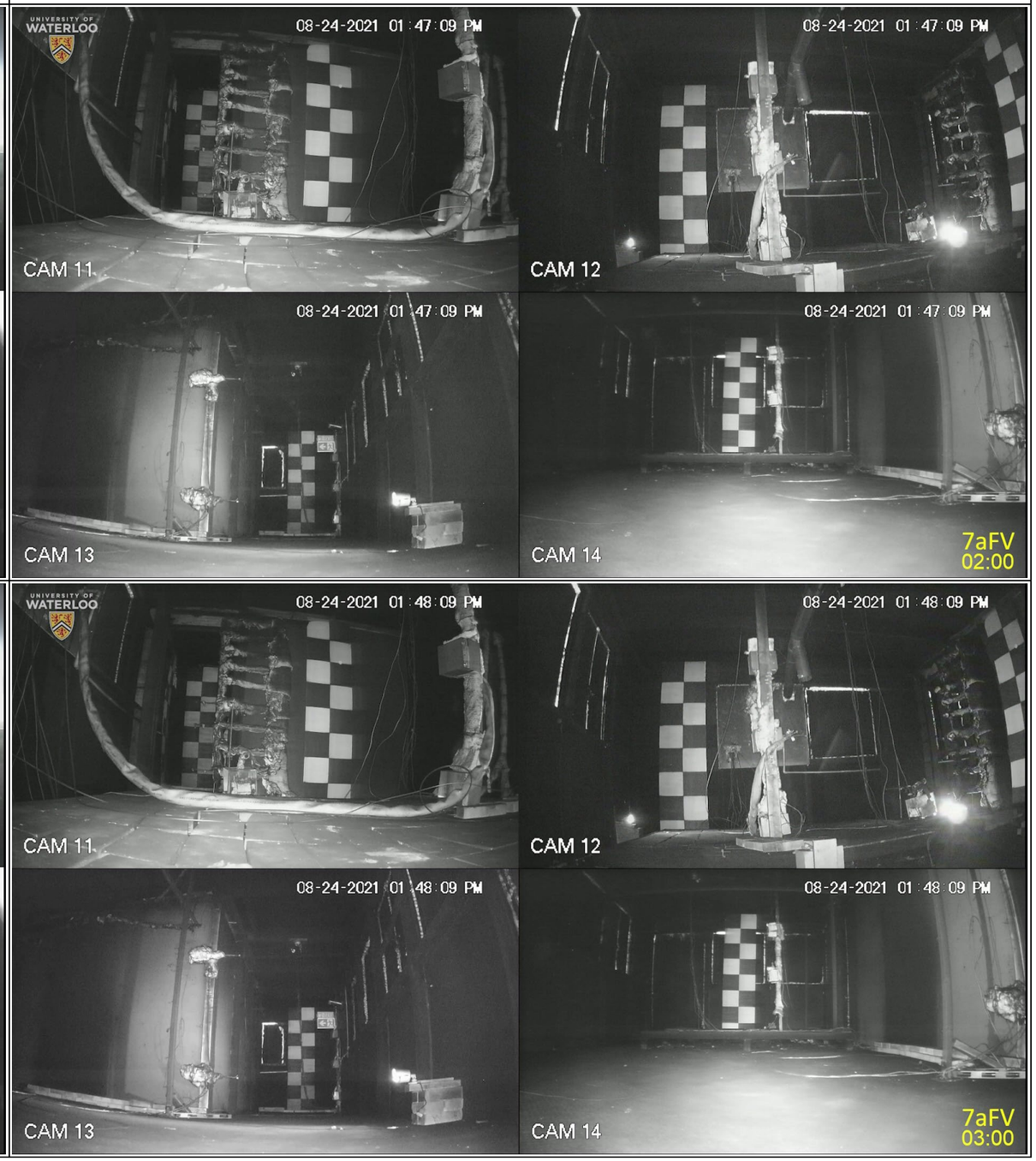






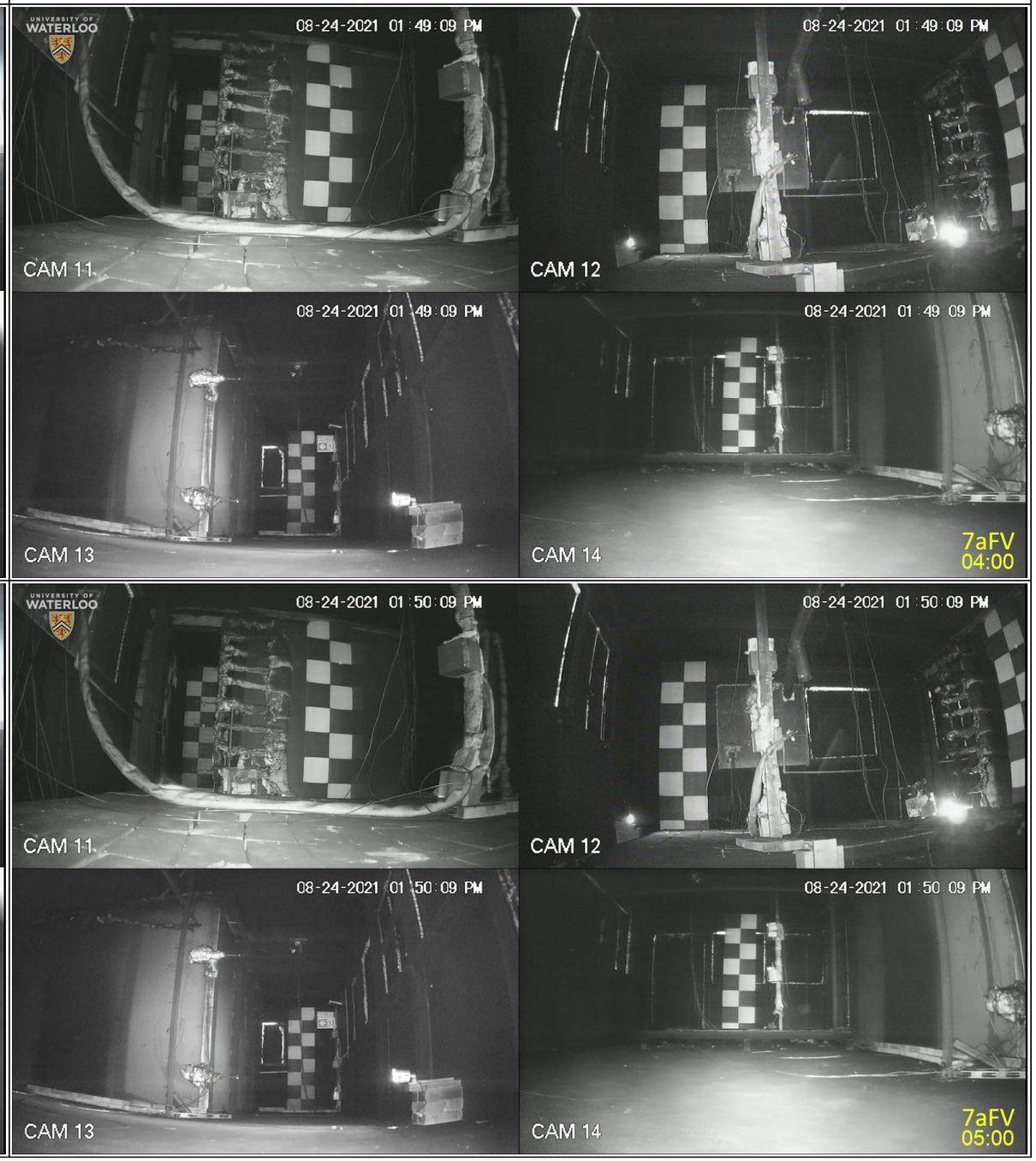
7aFV - Burn Room (UK Leather Couch – Crib 5)	**7bFV** – Upper Level (UK Leather Couch – Crib 5)





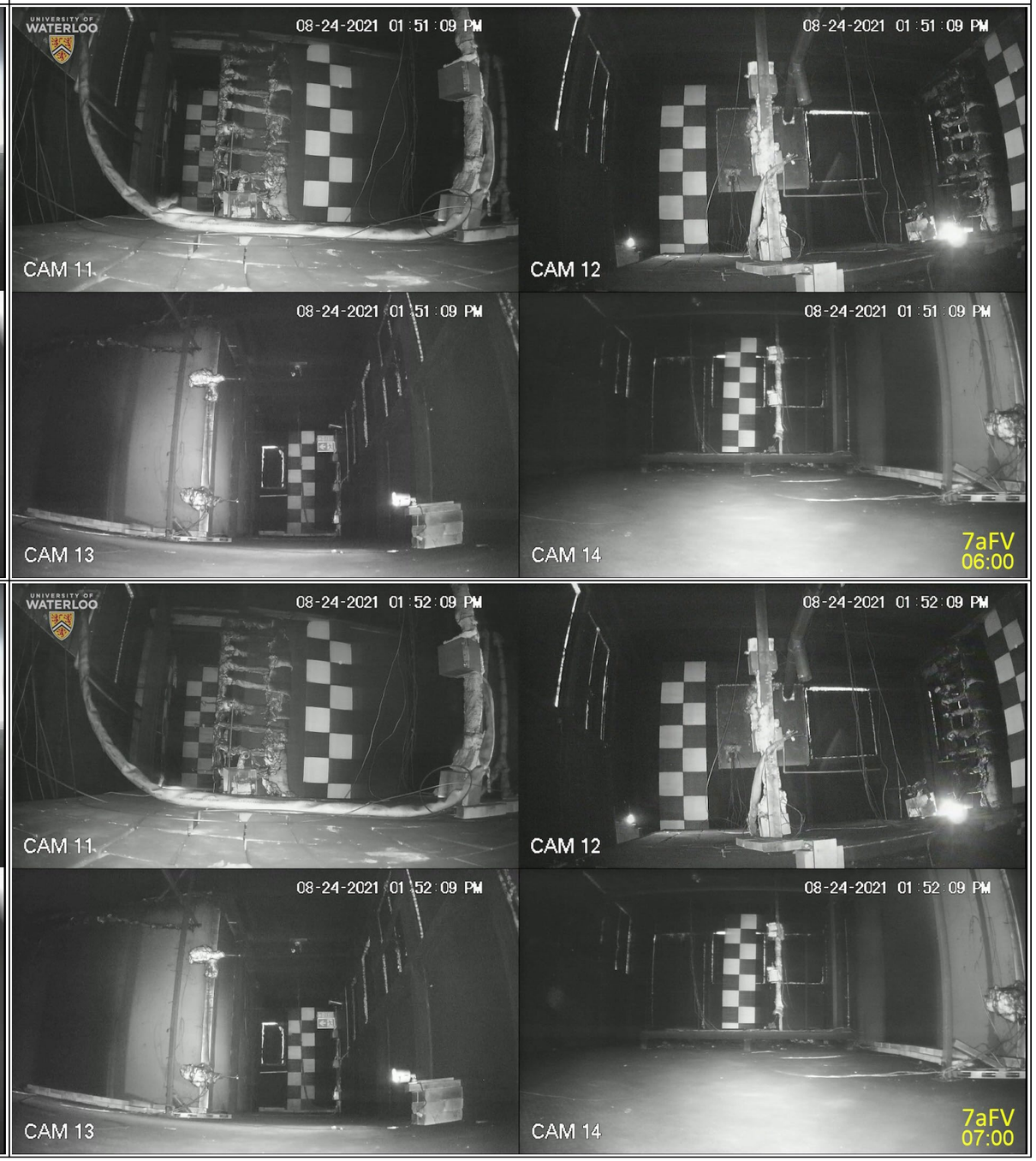
7aFV - Burn Room (UK Leather Couch – Crib 5)	**7bFV** – Upper Level (UK Leather Couch – Crib 5)

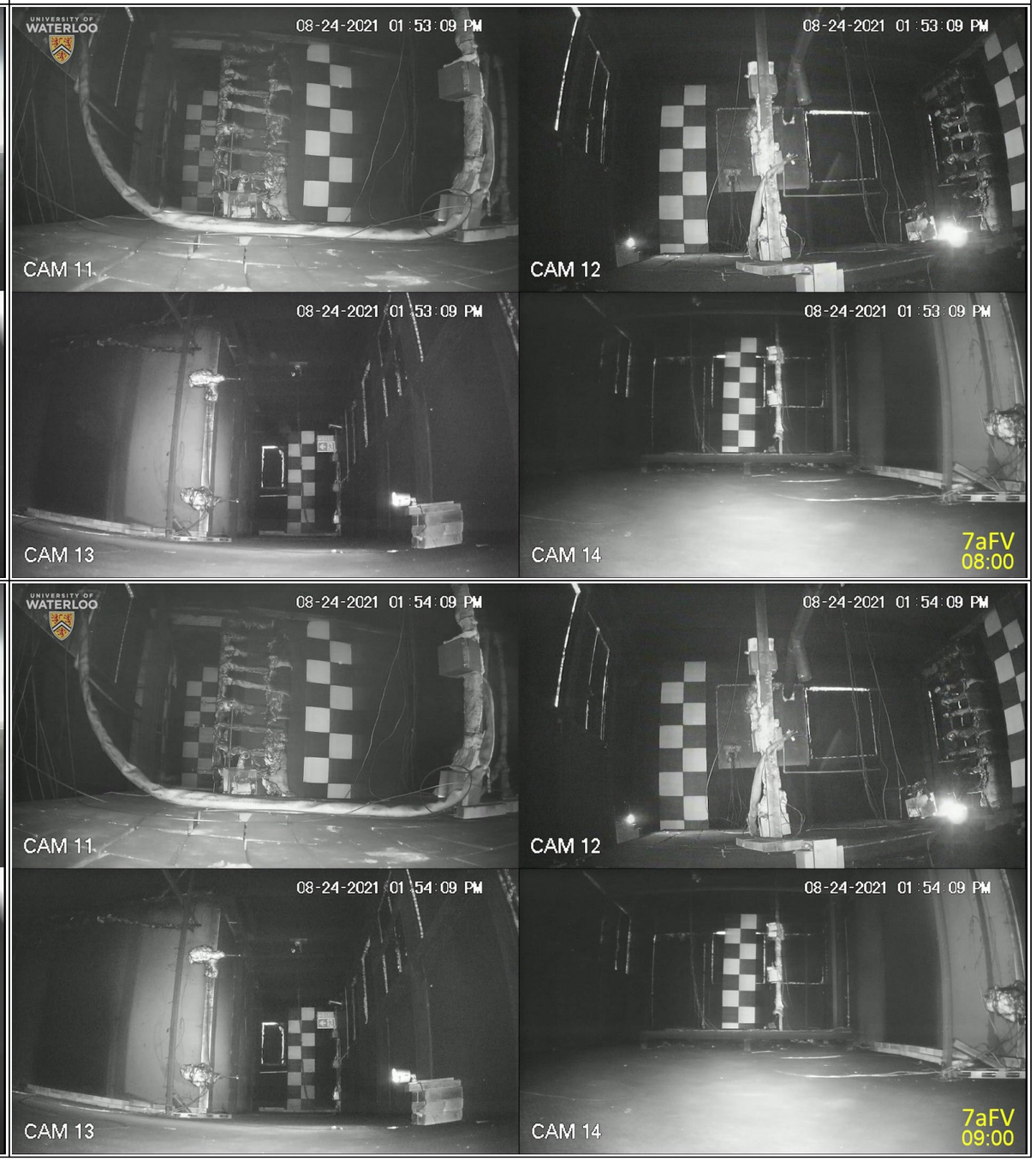




7aFV - Burn Room (UK Leather Couch – Crib 5)	**7bFV** – Upper Level (UK Leather Couch – Crib 5)

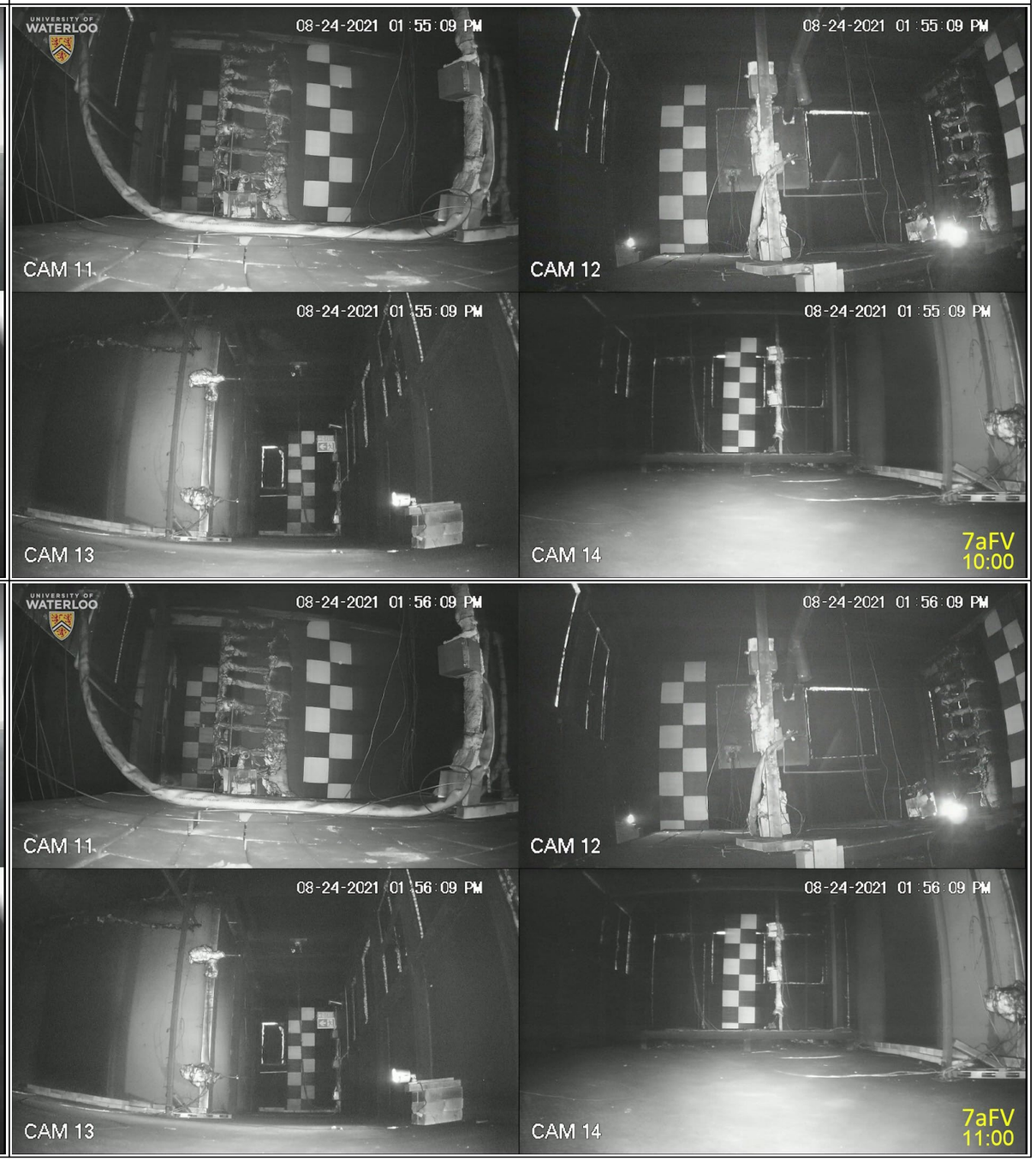




7aFV - Burn Room (UK Leather Couch – Crib 5)	**7bFV** – Upper Level (UK Leather Couch – Crib 5)
	

7aFV - Burn Room (UK Leather Couch – Crib 5)	**7bFV** – Upper Level (UK Leather Couch – Crib 5)





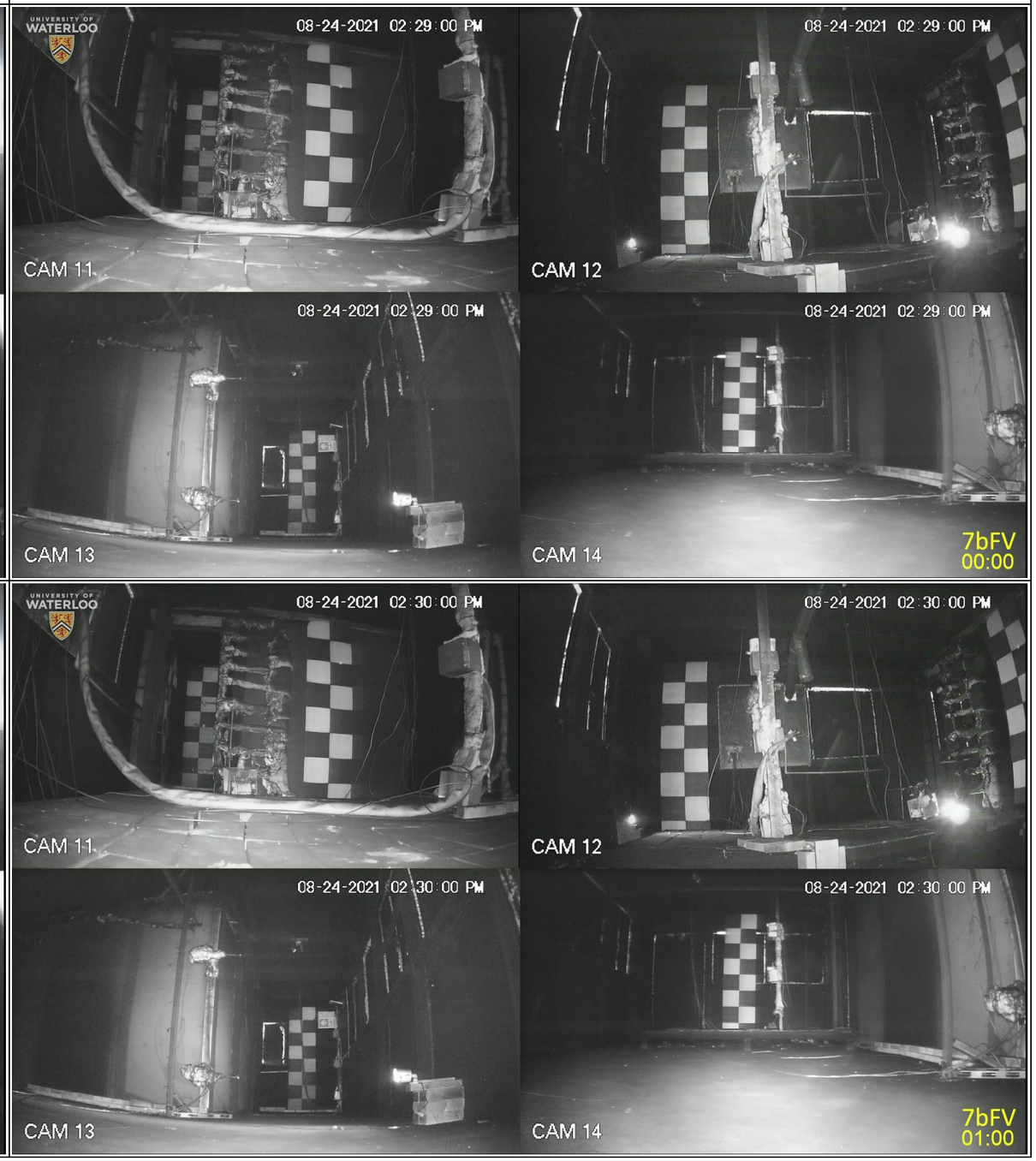
7aFV - Burn Room (UK Leather Couch – Crib 5)	**7bFV** – Upper Level (UK Leather Couch – Crib 5)





7bFV - Burn Room (UK Leather Couch – Crib 7)	**7bFV** – Upper Level (UK Leather Couch – Crib 7)

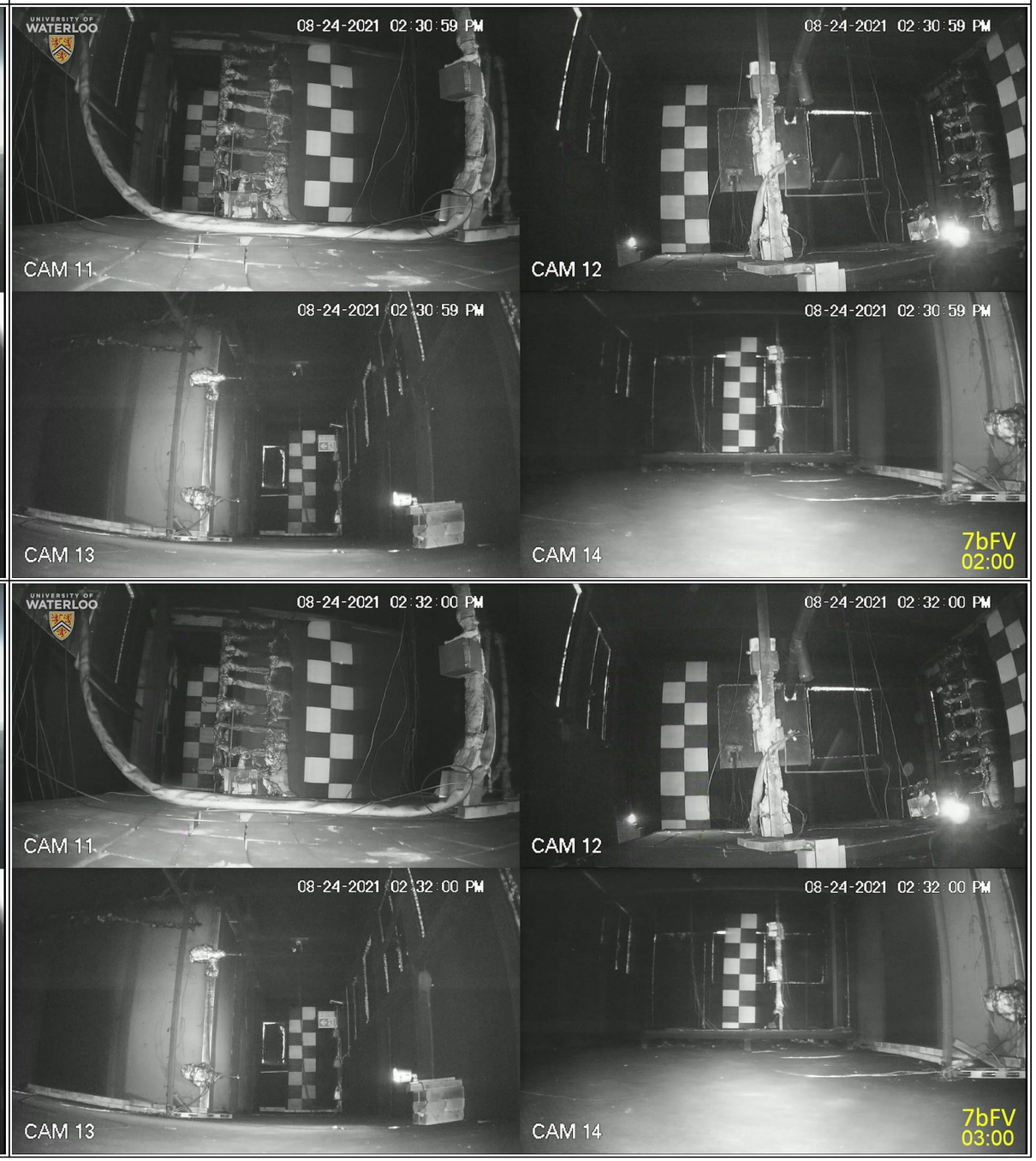




7bFV - Burn Room (UK Leather Couch – Crib 7)

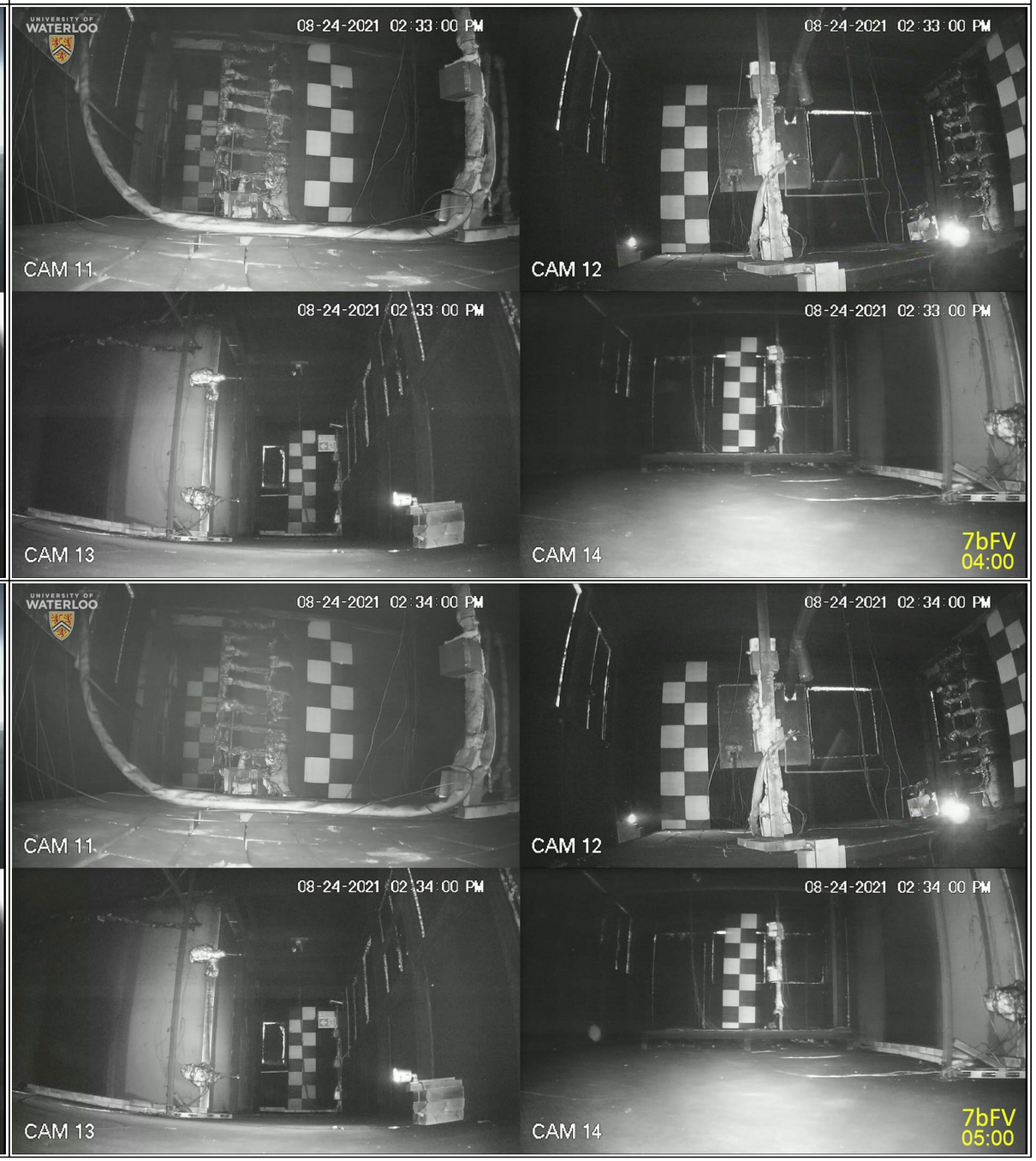


7bFV – Upper Level (UK Leather Couch – Crib 7)



7bFV - Burn Room (UK Leather Couch – Crib 7)	**7bFV** – Upper Level (UK Leather Couch – Crib 7)





7bFV - Burn Room (UK Leather Couch – Crib 7)	**7bFV** – Upper Level (UK Leather Couch – Crib 7)





7bFV - Burn Room (UK Leather Couch – Crib 7)	**7bFV** – Upper Level (UK Leather Couch – Crib 7)





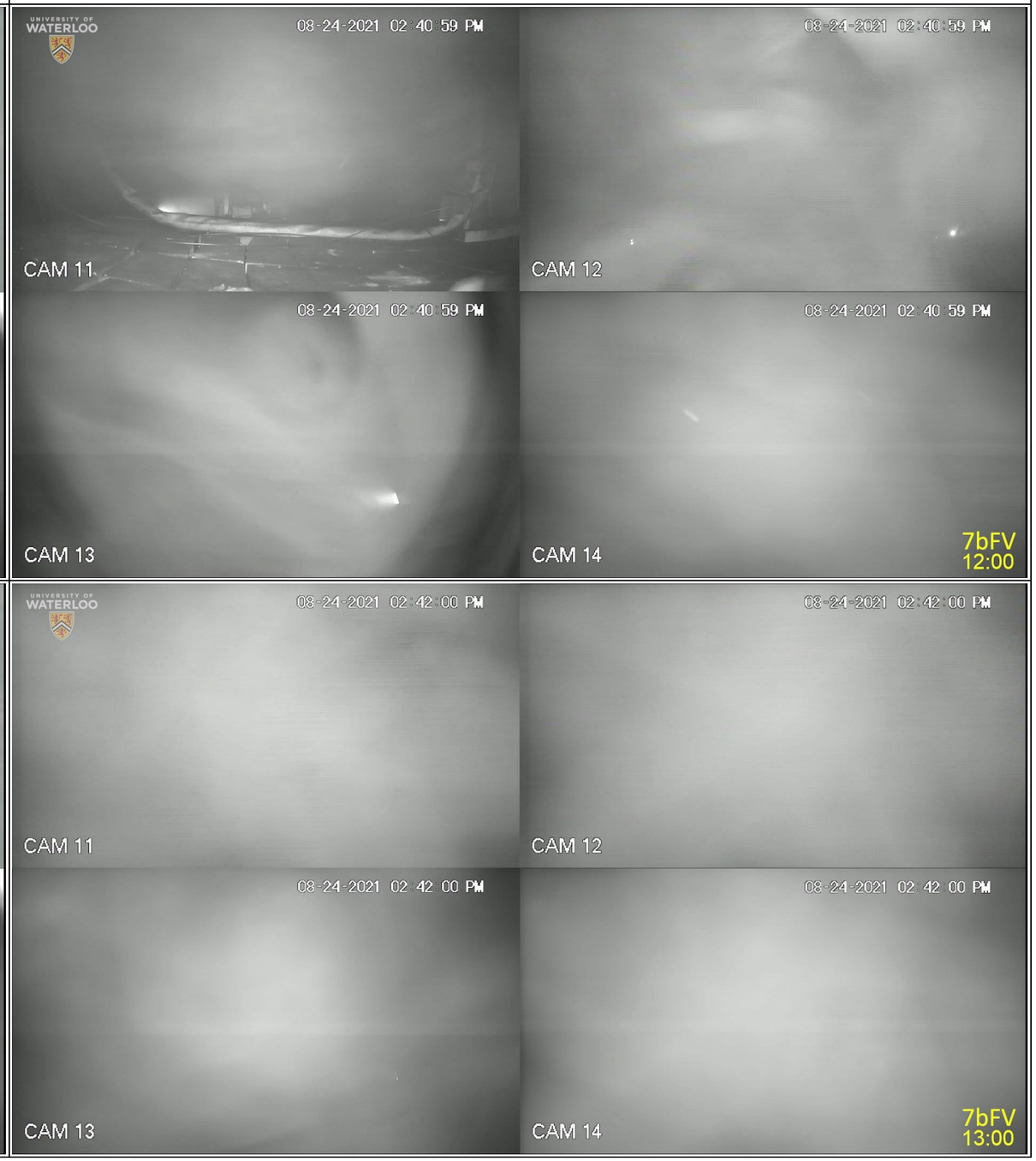
7bFV - Burn Room (UK Leather Couch – Crib 7)	**7bFV** – Upper Level (UK Leather Couch – Crib 7)





7bFV - Burn Room (UK Leather Couch – Crib 7)	**7bFV** – Upper Level (UK Leather Couch – Crib 7)



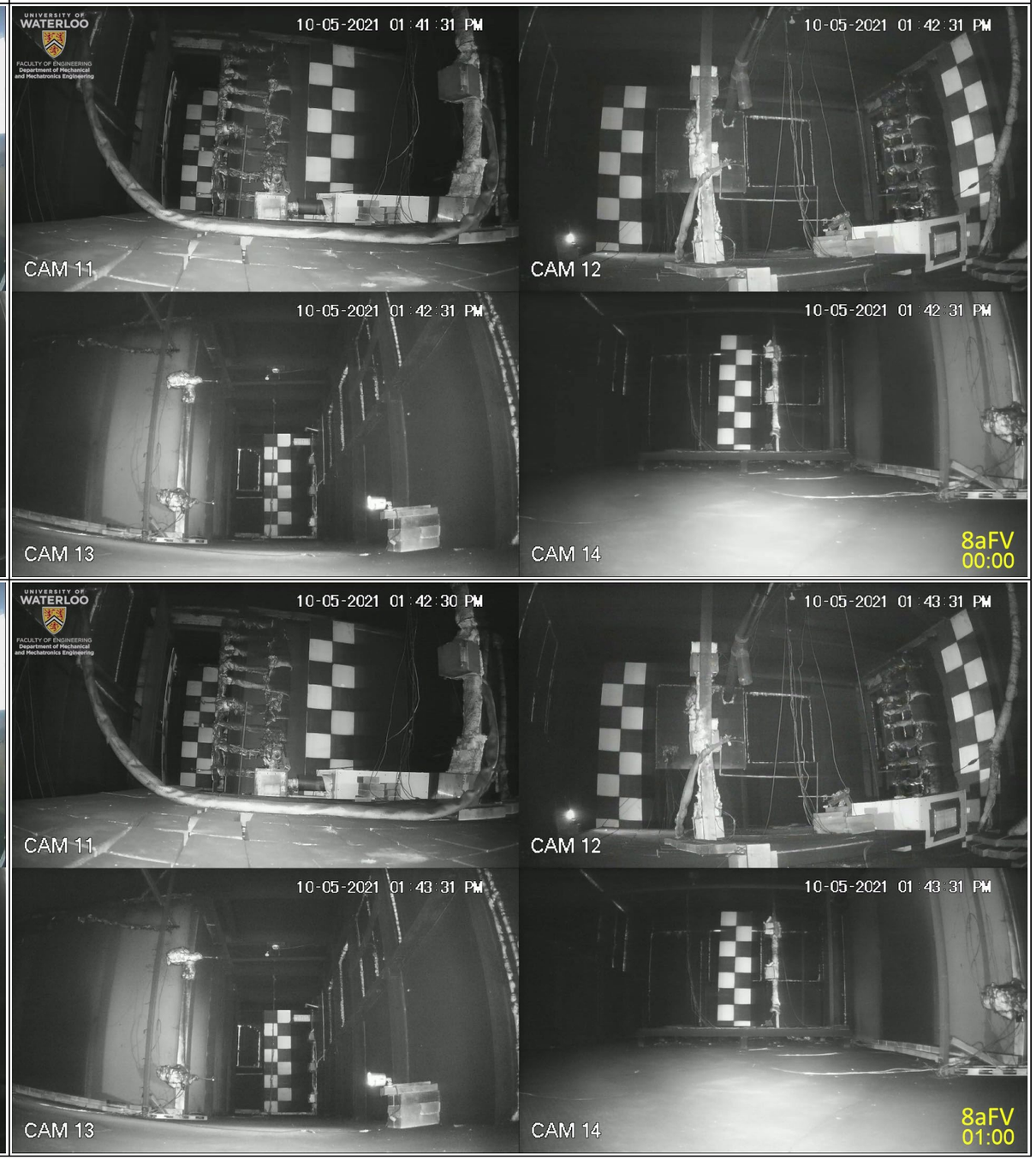


7bFV - Burn Room (UK Leather Couch – Crib 7)	**7bFV** – Upper Level (UK Leather Couch – Crib 7)
	

8aFV - Burn Room (US TB133 Faux-Leather Couch – Crib 7)



8aFV – Upper Level (US TB133 Leather Couch – Crib 7)



8aFV - Burn Room (US TB133 Faux-Leather Couch – Crib 7)	**8aFV** – Upper Level (US TB133 Leather Couch – Crib 7)

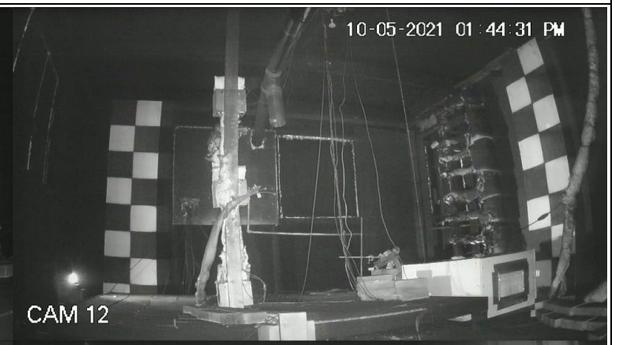












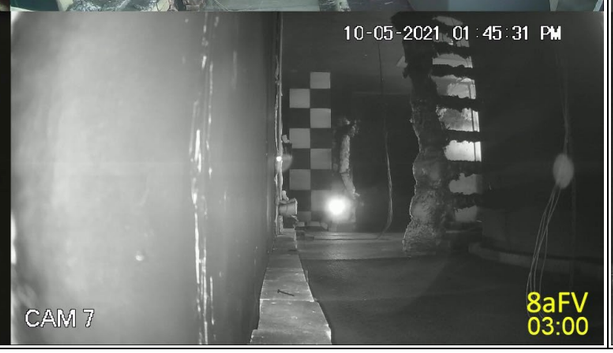




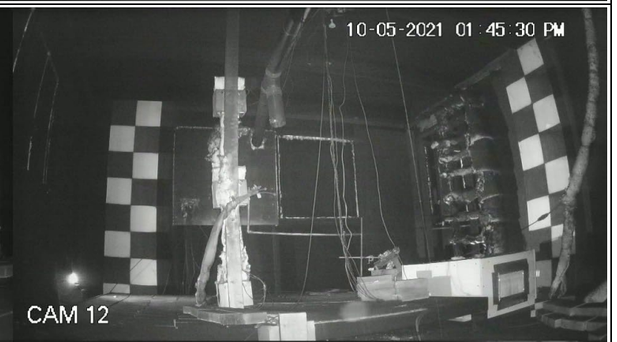
















8aFV - Burn Room (US TB133 Faux-Leather Couch – Crib 7)	**8aFV** – Upper Level (US TB133 Leather Couch – Crib 7)

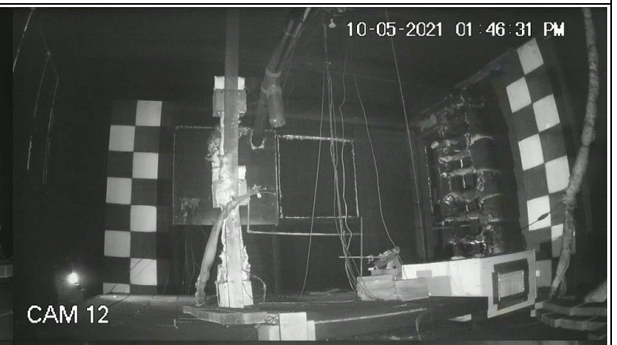
















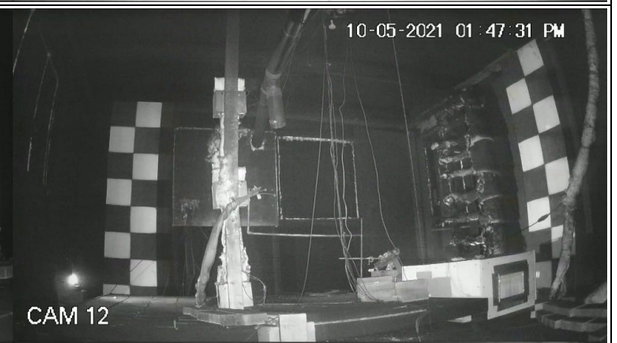
















8aFV - Burn Room (US TB133 Faux-Leather Couch – Crib 7)	**8aFV** – Upper Level (US TB133 Leather Couch – Crib 7)

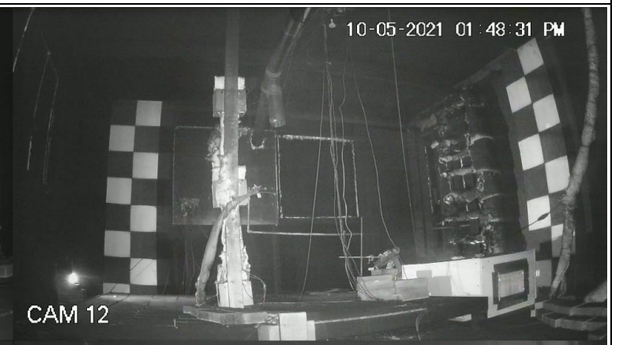
















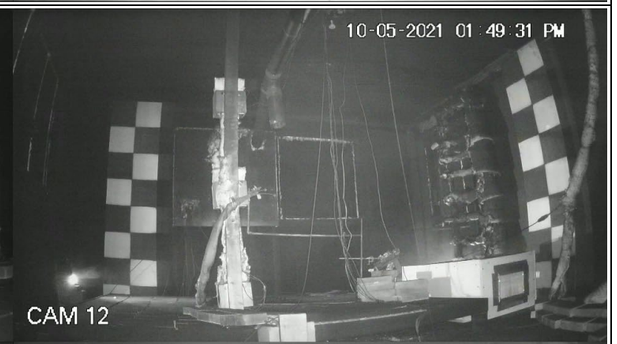
















8aFV - Burn Room (US TB133 Faux-Leather Couch – Crib 7)

















8aFV – Upper Level (US TB133 Leather Couch – Crib 7)

















8aFV - Burn Room (US TB133 Faux-Leather Couch – Crib 7)	**8aFV** – Upper Level (US TB133 Leather Couch – Crib 7)

































8aFV - Burn Room (US TB133 Faux-Leather Couch – Crib 7)	**8aFV** – Upper Level (US TB133 Leather Couch – Crib 7)

































8aFV - Burn Room (US TB133 Faux-Leather Couch – Crib 7)	**8aFV** – Upper Level (US TB133 Leather Couch – Crib 7)



8aFV - Burn Room (US TB133 Faux-Leather Couch – Crib 7)	**8aFV** – Upper Level (US TB133 Leather Couch – Crib 7)









8aFV - Burn Room (US TB133 Faux-Leather Couch – Crib 7)	**8aFV** – Upper Level (US TB133 Leather Couch – Crib 7)



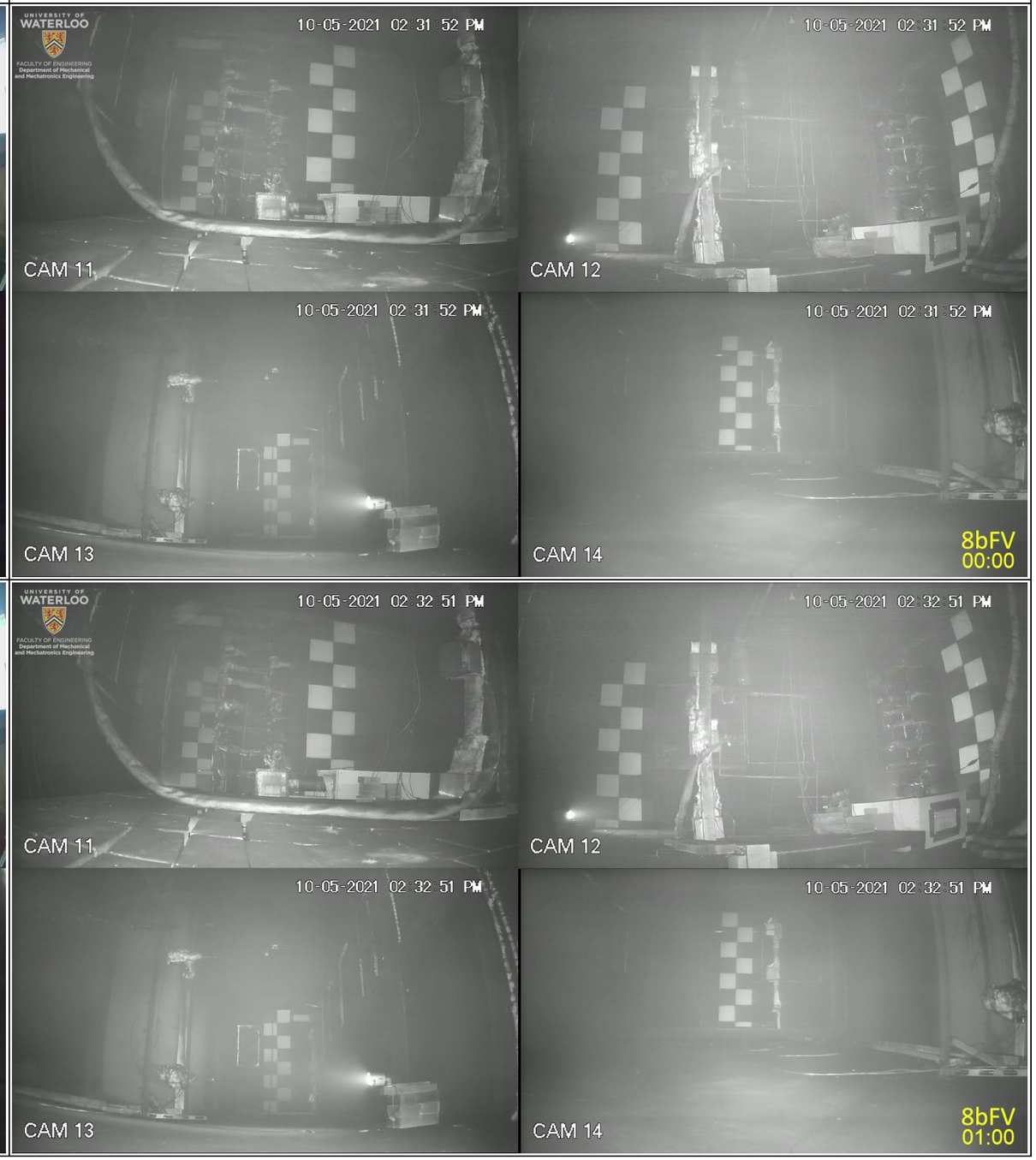






8bFV - Burn Room (US TB133 Faux-Leather Couch – Burner)	**8bFV** – Upper Level (US TB133 Leather Couch – Burner)





8bFV - Burn Room (US TB133 Faux-Leather Couch – Burner)	**8bFV** – Upper Level (US TB133 Leather Couch – Burner)



























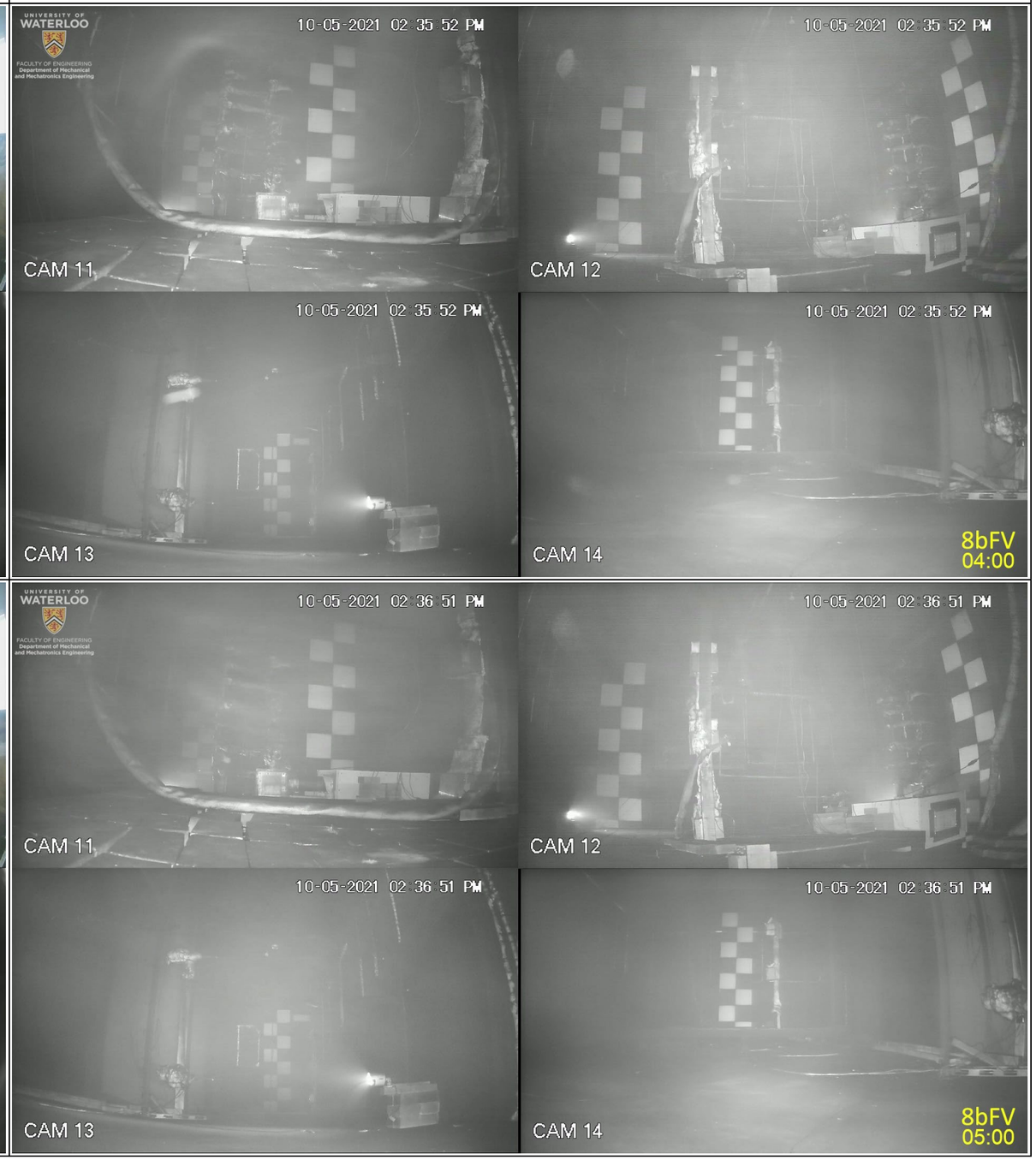






8bFV - Burn Room (US TB133 Faux-Leather Couch – Burner)	**8bFV** – Upper Level (US TB133 Leather Couch – Burner)





8bFV - Burn Room (US TB133 Faux-Leather Couch – Burner)	**8bFV** – Upper Level (US TB133 Leather Couch – Burner)

































8bFV - Burn Room (US TB133 Faux-Leather Couch – Burner)	**8bFV** – Upper Level (US TB133 Leather Couch – Burner)





8bFV - Burn Room (US TB133 Faux-Leather Couch – Burner)	**8bFV** – Upper Level (US TB133 Leather Couch – Burner)





8bFV - Burn Room (US TB133 Faux-Leather Couch – Burner)	**8bFV** – Upper Level (US TB133 Leather Couch – Burner)





8bFV - Burn Room (US TB133 Faux-Leather Couch – Burner)	**8bFV** – Upper Level (US TB133 Leather Couch – Burner)





8bFV - Burn Room (US TB133 Faux-Leather Couch – Burner)	**8bFV** – Upper Level (US TB133 Leather Couch – Burner)





8bFV - Burn Room (US TB133 Faux-Leather Couch – Burner)	**8bFV** – Upper Level (US TB133 Leather Couch – Burner)

































9FV - Burn Room (US TB133 Faux-Leather Couch – Crib 7)	**9FV** – Upper Level (US TB133 Leather Couch – Crib 7)

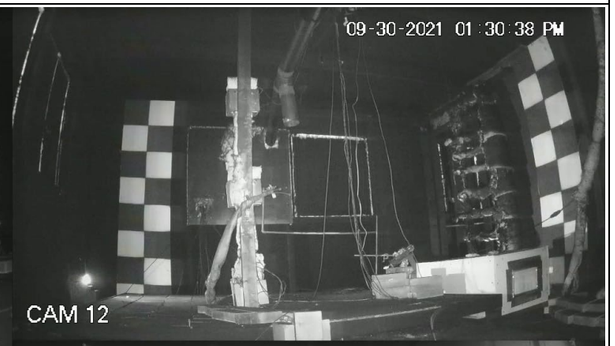
















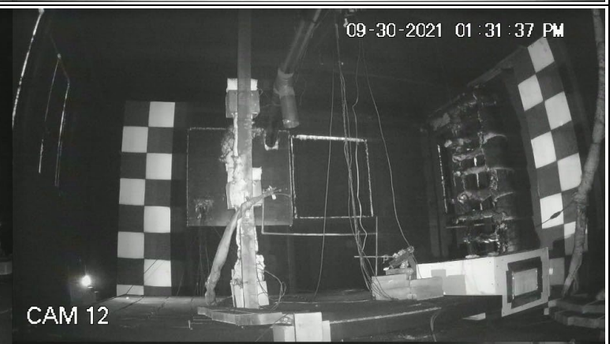
















9FV - Burn Room (US TB133 Faux-Leather Couch – Crib 7)	**9FV** – Upper Level (US TB133 Leather Couch – Crib 7)

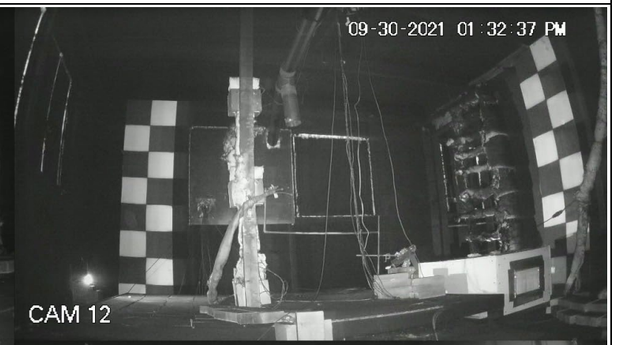
















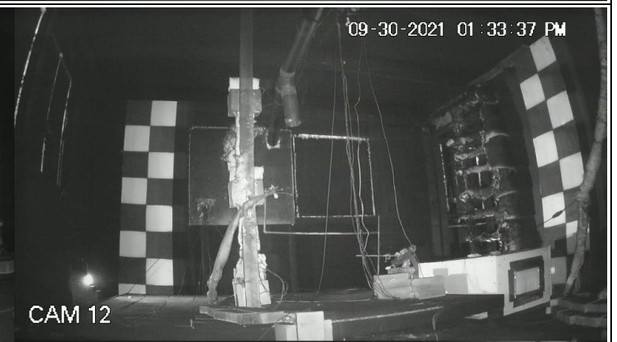
















9FV - Burn Room (US TB133 Faux-Leather Couch – Crib 7)











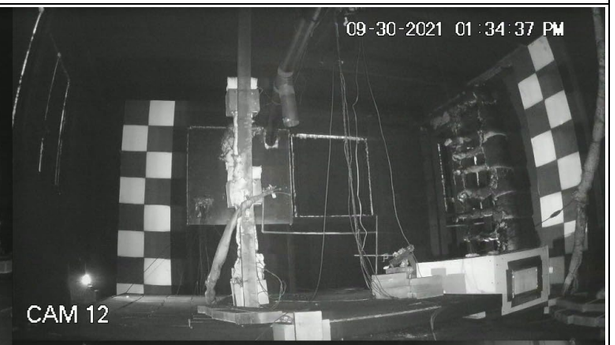


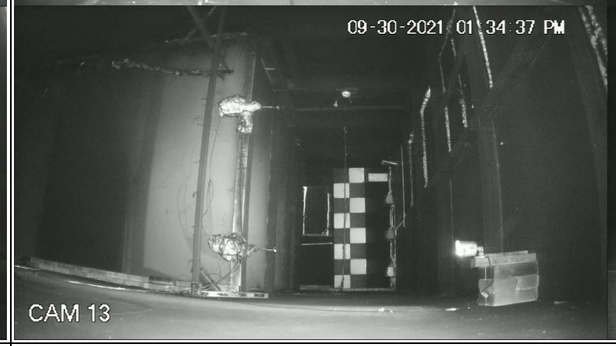




9FV – Upper Level (US TB133 Leather Couch – Crib 7)

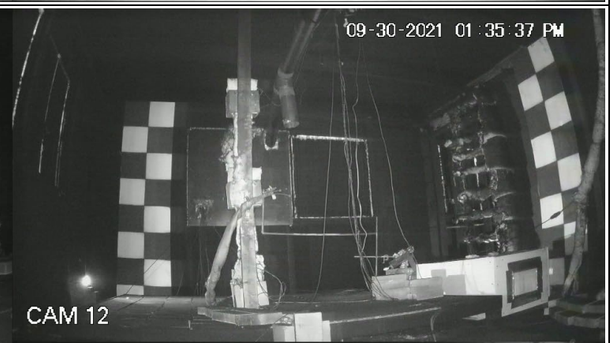
















9FV - Burn Room (US TB133 Faux-Leather Couch – Crib 7)	**9FV** – Upper Level (US TB133 Leather Couch – Crib 7)

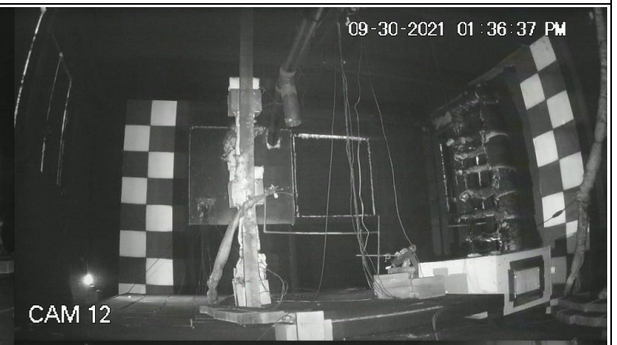
















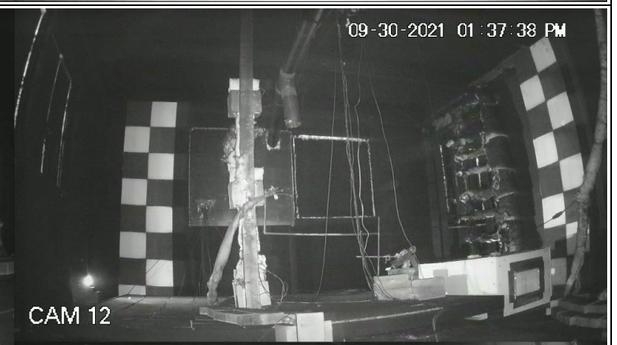














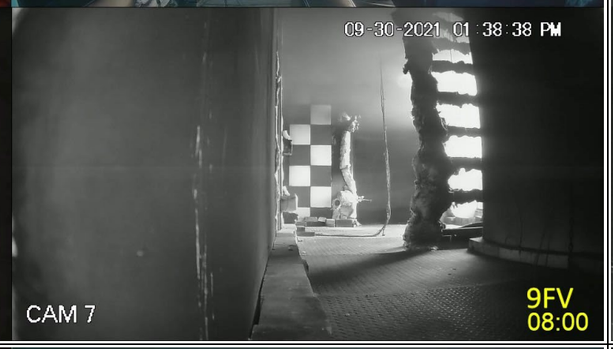


9FV - Burn Room (US TB133 Faux-Leather Couch – Crib 7)	**9FV** – Upper Level (US TB133 Leather Couch – Crib 7)

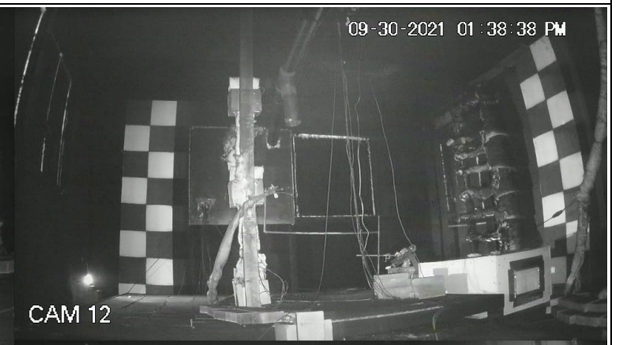
























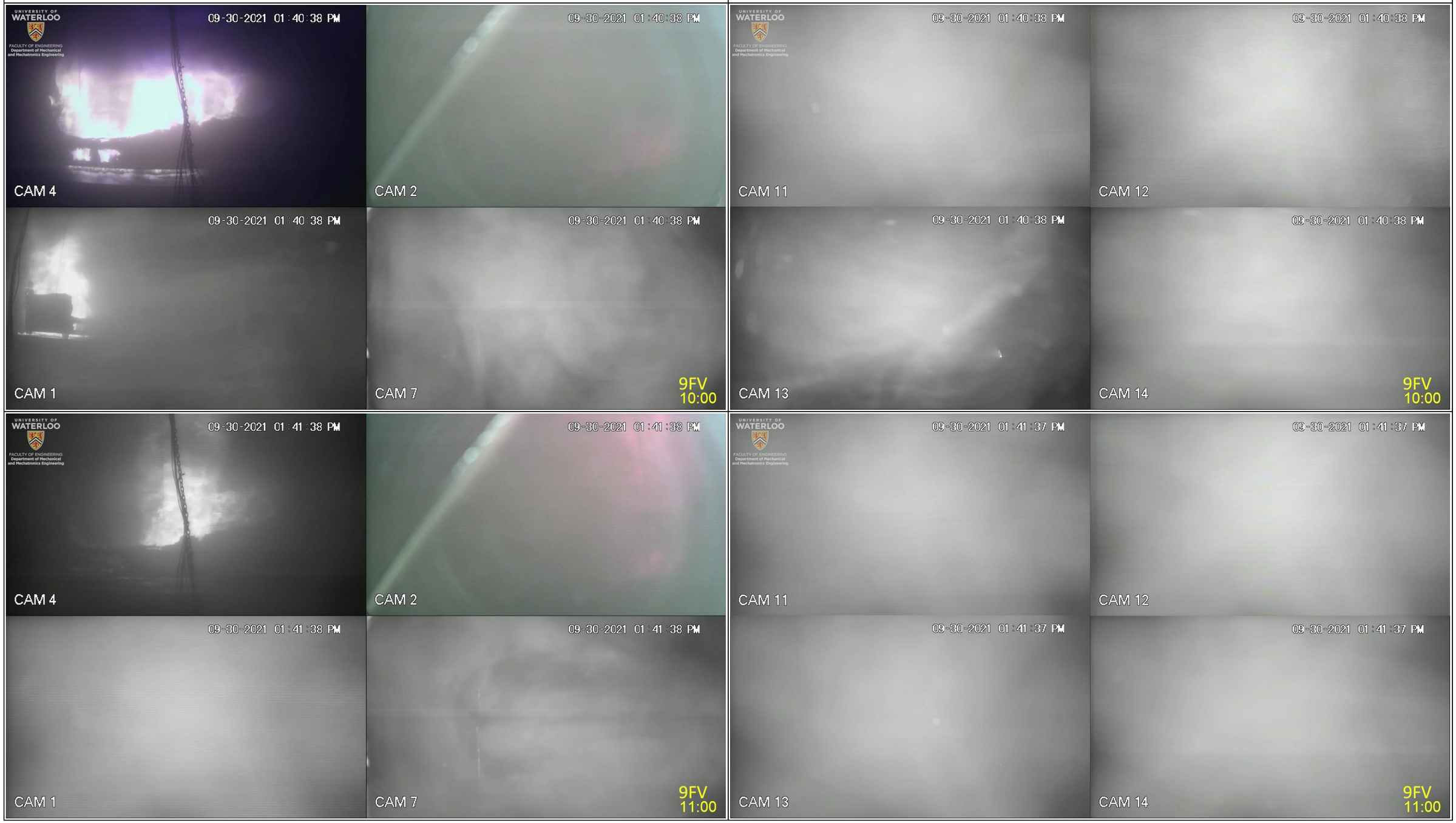






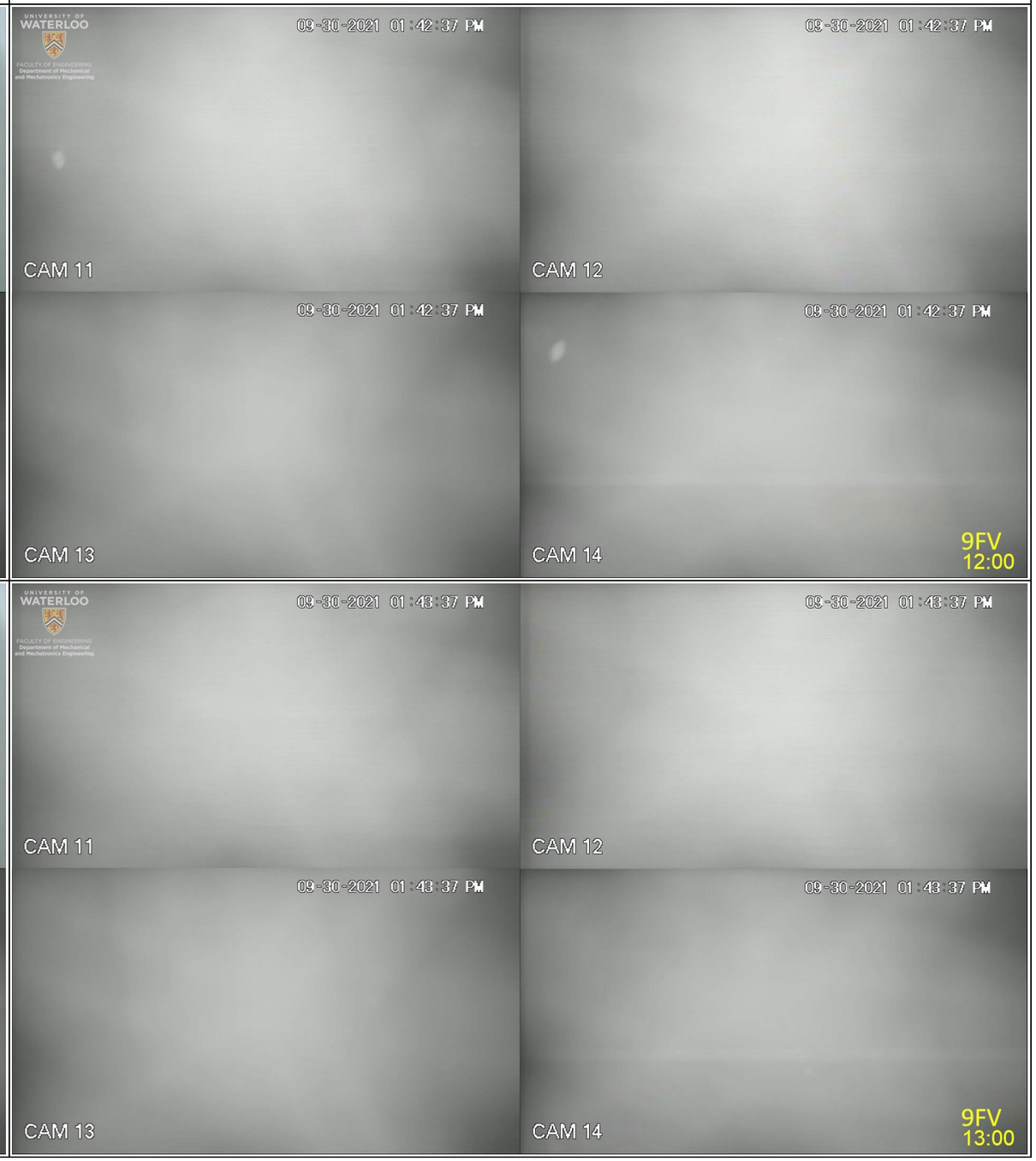


9FV - Burn Room (US TB133 Faux-Leather Couch – Crib 7)	**9FV** – Upper Level (US TB133 Leather Couch – Crib 7)



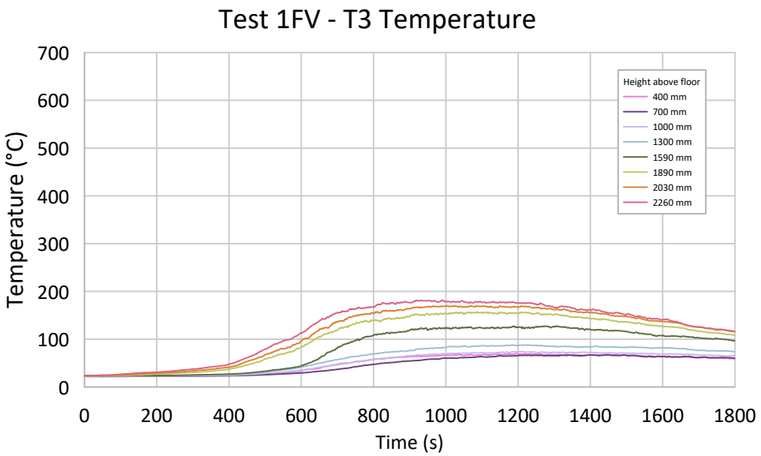
9FV - Burn Room (US TB133 Faux-Leather Couch – Crib 7)	**9FV** – Upper Level (US TB133 Leather Couch – Crib 7)

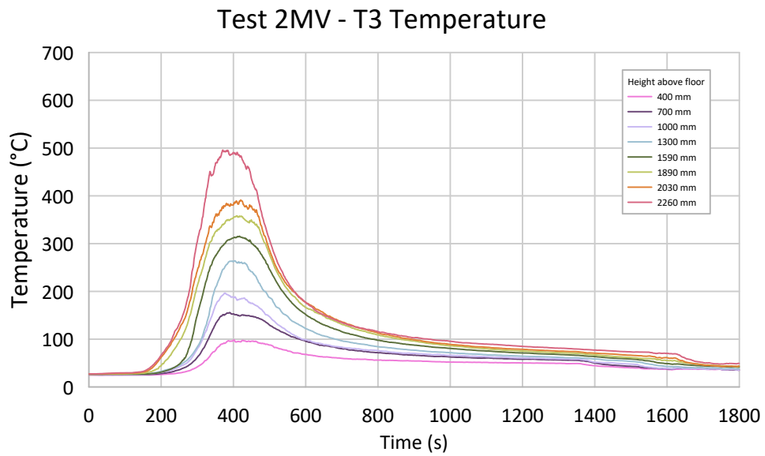


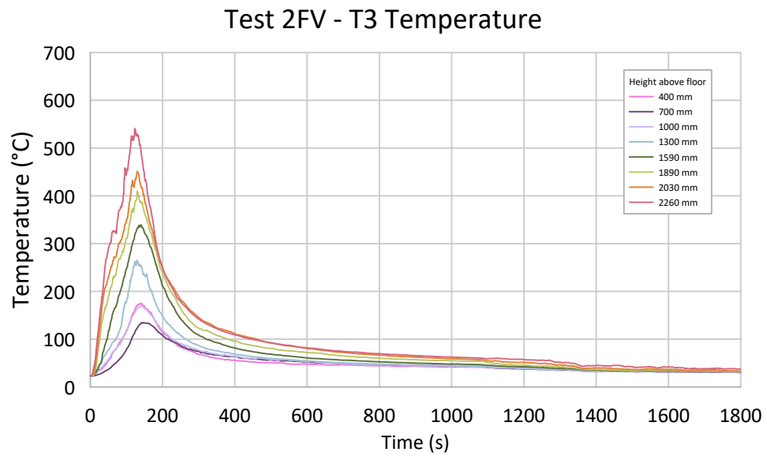


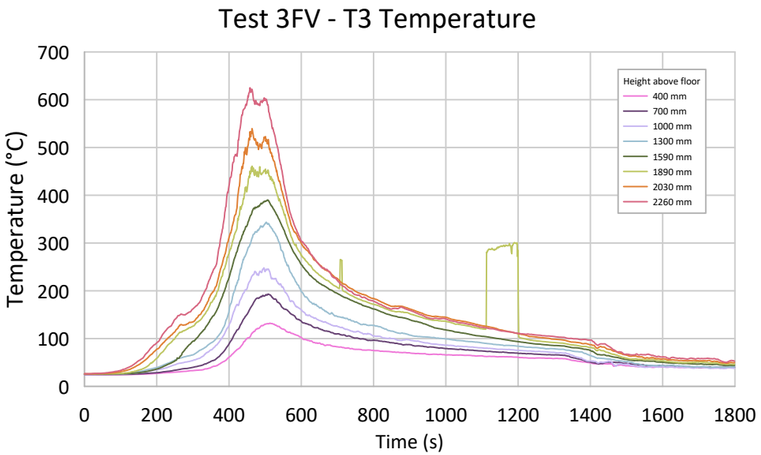
Appendix B:

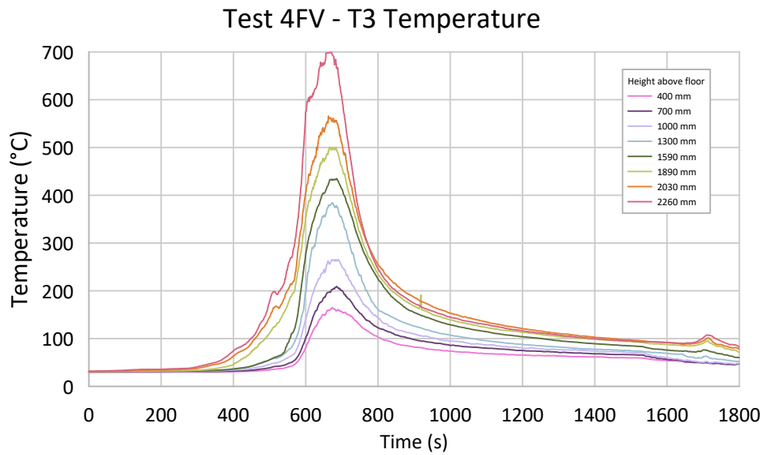
Temperature Time Curves for Select Thermocouple Locations

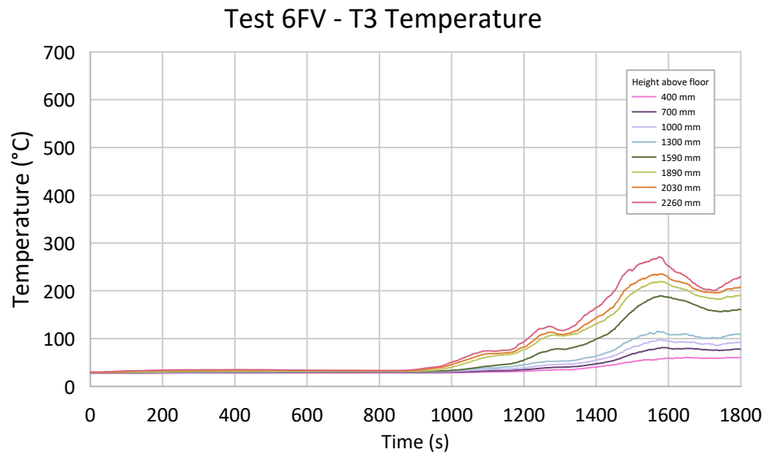

Test 1FV - T3 Temperature
Temperature (°C)
Time (s)
Height above floor
400 mm
700 mm
1000 mm
1300 mm
1590 mm
1890 mm
2030 mm
2260 mm

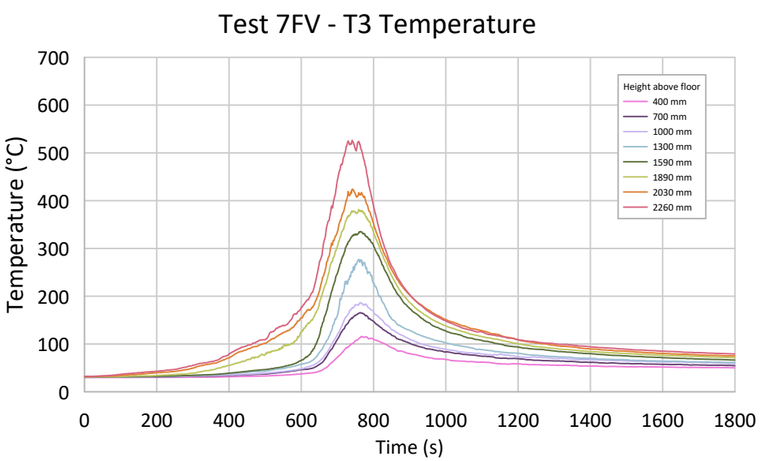

Test 2MV - T3 Temperature
Temperature (°C)
Time (s)
Height above floor
400 mm
700 mm
1000 mm
1300 mm
1590 mm
1890 mm
2030 mm
2260 mm

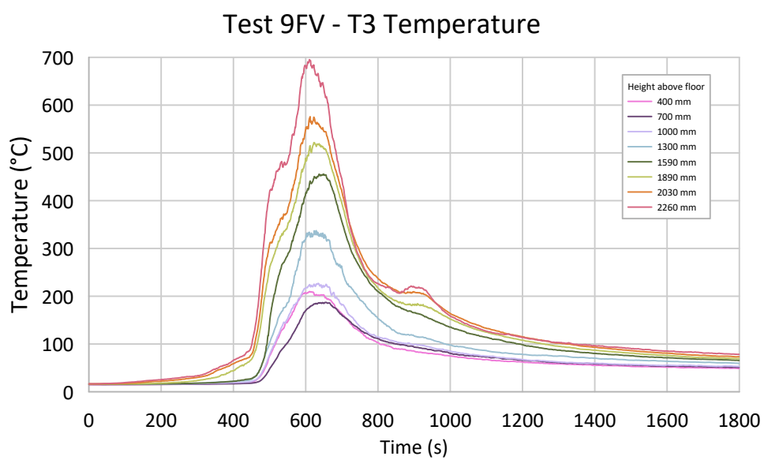

Test 2FV - T3 Temperature
Temperature (°C)
Time (s)
Height above floor
400 mm
700 mm
1000 mm
1300 mm
1590 mm
1890 mm
2030 mm
2260 mm

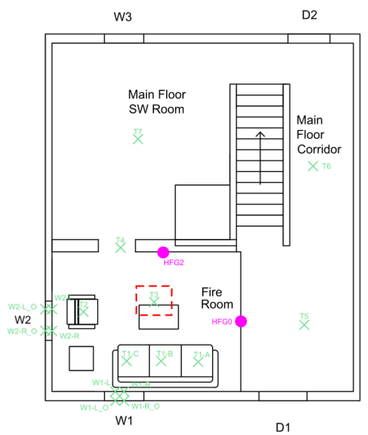

Test 3FV - T3 Temperature
Temperature (°C)
Time (s)
Height above floor
400 mm
700 mm
1000 mm
1300 mm
1590 mm
1890 mm
2030 mm
2260 mm

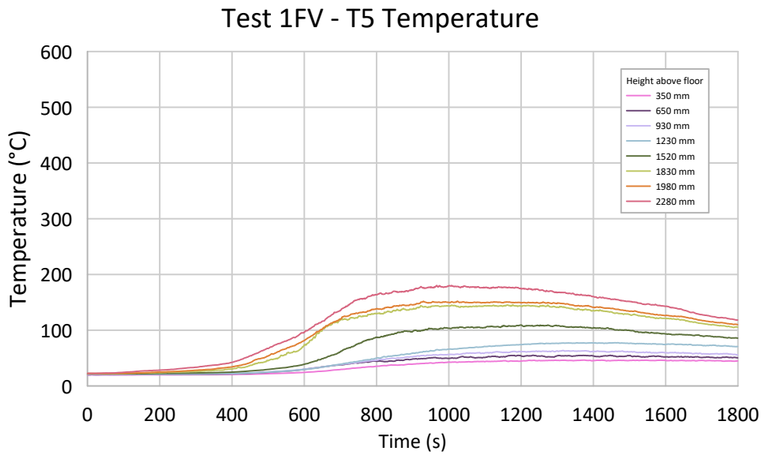

Test 4FV - T3 Temperature
Temperature (°C)
Time (s)
Height above floor
400 mm
700 mm
1000 mm
1300 mm
1590 mm
1890 mm
2030 mm
2260 mm

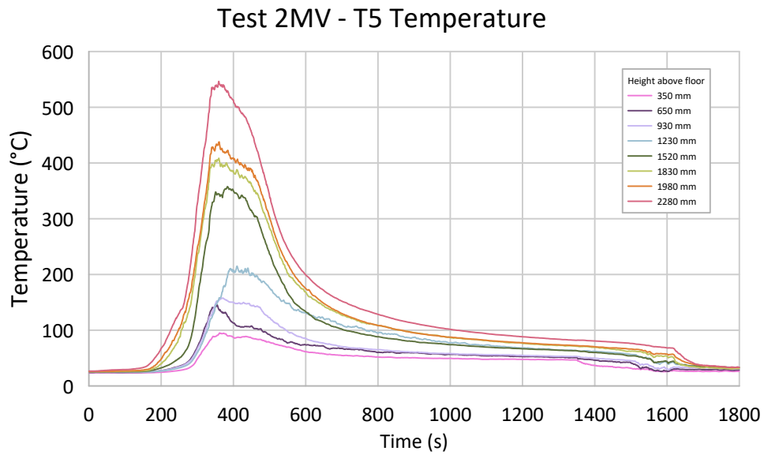

Test 6FV - T3 Temperature
Temperature (°C)
Time (s)
Height above floor
400 mm
700 mm
1000 mm
1300 mm
1590 mm
1890 mm
2030 mm
2260 mm

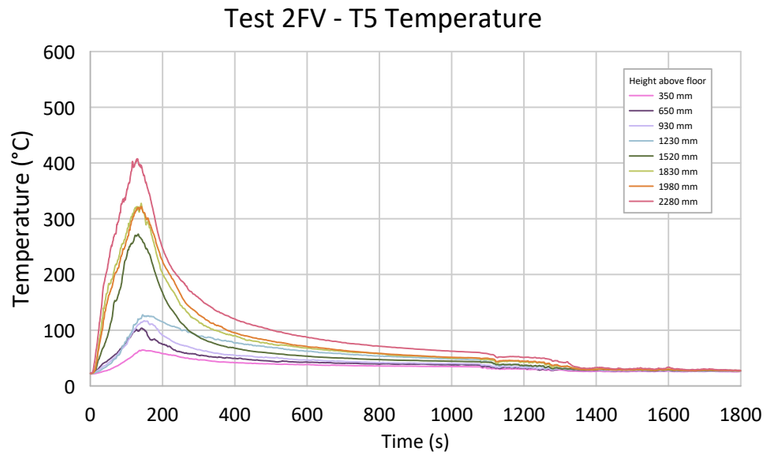

Test 7FV - T3 Temperature
Temperature (°C)
Time (s)
Height above floor
400 mm
700 mm
1000 mm
1300 mm
1590 mm
1890 mm
2030 mm
2260 mm

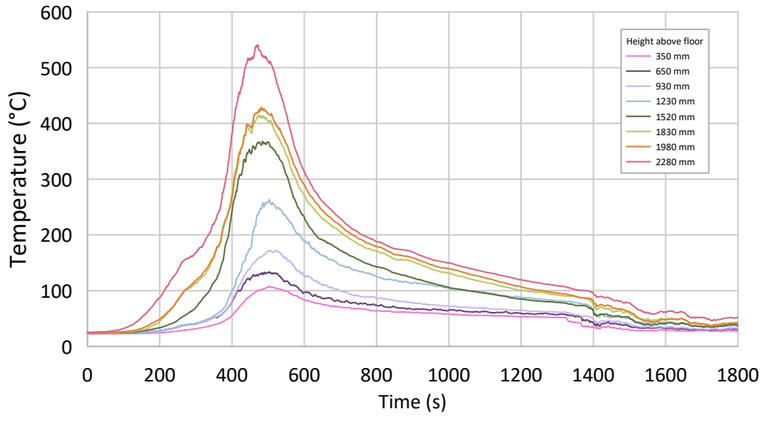

Test 9FV - T3 Temperature
Temperature (°C)
Time (s)
Height above floor
400 mm
700 mm
1000 mm
1300 mm
1590 mm
1890 mm
2030 mm
2260 mm

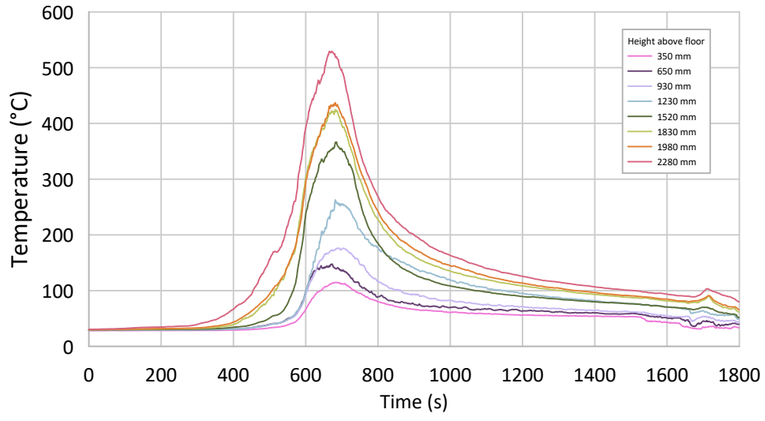

W3
D2
Main Floor
SW Room
Main
Floor
Corridor
Fire
Room
W2
W1
D1

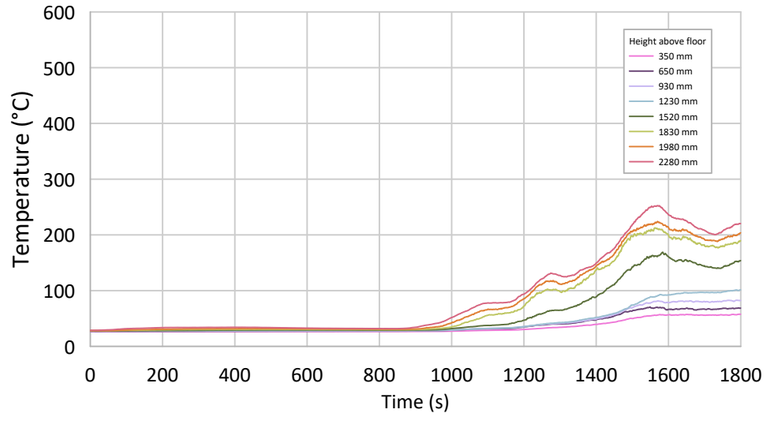

Test 1FV - T5 Temperature
Temperature (°C)
Time (s)
Height above floor
350 mm
650 mm
930 mm
1230 mm
1520 mm
1830 mm
1980 mm
2280 mm

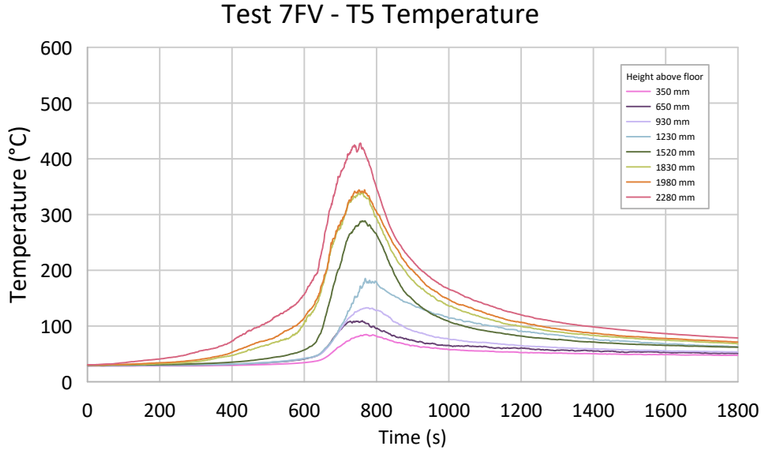

Test 2MV - T5 Temperature
Temperature (°C)
Time (s)
Height above floor
350 mm
650 mm
930 mm
1230 mm
1520 mm
1830 mm
1980 mm
2280 mm

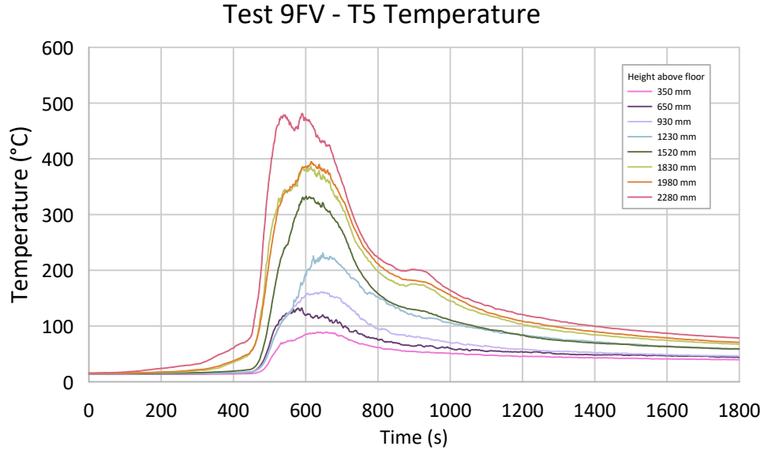

Test 2FV - T5 Temperature
Temperature (°C)
Time (s)
Height above floor
350 mm
650 mm
930 mm
1230 mm
1520 mm
1830 mm
1980 mm
2280 mm

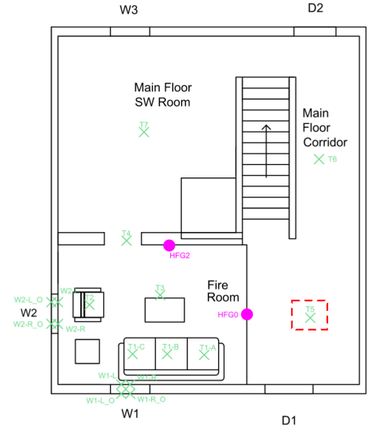

Test 3FV - T5 Temperature
Temperature (°C)
Time (s)
Height above floor
350 mm
650 mm
930 mm
1230 mm
1520 mm
1830 mm
1980 mm
2280 mm

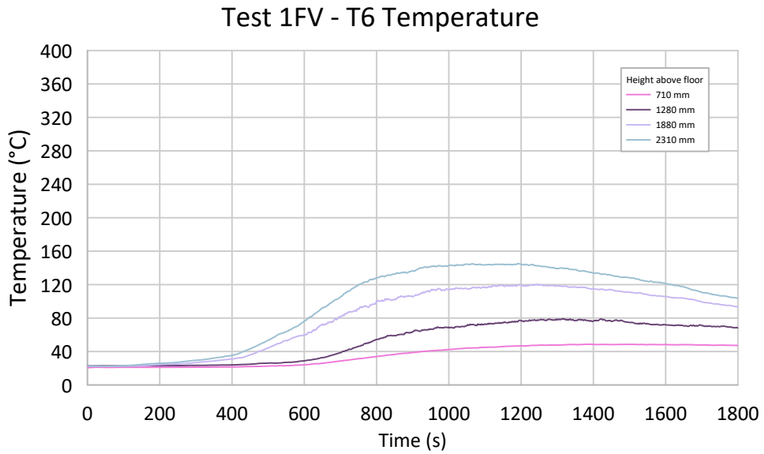

Test 4FV - T5 Temperature
Temperature (°C)
Time (s)
Height above floor
350 mm
650 mm
930 mm
1230 mm
1520 mm
1830 mm
1980 mm
2280 mm

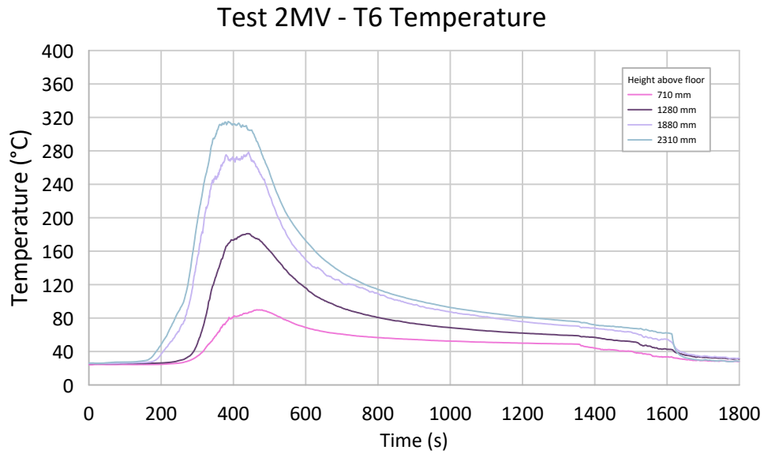

Test 6FV - T5 Temperature
Temperature (°C)
Time (s)
Height above floor
350 mm
650 mm
930 mm
1230 mm
1520 mm
1830 mm
1980 mm
2280 mm

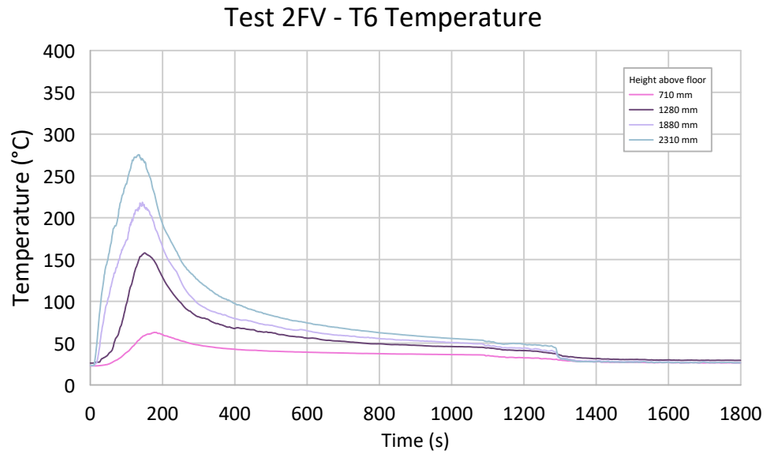

Test 7FV - T5 Temperature
Temperature (°C)
Time (s)
Height above floor
350 mm
650 mm
930 mm
1230 mm
1520 mm
1830 mm
1980 mm
2280 mm

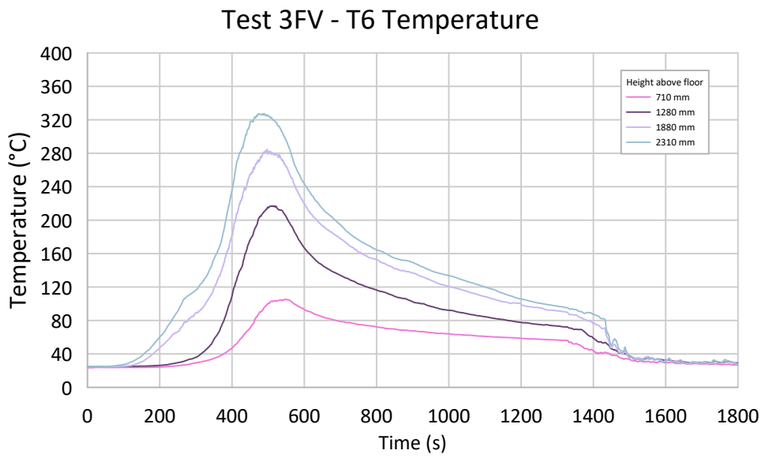

Test 9FV - T5 Temperature
Temperature (°C)
Time (s)
Height above floor
350 mm
650 mm
930 mm
1230 mm
1520 mm
1830 mm
1980 mm
2280 mm

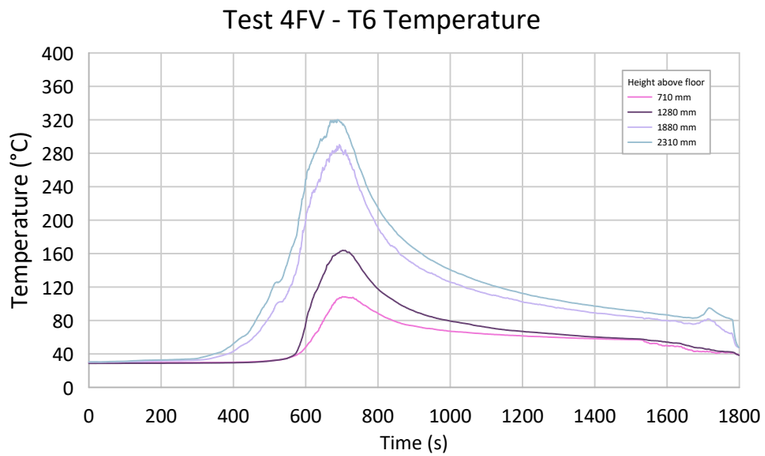

W3
D2
Main Floor
SW Room
Main
Floor
Corridor
T7
T6
T4
HFG2
T3
Fire
Room
HFG0
T5
W2
W2-L_O
W2-L_I
W2-R_O
W2-R_I
W2-R
T1-C
T1-B
T1-A
W1-L_O
W1-L_I
W1-R_I
W1-R_O
W1
D1

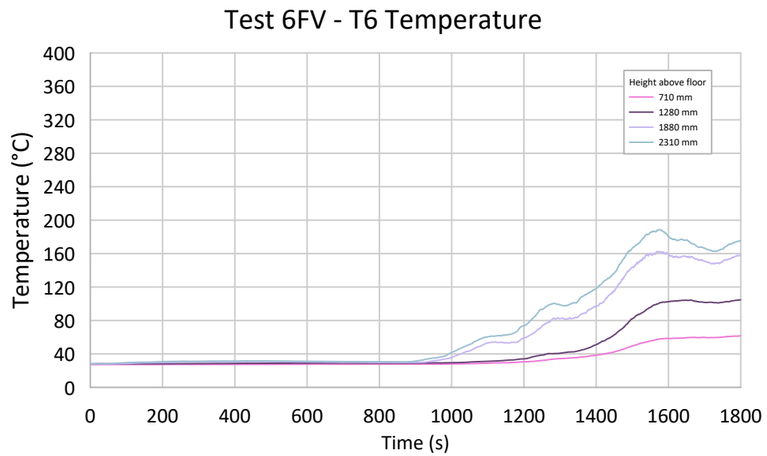

Test 1FV - T6 Temperature
Temperature (°C)
Time (s)
Height above floor
710 mm
1280 mm
1880 mm
2310 mm

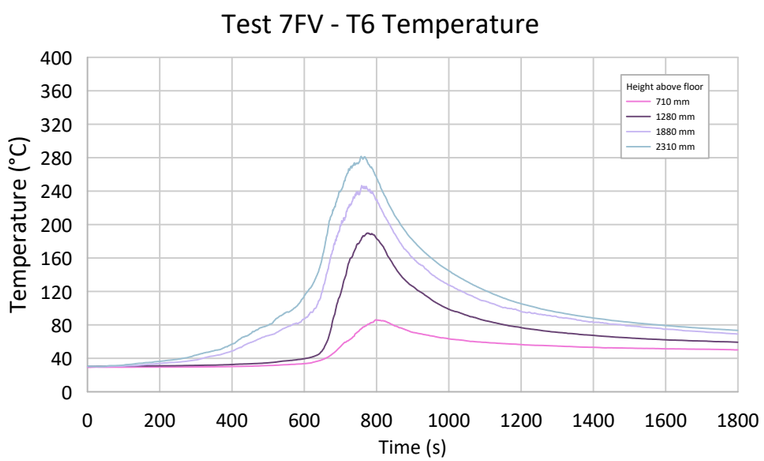

Test 2MV - T6 Temperature
Temperature (°C)
Time (s)
Height above floor
710 mm
1280 mm
1880 mm
2310 mm

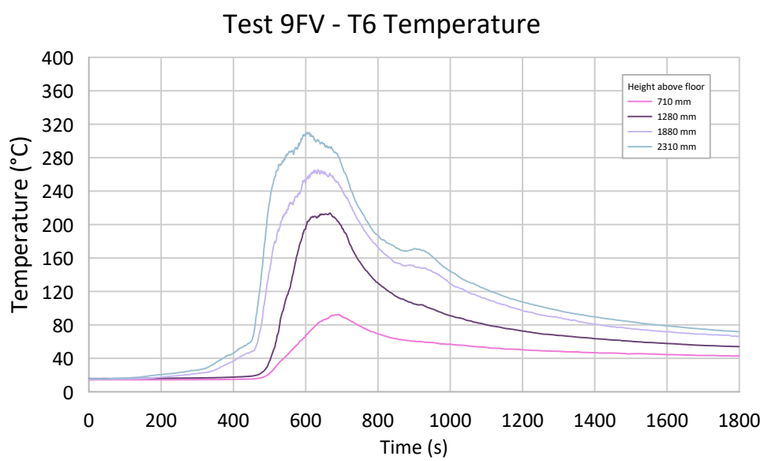

Test 2FV - T6 Temperature
Temperature (°C)
Time (s)
Height above floor
710 mm
1280 mm
1880 mm
2310 mm

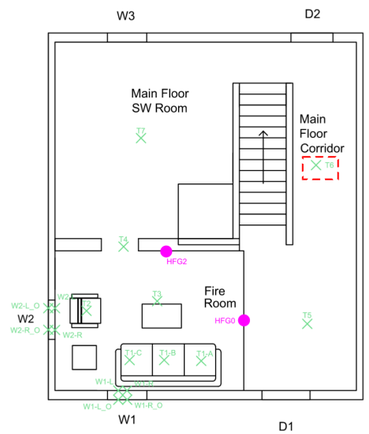

Test 3FV - T6 Temperature
Temperature (°C)
Time (s)
Height above floor
710 mm
1280 mm
1880 mm
2310 mm

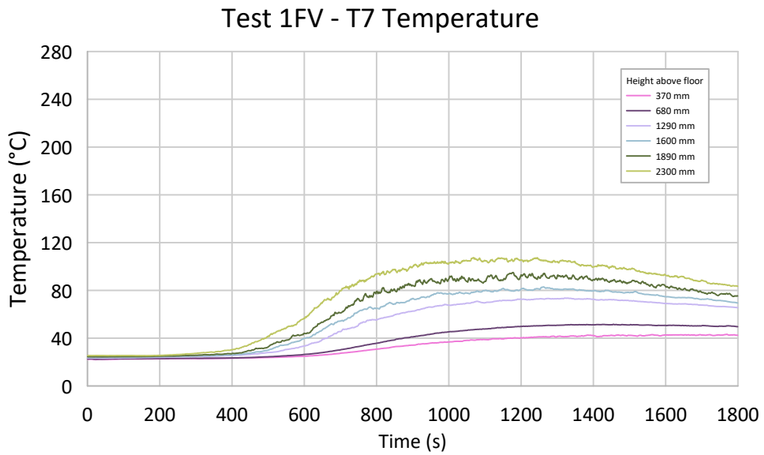

Test 4FV - T6 Temperature
Temperature (°C)
Time (s)
Height above floor
710 mm
1280 mm
1880 mm
2310 mm

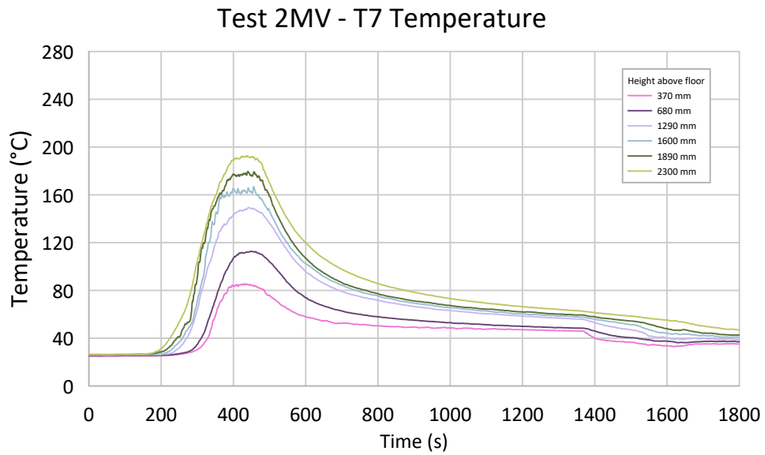

Test 6FV - T6 Temperature
Temperature (°C)
Time (s)
Height above floor
710 mm
1280 mm
1880 mm
2310 mm

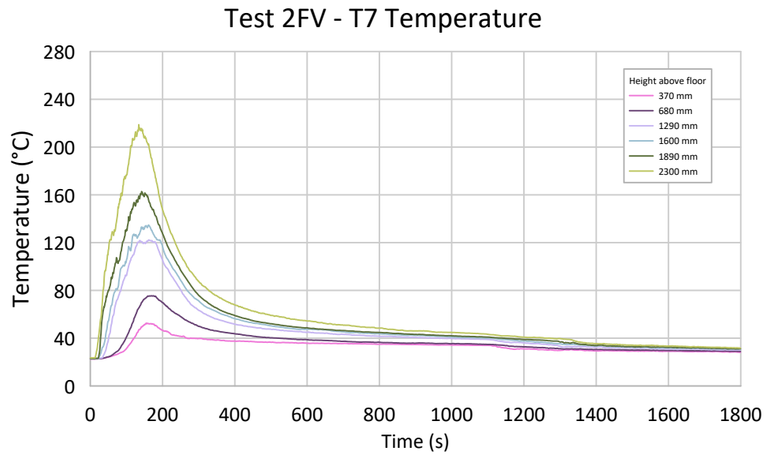

Test 7FV - T6 Temperature
Temperature (°C)
Time (s)
Height above floor
710 mm
1280 mm
1880 mm
2310 mm

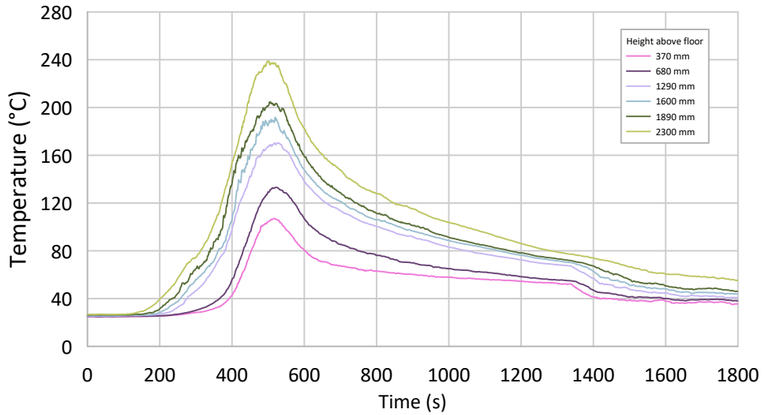

Test 9FV - T6 Temperature
Temperature (°C)
Time (s)
Height above floor
710 mm
1280 mm
1880 mm
2310 mm

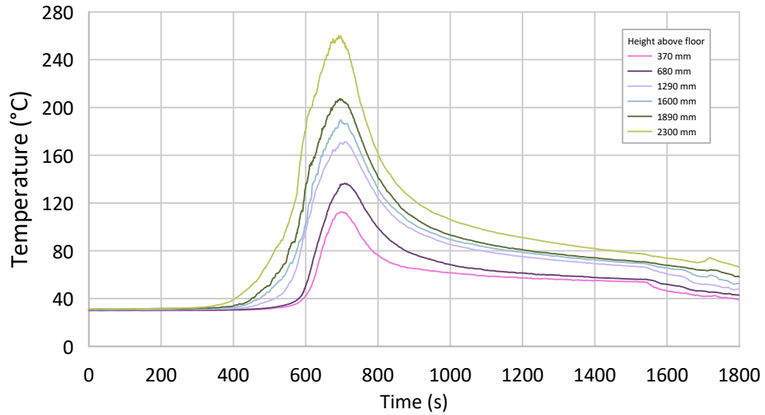

W3
D2
Main Floor
SW Room
Main
Floor
Corridor
Fire
Room
W2
W1
D1
HFG2
HFG0

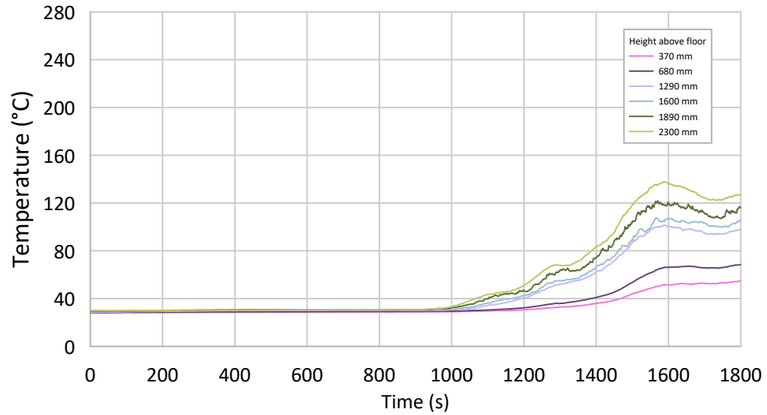

Test 1FV - T7 Temperature
Temperature (°C)
Time (s)
Height above floor
370 mm
680 mm
1290 mm
1600 mm
1890 mm
2300 mm

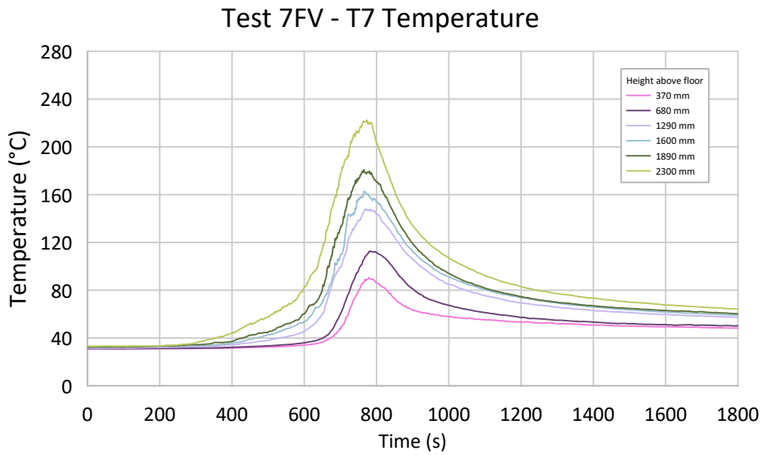

Test 2MV - T7 Temperature
Temperature (°C)
Time (s)
Height above floor
370 mm
680 mm
1290 mm
1600 mm
1890 mm
2300 mm

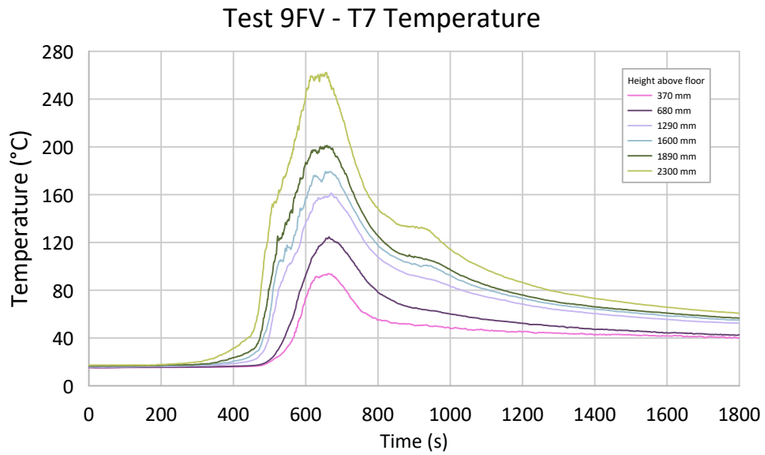

Test 2FV - T7 Temperature
Temperature (°C)
Time (s)
Height above floor
370 mm
680 mm
1290 mm
1600 mm
1890 mm
2300 mm

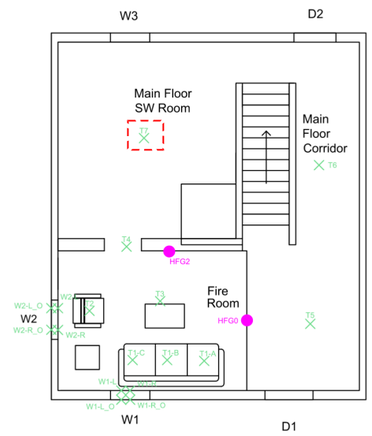

Test 3FV - T7 Temperature
Temperature (°C)
Time (s)
Height above floor
370 mm
680 mm
1290 mm
1600 mm
1890 mm
2300 mm

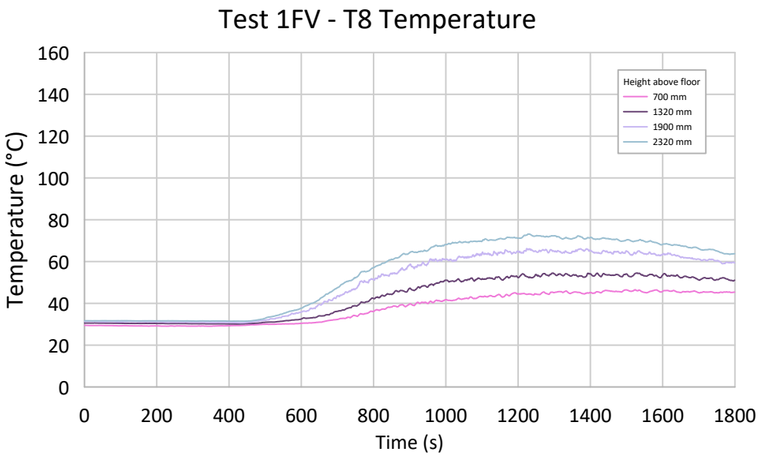

Test 4FV - T7 Temperature
Temperature (°C)
Time (s)
Height above floor
370 mm
680 mm
1290 mm
1600 mm
1890 mm
2300 mm

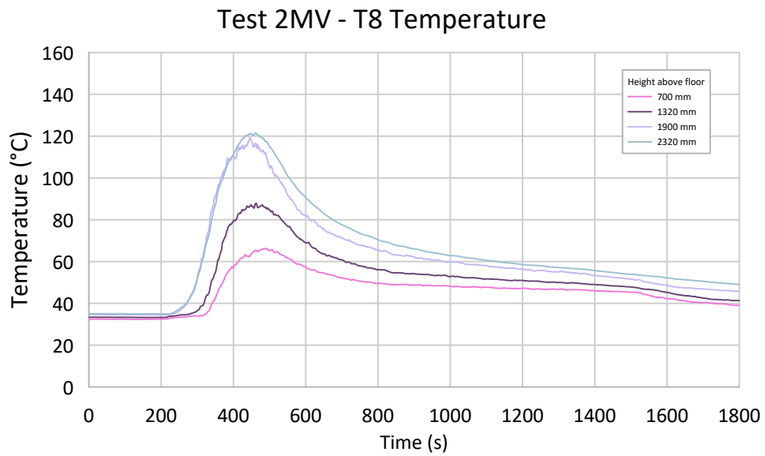

Test 6FV - T7 Temperature
Temperature (°C)
Time (s)
Height above floor
370 mm
680 mm
1290 mm
1600 mm
1890 mm
2300 mm

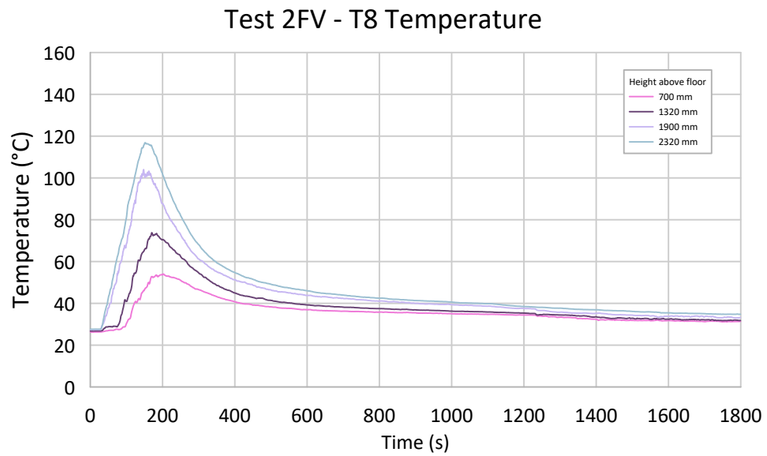

Test 7FV - T7 Temperature
Temperature (°C)
Time (s)
Height above floor
370 mm
680 mm
1290 mm
1600 mm
1890 mm
2300 mm

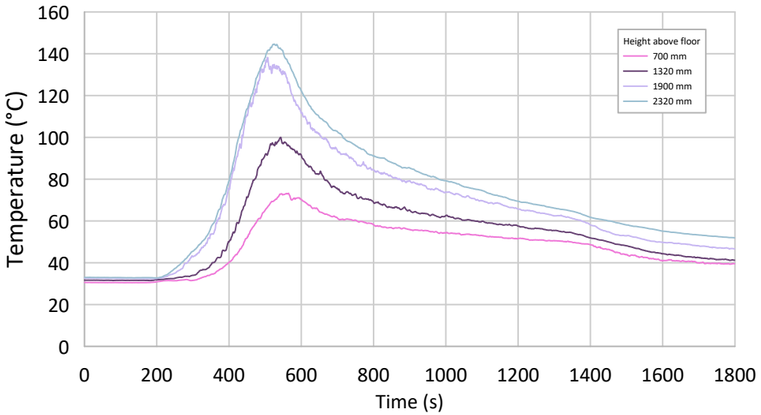

Test 9FV - T7 Temperature
Temperature (°C)
Time (s)
Height above floor
370 mm
680 mm
1290 mm
1600 mm
1890 mm
2300 mm

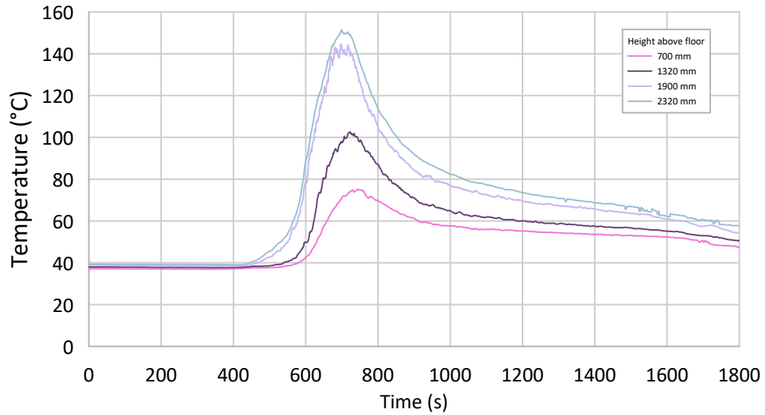

W3
D2
Main Floor SW Room
Main Floor Corridor
Fire Room
W2
W1
D1
HFG2
HFG0

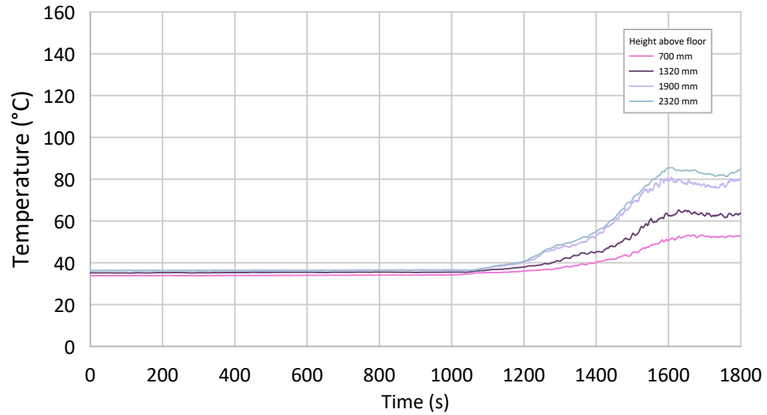

Test 1FV - T8 Temperature
Temperature (°C)
Time (s)
Height above floor
700 mm
1320 mm
1900 mm
2320 mm

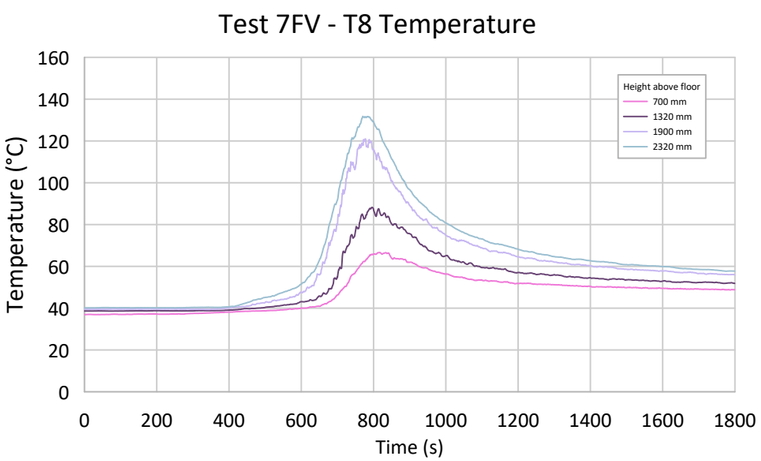

Test 2MV - T8 Temperature
Temperature (°C)
Time (s)
Height above floor
700 mm
1320 mm
1900 mm
2320 mm

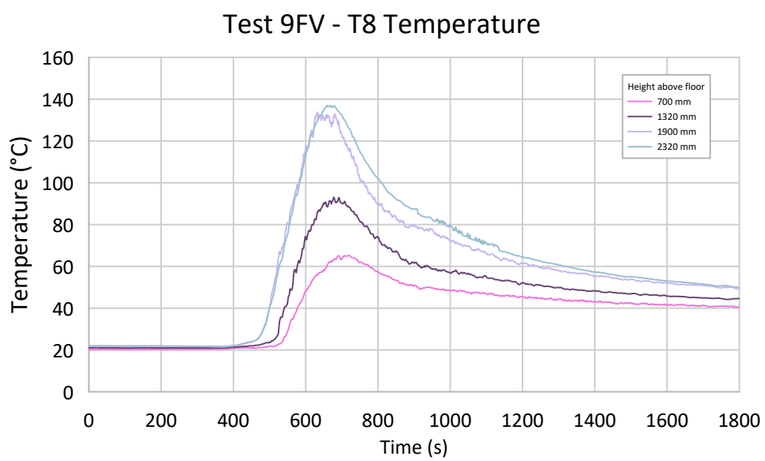

Test 2FV - T8 Temperature
Temperature (°C)
Time (s)
Height above floor
700 mm
1320 mm
1900 mm
2320 mm

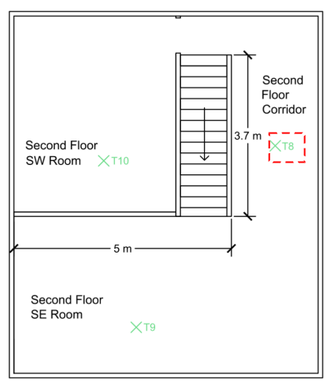

Test 3FV - T8 Temperature
Temperature (°C)
Time (s)
Height above floor
700 mm
1320 mm
1900 mm
2320 mm

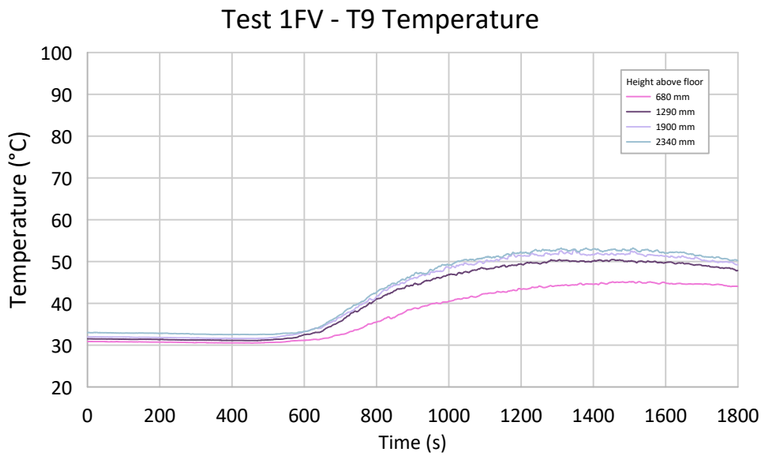

Test 4FV - T8 Temperature
Temperature (°C)
Time (s)
Height above floor
700 mm
1320 mm
1900 mm
2320 mm

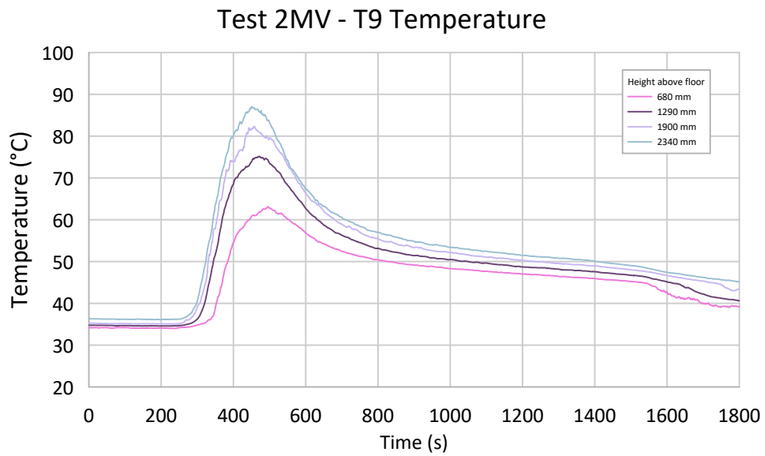

Test 6FV - T8 Temperature
Temperature (°C)
Time (s)
Height above floor
700 mm
1320 mm
1900 mm
2320 mm

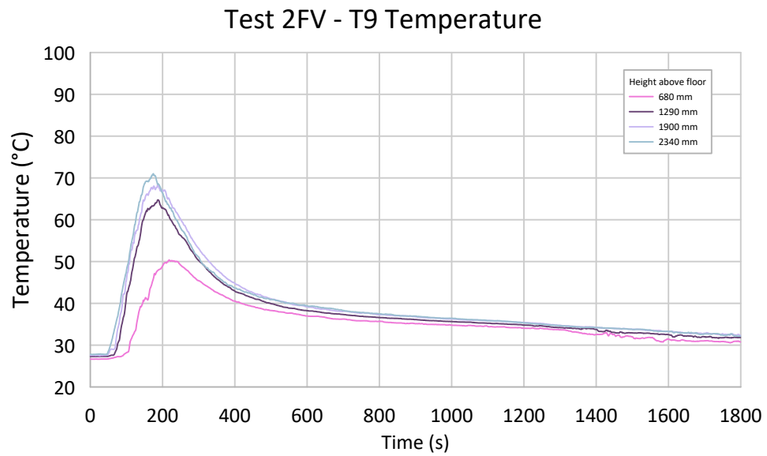

Test 7FV - T8 Temperature
Temperature (°C)
Time (s)
Height above floor
700 mm
1320 mm
1900 mm
2320 mm

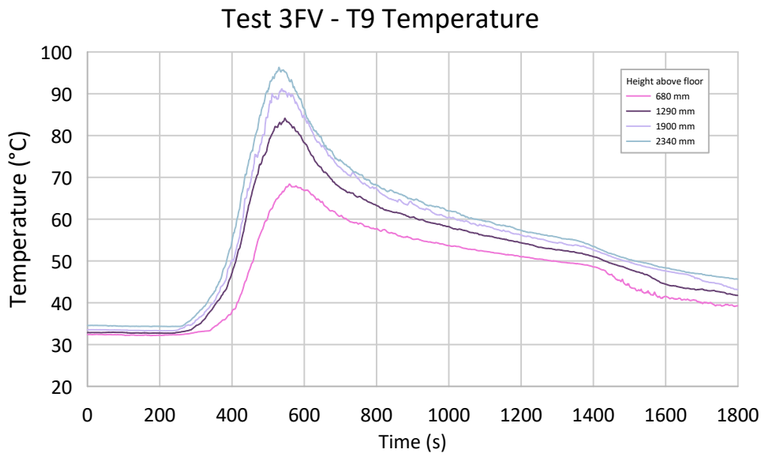

Test 9FV - T8 Temperature
Temperature (°C)
Time (s)
Height above floor
700 mm
1320 mm
1900 mm
2320 mm

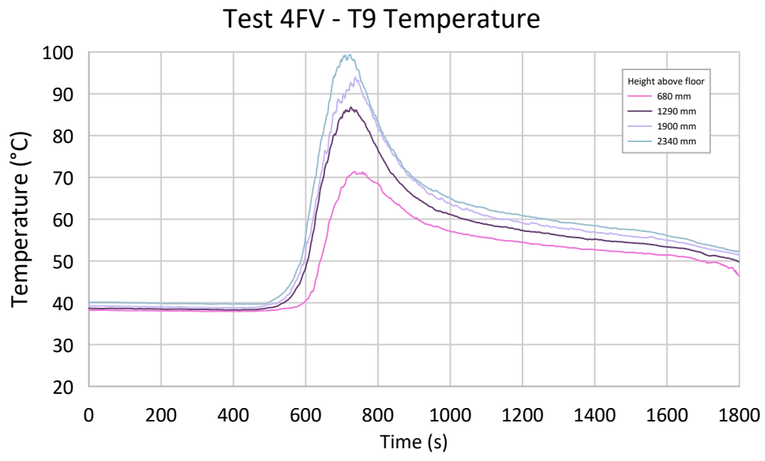

Second Floor Corridor
3.7 m
T8
Second Floor SW Room
T10
5 m
Second Floor SE Room
T9

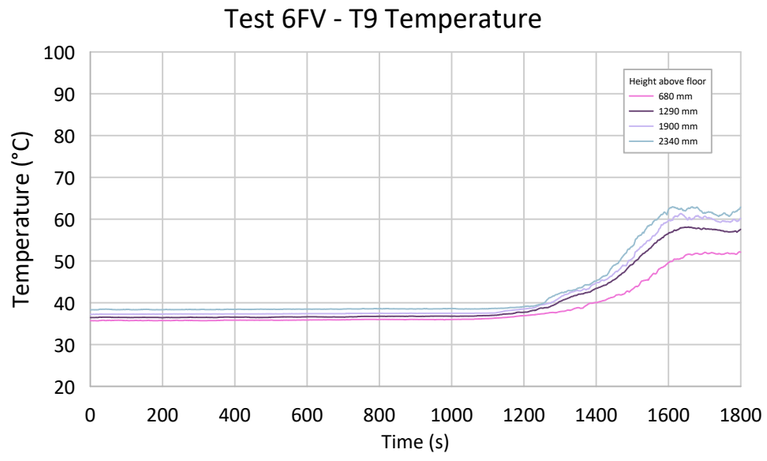

Test 1FV - T9 Temperature
Temperature (°C)
Time (s)
Height above floor
680 mm
1290 mm
1900 mm
2340 mm

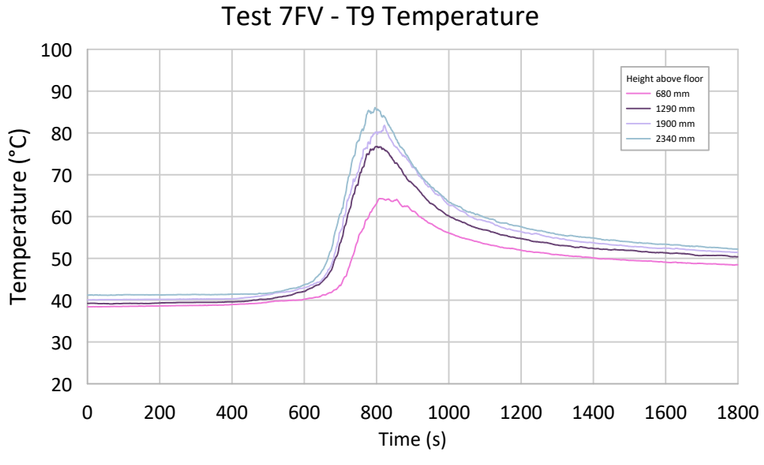

Test 2MV - T9 Temperature
Temperature (°C)
Time (s)
Height above floor
680 mm
1290 mm
1900 mm
2340 mm

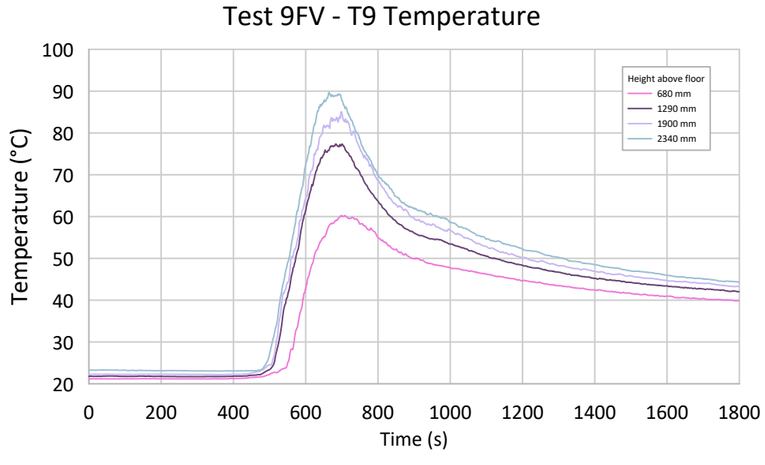

Test 2FV - T9 Temperature
Temperature (°C)
Time (s)
Height above floor
680 mm
1290 mm
1900 mm
2340 mm

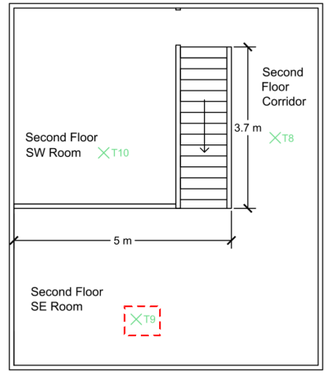

Test 3FV - T9 Temperature
Temperature (°C)
Time (s)
Height above floor
680 mm
1290 mm
1900 mm
2340 mm

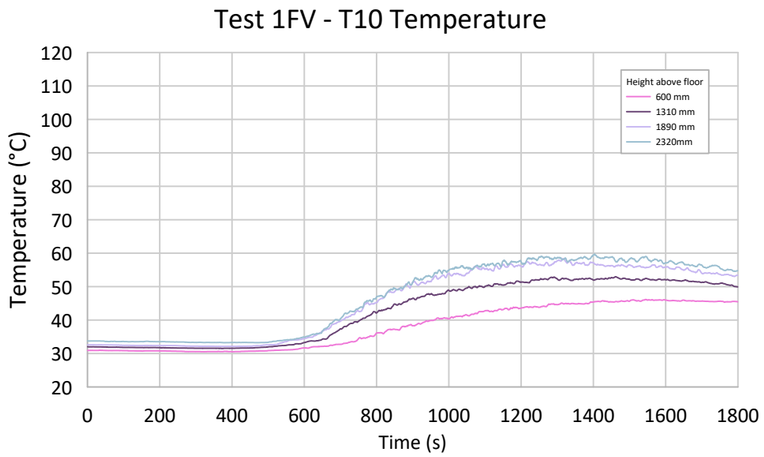

Test 4FV - T9 Temperature
Temperature (°C)
Time (s)
Height above floor
680 mm
1290 mm
1900 mm
2340 mm

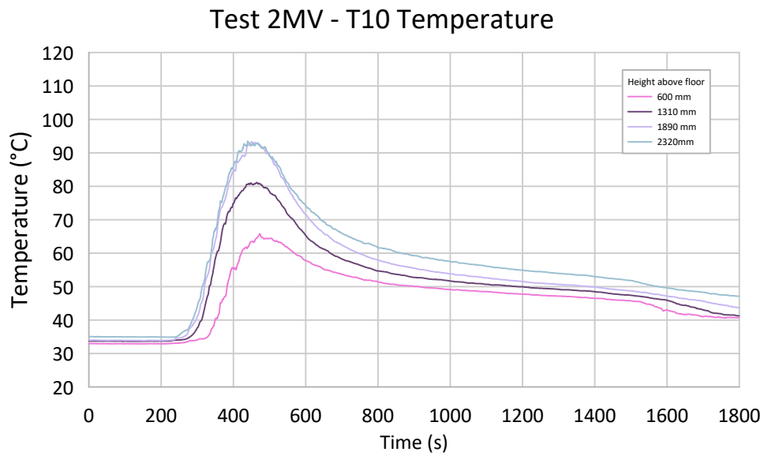

Test 6FV - T9 Temperature
Temperature (°C)
Time (s)
Height above floor
680 mm
1290 mm
1900 mm
2340 mm

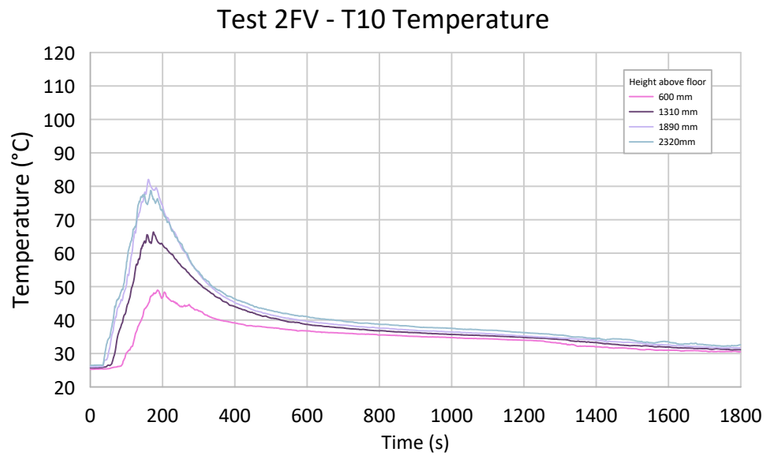

Test 7FV - T9 Temperature
Temperature (°C)
Time (s)
Height above floor
680 mm
1290 mm
1900 mm
2340 mm

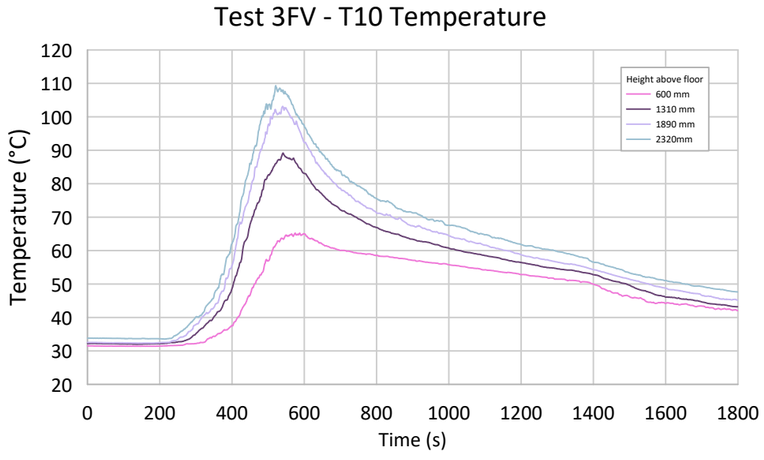

Test 9FV - T9 Temperature
Temperature (°C)
Time (s)
Height above floor
680 mm
1290 mm
1900 mm
2340 mm

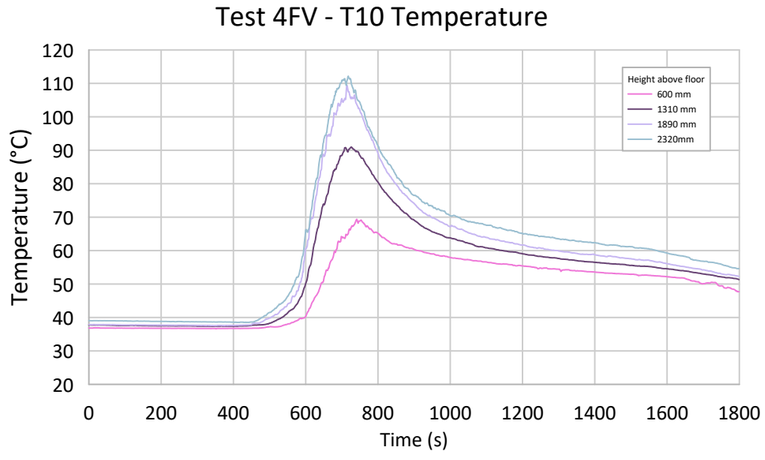

Second Floor Corridor
3.7 m
T8
Second Floor SW Room
T10
5 m
Second Floor SE Room
T9

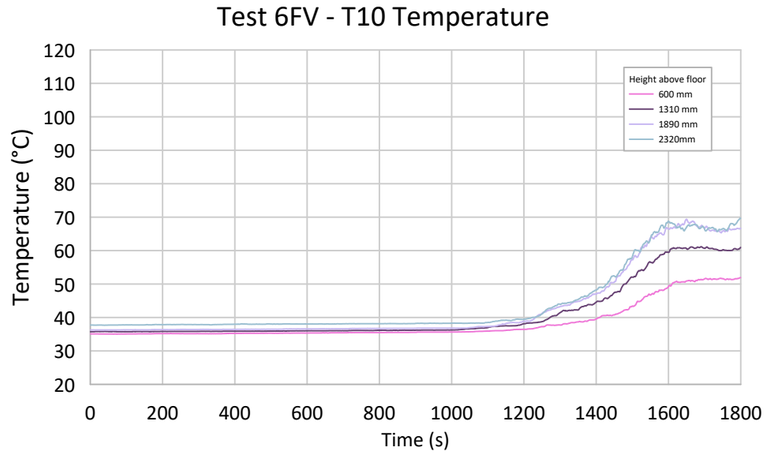

Test 1FV - T10 Temperature
Temperature (°C)
Time (s)
Height above floor
600 mm
1310 mm
1890 mm
2320mm

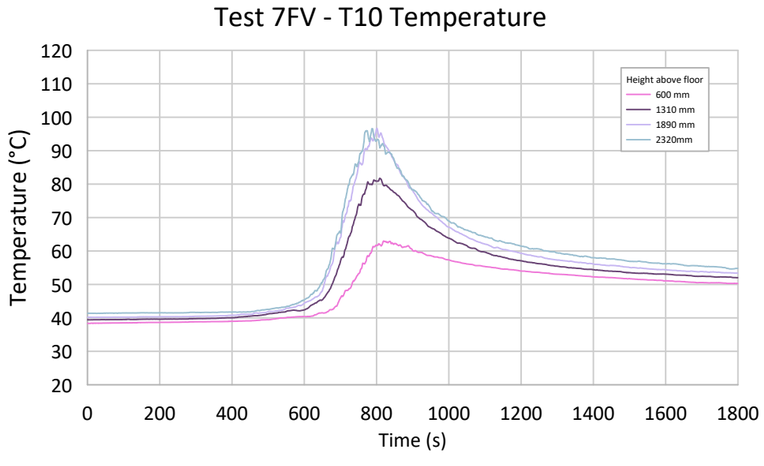

Test 2MV - T10 Temperature
Temperature (°C)
Time (s)
Height above floor
600 mm
1310 mm
1890 mm
2320mm

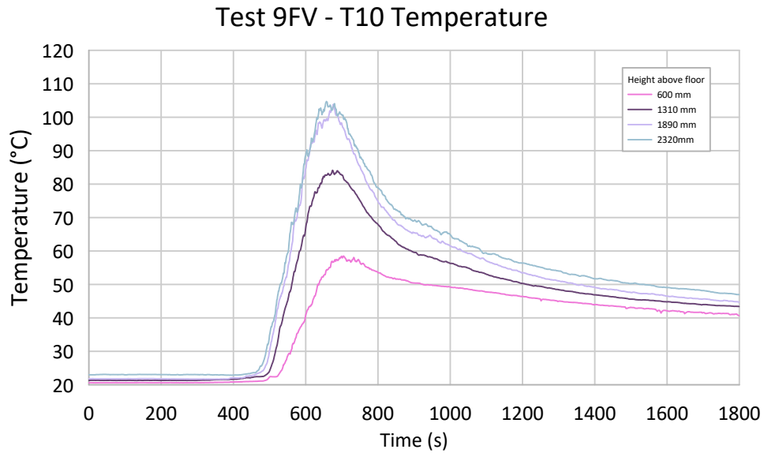

Test 2FV - T10 Temperature
Temperature (°C)
Time (s)
Height above floor
600 mm
1310 mm
1890 mm
2320mm

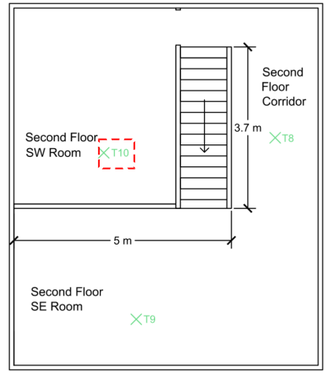

Test 3FV - T10 Temperature
Temperature (°C)
Time (s)
Height above floor
600 mm
1310 mm
1890 mm
2320mm


Test 4FV - T10 Temperature
Temperature (°C)
Time (s)
Height above floor
600 mm
1310 mm
1890 mm
2320mm


Test 6FV - T10 Temperature
Temperature (°C)
Time (s)
Height above floor
600 mm
1310 mm
1890 mm
2320mm


Test 7FV - T10 Temperature
Temperature (°C)
Time (s)
Height above floor
600 mm
1310 mm
1890 mm
2320mm

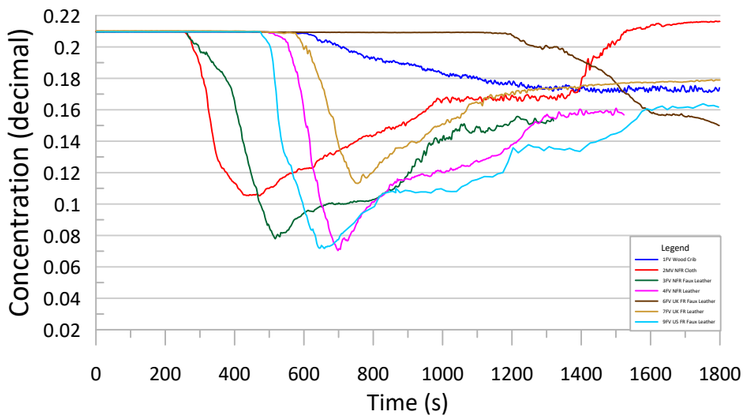

Test 9FV - T10 Temperature
Temperature (°C)
Time (s)
Height above floor
600 mm
1310 mm
1890 mm
2320mm


Second Floor Corridor
3.7 m
Second Floor SW Room
T10
T8
5 m
Second Floor SE Room
T9

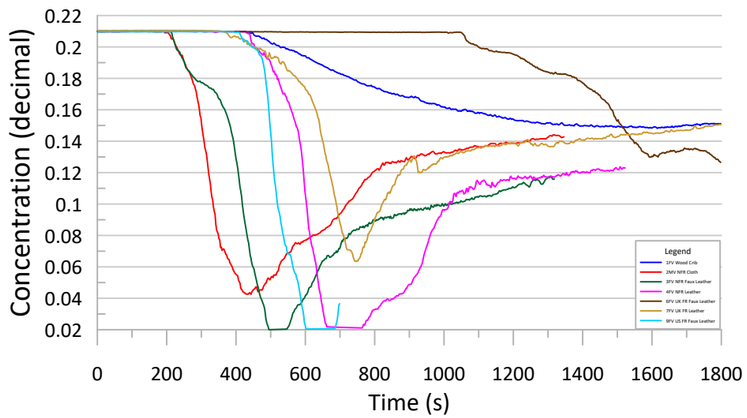
Appendix C:

Gas Instrumentation Stations (GIS) Graphs

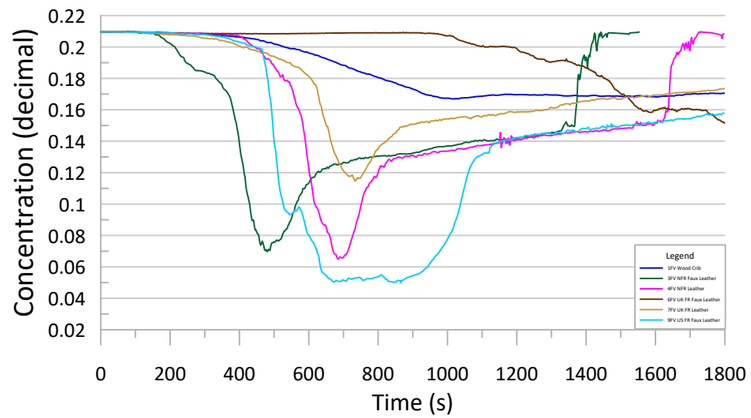
O2 Concentration at LBR 0.9 m GIS2



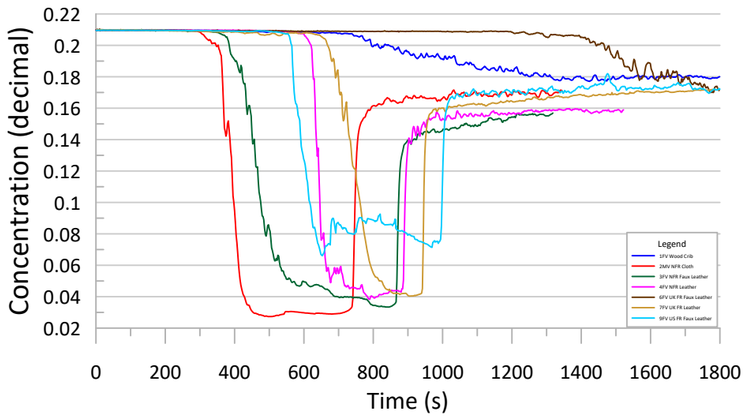
O2 Concentration at LSW 1.5 m GIS3



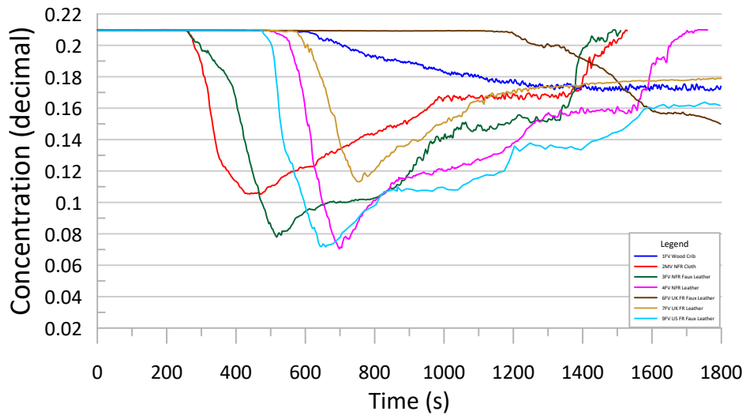
O2 Concentration at LHA 1.5 m GIS4



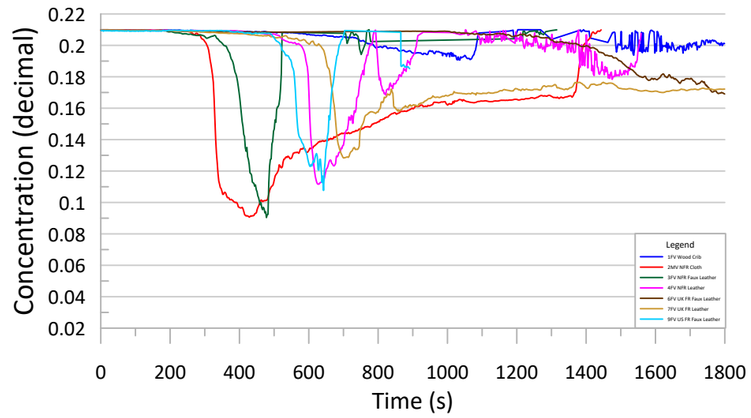
O2 Concentration at LBR 3ft 0.9 m GIS1



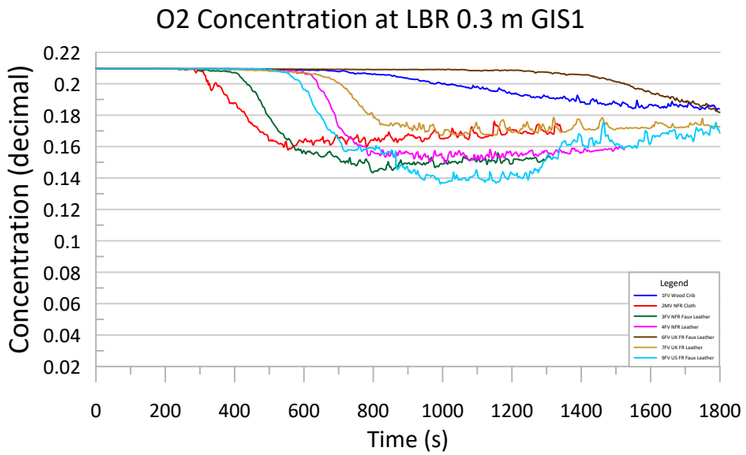
O2 Concentration at LSW 0.9 m GIS3



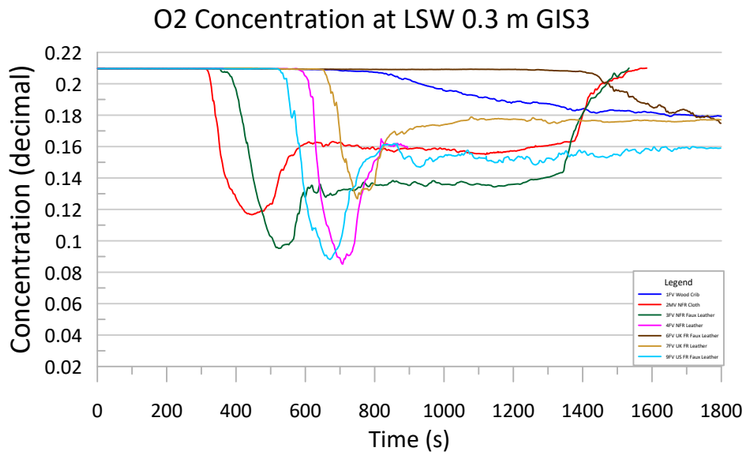
O2 Concentration at LHA 0.9 m GIS4



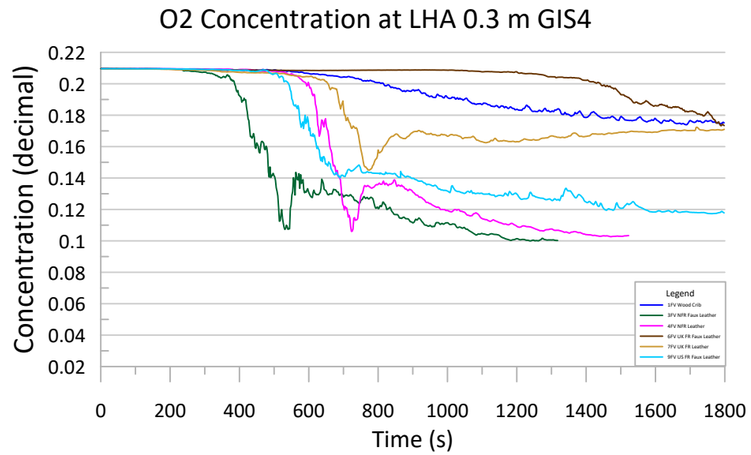
O2 Concentration at LBR 0.3 m GIS1

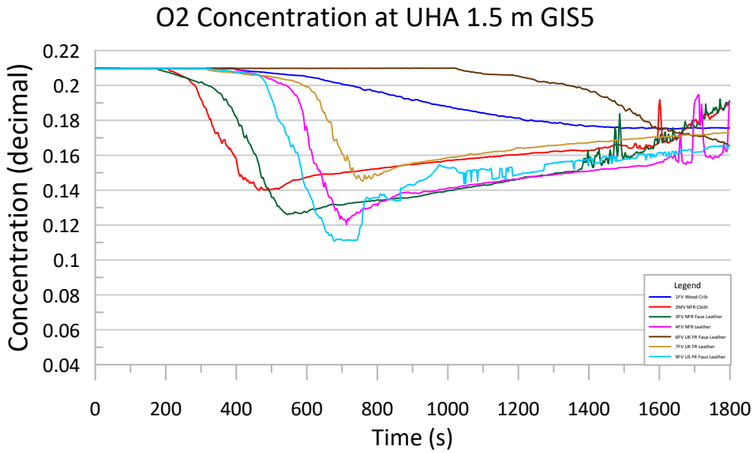


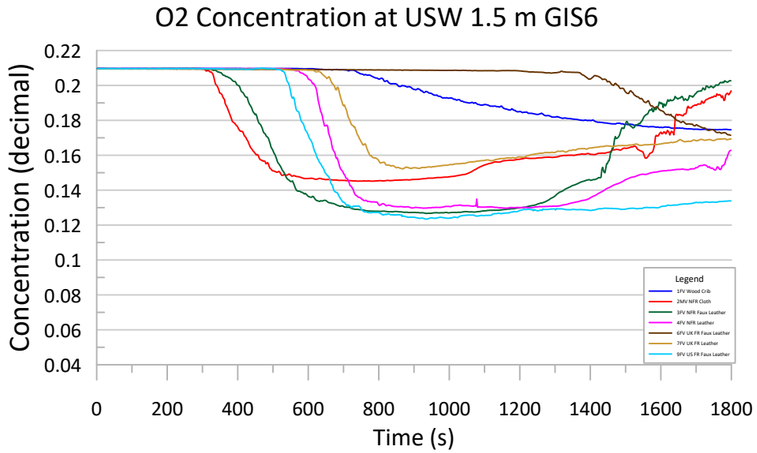
O2 Concentration at LSW 0.3 m GIS3

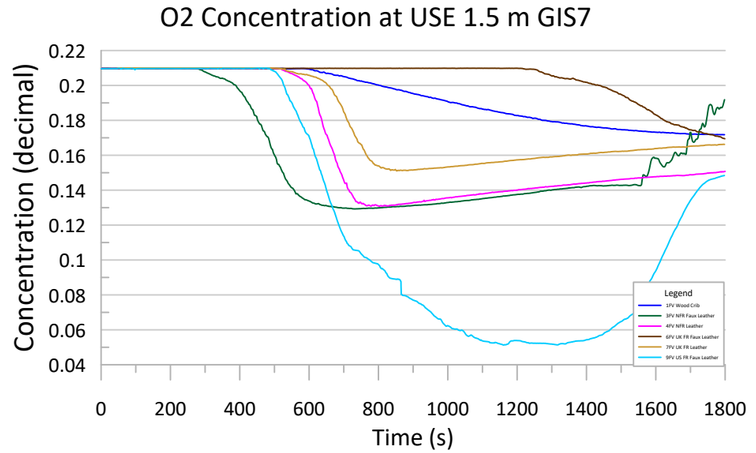


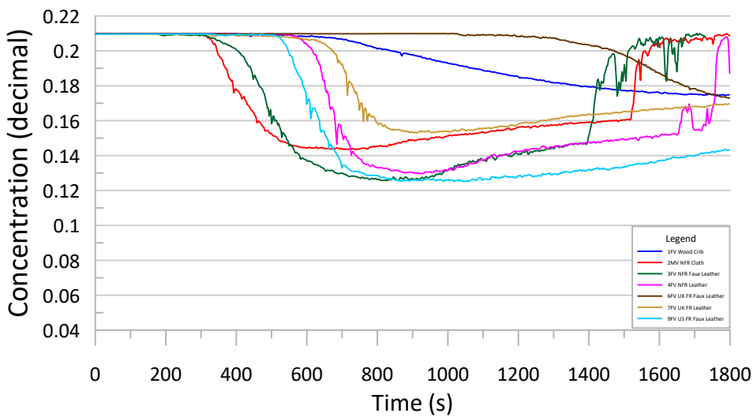
O2 Concentration at LHA 0.3 m GIS4

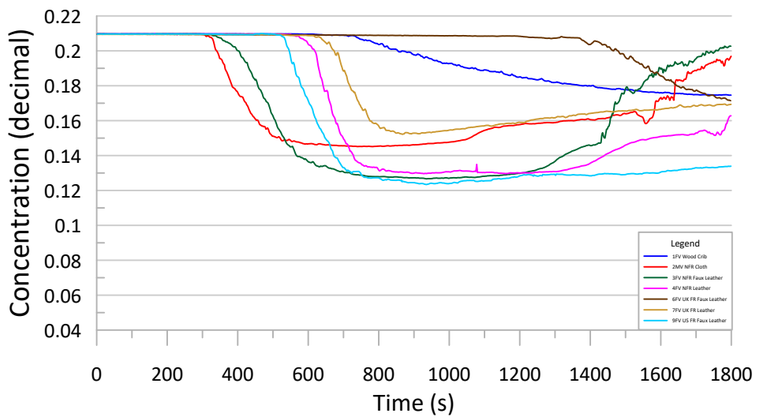


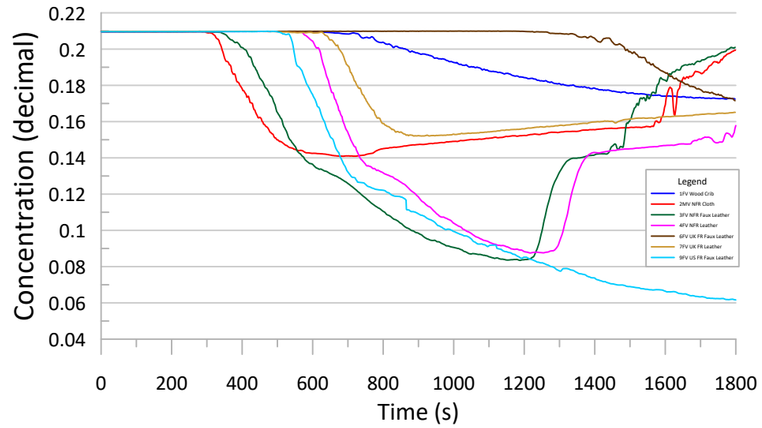

O2 Concentration at UHA 1.5 m GIS5
Concentration (decimal)
0.22
0.2
0.18
0.16
0.14
0.12
0.1
0.08
0.06
0.04
0
200
400
600
800
1000
1200
1400
1600
1800
Time (s)
Legend
1FV Wood Crib
2MV NFR Cloth
3FV NFR Faux Leather
4FV NFR Leather
6FV UK FR Faux Leather
7FV UK FR Leather
9FV US FR Faux Leather

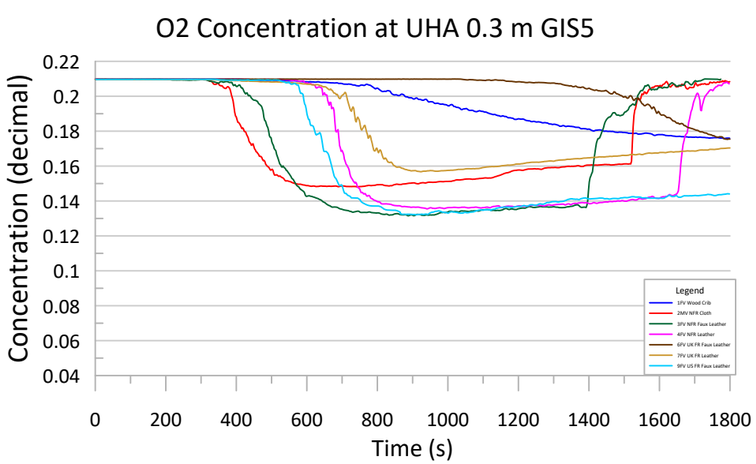

O2 Concentration at USW 1.5 m GIS6
Concentration (decimal)
0.22
0.2
0.18
0.16
0.14
0.12
0.1
0.08
0.06
0.04
0
200
400
600
800
1000
1200
1400
1600
1800
Time (s)
Legend
1FV Wood Crib
2MV NFR Cloth
3FV NFR Faux Leather
4FV NFR Leather
6FV UK FR Faux Leather
7FV UK FR Leather
9FV US FR Faux Leather

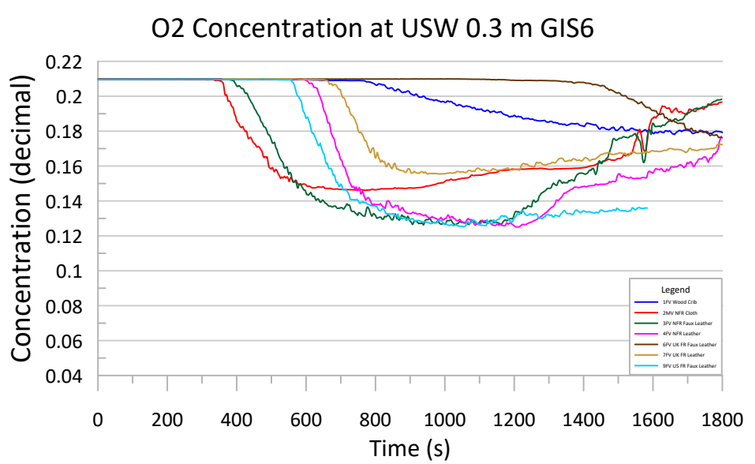

O2 Concentration at USE 1.5 m GIS7
Concentration (decimal)
0.22
0.2
0.18
0.16
0.14
0.12
0.1
0.08
0.06
0.04
0
200
400
600
800
1000
1200
1400
1600
1800
Time (s)
Legend
1FV Wood Crib
3FV NFR Faux Leather
4FV NFR Leather
6FV UK FR Faux Leather
7FV UK FR Leather
9FV US FR Faux Leather

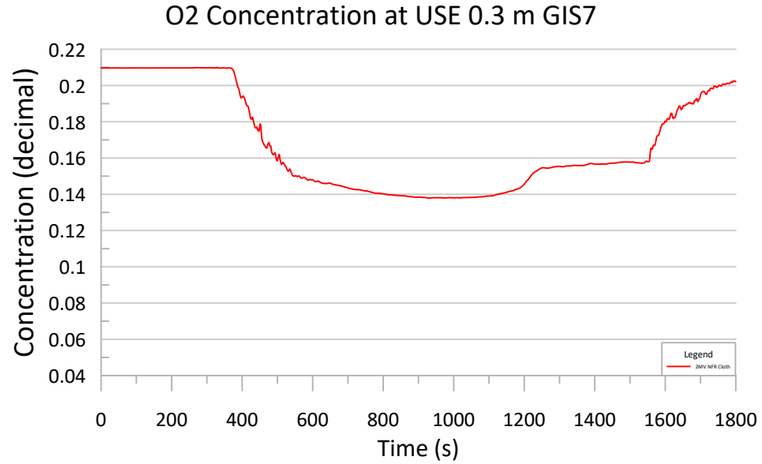

O2 Concentration at UHA 0.9 m GIS5
Concentration (decimal)
0.22
0.2
0.18
0.16
0.14
0.12
0.1
0.08
0.06
0.04
0
200
400
600
800
1000
1200
1400
1600
1800
Time (s)
Legend
1FV Wood Crib
2MV NFR Cloth
3FV NFR Faux Leather
4FV NFR Leather
6FV UK FR Faux Leather
7FV UK FR Leather
9FV US FR Faux Leather


O2 Concentration at USW 0.9 m GIS6
Concentration (decimal)
0.22
0.2
0.18
0.16
0.14
0.12
0.1
0.08
0.06
0.04
0
200
400
600
800
1000
1200
1400
1600
1800
Time (s)
Legend
1FV Wood Crib
2MV NFR Cloth
3FV NFR Faux Leather
4FV NFR Leather
6FV UK FR Faux Leather
7FV UK FR Leather
9FV US FR Faux Leather

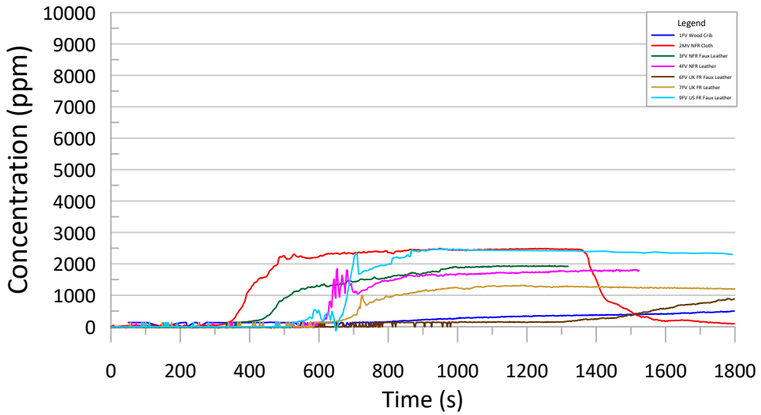

O2 Concentration at USE 0.9 m GIS7
Concentration (decimal)
0.22
0.2
0.18
0.16
0.14
0.12
0.1
0.08
0.06
0.04
0
200
400
600
800
1000
1200
1400
1600
1800
Time (s)
Legend
1FV Wood Crib
2MV NFR Cloth
3FV NFR Faux Leather
4FV NFR Leather
6FV UK FR Faux Leather
7FV UK FR Leather
9FV US FR Faux Leather


O2 Concentration at UHA 0.3 m GIS5
Concentration (decimal)
0.22
0.2
0.18
0.16
0.14
0.12
0.1
0.08
0.06
0.04
0
200
400
600
800
1000
1200
1400
1600
1800
Time (s)
Legend
1FV Wood Crib
2MV NFR Cloth
3FV NFR Faux Leather
4FV NFR Leather
6FV UK FR Faux Leather
7FV UK FR Leather
9FV US FR Faux Leather

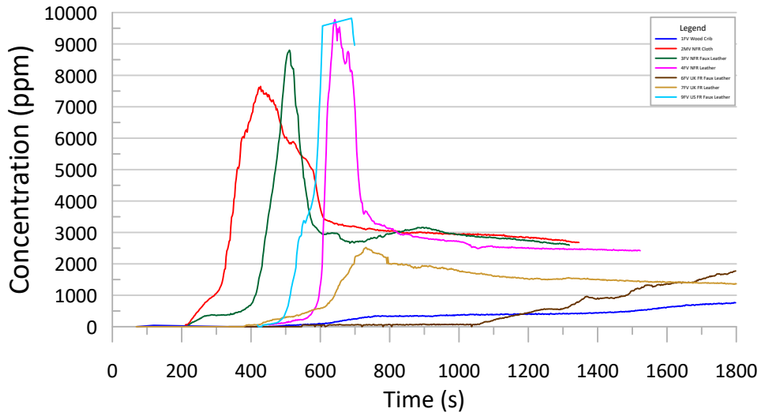

O2 Concentration at USW 0.3 m GIS6
Concentration (decimal)
0.22
0.2
0.18
0.16
0.14
0.12
0.1
0.08
0.06
0.04
0
200
400
600
800
1000
1200
1400
1600
1800
Time (s)
Legend
1FV Wood Crib
2MV NFR Cloth
3FV NFR Faux Leather
4FV NFR Leather
6FV UK FR Faux Leather
7FV UK FR Leather
9FV US FR Faux Leather


O2 Concentration at USE 0.3 m GIS7
Concentration (decimal)
0.22
0.2
0.18
0.16
0.14
0.12
0.1
0.08
0.06
0.04
0
200
400
600
800
1000
1200
1400
1600
1800
Time (s)
Legend
2MV NFR Cloth

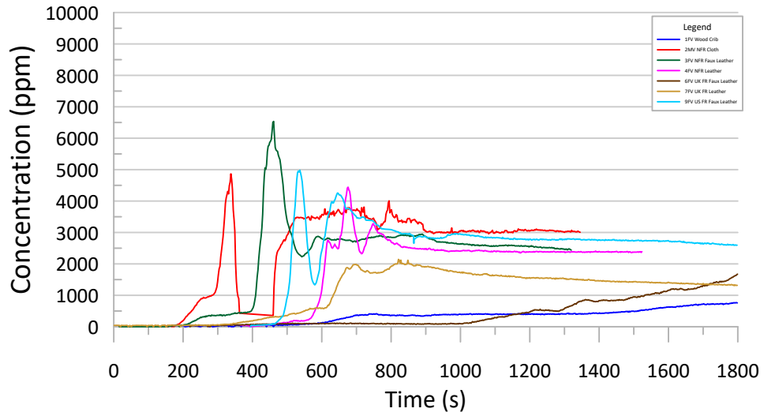
CO Concentration at LBR 0.9 GIS2



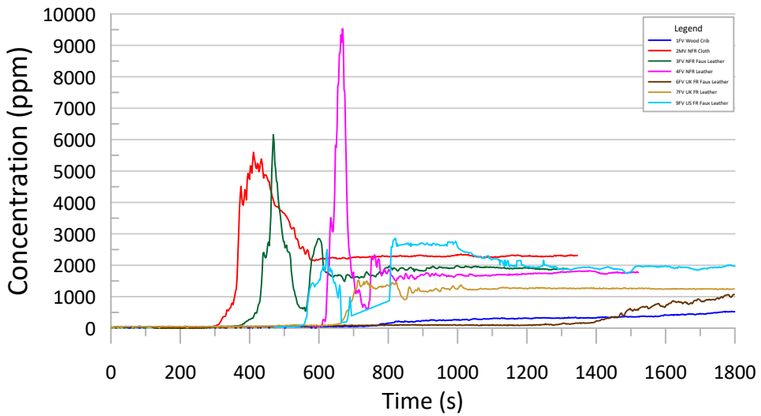
CO Concentration at LSW 1.5 m GIS3



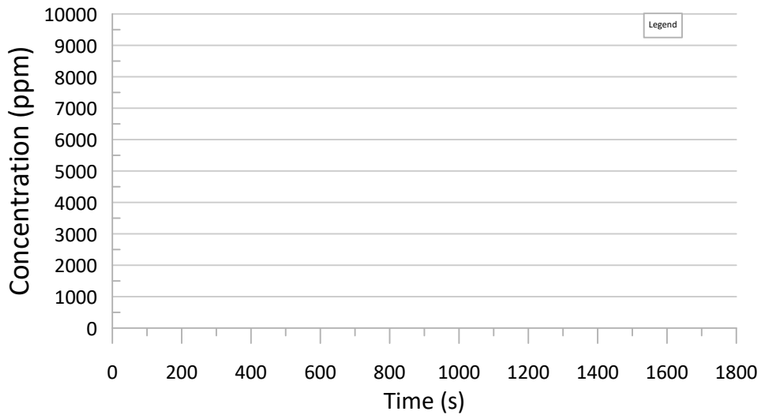
CO Concentration at LHA 1.5m GIS4



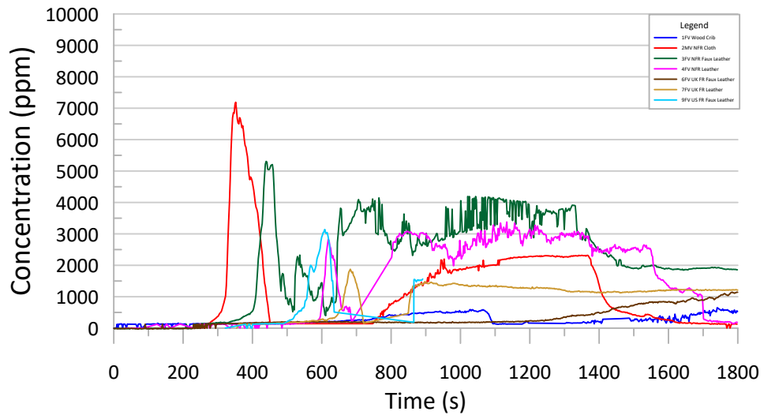
CO Concentration at LBR 0.9 m GIS1



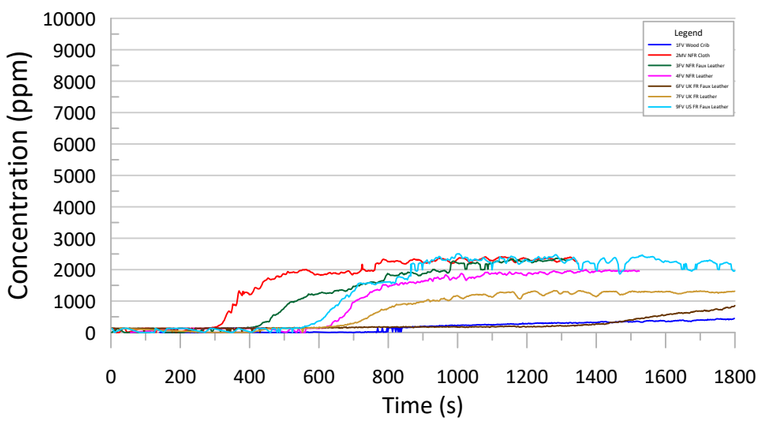
CO Concentration at LSW 0.9 m GIS3



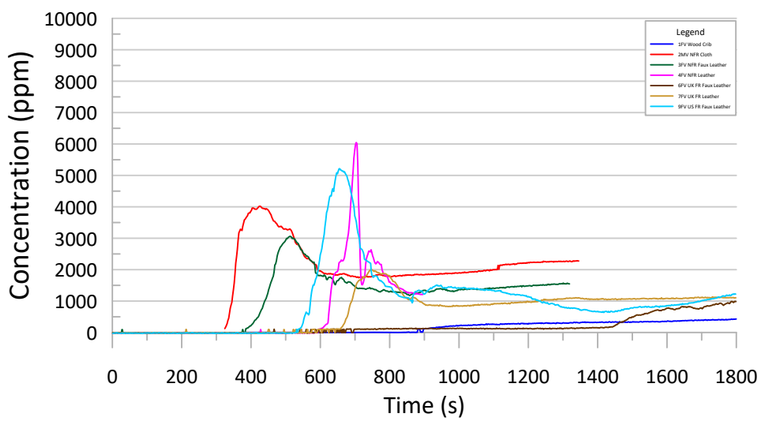
CO Concentration at LHA 0.9 m GIS4



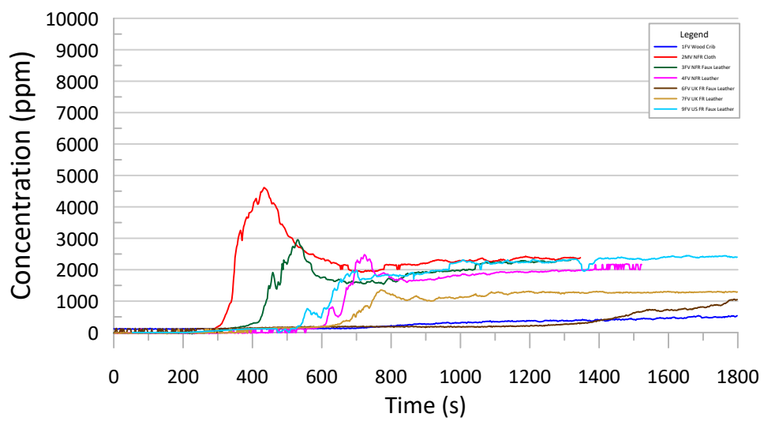
CO Concentration at LBR 0.3 m GIS1



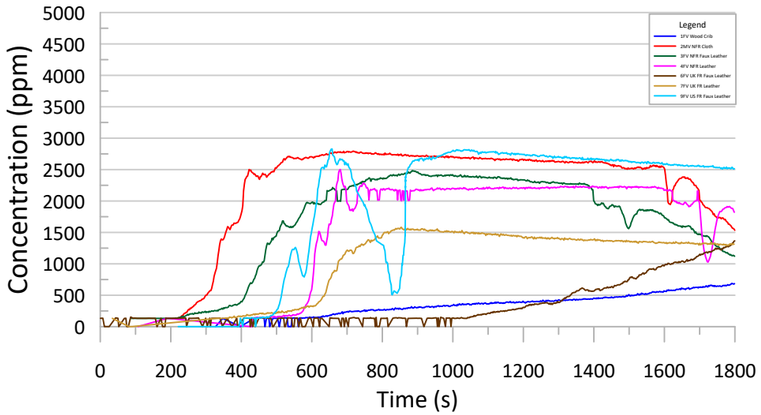
CO Concentration at LSW 0.3 m GIS3



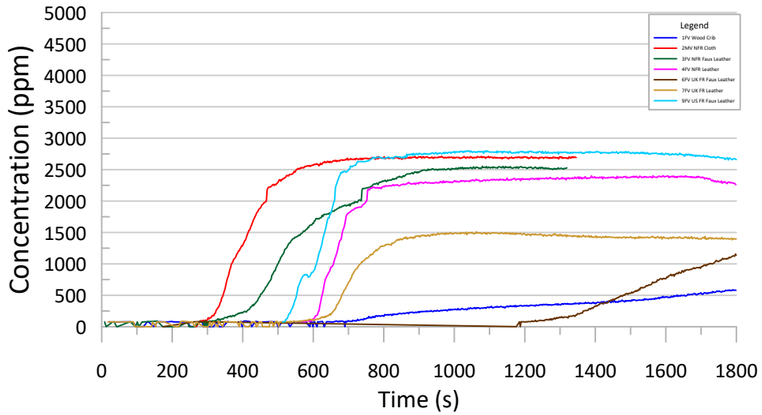
CO Concentration at LHA 0.3 m GIS4



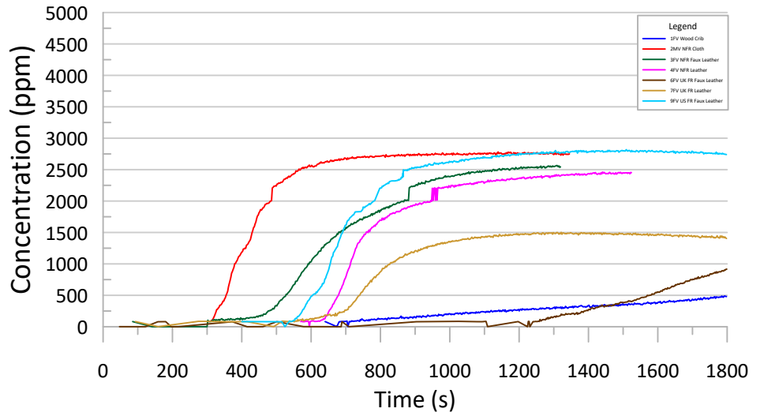
CO Concentration at UHA 1.5 m GIS5



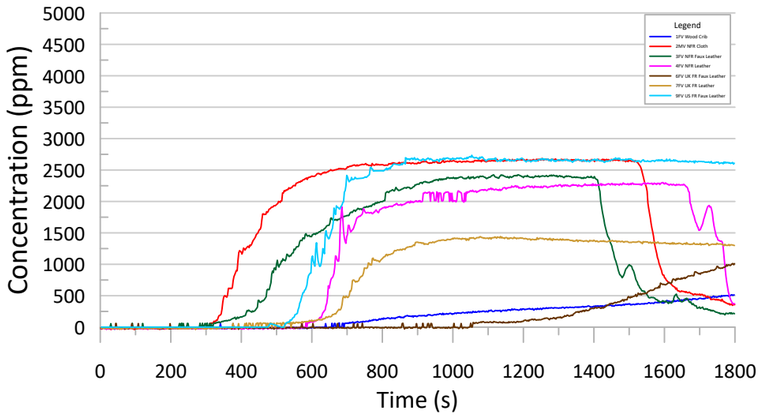
CO Concentration at USW 1.5 m GIS6



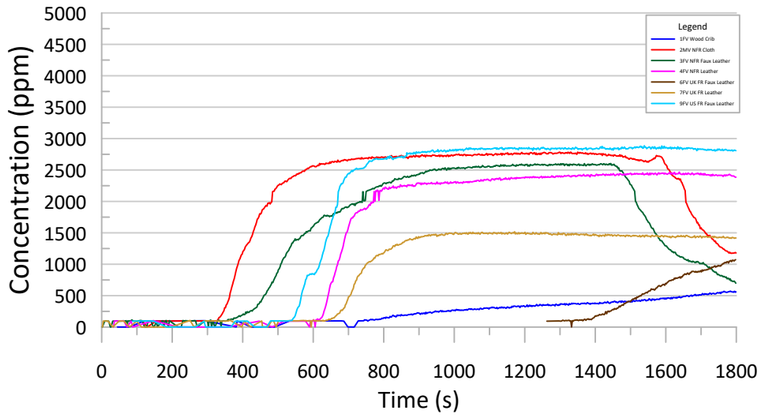
CO Concentration at USE 1.5 m GIS7



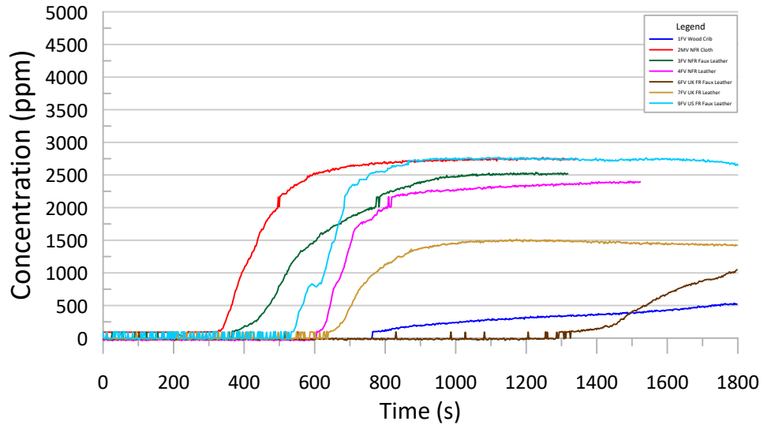
CO Concentration at UHA 0.9 GIS5



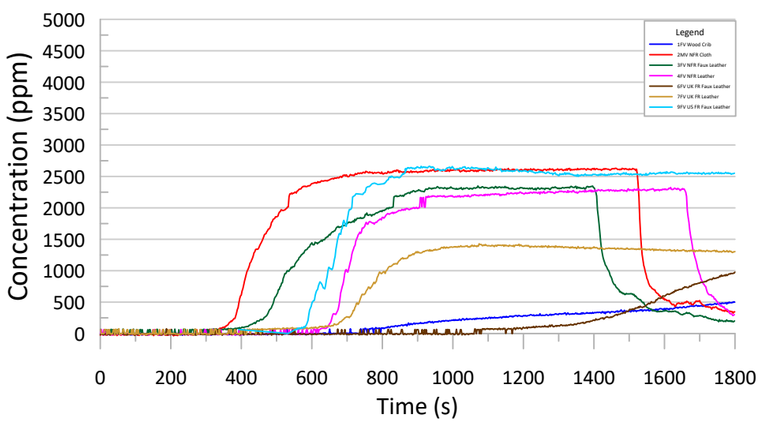
CO Concentration at USW 0.9 GIS6



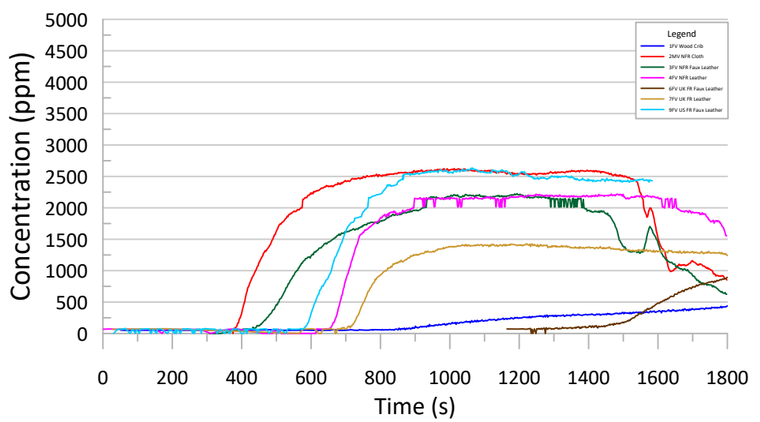
CO Concentration at USE 0.9 GIS7



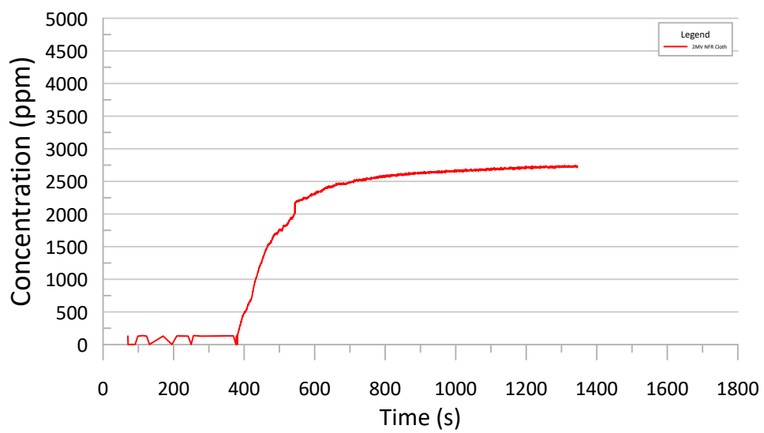
CO Concentration at UHA 0.3 m GIS5



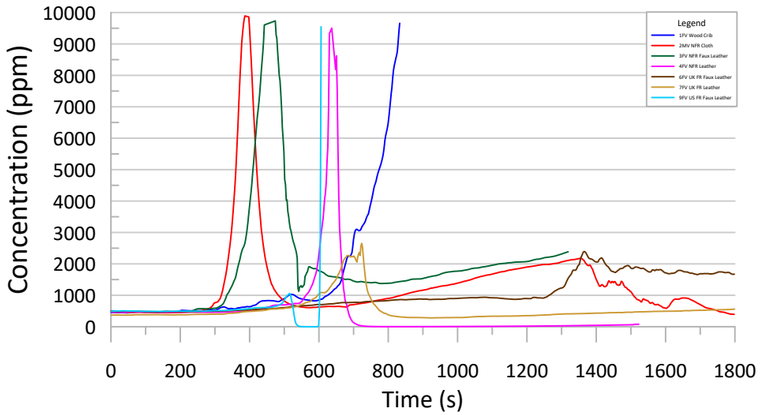
CO Concentration at USW 0.3 m GIS6



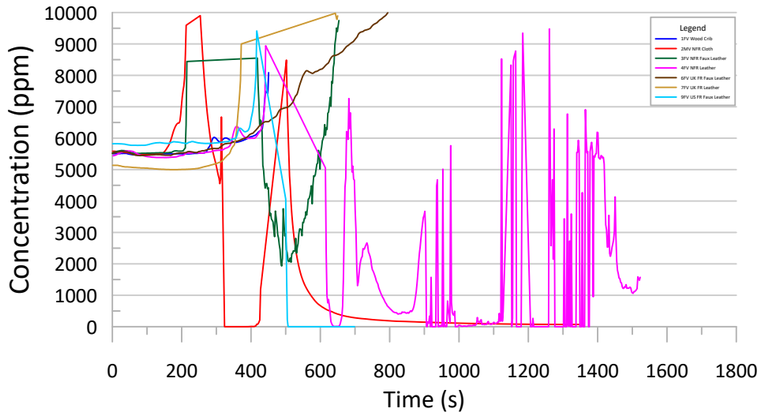
CO Concentration at USE 0.3 m GIS7



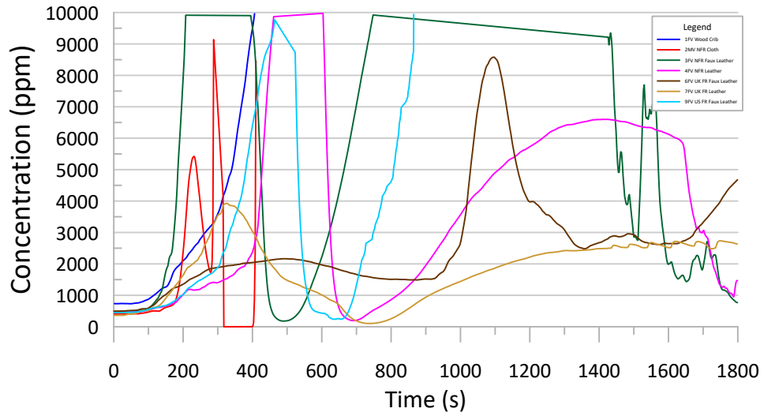
CO2 Concentration at LBR 0.9 GIS2



CO2 Concentration at LSW 1.5 GIS3



CO2 Concentration at LHA 1.5 GIS4



CO2 Concentration at LBR 0.9 GIS1

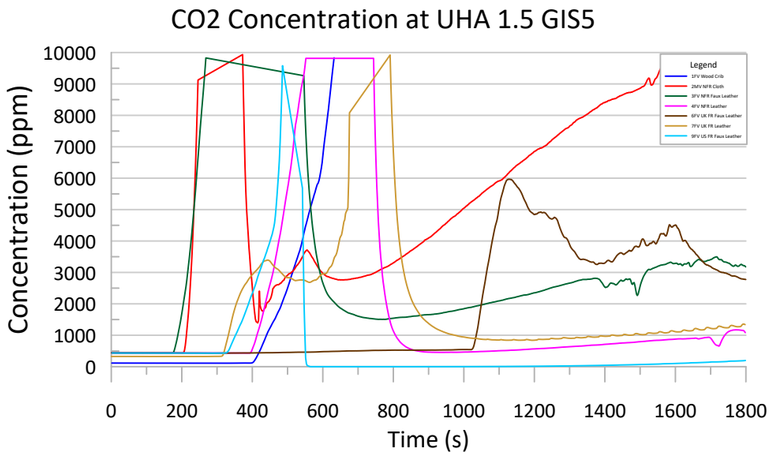
CO2 Concentration at LSW 0.9 GIS3

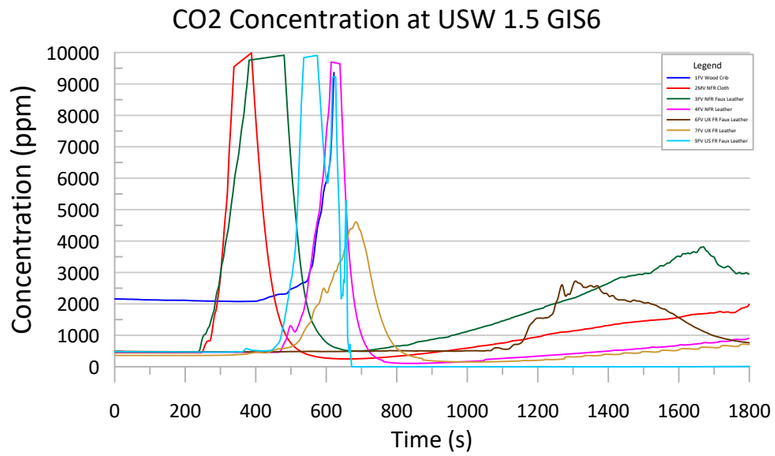
CO2 Concentration at LHA 0.9 GIS4

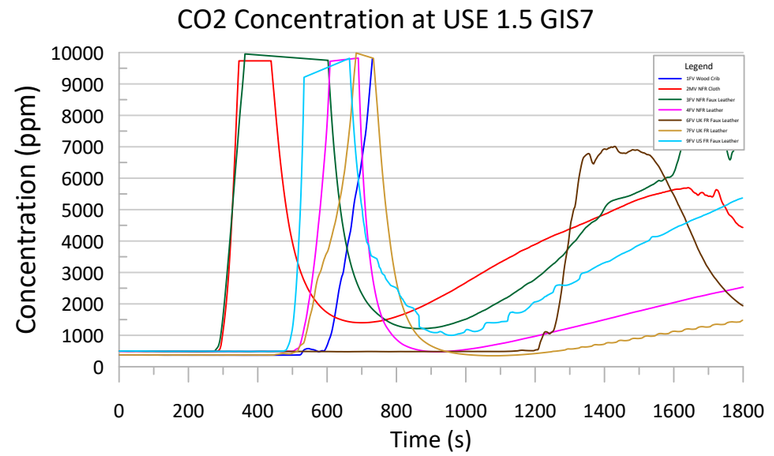
CO2 Concentration at LBR 0.3 m GIS1

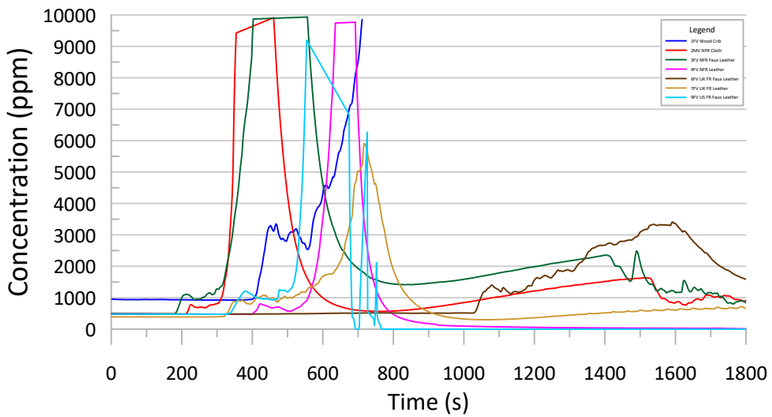
CO2 Concentration at LSW 0.3 m GIS3

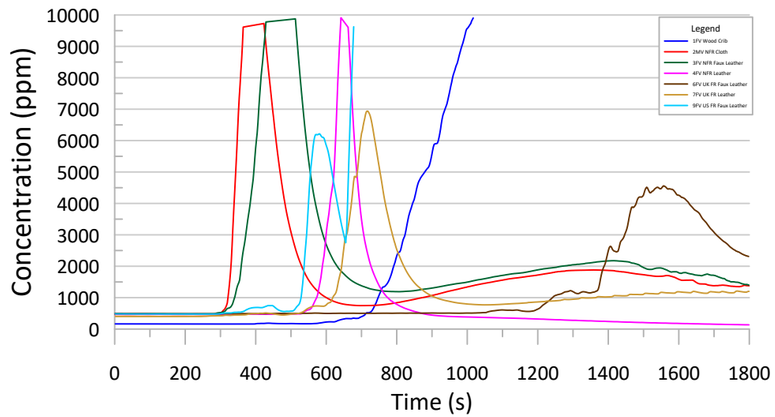
CO2 Concentration at LHA 0.3 m GIS4

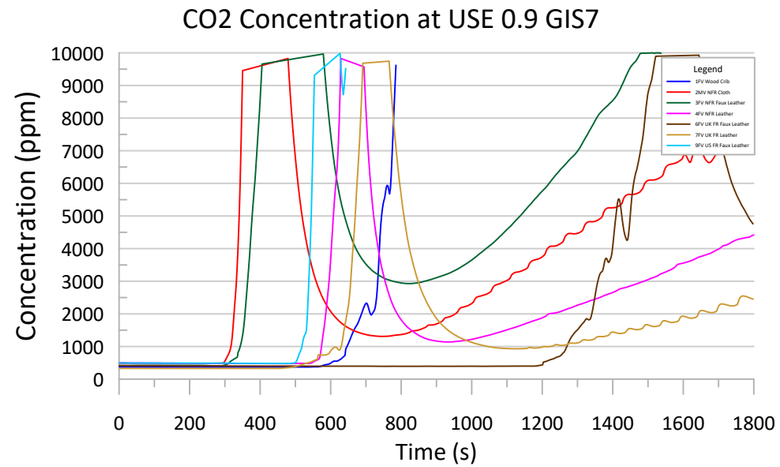

CO2 Concentration at UHA 1.5 GIS5
Concentration (ppm)
Time (s)
Legend
1FV Wood Crib
2MV NFR Cloth
3FV NFR Faux Leather
4FV NFR Leather
6FV UK FR Faux Leather
7FV UK FR Leather
9FV US FR Faux Leather

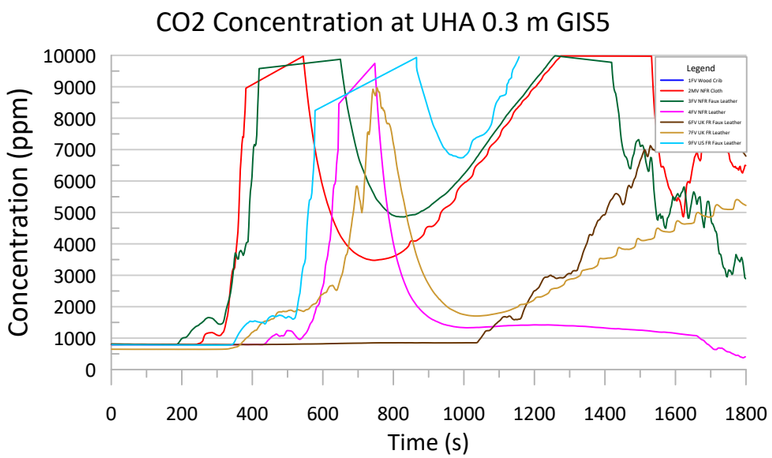

CO2 Concentration at USW 1.5 GIS6
Concentration (ppm)
Time (s)
Legend
1FV Wood Crib
2MV NFR Cloth
3FV NFR Faux Leather
4FV NFR Leather
6FV UK FR Faux Leather
7FV UK FR Leather
9FV US FR Faux Leather

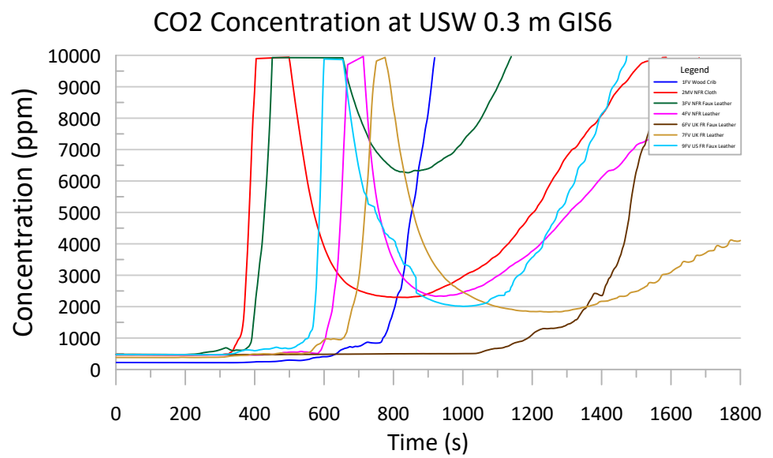

CO2 Concentration at USE 1.5 GIS7
Concentration (ppm)
Time (s)
Legend
1FV Wood Crib
2MV NFR Cloth
3FV NFR Faux Leather
4FV NFR Leather
6FV UK FR Faux Leather
7FV UK FR Leather
9FV US FR Faux Leather

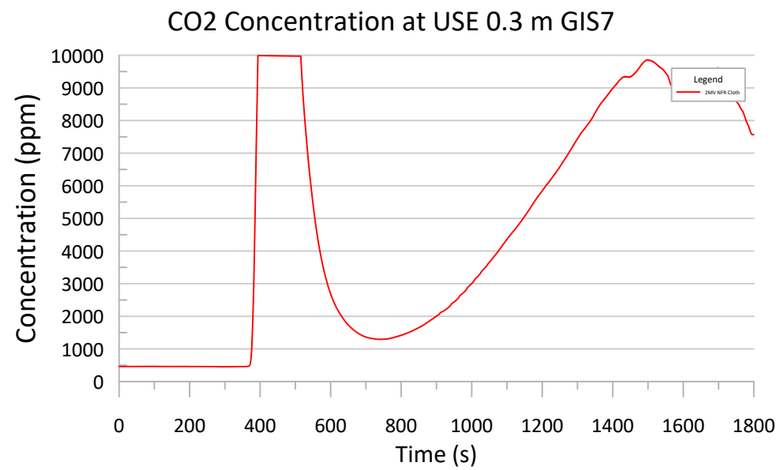

CO2 Concentration at UHA 0.9 GIS5
Concentration (ppm)
Time (s)
Legend
1FV Wood Crib
2MV NFR Cloth
3FV NFR Faux Leather
4FV NFR Leather
6FV UK FR Faux Leather
7FV UK FR Leather
9FV US FR Faux Leather


CO2 Concentration at USW 0.9 GIS6
Concentration (ppm)
Time (s)
Legend
1FV Wood Crib
2MV NFR Cloth
3FV NFR Faux Leather
4FV NFR Leather
6FV UK FR Faux Leather
7FV UK FR Leather
9FV US FR Faux Leather

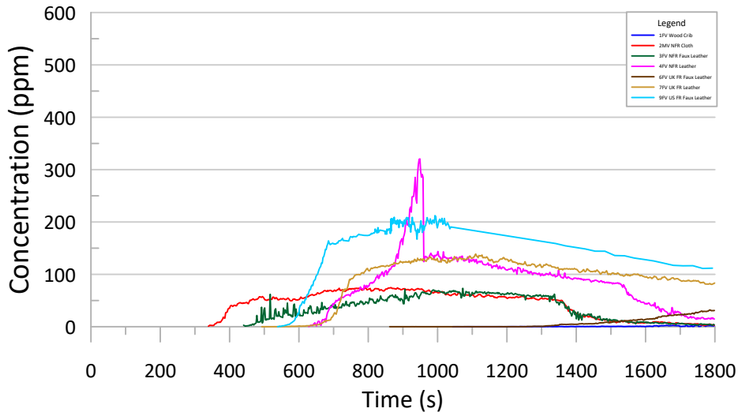

CO2 Concentration at USE 0.9 GIS7
Concentration (ppm)
Time (s)
Legend
1FV Wood Crib
2MV NFR Cloth
3FV NFR Faux Leather
4FV NFR Leather
6FV UK FR Faux Leather
7FV UK FR Leather
9FV US FR Faux Leather


CO2 Concentration at UHA 0.3 m GIS5
Concentration (ppm)
Time (s)
Legend
1FV Wood Crib
2MV NFR Cloth
3FV NFR Faux Leather
4FV NFR Leather
6FV UK FR Faux Leather
7FV UK FR Leather
9FV US FR Faux Leather

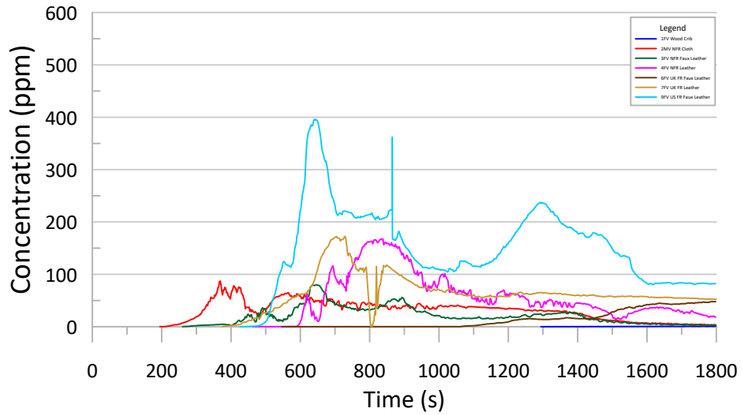

CO2 Concentration at USW 0.3 m GIS6
Concentration (ppm)
Time (s)
Legend
1FV Wood Crib
2MV NFR Cloth
3FV NFR Faux Leather
4FV NFR Leather
6FV UK FR Faux Leather
7FV UK FR Leather
9FV US FR Faux Leather


CO2 Concentration at USE 0.3 m GIS7
Concentration (ppm)
Time (s)
Legend
2MV NFR Cloth

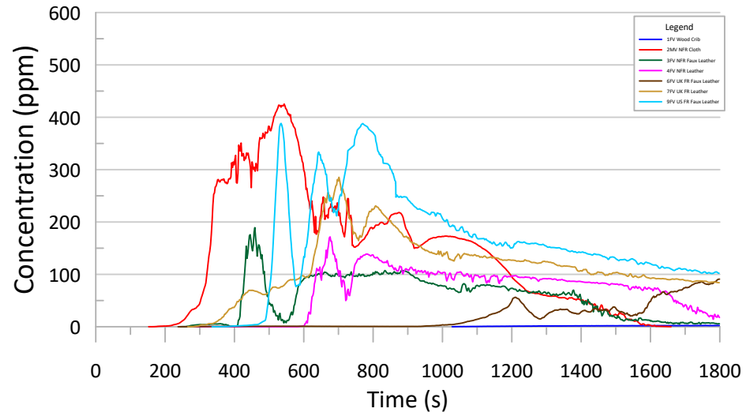
HCN Concentration at LBR 0.9 GIS2



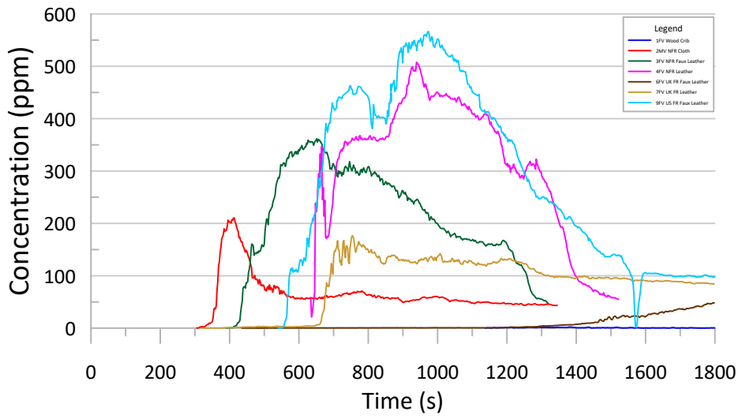
HCN Concentration at LSW 1.5 GIS3



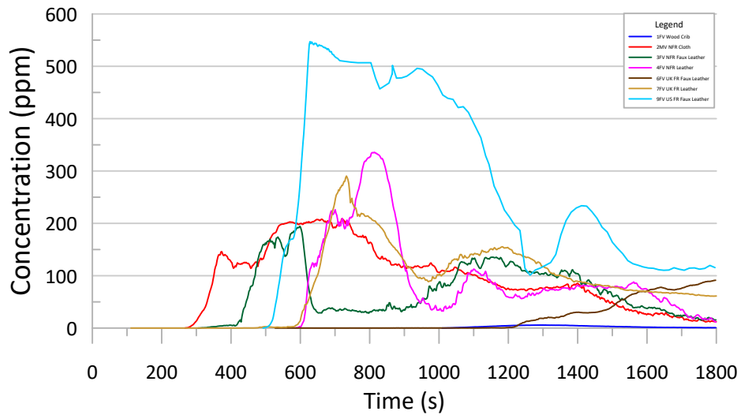
HCN Concentration at LHA 1.5 GIS4



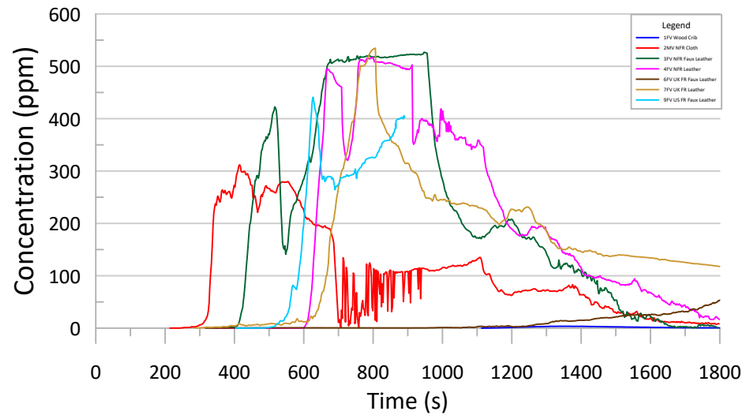
HCN Concentration at LBR 0.9 GIS1



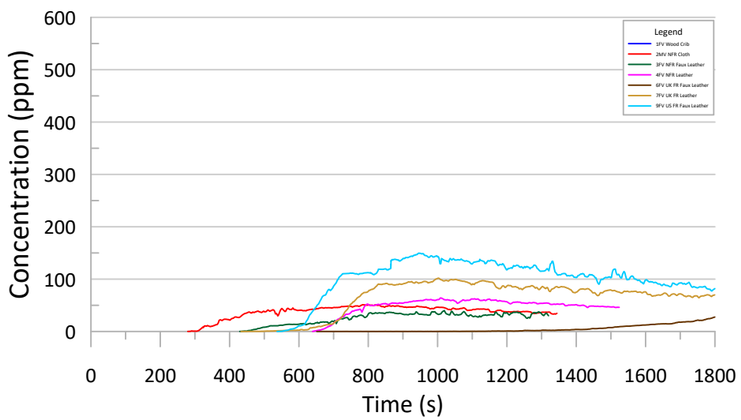
HCN Concentration at LSW 0.9 GIS3



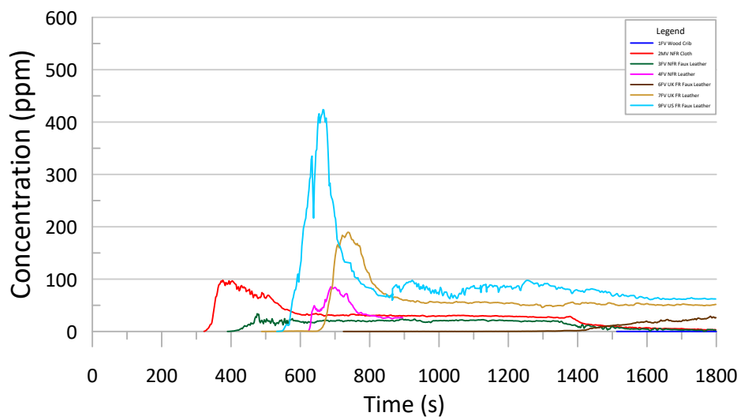
HCN Concentration at LHA 0.9 GIS4



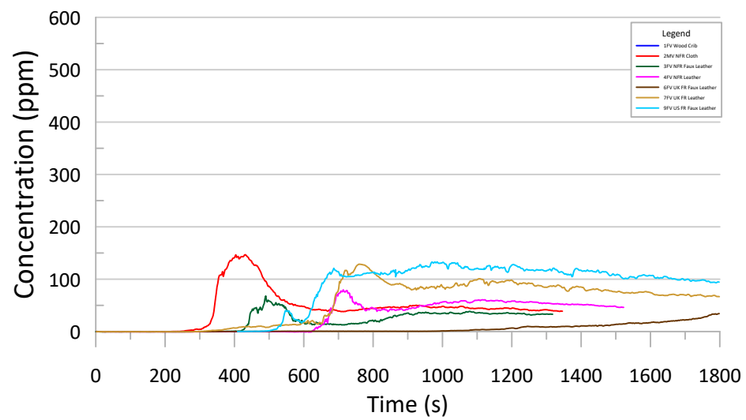
HCN Concentration at LBR 0.3 m GIS1



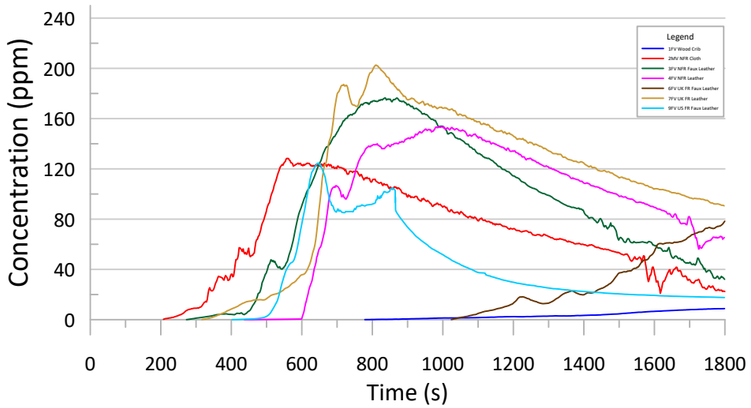
HCN Concentration at LSW 0.3 m GIS3



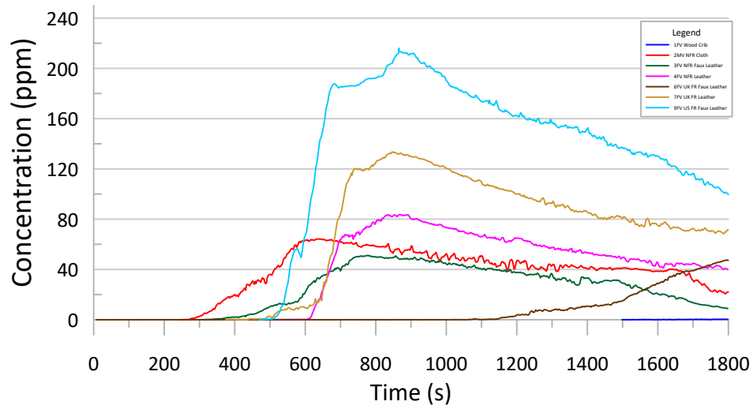
HCN Concentration at LHA 0.3 m GIS4



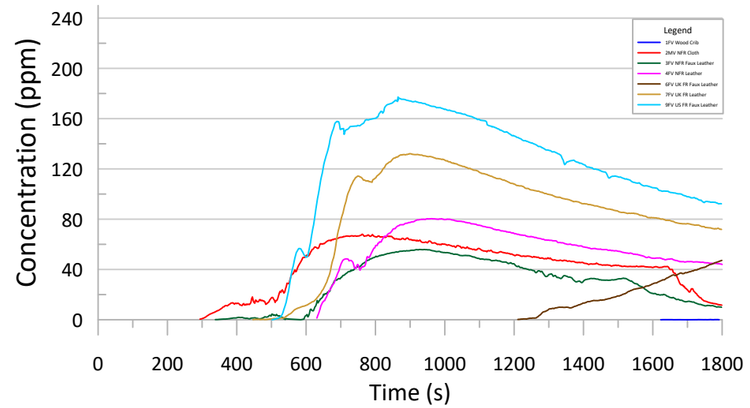
HCN Concentration at UHA 1.5 GIS5



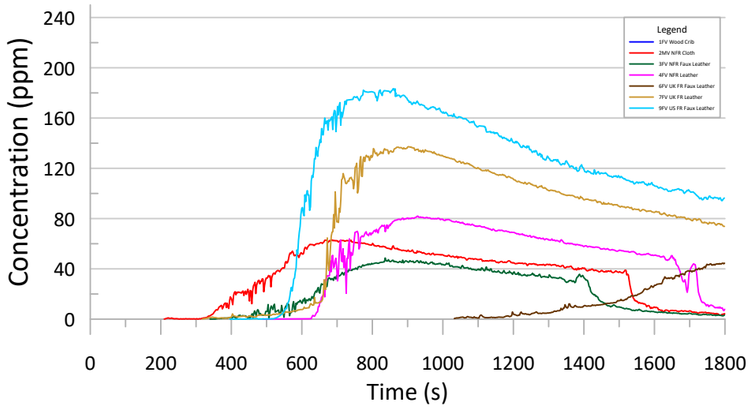
HCN Concentration at USW 1.5 GIS6



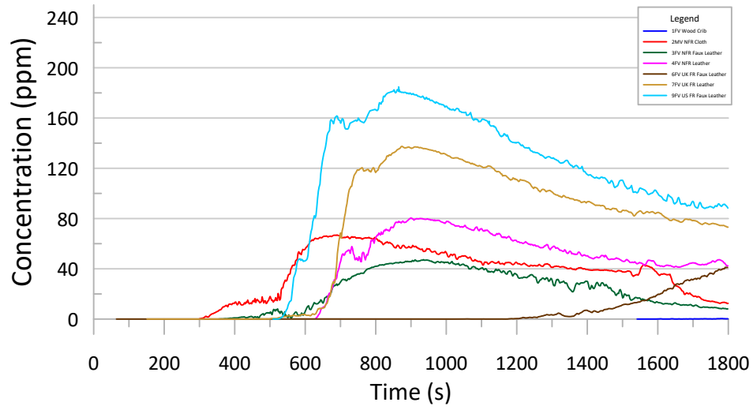
HCN Concentration at USE 1.5 GIS7



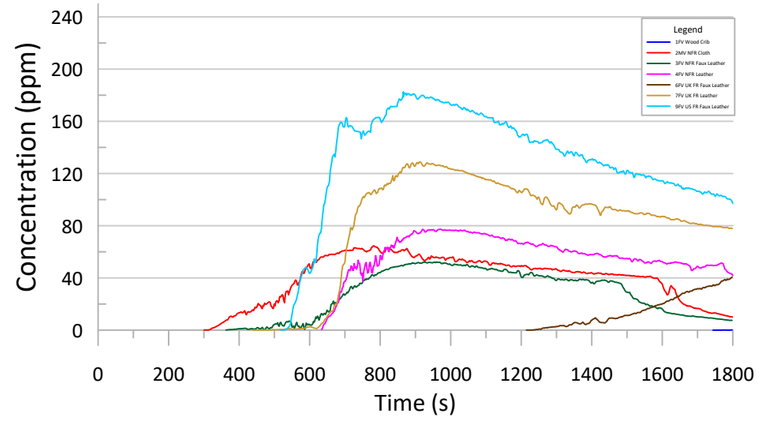
HCN Concentration at UHA 3ft 0.9 GIS5



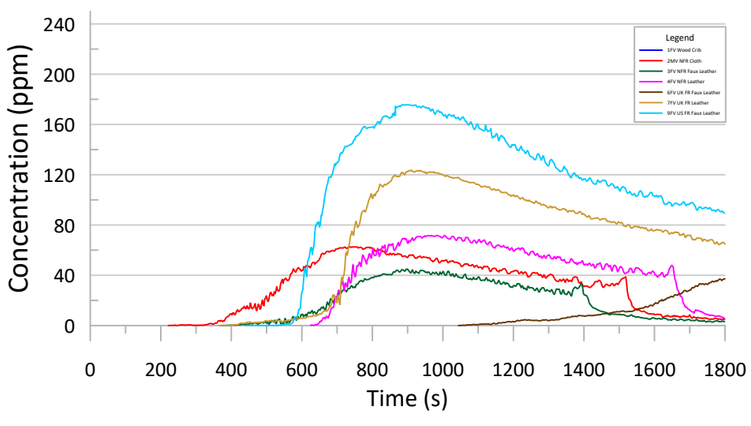
HCN Concentration at USW 0.9 GIS6



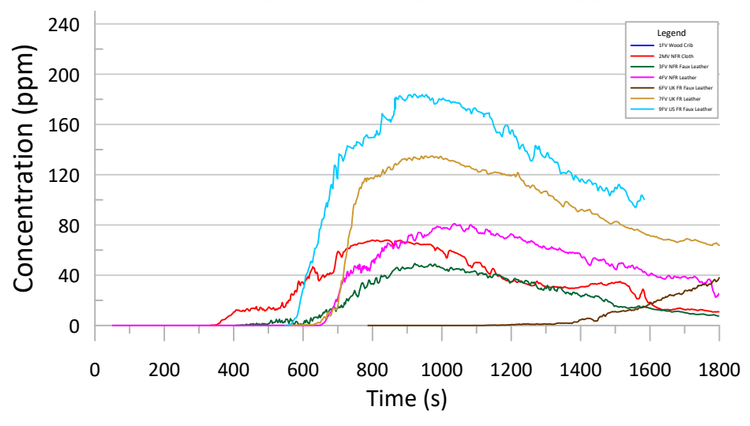
HCN Concentration at USE 0.9 GIS7



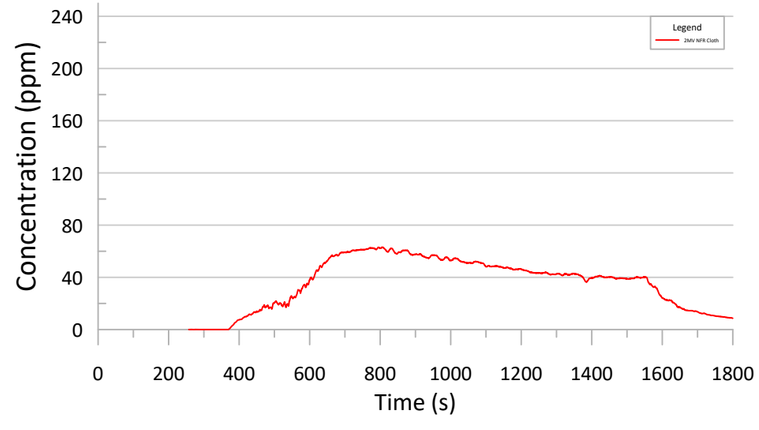
HCN Concentration at UHA 0.3 m GIS5



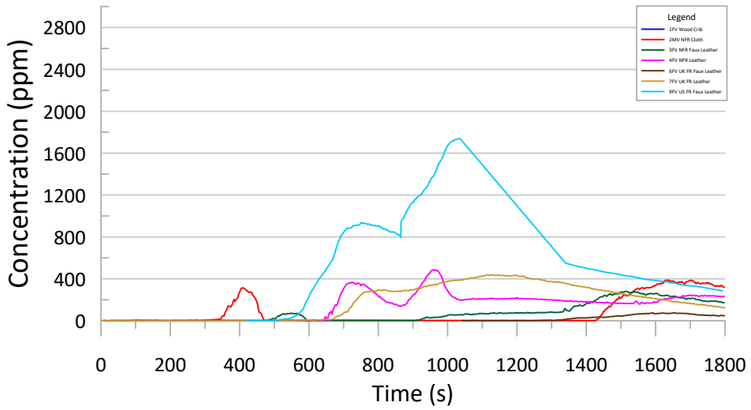
HCN Concentration at USW 0.3 m GIS6



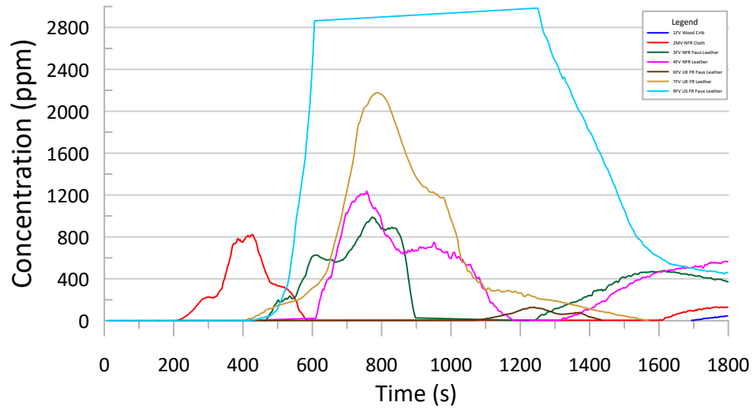
HCN Concentration at USE 0.3 m GIS7



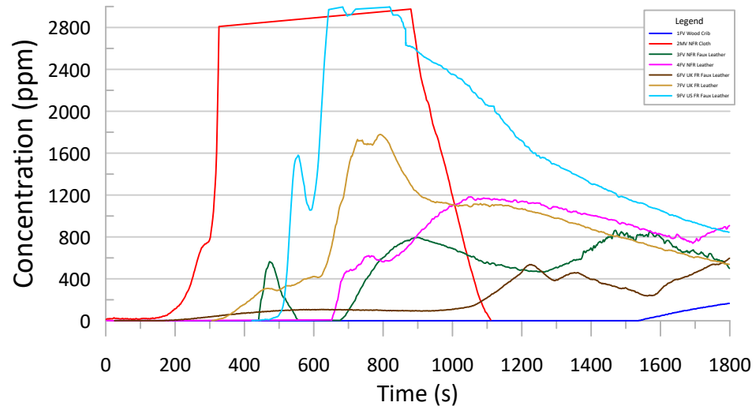
HCL Concentration at LBR 0.9 GIS2



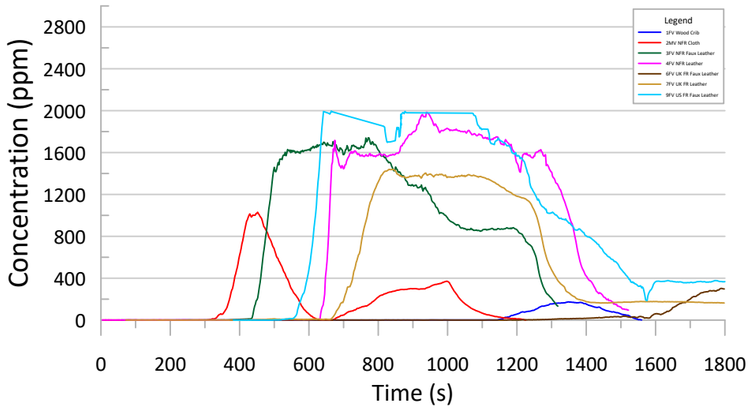
HCL Concentration at LSW 1.5 GIS3



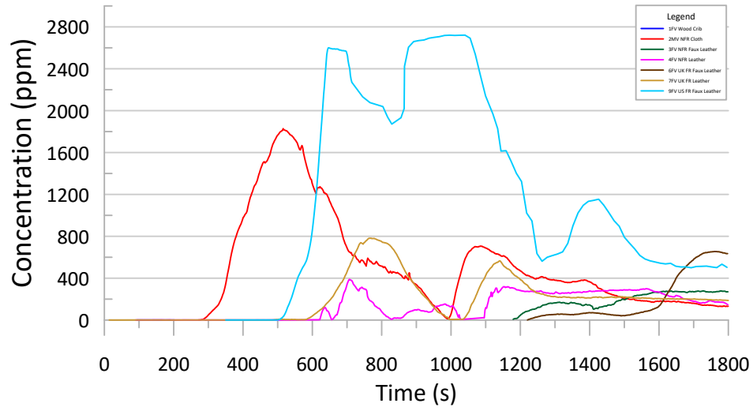
HCL Concentration at LHA 1.5 GIS4



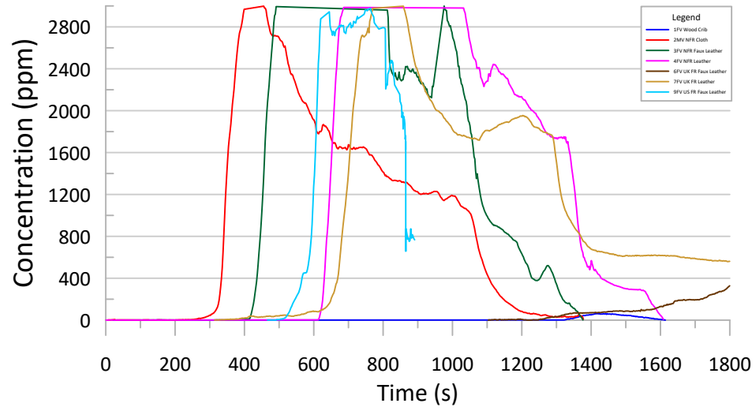
HCL Concentration at LBR 0.9 GIS1



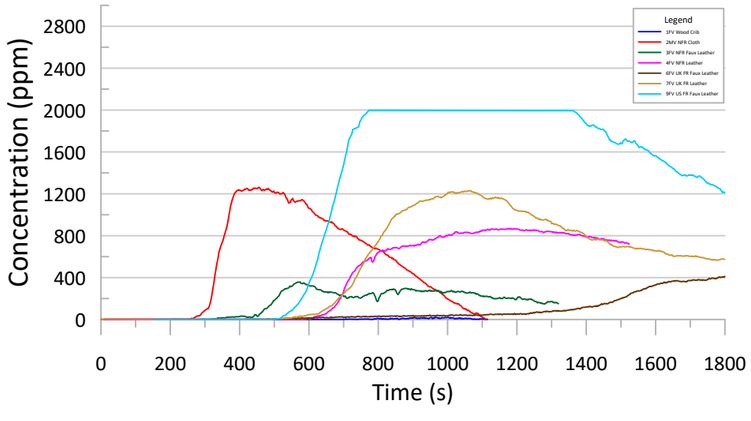
HCL Concentration at LSW 0.9 GIS3



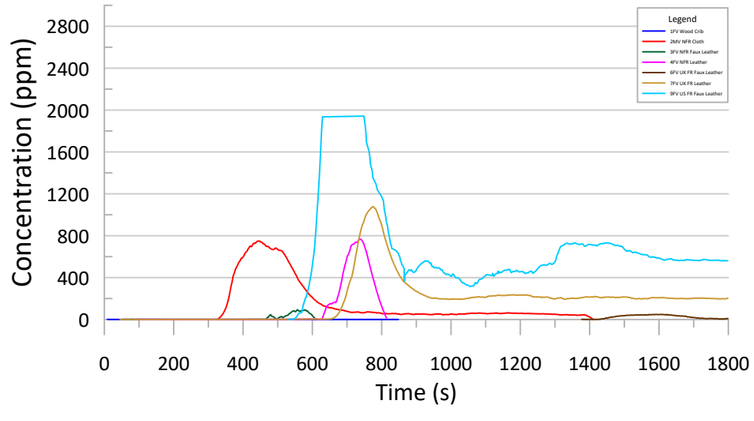
HCL Concentration at LHA 0.9 GIS4



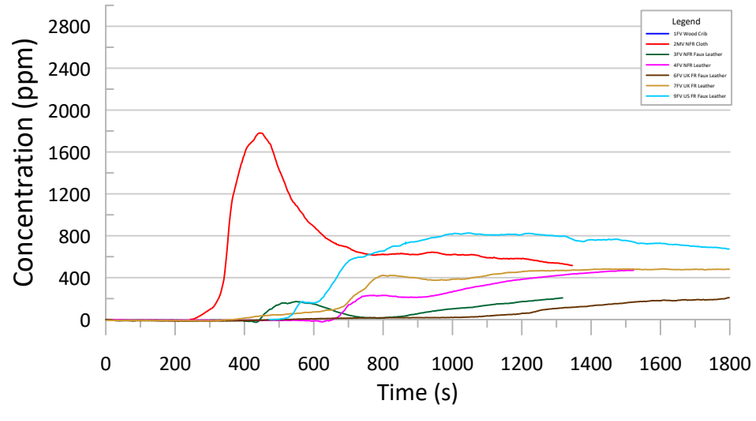
HCL Concentration at LBR 0.3 m GIS1



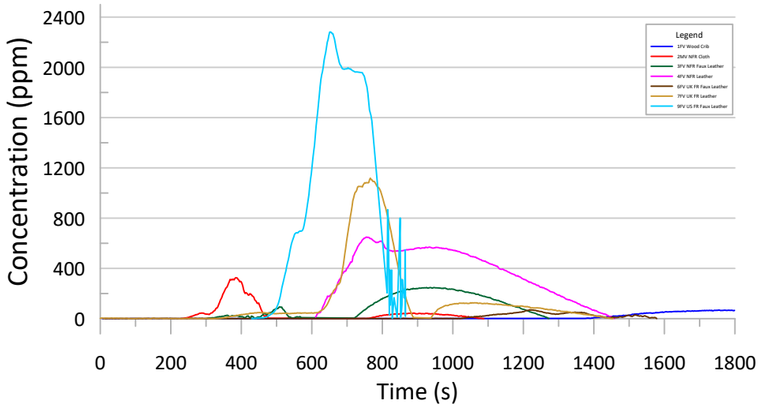
HCL Concentration at LSW 0.3 m GIS3



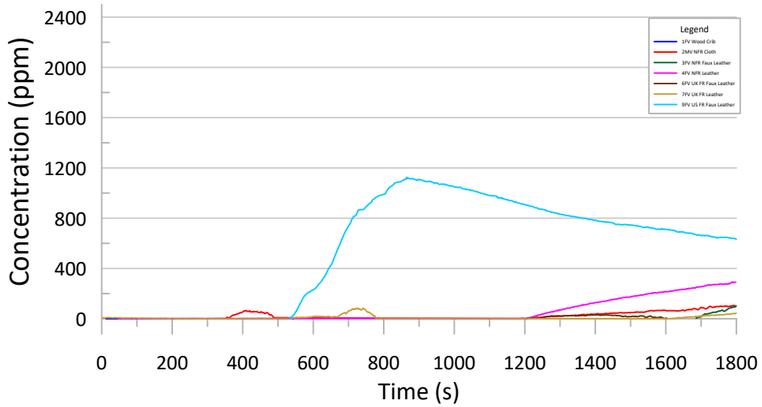
HCL Concentration at LHA 0.3 m GIS4



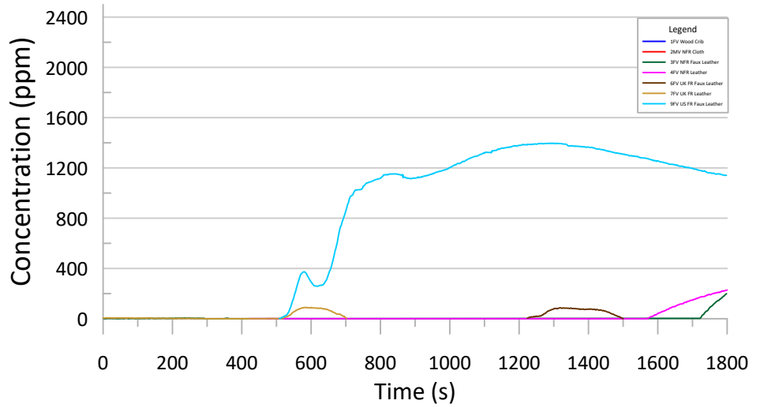
HCL Concentration at UHA 1.5 GIS5



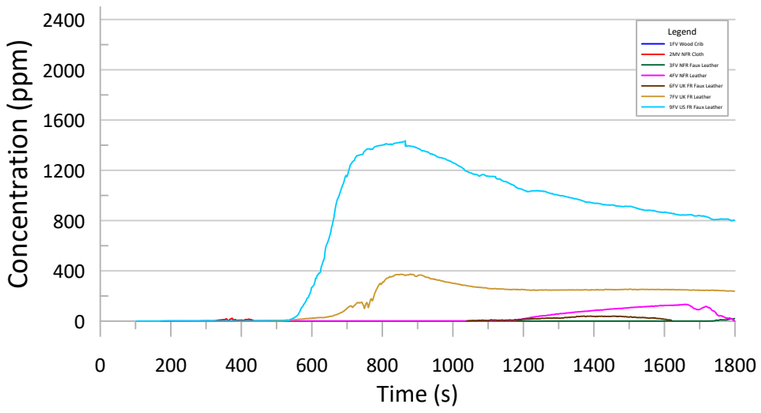
HCL Concentration at USW 1.5 GIS6



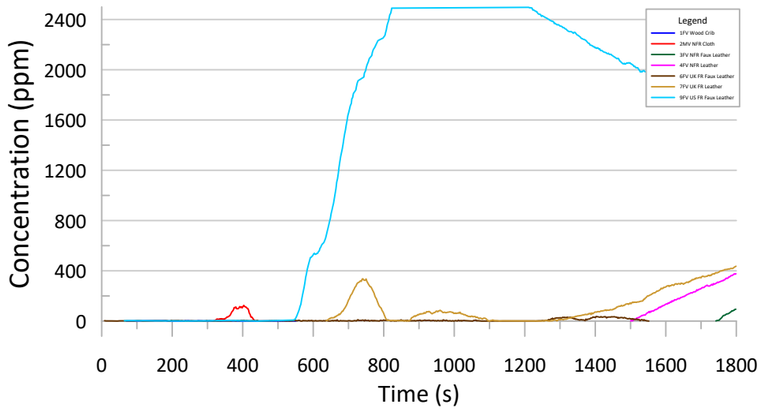
HCL Concentration at USE 1.5 GIS7



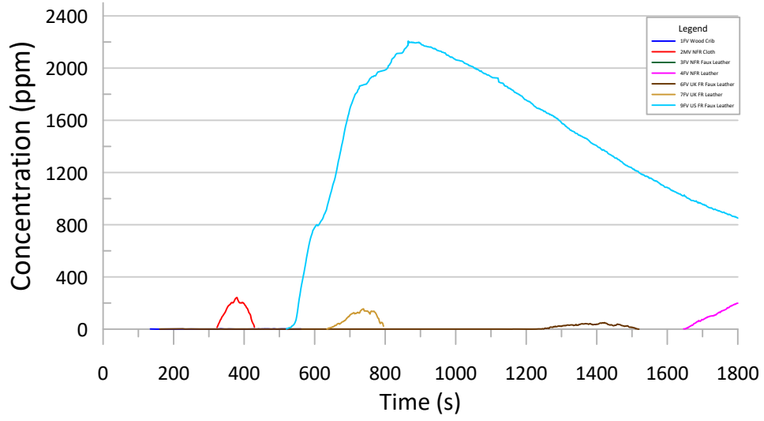
HCL Concentration at UHA 0.9 GIS5



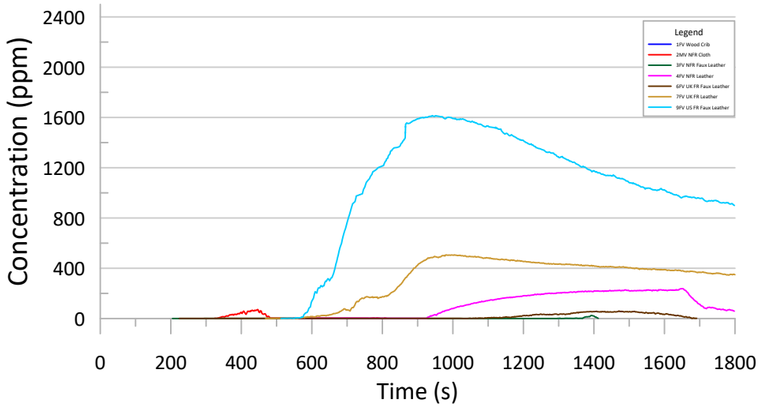
HCL Concentration at USW 0.9 GIS6



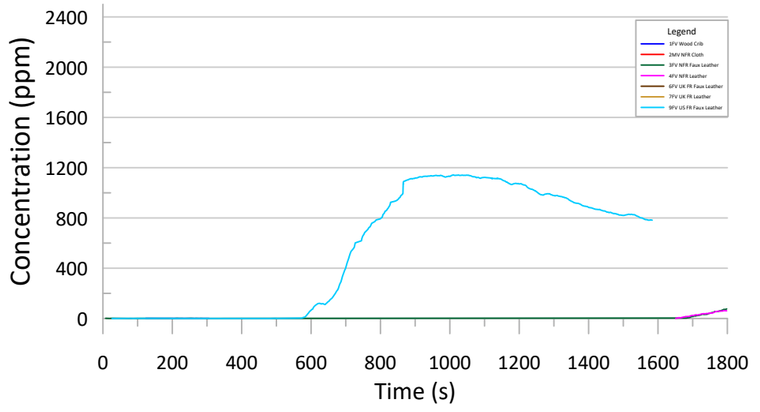
HCL Concentration at USE 3ft Large Bedroom



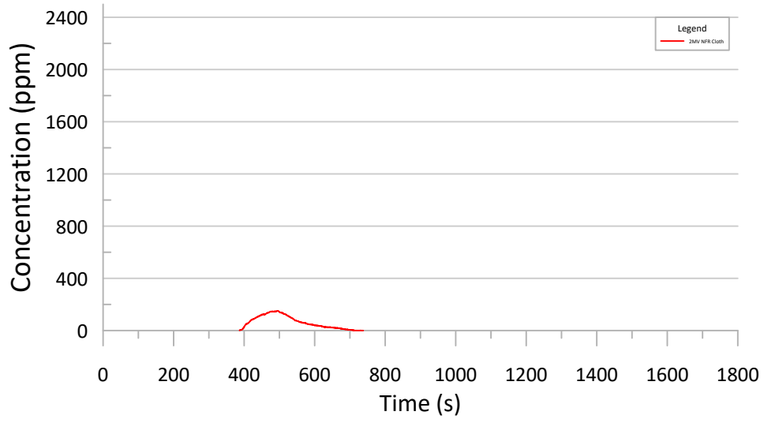
HCL Concentration at UHA 0.3 m GIS5



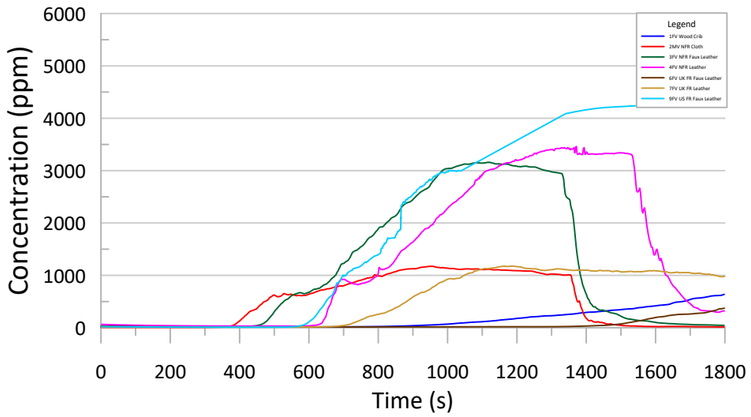
HCL Concentration at USW 0.3 m GIS6



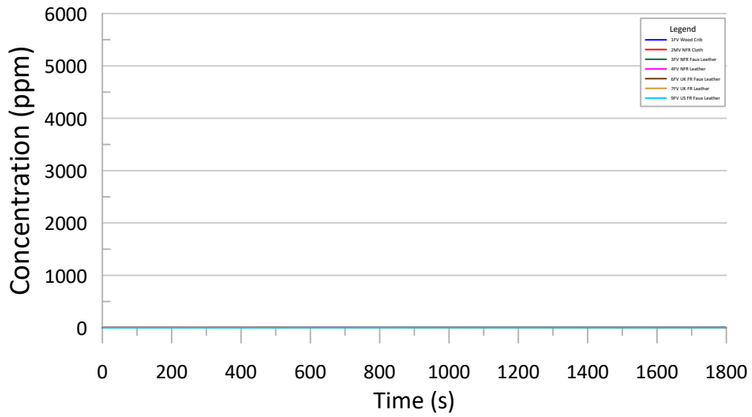
HCL Concentration at USE 0.3 m GIS7



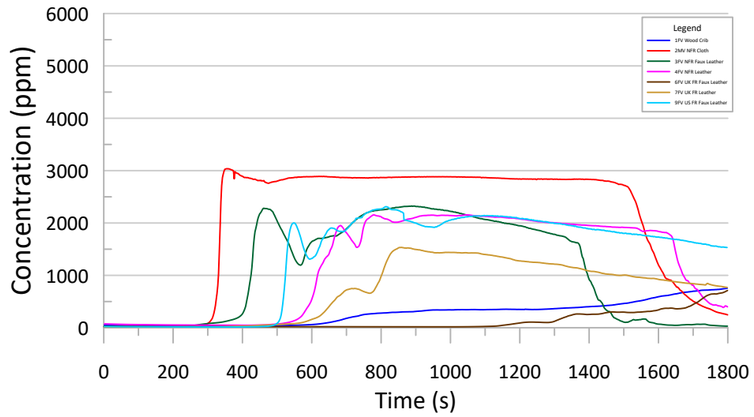
NH3 Concentration at LBR 0.9 GIS2



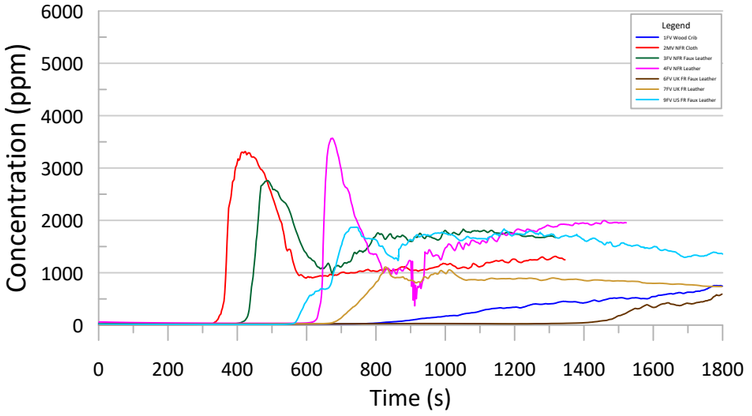
NH3 Concentration at LSW 1.5 GIS3



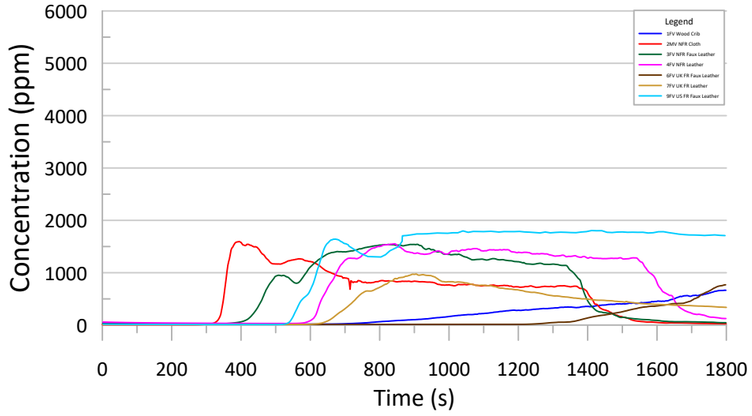
NH3 Concentration at LHA 1.5 GIS4



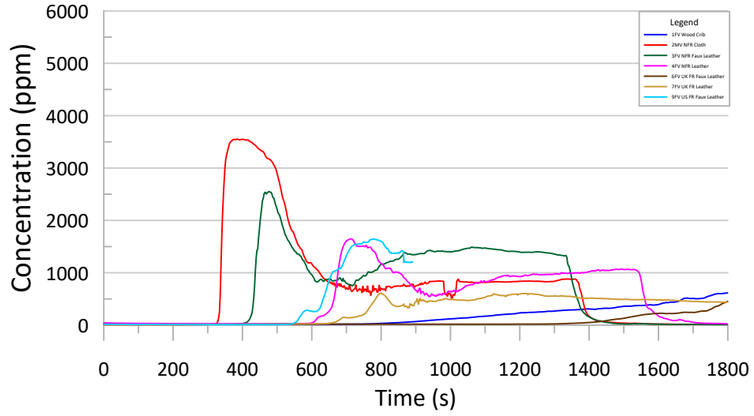
NH3 Concentration at LBR 0.9 GIS1



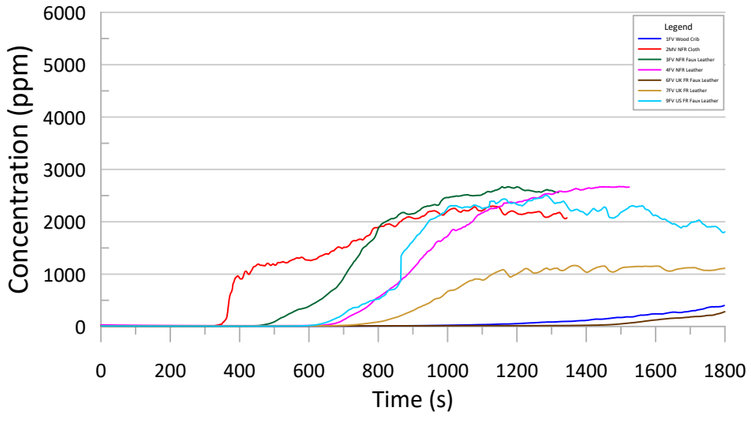
NH3 Concentration at LSW 0.9 GIS3



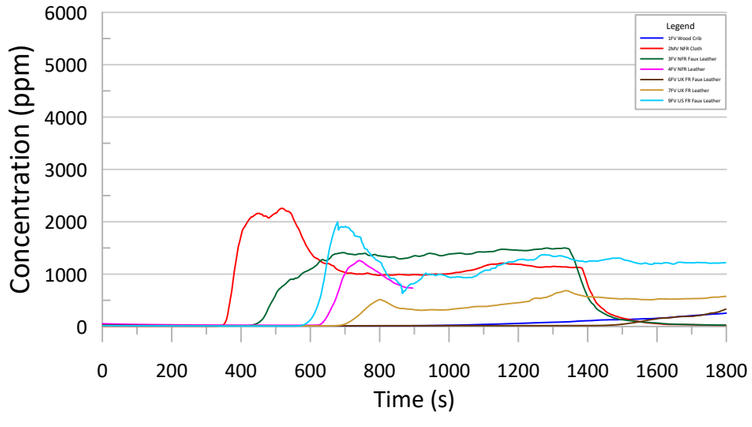
NH3 Concentration at LHA 0.9 GIS4



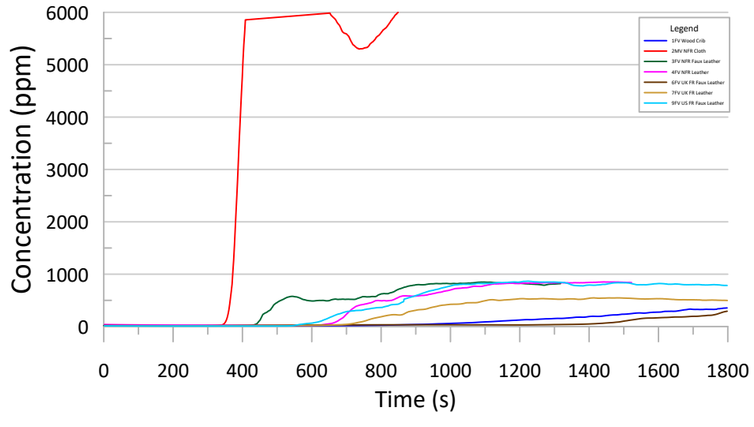
NH3 Concentration at LBR 0.3 m GIS1

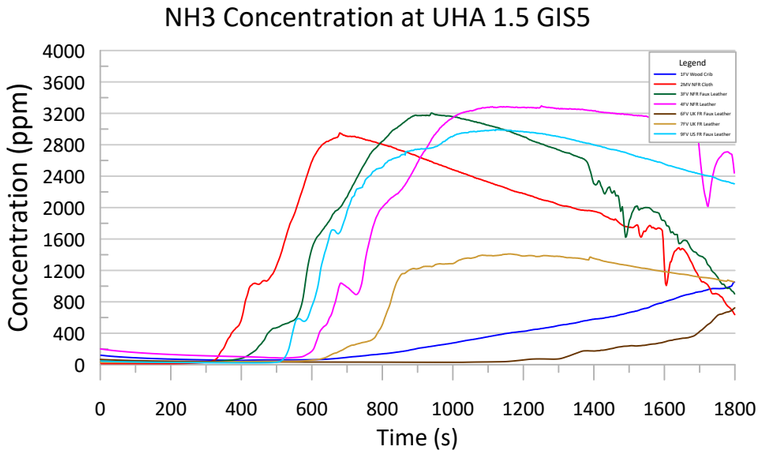


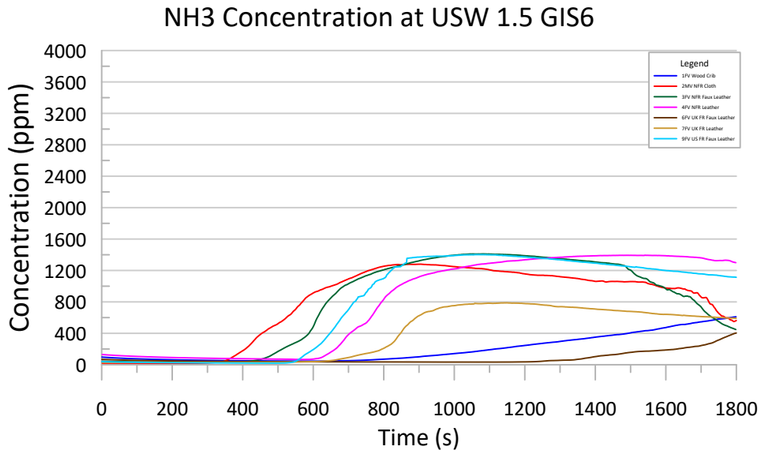
NH3 Concentration at LSW 0.3 m GIS3

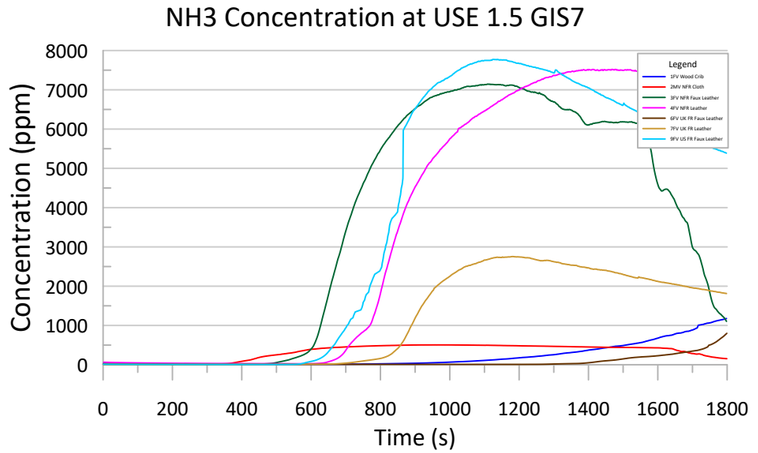


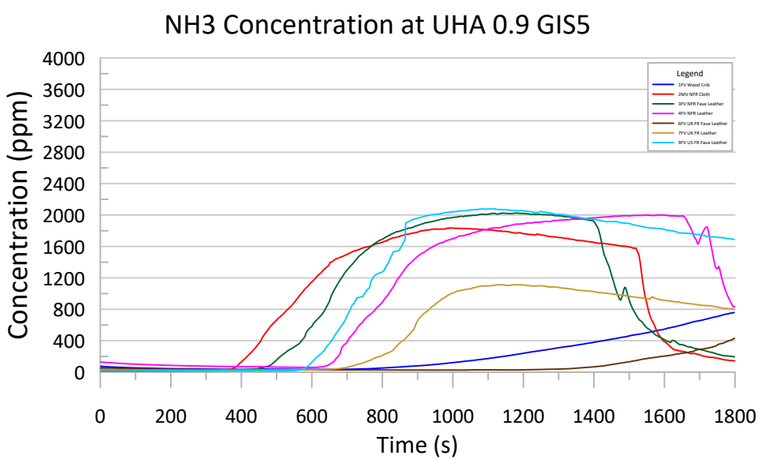
NH3 Concentration at LHA 0.3 m GIS4

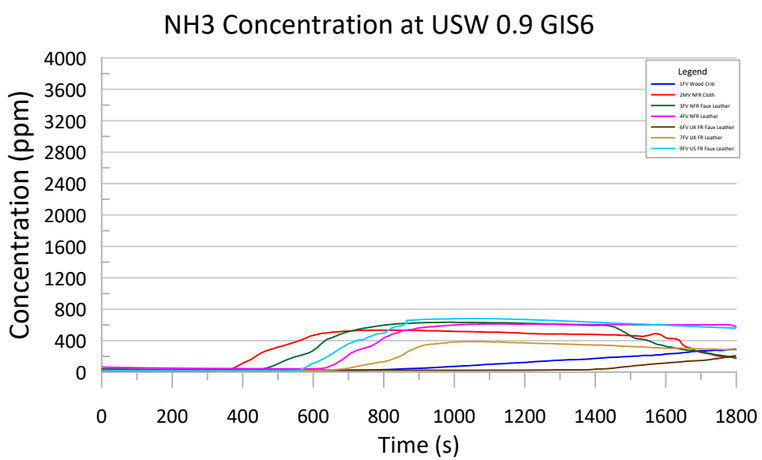


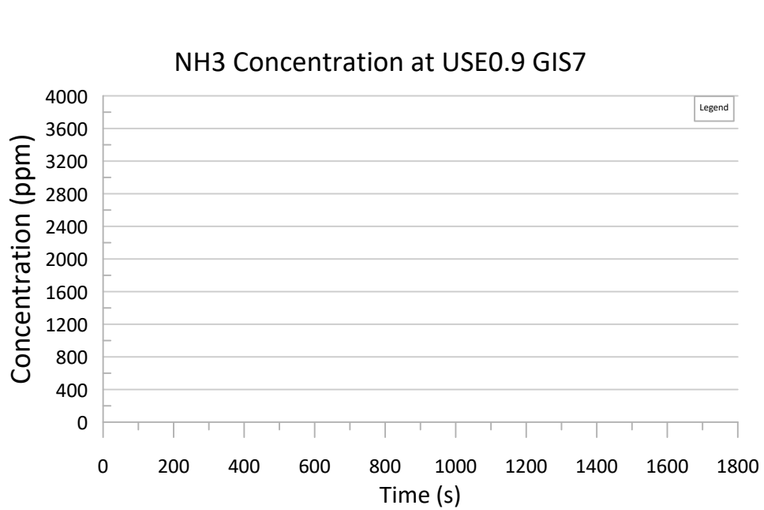

NH3 Concentration at UHA 1.5 GIS5
Concentration (ppm)
Time (s)
Legend
1FV Wood Crib
2MV NFR Cloth
3FV NFR Faux Leather
4FV NFR Leather
6FV UK FR Faux Leather
7FV UK FR Leather
9FV US FR Faux Leather

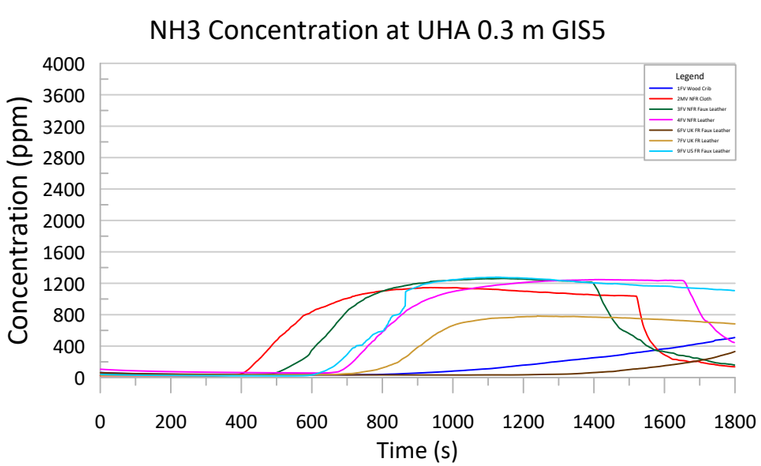

NH3 Concentration at USW 1.5 GIS6
Concentration (ppm)
Time (s)
Legend
1FV Wood Crib
2MV NFR Cloth
3FV NFR Faux Leather
4FV NFR Leather
6FV UK FR Faux Leather
7FV UK FR Leather
9FV US FR Faux Leather

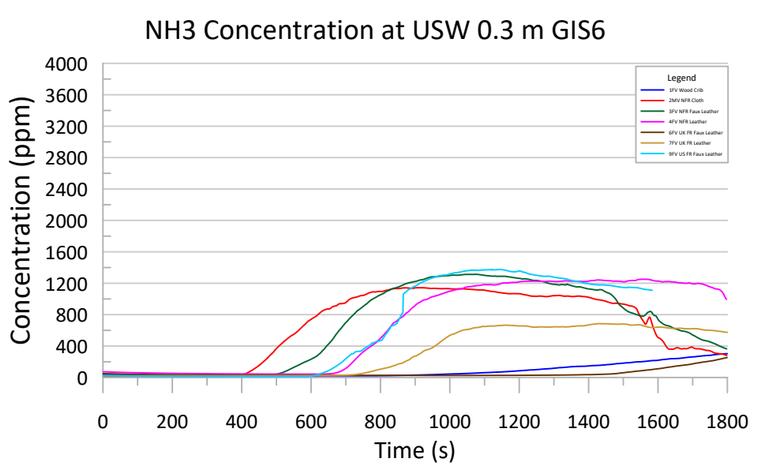

NH3 Concentration at USE 1.5 GIS7
Concentration (ppm)
Time (s)
Legend
1FV Wood Crib
2MV NFR Cloth
3FV NFR Faux Leather
4FV NFR Leather
6FV UK FR Faux Leather
7FV UK FR Leather
9FV US FR Faux Leather

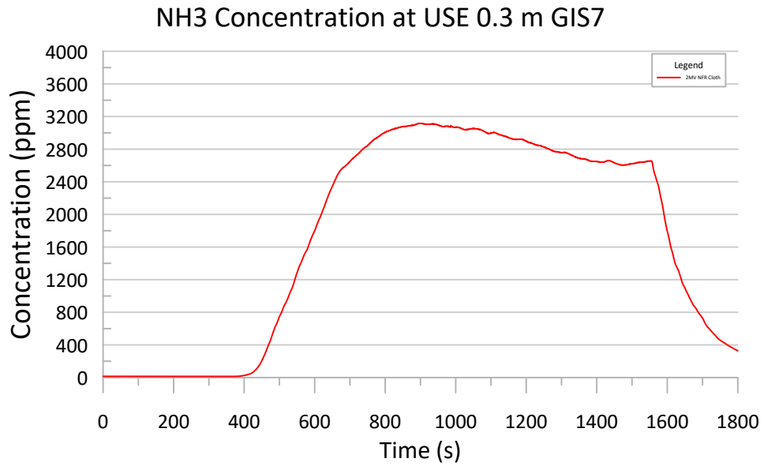

NH3 Concentration at UHA 0.9 GIS5
Concentration (ppm)
Time (s)
Legend
1FV Wood Crib
2MV NFR Cloth
3FV NFR Faux Leather
4FV NFR Leather
6FV UK FR Faux Leather
7FV UK FR Leather
9FV US FR Faux Leather


NH3 Concentration at USW 0.9 GIS6
Concentration (ppm)
Time (s)
Legend
1FV Wood Crib
2MV NFR Cloth
3FV NFR Faux Leather
4FV NFR Leather
6FV UK FR Faux Leather
7FV UK FR Leather
9FV US FR Faux Leather

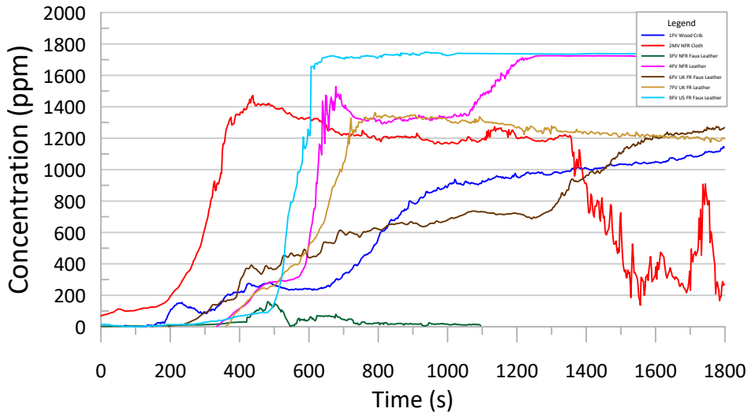

NH3 Concentration at USE0.9 GIS7
Concentration (ppm)
Time (s)
Legend


NH3 Concentration at UHA 0.3 m GIS5
Concentration (ppm)
Time (s)
Legend
1FV Wood Crib
2MV NFR Cloth
3FV NFR Faux Leather
4FV NFR Leather
6FV UK FR Faux Leather
7FV UK FR Leather
9FV US FR Faux Leather

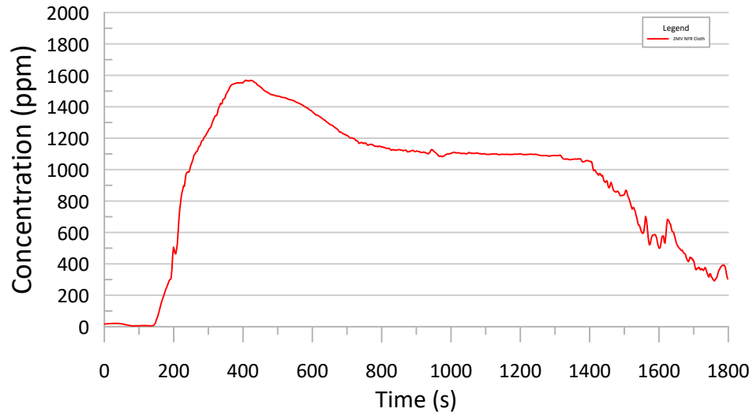

NH3 Concentration at USW 0.3 m GIS6
Concentration (ppm)
Time (s)
Legend
1FV Wood Crib
2MV NFR Cloth
3FV NFR Faux Leather
4FV NFR Leather
6FV UK FR Faux Leather
7FV UK FR Leather
9FV US FR Faux Leather


NH3 Concentration at USE 0.3 m GIS7
Concentration (ppm)
Time (s)
Legend
2MV NFR Cloth

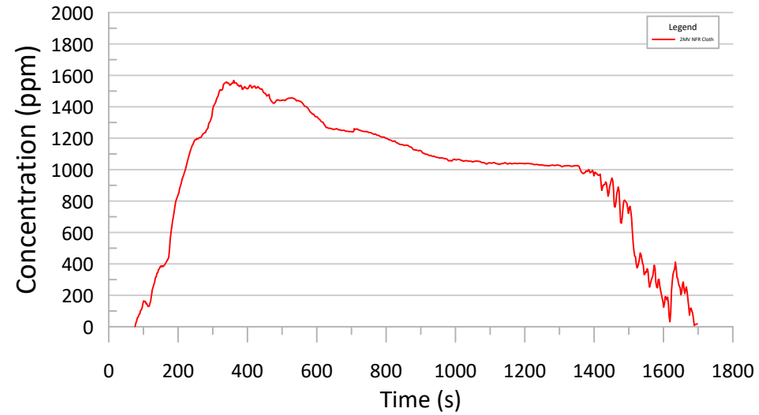
VOC Concentration at LBR 3ft 0.9 GIS2



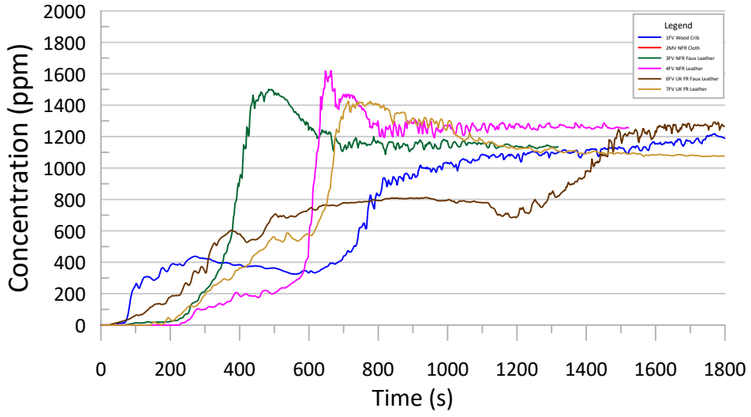
VOC Concentration at LSW 1.5 GIS3



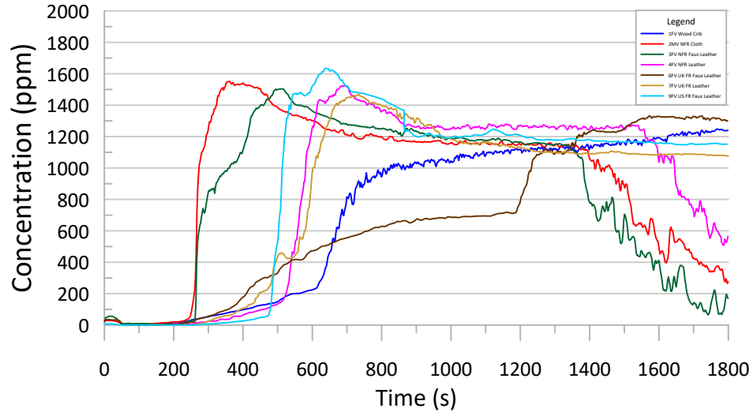
VOC Concentration at LHA 1.5 GIS4



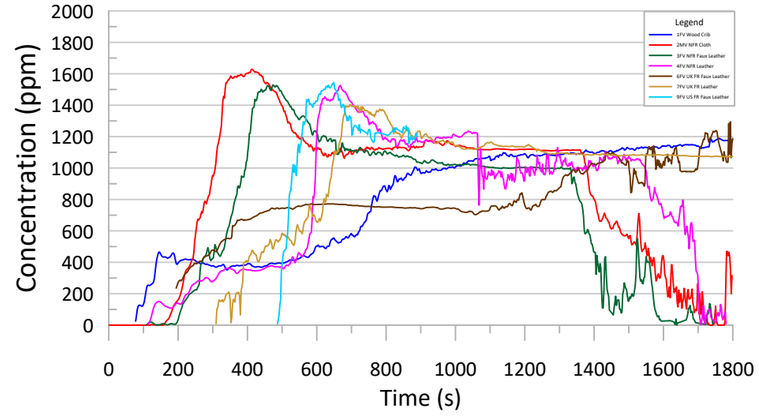
VOC Concentration at LBR 3ft 0.9 GIS1



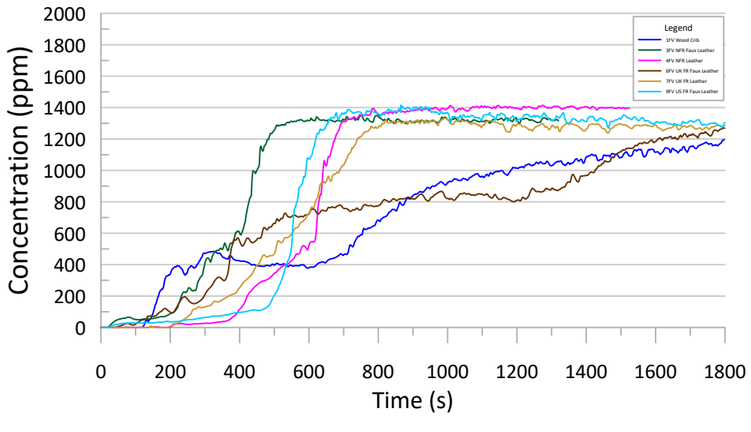
VOC Concentration at LSW 0.9 GIS3



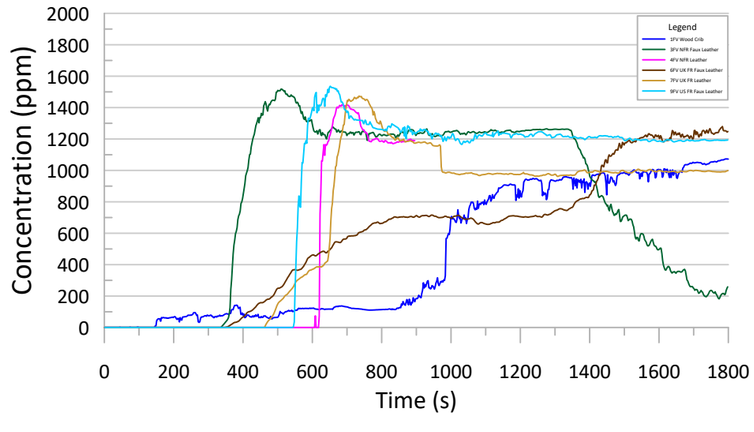
VOC Concentration at LHA 0.9 GIS4



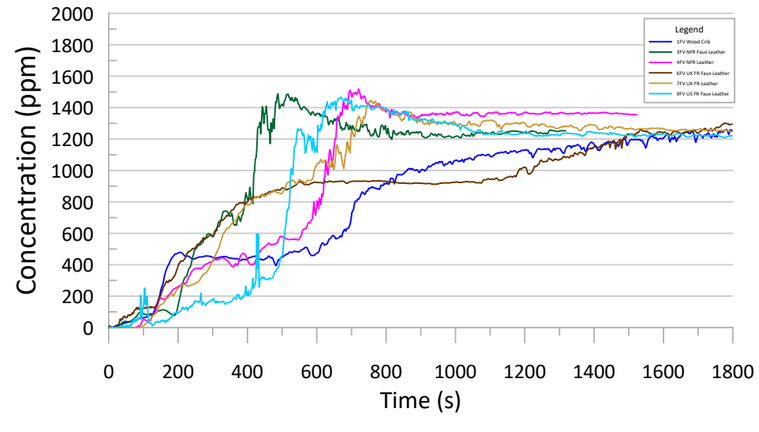
VOC Concentration at LBR 0.3 m GIS1



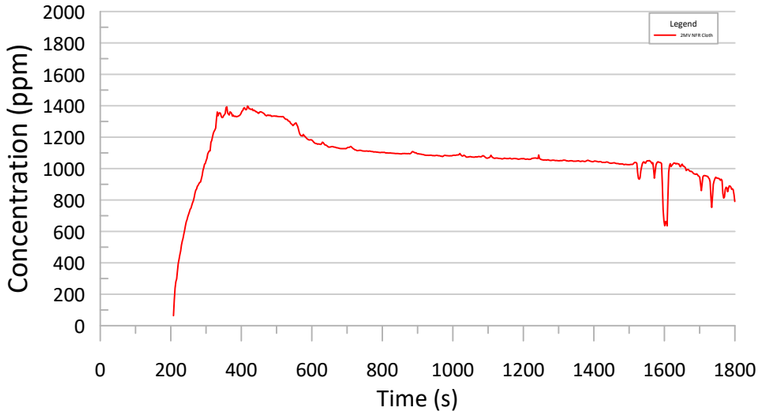
VOC Concentration at LSW 0.3 m GIS3



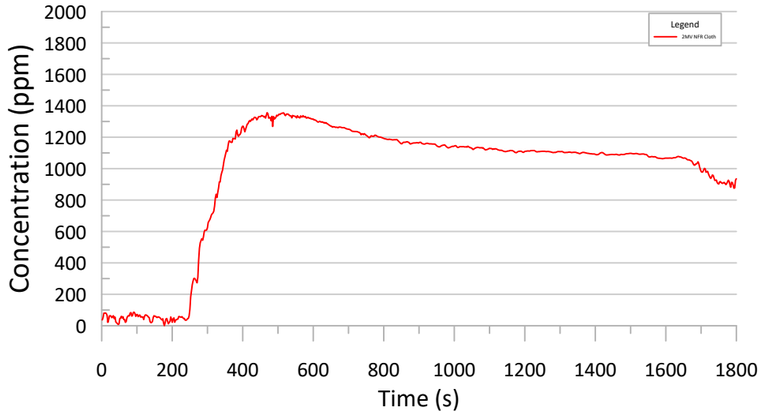
VOC Concentration at LHA 1ft 0.3 m GIS4



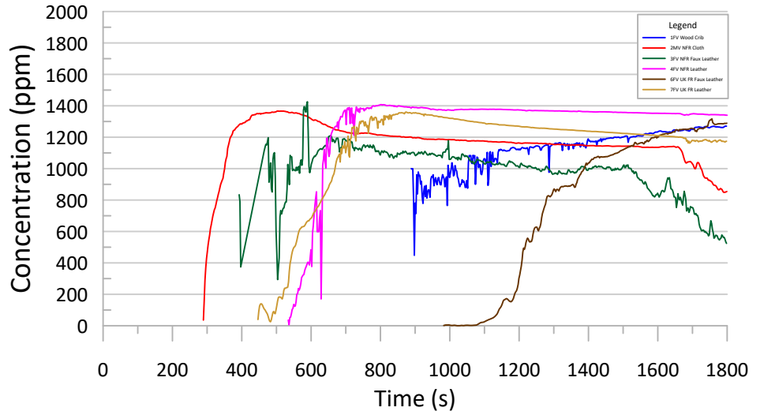
VOC Concentration at UHA 1.5 GIS5



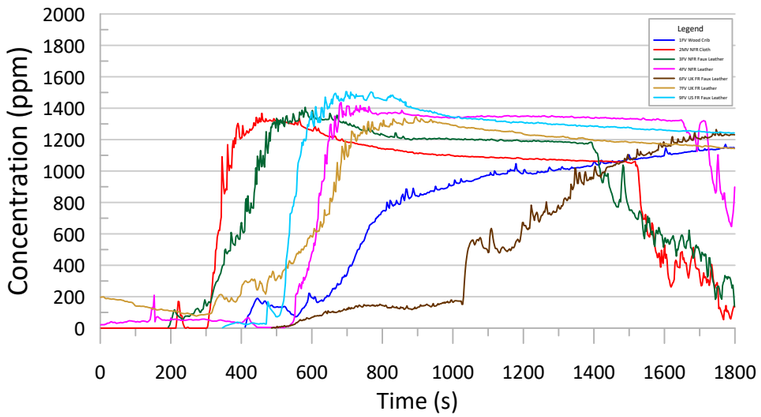
VOC Concentration at USW 1.5 GIS6



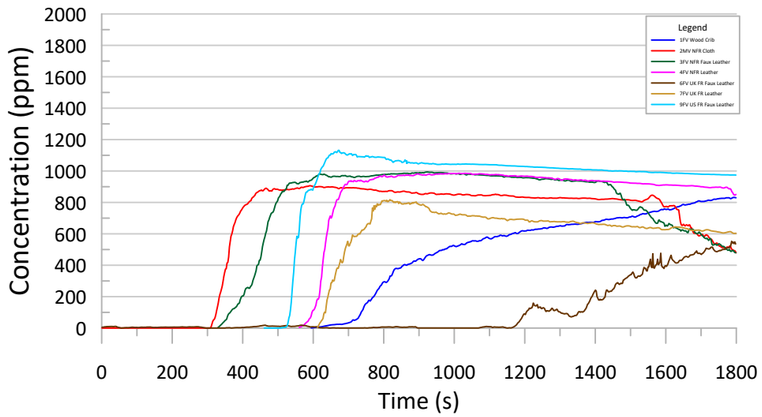
VOC Concentration at USE 1.5 GIS7



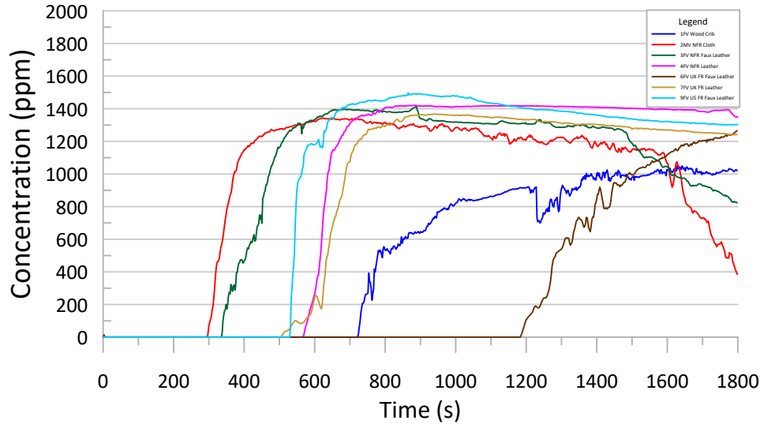
VOC Concentration at UHA 0.9 GIS5



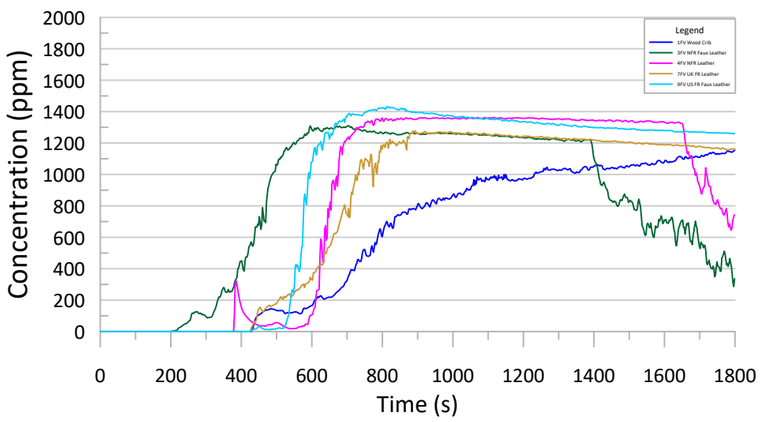
VOC Concentration at USW 0.9 GIS6



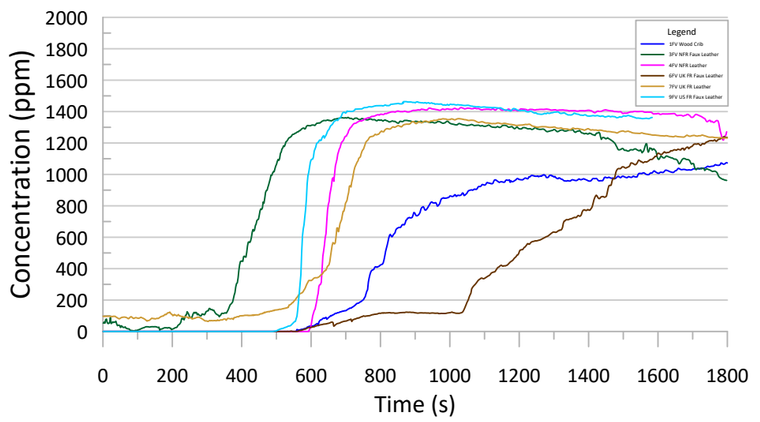
VOC Concentration at USE 0.9 GIS7



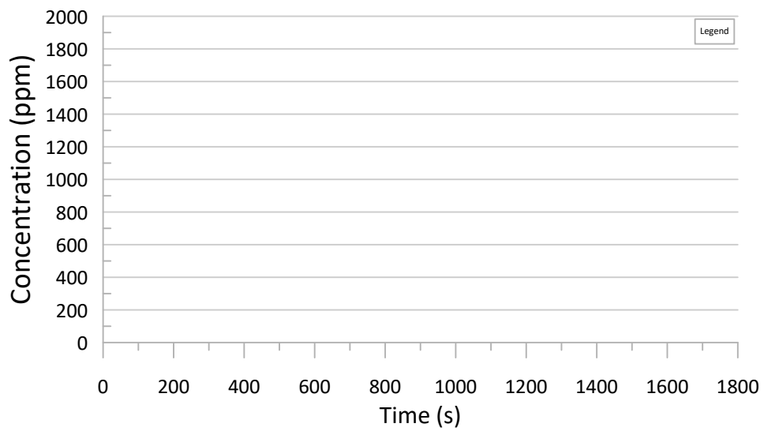
VOC Concentration at 0.3 m GIS5



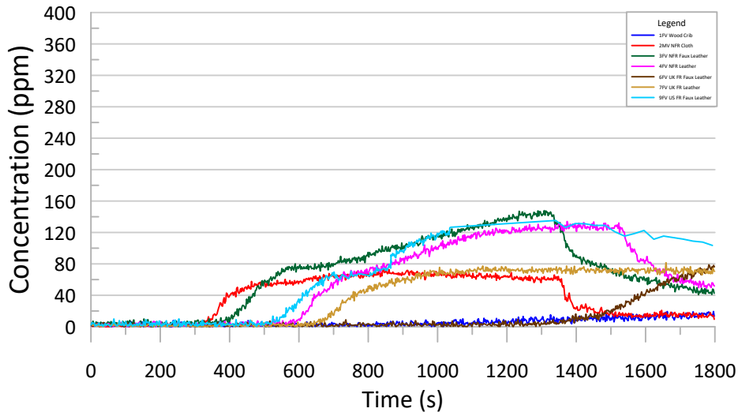
VOC Concentration at USW 0.3 m GIS6



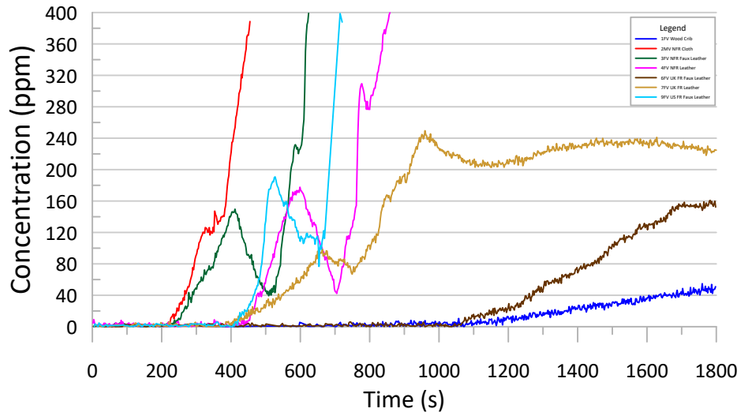
VOC Concentration at USE 0.3 m GIS7



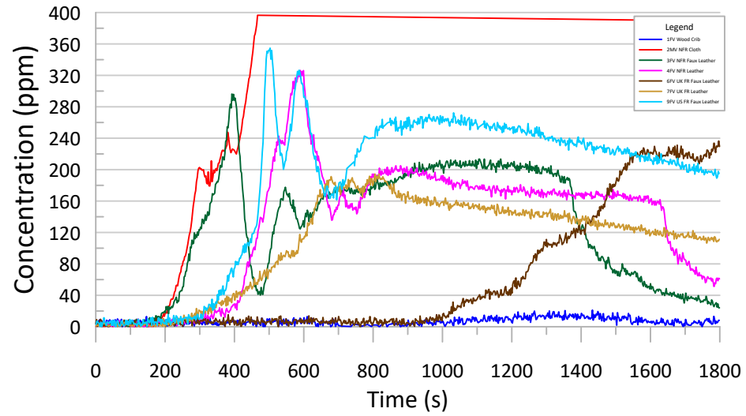
NO Concentration at LBR 0.9 GIS2



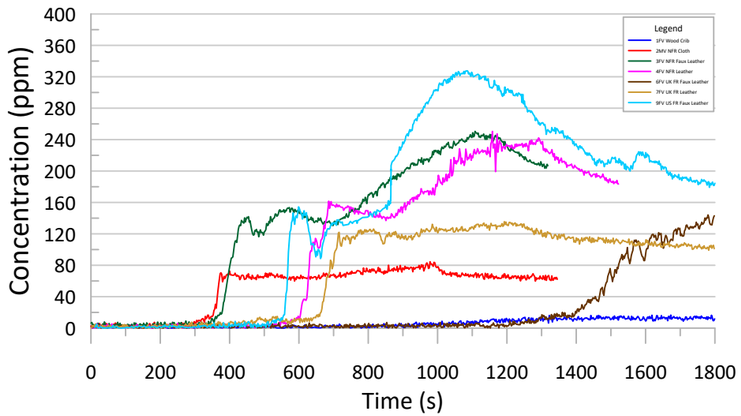
NO Concentration at LSW 1.5 GIS3



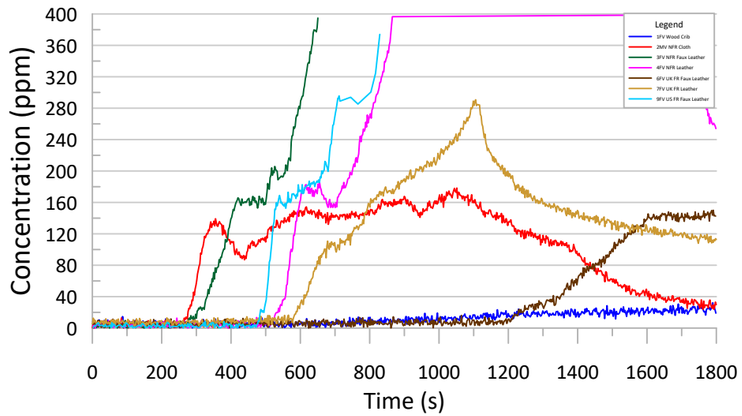
NO Concentration at LHA 1.5 GIS4



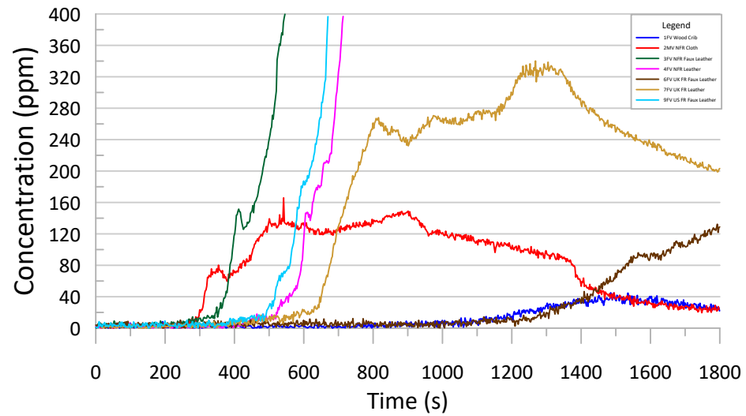
NO Concentration at LBR 3ft Burn Room North Wall



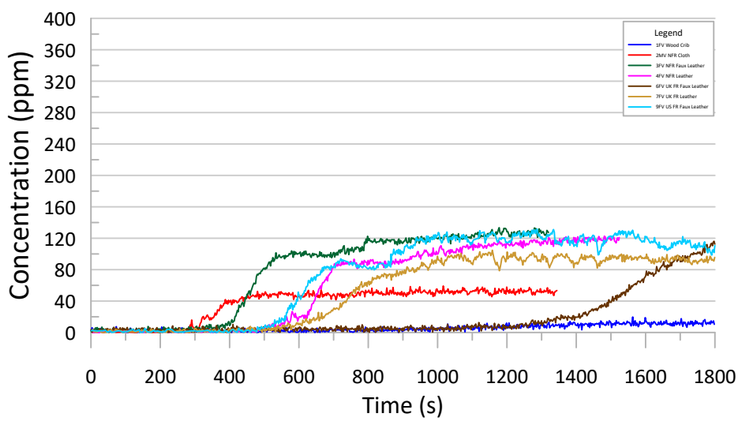
NO Concentration at LSW 0.9 GIS3



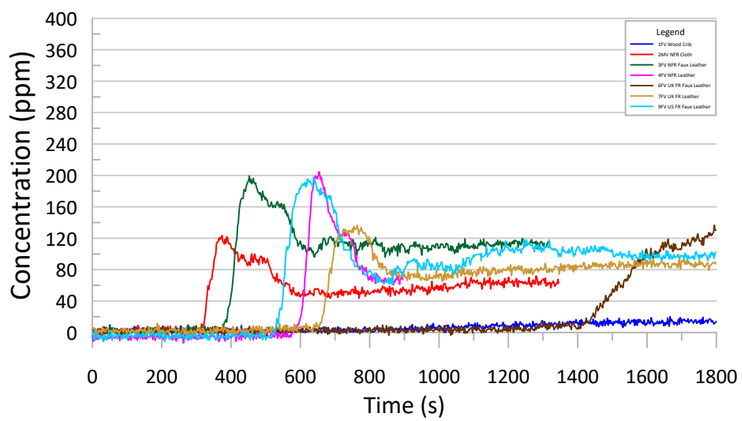
NO Concentration at LHA 0.9 GIS4



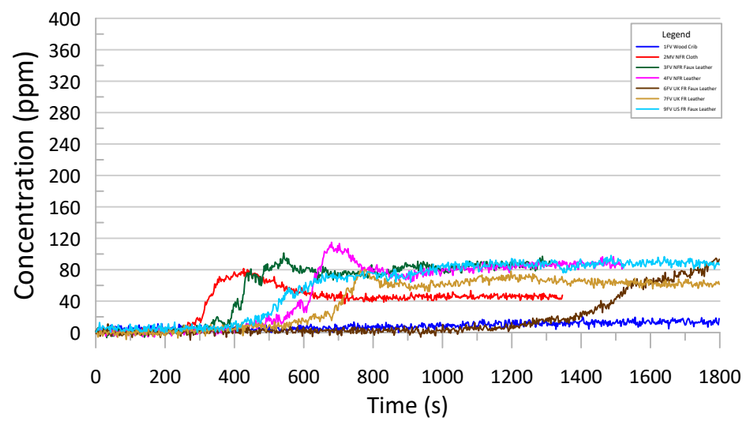
NO Concentration at LBR 0.3 m GIS1



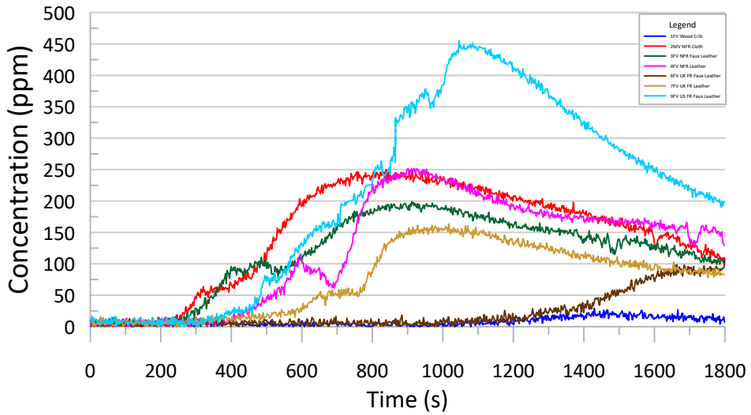
NO Concentration at LSW 0.9 GIS1



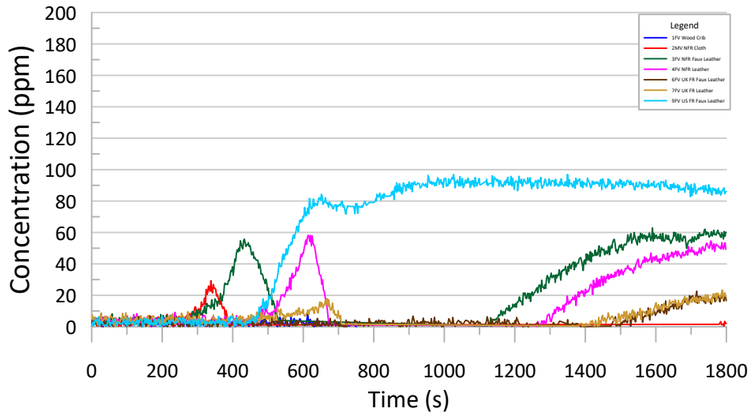
NO2 Concentration at LHA 0.3 m GIS4



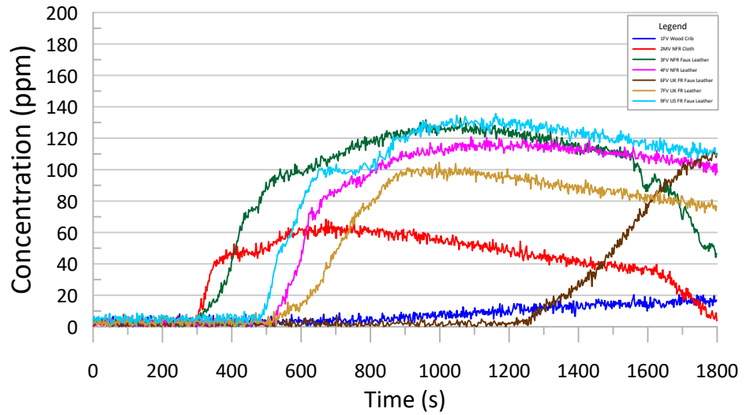
NO Concentration at UHA 1.5 GIS5



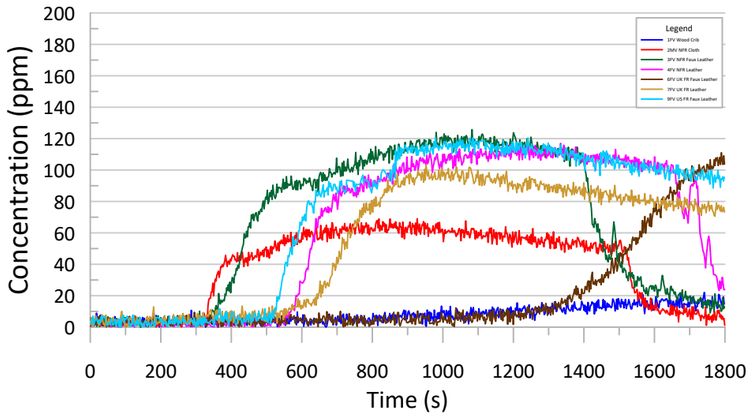
NO Concentration at USW 1.5 GIS6



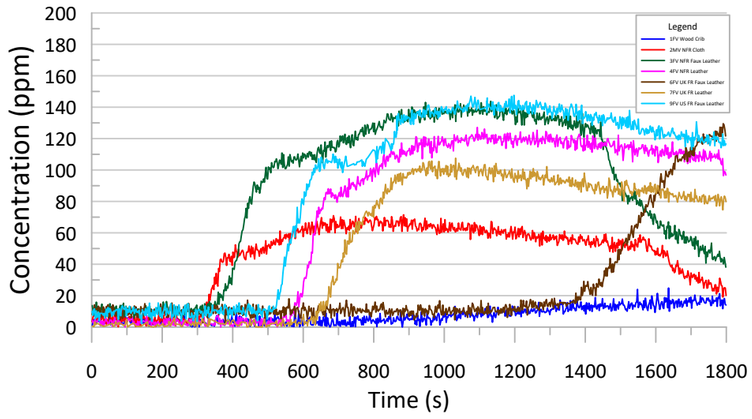
NO Concentration at USE 1.5 GIS7



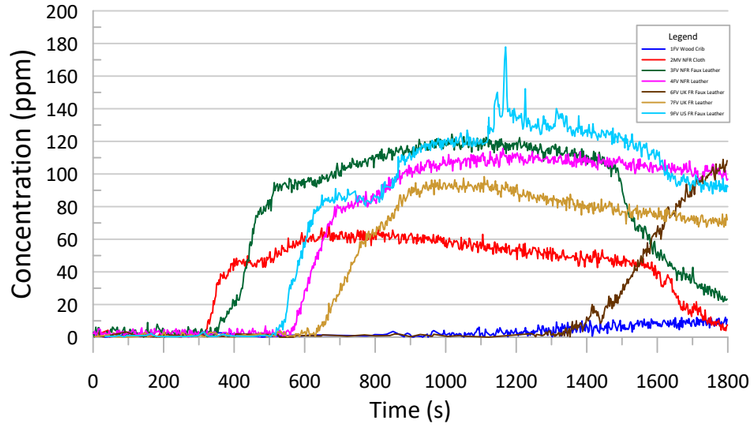
NO Concentration at UHA 0.9 GIS5



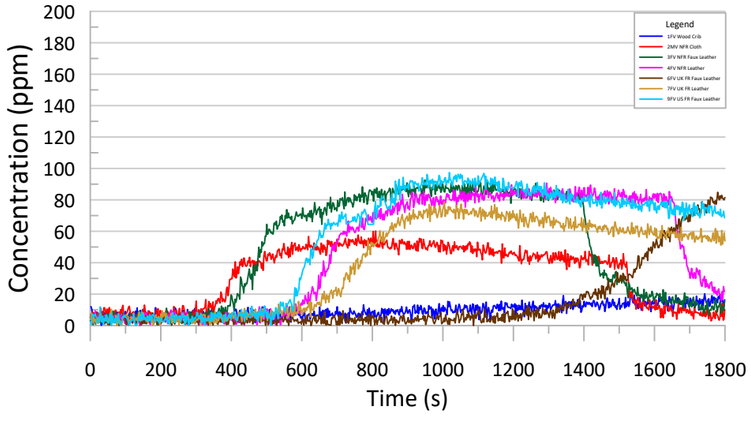
NO Concentration at USW 0.9 GIS6



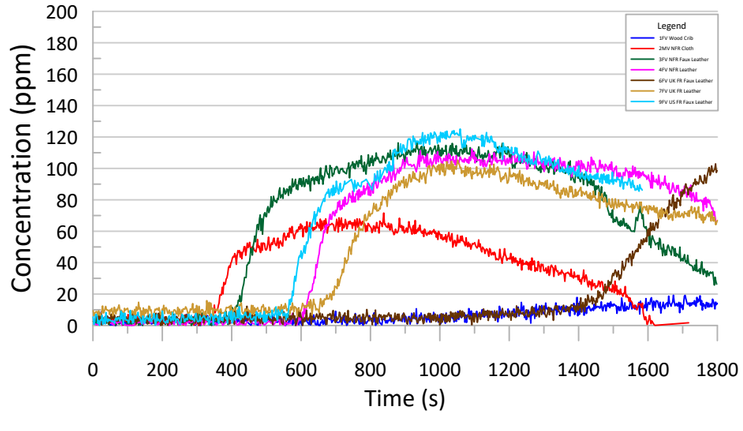
NO Concentration at USE 0.9 GIS7



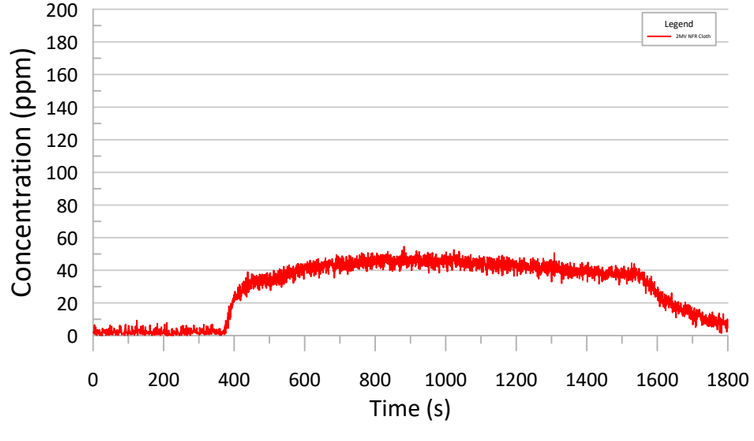
NO Concentration at UHA 0.3 m GIS5

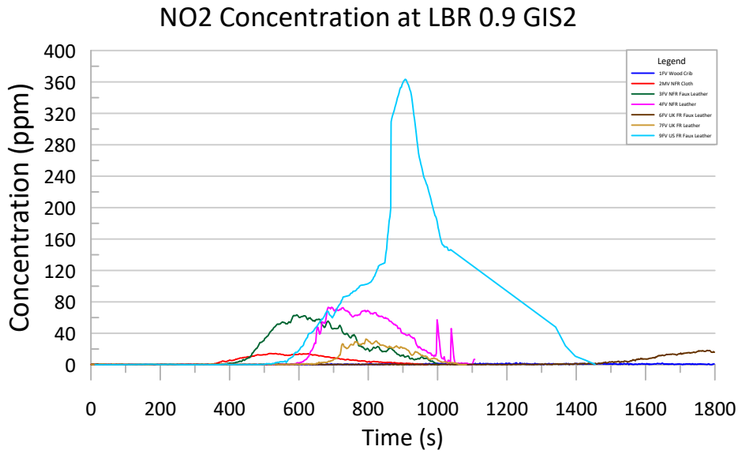


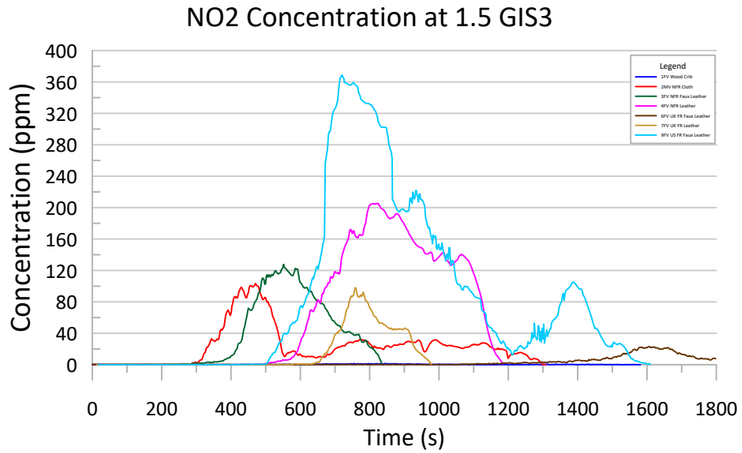
NO Concentration at USW 0.3 m GIS6

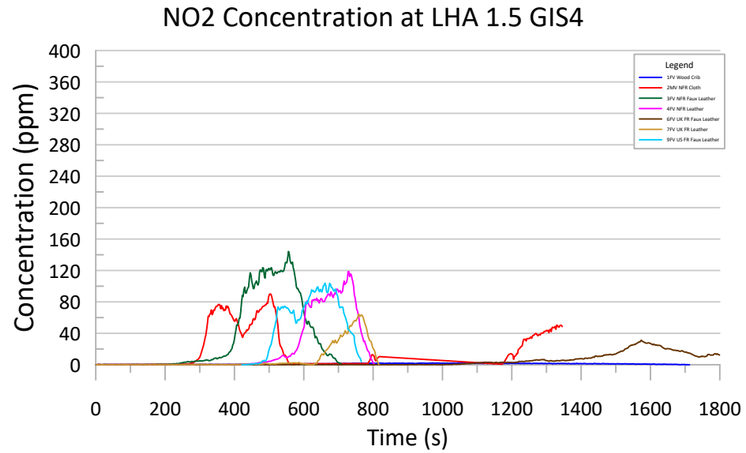


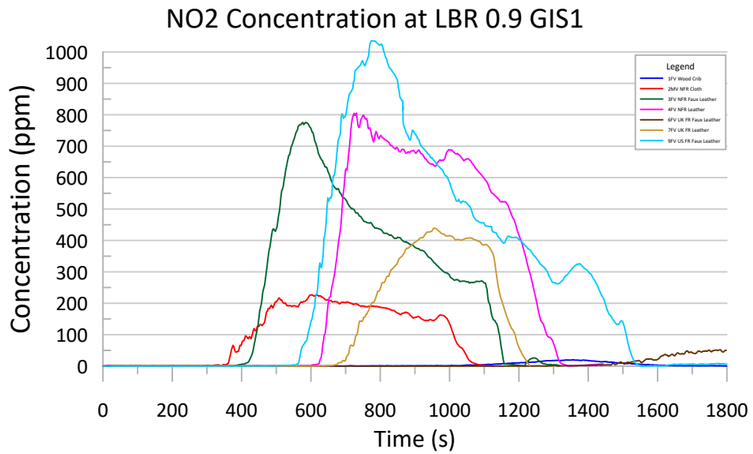
NO Concentration at USE 0.3 m GIS7

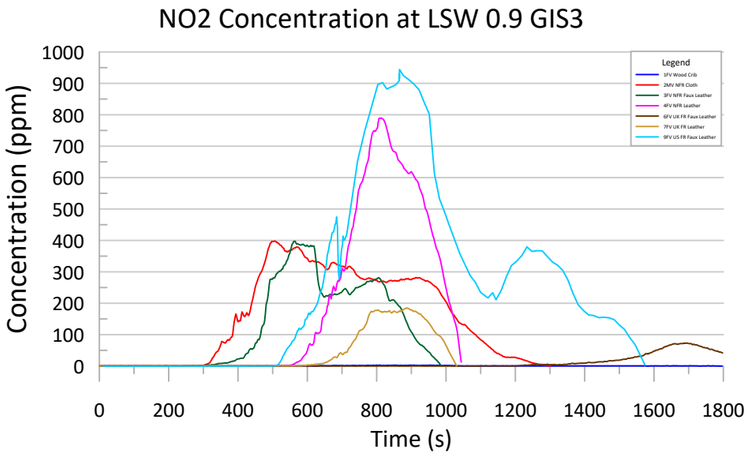


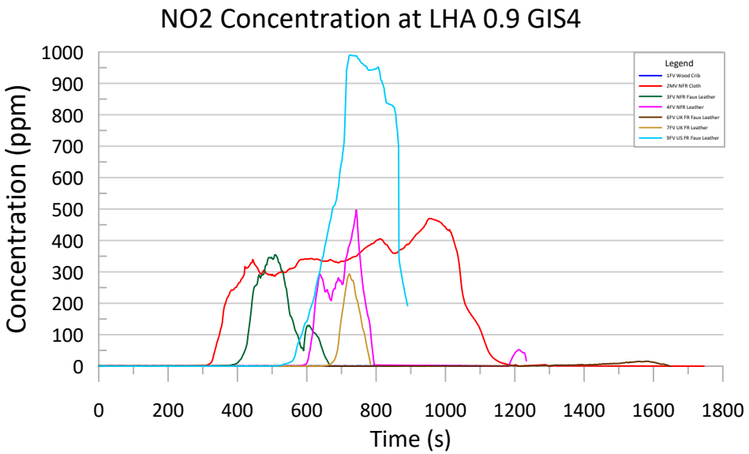

NO2 Concentration at LBR 0.9 GIS2
Concentration (ppm)
Time (s)
Legend
1FV Wood Crib
2MV NFR Cloth
3FV NFR Faux Leather
4FV NFR Leather
6FV UK FR Faux Leather
7FV UK FR Leather
9FV US FR Faux Leather

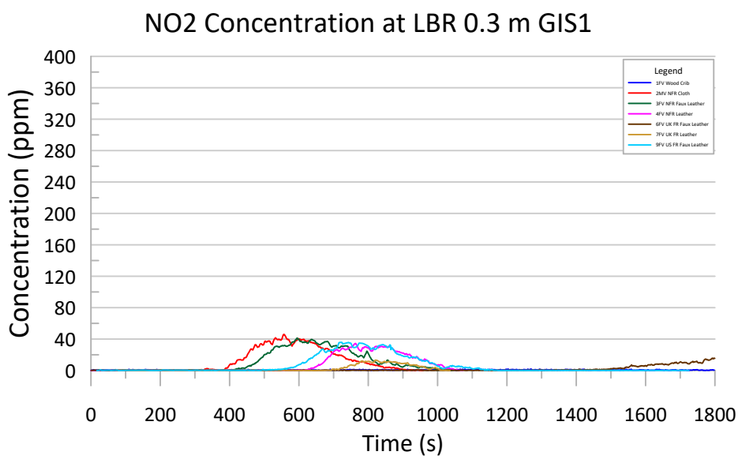

NO2 Concentration at 1.5 GIS3
Concentration (ppm)
Time (s)
Legend
1FV Wood Crib
2MV NFR Cloth
3FV NFR Faux Leather
4FV NFR Leather
6FV UK FR Faux Leather
7FV UK FR Leather
9FV US FR Faux Leather

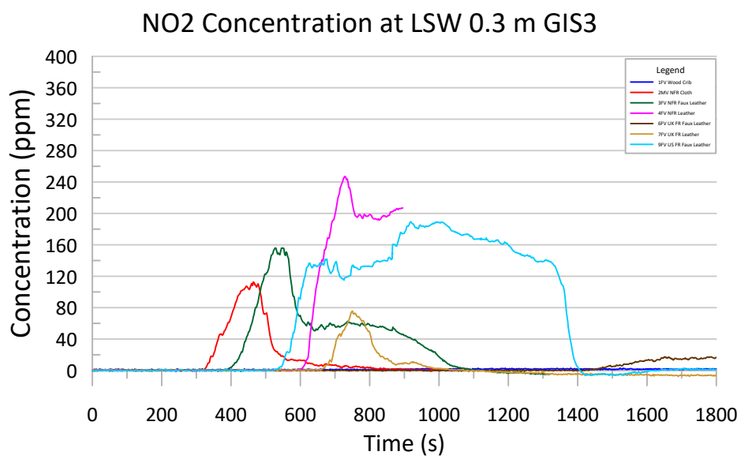

NO2 Concentration at LHA 1.5 GIS4
Concentration (ppm)
Time (s)
Legend
1FV Wood Crib
2MV NFR Cloth
3FV NFR Faux Leather
4FV NFR Leather
6FV UK FR Faux Leather
7FV UK FR Leather
9FV US FR Faux Leather

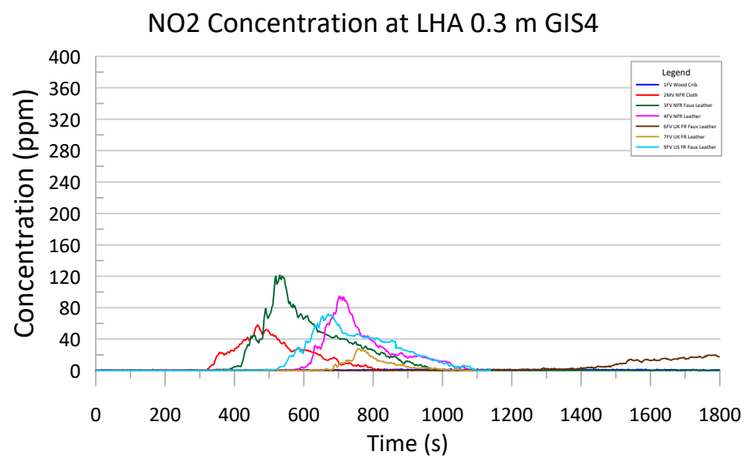

NO2 Concentration at LBR 0.9 GIS1
Concentration (ppm)
Time (s)
Legend
1FV Wood Crib
2MV NFR Cloth
3FV NFR Faux Leather
4FV NFR Leather
6FV UK FR Faux Leather
7FV UK FR Leather
9FV US FR Faux Leather

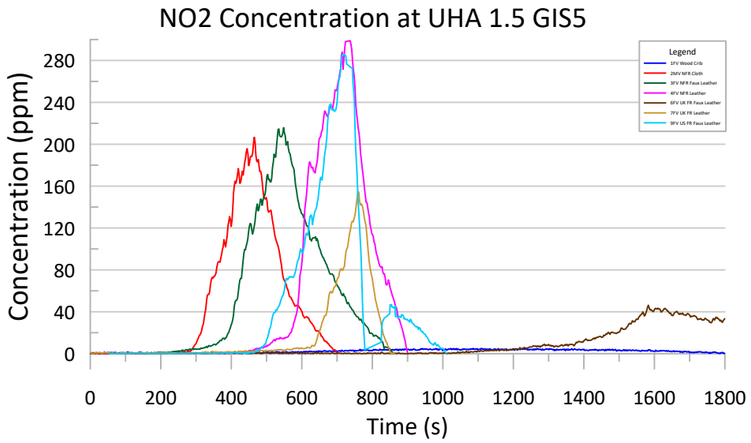

NO2 Concentration at LSW 0.9 GIS3
Concentration (ppm)
Time (s)
Legend
1FV Wood Crib
2MV NFR Cloth
3FV NFR Faux Leather
4FV NFR Leather
6FV UK FR Faux Leather
7FV UK FR Leather
9FV US FR Faux Leather

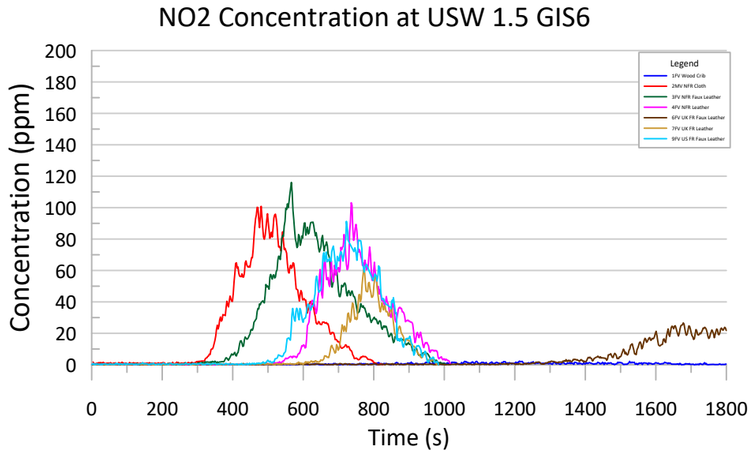

NO2 Concentration at LHA 0.9 GIS4
Concentration (ppm)
Time (s)
Legend
1FV Wood Crib
2MV NFR Cloth
3FV NFR Faux Leather
4FV NFR Leather
6FV UK FR Faux Leather
7FV UK FR Leather
9FV US FR Faux Leather

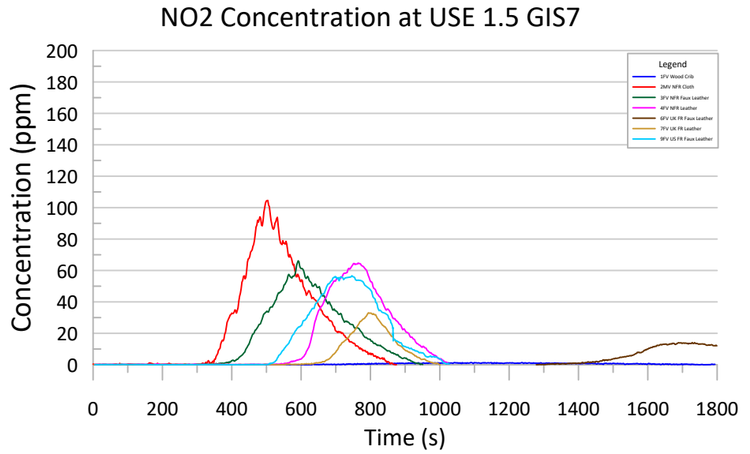

NO2 Concentration at LBR 0.3 m GIS1
Concentration (ppm)
Time (s)
Legend
1FV Wood Crib
2MV NFR Cloth
3FV NFR Faux Leather
4FV NFR Leather
6FV UK FR Faux Leather
7FV UK FR Leather
9FV US FR Faux Leather

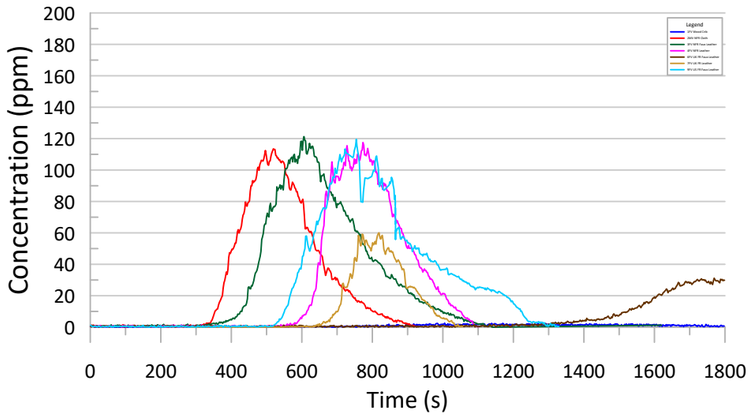

NO2 Concentration at LSW 0.3 m GIS3
Concentration (ppm)
Time (s)
Legend
1FV Wood Crib
2MV NFR Cloth
3FV NFR Faux Leather
4FV NFR Leather
6FV UK FR Faux Leather
7FV UK FR Leather
9FV US FR Faux Leather

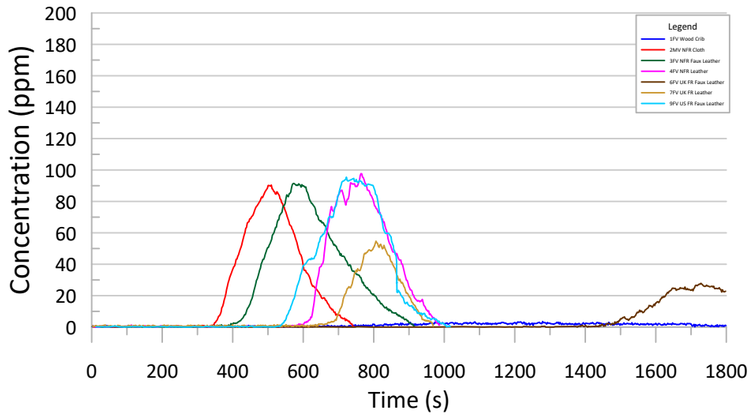

NO2 Concentration at LHA 0.3 m GIS4
Concentration (ppm)
Time (s)
Legend
1FV Wood Crib
2MV NFR Cloth
3FV NFR Faux Leather
4FV NFR Leather
6FV UK FR Faux Leather
7FV UK FR Leather
9FV US FR Faux Leather

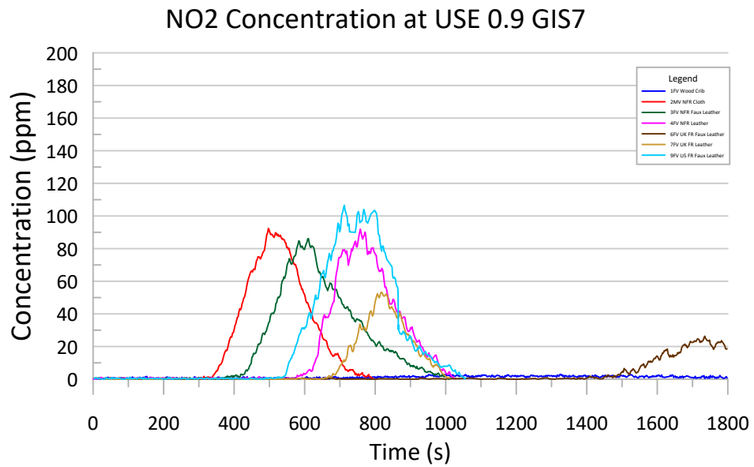

NO2 Concentration at UHA 1.5 GIS5
Concentration (ppm)
Time (s)
Legend
1FV Wood Crib
2MV NFR Cloth
3FV NFR Faux Leather
4FV NFR Leather
6FV UK FR Faux Leather
7FV UK FR Leather
9FV US FR Faux Leather

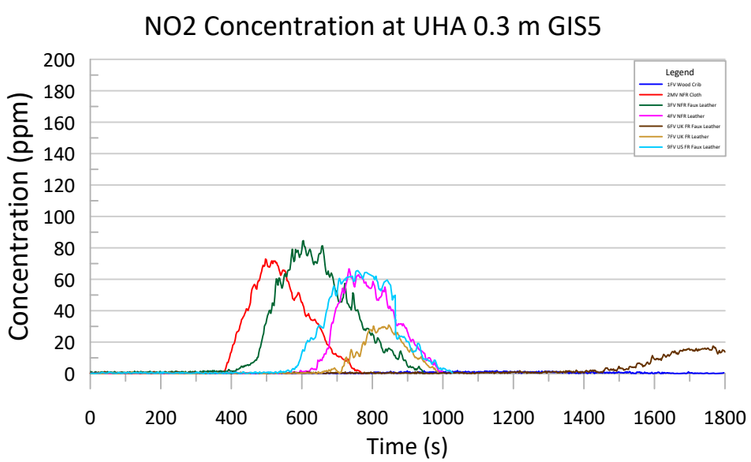

NO2 Concentration at USW 1.5 GIS6
Concentration (ppm)
Time (s)
Legend
1FV Wood Crib
2MV NFR Cloth
3FV NFR Faux Leather
4FV NFR Leather
6FV UK FR Faux Leather
7FV UK FR Leather
9FV US FR Faux Leather

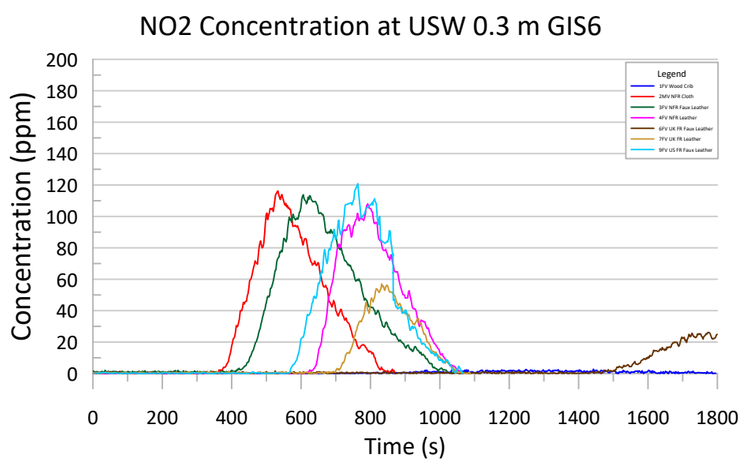

NO2 Concentration at USE 1.5 GIS7
Concentration (ppm)
Time (s)
Legend
1FV Wood Crib
2MV NFR Cloth
3FV NFR Faux Leather
4FV NFR Leather
6FV UK FR Faux Leather
7FV UK FR Leather
9FV US FR Faux Leather

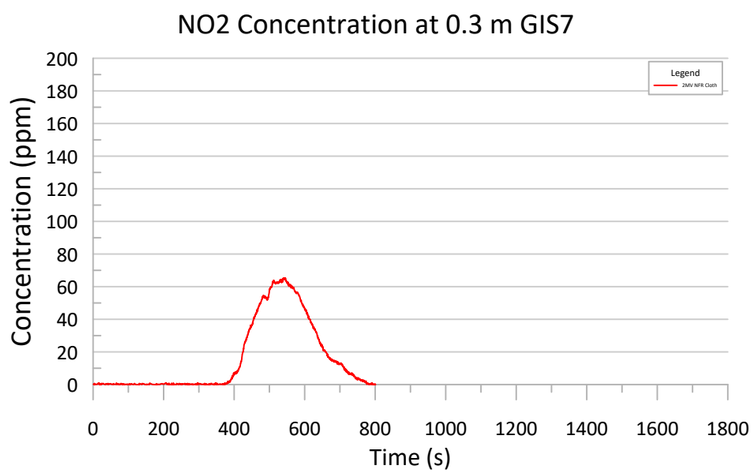

NO2 Concentration at UHA 0.9 GIS5
Concentration (ppm)
Time (s)


NO2 Concentration at USW 0.9 GIS6
Concentration (ppm)
Time (s)
Legend
1FV Wood Crib
2MV NFR Cloth
3FV NFR Faux Leather
4FV NFR Leather
6FV UK FR Faux Leather
7FV UK FR Leather
9FV US FR Faux Leather

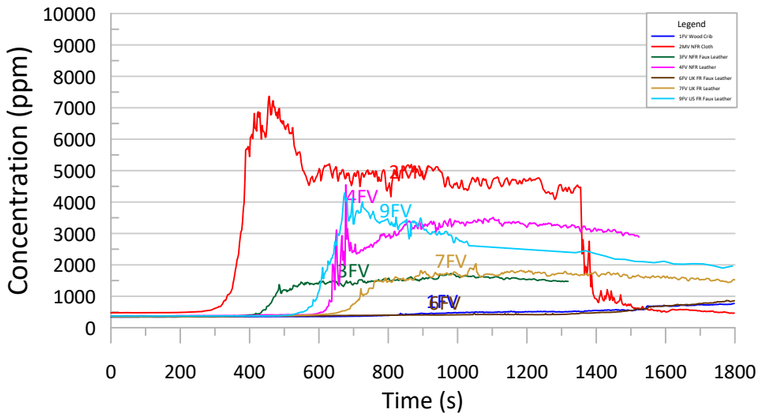

NO2 Concentration at USE 0.9 GIS7
Concentration (ppm)
Time (s)
Legend
1FV Wood Crib
2MV NFR Cloth
3FV NFR Faux Leather
4FV NFR Leather
6FV UK FR Faux Leather
7FV UK FR Leather
9FV US FR Faux Leather


NO2 Concentration at UHA 0.3 m GIS5
Concentration (ppm)
Time (s)
Legend
1FV Wood Crib
2MV NFR Cloth
3FV NFR Faux Leather
4FV NFR Leather
6FV UK FR Faux Leather
7FV UK FR Leather
9FV US FR Faux Leather

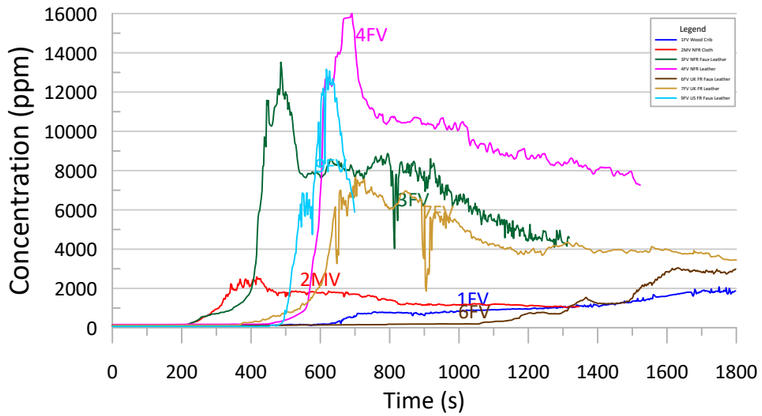

NO2 Concentration at USW 0.3 m GIS6
Concentration (ppm)
Time (s)
Legend
1FV Wood Crib
2MV NFR Cloth
3FV NFR Faux Leather
4FV NFR Leather
6FV UK FR Faux Leather
7FV UK FR Leather
9FV US FR Faux Leather


NO2 Concentration at 0.3 m GIS7
Concentration (ppm)
Time (s)
Legend
2MV NFR Cloth

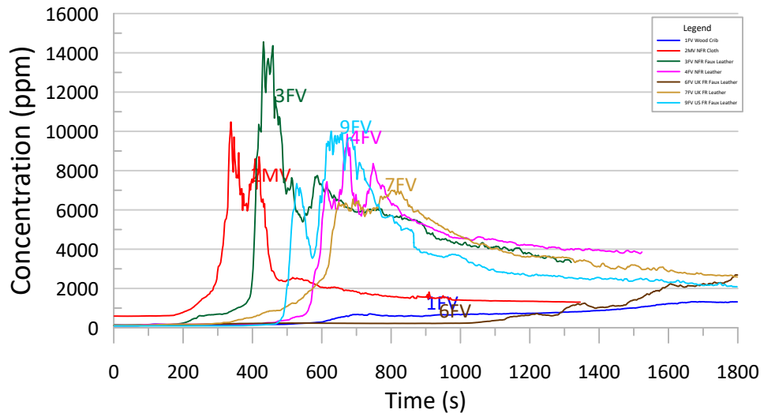
CH4 Concentration at LBR 0.9 GIS2



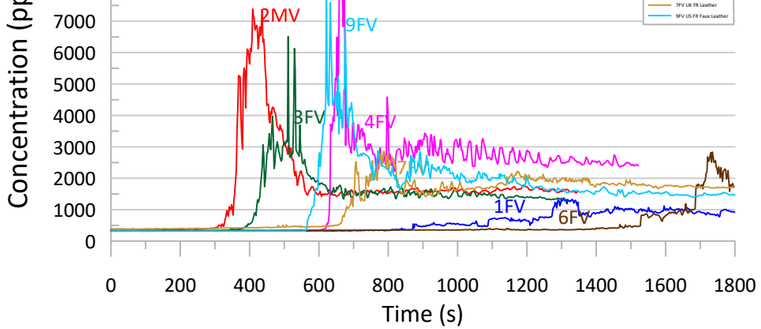
CH4 Concentration at 1.5 GIS3



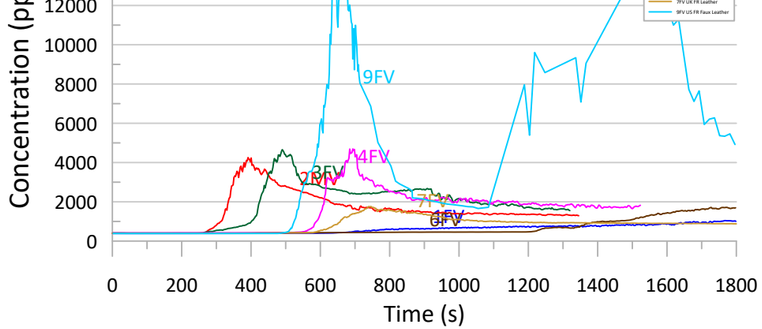
CH4 Concentration at LHA 1.5 GIS4



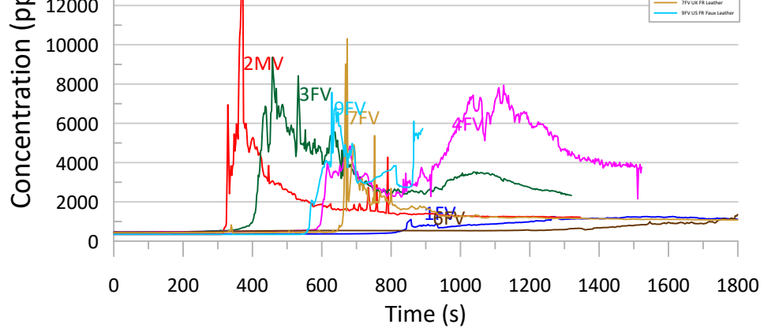
CH4 Concentration at LBR 0.9 GIS1



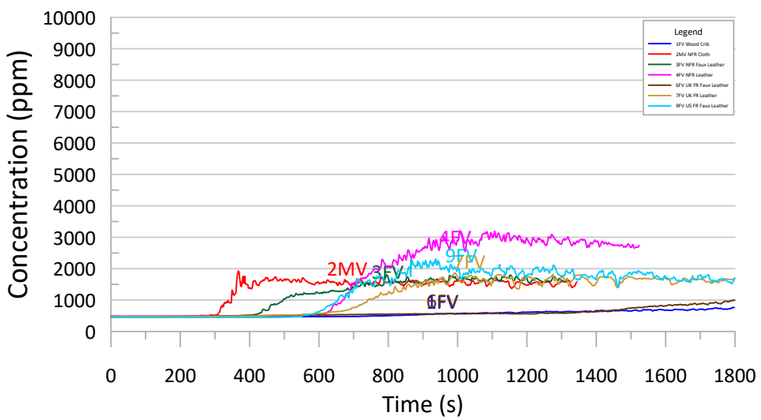
CH4 Concentration at LSW 0.9 GIS3



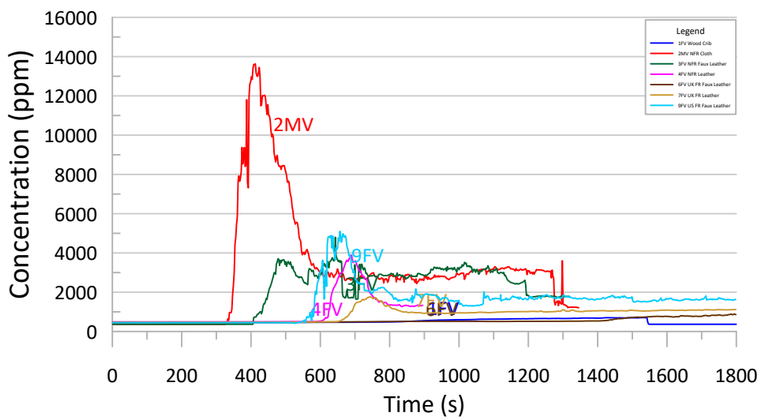
CH4 Concentration at LHA 0.9 GIS4



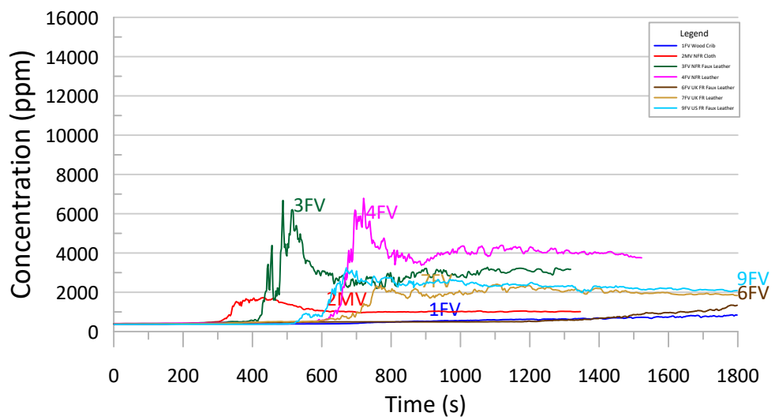
CH4 Concentration at LBR 0.3 m GIS1



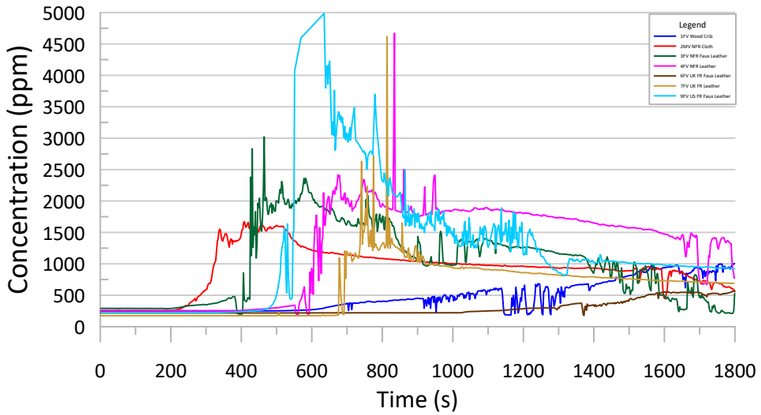
CH4 Concentration at LSW 0.3 m GIS3



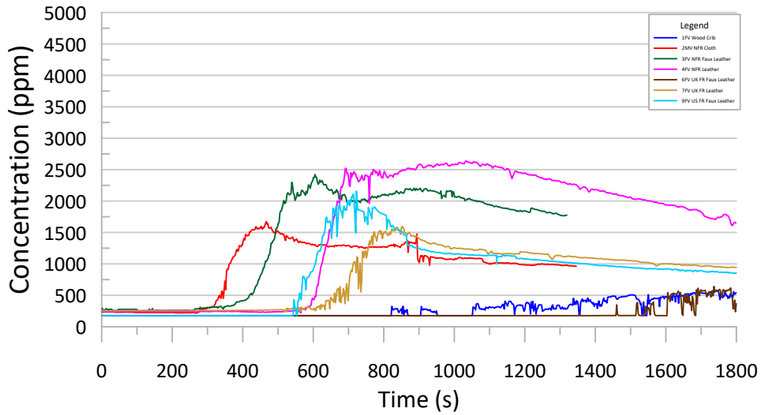
CH4 Concentration at LHA 0.3 m GIS4



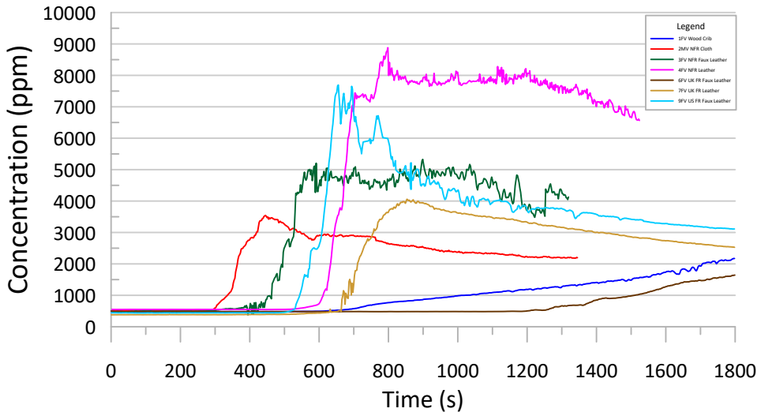
CH4 Concentration at UHA 1.5 GIS5



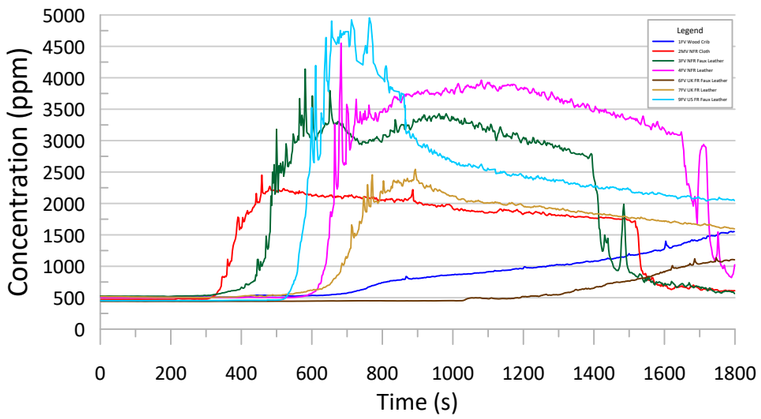
CH4 Concentration at USW 1.5 GIS6



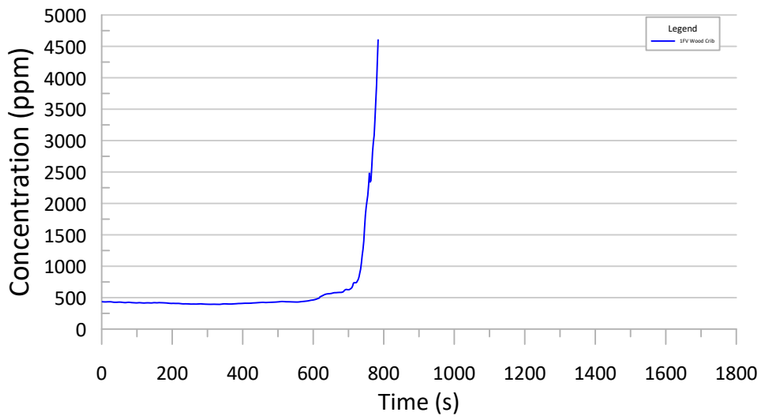
CH4 Concentration at USE 1.5 GIS7



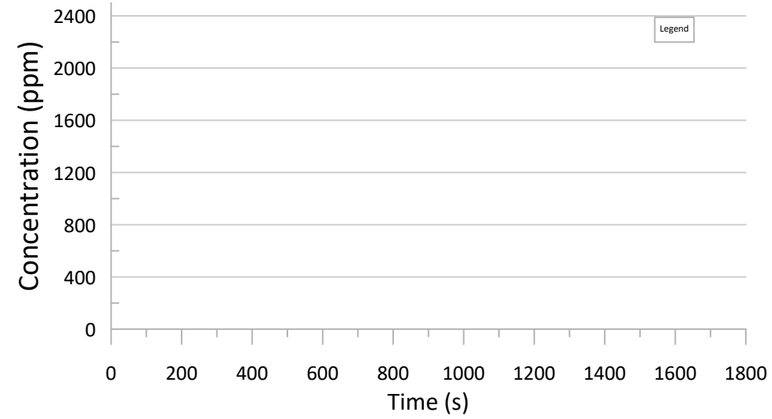
CH4 Concentration at UHA 0.9 GIS5



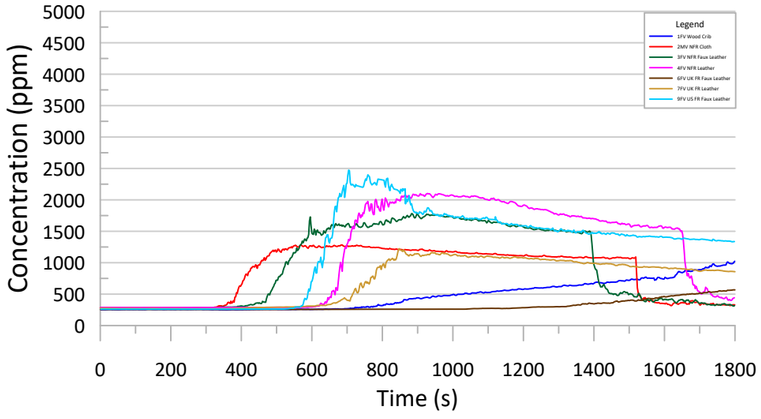
CH4 Concentration at USW 0.9 GIS6



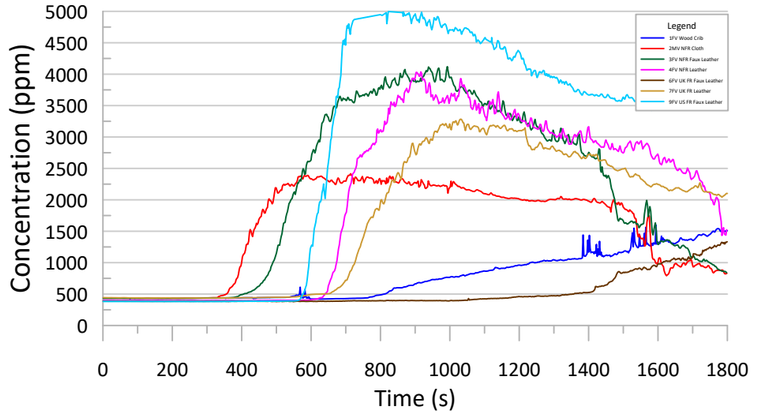
CH4 Concentration at USE 0.9 GIS7



CH4 Concentration at UHA 0.3 m GIS5



CH4 Concentration at USW 0.3 m GIS6



CH4 Concentration at USE 0.3 m GIS7

